METAL-CATALYZED OXIDATIVE TRANSFORMATIONS OF CARBONYL COMPOUNDS: DOMINO REACTIONS, REARRANGEMENTS, AND CONTINUOUS FLOW APPLICATIONS

A THESIS

SUBMITTED IN PARTIAL FULFILLMENT OF THE REQUIREMENTS

FOR THE DEGREE OF

DOCTOR OF PHILOSOPHY

IN CHEMISTRY

BY

MORESHWAR B. CHAUDHARI

(ID: 20153378)

UNDER THE GUIDANCE OF Dr. BOOPATHY GNANAPRAKASAM

AT

DEPARTMENT OF CHEMISTRY
INDIAN INSTITUTE OF SCIENCE EDUCATION AND RESEARCH
PUNE, MAHARASHTRA, INDIA-411008

DECEMBER- 2019

This Thesis is Dedicated to My Family, Teachers, and Friends for Making All of My Success Possible

भारतीय विज्ञान शिक्षा एवं अनुसंधान संस्थान पुणे
INDIAN INSTITUTE OF SCIENCE EDUCATION AND RESEARCH PUNE
डॉ. होमी भाभा मार्ग, पुणे 411008, महाराष्ट्र, भारत | Dr. Homi Bhabha Road, Pune 411008, Maharashtra, India
T +91 20 2590 8001 W www.iiserpune.ac.in

IISER PUNE

CERTIFICATE

Certified that the work incorporated in the thesis entitled ("Metal-Catalyzed Oxidative Transformations of Carbonyl Compounds: Domino Reactions, Rearrangements, and Continuous Flow Applications") Submitted by (**Moreshwar B. Chaudhari**) was carried out by the candidate, under my supervision. The work presented here or any part of it has not been included in any other thesis submitted previously for the award of any degree or diploma from any other University or institution.

Date: 15/10/2019

(Supervisor)

Dr. Boopathy Gnanaprakasam
(Assistant Professor)

DECLARATION

I declare that this written submission represents my ideas in my own words and where others' ideas have been included, I have adequately cited and referenced the original sources. I also declare that I have adhered to all principles of academic honesty and integrity and have not misrepresented or fabricated or falsified any idea/data/fact/source in my submission. I understand that violation of the above will be cause for disciplinary action by the Institute and can also evoke penal action from the sources which have thus not been properly cited or from whom proper permission has not been taken when needed.

Date: 15/10/2019 (Signature)

(Moreshwar B. Chaudhari)
Roll No. 20153378

Acknowledgments

Having completed this Ph.D., I would like to extend my gratitude to many people who made these five years possible. First and foremost, I would like to express my sincere gratitude to my advisor, **Dr. Boopathy Gnanaprakasam**, for giving me all opportunities, advice, active guidance, constant encouragement, motivation, and profound understanding during the Ph.D. study. Being a first student, it was a great opportunity for me to gain remarkable knowledge from Prof. Gnanaprakasam. I doubt that I will ever be able to express my appreciation fully, but I owe him my deepest gratitude.

No words are adequate to thanks my loving mother, Mrs. **Suman Chaudhari,** and father, Mr. **Bhagwan G. Chaudhari,** for their dedication, motivation, patient, and caring throughout my life. I wish to express my extreme indebtedness to loving sisters Mrs. Archana, Manisha, Shital, and Nayana, for their contribution to my achievements. I am also thankful to my brothers-in-law for their constant support and cheering throughout my Ph.D. studies.

I am extremely thankful to our former director, Prof. K. N. Ganesh, and current director Prof. Jayant Udgaonkar for providing excellent research platform, financial support, and facilities at the Indian Institute of Science Education and Research (IISER), Pune, India. I also would like to extend my gratitude to my thesis Research Advisory Committee members, Dr. Ravindar Kontham, Dr. E. Balaraman, and Dr. Ramakrishna G. Bhat for their valuable inputs during my RAC meetings. I want to thank former Chair chemistry Prof. M. Jayakannan and current Chair Prof. H. N. Gopi for their support and various departmental activities, including Chemsymphoria. I want to thank our collaborators, Dr. Karmodiya and Dr. Sudipta Basu, from IISER-Pune. Special thanks to Prof. V. G. Anand for discussion on EPR analysis, and I am also thankful to all the chemistry faculty members at IISER-Pune for their support. I also thank all administrative staff (Mahesh, Yathish, Ganesh, Mayuresh, Megha, Sanjay, Tushar, Sayalee) and instrument operators (Sandeep, Nitin, Ravindar, Chinmay).

I am amazingly fortunate to get the cheerful and friendly lab members: Girish, Dr. Sandip, Akanksha, Nirmala, Akash Ubale, Moseen, Parvathalu, Akash Jamdade, and Dashrath Sutar without them working would have become boring in the lab. I am thankful for every one of my research group for their timely help. I owe my gratitude to Dr. Trimbak, Dr. Prabhakar, Dr. Tushar, Dr. Shahaji, Dr. Nitin, Dr. Satish E., Dr. Vijay, and Dr. Dutta for valuable suggestions and guidance. I am indebted to my loving batch-mates of 2015 batch, Mr. Ravindra, Soumendu, Debanjan, Naveen, Suraj, Pooja, Jagan, Rishabh, Nasrina, Rajashree, Yogeshwar, Somraj, Gayathri, Sachin and IISER friends Prachi, Iranna, Madan, Pramod, Sohan, Ganesh, Shraddha and non-IISER friends, Yogesh Jagtap, Sagar Deshmukh, Prabhakar Kshirsagar, Sanhita and Amardeep for their ardent and assiduous support, care and attention. Many thanks to my M.Sc., classmates, Satish, Gulab, Vinayak, Vishakha, Bapusaheb, Samadhan, Sagar, Daya, Shital, Dhanashri, Girish and Avinash for their timely support.

I wish to express my extreme indebtedness to Dr. T. K. Paine (IACS, Kolkata) for isotope labeling experiments. Dr. Gopinath (NCL, Pune) for GC analysis and Dr. E. Balaraman for TEM analysis. I would like to acknowledge SAIF and ESCA, IIT-Bombay, India, for the instrumentation facility.

Financial assistance as JRF/SRF by the IISER- Pune, and CSIR, New Delhi is gratefully acknowledged. Last but not least, my words are insufficient to thank **almighty God** without whom anything is impossible by this little man as his ubiquitous presence and the omniscient role is gargantuan indeed.

MORESHWAR B. CHAUDHARI

TABLE OF CONTENTS

Abbreviation

° C	Degrees Celsius	EtOAc	Ethyl acetate
M	Micro	FTIR	Fourier-transform infrared spectroscopy
t_R	Residence time (in flow)	g	gram(s)
Ac	Acetyl	GC	Gas chromatography
Ar	Aryl	GC-MS	Gas chromatography-mass spectrometry
Atm	Atmospheric	h	Hour (s)
Aq	Aqueous	Hz	Hertz
Bn	Benzyl	HRMS	High-resolution mass spectroscopy
bs	Broad singlet	IR	Infra-red
Bu	Butyl	J	Coupling constant in NMR
bpy	Bipyridyl	L	Ligand
calcd.	Calculated	LA	Lewis-acid
cat.	Catalytic	M	Molar (mol L^{-1})
conc.	Concentrated	m/z	mass to charge ratio
$CDCl_3$	Deuterated chloroform	m	multiplet (in NMR)
DBU	1,8-Diazabicyclo[5.4.0]undec-7-ene	Me	Methyl
DCM	Dichloromethane	MS	Mass spectroscopy
DCE	Dichloroethane	Mp	Melting point
THF	Tetrahydrofuran	mg	Milligram
DEPT	Distortionless enhancement by polarization transfer	mmol	Millimoles
DMF	*N, N*-Dimethyl formamide	NMR	Nuclear magnetic resonance
DMSO	Dimethyl sulfoxide	OAc	Acetate
DMSO-d_6	Duterated dimethyl sulfoxide	Ph	Phenyl
DMA	*N,N'*-Dimethylacetmide	PTSA	*Para*-toluenesulfonic acid
dppf	1,1′-Bis(diphenylphosphino)ferrocene	pybox	(2,6-Bis[(*4S*)-(−)-isopropyl-2-oxazolin-2-yl]pyridine)
DMAP	4-Dimethylaminopyridine	rt	Room temperature
DTBP	Di-tert-butyl peroxide	Sn	Tin
dr	Diastereomeric ratio	*tert*	Tertiary
ee	Enantiomeric excess	TBHP	*tert*-butyl hydroperoxide
equiv	Equivalents	TLC	Thin layer chromatography
ESI TOF	Electrospray ionization time-of-flight	TMS	Tetramethyl silane
EI	Electron impact	THF	Tetrahydrofuran
ESI	Electron spray ionization	TON	Turnover number
Et	Ethyl	TS	Transition state

PREFACE

The metal-catalyzed reactions have pivotal importance in chemical synthesis, which can be utilized to construct challenging organic scaffold of biological importance with improved sustainability and atom economy. In particular, the oxidation reactions are profoundly important in chemical/biological synthesis, and it provides a breakthrough for the synthesis of building blocks/precursors towards natural/unnatural targets. Accordingly, the metal-catalyzed oxidative C-H functionalization offers a direct route to construct the C-C, C-O and C-N bond formation and gives access to novel bioactive compounds, commercial drugs, natural products, household products, petrochemicals, *etc*. The present investigation of this thesis describes C-C bond formation by α-alkylation of unactivated amides, C-O bond formation *via* sp^3-C-H peroxidation in batch/continuous-flow, hydroxylation of carbonyl compounds and novel rearrangement of peroxides using Lewis or Brønsted acid to afford the biologically important scaffolds.

This thesis describes research findings in the development of "Metal-Catalyzed Oxidative Transformations of Carbonyl Compounds: Domino Reactions, Rearrangements, and Continuous Flow Applications," and which comprises of four chapters.

Chapter 1: Introduction to Oxidative C-H Functionalization

At the outset, the brief introduction of metal catalysis is described concerning the field of chemistry. Later, the fundamental of oxidation reactions, along with an overview of C-H functionalization is discussed. Then, the aim and rationale of the thesis are described.

Chapter 2: Ruthenium-Catalyzed Direct α-Alkylation of Amides Using Alcohols and C-H Hydroxylation of Carbonyl Compounds

In this chapter, we present a ruthenium-catalyzed direct α-alkylation of unactivated amides and 2-oxindoles, using alcohol as an alkylating agent and transition-metal-free C-H hydroxylation of carbonyl compounds. Chapter 2 is subdivided into two sections. Section A describes a highly efficient protocol for ruthenium-pincer catalyzed direct α-alkylation of amides using alcohol with an astonishing turnover number. A variety of pincer catalysts were screened for this transformation, and out of that, Ru-PNN catalyst was found to be the best. In section B, we describe transition-metal-free C-H hydroxylation of carbonyl derivatives using atmospheric oxygen and inexpensive base. Both the section includes a literature background, the rationale for work, optimization studies, substrate scope, and mechanistic studies.

Chapter 3: Metal-Catalyzed Batch/Continuous Flow Synthesis of Peroxides and Evaluation of Biological Properties

This chapter describes the simple and efficient method for the synthesis of quaternary peroxides using homogeneous as well as a heterogeneous catalyst in batch/flow and evaluation of biological properties. This chapter is also subdivided into two sections, A and B. In section A, the use of homogeneous Fe-catalyst is demonstrated for the C-H peroxidation of derivatives of 2-oxindole, coumarin and barbituric acid. The peroxidation is accomplished using continuous flow with a shorter reaction time. At the outset, the introduction to continuous flow chemistry and literature precedence for the metal-catalyzed peroxidation reactions is described. Then, the optimization of reaction conditions in batch/flow and broad substrate scope is demonstrated. Subsequently, the mechanistic studies (EPR and radical quenching experiments) on the peroxidation reaction are shown. Finally, in biological studies, the anticancer activity of the synthesized peroxides is demonstrated. In section B, the synthesis and characterization of supported magnetic iron oxide nanoparticles and its catalytic property for the C-H peroxidation reaction using batch/flow are described. The extensive optimization and substrate scope using batch/flow is demonstrated. Eventually, the antimalarial property of the quaternary peroxides is evaluated against the malarial parasite.

Chapter 4: The Novel Rearrangements of Peroxide on Electron Deficient Oxygen

The present chapter showcase the discovery of two novel rearrangements in peroxyoxindole derivatives to afford 1,4-Benzoxazin-3-one derivatives and substituted-2*H*-benzo[*b*][1,4]oxazin-3(4*H*)-one. This chapter is also subdivided into two sections. In the first section, highly selective synthesis of (*Z*)-2-arylidene and alkylidene-2*H*-benzo[*b*][1,4]oxazin-3(4*H*)-one derivatives using Sn-catalyst is discussed. The results on $FeCl_3$ catalyzed Hock fragmentation products *via* C−C bond cleavage are also described. In the second section, novel rearrangement of *in situ* generated peresters is presented. This reaction utilizes the feedstocks chemicals such as esters for the synthesis of perester intermediate as a key step for the skeletal rearrangement. In the beginning, the introduction and literature background delineates the variety of reported rearrangements in the peroxide scaffold. Next, the optimization and substrate scope for the novel rearrangement is described. To gain mechanistic insights, the isotope labeling experiments were performed. Furthermore, 2-oxindole hydroperoxide or perester intermediate was prepared separately, and their reactions were investigated. Finally, based on the preliminary experimental shreds of evidence, the plausible reaction mechanism is depicted for molecular rearrangement reactions.

LIST OF PUBLICATIONS

(1) **Chaudhari, M. B.**; Jayan, K.; Gnanaprakasam, B. Sn-Catalyzed Criegee-Type Rearrangement of Peroxyoxindoles Enabled by Catalytic Dual Activation of Esters and Peroxides (manuscript under revision).

(2) **Chaudhari, M. B**.; Mohanta, N.; Pandey, A. M.; Vandana, M.; Karmodiya, K.; Gnanaprakasam, B. Peroxidation of 2-Oxindole and Barbituric Acid Derivatives under Batch and Continuous Flow Using an Eco-Friendly Ethyl Acetate Solvent. *React. Chem. Eng*. **2019**, *4*, 1277.

(3) **Chaudhari, M. B.**; Chaudhary, A.; Kumar, V.; Gnanaprakasam, B. The Rearrangement of Peroxides for the Construction of Fluorophoric 1,4-benzoxazin-3-one Derivatives. *Org. Lett*. **2019**, *21*, 1617.

(4) **Chaudhari, M. B.**; Gnanaprakasam, B. Recent Advances in Metal-Catalyzed Amide Bond Activation. *Chem. Asian. J*. **2019**, *14*, 76 **(FOCUS REVIEW).**

(5) **Chaudhari, M. B.**; Moorthy S.; Patil, S.; Bisht, G. S.; Haneef, M.; Gnanaprakasam, B. Iron-Catalyzed Batch/Continuous Flow C−H Functionalization Module for the Synthesis of Anticancer Peroxides. *J. Org. Chem.* **2018**, *83*, 1358.

(6) **Chaudhari, M. B.**; Malpathak, S.; Hazra, A.; Gnanaprakasam, B. Transition-Metal-Free C–H Hydroxylation of Carbonyl Compounds. *Org. Lett*. **2017**, *19*, 3628 (most-read article in the month of July-2017 in *Organic Letters*).

(7) **Chaudhari, M. B.**; Bisht, G. S.; Kumari, P.; Gnanaprakasam, B. Ruthenium-Catalyzed Direct α-Alkylation of Amides Using Alcohols. *Org. Biomol. Chem.* **2016**, *14*, 9215.

(8) Mohanta, N.; **Chaudhari, M. B**.; Digrawal, N. K.; Gnanaprakasam, B. Rapid and Multi-gram Synthesis of Vinylogous Esters under Continuous-Flow: An Access to Transetherification and Reverse Reaction of Vinylogous Esters. *Org. Process Res. Dev*. **2019**, *23*, 1034.

(9) Bisht, G. S.; Pandey, A. M.; **Chaudhari, M. B**.; Agalave, S. G.; Kanyal, A.; Karmodiya, K.; Gnanaprakasam, B. Ru-Catalyzed Dehydrogenative Synthesis of Antimalarial Arylidene Oxindoles. *Org. Biomol. Chem.* **2018,** *16*, 7223.

(10) Agalave, S. G.; **Chaudhari, M. B**.; Bisht, G. S.; Gnanaprakasam, B. Additive Free Fe-Catalyzed Conversion of Nitro to Aldehyde under Continuous Flow Module. *ACS Sustainable Chem. Eng*. **2018**, *6*, 12845.

(11) Bisht, G. S.; **Chaudhari, M. B**.; Gupte, V. S.; Gnanaprakasam, B. Ru-NHC Catalysed Domino Reaction of Carbonyl Compounds and Alcohols: A Short Synthesis of Donaxaridine. *ACS Omega* **2017**, *2*, 8234.

BOOK CHAPTERS:

(1) Gnanaprakasam, B.; ***Chaudhari, M. B.*** *Metal-Catalyzed Synthesis of Peroxides,* Volume Editor: Prof. Alexander Terent'ev, *Vol*. 38: Peroxides, *Science of Synthesis Knowledge Updates,* (**2019**), 2, 407, Houben-Weyl, Thieme.

Chapter 1

Introduction to Metal-Catalyzed Oxidative C-H Functionalization

1. Introduction to Metal-Catalyzed Oxidative C-H Functionalization

1.1. Abstract

In the present chapter, a summary of applications of metal catalysis in chemistry is depicted. Subsequently, the fundamental oxidation reactions and definitions are described. Further, the general overview of oxidative C-H functionalization, including classical and catalytic C-H functionalization, is also presented. The selected representative examples of oxidative C-H functionalization are also summarized in this chapter. The various types of substrate for the direct oxidative C-H functionalization were recapitulated. Finally, the aim and rationale for the thesis work are described.

1.2. Introduction to metal catalysis and oxidation

Nature performs the sundry of chemical reactions using an enzyme as a catalyst. However, to mimic such transformations, the science of organic synthesis arises. Organic synthesis is a discipline which is utilized for the construction of natural/unnatural molecules by the scientific community from across the world. In this context, the use of metal catalysis is an alternative coherent strategy to enzymatic transformations for the synthesis of complex organic architectures.[1] For instance, Robert Grubbs was awarded a noble prize for the path-breaking discovery of a ruthenium-based catalyst for the metathesis reaction. Moreover, in 2010, Heck, Negishi, and Suzuki awarded the noble prize for their excellent work on palladium-catalyzed cross-coupling reactions. The recognition for the catalysis by the highest award in science signifies the power of metal catalysis in organic synthesis. As a result, almost all types of chemical transformations such as cross-coupling reactions, C-H functionalization, oxidation-reduction, radical reactions, as well as target-oriented natural products synthesis and polymer synthesis, *etc.* could be achieved using metal catalysis.[2]

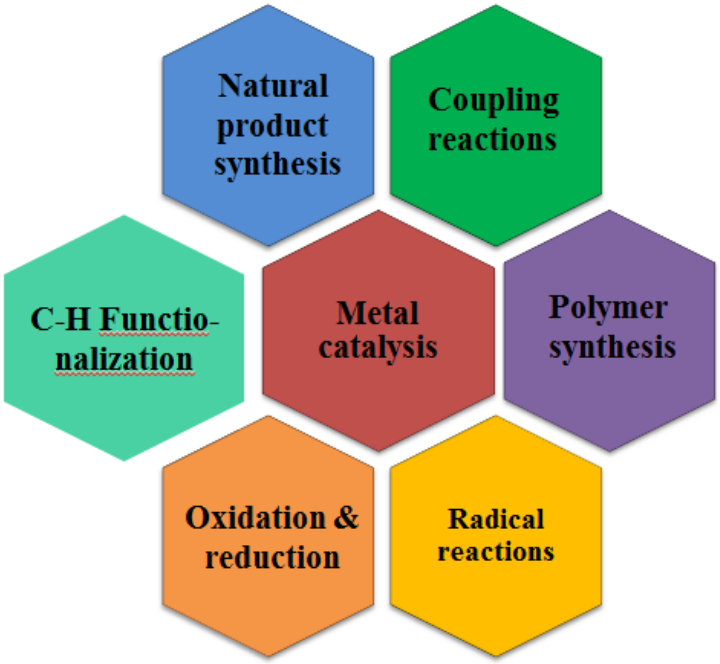

Figure 1. An important application of metal catalysis in chemistry

The selection of a homogeneous or heterogeneous catalyst depends on the choice of reaction and chemical transformation. The reactions employing heterogeneous catalysis are more relevant at industrial scale owing to their properties such as high thermal stability, easy recovery, and recyclability. However, homogeneous catalysts are industrially less relevant due to non-reusability and decomposition at higher temperatures.[3] It would be difficult to draw the direct conclusion which one is better out of homogeneous and heterogeneous catalysis. Among the several types of chemical transformations, oxidation reactions catalyzed by the transition metals are most widely employed in organic synthesis and known for several decades. The oxidation reactions are generally defined in three categories.

(i) **Definition in terms of hydrogen transfer:** The oxidation is defined as the loss of hydrogen.

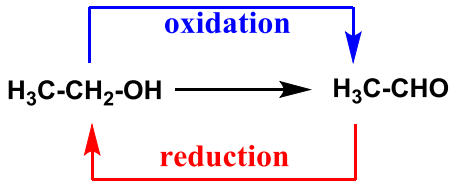

(ii) **Definition with respect to oxygen transfer:** The oxidation is defined as a gain of oxygen.

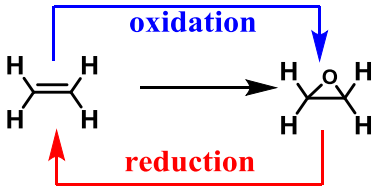

(iii) **Definition in terms of electron transfer:** The oxidation is defined as a loss of electrons.

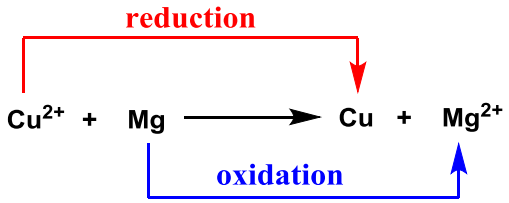

Further, any chemical transformation which falls under the categories mentioned above such as dehydrogenation, peroxidation, oxygen insertion or loss of electrons and involvement of oxygen (O_2) are considered as oxidative transformation.[4]

1.3. Overview on Oxidative C-H functionalization

1.3.1. C-H Functionalization

The C-H functionalization is defined as catalytic or stoichiometric reactions of metal complexes with the unreactive C-H bonds to provide the products comprising a new C-C, C-O, C-N, and C-X bonds.

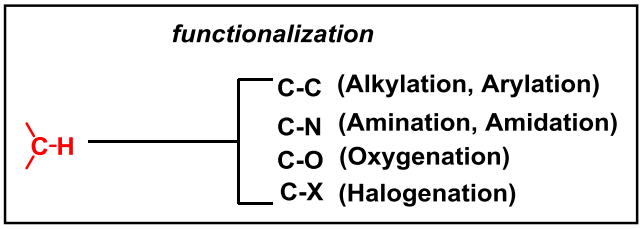

Figure 2. Functionalization of C-H bond

In classical organic synthesis, the presence of electron-withdrawing functional group makes adjacent C-H bond acidic and thus, base mediated deprotonation offers nucleophiles which react with electrophiles to afford desired products. In contrast, in catalytic C-H functionalization reactions, the substitution of a C-H bond is challenging regardless of functional group influence (unactivated).[5]

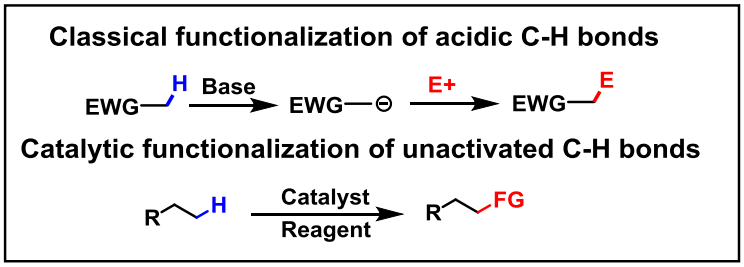

Scheme 1. Classical *vs.* catalytic functionalization of C-H bond

In modern synthetic transformations, C-H activation and C-H functionalization are two different strategies. There is substantial dissimilarity between these two strategies. In the case of C-H activation, hydrocarbon (C-H bond) is coordinated to the metal *via* "agostic" interaction, and these reactions proceed *via* a concerted pathway.[6] However, in C-H functionalization, there is coordination or no coordination of hydrocarbon (C-H bond) to a metal center, and these reactions proceed in a stepwise pathway. The general conclusion can be made, all the C-H activations are C-H functionalization, but not all the C-H functionalizations are C-H activation.

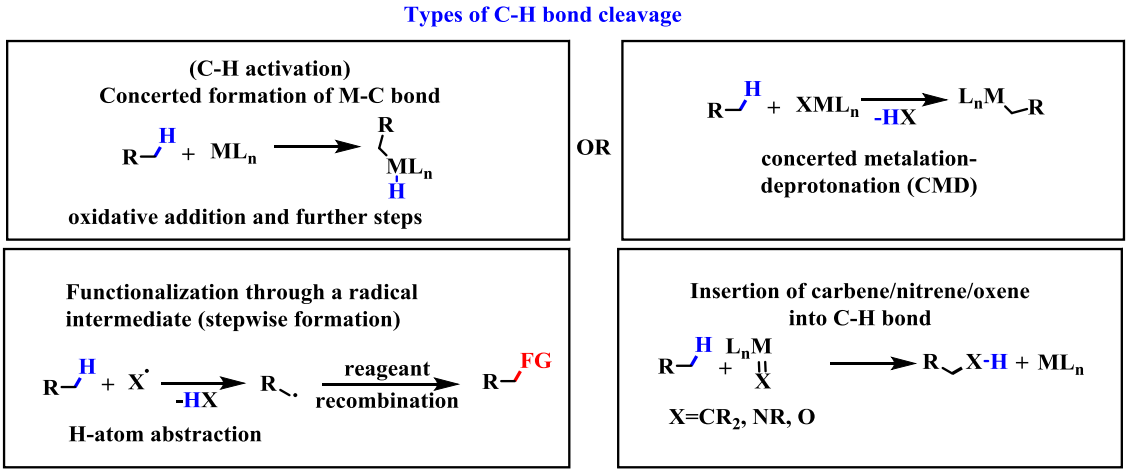

Scheme 2. Types of C-H bond cleavage

There are mainly three types of bond cleavage. Type 1 is C-H bond cleavage by C-H activation, which precedes the concerted formation of M-C bond *via* oxidative addition, transmetallation, and reductive elimination steps. The other possibility for C-H activation is concerted metalation-deprotonation (CMD). Type 2 involves the functionalization of a C-H bond through a radical intermediate by the stepwise formation of radical species, which recombines to give the desired radical-radical cross-coupled products. The last type involves the insertion of reactive chemical species such as carbene/nitrene/oxene into a C-H bond to afford desired products.[5]

1.3.2. C-H Functionalization *via* Borrowing Hydrogen Catalysis (BHC):

Borrowing hydrogen catalysis (BHC) is a combination of oxidation-condensation-reduction sequence in one pot. It is considered as one of the finest environmentally benign approaches owing to its inherent properties such as atom economy, use of alcohols as alkylating agents, and green by-products. For instance, BHC relies on giving and take processes. The α-functionalization of ketone, amide, and ester is possible using this approach. [7-15]

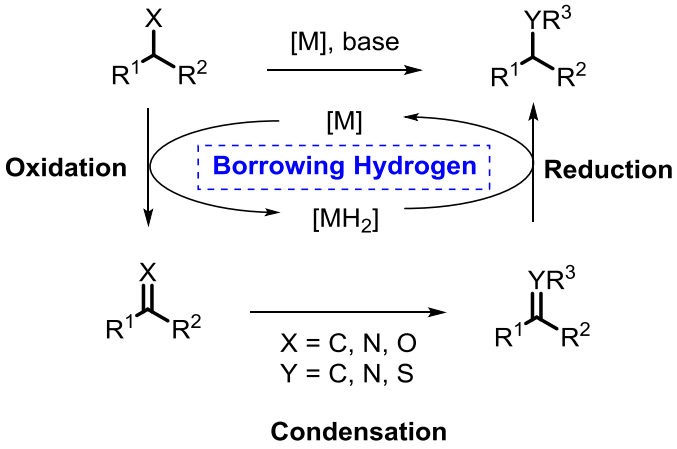

Figure 3. General overview on borrowing hydrogen catalysis

The key step involves catalytic oxidation of alcohol to produce aldehyde and metal hydride species. Subsequently, the reaction of base mediated enolate of ketone, ester, or amide with an aldehyde affords desired unsaturated product, which is reduced by the in situ generated metal hydride during the oxidation process. Hence, using BHC, it is possible to functionalize the C-H bond of amide, ketones, and esters.

1.3.3. Oxidative C-H Functionalization

The oxidative C-H functionalization is related to the oxidation process or being produced by the oxidation. This type of reaction involves one of the steps as oxidation or peroxidation, use of oxygen as an oxidant or reagent, or ring expansion by the oxygen insertion. There are numerous reports available for oxidative C-H functionalization, and a majority of them use peroxides or atmospheric oxygen as an oxidant or reagent; however, it is not possible to include all the literature reports. Thus, in this chapter, we describe the few pioneering examples for the major category of the oxidative C-H functionalization in which peroxides or oxygen has been used along with metal catalysts. The pioneering work on the radical oxidation of allylic alkenes using a copper catalyst and *tert*-butyl benzoperoxoate to afford allylic benzoate derivatives *via* oxidative C-H functionalization. The peroxide was used as an

oxidant as well as a reagent in this transformation. The overall transformation is named Kharasch-Sosnovsky reaction that discovered it the first time in 1958.[16]

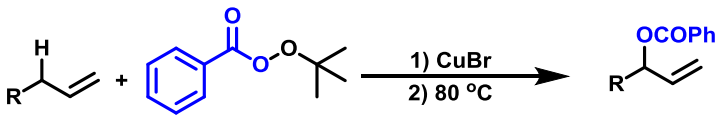

Scheme 3. Kharasch and Sosnovsky reaction

The Kharasch-Sosnovsky reported the peroxidation of carbonyl compounds using CuCl as catalyst and TBHP as a radical initiator, as well as a reagent. If there is no substituent on α-position, the reaction afforded very poor yield owing to other by-products formation. Thus, the introduction of a substituent on α-position to carbonyl produced excellent of the peroxylated product (Scheme 4).[17]

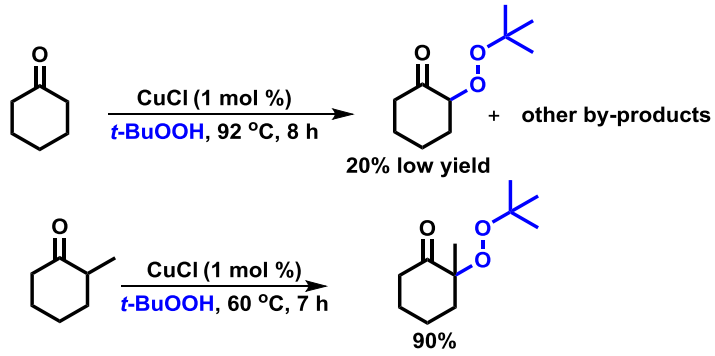

Scheme 4. Kharash approach for peroxidation of carbonyl compounds

In 1996, Singh and co-workers reported the allylic benzoxylation of olefins in the presence of catalytic $Cu(OTf)_2$ and DBU at room temperature or 60 °C.[18] In this report, the DBU was used to accelerate the rate of the reaction and to increase the yield of the reaction.

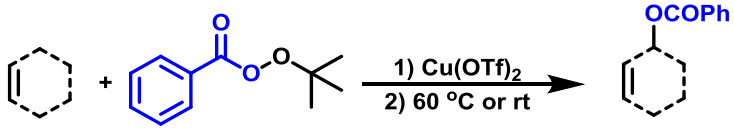

Scheme 5. Singh's approach for benzoxylation of allylic olefins

Subsequently, Singh and co-workers demonstrated the asymmetric Kharasch reaction of allylic olefins using chiral Bis(diphenyloxazoline)-copper complexes and *tert*-Butyl Perbenzoate. [19] The reaction proceeded at fairly mild conditions (at room temperature), and the addition of chiral ligand has controlled enantioselectivity.

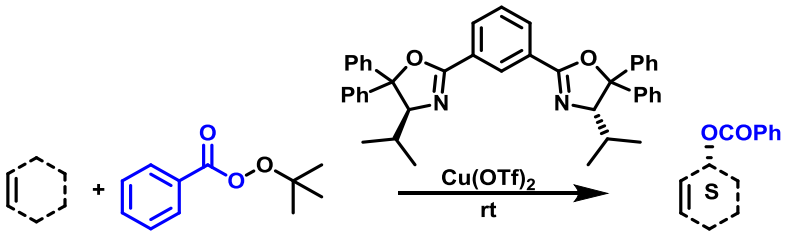

Scheme 6. Singh's approach for asymmetric benzoxylation of olefins

While attempting the epoxidation of styrene derivatives; interestingly the Feringa and co-workers observed the vicinal bisperoxidtion of styrene derivatives in presence of TBHP and Nickel catalyst. The addition of peroxide group across olefin (vicinal bisperoxidation) underwent *via* dinuclear nickel catalyst and proceeded *via* a radical process.[20]

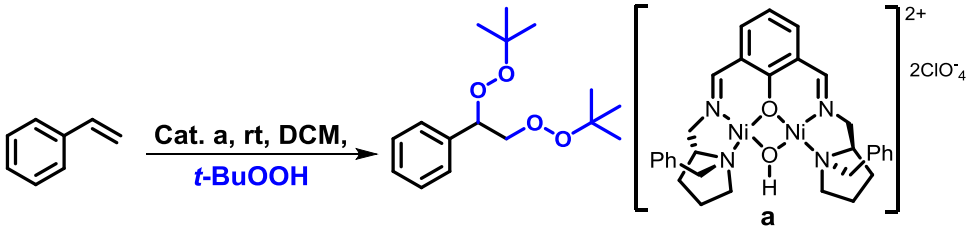

Scheme 7. Feringa's approach for bisperoxidation of olefin

Similarly, in 2002, while performing the epoxidation of alkene derivatives using TBHP and palladium catalyst, Corey and co-workers observed the formation of bisperoxylated product in 85% yield.[21] Notably, the reaction of allylic olefins in the presence of *t*-BuOOH-Pd(OAc)$_2$-K$_2$CO$_3$ in CH$_2$Cl$_2$ at 0 °C favored allylic peroxidation of olefins. However, the non-allylic substrates underwent an epoxidation reaction under the same conditions.

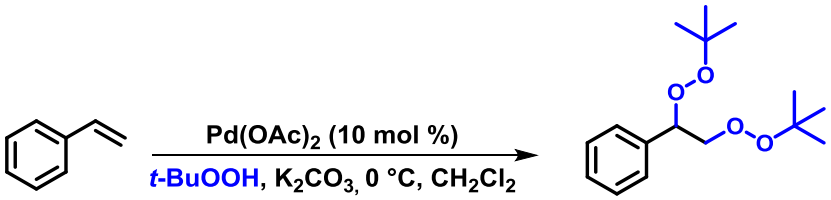

Scheme 8. Corey's approach for bisperoxidation of olefin

Accordingly, Terente'v and co-workers reported the Mn(OAc)$_3$-catalyzed bisperoxidation of alkenes in better yield than Feringas approach.[22] To get the best catalyst, the authors have screened a variety of catalysts such as MnO$_2$, KMnO$_4$, Mn(OAc)$_2$·4H$_2$O, MnCl$_2$·4H$_2$O. Out of all, Mn(OAc)$_2$·4H$_2$O, TBHP, and acetonitrile were found to be the best in terms of yield and selectivity.

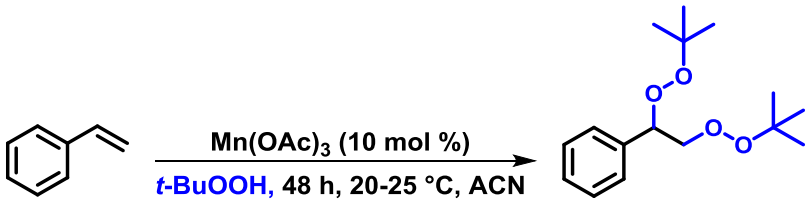

Scheme 9. Terente'v approach for bisperoxidation of olefin

Interestingly, Li and co-workers reported the Iron-catalyzed regioselective peroxidation-carbonylation of olefins using aldehyde and TBHP by radical pathway.[23] In this protocol, a wide substrate scope has been demonstrated for the difunctionalization reaction. Moreover, the synthesized peroxides have been utilized for the formation of epoxides using DBU as a base.

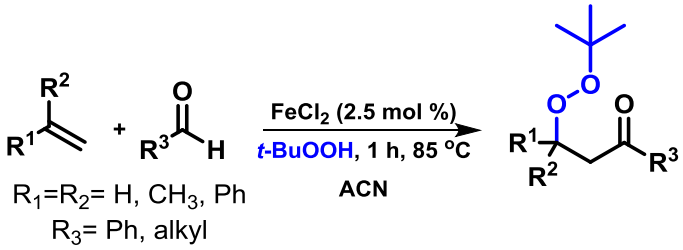

Scheme 10. Li's approach for di-functionalization of alkene

The C-C and C-N bond formation *via* cross-dehydrogenative coupling of *N*-allylbenzamides with indole has been accomplished using a copper catalyst and TBHP as an oxidant. The reaction afforded a variety of α-substituted-*N*-allyl-benzamides under mild reaction conditions.[24]

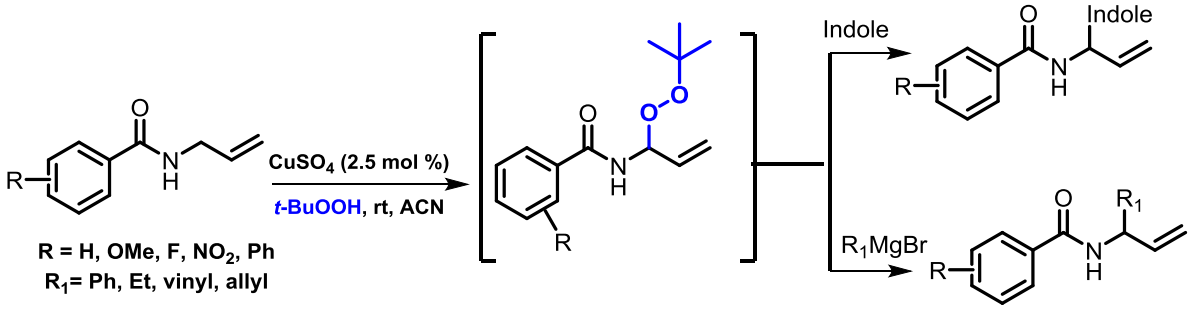

Scheme 11. Krishna's approach for C-H bond functionalization

In previous decades, molecular oxygen has been used as a source of hydroxyl group for the selective oxidation of C-H bonds in the presence of metal or enzymes.[25] In 1989, Yoshida and co-workers reported the direct hydroxylation of benzene derivatives using catecholato-Fe complex as catalyst and *tert*-butylhydroquinone (TBHQ) as reductant.[26]

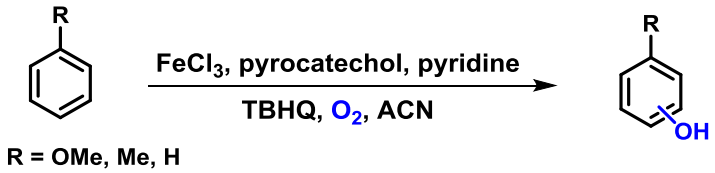

Scheme 12. Yoshida's approach for hydroxylation of benzene derivatives

The Pd-catalyzed ortho-hydroxylation of benzoic acids with molecular oxygen or air was documented. In the control experiments no reaction was observed in the presence of a stoichiometric amount of $Pd(OAc)_2$ under an argon atmosphere, thus O_2 involved in the product formation rather than reoxidation of Pd(0).[27]

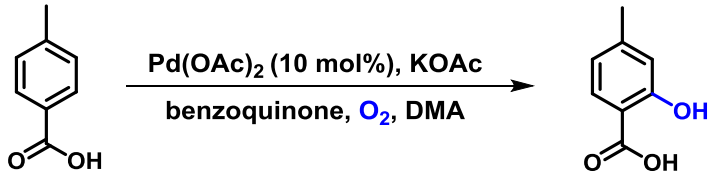

Scheme 13. Yu's approach for hydroxylation of benzoic acid derivatives

Moreover, the use of molecular oxygen for the C-H oxidation of the Sp^3 C-H bond also documented in the literature. Remarkably, ritter and co-workers reported the dinuclear Pd-catalyzed hydroxylation of a variety of carbonyl compounds.[28]

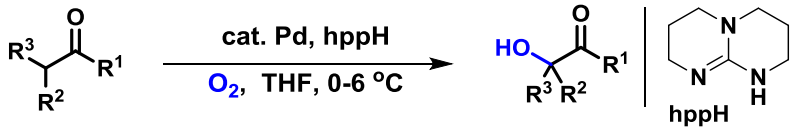

Scheme 14. Ritter's approach for hydroxylation of carbonyl compounds

In 2001, Sen and co-workers reported the Na_2PtCl_6-$CuCl_2$-Catalyzed oxidation of unactivated aliphatic compounds molecular oxygen. In this report, Sen showed that $CuCl_2$ acts as co-catalyst and molecular oxygen as the oxidant.[29]

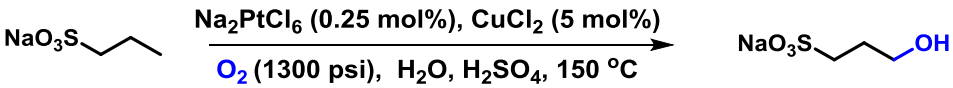

Scheme 15. Sen's approach for hydroxylation of a terminal methyl group

On the other hand, the use of oxygen and peroxide as an oxidant has been employed for several examples of oxidative C-H functionalization. Gaunt and co-workers reported the C2-alkenylation of *N*-protected pyrrole derivatives by employing $Pd(OAc)_2$, *di-tert*-butylbenzylperoxide and O_2 was reported.[30]

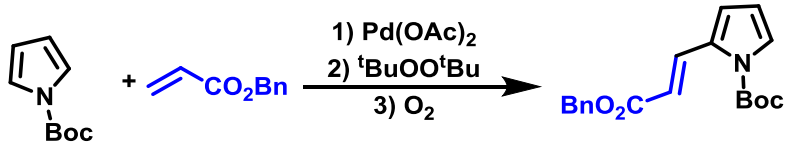

Scheme 16. Gaunt's approach for C-2 alkenylation of pyrrole derivatives

Stahl and co-workers have reported pioneering work on oxidative C-H functionalization by using peroxides and molecular oxygen as a source of oxidant. For instance, the palladium-catalyzed acyloxylation of olefins was demonstrated by Stahl and co-workers in the presence of diazaflurenone (DAF), 2,5-dimethyl-1,4-benzoquinone (Me_2BQ), iron-phthalocyanine (Fe-Pc).[31] Besides, the same group also reported the copper-catalyzed oxidative arylation of alkylarenes using phenanthroline as a ligand.[32]

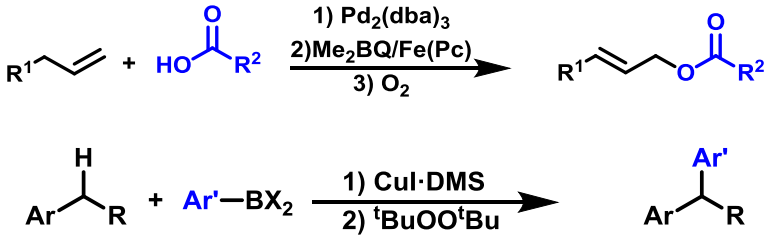

Scheme 17. Stahl's approach for acyloxylation of olefins and arylation of alkylarenes

1.4 Aim and rationale of thesis work

In the past decades, oxidative C-H functionalization is widely utilized for the formation of C-C, C-O, and C-N bond formation reactions. The type of substrates for oxidative C-H functionalization is ranging from alkanes, ethers, amines, and olefin, *etc*.

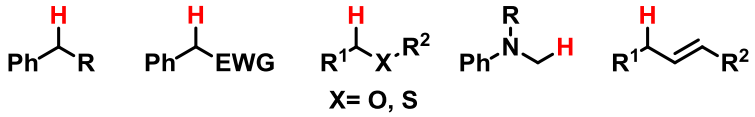

General substrate type for oxidative transformations of sp^3 C-H bonds

Figure 4. Type of substrates for C-H functionalization

The C-H functionalization of amides and heterocyclic moieties is a fascinating and challenging scaffold among the various functionalities owing to their important biological properties and its existence in natural products. Other interesting substrates such as 2-oxindole, barbituric acid, coumarin, and tetralone derivatives are considered as pharmacophores, easily available, and less explored towards direct C-H

functionalization. However, the functionalization of such types of moieties requires special reagents, a stoichiometric amount of additives/oxidants, a higher temperature, which limits their utilization in several organic transformations. In this context, organic chemists are on virtue for the development of a sustainable, efficient, and elegant approach for the C-H functionalization of amides and other heterocyclic cores in modern chemical synthesis.

Hence, we have focused our research on the catalytic C-H functionalization of various carbonyl compounds having ketones, amides, and esters functionality.

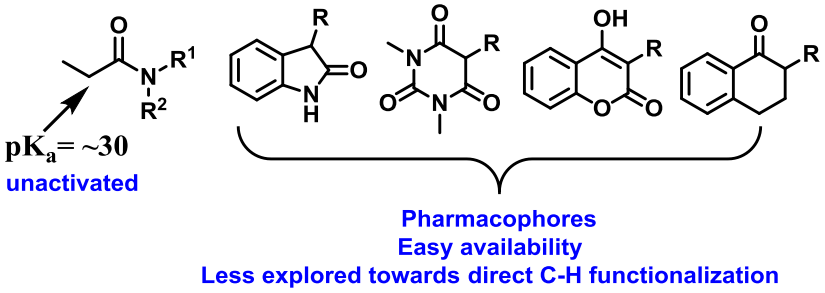

Figure 5. Unactivated amide and heterocyclic scaffolds for oxidative C-H functionalization

Objectives of the project:

- **α-alkylation of unactivated amides and 2-oxindoles *via* borrowing hydrogen catalysis**

Traditionally, the α-alkylation of unactivated amides was achieved using a stoichiometric amount of strong base such as *NaH*, *Na*NH_2, LDA, *n*-BuLi, KHMDS with mutagenic halogenated alkyl halides as an alkylating partner. Thus, to avoid the use of strong base and copious waste, we envisioned the environmentally benign protocol for α-alkylation of unactivated amides using alcohols as any alkylating agents, which gives by-products such as H_2 or H_2O. Next, the C-H hydroxylation of carbonyl compounds requires cryogenic conditions, metals, reductant, and higher temperatures. Thus we have inspired to develop a transition-metal-free approach for C-H hydroxylation of carbonyl compounds using naturally available source O_2 and bench stable base, KO-*t*-Bu at room temperature.

- **Fe-catalyzed direct C-H peroxidation of carbonyl compounds under batch/continuous-flow**

On the other hand, the metal-catalyzed peroxidation reaction limits their utilities on a large scale in academics as well as in industrial-scale owing to safety hazards.

Thus, we projected the safe, green, and mild protocol for C-H peroxidation using an earth-abundant metal catalyst in batch/flow. The peroxidation reactions preceded smoothly using a homogeneous $FeCl_3$ catalyst. Moreover, we have extended our research findings using supported catalyst (magnetic iron nanoparticles) in for C-H peroxidation using batch/continuous flow. To our delight, the synthesized quaternary peroxides exhibited the good anticancer and antimalarial activities and could be synthesized on-demand on a large scale with shorter duration using continuous flow.

- **The novel rearrangements of peroxides on electron-deficient atom**

The unique properties of quaternary peroxides such as reactive O-O bond can be used to trigger the unprecedented rearrangement reactions. We anticipated the fundamental possibility of rearrangement using metals to undergo the ring expansion of peroxyindoles. Our anticipation turned out to be practical, and we observed two novel rearrangements. In the first rearrangement, the reaction of 3-alkyl or benzyl-3-(*tert*-butylperoxy)indolin-2-one derivatives in the presence of a catalytic amount of metal triflate produces series of fluorophoric (Z)-2-arylidene and alkylidene-2*H*-benzo[*b*][1,4]oxazin-3(4*H*)-ones in good to excellent yield. However, the second novel rearrangement reaction is highly dependent on the solvent and substrate. For instance, the reaction 3-(*tert*-butylperoxy)-3-methyl or aryl indolin-2-one derivatives and esters in the presence of metal triflates lead to give the substituted-2*H*-benzo[*b*][1,4]oxazin-3(4*H*)-one.

Overall, this thesis dealt with the oxidative C-H functionalization of carbonyl derivatives to develop a newer approach for transformations such as α-alkylation, C-H hydroxylation, C-H peroxidation and domino rearrangement of peroxides (intermolecular oxygen insertion). All the chapters are interconnected with each other. After the current general introduction, to get a clear idea, the introduction and literature background for each chapter are written separately.

1.5 References:

(1) Chorkendorff, I.; Niemantsverdriet, J. W. *Concepts of Modern Catalysis and Kinetics*, Wiley-VCH Verlag GmbH & Co. KGaA Weinheim, 2003.
(2) (a) Tsuji, J. *Organic Synthesis by Means of Transition Metal Complexes*, Springer-Verlag Berlin Heidelberg, 1975. (b) Brandsma, L.; Vasilevsky, S.F.; Verkruijsse, H. D. *Application of Transition Metal Catalysts in Organic Synthesis,* Springer-Verlag Berlin Heidelberg, 1999.
(3) *Bridging Heterogeneous and Homogeneous Catalysis: Concepts, Strategies, and Applications*, Ed. by Can, Li.; Y, Liu, Wiley-VCH Verlag GmbH & Co. KGaA, 2014.

(4) (a) Sheldon and Kochi, *Metal-Catalyzed Oxidations of Organic Compounds*, **1981,** 1-13; (b) Clive, D. L. J.; Wickens, P. L. *J. Chem. Soc., Chem. Commun.* **1993,** 923; (c) Punniyamurthy, T.; Velusamy, S.; Iqbal, J. *Chem. Rev*. **2005**, *105*, 2329.
(5) (a) Hartwig, J. F.; Larsen, M. A. *ACS Cent. Sci.* **2016**, *2*, 281; (b) Jia, F.; Li, Z. *Org. Chem. Front*. **2014**, *1*, 194.
(6) Brookhart, M.; Green, M. L. H.; Parkin, G. *PNAS*, **2007**, *104*, 6908.
(7) Gunanathan, C.; Milstein, D. *Science* **2013**, *341*, 1229712.
(8) Corma, A.; Navas, J.; Sabater, M. J. *Chem. Rev.* **2018**, *118*, 1410.
(9) Watson, A. J. A.; Williams, J. M. J. *Science* **2010**, *329*, 635.
(10) Deibl, N.; Kempe, R. *J. Am. Chem. Soc*. **2016**, *138*, 10786.
(11) Reed-Berendt, B. G.; Polidano, K.; Morrill, L. C. *Org. Biomol. Chem*. **2019**, *17*, 1595.
(12) Elangovan, S.; Neumann, J.; Sortais, J.-B.; Junge, K.; Darcel, C.; Beller, M. *Nat. Commun*. **2016**, *7*, 12641.
(13) Bala, M.; Verma, P. K.; Sharma, U.; Kumar, N.; Singh, B. *Green Chem*., **2013**, *15*, 1687.
(14) Obora, Y. *ACS Catal.* **2014**, *4*, 3972.
(15) Sawaguchi, T.; Obora, Y. *Chem. Lett*. **2011**, *40*, 1055.
(16) Kharasch, M. S.; Sosnovsky, G. *J. Am. Chem. Soc*. **1958**, *80*, 756.
(17) Kharasch, M. S.; Fono, A. *J. Org. Chem.* **1959**, *24*, 72.
(18) Sekar, G.; DattaGupta, A.; Singh, V. K. *Tetrahedron Lett*. **1996**, *37*, 8435.
(19) Sekar, G.; DattaGupta, A.; Singh, V. K. *J. Org. Chem*. **1998**, *63*, 2961.
(20) Rispens, M. T.; Gelling, O. J.; de Vries, A. H. M.; Meetsma, A.; van Bolhuis, F.; Feringa, B. L. *Tetrahedron* **1996**, *52*, 3521.
(21) Yu, J. Q.; Corey, E. J. *Org. Lett*. **2002**, *4*, 2727.
(22) Terent'ev, A. O.; Sharipov, M. Y.; Krylov, I. B.; Gaidarenko, D. V.; Nikishin, G. I. *Org. Biomol. Chem*. **2015**, *13*, 1439.
(23) Liu, W.; Li, Y.; Liu, K.; Li, Z. *J. Am. Chem. Soc.* **2011**, *133*, 10756.
(24) Jala, R.; Palakodety, R. K. *Tetrahedron Lett.* **2019**, *60*, 1437.
(25) Roduner, E.; Kaim, W.; Sarkar, B.; Urlacher, V. B.; Pleiss, J.; Glaser, R.; Einicke, W.-D.; Sprenger, G. A.; Beifuß, U.; Klemm, E.; Liebner, C.; Hieronymus, H.; Hsu, S.-F.; Plietker, B.; Laschat, S. *ChemCatChem.* **2013**, *5*, 82.
(26) Funabiki, T.; Tsujimoto, M.; Ozawa, S.; Yoshida, S. *Chem. Lett*. **1989**, *7*, 1267.
(27) Zhang, Y.-H.; Yu, J.-Q. *J. Am. Chem. Soc.* **2009**, *131*, 14654.
(28) Chuang, G. J.; Wang, W.; Lee, E.; Ritter, T. *J. Am. Chem. Soc.* **2011**, *133*, 1760.
(29) Lin, M.; Shen, C.; Garcia-Zayas, E. A.; Sen, A. *J. Am. Chem. Soc.* **2001**, *123*, 1000.

(30) Beck. E. M.; Grimster, N. P.; Hatley. R.; Gaunt, M. J. *J. Am. Chem. Soc.* **2006**, *128*, 2528.
(31) Kozack, C. V.; Sowin, J. A.; Jaworski, J. N.; Iosub, A. V.; Stahl, S. S. *ChemSusChem*, **2019**, *12*, 3003.
(32) Vasilopoulos, A.; Zultanski, S. L.; Stahl, S. S. *J. Am. Chem. Soc.* **2017**, *139*, 7705.

Chapter 2

Section A

Ruthenium-Catalyzed Direct α-Alkylation of Amides using Alcohols *via* Borrowing Hydrogen Concept

2A. Ruthenium-Catalyzed Direct α-Alkylation of Amides using Alcohols *via* Borrowing Hydrogen Concept

2A.1. Abstract

The present chapter describes a highly efficient α-alkylation of unactivated amides using alcohol in the presence of a Ru-pincer catalyst (0.1 mol%). This process is demonstrated with a wide variety of examples by avoiding hazardous halogenated alkylating reagents. The reaction proceeds *via* dehydrogenation-condensation-hydrogenation steps in a domino manner with water as a by-product. Furthermore, the α-alkylation reaction of 2-oxindole with alcohol produces quaternary C3-alkylated, 3-hydroxyindolin-2-one *via* domino dehydrogenation-condensation- hydrogenation-hydration process. Phosphine based pincer complex provides a higher turnover number (390-570), emphasizing the significance of the phosphine arm of the pincer ligand. The simplicity, generality, and efficiency of this "green" process make it an attractive alternative method for the preparation of α-alkylated amides/heterocyclic compounds.

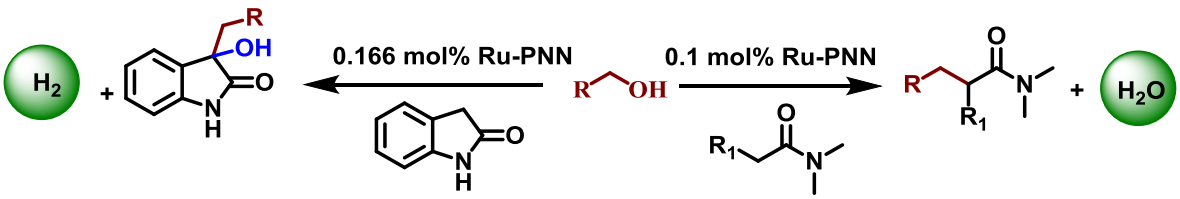

2A.2. Introduction:

2A.2.1 Borrowing Hydrogen Concept

In 1998, Paul Anastas and co-workers published a set of twelve principles to guide the ideal practices for chemical reactions. The twelve principles include ways to minimize environmental and human health hazards. However, the principles of green chemistry are fascinating but difficult to implement for all chemical transformations.[1] One of the important principles is based on the term atom economy, which was the first time coined by Trost in 1991.[2] The superlative way to get a good atom economy can be accomplished by simple additions and rearrangements which results in the same number of atoms in the reactants and the products. Further, the true catalyst should be present in very catalytic amounts and prerequisites no additives.

The alkylation reaction is one of the widely used and studied reactions in synthetic organic chemistry. A strong base achieved the classical α-alkylation reaction of unactivated carbonyl compounds (Na*H*, $NaNH_2$, LDA, *n*-BuLi, KHMDS, *etc*.) mediated SN_2 substitution reaction of the enolate nucleophile with alkyl halides. These methods require a stoichiometric amount of genotoxic activated reagents such as alkyl halides, needing cryogenic conditions and moisture-sensitive bases, which produce a stoichiometric amount of the metal salt as waste.[3] Recently, alcohols have been effectively used as acylating as well as versatile alkylating reagents in several borrowing hydrogen concepts due to their environmentally benign properties[4-5]; the only by-product of this transformation being water. Activated reagents, allylic acetate or imines were also used for the α-substitution of unactivated amides in the presence of a Lewis acid catalyst[6] (20 mol%) or Pd catalyst.[7]

Borrowing hydrogen (BH) catalysis, also known as hydrogen auto transfer, is an important catalytic concept and as one of the best examples of Green Chemistry. The process is mainly based on the oxidation of an alcohol (**a**) to give an aldehyde or ketone (**b**) using metal catalyst; the oxidized product then condensed with a nucleophile such as amines or enolates to give an unsaturated intermediate (**d**). The *in situ* generated H_2 *via* dehydrogenation of alcohols can be used for the reduction of an unsaturated compound to afford the desired product (**e**). Eventually, water is formed as the only by-product, thus making the BH process atom-economical and environmentally benign (Figure 2A.1.).[8-10]

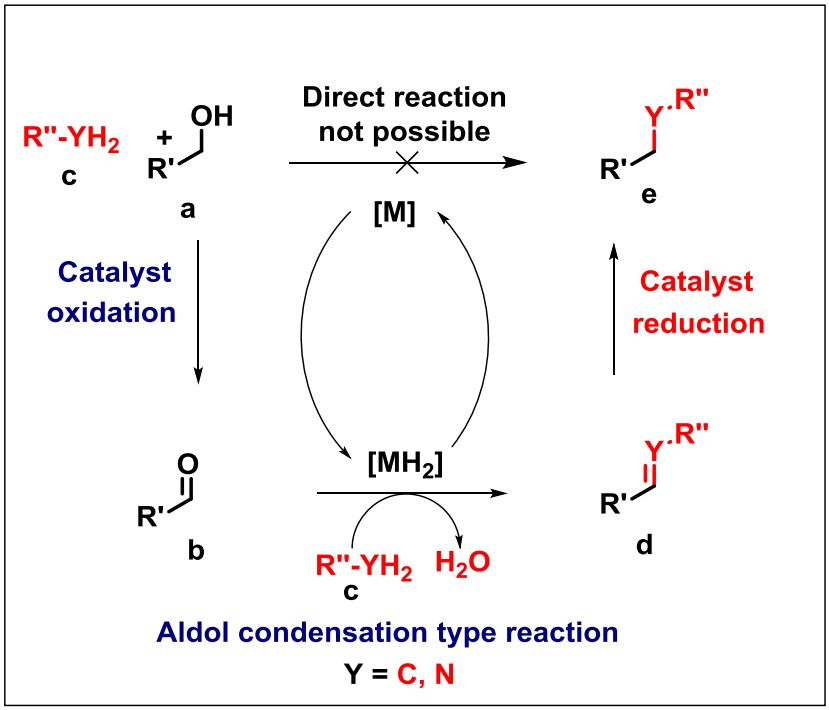

Figure 2A.1. Transition metal-catalyzed borrowing hydrogen concept

2A.2.2. Literature background on borrowing hydrogen concept and acceptorless dehydrogenation

A variety of homogeneous and heterogeneous transition metal catalysts has been known for this transformation, thus representing the BH processes that are favorable for replacing those procedures that use traditional mutagenic halogenated alkylating agents. Pioneering work on borrowing hydrogen catalysis using alcohol as an alkylating reagent was achieved by Grigg, Watanabe, and Murahashi. In 1981, Grigg and co-workers reported the *N*-alkylation of amines in the presence of Rhodium (Rh), Iridium (Ir) or Ruthenium (Ru) complex at 100 ^{o}C.[11]

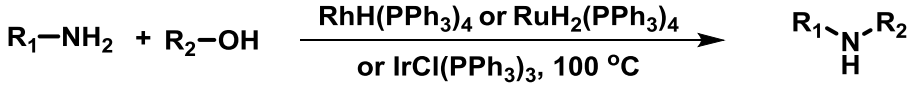

Scheme 2A.1. Grigg's approach for *N*-alkylation of amines using alcohols

At the same time, Watanabe and co-workers also reported the *N*-alkylation of amines in the presence of ruthenium complex at 180 ^{o}C.[12,13]

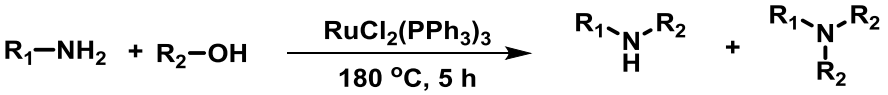

Scheme 2A.2. Watanabe's approach for *N*-alkylation of amines using alcohols

Similarly, Murahashi and co-workers reported the Ru-catalyzed alkylation of amines using alcohols to get the secondary or tertiary amines.[14]

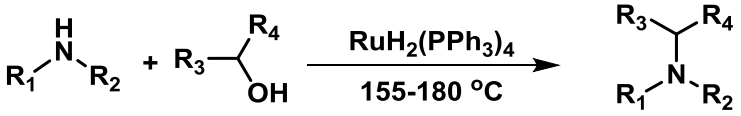

Scheme 2A.3. Murahashi's approach for *N*-alkylation of amines using alcohols

In 2009, Williams and co-workers reported the *N*-alkylation of amines using $RuCl_2$(p-cymene)$_2$ complex.[15]

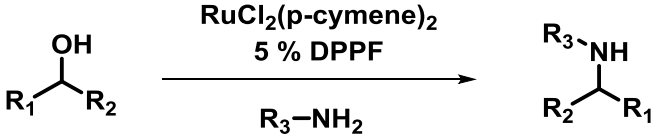

Scheme 2A.4. Williams approach for *N*-alkylation of amines using alcohols

Milstein and co-workers reported the direct synthesis of imines using amine and alcohol in the presence of a Ru-PNP catalyst.[16]

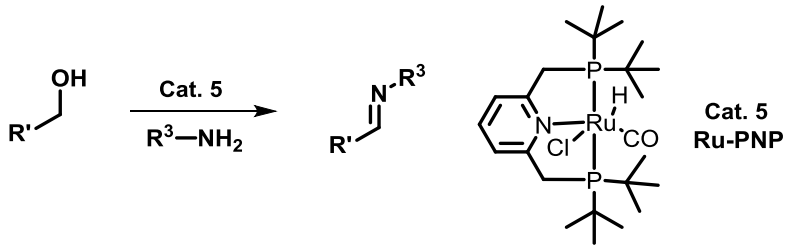

Scheme 2A.5. Milstein's approach for direct synthesis of imine using amine and alcohol

Moreover, in 2005, Milstein and co-workers reported the esterification of alcohols using a catalytic amount of pincer type catalyst. However, a similar type of transformation was achieved by Madson and co-workers using Ru-NHC catalyst (Scheme 2A.6).[17,18]

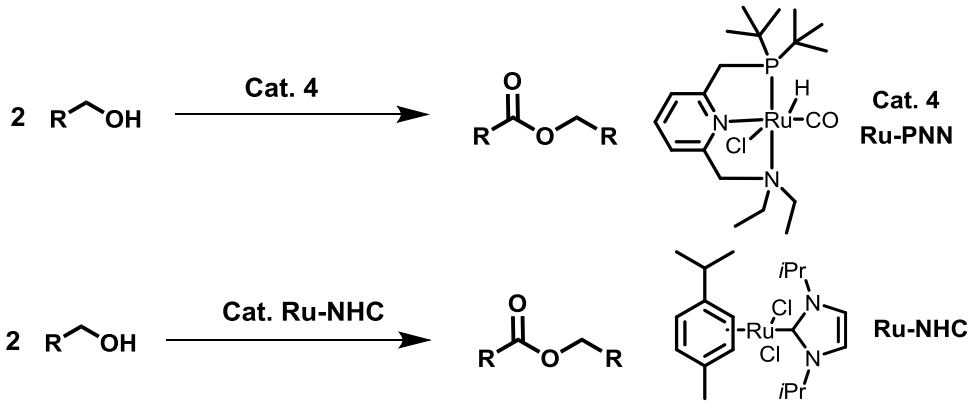

Scheme 2A.6. Milstein and Madson's approach for the synthesis of esters from alcohols

Milstein and co-workers reported the pathbreaking report for the direct synthesis of an amide using a Ru-PNN catalyst.[19]

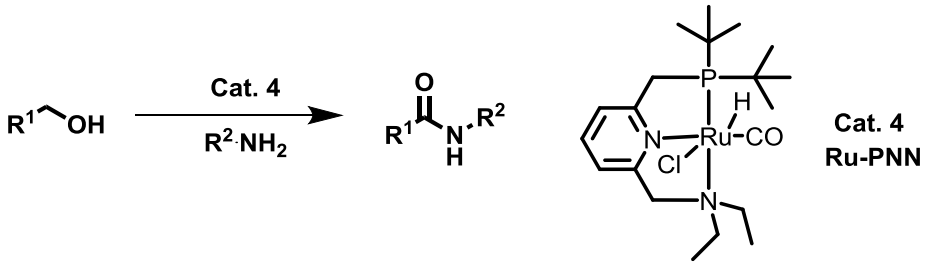

Scheme 2A.7. Milstein's approach for the direct synthesis of amides using amine and alcohols

Interestingly, the α-alkylation of ketones was reported by Ryu and co-workers using $RuHCl(CO)(PPh_3)_3$ using alcohols as alkylating reagents .[20]

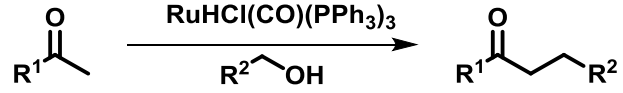

Scheme 2A.8. Ryu's approach for direct α-alkylation of ketones using alcohols

Huang[21] and Ryu[22] achieved pioneering research work on the α-alkylation reaction of amides using alcohol. This transformation was rarely studied and achieved by a higher loading of iridium or ruthenium catalyst. The α-alkylation of amides was first time reported by using the iridium (PNNNP) complex using alcohol as an alkylating agent with a TON of 40. Similarly, the use of $RuHCl(CO)(PPh_3)_3$ provided a TON of 13. When we were working on this project, only two reports were documented for the α-alkylation of unactivated amides (Scheme 2A.9).

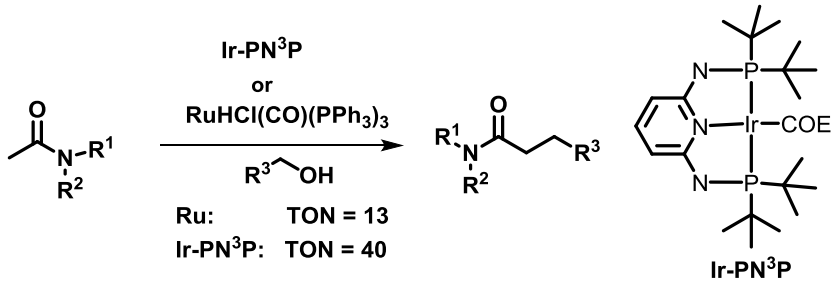

Scheme 2A.9. Huang and Ryu's approach for direct α-alkylation of unactivated amides using alcohols

However, the C3-alkylation of 2-oxindole was reported using Ru,[23a] Rh,[23b] Pt/CeO2,[23C], and Pd/C[23d] catalyst.

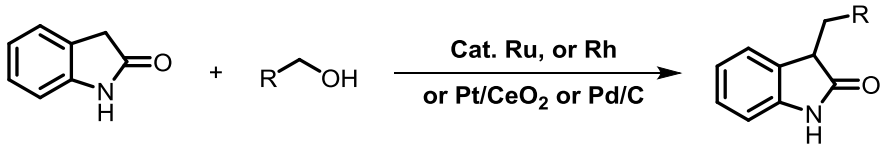

Scheme 2A.10. Miscellaneous approaches for direct C-alkylation of 2-oxindole using alcohols

2A.3 Rationale of present work

Amide is a ubiquitous functional group of pharmaceutical compounds, natural products, peptides, proteins, and polymers.[24] The C3-hydroxy functionalized 2-oxindole represents an important class of cyclic amides by its broad biological activity and as a key intermediate in the synthesis of natural products (Figure 2A.3.).[25]

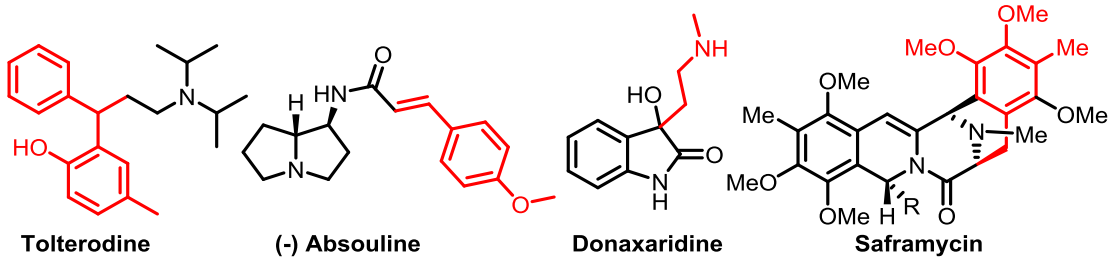

Figure 2A.3. Bioactive natural products/drugs can be synthesized using borrowing hydrogen concept

The α-functionalization of amides *via* C–C bond formation is highly important due to a wide range of applications in the total synthesis of natural products and pharmaceutically active compounds. The α-alkylation reactions of amides and esters are more challenging tasks due to their lower Brønsted acidity of α-hydrogen than ketones and aldehydes (Figure 2A.4.).

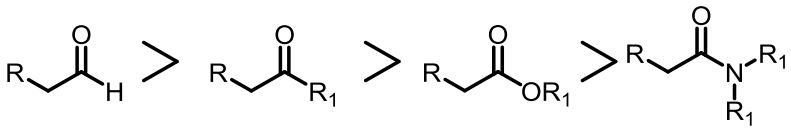

Figure 2A.4. Decreasing order of Brønsted acidity of α-Hydrogen in various carbonyl compounds

The reported methods pose severe drawbacks such as high catalyst loading, use of additives, activated reagents, multi-step, and limited substrate scope, which represent a less efficient process. Hence, considering the existing limitations of the α-alkylation of amides, an efficient and sustainable catalytic approach is required. Presently, Ru-complexes derived from PNN, and PNP pincer ligands have shown remarkable catalytic activity in alcohol activation, which led to several new catalytic reactions towards C-O and C-N bond formation. Moreover, these complexes have not been studied for C-C bond formation. On the other hand, in the conventional approach, the C-3 hydroxylation of substituted 2-oxindole has been accomplished by multi-steps with the need for an additional step for the oxidation of C3-alkyl-2-oxindole using a stoichiometric amount of reductant.[26] Although a few reports exist for the C3-alkylation of 2-oxindole with a lower turnover number (TON). However, the direct synthesis of C3-hydroxy functionalized 2-oxindole from 2-oxindole using alcohol and metal catalysts has not been reported. Therefore, we questioned whether the Ru-PNN and Ru-MACHO catalysts and their derivatives could perform the α-alkylation reactions? If yes, then which catalytic system will be suitable for such transformations? By considering these facts, we decided to synthesize as well as

screen existing metal catalysts and develop a very simple protocol for the challenging task. Thus, we inspired by the excellent catalytic activity of Ru-Pincer type complexes and sought to implement them for α-alkylation of amides/2-oxindoles.

2A.4. Results and discussion

To achieve the specified objective, we have developed a highly efficient method for the direct α-alkylation of unactivated amides using alcohol in the presence of a Ru-PNN catalyst with a high turnover number in a domino fashion (Figure 2A.5.). Using this approach, 2-oxindole is directly converted into C3-alkylated 3-hydroxyindolin-2-one *via* domino dehydrogenation-condensation-hydrogenation-hydroxylation processes without the use of any oxidant in a single step. To the best of our knowledge, this is the first report for the direct synthesis of C3-hydroxy functionalized 2-oxindole *via* successive alkylation and hydroxylation at α-position of 2-oxindole using Ru-catalyst.

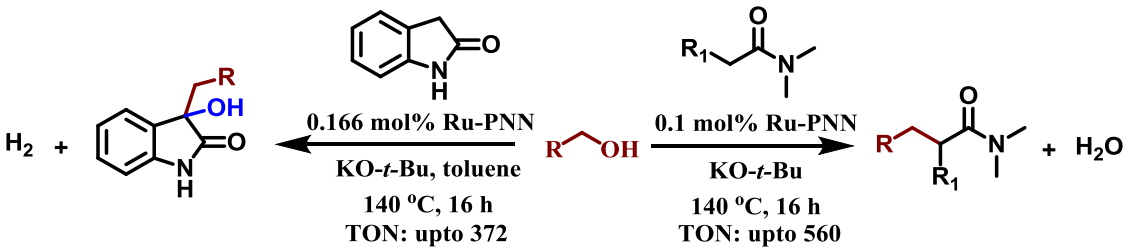

Figure 2A.5. General scheme for α-alkylation of amides

2A.4.1. Optimization studies

Initially, the reaction conditions for the α-alkylation reaction of *N*,*N*-dimethylacetamide (DMA) with benzyl alcohol using Ru-PNN catalyst were optimized by varying concentration of catalyst, base, and *N*,*N*-dimethylacetamide - (Table 2A.1). When a toluene solution containing 1 mmol of benzyl alcohol (**1**), 2 mmol of *N*,*N*-dimethylacetamide (**2**), 2 mmol of KO-*t*-Bu and 0.5 mol% of catalyst **4** was heated at 140 ^{o}C in a sealed tube, 75% conversion of benzyl alcohol was observed by GC after 16 h, to give *N*,*N*-dimethyl-3-phenylpropanamide **3a** in 55% isolated yield after column purification (Table 2A.1, entry 2). A control experiment was performed for this reaction in the absence of the catalyst **4** (Ru-PNN), which showed a 40% conversion of the benzyl alcohol by GC analysis, which led to only dibenzyl ether in 35% yield. The absence of *N*,*N*-dimethyl-3-phenylpropanamide **3a**, emphasizes the importance of the Ru-PNN catalyst for this reaction (Table 2A.1, entry 1).

Table. 2A.1- Optimization of reaction conditions for Ru-PNN pincer catalyst

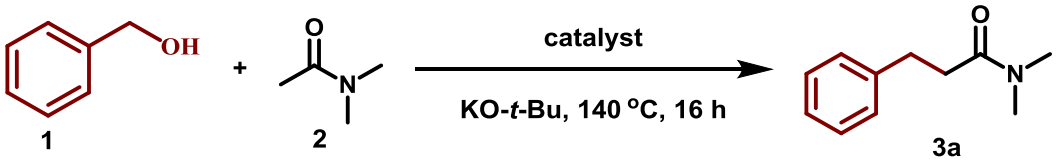

Entry	Catalyst in mol%	KO-*t*-Bu: DMA	Conversion	Yield of 3a	TON
1[a]	-	2:2	40	0	-
2[a]	0.5	2:2	75	55	110
3[b]	0.1	2:2	70	40	400
4[b,c]	-	1.3:10	44	0	-
5[b,c]	**0.1**	**1.3:10**	**62**	**56**	**560**
6[c,d]	0.125	1.3:10	72	64	512
7[c,e]	0.17	1.3:10	92	76	456

Reaction Condition- [a)] catalyst **4** (0.005 mmol), benzyl alcohol (1 mmol), KO-*t*-Bu (2 mmol), *N*,*N*-dimethylacetamide (2 mmol) and toluene (1 mL) were heated at 140 °C in a sealed tube for 16 h. Conversion of benzyl alcohol was analyzed by GC using mesitylene as an internal standard. [b)] benzyl alcohol (5 mmol) was used. [c)] neat condition. [d)] benzyl alcohol (4 mmol) was used. [e)] benzyl alcohol (3 mmol) was used.

However, the same reaction in the presence of 0.1 mol% of the catalyst **4**, afforded 70% conversion of benzyl alcohol, led to **3a** in 40% isolated yield (Table 2A.1, entry 3). Remarkably, heating of the reaction mixture containing 0.1 mol% of the catalyst **4**, 5 mmol of benzyl alcohol, 6.5 mmol of KO-*t*-Bu and 50 mmol of *N*,*N*-dimethylacetamide at 140 °C for 16 h, provided **3a** in 56% yield with high TON (Table 2A.1, entry 5). A control experiment was performed in the absence of catalyst **4**, showed the absence of product **3a** (Table 2A.1, entry 4), revealing the necessity of the metal catalyst for the oxidation of benzyl alcohol. Although a better conversion of benzyl alcohol and moderate yield of the product **3a** was observed by increasing catalyst loading (0.125 and 0.17 mol%), the TON was noticeably decreased (Table 2A.1, entries 6,7).

Table 2A.2 Catalyst Screening

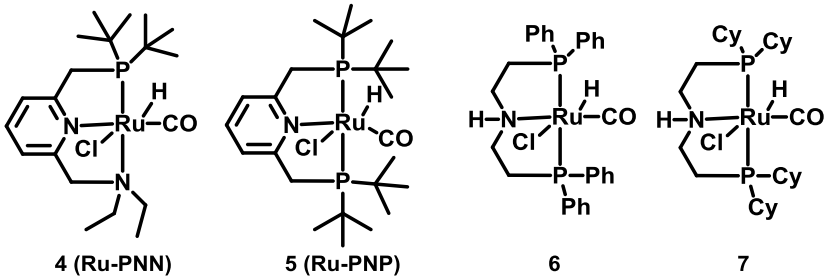

Entry	Catalyst in mol%	Conversion	Yield of 3a	TON
1	**Catalyst 4 (0.1 mol%)**	**62**	**56**	**560**
2	Catalyst **5** (0.1 mol%)	53	41	410
3	Catalyst **6** (0.1 mol%)	65	37	370
4	Catalyst **7** (0.1 mol%)	48	47	470

Reaction condition- catalyst (0.005 mmol), benzyl alcohol (5 mmol), KO-*t*-Bu (6.5 mmol), and *N*,*N*-dimethylacetamide (5 mL) were heated at 140 ^{o}C in a sealed tube for 16 h. Conversion of benzyl alcohol was analyzed by GC using mesitylene as an internal standard.

Keeping the standard reaction conditions, a detailed screening was carried out with a variety of cooperative metal complexes (Table 2A.2). Accordingly, the α-alkylation reaction of *N*,*N*-dimethylacetamide with benzyl alcohol in the presence of 0.1 mol% of catalyst **5** furnished 53% conversion of benzyl alcohol, to give the desired product **3a** in 41% yield (Table 2A.2, entry 2). This reaction was also driven by catalyst **6** and **7**, led to 65% and 48% conversion, to give the respective product **3a** in 37% and 47% isolated yield (Table 2A.2, entry 3, 4). After screening experiments with other Ru-pincer complexes, Ru-PNN was noted as the most efficient pre-catalyst for this reaction.

2A.4.2. Substrate scope for α-alkylation of unactivated amides

To explore the scope of the α-alkylation reaction, several aromatic and aliphatic alcohols were examined in the presence of catalyst **4** (Figure 2A.6.). The reaction of 2-methylbenzyl alcohol and *N*,*N*-dimethylacetamide was occurred in the presence of 0.1 mol% of catalyst **4**, to give 64% conversion with the isolation of *N*,*N*-dimethyl-3-(o-tolyl)propanamide **3b** in 63% yield (Figure 2A.6.). The α-alkylation of *N*,*N*-dimethylacetamide with 3-methylbenzyl alcohol, and 4-methylbenzyl alcohol afforded the corresponding products **3c, 3d** in 68% and 70% yield, respectively (Figure 2A.6.). Other aromatic alcohols, 2-methoxy, 3-methoxy- and 4-methoxybenzyl alcohols were also reacted. Similarly, with *N*,*N*-dimethylacetamide to obtain the corresponding products **3e, 3f, 3g** in 60, 52, and 55% yield, respectively (Figure 2A.6.). The possibilities of expanding this reaction for the synthesis of long-chain carboxylic amides were also explored by reacting them with various aliphatic alcohols. Unlike the aromatic alcohols, reactions with aliphatic alcohols require longer duration and higher catalyst loading. For instance, the reaction of *N*,*N*-dimethylacetamide with 1-butanol in the presence of 0.2 mol% complex **4**, provided

70% conversion, to afford *N*,*N*-dimethylhexanamide **3h** in 55% isolated yield (Figure 2A.6.). The reaction of *N*,*N*-dimethylacetamide with 1-hexanol, 1-octanol, and 3-methylbutan-1-ol led to 70, 48, and 86% conversion of respective alcohol. Further, silica-gel column purification of the reaction mixture provided the alkyl tethered amide products **3i, 3j, 3k** in 60, 36 and 66% yield, respectively (Figure 2A.6.). Next, we studied the α-alkylation reaction of the *N*-acetyl heterocyclic system using catalyst **4**. A mixture containing *N*-acetyl-pyrrolidine, benzyl alcohol, and 0.1 mol% of catalyst **4** was heated for 24 h, led to 69% conversion, to afford the amide **3l** in 44% yield (Figure 2A.6.). *N*-acetyl piperidine and *N*-acetyl morpholine were also alkylated using benzyl alcohol, led to 74 and 42% conversion, resulting in **3m** and **3n** in 54 and 32% isolated yield (Figure 2A.6.).

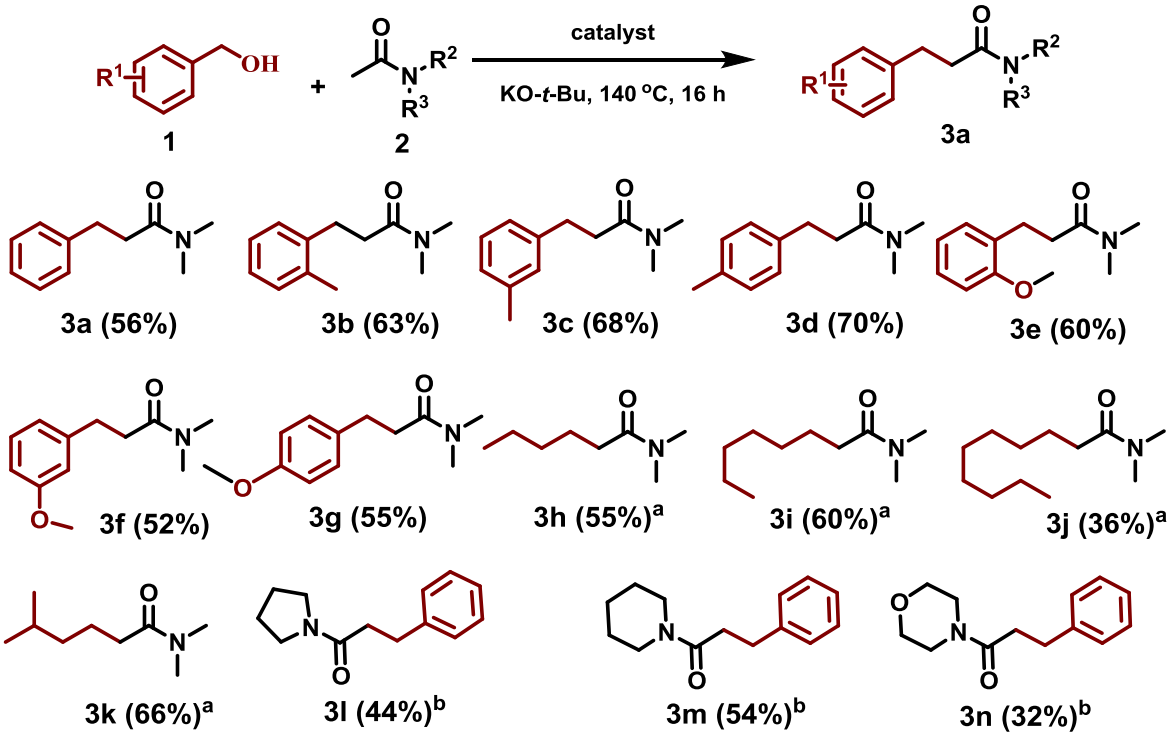

Figure 2A.6. Substrate scope for α-alkylation of unactivated amides

Reaction condition: Catalyst **4** (0.005 mmol), alcohol (5 mmol), amide (5 mL), and KO-*t*-Bu (6.5 mmol) were heated at 140 °C in a sealed tube for 16 h. Conversion of alcohol was analyzed by GC using mesitylene as an internal standard. [a] 0.2 mol% of catalyst **4** was used for aliphatic alcohols and heated for 24 h. [b] 2 equiv of amide and 5 mL of toluene was used and heated for 24 h.

Surprisingly, the reactions of 2-oxindole (**8**) with various alcohols in the presence of 0.166 mol% complex **4** led to 3-alkylated-3-hydroxy functionalized 2-oxindole (**9**). For instance, the reaction of 2-oxindole and benzyl alcohol furnished 92% conversion of benzyl alcohol to give 62% of 3-benzyl-3-hydroxyindolin-2-one **9a** (Figure 2A.7.).

Notably, these transformations led to the formation of a C3 quaternary stereocentre directly from the methylene group of the 2-oxindole in a single step. NMR and mass analysis explicitly characterized the product. Further, the structure of the product was confirmed by X-ray analysis (Figure 2A.7., entry **9a**). The ^{1}H-NMR of the crude reaction mixture showed the absence of C3–H of **10** (Figure 2A.8.). This observation supported the structure of **9a**, ruling out the possibility of aerial oxidation in column chromatography. This reaction was also generalized with other alcohols. The reaction of 2-oxindole with 3-methoxybenzyl alcohol, 3-methylbenzyl alcohol and 4-methylbenzyl alcohol afforded the corresponding hydroxyl functionalized products **9b–d** in 54%, 72%, and 48% yields, respectively (Figure 2A.7.).

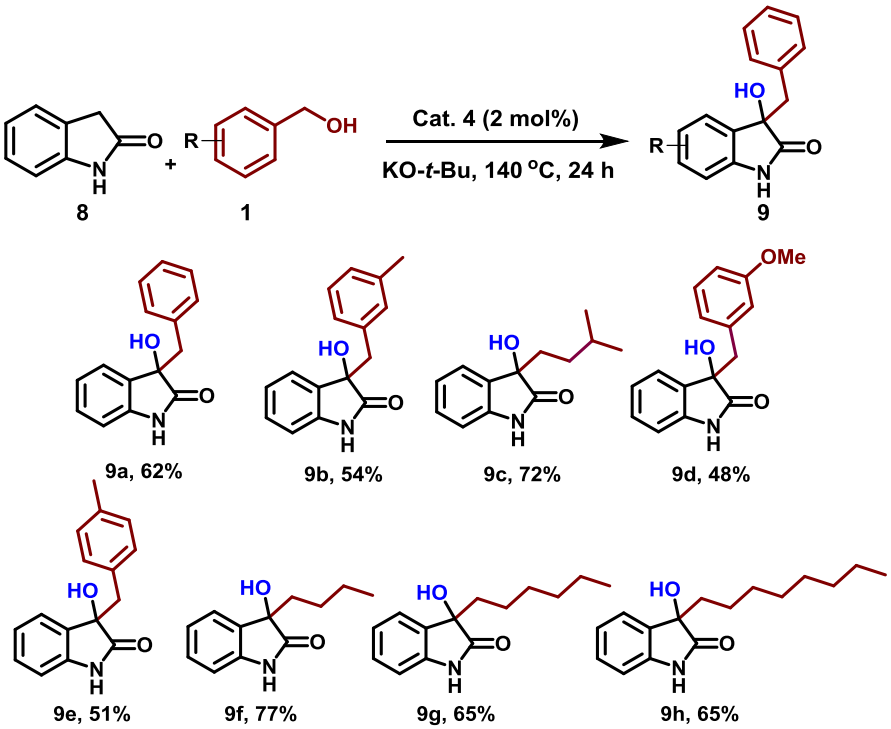

Figure 2A.7. Substrate scope for α-alkylation-hydroxylation of 2-oxindole

The scope of this reaction was also examined with several aliphatic alcohols. Heating a toluene solution of 2-oxindole, 1-butanol, KO-*t*-Bu, and 2 mol% of catalyst **4** for 24 h led to 3-butyl-3-hydroxyindolin-2-one (**9e**) in 77% yield (Figure 2A.7.). A similar reaction with 1-hexanol afforded the corresponding hydroxyl functionalized products **9f** in moderate yields. This reaction was also effective with other aliphatic alcohols such as 3-methylbutan-1-ol, 1-hexanol, and 1-octanol, to afford the appropriate products **9f, g,** and **h** in good yield (Figure 2A.7).

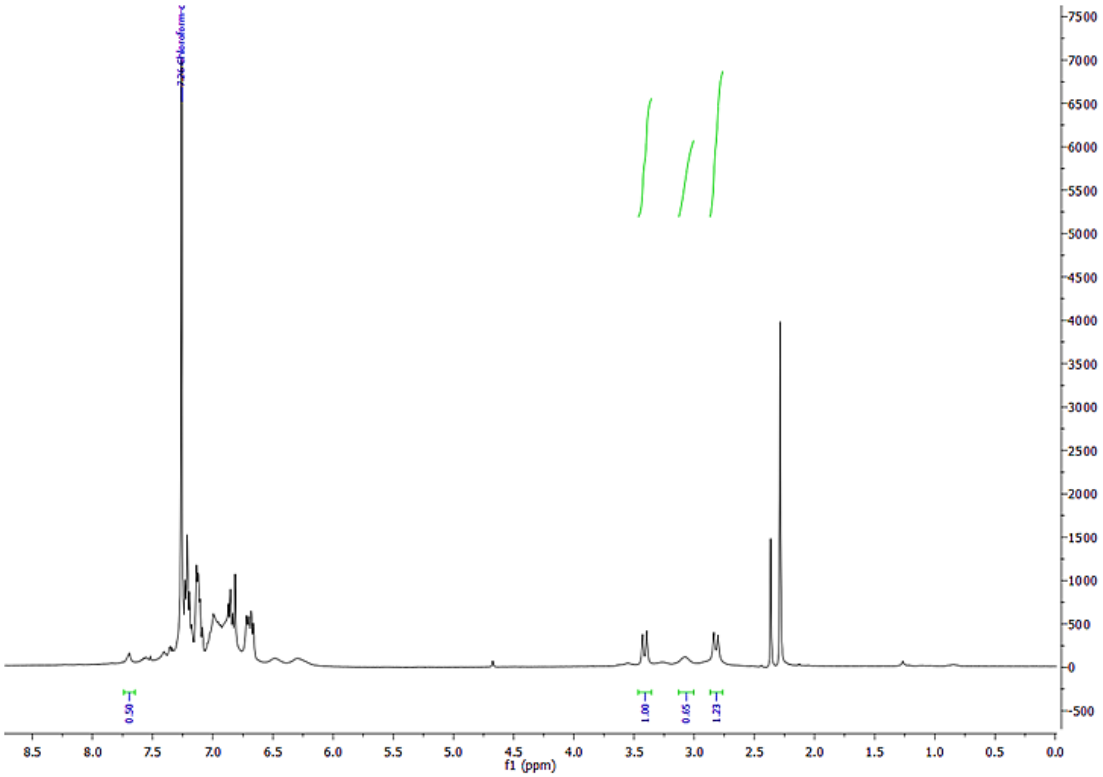

Figure 2A.8. ^{1}H NMR spectra for the crude reaction mixture in $CDCl_3$ which shows the absence of C3-H (~3.7 ppm) proton and thus ruling out the possibility of aerial oxidation in column chromatography.

2A.5. Mechanistic investigation

To investigate the reaction pathway, a toluene solution containing an equiv amount of compound **11** and water in the presence of 1 mol % of catalyst **4** was heated at 140 °C for 16 h and indicated no reaction (Scheme 2A.1.). Therefore, the possibility of the formation of product **9a** *via* hydration across the olefin was ruled out. Again, the addition of 1 N aqueous KOH failed to afford product **9a**. To check the C–H hydroxylation possibility, an equiv amount of compound **10**, water, and 1 mol% of catalyst **4** was heated at 140 °C for 16 h which afforded 25% yield of **9a**.

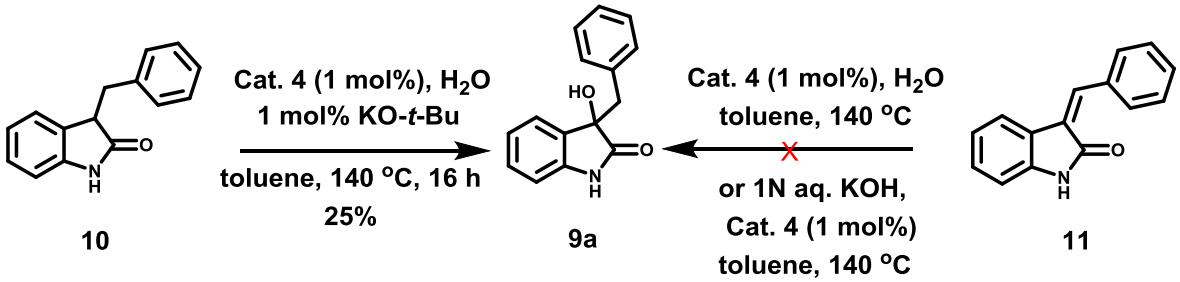

Scheme 2A.11. Control experiments for mechanistic investigations

2A.5.1. H_2 liberation studies

To confirm the liberation of hydrogen, the gaseous component of the reaction mixture from the sealed tube was taken using a gas-tight syringe and injected to the gas chromatography (GC) instrument. The GC analysis showed the liberation of H_2 during a reaction (Figure 2A.9.). This experiment proves that there is a formation of H_2 which is not utilized for the reduction of olefin across 2-oxindole moiety.

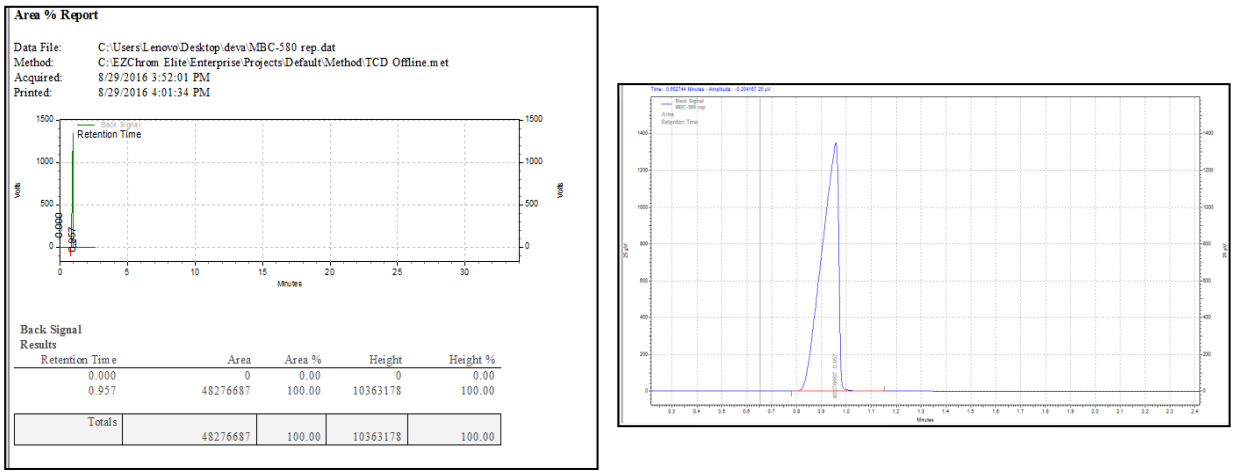

Figure 2A.9. GC chromatograph for H_2 liberation

2A.6. The possible reaction mechanism

Based on a previous report[27] and preliminary results such as H_2 liberation and control experiments, a plausible catalytic cycle is postulated in Figure 2A.10. Initially, the pre-catalyst **4** undergoes H-Cl liberation with the addition of base to give the active catalyst **A**. Then, the O–H activation of alcohol by catalyst **A** results in the intermediate **B**. The β-H elimination followed by aldehyde dissociation gives the intermediate **C** and free aldehyde. Next, the base-mediated condensation of an aldehyde with the amide provides the unsaturated amide **11**. The addition of Ru–H from the intermediate **C** to the β-carbon of compound **11** results in intermediate **D**. The intermediate **D** may shift to the more stable form **E** through enolate coordination on the Ru-centre. Perhaps, the addition of water to the C3-position of the oxindole bound ruthenium intermediate **E** followed by proton abstraction by the Ru-centre affords the intermediate **C**, which subsequently liberates molecular hydrogen to form the active catalyst.

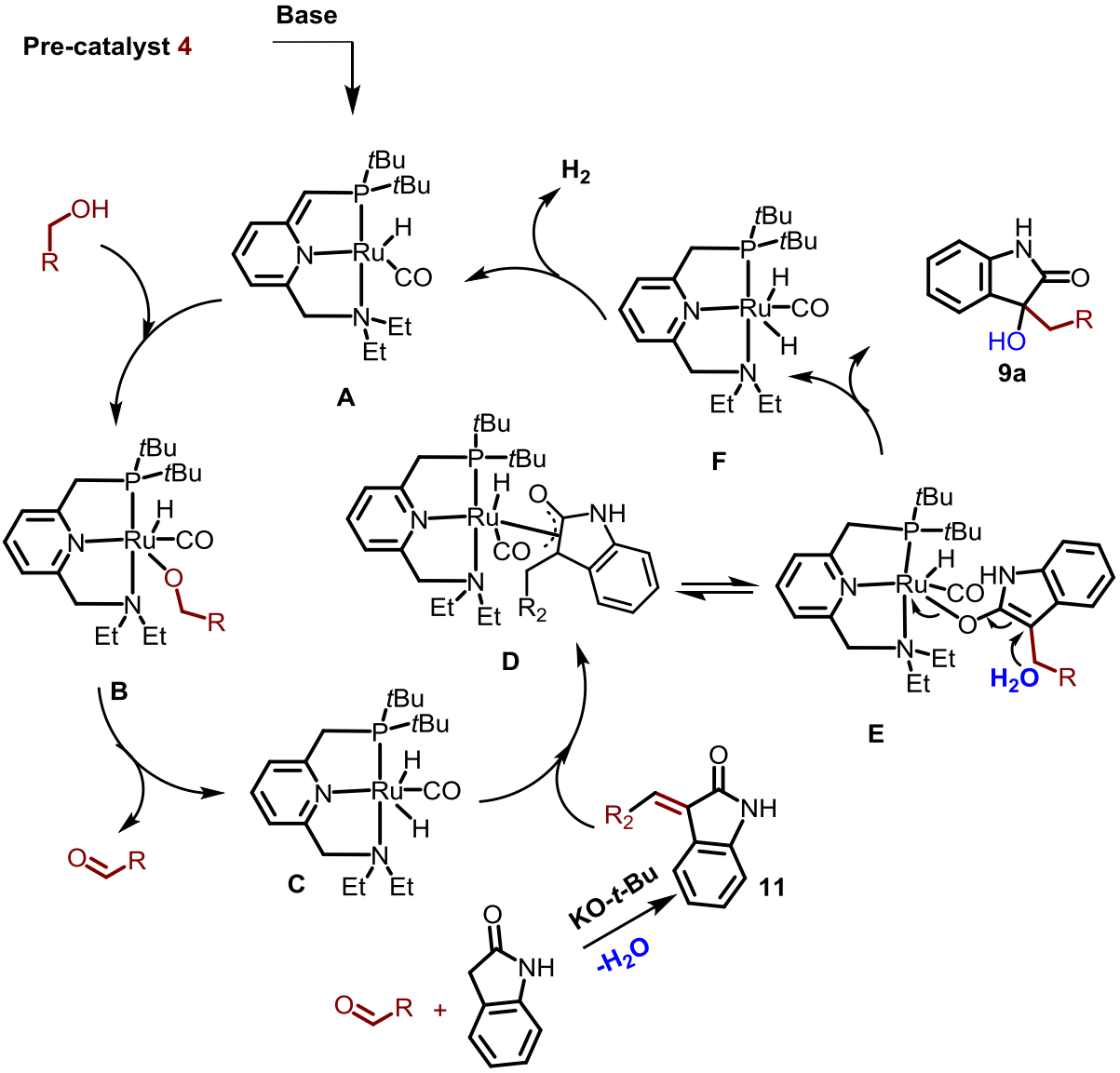

Figure 2A.10. Plausible reaction mechanism

2A.7. Conclusion

In conclusion, we have developed Ru-PNN catalyzed direct α-alkylation of amides using alcohol as an alkylating partner, and the transformation proceeds *via* dehydrogenation–condensation–hydrogenation steps under simple reaction conditions with a good turnover number (TON). Unlike the other Ru-catalysts, the phosphine based pincer complex exhibited an effective catalytic function for α-alkylation reactions of several amides with a wide variety of alcohols. A new approach was discovered for the synthesis of C3-hydroxy 2-oxindole directly from 2-oxindole using alcohol and Ru-PNN catalyst without the use of any oxidant. This reaction was enabled *via* double functionalization (C3-alkylation and C3-hydroxylation) in one step with a high TON. Moreover, the structure of the product

is explicitly characterized and evidenced by single-crystal XRD. The simplicity, wide substrate, and atom economy of this process make it an attractive alternative method for the preparation of α-alkylated amides and C3-alkylated 3-hydroxyindolin-2-one.

2A.8. Experimental section and characterization data

2A.8.1. General information and data collection

All experiments with metal complexes and phosphine ligands were carried out under an atmosphere of nitrogen. All the alcohols and amides were purchased from Sigma-Aldrich or Alfa-Aesar and stored over molecular sieves. Deuterated solvents were used as received. All the solvents used were dry grade and stored over 4Å molecular sieves. Column chromatographic separations performed over 100-200 Silica-gel. Visualization was accomplished with UV light and PMA, CAM stain followed by heating. Ruthenium complexes **5** and **7** were prepared according to literature procedures. The complex **4** and **6** were purchased from Sigma-Aldrich. ^{1}H and ^{13}C NMR spectra were recorded on 400 and 100 MHz, respectively, using a Bruker 400 MHz or JEOL 400 MHz spectrometers. Abbreviations used in the NMR follow-up experiments: b, broad; s, singlet; d, doublet; t, triplet; q, quartet; quin, quintet; m, multiplet. Conversion of reactants was monitored using Gas Chromatography, with GC 2014, Shimadzu.

2A.8.2. Experimental procedure

(i) General experimental procedure for the α-alkylation of unactivated amides (method A):

To an oven-dried 20 mL resealable pressure tube (equipped with rubber septum), catalyst **4** (0.005 mmol), KO-*t*-Bu (6.5 mmol), alcohol (5 mmol) and *N*,*N*-dimethylacetamide (5 mL) were added under N_2 atmosphere using a balloon. Then, the tube was purged with N_2 and quickly removed septum and sealed with a cap using a crimper. The reaction mixture was stirred at 140 ^{o}C for 16 h. After cooling to room temperature, mesitylene (1 mmol) was added and the products were analyzed by GC. The reaction mixture was quenched with water (20 mL) and extracted with ethyl acetate (3 x 40 mL). The entire ethyl acetate layer was combined, washed with brine (50 mL) and then dried over Na_2SO_4. After concentration under reduced pressure, the residue was purified by 100-200 mesh silica-gel column chromatography using ethyl acetate/petroleum ether (1:4) to afford the pure product **3**. (In case of aliphatic alcohols and cyclic amides heated for 24 h).

(ii) Experimental procedure for α-alkylation-hydroxylation of 2-oxindole (method B):

Catalyst **4** (0.0025 mmol), KO-*t*-Bu (1.95 mmol), alcohol (1.5 mmol), 2-oxindole (3 mmol), and toluene (2 mL) were added to 20 mL resealable pressure tube under N_2

atmosphere using balloon (equipped with rubber septum). Then, the tube was purged with N_2 and quickly removed septum and sealed with a cap using a crimper. The reaction mixture was stirred at 140 ^oC for 16 h. After cooling to room temperature, mesitylene (1 mmol) was added and the products were analyzed by GC using an Rtx-5 column on a GC-2014 Shimadzu series GC system. The reaction mixture was concentrated under vacuum. DCM was added to the reaction mixture and passed through a plug of celite bed. After concentrating the filtrate under reduced pressure, the residue was purified by 100-200 mesh silica-gel column chromatography using ethyl acetate/petroleum ether (3:7) to afford the pure product **9**.

(iii) Experimental procedure for α-hydroxylation of 3-benzylindolin-2-one:

The catalyst **4** (0.01 mmol), KO-*t*-Bu (0.15 mmol), 3-benzylindolin-2-one (0.5 mmol), toluene (1 mL) were added to 20 mL glass tube (equipped with rubber septum) under N_2 atmosphere using balloon and reaction mixture was stirred at RT for 15 minutes under N_2 atmosphere and finally water (1 mmol) was added. Then, the tube was purged with N_2 and quickly removed septum and sealed with a cap using a crimper. The reaction mixture was stirred at 140 ^oC for 16 h. The reaction mixture was concentrated under vacuum, and dichloromethane was added to the reaction mixture and passed through a plug of a celite bed. After concentrating the filtrate under reduced pressure, the residue was purified by 100-200 mesh silica-gel column chromatography using ethyl acetate/petroleum ether (3:7) to afford the pure product **9a**.

(iv) Experimental procedure for control experiment:

KO-*t*-Bu (6.5 mmol), benzyl alcohol (5 mmol), and *N*,*N*-dimethylacetamide (5 mL) were added to 20 mL resealable pressure tube (equipped with rubber septum) under N_2 atmosphere using a balloon. Then, the tube was purged with N_2 and quickly removed septum and sealed with a cap using a crimper. The reaction mixture was stirred at 140 ^oC for 16 h. After cooling to room temperature, mesitylene (1 mmol) was added, and the products were analyzed by GC using an Rtx-5 column on a GC-2014 Shimadzu series GC system.

2A.8.3. Spectroscopic data for the product

***N*,*N*-Dimethyl-3-phenylpropanamide (3a)[21]:** Catalyst **4** (2.44 mg, 0.005 mmol), KO-*t*-Bu (728 mg, 6.5 mmol), benzyl alcohol (540 mg, 5 mmol) and *N*,*N*-dimethylacetamide (5 mL) were allowed to react in 20 mL resealable pressure tube according to method A to afford the amide **3a** (495 mg, 56%) as a colorless liquid. **^{1}H NMR** (400 MHz, $CDCl_3$,) δ 7.34–7.21 (m, 5H), 3.02-2.96 (m, 8H), 2.64 (m, 2H). **^{13}C NMR** (100 MHz ,$CDCl_3$) δ 172.33, 141.62, 128.58, 128.54, 128.45, 127.16, 126.21, 37.28, 35.56, 35.42, 31.51. **FTIR** (neat) 1642 cm^{-1}. **HRMS** (ESI) m/z calculated for $C_{11}H_{15}NO$ $(M+H)^+$: 178.1232, found: 178.1235.

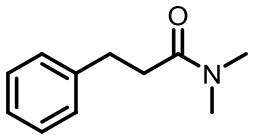

***N*,*N*-Dimethyl-3-o-tolylpropanamide (3b)[21]:** Catalyst **4** (2.44 mg, 0.005 mmol), KO-*t*-Bu (728 mg, 6.5 mmol), 2-methylbenzylalcohol (610 mg , 5 mmol) and *N*,*N*-dimethylacetamide (5 mL) were allowed to react in 20 mL

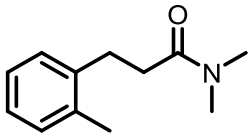

resealable pressure tube according to method A to afford the amide **3b** (605 mg, 63%) as a pale yellow liquid. **^{1}H NMR** (400 MHz, $CDCl_3$,) δ 7.17-7.09 (m, 4H), 2.98-2.93 (m, 8H), 2.56 (m, 2H), 2.33 (s, 3H). **^{13}C NMR** (100 MHz ,$CDCl_3$) δ 172.48, 139.67, 136.1, 130.39, 128.89, 126.39, 126.22, 37.27, 35.57, 34.04, 28.82, 19.41. **FTIR** (neat) 1641.9 cm^{-1}. **HRMS** (ESI) m/z calculated for $C_{12}H_{17}NO$ $(M+H)^+$: 192.1388, found: 192.1391.

***N*,*N*-Dimethyl-3-m-tolylpropanamide (3c)[21]:** Catalyst **4** (2.44 mg, 0.005 mmol), KO-*t*-Bu (728 mg, 6.5 mmol), 3-methylbenzylalcohol (610 mg, 5 mmol) and *N*,*N*-dimethylacetamide (5 mL) were allowed to react in 20 mL resealable pressure tube according to method A to afford the amide **3c** (650 mg, 68%) as a pale yellow liquid. **^{1}H NMR** (400 MHz, $CDCl_3$) δ 7.18 (t, 1H), 7.03-7.01 (m, 3H), 2.95-2.90 (m, 8H), 2.60 (m, 2H), 2.33 (s, 3H). **^{13}C NMR** (100 MHz, $CDCl_3$) δ 172.43, 141.57, 138.17, 129.36, 128.5, 126.96, 125.52, 37.31, 35.52, 35.57, 31.45, 21.51. **FTIR** (neat) 1642.7 cm^{-1}. **HRMS** (ESI) m/z calculated for $C_{12}H_{17}NO$ $(M+H)^+$: 192.1388, found: 192.1390.

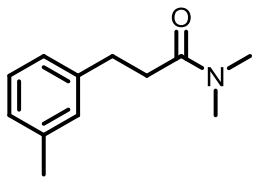

***N*,*N*-Dimethyl-3-p-tolylpropanamide (3d)[21]:** Catalyst **4** (2.44 mg, 0.005 mmol), KO-*t*-Bu (728 mg, 6.5 mmol), 4-methylbenzylalcohol (610 mg, 5 mmol) and *N*,*N*-dimethylacetamide (5 mL) were allowed to react in 20 mL resealable pressure tube according to method A to afford the amide **3d** (670 mg, 70%) as a pale yellow liquid. **^{1}H NMR** (400 MHz, $CDCl_3$) δ 7.13-7.08 (m, 4H), 2.95-2.90 (m, 8H), 2.59 (m, 2H), 2.32 (s, 3H). **^{13}C NMR** (100 MHz, $CDCl_3$) δ 172.42, 138.52, 135.69, 129.25, 128.41, 37.29, 35.61, 35.55, 31.06, 21.12. **FTIR** (neat) 1641.04 cm^{-1}. **HRMS** (ESI) m/z calculated for $C_{12}H_{17}NO$ $(M+H)^+$: 192.1388, found: 192.1393.

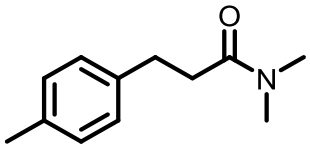

3-(2-Methoxyphenyl)-*N*,*N*-dimethylpropanamide (3e)[21]: Catalyst **4** (2.44 mg, 0.005 mmol), KO-*t*-Bu (728 mg, 6.5 mmol), 2-methoxybenzylalcohol (690 mg, 5 mmol) and *N*,*N*-dimethylacetamide (5 mL) were allowed to react in 20 mL resealable pressure tube according to method A to afford the amide **3e** (625 mg, 60%) as a pale yellow liquid. **^{1}H NMR** (400 MHz, $CDCl_3$) δ 7.21-7.16 (m, 2H), 6.89-6.83 (m, 2H), 3.82 (s, 3H), 2.95-2.94 (m, 8H), 2.59 (m, 2H). **^{13}C NMR** (100 MHz, $CDCl_3$) δ 173.04, 157.59, 130.3, 127.58, 120.63, 114.32, 110.29, 55.30, 37.28, 35.49, 33.84, 26.80. **FTIR** (neat) 1643.9 cm^{-1}. **HRMS** (ESI) m/z calculated for $C_{12}H_{17}NO_2$ $(M+H)^+$: 208.1337, found: 208.1340.

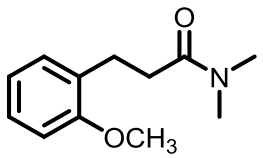

3-(3-Methoxyphenyl)-*N*,*N*-dimethylpropanamide (3f)[21]: Catalyst **4** (2.44 mg, 0.005 mmol), KO-*t*-Bu (728 mg, 6.5 mmol), 3-methoxybenzylalcohol (690 mg, 5 mmol) and *N*,*N*-dimethylacetamide (5 mL) were allowed to react in 20 mL resealable pressure tube according to method A to afford the amide **3f** (540 mg, 52%) as a pale yellow liquid. **^{1}H NMR** (400 MHz, $CDCl_3$) δ 7.22-7.18 (m, 1H), 6.82-6.73 (m, 3H), 3.79 (s, 3H), 2.95-2.93 (m, 8H), 2.60 (m, 2H). **^{13}C NMR** (100 MHz,

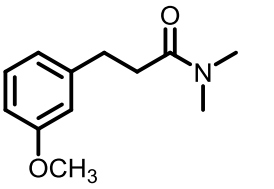

cryCDCl$_3$) δ 172.30, 159.81, 143.26, 129.57, 120.89, 114.30, 111.50, 55.29, 37.30, 35.58, 35.35, 31.55. **FTIR** (neat) 1640.4 cm^{-1}. **HRMS** (ESI) m/z calculated for $C_{12}H_{17}NO_2$ $(M+H)^+$: 208.1337, found: 208.1344.

3-(4-Methoxyphenyl)-*N*,*N*-dimethylpropanamide (3g)[21]: Catalyst **4** (2.44 mg, 0.005 mmol), KO-*t*-Bu (728 mg, 6.5 mmol), 4-methoxybenzylalcohol (690 mg, 5 mmol) and *N*,*N*-dimethylacetamide (5 mL) were allowed to react in 20 mL resealable pressure tube according to method A to afford the amide **3g** (566 mg, 55%) as a pale yellow liquid. **^{1}H NMR** (400 MHz, CDCl$_3$) δ 7.13 (d, *J* = 8 Hz, 2H), 6.82 (d, *J* = 8 Hz, 2H), 3.78 (s, 3H), 2.94-2.92 (m, 8H), 2.58 (m, 2H). **^{13}C NMR** (100 MHz, CDCl$_3$) δ 172.54, 158.08, 133.61, 129.48, 113.98, 55.38, 37.34, 35.69, 35.58, 30.62. **FTIR** (neat) 1640.85 cm^{-1}. **HRMS** (ESI) m/z calculated for $C_{12}H_{17}NO_2$ $(M+H)^+$: 208.1337, found: 208.1339.

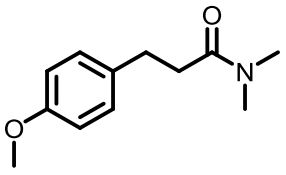

***N*,*N*-Dimethylhexanamide (3h)[21]:** Catalyst 4 (4.88 mg, 0.01 mmol), KO-*t*-Bu (728 mg, 6.5 mmol), butanol (370 mg, 5 mmol) and *N*,*N*-dimethylacetamide (5 mL) were allowed to react in 20 mL resealable pressure tube according to method A to afford the amide **3h** (393 mg, 55%) as a colorless liquid. **^{1}H NMR** (400 MHz, CDCl$_3$) δ 2.99 (s, 3H), 2.93 (s, 3H), 2.29 (t, *J* = 8 Hz, 2H), 1.62 (quin, *J* = 8 Hz, 2H), 1.30-1.33 (m, 4H), 0.89 (m, 3H). **^{13}C NMR** (100 MHz, CDCl$_3$) 173.55, 37.46, 35.51, 33.51, 31.81, 25.01, 22.62, 14.1. **FTIR** (neat) 1643 cm^{-1}. **HRMS** (ESI) m/z calculated for $C_8H_{17}NO$ $(M+H)^+$: 144.1388, found: 144.1390.

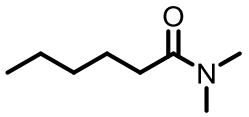

***N*,*N*-Dimethyloctanamide (3i)[22]:** Catalyst **4** (4.88 mg, 0.01 mmol), KO-*t*-Bu (728 mg, 6.5 mmol), hexanol (510 mg, 5 mmol) and *N*,*N*-dimethylacetamide (5 mL) were allowed to react in 20 mL resealable pressure tube according to method A to afford the amide **3i** (513 mg, 60%) as a colorless liquid. **^{1}H NMR** (400 MHz, CDCl$_3$) δ 2.99 (s, 3H),2.93 (s, 3H), 2.29 (t, *J* = 8 Hz, 2H), 1.61 (quintet, *J* = 8 Hz, 2H), 1.30-1.27 (m, 8H), 0.86 (m, 3H). **^{13}C NMR** (100 MHz, CDCl$_3$) 173.44, 37.44, 35.49, 33.57, 31.87, 29.62, 29.25, 22.76, 14.21. **FTIR** (neat) 1642.8 cm^{-1}. **HRMS** (ESI) m/z calculated for $C_{10}H_{21}NO$ $(M+H)^+$: 172.1701, found: 172.1701.

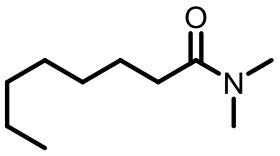

***N*,*N*-Dimethyldecanamide (3j)[21]:** Catalyst **4** (4.88 mg, 0.01 mmol), KO-*t*-Bu (728 mg, 6.5 mmol), octanol (650 mg, 5 mmol) and *N*,*N*-dimethylacetamide (5 mL) were allowed to react in 20 mL resealable pressure tube according to method A to afford the amide **3j** (398 mg, 36%) as a colorless liquid. **^{1}H NMR** (400 MHz, CDCl$_3$) δ 2.99 (s, 3H), 2.92 (s, 3H), 2.28 (t, *J* = 8 Hz, 2H), 1.60 (quin, *J* = 8Hz, 2H), 1.28-1.24 (m, 12H), 0.86(m, 3H). **^{13}C NMR** (100 MHz, CDCl$_3$) 173.48, 37.43, 33.55, 31.99, 29.64, 29.6, 29.58, 29.4, 25.33, 22.77, 14.19. **FTIR** (neat) 1645.6 cm^{-1}. **HRMS** (ESI) m/z calculated for $C_{12}H_{25}NO$ $(M+H)^+$: 200.2014, found: 200.2016.

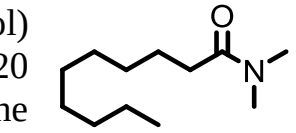

***N*,*N*-Dimethyl-5-methylhexanamide (3k):** Catalyst **4** (4.88 mg, 0.01 mmol), KO-*t*-Bu (728 mg, 6.5 mmol), isoamyl alcohol (440 mg, 5 mmol) and *N*,*N*-

dimethylacetamide (5 mL) were allowed to react in 20 mL resealable pressure tube according to method A to afford the amide **3k** (519 mg, 66%) as a yellow liquid. 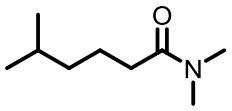 **^{1}H NMR** (400 MHz, $CDCl_3$) δ 3.00 (s, 3H), 2.94 (s, 3H), 2.28 (t, *J* = 8 Hz, 2H), 1.66-1.56 (m, 5H), 1.21 (m, 2H), 0.88(d, *J* = 6.4 Hz, 6H). **^{13}C NMR** (100 MHz, $CDCl_3$) δ 173.45, 38.88, 37.43, 35.49, 33.77, 28.03, 23.18, 22.67. **FTIR** (neat) 1644.8 cm^{-1}. **HRMS** (ESI) m/z calculated for $C_9H_{19}NO$ $(M+H)^+$: 158.1545, found: 158.1548.

3-Phenyl-1-(pyrrolidin-1-yl)propan-1-one (3l): Catalyst **4** (2.44 mg, 0.005 mmol), KO-*t*-Bu (728 mg, 6.5 mmol), benzyl alcohol (440 mg, 5 mmol) and *N*-acetylpyrrolidine (1130 mg, 10 mmol) were allowed to react in 20 mL resealable pressure tube according to method A to afford the cyclic amide **3l** (450 mg, 44%) as a yellow liquid. 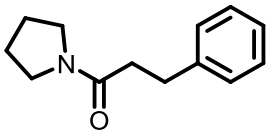 **^{1}H NMR** (400 MHz, $CDCl_3$) δ 7.28-7.21 (m, 5H), 3.46 (t, *J* = 6.7 Hz, 2H), 3.28 (t, *J* = 6.6 Hz, 2H), 2.98 (t, *J* = 8 Hz, 2H), 2.56 (t, *J* = 8.0 Hz, 2H), 1.89-1.80 (m, 4H). **^{13}C NMR** (100 MHz, $CDCl_3$) 170.97, 141.64, 128.88, 128.57, 127.96,126.19, 46.71, 45.79, 36.89, 31.36, 26.18, 24.51. **FTIR** (neat) 1641.8 cm^{-1}. **HRMS** (ESI) m/z calculated for $C_{13}H_{17}NO$ $(M+H)^+$: 204.1388, found: 204.1389.

3-Phenyl-1-(piperidin-1-yl)propan-1-one (3m)[21]: Catalyst **4** (2.44 mg, 0.005 mmol), KO-*t*-Bu (728 mg, 6.5 mmol), benzyl alcohol (440 mg, 5 mmol) and *N*-acetylpiperidine (1270 mg, 10 mmol) were allowed to react in 20 mL resealable pressure tube according to method A to afford the cyclic amide **3m** (585 mg, 54%) as a yellow liquid. 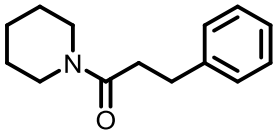 **^{1}H NMR** (400 MHz, $CDCl_3$) δ 7.18-7.05 (m, 5H), 3.43 (m, 2H), 3.20 (m, 2H), 2.84 (t, *J* = 8 Hz, 2H), 2.49 (t, *J* = 8.0 Hz, 2H), 1.31-1.48 (m, 6H). **^{13}C NMR** (100 MHz, $CDCl_3$) 170.58, 141.63, 128.6, 128.58, 126.93, 126.22, 46.77, 42.87, 35.33, 31.77, 26.54, 25.69, 24.76, 24.68. **FTIR** (neat) 1633.9 cm^{-1}. **HRMS** (ESI) m/z calculated for $C_{14}H_{19}NO$ $(M+H)^+$: 218.1545, found: 218.1547.

1-Morpholino-3-phenylpropan-1-one (3n)[22]: Catalyst **4** (2.44 mg, 0.005 mmol), KO-*t*-Bu (728 mg, 6.5 mmol), benzyl alcohol (440 mg, 5 mmol) and *N*-acetyl piperidine (1290 mg, 10 mmol) were allowed to react in 20 mL resealable pressure tube according to method A to afford the cyclic amide **3n** (360 mg, 32%) as a pale yellow liquid. 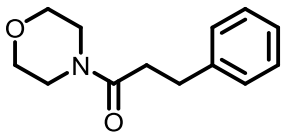 **^{1}H NMR** (400 MHz, $CDCl_3$) δ 7.16-7.05 (m, 5H), 3.47 (s, 4H), 3.35 (t, *J* = 4 Hz, 2H), 3.2 (t, *J* = 4 Hz, 2H), 2.82 (t, *J* = 8 Hz, 2H), 2.46 (t, *J* = 8 Hz, 2H). **^{13}C NMR** (100 Hz, $CDCl_3$) 171.05, 141.16, 128.68, 128.59, 127.21,126.41, 66.98, 66.59, 46.1, 42.07, 34.94, 31.61. **FTIR** (neat) 1639 cm^{-1}. **HRMS** (ESI) m/z calculated for $C_{13}H_{17}NO_2$ $(M+H)^+$: 220.1337, found: 220.1343.

3-Benzyl-3-hydroxyindolin-2-one (9a)[28]: Catalyst **4** (1.22 mg, 0.0025 mmol), KO-*t*-Bu (218.4 mg, 1.95 mmol), benzyl alcohol (162 mg, 1.5 mmol), 2-oxindole (399 mg, 3 mmol) and toluene (2 mL) were allowed to react in 20 mL resealable pressure tube according to method B to afford the C3-hydroxy 2-oxindole **9a** (223 mg, 62%) as a white solid. 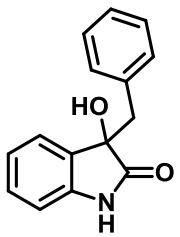

Melting point: 165-168 ^oC. **^{1}H NMR** (400 MHz, $CDCl_3$): δ 7.76 (bs,

1H), 7.22-7.11 (m, 5H), 7.05-6.98 (m, 3H), 6.71 (d, *J* = 7.6 Hz, 1H), 3.31 (d, *J* = 13.2 Hz, 1H), 3.14 (d, *J* = 12.8 Hz, 1H).**^{13}C NMR** (100 MHz, $CDCl_3$) δ 179.6, 140.28, 133.92,130.57, 129.85, 128.06, 127.12, 125.11, 122.99, 110.19, 77.36, 44.79. **FTIR** (neat) 3264.7, 1710.94 cm^{-1}. **HRMS** (ESI) m/z calculated for $C_{15}H_{13}NO_2$ $(M+H)^+$: 240.1024, found: 240.1030. **Crystal data for the compound 9a**: CCDC Number : 1451682.

3-Hydroxy-3-(3-methoxybenzyl)indolin-2-one (9b): Catalyst **4** (1.22 mg, 0.0025 mmol), KO-*t*-Bu (218.4 mg, 1.95 mmol), 3-methoxybenzyl alcohol (207 mg, 1.5 mmol), 2-oxindole (399 mg, 3 mmol) and toluene (2 mL) were allowed to react in 20 mL resealable pressure tube according to method B to afford the C3-hydroxy 2-oxindole **9b** (195 mg, 48%) as a light brown solid. **Melting point**: 125-127 °C. **^{1}H NMR** (400 MHz, $CDCl_3$) δ 7.89 (bs, 1H), 7.20-7.17 (m, 2H), 7.03(m, 2H), 6.70-6.68 (m, 2H), 6.57 (m, 1H), 6.48 (m, 1H), 3.61 (s, 3H), 3.43 (bs,1H), 3.28(d, *J* = 12.8 Hz, 1H), 3.11(d, *J* = 13.2 Hz, 1H). **^{13}C NMR** (100 MHz, $CDCl_3$) δ 180.34, 159.44, 140.74, 135.75, 130.25, 130.14, 129.3, 125.34, 123.35, 123.27, 115.96, 113.44, 110.70, 77.95, 55.51, 45.04. **FTIR** (neat) 3228.8, 1704.7 cm^{-1}. **HRMS** (ESI) m/z calculated for $C_{16}H_{15}NO_3$ $(M+Na)^+$: 292.0949, found: 292.0948.

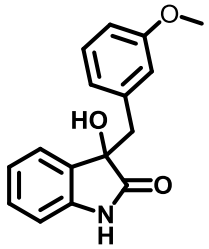

3-Hydroxy-3-(3-methylbenzyl)indolin-2-one (9c): Catalyst **4** (1.22 mg, 0.0025 mmol), KO-*t*-Bu (218.4 mg, 1.95 mmol), 3-methylbenzyl alcohol (183 mg, 1.5 mmol), 2-oxindole (399 mg, 3 mmol) and toluene (2 mL) were allowed to react in 20 mL resealable pressure tube according to method B to afford the C3-hydroxy 2-oxindole **9c** (206 mg, 54%) as a white solid. **Melting point** : 170-172 °C. **^{1}H NMR** (400 MHz, $CDCl_3$) δ 7.73 (bs, 1H), 7.23-7.15 (m, 2H), 7.05-6.96 (m, 3H), 6.81-6.71 (m, 3H), 3.27 (d, *J* =12.8 Hz, 1H), 3.19 (bs, 1H), 3.09 (d, *J* = 12.8 Hz, 1H), 2.20 (s, 3H). **^{13}C NMR** (100 MHz, $CDCl_3$) δ 179.73, 140.31, 137.59, 133.79, 131.38, 129.88, 129.79, 127.90, 127.85, 127.58, 125.15, 122.91, 110.19, 44.72, 21.41. **FTIR** (neat) 3267.7, 1713.5 cm^{-1}. **HRMS** (ESI) m/z calculated for $C_{16}H_{15}NO_2$ $(M+Na)^+$: 276.1000, found: 276.0999. **Crystal data for the compound 9c**: CCDC Number: 1451683.

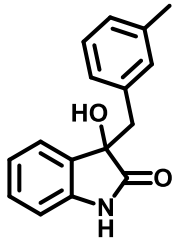

3-Hydroxy-3-(4-methylbenzyl)indolin-2-one (9d)[28]: Catalyst **4** (1.22 mg, 0.0025 mmol), KO-*t*-Bu (218.4 mg, 1.95 mmol), 4-methylbenzyl alcohol (183 mg, 1.5 mmol), 2-oxindole (399 mg, 3 mmol) and toluene (2 mL) were allowed to react in 20 mL resealable pressure tube according to method B to afford the C3-hydroxy 2-oxindole **9d** (196 mg, 51%) as a light brown solid. **Melting point** : 185-186 °C. **^{1}H NMR** (400 MHz, $CDCl_3$) δ 7.28 (bs, 1H), 7.23-7.18 (m, 2H), 7.04 (dt, *J* = 8 Hz, 1H), 6.96 (d, *J* = 8 Hz, 2H), 6.88 (d, *J* = 8 Hz, 2H), 6.71 (d, *J* = 8 Hz, 1H), 3.26 (d, *J* = 13.2 Hz, 1H), 3.10 (d, *J* = 12.8 Hz, 1H), 2.20 (s, 3H). **^{13}C NMR** (100 MHz, $CDCl_3$) δ 179.09, 140.11, 138.63, 136.57, 130.55, 130.27, 129.67, 128.66, 124.96, 122.82, 109.96, 44.29, 21.06. **FTIR** (neat) 3261.79, 1693 cm^{-1}. **HRMS** (ESI) m/z calculated for $C_{16}H_{15}NO_2$ $(M+Na)^+$: 276.1000, found: 276.0998.

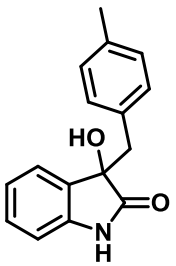

3-Butyl-3-hydroxyindolin-2-one (9e): Catalyst **4** (4.88 mg, 0.01 mmol), KO-*t*-Bu (218.4 mg, 1.95 mmol), butanol (111 mg, 1.5 mmol), 2-oxindole (399 mg, 3 mmol) and toluene (2 mL) were allowed to react in 20 mL resealable pressure tube according to method B to afford the C3-hydroxy 2-oxindole **9e** (238 mg, 77%) as a light yellow solid. **Melting point**: 95-98 ^{o}C. **^{1}H NMR** (400 MHz, $CDCl_3$) δ 8.33 (bs, 1H), 7.36 (d, *J* = 7.4 Hz, 1H), 7.28-7.24 (m, 1H), 7.08 (td, *J* = 7.6, 0.9 Hz, 1H), 6.89 (d, *J* = 7.7 Hz, 1H), 3.18 (bs, 1H), 1.99-1.93 (m, 2H), 1.29 - 1.04 (m, 4H), 0.82 (t, *J* = 7.2 Hz, 3H). **^{13}C NMR** (100 MHz, $CDCl_3$) δ 180.74, 140.60, 130.69, 129.72, 124.43, 123.27, 110.40, 38.44, 25.32, 22.86, 13.95. **FTIR** (neat) 3678, 3183, 1710 cm^{-1}. **HRMS** (ESI) m/z calculated for $C_{12}H_{15}NO_2$ $(M+Na)^+$: 228.1000, found: 228.1010.

3-Hydroxy-3-isopentylindolin-2-one (9f): Catalyst **4** (4.88 mg,0.01 mmol), KO-*t*-Bu (218.4 mg, 1.95 mmol), isoamyl alcohol (132 mg, 1.5 mmol), 2-oxindole (399 mg, 3 mmol) and toluene (2 mL) were allowed to react in 20 mL resealable pressure tube according to method B to afford the C3-hydroxy 2-oxindole **9f** (237 mg, 72%) as a light yellow solid.

Melting point : 117-119 ^{o}C. **^{1}H NMR** (400 MHz, $CDCl_3$) δ 8.63 (bs, 1H), 7.34 (d, *J* = 7.4 Hz, 1H), 7.23 (d, *J* = 7.7 Hz, 1H), 7.07 (t, *J* = 7.2 Hz, 1H), 6.88 (d, *J* = 7.7 Hz, 1H), 3.49 (bs, 1H), 1.99-1.89 (m, 2H), 1.49-1.43 (m, 1H), 1.15-0.95 (m, 2H), 0.8 (d, *J* = 6.6 Hz, 6H). **^{13}C NMR** (100 MHz, $CDCl_3$) δ 181.33, 140.69, 130.79, 129.64, 124.32, 123.24, 110.61, 77.01, 36.43, 31.82, 28.21, 22.52, 22.41. **FTIR** (neat) 3389, 3680, 1711 cm^{-1}. **HRMS** (ESI) m/z calculated for $C_{13}H_{17}NO_2$ $(M+Na)^+$: 242.1157, found : 242.1164.

3-Hexyl-3-hydroxyindolin-2-one (9g)[28]: Catalyst **4** (4.88 mg, 0.01 mmol), KO-*t*-Bu (218.4 mg, 1.95 mmol), hexanol (153 mg, 1.5 mmol), 2-oxindole (399 mg, 3 mmol) and toluene (2 mL) were allowed to react in 20 mL resealable pressure tube according to method B to afford the C3-hydroxy 2-oxindole **9g** (228 mg, 65%) as a white solid. **Melting point**: 90-92 ^{o}C. **^{1}H NMR** (400 MHz, $CDCl_3$) δ 8.30 (bs, 1H), 7.35 (d, *J* = 7.3 Hz, 1H), 7.27-7.25 (m, 1H), 7.07 (dd, *J* = 8.4, 0.8 Hz 1H), 6.88 (d, *J* = 7.7 Hz, 1H), 3.15 (bs, 1H), 1.96-1.93 (m, 2H), 1.22-1.19 (m, 8H), 0.82 (t, *J* = 6.9 Hz, 3H). **^{13}C NMR** (100 MHz, $CDCl_3$) δ 181.01, 140.62, 130.72, 129.68, 124.37, 123.25, 110.49, 77.25, 38.60, 31.63, 29.40, 23.14, 22.63, 14.14. **FTIR** (neat) 3678, 3324, 1711 cm^{-1}. **HRMS** (ESI) m/z calculated for $C_{14}H_{19}NO_2$ $(M+Na)^+$: 256.1313, found: 256.1319.

3-Hydroxy-3-octylindolin-2-one (9h): Catalyst **4** (4.88 mg,0.01 mmol), KO-*t*-Bu (218.4 mg, 1.95 mmol), octanol (195 mg, 1.5 mmol), 2-oxindole (399 mg, 3 mmol) and toluene (2 mL) were allowed to react in 20 mL resealable pressure tube according to method B to afford the C3-hydroxy 2-oxindole **9h** (254 mg, 65%) as a light yellow solid. **Melting point**: 102-105 ^{o}C. **^{1}H NMR** (400 MHz, $CDCl_3$) δ 7.77 (bs, 1H), 7.36 (d, *J* = 7.4 Hz, 1H), 7.29-7.25 (m, 1H), 7.08 (td, *J* = 7.6,

0.9 Hz, 1H), 6.87 (d, J = 7.8 Hz, 1H), 2.76 (bs, 1H), 1.96-1.94 (m, 2H), 1.25-1.19 (m, 12H), 0.85 (t, J = 7.0 Hz, 3H). **^{13}C NMR** (100 MHz, $CDCl_3$) δ 180.31, 140.51, 130.56, 129.75, 124.46, 123.28, 110.29, 77.07, 38.72, 31.91, 29.74, 29.41, 29.28, 23.20, 22.75, 14.23. **FTIR** (neat) 3267.7, 1713.5 cm^{-1}. **HRMS** (ESI) m/z calculated for $C_{16}H_{23}NO_2$ $(M+Na)^+$: 284.1626, found: 284.1632.

2A.8.4. Appendix I: Copies of ^{1}H and ^{13}C NMR spectra and crystal structure of representative compounds

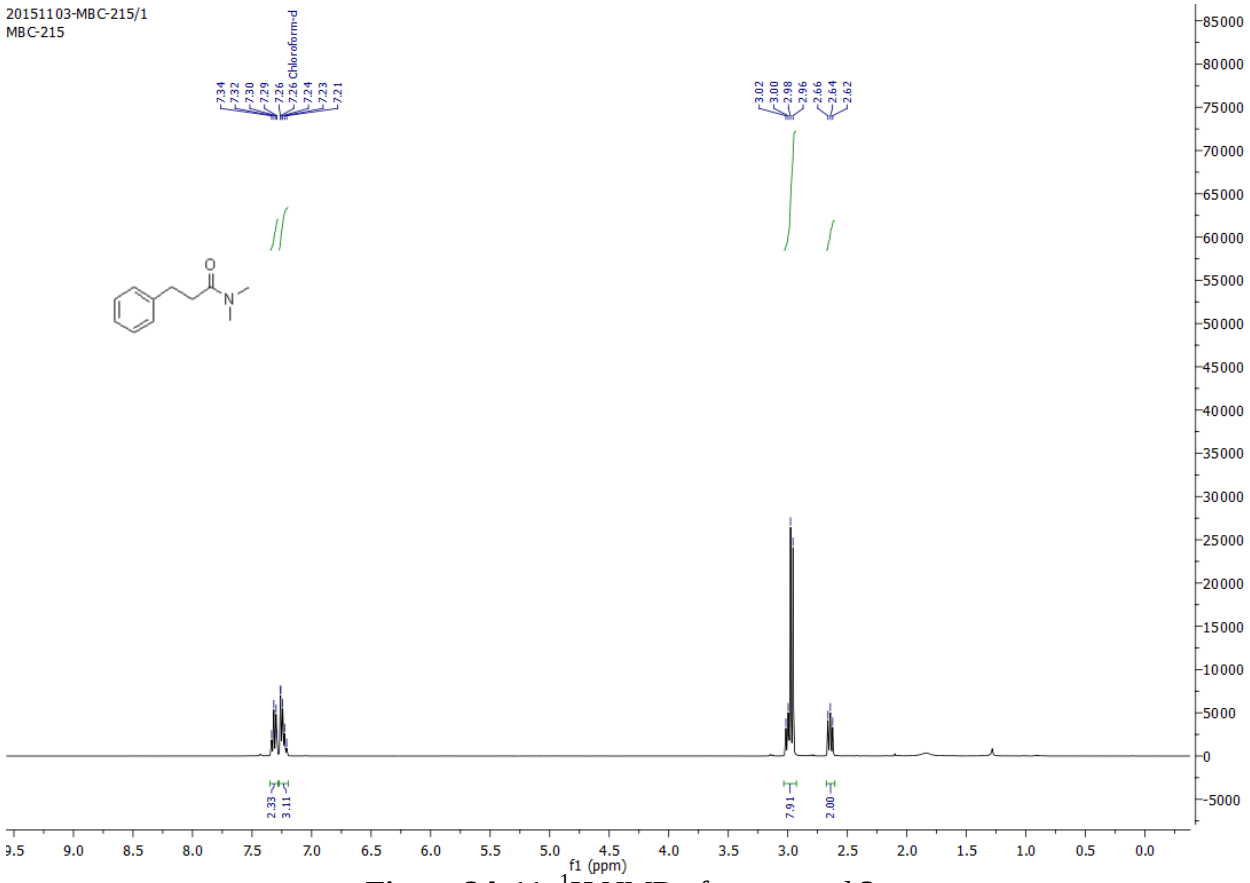

Figure 2A.11. ^{1}H NMR of compound **3a**

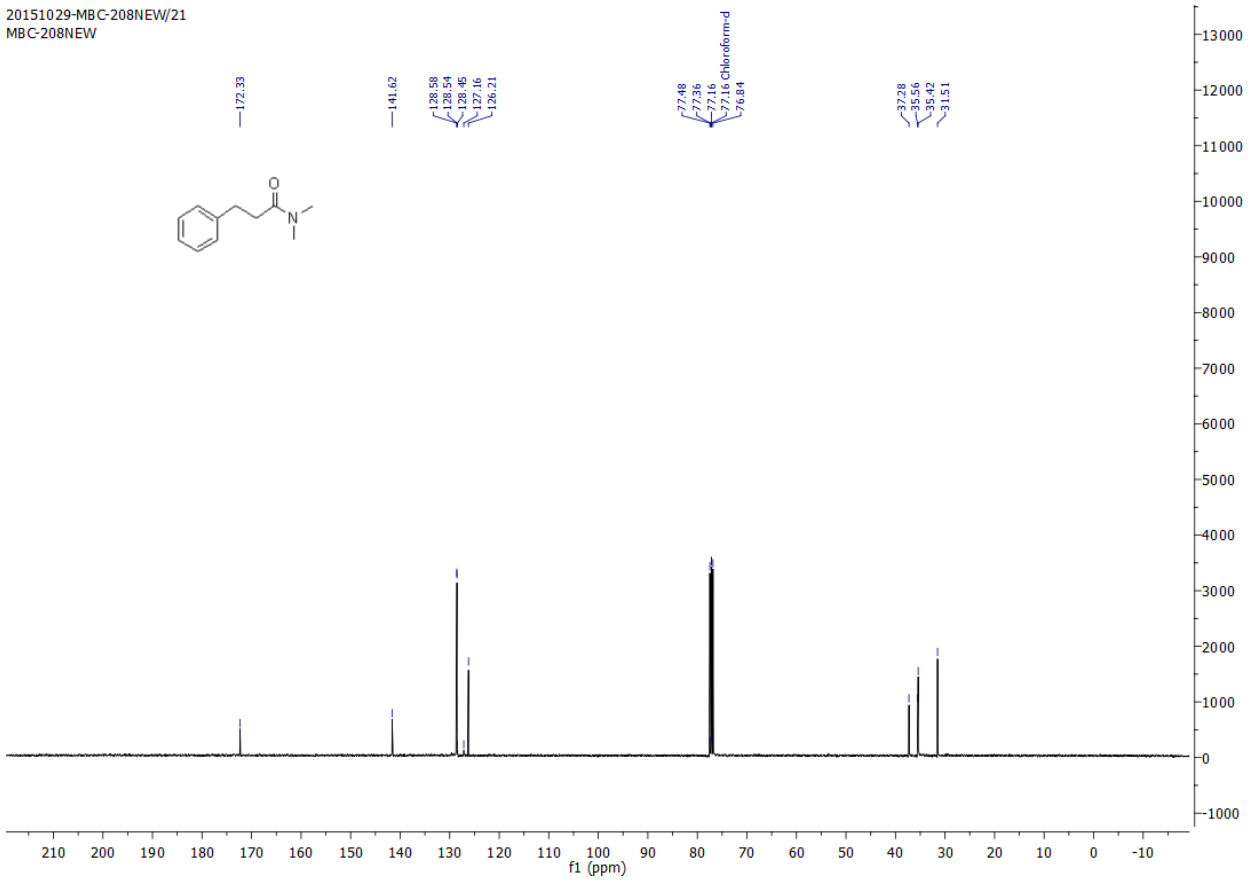

Figure 2A.12. ^{13}C NMR of compound **3a**

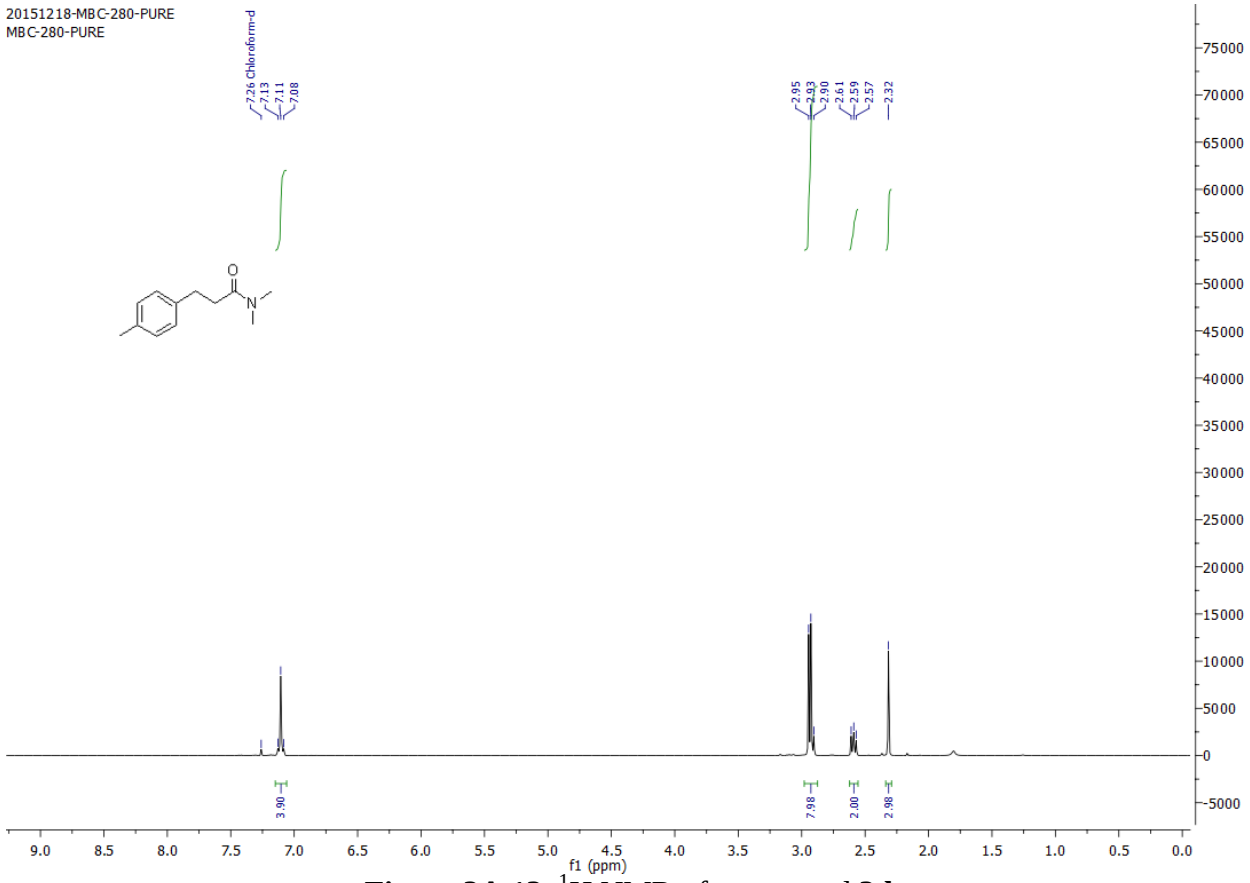

Figure 2A.13. ^{1}H NMR of compound **3d**

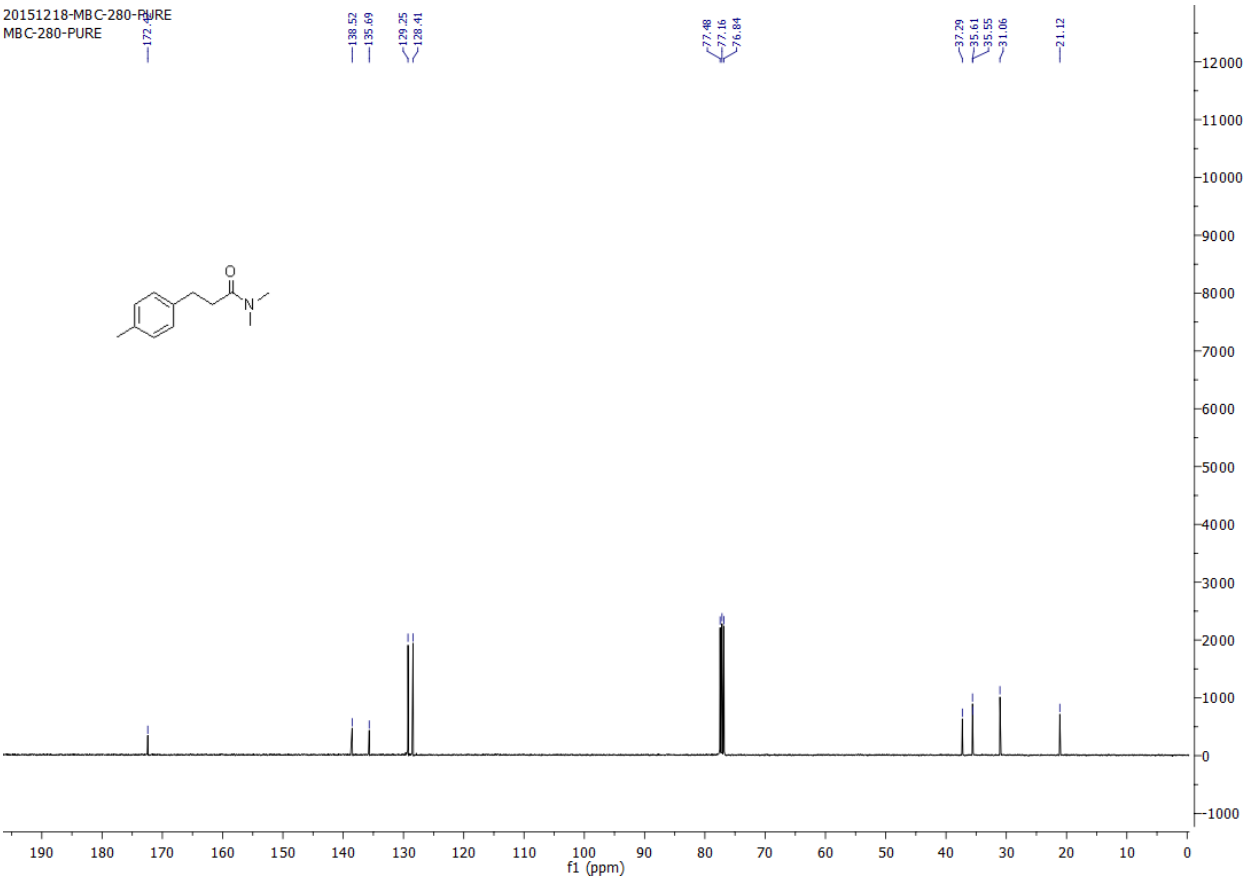

Figure 2A.14. ^{13}C NMR of compound **3d**

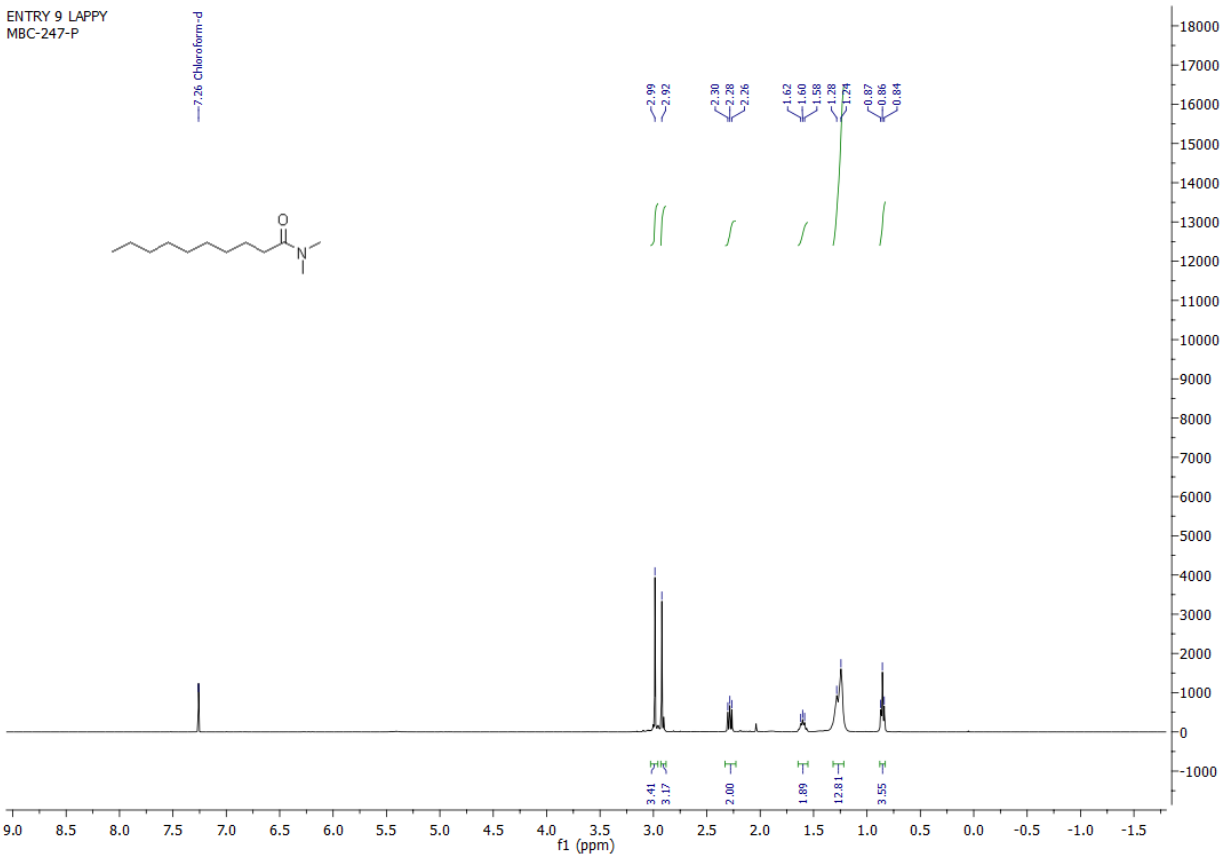

Figure 2A.15. ^{1}H NMR of compound **3j**

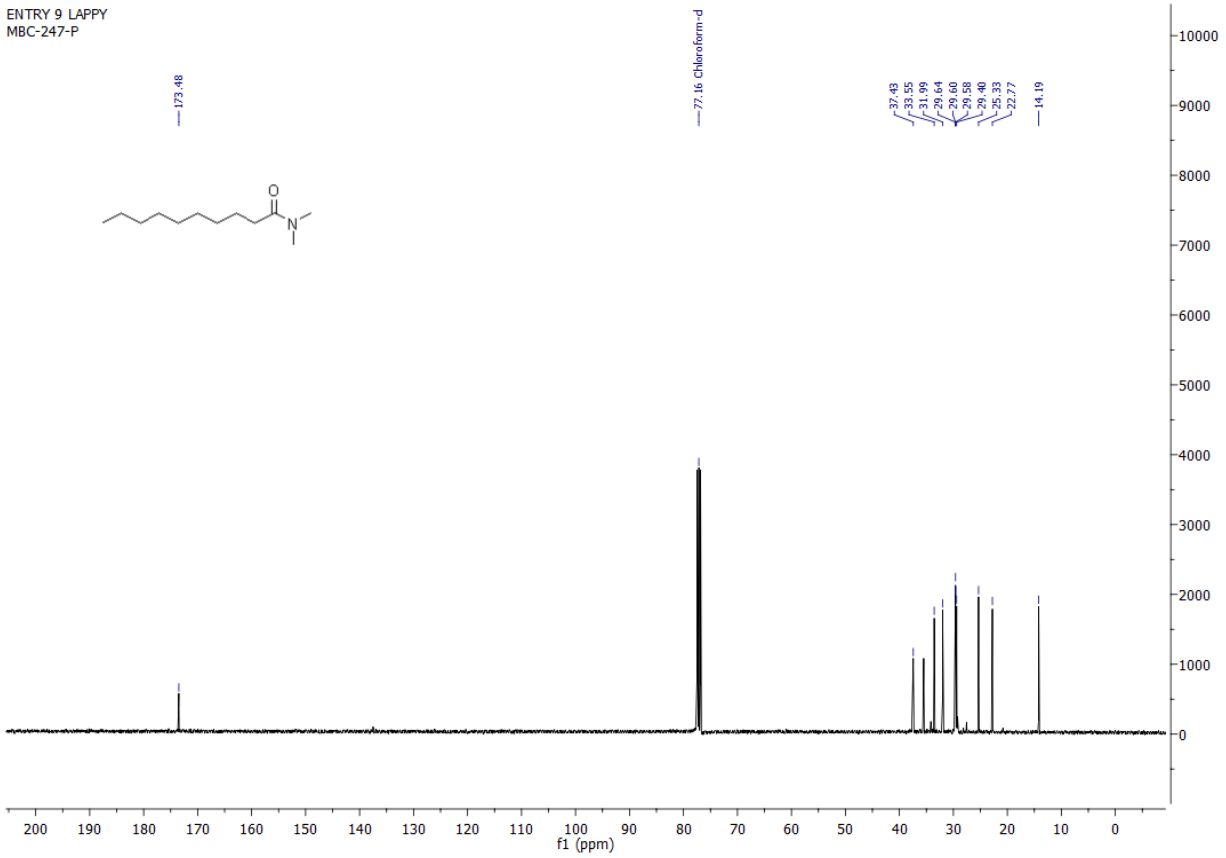

Figure 2A.16. ^{13}C NMR of compound **3j**

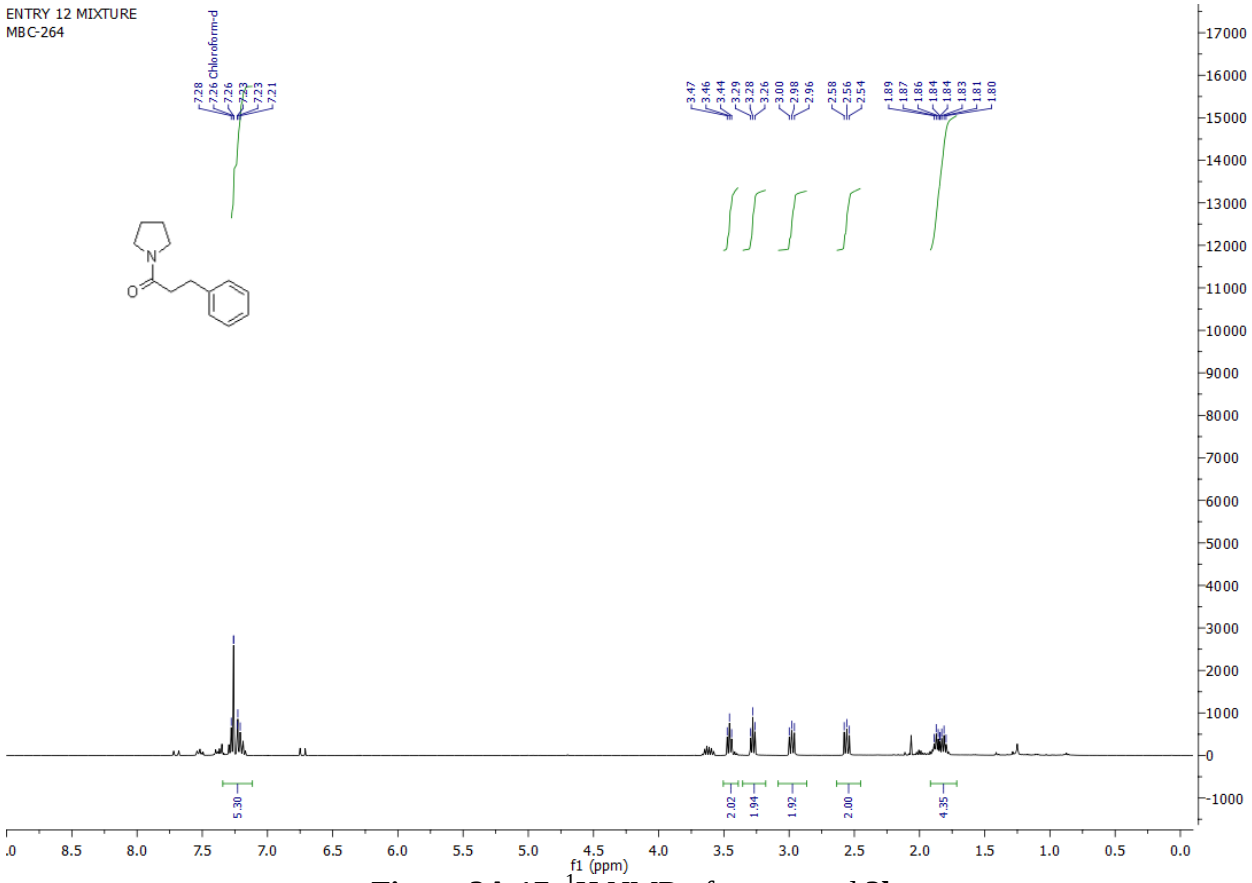

Figure 2A.17. ^{1}H NMR of compound **3l**

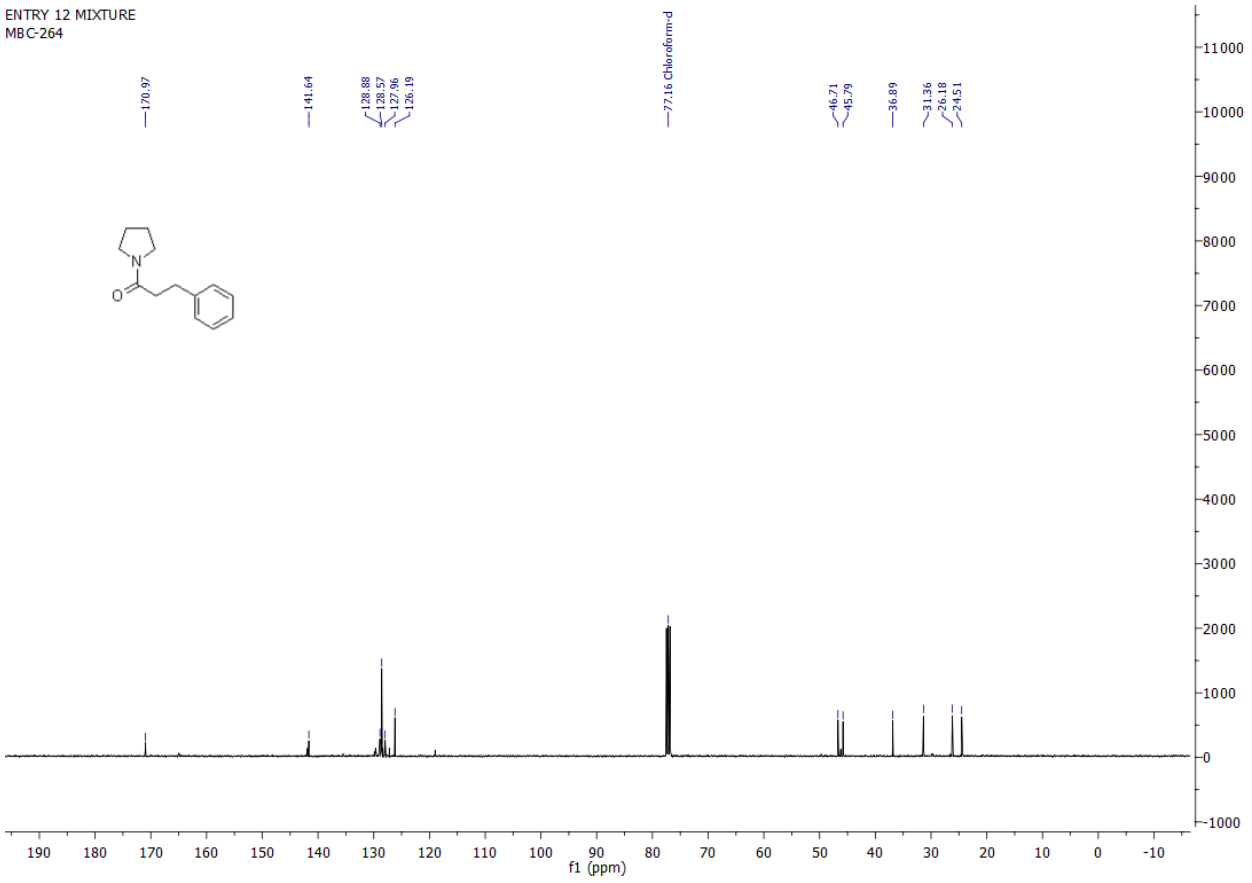

Figure 2A.18. ^{13}C NMR of compound **3l**

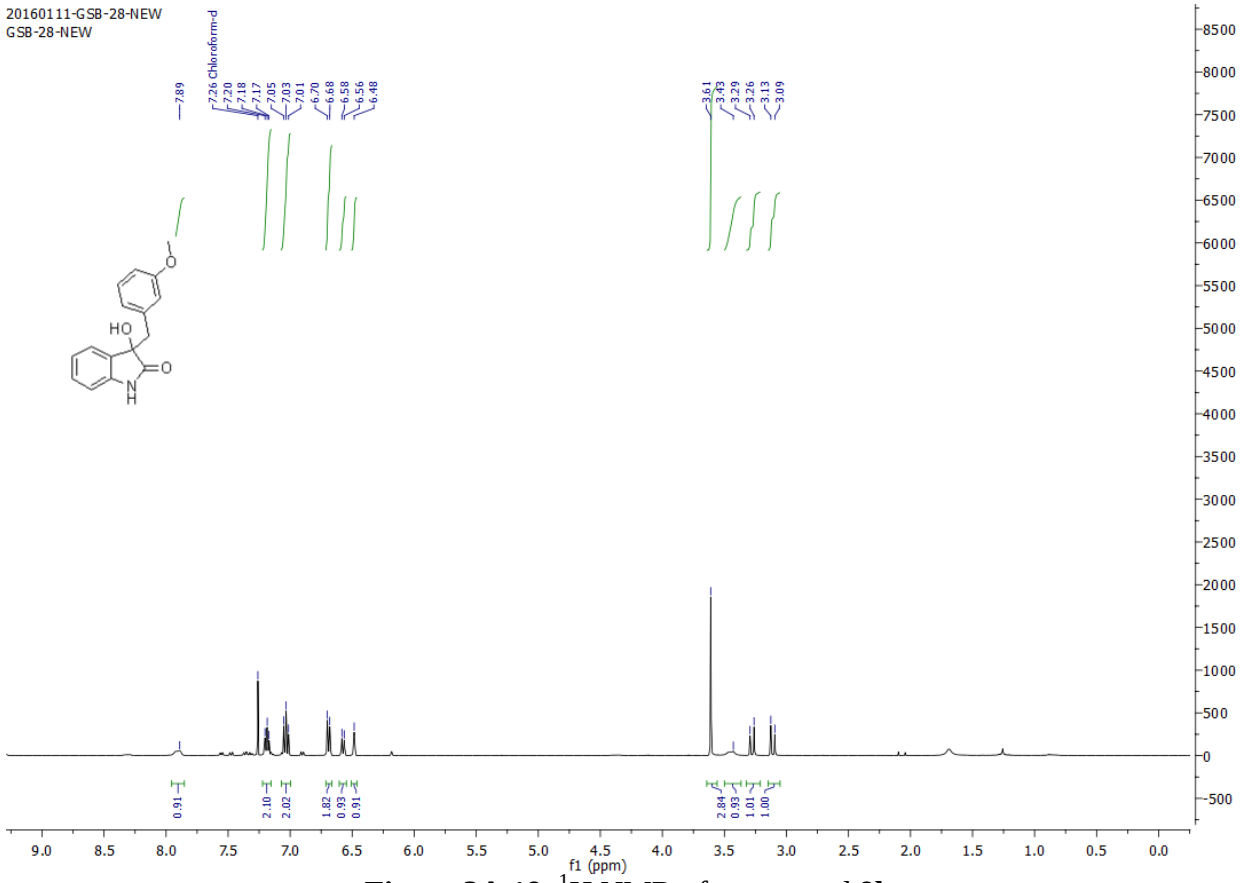

Figure 2A.19. ^{1}H NMR of compound **9b**

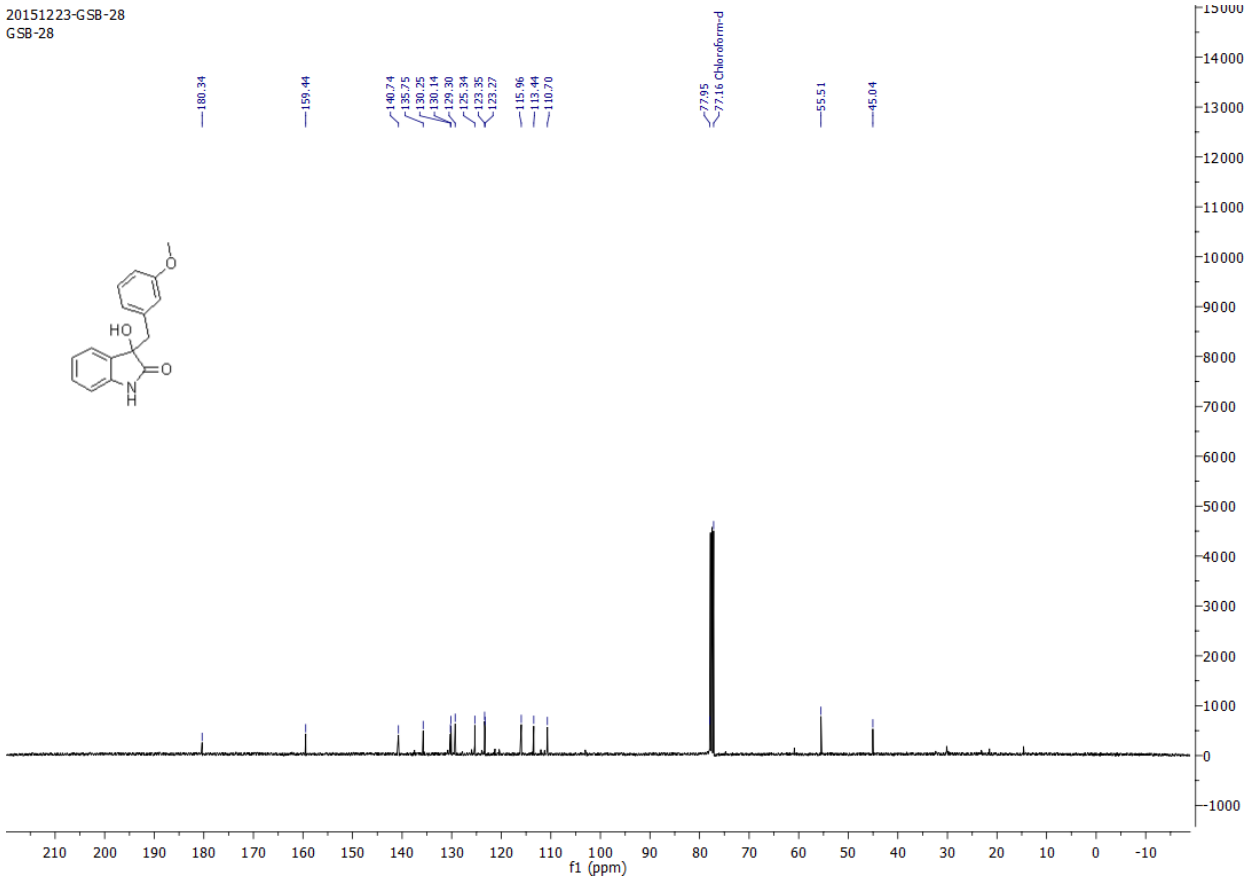

Figure 2A.20. ^{13}C NMR of compound **9b**

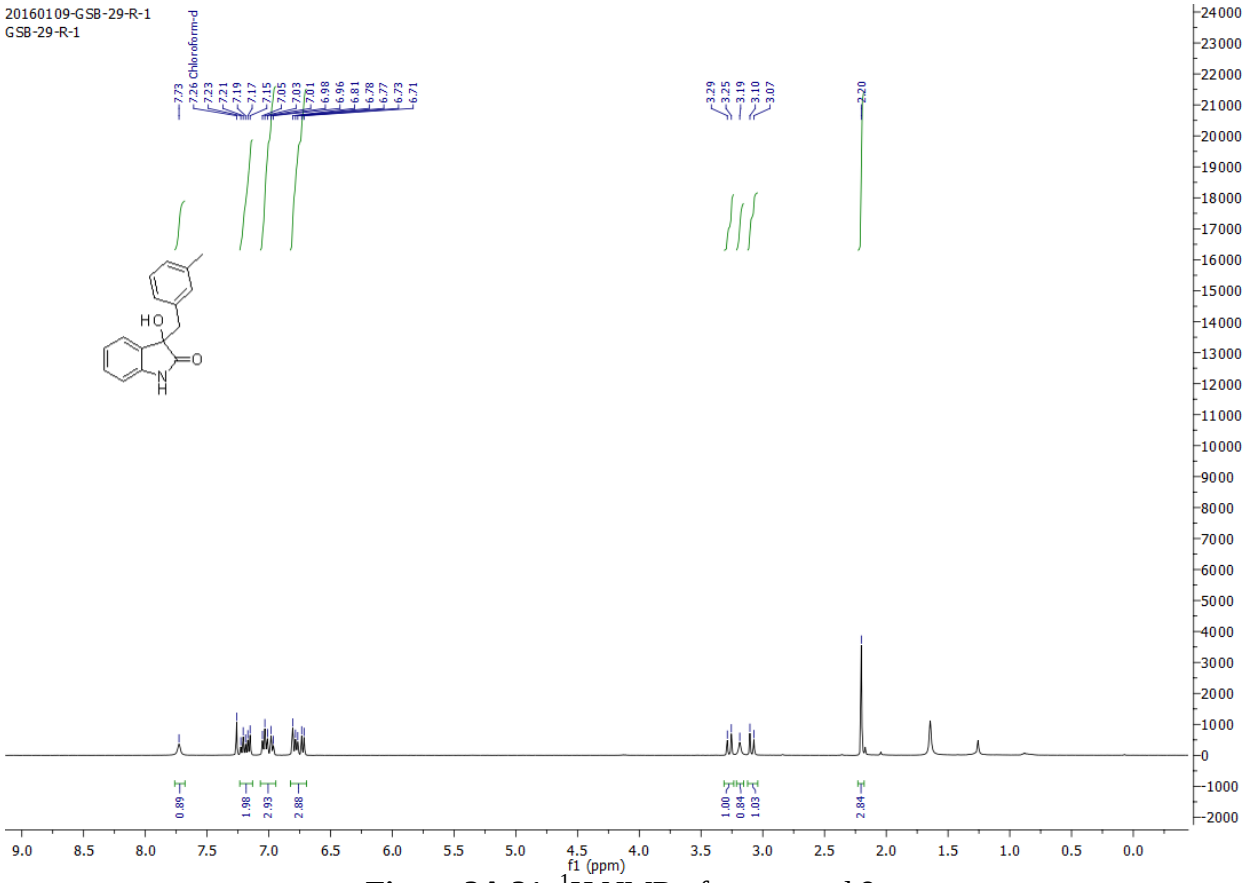

Figure 2A.21. ^{1}H NMR of compound **9c**

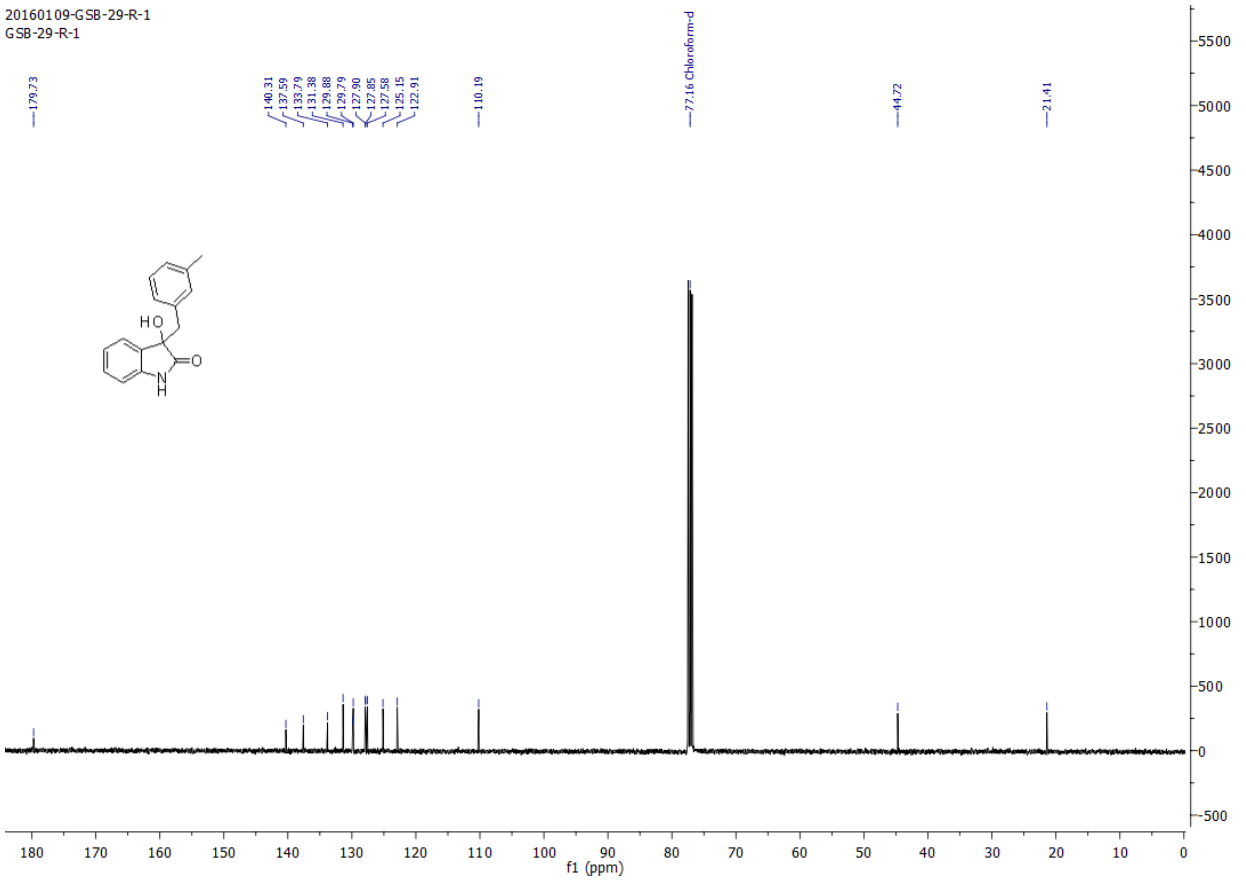

Figure 2A.22. ^{13}C NMR of compound **9c**

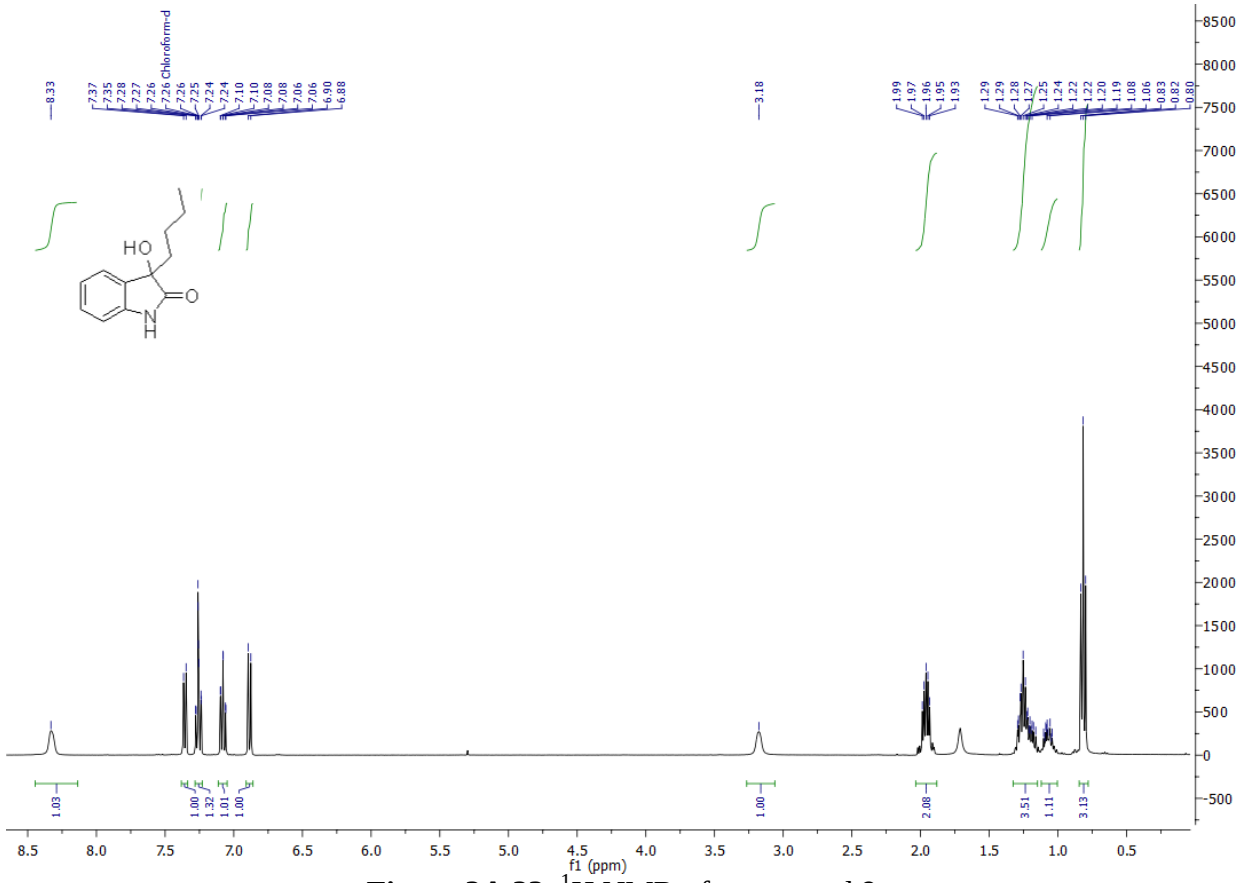

Figure 2A.23. ^{1}H NMR of compound **9e**

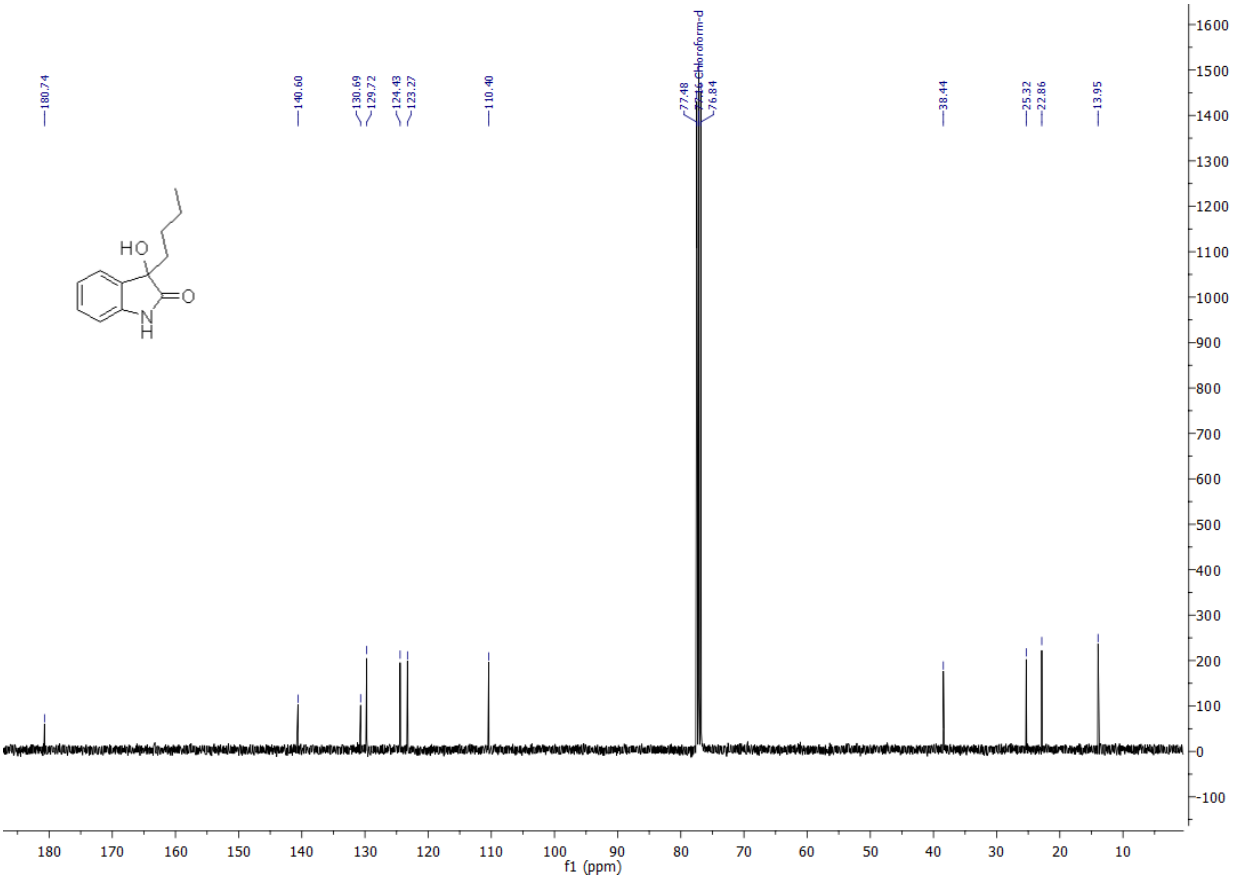

Figure 2A.24. ^{13}C NMR of compound **9e**

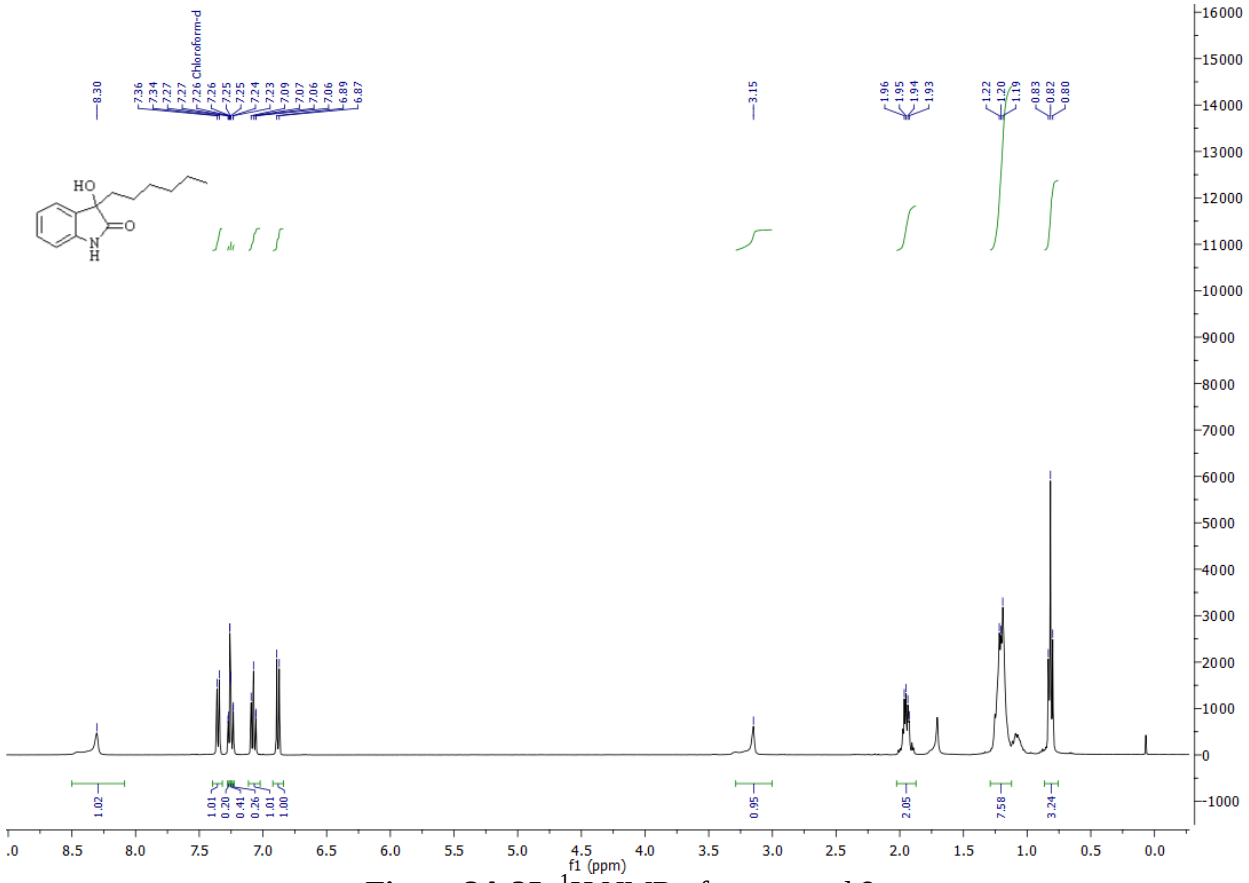

Figure 2A.25. ^{1}H NMR of compound **9g**

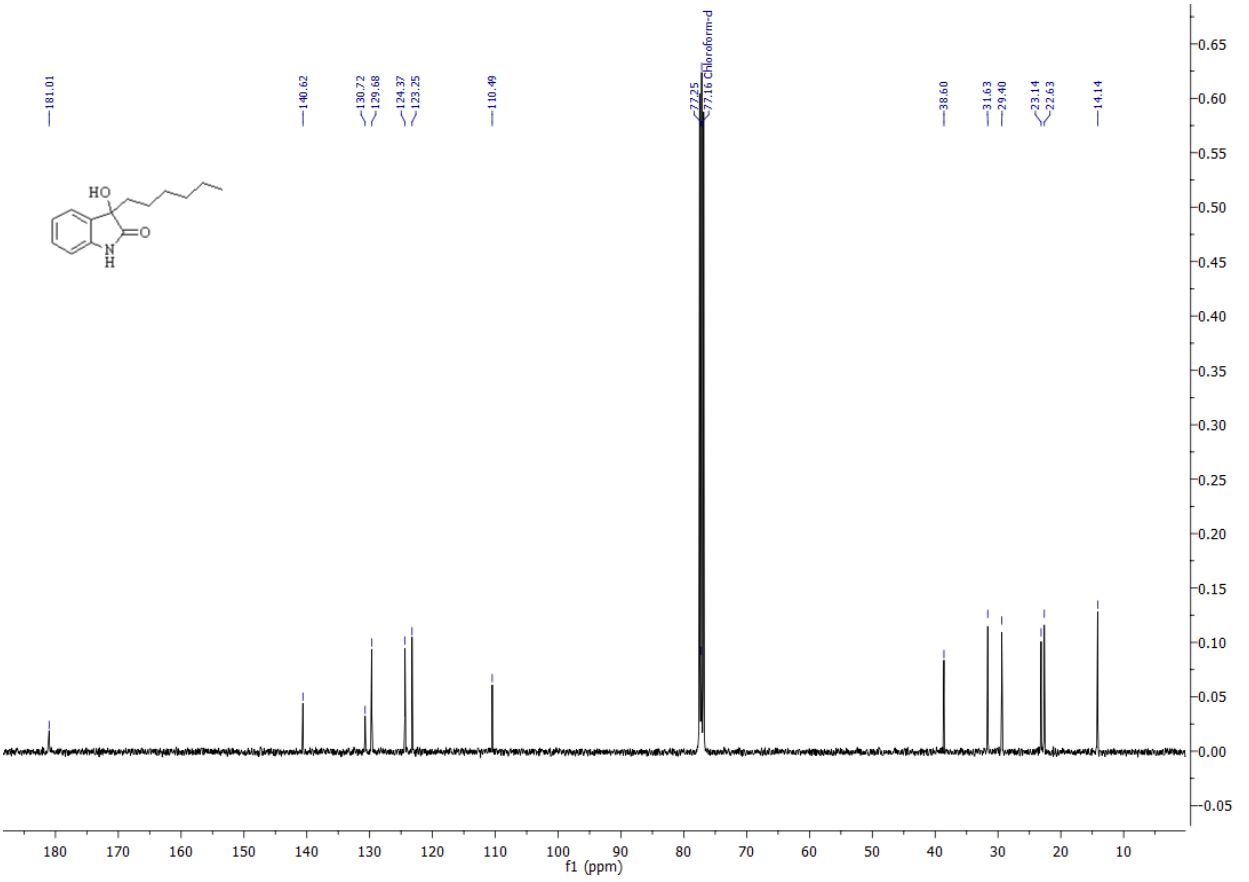

Figure 2A.26. ^{13}C NMR of compound **9g**

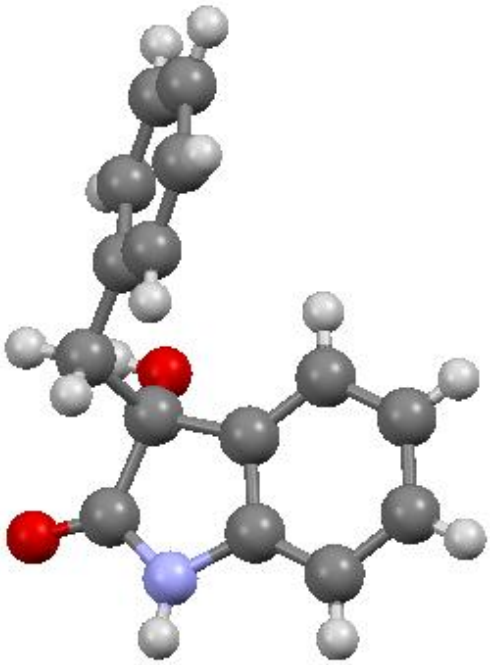

Figure 2A.27. Single crystal structure for compound **9a**

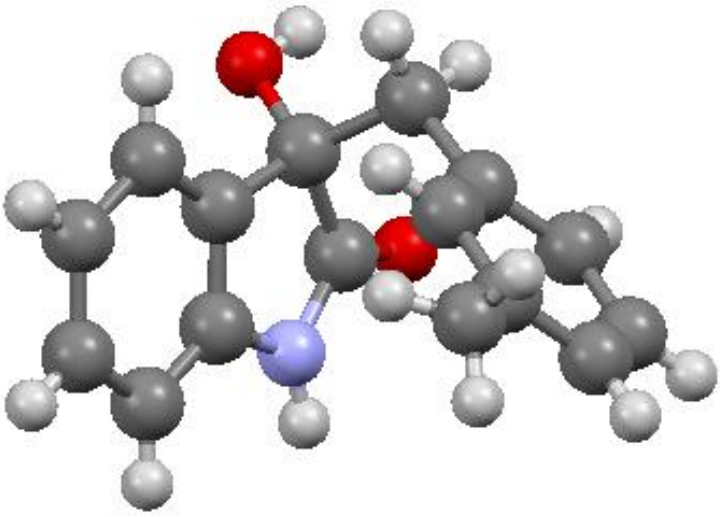

Figure 2A.28. Single crystal structure for compound **9c**

2A.9. References:

(1) Anastas, P. T.; Warner, J. C. 1998, *Green chemistry*: *theory and practice*

(2) Trost, B. M. *Science* **1991**, *254*, 1471.

(3) (a) Matsuo J-i.; Murakami, M. *Angew. Chem. Int. Ed*. **2013**, *52*, 9109. (b) Davies, S. G.; Goodwin, C. J.; Hepworth, D.; Roberts, P. M.; Thomson, J. E. *J. Org. Chem*., **2010**, *75*, 1214. (c) Kim, H.; Lee, D.; Kim S.; Kim, D. *J. Am. Chem. Soc*. **2007**, *129*, 2269. (d) Casiraghi, G.; Battistini, L.; Curti, C.; Rassu, G.; Zanardi, F. *Chem. Rev.* **2011**, *111*, 3076. (e) Palomo, C.; Oiarbide M.; Garcia, J. M. *Chem. Soc. Rev.* **2004**, *33*, 6. (f) Evans, D. A.; Downey, C. W.; Hubbs, J. L. *J. Am. Chem. Soc*. **2003**, *125*, 8706. (g) O'Donnell, C.; Zhou, W. L.; Scott, J. *J. Am. Chem. Soc.* **1996**, *118*, 6070.

(4) (a) Huang, F.; Liu, Z.; Yu, Z. *Angew. Chem. Int. Ed.* **2016**, *55*, 862. (b) Allen, C. L.; Williams, J. M. J. *Chem. Soc. Rev.* **2011**, *40*, 3405. (c) Pattabiraman, V. R.; Bode, J. W. *Nature* **2011**, *480*, 471.

(5) (a) Obora, Y. *ACS Catal.* **2014**, *4*, 3972. (b) Pan, S.; Shibata, T. *ACS Catal.* **2013**, *3*, 704. (b) Elangovan, E.; Sortais, J-B.; Beller, M.; Darcel, C. *Angew. Chem. Int. Ed*. **2015**, *54*, 14483.

(6) Kobayashi, S.; Kiyohara, H.; Yamaguchi, M. *J. Am. Chem. Soc.* **2011**, *133*.

(7) Zhang, K.; Peng, Q.; Hou, X-L.; Wu, Y-D. *Angew. Chem. Int. Ed*. **2008**, *47*, 1741.

(8) Gunanathan, C.; Milstein, D. *Science* **2013**, *341*, 1229712.

(9) Corma, A.; Navas, J.; Sabater, M. J. *Chem. Rev.* **2018**, *118*, 1410.

(10) Reed-Berendt, B. G.; Polidano, K.; Morrill, L. C. *Org. Biomol. Chem*. **2019**, *17*, 1595.

(11) Grigg, R.; Mitchell, T. R. B.; Sutthivaiyakit, S.; Tongpenyai, N. *J. Chem. Soc. Chem. Commun.* **1981**, 611.

(12) Watanabe, Y.; Tsuji, Y.; Ohsugi, Y. *Tetrahedron Lett*. **1981**, *22*, 2667.

(13) Watanabe, Y.; Tsuji, Y.; Ige, H.; Ohsugi, Y.; Ohta, T. *J. Org. Chem*. **1984**, *49*, 3359.

(14) Murahashi, S.; Rondo, R.; Hakata, T. *Tetrahedron Lett*. **1982**, *23*, 229.

(15) Hamid, M. H. S. A.; Allen, C. L.; Lamb, G. W.; Maxwell, A. C.; Maytum, H. C.; Watson, A. J. A.; Williams, J. M. J. *J. Am. Chem. Soc.* 2009, *131*, 1766.

(16) Gnanaprakasam, B.; Zhang, J.; Milstein, D. *Angew. Chem. Int. Ed.* **2010**, *49*, 1468.

(17) Zhang, J.; Leitus, G.; Ben-David, Y.; Milstein, D. *J. Am. Chem. Soc.* **2005**, 127, 10840.

(18) Sølvhøj, A.; Madson, R. *Organometallics* **2011**, *30*, 6044

(19) Gunanathan, C.; Ben-David, Y.; Milstien, D. *Science* **2007**, *317*, 790.

(20) Kuwahara, T.; Fukuyama, T.; Ryu, I. *Org. Lett*. **2012**, *14*, 4703.

(21) Guo, L.; Liu, Y.; Yao, W.; Leng, X.; Huang, Z. *Org. Lett.* **2013**, *15*, 1144.
(22) Kuwahara, T.; Fukuyama, T.; Ryu, I. *RSC Adv.* **2013**, *3*, 13702.
(23) (a) Jensen, T.; Madsen, R. *J. Org. Chem.* **2009,** *74*, 3990. (b) Jin, H.; Xie, J.; Pan, C.; Zhu, Z.; Cheng, Y.; Zhu, C. *ACS Catal.* **2013**, *3*, 2195. (c) Chaudhari, C.; Siddiki, S. M. A. H.; Kon, K.; Tomita, A.; Tai, Y.; Shimizu, K-I. *Catal. Sci. Technol.* **2014**, *4*, 1064. (d) Putra, A. E.; Oe, Y.; Ohta, T. *Eur. J. Org. Chem.* **2015**, 7799.
(24) Challis, B. C. and Challis, J. In the *Chemistry of Amides*; J. Zabicky, Ed.; John Wiley & Sons: London, **1970**; pp 73.
(25) (a) Peddibhotla, S. *Curr. Bioact. Compd.* **2009**, *5*, 20. (b) Lin, S.; Kwok, B. H. B.; Koldobskiy, M.; Crews, C. M.; Danishefsky, S. J. *J. Am. Chem. Soc.* **2004**, *126*, 6347. (c) Albrecht, B. K.; Williams, R. M. *Proc. Natl. Acad. Sci.* **2004**, *101*, 11949.
(26) (a) Tsang, A. S-K.; Kapat, A.; Schoenebeck, F. *J. Am. Chem. Soc.* **2016**, *138*, 518. (b) Zhang, Q-B.; Jia, W-L.; Ban, Y-L.; Zheng, Y.; Liu, Q.; Wu, L-Z. *Chem. Eur. J.* **2016**, *22*, 2595. (c) Liang, Y-F.; Jiao, N. *Angew. Chem. Int. Ed.* ***2014***, *53*, 548.
(27) (a) Hu, J.; Lan, T.; Sun, Y.; Chen, H.; Yao, J.; Rao, Y. *Chem Commun*. **2015**, *51*,14929. (b) Kohl, S. W.; Weiner, L.; Schwartsburd, L.; Konstantinovski, L.; Shimon, L. J. W.; Ben-David, Y.; Iron, M. A.; Milstein, D. *Science* **2009**, *324*, 74. (c) Balaraman, E.; Khaskin, E.; Leitus, G.; Milstein, D. *Nat. Chem.* **2013**, *5*, 122. (d) Bandini, M. *Org. Biomol. Chem.* **2013**, *11*, 5206.
(28) Chouhan, M.; Sharma, R.; Nair, V.A. *Appl. Organometal. Chem.* **2011**, *25*, 470.

The content of the Chapter 2A is reproduced from Ref. "*Org. Biomol. Chem*. **2016**,*14*, 9215" with permission from the Royal Society of Chemistry.

Chapter 2

Section B

C-H Hydroxylation of Carbonyl Compounds

2B. C-H Hydroxylation of Carbonyl Compounds

2B.1. Abstract

The coherent strategy for the hydroxylation of C-(sp^3)-H bond has been developed using a readily available base such as KO-*t*-Bu, as an inexpensive, commercially available, and bench stable reactant. The present finding uses air (O_2), which acts as an oxidant and can be accessible at virtually no cost and the most environmentally friendly reagent. This unified strategy is very facile for hydroxylation of various carbonyl compound derivatives to obtain quaternary hydroxyl compounds in an excellent yield at room temperature. A preliminary mechanistic investigation, supported by isotope labeling and computational studies, suggests the formation of a peroxide bond and its cleavage by *in situ* generated enolate.

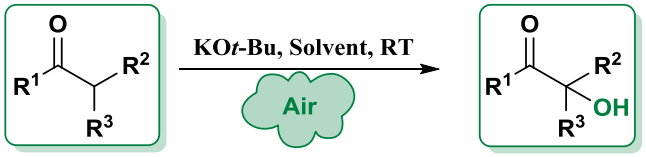

2B.2. Introduction and literature background on C-H hydroxylation

Gases like nitrogen and oxygen are the main constitutes in the atmospheric air on planet earth. The consumption of molecular oxygen as an oxidant accessible from air and utilization of such an oxygen atom source for oxygen incorporation (oxygenase activity) in organic synthesis has fascinated substantial attention. Oxygen is abundant and environmentally benign, which makes it an attractive reagent for plentiful chemical reactions. The oxidation reaction is a fundamentally important transformation in organic synthesis by which hydrocarbons are converted into valuable oxygenated products as feedstock for chemical and pharmaceutical industry.[1] Of which, α C-H hydroxylation of α-substituted carbonyl compounds to get quaternary α-hydroxyl carbonyl compounds perceives more attention in synthetic community, since such a quaternary α-hydroxyl functionality is central motif in all facets of chemistry ranging from several natural products (Figure 2B.1.) to synthetic drugs such as tephrosin[2], doxycycline[3], bicalutamide[4], aryloxindole,[5] and donaxaridine.[6] Furthermore, this type of quaternary α-hydroxyl carbonyl compounds serves as efficient photo-initiator in the coating industry.[7,8] Similarly the hydroxyl derivatives of barbituric acid are responsible for improving the durability of a polarizing plate.[9] While significant progress has been documented for the oxidation of the C-H bond by catalytic/non-catalytic approaches in the presence of various oxidant sources, there is

an increasing demand for more environmentally benign approaches avoiding the use of expensive metal catalysts, hazardous stoichiometric oxidants, and reductants.

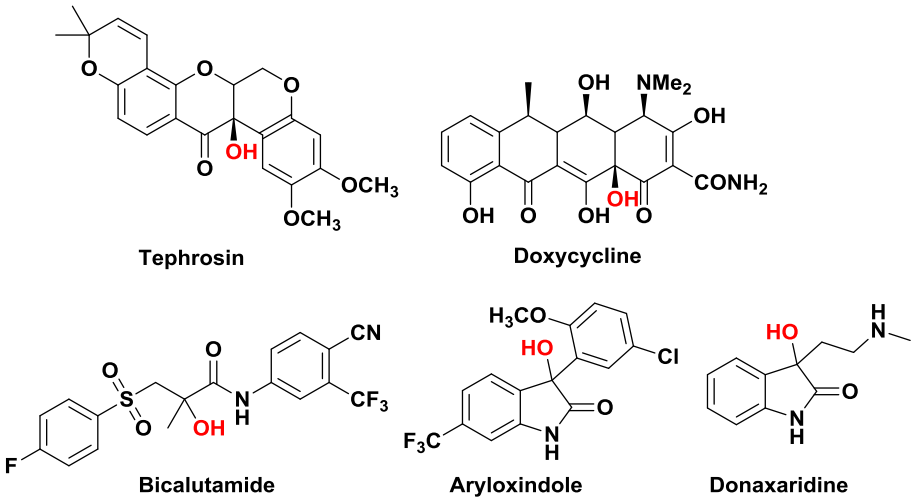

Figure 2B.1. Quaternary hydroxyl functionalized biologically active molecules

Recently, the direct hydroxylation of C(sp^3)-H bond can be achieved using a stoichiometric amount of oxidants.[10] The consumption of molecular oxygen as an oxidant accessible from air and utilization for oxygen incorporation in organic synthesis has attracted substantial attention.[11,12]

In 2002, Qaseer and co-workers reported the pioneering work on C-H hydroxylation of ketones using oxygen and bimetallic palladium. The conditions also require the use of hexahydropyrimidopyrimidine (hppH) at 0-6 ^{o}C (Figure 2B.2.).[13] The established protocol is only applicable for selected cyclic and acyclic ketone derivatives.

Later, in 2011, Ritter and co-workers reported the chemo and regioselective C-H hydroxylation of a variety of tetralone and other carbonyl compounds using molecular oxygen and dinuclear palladium catalyst at 0-6 ^{o}C. The use of hppH is necessary for the reaction to occur (Figure 2B.2.).[14]

In 2014, the Jiao group reported a transition-metal-free protocol for C-H hydroxylation of carbonyl derivatives. They have employed a catalytic amount of Cs_2CO_3, molecular oxygen, and a stoichiometric amount of phosphine as a reductant at room temperature. Although, the reported reaction conditions are mild, but the reaction requires a stoichiometric amount of phosphine as reductant (Figure 2B.2.).[15]

Notably, in 2015, Zhao and co-workers demonstrated an enantioselective version of C-H hydroxylation of carbonyl compounds using phase transfer catalyst,

aqueous NaOH, molecular oxygen along with phosphine as a reductant (Figure 2B.2.).[16]

Later, in 2016, Schoenebeck and co-workers reported CuO catalyzed C-H hydroxylation of carbonyls such as tetralone, derivatives of 2-oxindole, and cyclohexanone using hppH as base and phosphine as a reductant. In this protocol, they have also demonstrated the factors responsible for C-C bond cleavage (Figure 2B.2.).[17]

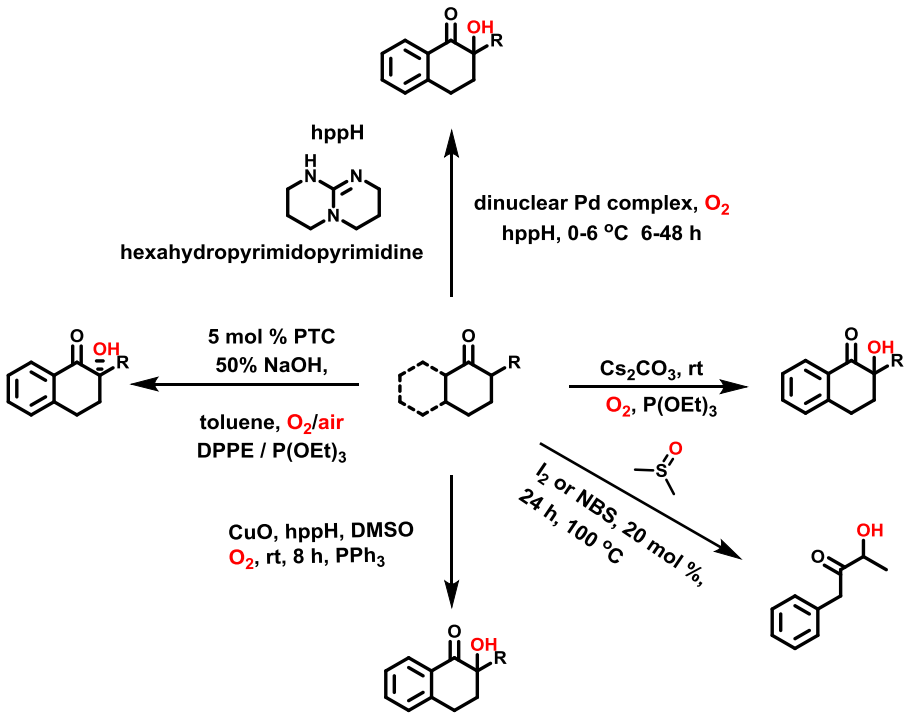

Figure 2B.2. State-of-the-art on C-H hydroxylation of ketones (tetralones)

Likewise, the enantioselective C-H hydroxylation of substituted 2-oxindole derivatives using $Zn(OAC)_2$, DBFOX (Dibenzofuran-4,6-bis(oxazoline) as a chiral ligand and oxaziridine as an oxidant is reported by Kanemasa and co-workers (Figure 2B.3.).[18]

In 2008, Itoh and coworkers reported PTC (cinchona alkaloid) catalyzed enantioselective C-H hydroxylation by employing molecular O_2 and alkaline solution of KOH at cryogenic conditions (Figure 2B.3).[19]

In 2012, Tan and co-workers reported PTC (pentadinium) catalyzed C-H hydroxylation of 2-oxindole derivatives. This reaction needed longer reaction time and cryogenic conditions (Figure 2B.3).[10g]

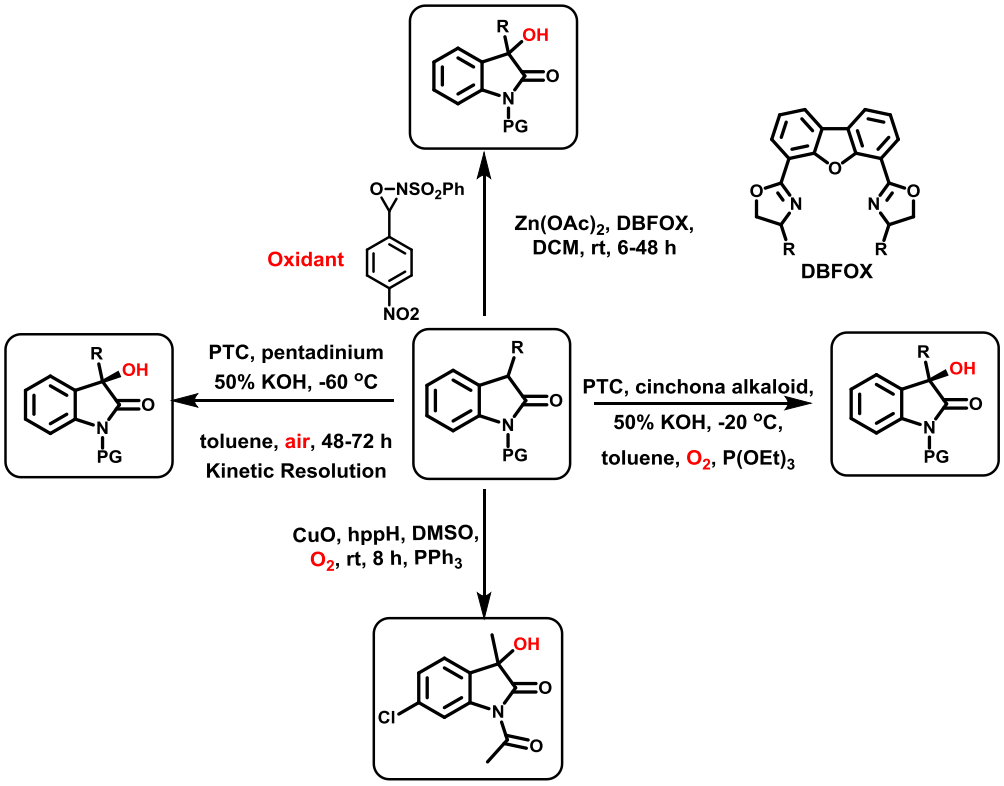

Figure 2B.3. State-of-the-art on C-H hydroxylation of C3-substituted-2-oxindole

2B.3. The rationale of present work

There are several reports available for the synthesis of quaternary α-hydroxy carbonyl compounds, but they also have few limitations. Some of them are the use of metal catalysts along with a special base, the use of oxidants such oxaziridine, cumene hydroperoxide (CHP), phenyliodine(III) diacetate (PIDA), *tert*-butyl hydroperoxide, oxone, and H_2O_2 are not safe to practice. Additionally, the use of phosphine based reductant such triphenylphosphine (PPh_3), (1,2-Bis(diphenylphosphino)ethane) DPPE, or triethyl phosphite ($P(OEt)_3$) or a special base such as hppH is necessary for all the previous reports (selected examples shown in figure 2B.4, 2B.5).

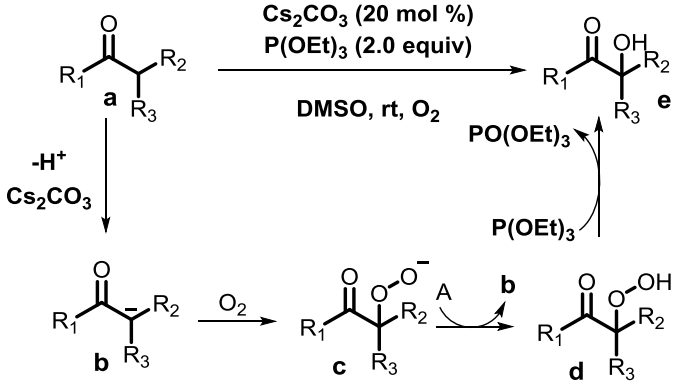

Figure 2B.4. Jiao's mechanism for transition-metal-free C-H hydroxylation

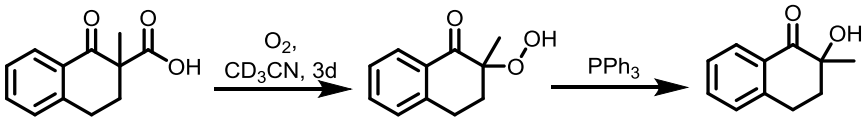

Figure 2B.5. Schoenebeck's mechanism for transition-metal-free C-H hydroxylation

By considering the above limitations, there is a demand to develop a variant protocol which enables the C-H hydroxylation with easy operation for the synthesis of quaternary α-hydroxyl carbonyl compounds and avoids the use of an expensive metal catalyst, special bases, hazardous phosphine based additives, longer reaction time, cryogenic conditions and protecting groups. Therefore, we have planned to use environmentally benign oxidants such as oxygen (air) and develop a strategy for the C-H hydroxylation reaction.

2B.4. Results and discussion

We have developed a KO-*t*-Bu, as a base, mediated aerobic C-H hydroxylation of various carbonyl compounds under simple reaction conditions without using any additives and reductants. The present finding comprises of following notable results: i) air as a source of hydroxyl functionality, which makes this protocol environmentally benign; ii) readily available, inexpensive base KO-*t*-Bu rather than expensive metal catalyst; iii) avoids the use of stoichiometry amount of hazardous phosphine compounds as an additive and reductant.

2B.4.1. Optimization studies

We commenced our reaction studies using cyclic ketone **12a.** A control experiment was performed by stirring ketone **12a** in DMSO under air at room temperature for 24 h, which showed no reaction (Table 2B.1, entry 1). To identify an optimal reaction condition for metal-free base mediated aerobic C-H hydroxylation, the various concentration of KO-*t*-Bu (10, 30 and 50 mol%) was added to the solution of **12a** in DMSO and allowed to stir at room temperature under air for 24 h. These results indicated that a gradual increase of the amount of KO-*t*-Bu considerably increased the formation of the product **13a**, led to 31, 45, 56% yield, respectively (Table 2B.1, entries 2, 3, 4). This reaction was also monitored at a different course of time (8-24 h) and showed the disappearance of the starting material in 24 h. To our delight, the addition of a stoichiometric amount of KO-*t*-Bu afforded desired product **13a** in excellent yield (90%) (Table 2B.1, entry 5). Similarly, the solvent effect on the C-H hydroxylation of compound **12a** was studied. The higher yield was observed when the C-H hydroxylation reaction was performed in DMSO. Other solvents such as

toluene, THF and 1,4-dioxane were ineffective in producing the product **13a** in higher yield (Table 2B.1, entries 6, 7, 8). Further, this reaction did not proceed to form the product **13a** under the argon atmosphere, which ruled out the DMSO acting as an oxidant source (Table 2B.1, entry 9). Additionally, we performed C-H hydroxylation using Cs_2CO_3 (Table 2B.1, entry 10 and 11), as developed by Jiao and co-workers[9], without the addition of any phosphine reductant, showed only trace amount of C-H hydroxylated product (Table 2B.1, entry 10, 11).

Table. 2B.1 Optimization of reaction conditions for ketones

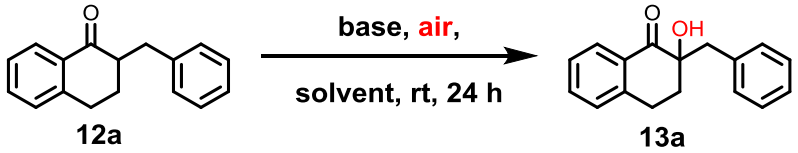

Entry	Base	Solvent	Yield of 13a
1	-	DMSO	no reaction
2	KO-*t*-Bu (0.1 equiv)	DMSO	31
3	KO-*t*-Bu (0.3 equiv)	DMSO	45
4	KO-*t*-Bu (0.5 equiv)	DMSO	56
5	**KO-*t*-Bu**	**DMSO**	**90**
6	KO-*t*-Bu	toluene	40
7	KO-*t*-Bu	THF	52
8	KO-*t*-Bu	1,4-dioxane	56
9[b]	KO-*t*-Bu	DMSO	no reaction
10	Cs_2CO_3 (0.1 equiv)	DMSO	Traces
11	Cs_2CO_3 (1 equiv)	DMSO	Traces
12	NaO-*t*-Bu	DMSO	67
13	LiO-*t*-Bu	DMSO	88

[a] **Reaction condition**: Base (0.25 mmol), ketone (0.25 mmol), solvent (1 mL); reaction mixture was stirred at room temperature for 24 h in air atmosphere. [b] The reaction was carried out under argon atmosphere.

These observations proved that changing the base from Cs_2CO_3 to KO-*t*-Bu allows the reaction to occur without the need for phosphine reductant. Other strong bases such as NaO-*t*-Bu and LiO-*t*-Bu also afforded the product **13a** in 67 and 88% yield, respectively (Table 2B.1, entries 12,13) suggesting an important role of the strength of the base.

2B.4.2. The substrate scope of ketone derivatives

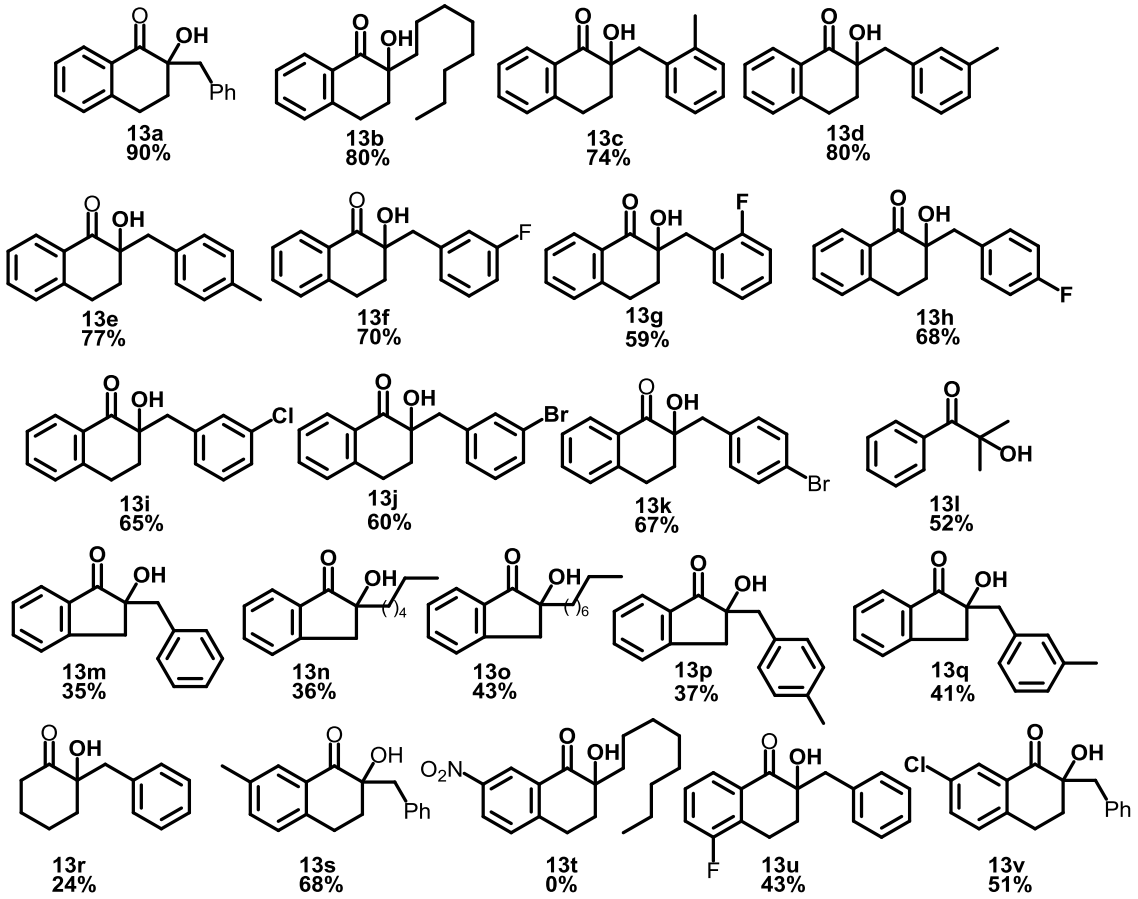

Figure 2B.6. Substrate scope for ketones

Using the optimized condition, the scope of the reaction was investigated with a variety of substrates. Thus, the reaction of 2-benzyl-3,4-dihydronaphthalen-1(2*H*)-one with optimized conditions gave **13a** (2-benzyl-2-hydroxy-3,4-dihydronaphthalen-1(2*H*)-one) in 90% yield. The reaction product was characterized by spectroscopic techniques and X-ray analysis. In the case of 2-octyl-3,4-dihydronaphthalen-1(2*H*)-one, this reaction proceeded smoothly to afford the product **13b** in 80% yield (Figure 2B.6.). Electron donating or electron-withdrawing group substitutions on the phenyl ring decreased the yield of the products. This aerobic α-hydroxylation reaction with 2-(2 or 3 or 4-methylbenzyl)-3,4-dihydronaphthalen-1(2*H*)-one furnished the corresponding products **13c-e** in 74, 80, 77% yield, respectively (Figure 2B.6.). This reaction condition was also compatible with the halogenated substrate, especially with fluorine substituent, and provided a moderate yield of **13f-k** (Figure 2B.6.). Encouraged by the results obtained with cyclic ketones, we subjected the same reaction condition to acyclic ketone **13l,** which serves as an ultraviolet (UV) curing agent,[7-9] gave a moderate yield of 52%. This α-hydroxylation reaction was also

generalized with various α-substituted 1-indanone to give the quaternary hydroxyl functionalized products **13m-q** (Figure 2B.6.). In the case of benzyl cyclohexanone (tertiary non-aromatic ketone), a 24% isolated yield of **13r** was observed. The reaction worked well with electron-donating as well as electron-withdrawing tetralone skeleton, which afforded a moderate yield of **13s, 13u,** and **13v**. Unfortunately, no desired product was observed with 2-benzyl-7-nitro-3,4-dihydronaphthalen-1(2*H*)-one (Figure. 2B., entry **13t)**.

2B.4.3. The substrate scope of amides derivatives

Table. 2B.1 Optimization of reaction conditions for amides

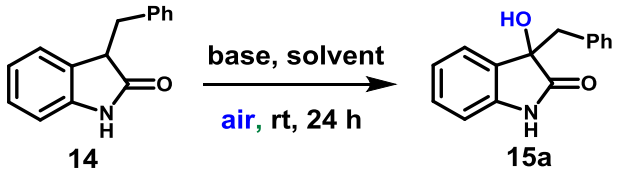

Entry	Base	Solvent	Yield of 15a
1	-	toluene	no reaction
2	KO-*t*-Bu (0.1 equiv)	toluene	31
3	KO-*t*-Bu (0.3 equiv)	toluene	53
4	KO-*t*-Bu (0.5 equiv)	toluene	77
5	KO-*t*-Bu	toluene	93
6	KO-*t*-Bu	DMSO	40
7	*Na*H	toluene	67
8	Cs_2CO_3	toluene	52
9[b]	KO-*t*-Bu	toluene	no reaction
10	NaO-*t*-Bu	toluene	81
11	LiO-*t*-Bu	toluene	88

[a] **Reaction condition:** Base (0.25 mmol), C3-substituted-2-oxindole (0.25 mmol), and solvent (1 mL) were stirred at room temperature for 24 h under open-air condition. [b] Reaction was carried out under the argon atmosphere.

Prompted by the results obtained with ketones, the scope of this methodology was further extended with C3-substituted-2-oxindole derivatives to obtain the C-H hydroxylated products. In search of the transition-metal-free C-H hydroxylation of α-substituted 2-oxindole, C3-benzyl-2-oxindole was chosen as the model substrate and set of the experiment was performed to optimize the reaction conditions to get the corresponding C3-hydroxylated 2-oxindole in higher yield (Table 2B.2). This optimization study reveals that C3-hydroxylation of **14** (3-benzylindolin-2-one) under air in the presence of a stoichiometric amount of KO-*t*-Bu in toluene furnished **15a** (3-

benzyl-3-hydroxyindolin-2-one) in 93% isolated yield. To our delight, this reaction gave a fruitful result on a gram scale (5 mmol) to afford the product **15a** in 1.02 g (85%). Similarly, this hydroxylation reaction was also examined with several C3-substituted 2-oxindoles. Excellent yields were obtained with 3-(3 or 4-methoxybenzyl)indolin-2-one, provided **15b** and **15c** in 90% and 89%, respectively (Figure 2B.7.). Further, compounds having substituent like 3-(2 or 3 or 4-methylbenzyl)indolin-2-one group furnished hydroxylated products in good to very good yields **15d-15f** (Figure 2B.7.). The biphenyl substituted 2-oxindole such as 3-([1,1'-biphenyl]-4-ylmethyl)indolin-2-one and 3-([1,1'-biphenyl]-4-ylmethyl)-1-benzylindolin-2-one produced hydroxylated product **15g** and **15p** in 91 and 98% yield, respectively (Figure 2B.7.).

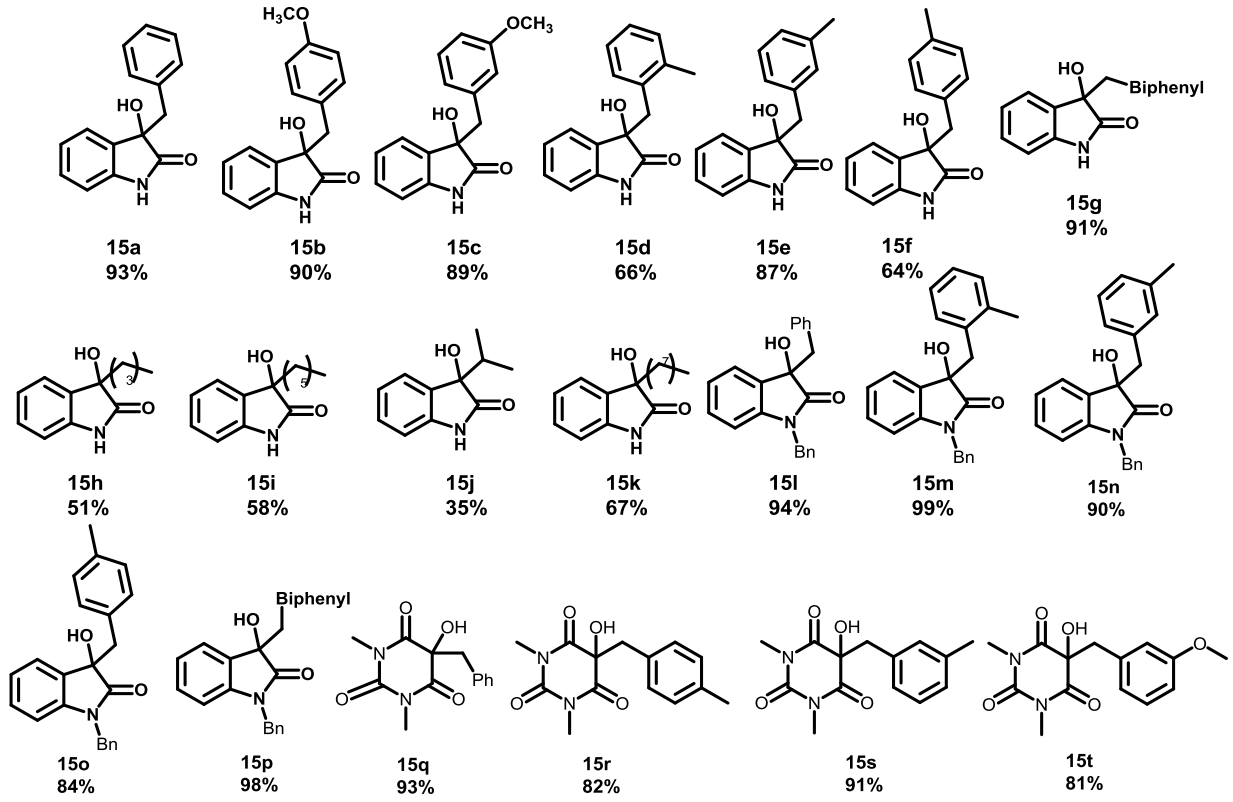

Figure 2B.7. Substrate scope for amide

Furthermore, the alkyl-substituted 2-oxindole was subjected to base mediated aerial oxidation, also provide the respective hydroxylated products **15h-k** in moderate yield (Figure 2B.7.). On the other hand, we explored the reactions of *N*-H protected 2-oxindoles, which proceeded smoothly and furnished product **15l-15o** in excellent yield (Figure 2B.7.). The obtained products were completely characterized by spectroscopic techniques. Further, this structure was supported with the help of the crystal structure of the product **15l**. Next, this C-H hydroxylation reaction was studied with several 1,3-

dimethyl barbituric acid derivatives. Thus, 5-benzyl-1,3-dimethylpyrimidine-2,4,6(1*H*,3*H*,5*H*)-trione was reacted with stoichiometric amount of KO-*t*-Bu under air for 24 h results in the formation of 5-benzyl-5-hydroxy-1,3-dimethylpyrimidine-2,4,6(1*H*,3*H*,5*H*)-trione **15q** in 93% yield (Figure 2B.7.). Other derivatives of barbituric acid were also successful for the C-H hydroxylation under this experimental condition to afford the respective hydroxylated products **15r, 15s,** and **15t** in good yields (Figure 2B.7.).

2B.5. Mechanistic investigations

2B.5.1. Isotope labeling and radical quenching experiments

To eliminate the possibility of trace metal involvement, we analyzed KO-*t*-Bu using MP-AES (Microwave Plasma-Atomic Emission Spectrometer) analysis and found acceptable quantities of such contaminants. We have performed an isotopic labeling experiment to check the source of oxygen incorporation. The GC-mass spectrum of the product **15a** (*m/z* = 239) is shifted two mass units higher to m/z = 241 (**15a'**) (91% ^{18}O labeled oxygen atom) when the reaction was carried out with $^{18}O_2$.

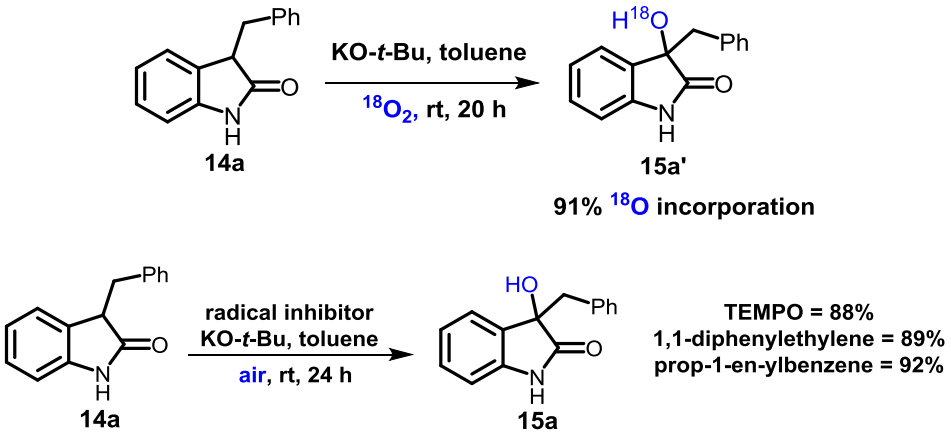

Scheme 2B.1. Experiments for the mechanistic studies

Reaction condition- C3-alkylated-2-oxindole (50 mg, 0.2242 mmol), 2,2,6,6-tetramethylpiperidine-1-oxyl (TEMPO) (1 equiv) or 1,1-diphenylethylene (1 equiv) or α-methyl styrene (1 equiv), KO-*t*-Bu (25 mg, 0.2242 mmol), toluene (1.0 mL) were added in a tube and the reaction mixture stirred under air at 25 ^{o}C for 24 h, afforded 88 or 89 or 92% isolated yield respectively after column chromatography.

These labeling studies indicate the incorporation of oxygen from the molecular oxygen. To check the involvement of a radical, the C-H hydroxylation reaction was performed under the addition of the radical quencher 2,2,6,6-tetramethylpiperidine-1-oxyl (TEMPO) or 1,1-diphenylethylene or prop-1-en-2-ylbenzene, but this did not

prevent the product formation **15a**. These results ruled out the involvement of free radical intermediates (Scheme 2B.1.).

2B.5.2. DFT calculations

To investigate the proposed reaction mechanism, computational studies were performed on a model reaction and the actual reaction giving the product **13a**. The transition state structure for the model compound (Figure 2B.8.a) shows a stretched peroxide bond (R_{O4-O5} = 1.68 Å) and the simultaneous formation of a C-O bond with the reductant (R_{C7-O5} = 2.41 Å). Furthermore a hydrogen bond between the hydrogen atom on the peroxide and the carbonyl oxygen on the reductant (R_{O9-H6} = 2.08 Å) stabilizes the transition state. The transition state for the ketone **12a** has a very similar structure (Figure 2B.8.). The calculated reaction barrier, relative stability of the product and key geometrical parameters for **13a** are shown in Figure 2B.8.

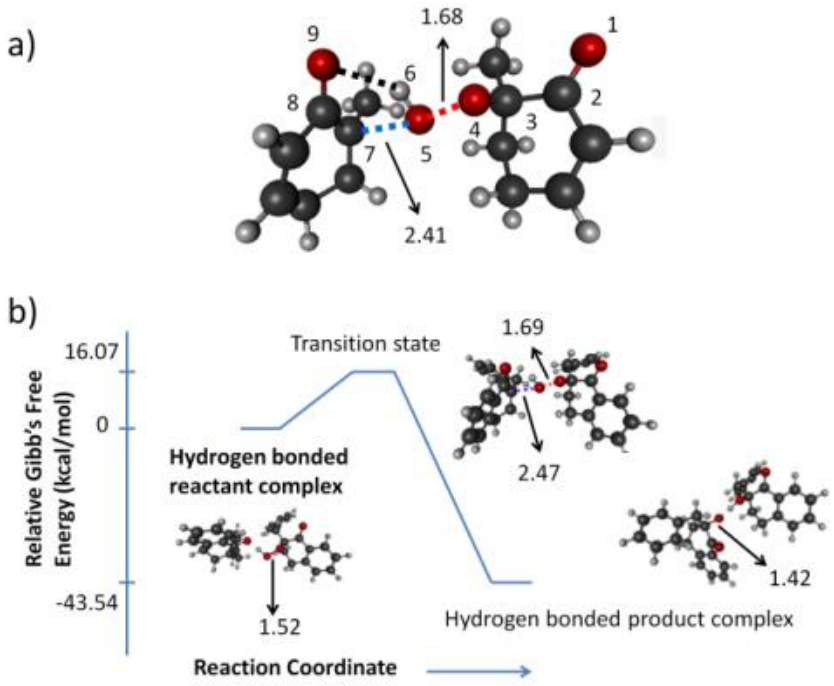

Figure 2B.8. a) Structure of the transition state for the model reaction and b) energy profile diagram for the reaction of ketone **12a**. The red, blue, and black dashed lines represent bonds being broken, bonds being formed and hydrogen bond interactions, respectively. The arrows indicate bond lengths in Å.

2B.6. The possible reaction mechanism

Based on our preliminary results, DFT computations, and previous studies,[10g] a plausible reaction mechanism involving base induced two-step hydroxylation has been

postulated (Figure 2B.9.). Initially, compound **A** undergoes base mediated deprotonation to give the enolate **B**. Next, the enolate **B** reacts with air (atmospheric O_2) to generate organic superoxide anion **C** that may abstract a proton from **A** to form **D** (confirmed by HRMS), which is subsequently cleaved by the *in situ* generated reductant enolate **B**, to give the expected product **E**.

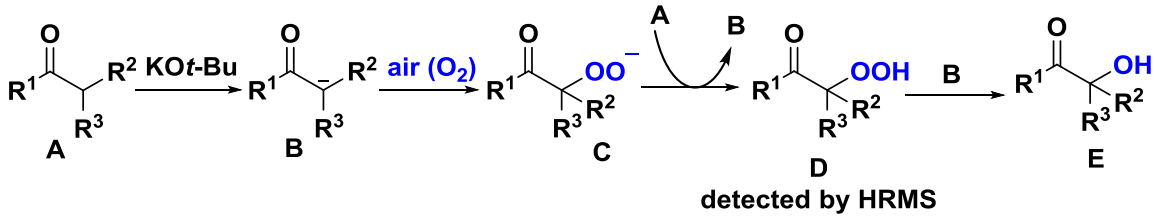

Figure 2B. 9. Our proposed reaction mechanism for C-H hydroxylation

It is believed that the enolate formed after deprotonation of **A** might be performing double duty to furnish the overall reaction. When Cs_2CO_3 was used as the base, a phosphine reductant is required for the reaction to occur.[9] The stronger bases used in our work appear to lead the formation of enolate in higher concentration, which allows it to be available as a reductant for the peroxide bond cleavage, avoiding the requirement of additional phosphine reductant.

2B.7. Conclusion

In conclusion, we have developed a mild and operationally simple transition-metal free protocol for C-H hydroxylation of various ketones and amides using inexpensive- base and environmentally benign atmospheric air as an oxidant. This methodology delivers a broad array of substrates and provides an alternate route for the synthesis of hydroxylated ketones and amides by avoiding the use of hazardous phosphine based reductant and an expensive metal catalyst. The DFT computations and isotope labeling studies support the mechanism.

2B.8. Experimental section and characterization data

2B.8.1. General information and data collection

All the solvents used for starting material synthesis were dry grade and stored over molecular sieves. The alcohols, 2-oxindole, KO-*t*-Bu reagent grade, ≥98% (156671 ALDRICH), and tetralone used for starting material synthesis and C-H hydroxylation were purchased from Sigma-Aldrich or Alfa-Aesar. Deuterated solvents were used as received. For C-H hydroxylation of carbonyl compounds, AR grade dry solvents were used. Column chromatographic separations performed over 100-200 Silica-gel. Visualization was accomplished with UV light and PMA, CAM stain

followed by heating. ^{1}H and ^{13}C NMR spectra were recorded on 400 and 100 MHz, respectively, using a Bruker 400 MHz or JEOL 400 MHz spectrometers. Abbreviations used in the NMR follow-up experiments: b, broad; s, singlet; d, doublet; t, triplet; q, quartet; m, multiplet. High-resolution mass spectra were obtained with Waters- synapt G2 using electrospray ionization (ESI). Fourier-transform infrared (FT-IR) spectra were obtained with a Bruker Alpha-E Fourier transform infrared spectrometer.

2B.8.2. Experimental procedure

A) General experimental procedure for C-H hydroxylation of ketone (Method A):

KO-*t*-Bu (28 mg, 0.25 mmol), DMSO (l mL) and ketone (0.25 mmol) were added to a 20 mL tube with a magnetic bar, and then the mixture was stirred at room temperature (25 ^{o}C) in an open-air for 24 h. The solution was then diluted with ethyl acetate (10 mL), washed with water (5 x 3), and brine (5 x 5 mL), dried over anhydrous Na_2SO_4, filtered and evaporated under vacuum. The crude reaction mixture was purified by column chromatography on silica gel. (EtOAc: n-hexane = 10:90). Note: After aqueous workup, most of the compounds do not require further purification using column chromatography.

B) General experimental procedure for C-H hydroxylation of amide:

KO-*t*-Bu (28mg, 0.25 mmol), toluene (l mL) and amide (0.25 mmol) were added to a 20 mL tube with a magnetic bar, and then the mixture was stirred at room temperature (25 ^{o}C) in an open-air for 24 h. The volatile solvent was removed using a vacuum, and the crude reaction mixture was directly purified by column chromatography on silica gel to afford the product **15** (EtOAc: n-hexane= 30:70).

C) Experimental procedure for C-H hydroxylation of amide (1 mmol scale):

3-Benzyl-3-hydroxyindolin-2-one (15a): The reaction of 3-benzylindolin-2-one (223 mg, 1 mmol), KO-*t*-Bu (112 mg, 1 mmol), in toluene (5 mL), at 25 ^{o}C, stirred under air for 24 h. After reaction completion, the volatile solvent was removed using a vacuum, and the crude reaction mixture was directly purified by column chromatography on silica gel with eluent (EtOAc: n-hexane= 30:70) afforded (212, mg 89%) of **15a** as a white solid. Spectroscopic data matches with the previously reported compound.

D) Experimental procedure for C-H hydroxylation of amide (gram-scale synthesis):

3-Benzyl-3-hydroxyindolin-2-one (15a): The reaction of 3-benzylindolin-2-one (1115 mg, 5 mmol), KO-*t*-Bu (560 mg, 5 mmol), in toluene (20 mL), at 25 ^{o}C, stirred under air for 24 h. After reaction completion, the volatile solvent was removed using a

vacuum, and the crude reaction mixture was directly purified by column chromatography on silica gel with eluent (EtOAc: n-hexane= 30:70) afforded (1020, mg 85%) of **15a** as a white solid. Spectroscopic data matches with the previously reported compound.

E) Experimental procedure for C-H hydroxylation of amide (Detection of intermediate peroxide):

The reaction of 3-benzylindolin-2-one (50 mg, 0.2242 mmol), KO-*t*-Bu (25 mg, 0.2242 mmol), in toluene (1 mL), at 25 ^{o}C, stirred under air, for 2 h. Then the reaction mixture was freeze using liquid nitrogen and allowed to attain room temperature followed by immediate injection in HRMS instrument. **HRMS:** 3-benzyl-3-hydroperoxyindolin-2-one (ESI) m/z calculated for $C_{15}H_{13}NO_3$ $(M+H)^+$: 256.0974, found: 256.0990.

2B.8.3. Isotope labeling experiment

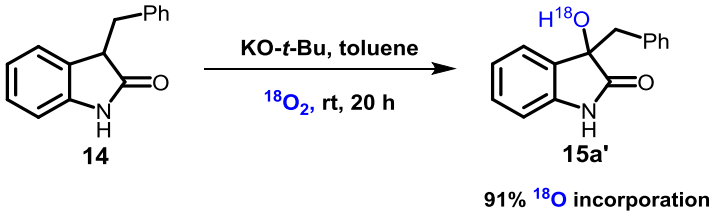

Scheme 2B.3. ^{18}O labeling experiment

Isotope labeling experiment carried out at the Department of Inorganic Chemistry, IACS, Kolkata, India. ^{18}O was purchased from Icon Services Inc., USA, with 98% isotopic purity. The experiment was carried out according to the standard reaction conditions of **14** to **15** under 1 atm of $^{18}O_2$. The percentage of ^{18}O enrichment was examined by mass spectrometry, as shown in Figure 2B.10. The calculated data showed 91% ^{18}O enrichment of **15a'**.

Reaction condition: C3-alkylated-2-oxindole (50 mg, 0.2242 mmol), KO-*t*-Bu (25 mg, 0.2242 mmol), toluene (1.0 mL) were added in a Schlenk tube inside the glove box. The reaction mixture stirred under $^{18}O_2$ (1 atm) at 25^{o}C, the reaction mixture was stirred for 20 h. The ^{18}O was determined in product **15a'** by GC-MS and HRMS. GC-MS data calculated for $C_{15}H_{13}N^{18}OO$ is 241, found 241. ESI-MS m/z calculated for $C_{15}H_{13}N^{18}OO$ $(M+Na)^+$ 264.0886, found **264.0706**. $C_{15}H_{13}N^{18}OO$ $(M+K)^+$ 280.0626, found **280.0499** (shown in Figure 2B.10.).

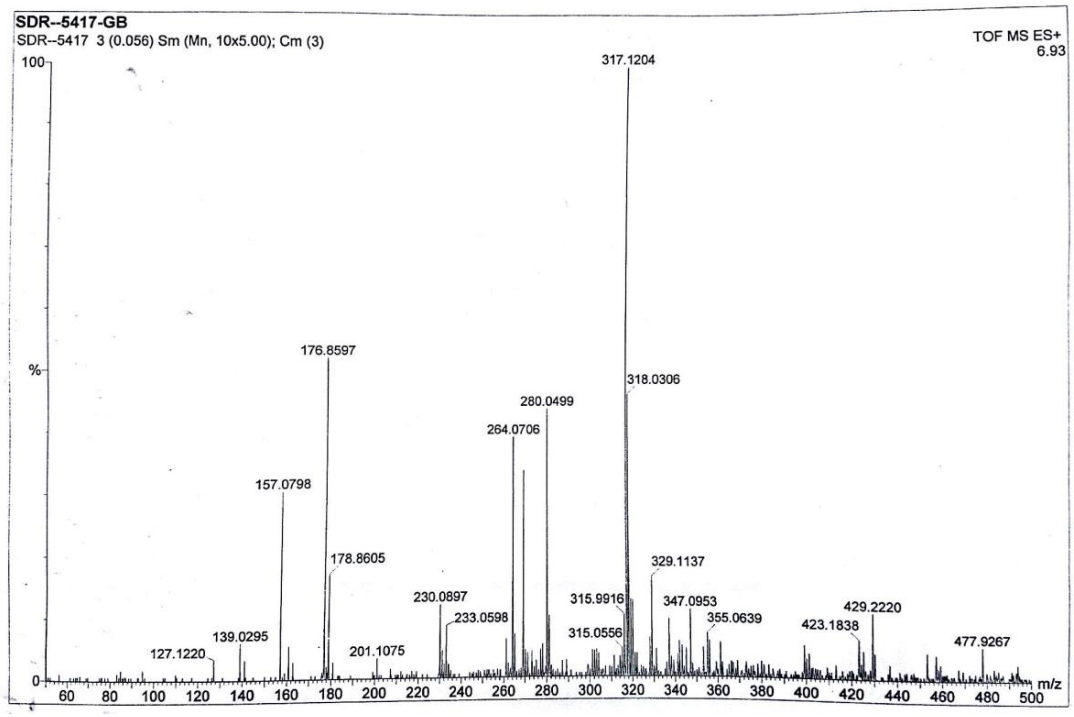

Figure 2B.10. HRMS data for ^{18}O labeled compounds

2B.8.4. Spectroscopic data for the product

2-Benzyl-2-hydroxy-3,4-dihydronaphthalen-1(2*H*)-one (13a): The reaction of 3,4-dihydronaphthalen-1(2*H*)-one (59 mg, 0.25 mmol), KO-*t*-Bu (28 mg, 0.25 mmol), in DMSO (1.0 mL), at 25 ^{o}C, under air, for 24 h, afforded (57 mg, 90%) of **13a** as a light yellow solid.

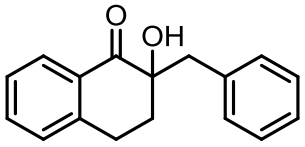

^{1}H NMR (400 MHz, $CDCl_3$) δ 8.02 (dd, *J* = 7.8, 1.2 Hz, 1H), 7.57 (dt, *J* = 7.5, 1.4 Hz, 1H), 7.38 (t, *J* = 7.5, 1H), 7.32-7.27 (m, 4H), 7.16-7.14 (m, 2H), 3.77 (bs, 1H), 3.31-3.22 (m, 1H), 3.07-3.03 (m, 1H), 3.0 (d, *J* = 13.8 Hz, 1H), 2.93 (d, *J* = 13.8 Hz, 1H), 2.30-2.25 (m, 1H), 2.19 (m, 1H). **^{13}C NMR** (100 MHz, $CDCl_3$) δ 201.04, 143.34, 135.48, 134.28, 130.55, 130.51, 129.26, 128.25, 128.16, 127.22, 127.02, 76.20, 42.10, 33.98, 26.53. **FTIR** (neat): 3488, 2926, 1684, 1289 cm^{-1}. **HRMS** (ESI) m/z calculated for $C_{17}H_{16}O_2$ $(M+Na)^+$: 275.1048, found: 275.1046.

2-Hydroxy-2-octyl-3,4-dihydronaphthalen-1(2*H*)-one (13b): The reaction of 2-octyl-3,4-dihydronaphthalen-1(2*H*)-one (64.5 mg, 0.25 mmol), KO-*t*-Bu (28 mg, 0.25 mmol), in DMSO (1.0 mL), at 25 ^{o}C, under air, for 24 h, afforded (55 mg, 80% yield without performing column chromatography, purity confirmed by NMR) **13b** as a yellow liquid.

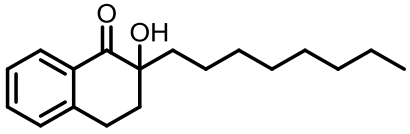

^{1}H NMR (400 MHz, $CDCl_3$) δ 8.01 (dd, *J* = 7.8, 1.2 Hz, 1H), 7.51 (dt, *J* = 7.5, 1.4 Hz, 1H), 7.34 (t, *J* = 7.5 Hz, 1H), 7.18-7.12 (m, 1H), 3.83 (bs, 1H), 3.14- 2.95 (m, 2H), 2.34 (m, 1H), 2.19-2.11 (m, 1H), 1.71-1.65 (m, 1H), 1.57-1.53 (m, 1H), 1.25-1.22 (m, 12H), 0.85 (t, *J* = 6.9 Hz, 3H). **^{13}C NMR** (100 MHz, $CDCl_3$,) δ 202.19, 143.59, 134.09, 130.40, 129.13, 128.06, 127.01, 75.90, 35.66, 34.01, 31.95, 29.96, 29.59, 29.33, 26.70, 23.03, 22.77, 14.23. **FTIR** (neat):

3498, 2926, 1687, 1226 cm^{-1}. **HRMS** (ESI) m/z calculated for $C_{18}H_{26}O_2$ $(M+Na)^+$: 297.1830, found: 297.1830.

2-Hydroxy-2-(2-methylbenzyl)-3,4-dihydronaphthalen-1(2*H*)-one (13c): The reaction of 2-(2-methylbenzyl)-3,4-dihydronaphthalen-1(2*H*)-one (62.5 mg, 0.25 mmol), KO-*t*-Bu (28 mg, 0.25 mmol), in DMSO (1.0 mL), at 25 ^oC, under air, for 24 h, afforded (49.5 mg, 74%) of **13c** as a yellow semisolid. **^{1}H NMR** (400 MHz, $CDCl_3$) δ 8.03 (dd, *J* = 7.8, 1.5 Hz, 1H), 7.57 (dt, *J* = 7.5, 1.5 Hz, 1H), 7.38 (t, *J* = 7.5 Hz, 1H), 7.32 (d, *J* = 7.8 Hz, 1H), 7.14-7.05 (m, 3H), 6.96 (d, *J* = 7.1 Hz, 1H), 3.70 (bs, 1H), 3.36-3.27 (m, 1H), 3.12 (d, *J* = 13.9 Hz, 1H), 3.10-3.06 (m, 1H), 3.01 (d, *J* = 13.9 Hz, 1H), 2.44 (m, 1H), 2.29 (m, 1H), 2.19 (s, 3H).**^{13}C NMR** (100 MHz, $CDCl_3$) δ 200.77, 143.22, 137.97, 134.22, 133.58, 131.17, 130.65, 130.59, 129.26, 128.22, 127.27, 127.06, 125.53, 76.69, 38.57, 35.44, 26.60, 20.29. **FTIR** (neat): 3490, 2926, 1685, 1287 cm^{-1}. **HRMS** (ESI) m/z calculated for $C_{18}H_{18}O_2$ $(M+Na)^+$: 289.1204, found: 289.1204

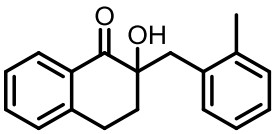

2-Hydroxy-2-(3-methylbenzyl)-3,4-dihydronaphthalen-1(2*H*)-one (13d): The reaction of 2-(3-methylbenzyl)-3,4-dihydronaphthalen-1(2*H*)-one (62.5 mg, 0.25 mmol), KO-*t*-Bu (28 mg, 0.25 mmol), in DMSO (1.0 mL), at 25 ^oC, under air, for 24 h, afforded (53 mg, 80%) of **13d** as a yellow liquid. **^{1}H NMR** (400 MHz, $CDCl_3$) δ 8.03 (dd, *J* = 8.2 Hz, 1H), 7.57 (dt, *J* = 8.2 Hz, 1H), 7.39 (t, *J* = 7.4 Hz, 1H), 7.31 (d, *J* = 7.8 Hz, 1H), 7.19-7.12 (m, 1H), 7.06 (d, *J* = 7.8 Hz, 1H), 6.98 (m, 1H), 6.93, (d, *J* = 7.3 Hz, 1H), 3.78 (bs, 1H), 3.31-3.22 (m, 1H), 3.08-3.01 (m, 1H), 2.96 (d, *J* = 13.7 Hz, 1H), 2.88 (d, *J* = 13.7 Hz, 1H), 2.32 (s, 3H), 2.30-2.26 (m, 1H), 2.19 (m, 1H). **^{13}C NMR** (100 MHz, $CDCl_3$) δ 201.09, 143.34, 137.77, 135.34, 134.25, 131.36, 130.57, 129.25, 128.11, 127.78, 127.44, 127.19, 125.78, 76.2, 41.98, 33.92, 26.52, 21.56. **FTIR** (neat): 3485, 2925, 1684, 1288, 1226 cm^{-1}. **HRMS** (ESI) m/z calculated for $C_{18}H_{18}O_2$ $(M+Na)^+$: 289.1204, found: 289.1211.

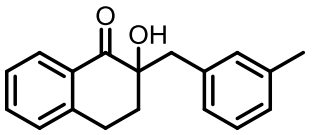

2-Hydroxy-2-(4-methylbenzyl)-3,4-dihydronaphthalen-1(2*H*)-one (13e): The reaction of 2-(4-methylbenzyl)-3,4-dihydronaphthalen-1(2*H*)-one (62.5 mg, 0.25 mmol), KO-*t*-Bu (28 mg, 0.25 mmol), in DMSO (1.0 mL), at 25 ^oC, under air, for 24 h, afforded (51 mg, 77%) of **13e** as a yellow solid. **^{1}H NMR** (400 MHz, $CDCl_3$) δ 8.02 (d, *J* = 8 Hz, 1H), 7.57 (m, 1H), 7.38 (t, *J* = 7.5 Hz, 1H), 7.30 (d, *J* = 7.7 Hz, 1H), 7.08 (d, *J* = 8.0 Hz, 2H), 7.03 (d, *J* = 8.0 Hz, 2H), 3.75 (bs, 1H), 3.31-3.22 (m, 1H), 3.07-3.00 (m, 1H), 2.96 (d, *J* = 13.8 Hz, 1H), 2.89 (d, *J* = 13.9 Hz, 1H), 2.32 (s, 3H), 2.27-2.15 (m, 2H). **^{13}C NMR** (100 MHz, $CDCl_3$) δ 201.13, 143.34, 136.57, 134.25, 132.26, 130.56, 130.35, 129.25, 128.98, 128.12, 127.19, 76.23, 41.65, 33.97, 26.53, 21.23. **FTIR** (neat): 3492, 2924, 1685, 1289 cm^{-1}. **HRMS** (ESI) m/z calculated for $C_{18}H_{18}O_2$ $(M+Na)^+$: 289.1204, found: 289.1210.

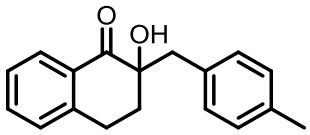

2-(3-Fluorobenzyl)-2-hydroxy-3,4-dihydronaphthalen-1(2*H*)-one (13f): The reaction of 2-(3-fluorobenzyl)-3,4-dihydronaphthalen-1(2*H*)-one (63.5 mg, 0.25 mmol), KO-*t*-Bu (28 mg, 0.25 mmol), in DMSO (1.0 mL), at 25 ^{o}C, under air, for 24 h, afforded (47.5 mg, 70%) of **13f** as a cream color solid. **^{1}H NMR** (400 MHz, $CDCl_3$) δ 8.02 (dd, *J* = 7.8, 1.2 Hz, 1H), 7.58 (dt, *J* = 7.5, 1.4 Hz, 1H), 7.39 (t, *J* = 7.6 Hz, 1H), 7.31 (d, *J* = 7.7 Hz, 1H), 7.23-7.20 (m, 1H), 6.97- 6.89 (m, 3H), 3.83 (bs, 1H), 3.28-3.19 (m, 1H), 3.08-3.02 (m, 1H), 2.97 (d, *J* = 13.8 Hz, 1H), 2.92 (d, *J* = 13.8 Hz, 1H), 2.30-2.30 (m, 1H), 2.23-2.15 (m, 1H). **^{13}C NMR** (100 MHz, $CDCl_3$) δ 200.82, 162.66 (d, *J* = 244.1 Hz), 143.25, 138.015 (d, *J* = 7.4 Hz), 134.45, 130.35, 129.585 (d, *J* = 8.2 Hz), 129.30, 128.19, 127.33, 126.14 (d, *J* = 2.8 Hz), 117.41 (d, *J* = 21.2 Hz), 113.975 (d, *J* = 20.9 Hz), 76.06, 41.77 (d, *J* = 1.8 Hz), 41.75, 33.91, 26.48. **FTIR** (neat): 3478, 2924, 1685, 1288 cm^{-1}. **HRMS** (ESI) m/z calculated for $C_{17}H_{15}FO_2$ $(M+H)^+$: 271.1134, found: 271.1142.

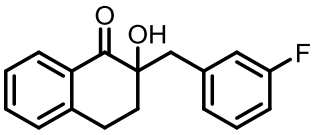

2-(2-Fluorobenzyl)-2-hydroxy-3,4-dihydronaphthalen-1(2*H*)-one (13g): The reaction of 2-(2-fluorobenzyl)-3,4-dihydronaphthalen-1(2*H*)-one (63.5 mg, 0.25 mmol), KO-*t*-Bu (28 mg, 0.25 mmol), in DMSO (1.0 mL), at 25 ^{o}C, under air, for 24 h, afforded (40 mg, 59%) of **13g** as a creamy wax. **^{1}H NMR** (400 MHz, $CDCl_3$) δ 8.05 (dd, *J* = 7.9, 1.6 Hz, 1H), 7.56 (dt, *J* = 7.5, 1.7 Hz, 1H), 7.38 (t, *J* = 7.5, 1H), 7.34-7.27 (m, 2H), 7.20-7.06 (m, 2H), 7.01-6.96 (m, 1H), 3.78 (bs, 1H), 3.38-3.29 (m, 1H), 3.10-2.98 (m, 3H), 2.33-2.18 (m, 2H). **^{13}C NMR** (100 MHz, $CDCl_3$) δ 200.75, 161.56 (d, *J* = 243.6 Hz), 143.44, 134.29, 133.33 (d, *J* = 4.4 Hz), 130.36, 129.18, 128.86 (d, *J* = 8.3 Hz), 128.31, 127.12, 123.895 (d, *J* = 3.4 Hz), 122.29 (d, *J* = 15.5 Hz), 115.255 (d, *J* = 22.6 Hz), 75.87, 34.61 (d, *J* = 47.1 Hz), 29.85, 26.34. **FTIR** (neat): 3289, 2928, 1735, 1685, 1227 cm^{-1}. **HRMS** (ESI) m/z calculated for $C_{17}H_{15}FO_2$ $(M+Na)^+$: 293.0953, found: 293.0961.

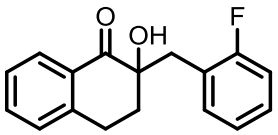

2-(4-Fluorobenzyl)-2-hydroxy-3,4-dihydronaphthalen-1(2*H*)-one (13h): The reaction of 2-(4-fluorobenzyl)-3,4-dihydronaphthalen-1(2*H*)-one (63.5 mg, 0.25 mmol), KO-*t*-Bu (28 mg, 0.25 mmol), in DMSO (1.0 mL), at 25 ^{o}C, under air, for 24 h, afforded (46 mg, 68%) of **13h** as a white solid. **^{1}H NMR** (400 MHz, $CDCl_3$) δ 8.01 (dd, *J* = 7.8 Hz, 1H), 7.57 (dt, *J* = 7.6, 1.3 Hz, 1H), 7.39 (t, *J* = 7.5 Hz, 1H), 7.31 (d, *J* = 7.7 Hz, 1H), 7.10 (d, *J* = 8.0 Hz, 2H), 6.93 (d, *J* = 8.0 Hz, 2H), 3.79 (bs, 1H), 3.28-3.19 (m, 1H), 3.08-3.01 (m, 1H), 2.96 (d, *J* = 14.0 Hz, 1H), 2.90 (d, *J* = 13.9 Hz, 1H), 2.29-2.16 (m, 2H). **^{13}C NMR** (100 MHz, $CDCl_3$) δ 200.95, 162.11 (d, *J* = 243.5 Hz), 143.26, 134. 39, 131.89 (d, *J* = 7.9 Hz), 131.12 (d, *J* = 2.9 Hz), 130.41, 129.29, 128.12, 127.28, 115.08 (d, *J* = 21.1 Hz), 76.08, 41.21, 33.94, 26.47. **FTIR** (neat): 3499, 2928, 1734, 1686, 1225 cm^{-1}. **HRMS** (ESI) m/z calculated for $C_{17}H_{15}FO_2$ $(M+Na)^+$: 293.0953, found: 293.0959.

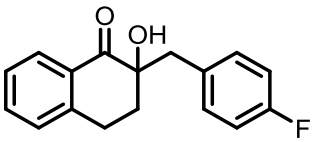

2-(3-Chlorobenzyl)-2-hydroxy-3,4-dihydronaphthalen-1(2*H*)-one (13i): The reaction of 2-(3-chlorobenzyl)-3,4-dihydronaphthalen-1(2*H*)-one (67.5 mg, 0.25 mmol), KO-*t*-Bu (28 mg, 0.25 mmol), in DMSO (1.0 mL), at 25 ^{o}C, under air, for 24 h, afforded (48.5, mg 65%) of **13i** as a yellow wax. **^{1}H NMR** (400 MHz, $CDCl_3$) δ 8.02 (d, *J* = 7.8 Hz, 1H), 7.58 (m, 1H), 7.39 (t, *J* = 7.5 Hz, 1H), 7.31 (d, *J* = 7.8 Hz, 1H), 7.22-7.17 (m, 3H), 7.03-7.02 (m, 1H), 3.83 (bs, 1H), 3.27-3.18 (m, 1H), 3.08-3.02 (m, 1H), 2.95 (d, *J* = 13.8 Hz, 1H), 2.88 (d, *J* = 13.8 Hz, 1H), 2.29-2.15 (m, 2H). **^{13}C NMR** (100 MHz, $CDCl_3$) δ 200.79, 143.24, 137.57, 134.47, 134.01, 130.56, 130.33, 129.43, 129.31, 128.64, 128.18, 127.34, 127.24, 76.03, 41.66, 33.87, 26.47. **FTIR** (neat): 3478, 2929, 1733, 1685, 1225 cm^{-1}. **HRMS** (ESI) m/z calculated for $C_{17}H_{15}ClO_2$ $(M+Na)^+$: 309.0658, found: 309.0661

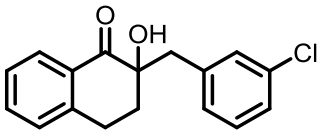

2-(3-Bromobenzyl)-2-hydroxy-3,4-dihydronaphthalen-1(2*H*)-one (13j): The reaction of 2-(3-bromobenzyl)-3,4-dihydronaphthalen-1(2*H*)-one (78.5 mg, 0.25 mmol), KO-*t*-Bu (28 mg, 0.25 mmol), in DMSO (1.0 mL), at 25 ^{o}C, under air, for 24 h, afforded (50 mg, 60%) of **13j** as a yellow liquid. **^{1}H NMR** (400 MHz, $CDCl_3$) δ 8.02 (dd, *J* = 7.9, 1.2 Hz, 1H), 7.58 (dt, *J* = 7.5, 1.4 Hz 1H), 7.41-7.36 (m, 2H), 7.34-7.32 (m, 1H), 7.19-7.12 (m, 2H), 7.06 (d, *J* = 7.7 Hz, 1H), 3.82 (bs, 1H), 3.27-3.18 (m, 1H), 3.08-3.02 (m, 1H), 2.94 (d, *J* = 13.8 Hz, 1H), 2.90 (d, *J* = 13.8 Hz, 1H), 2.30-2.15 (m, 2H). **^{13}C NMR** (100 MHz, $CDCl_3$) δ 200.79, 143.24, 137.57, 134.47, 134.01, 130.56, 130.33, 129.43, 129.31, 128.64, 128.18, 127.34, 127.24, 76.03, 41.66, 33.87, 26.47. **FTIR** (neat): 3482, 2929, 1735, 1685, 1226 cm^{-1}. **HRMS** (ESI) m/z calculated for $C_{17}H_{15}BrO_2$ $(M+H)^+$: 331.0334, found: 331.0344.

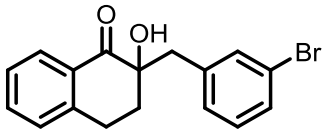

2-(4-Bromobenzyl)-2-hydroxy-3,4-dihydronaphthalen-1(2*H*)-one (13k): The reaction of 2-(4-bromobenzyl)-3,4-dihydronaphthalen-1(2*H*)-one (78.5 mg, 0.25 mmol), KO-*t*-Bu (28 mg, 0.25 mmol), in DMSO (1.0 mL), at 25 ^{o}C, under air, for 24 h, afforded (56 mg, 67%) of **13k** as a creamy solid. **^{1}H NMR** (400 MHz, $CDCl_3$) δ 8.00 (dd, *J* = 7.8, 1.3 Hz, 1H), 7.57 (dt, *J* = 7.5, 1.4 Hz, 1H), 7.40-7.37 (m, 3H), 7.3 (d, *J* = 7.8 Hz, 1H), 7.02 (d, *J* = 8.4 Hz, 2H), 3.80 (bs, 1H), 3.27-3.18 (m, 1H), 3.08-3.01 (m, 1H), 2.94 (d, *J* = 13.9 Hz, 1H), 2.88 (d, *J* = 13.8 Hz, 1H), 2.30-2.15 (m, 2H). **^{13}C NMR** (100 MHz, $CDCl_3$) δ 200.82, 143.24, 134.46, 132.17, 131.35, 130.55, 130.34, 129.31, 128.15, 127.32, 121.13, 75.99, 41.47, 33.98, 26.47. **FTIR** (neat): 3489, 2929, 1684, 1289 cm^{-1}. **HRMS** (ESI) m/z calculated for $C_{17}H_{15}BrO_2$ $(M+H)^+$: 331.0334, found: 331.0333.

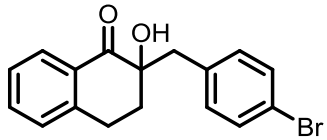

2-Hydroxy-2-methyl-1-phenylpropan-1-one (13l): The reaction of 2-methyl-1-phenylpropan-1-one (37 mg, 0.25 mmol), KO-*t*-Bu (28mg, 0.25 mmol), in DMSO (1.0 mL), at 25 ^{o}C, under air, for 24 h, afforded (21.5 mg, 52%) of **13l** as a colorless liquid. **^{1}H NMR** (400 MHz, $CDCl_3$) δ 8.01 (d, *J* = 7.2 Hz, 2H), 7.57 (t, *J* = 7.2 Hz, 1H), 7.47 (t, *J* =

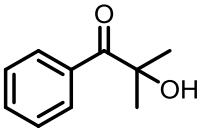

7.6 Hz, 2H), 4.08 (bs, 1H), 1.64 (s, 6H). **^{13}C NMR** (100 MHz, $CDCl_3$) δ 204.92, 133.88, 133.13, 129.77, 128.62, 76.39, 28.59. **FTIR** (neat): 3359, 2972, 1736, 1224, 1066 cm^{-1}. **HRMS** (ESI) m/z calculated for $C_{10}H_{12}O_2$ $(M+Na)^+$: 187.0735, found: 187.1128.

2-Benzyl-2-hydroxy-2,3-dihydro-1*H*-inden-1-one (13m): The reaction of 2-benzyl-2,3-dihydro-1*H*-inden-1-one (55.5 mg, 0.25 mmol), KO-*t*-Bu (28 mg, 0.25 mmol), in DMSO (1.0 mL), at 25 °C, under air, for 24 h, afforded (21 mg 35%) of **13m** as a yellow wax. **^{1}H NMR** (400 MHz, $CDCl_3$) δ 7.77 (dd, *J* = 6.1, 1.8 Hz, 1H), 7.59 (dt, *J* = 7.7, 1.1 Hz, 1H), 7.38 (t, *J* = 7.0 Hz, 2H), 7.26 – 7.17 (m, 5H), 3.36 (d, *J* = 17.0 Hz, 1H), 3.10 – 3.05 (d, *J* = 16.8 Hz, 1H), 3.01 (d, *J* = 13.7 Hz, 1H), 2.94 (d, *J* = 13.7 Hz, 1H), 2.74 (bs, 1H). **^{13}C NMR** (100 MHz, $CDCl_3$) δ 207.26, 151.38, 135.96, 135.59, 134.15, 130.42, 128.37, 128.04, 127.10, 126.77, 124.88, 80.19, 44.39, 39.68. **FTIR** (neat): 3431, 2924, 1711.85, 1216, 1052 cm^{-1}. **HRMS** (ESI) m/z calculated for $C_{16}H_{14}O_2$ $(M+Na)^+$: 261.0891, found: 261.0891.

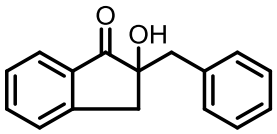

2-Hexyl-2-hydroxy-2,3-dihydro-1*H*-inden-1-one (13n): The reaction of 2-hexyl-2,3-dihydro-1*H*-inden-1-one (54 mg, 0.25 mmol), KO-*t*-Bu (28 mg, 0.25 mmol), in DMSO (1.0 mL), at 25 °C, under air, for 24 h, afforded (21 mg 36%) of **13n** as a yellow liquid. **^{1}H NMR** (400 MHz, $CDCl_3$) δ 7.76 (d, *J* = 7.7 Hz, 1H), 7.63 (dt, *J* = 7.5, 1.2 Hz,1H), 7.46 – 7.36 (m, 2H), 3.28 (d, *J* = 17.0 Hz, 1H), 3.15 (d, *J* = 17.0 Hz, 1H), 2.57 (bs, 1H), 1.71- 1.61 (m, 2H), 1.28 – 1.20 (m, 8H), 0.84 (t, *J* = 6.8 Hz, 3H). **^{13}C NMR** (100 MHz, $CDCl_3$) δ 208.34, 151.70, 135.92, 134.41, 127.99, 126.79, 124.81, 80.09, 77.48, 77.36, 76.84, 40.29, 38.94, 31.75, 29.85, 29.71, 23.67, 22.67, 14.16. **FTIR** (neat): 3435, 2927, 1714, 1213, 1079 cm^{-1}. **HRMS** (ESI) m/z calculated for $C_{15}H_{20}O_2$ $(M+Na)^+$: 255.1360, found: 255.1364.

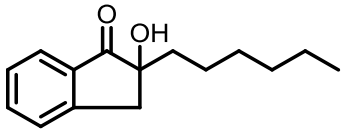

2-Hydroxy-2-octyl-2,3-dihydro-1*H*-inden-1-one (13o): The reaction of 2-octyl-2,3-dihydro-1*H*-inden-1-one (61 mg, 0.25 mmol), KO-*t*-Bu (28 mg, 0.25 mmol), in DMSO (1.0 mL), at 25 °C, under air, for 24 h, afforded (28 mg, 43%) of **13o** as a yellow liquid. **^{1}H NMR** (400 MHz, $CDCl_3$) δ 7.79 – 7.74 (m, 1H), 7.63 (dt, *J* = 7.5, 1.2 Hz, 1H), 7.45 – 7.37 (m, 2H), 3.28 (d, *J* = 17.0 Hz, 1H), 3.15 (d, *J* = 17.0 Hz, 1H), 2.57 (bs, 1H), 1.71 – 1.61 (m, 3H), 1.28-1.17 (m, 12H), 0.88 – 0.83 (t, 3H). **^{13}C NMR** (100 MHz, $CDCl_3$) δ 208.34, 151.70, 135.91, 134.42, 127.98, 126.79, 124.81, 80.09, 40.29, 38.94, 31.94, 30.06, 29.52, 29.32, 23.72, 22.76, 14.22. **FTIR** (neat): 3430, 2925, 1716, 1213, 1081 cm^{-1}. **HRMS** (ESI) m/z calculated for $C_{17}H_{24}O_2$ $(M+Na)^+$: 283.1673, found: 283.1668.

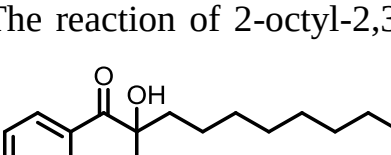

2-Hydroxy-2-(4-methylbenzyl)-2,3-dihydro-1*H*-inden-1-one (13p): The reaction of 2-(4-methylbenzyl)-2,3-dihydro-1*H*-inden-1-one (59 mg, 0.25 mmol), KO-*t*-Bu (28 mg, 0.25

mmol), in DMSO (1.0 mL), at 25 ^{o}C, under air, for 24 h, afforded (21.5 mg, 34%) of **13p** as a yellow liquid. **^{1}H NMR** (400 MHz, $CDCl_3$) δ 7.77 (d, *J* = 8.0 Hz, 1H), 7.60 (dt, 1H), 7.39 (m, 2H), 7.07 (m, 4H), 3.35 (d, *J* = 17.0 Hz, 1H), 3.07 (d, *J* = 17.0 Hz, 1H), 2.96 (d, *J* = 13.9 Hz, 1H), 2.90 (d, *J* = 13.7 Hz, 1H), 2.65 (bs, 1H), 2.31 (s, 3H). **^{13}C NMR** (100 MHz, $CDCl_3$) δ 201.59, 136.72, 135.91, 134.18, 130.31, 129.12, 128.75, 128.04, 126.80, 124.89, 123.91, 80.20, 43.96, 39.76, 21.20. **FTIR** (neat): 3437, 2923, 1711, 1377, 1218, 1055 cm^{-1}. **HRMS** (ESI) m/z calculated for $C_{17}H_{16}O_2$ $(M+Na)^+$: 275.1047, found: 275.1053.

2-Hydroxy-2-(3-methylbenzyl)-2,3-dihydro-1*H*-inden-1-one (13q): The reaction of 2-(3-methylbenzyl)-2,3-dihydro-1*H*-inden-1-one (59 mg, 0.25 mmol), KO-*t*-Bu (28 mg, 0.25 mmol), in DMSO (1.0 mL), at 25 ^{o}C, under air, for 24 h, afforded (26 mg, 41%) of **13q** as a yellow wax.

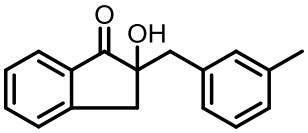

^{1}H NMR (400 MHz, $CDCl_3$) δ 7.79 – 7.76 (m, 1H), 7.59 (dt, *J* = 7.6, 1.2 Hz, 1H), 7.40 – 7.36 (m, 2H), 7.14 (m, 2H), 7.05 – 6.97 (m, 3H), 3.36 (d, *J* = 17.2 Hz, 1H), 3.07 (d, *J* = 16.8 Hz, 1H), 2.97 (d, *J* = 13.7 Hz, 1H), 2.89 (d, *J* = 13.7 Hz, 1H), 2.68 (bs, 1H), 2.31 (s, 3H). **^{13}C NMR** (100 MHz, $CDCl_3$) δ 207.24, 151.39, 137.96, 135.90, 135.50, 134.23, 131.22, 128.27, 128.02, 127.87, 127.46, 126.78, 124.86, 80.19, 44.31, 39.73, 21.53. **FTIR** (neat): 3434, 2925, 1715, 1377, 1219, 1056 cm^{-1}. **HRMS** (ESI) m/z calculated for $C_{17}H_{16}O_2$ $(M+Na)^+$: 275.1047, found: 275.1048.

2-Benzyl-2-hydroxycyclohexan-1-one (13r): The reaction of 2-benzylcyclohexan-1-one (47 mg, 0.25 mmol), KO-*t*-Bu (28 mg, 0.25 mmol), in DMSO (1.0 mL), at 25 ^{o}C, under air, for 24 h, afforded (12.5 mg, 24%) of **13r** as a white semi solid.

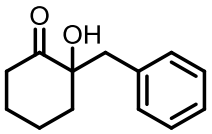

^{1}H NMR (400 MHz, $CDCl_3$) δ 7.28-7.18 (m, 5 H), 3.86 (brs, 1 H), 3.14 (d, *J* = 14.0 Hz, 1 H), 2.98 (d, *J* = 14.0 Hz, 1 H), 2.74-2.66 (m, 1 H), 2.57-2.51 (m, 1 H), 2.25-2.15 (m, 2 H), 1.93-1.81 (m, 2 H), 1.76-1.58 (m, 2 H). **^{13}C NMR** (100 MHz, $CDCl_3$) δ 213.6, 135.42, 130.19, 128.36, 127.10, 79.42, 43.42, 40.53, 38.72, 29.85, 22.93. **FTIR** (neat): 3482, 2925, 1714, 1098 cm^{-1}. **HRMS** (ESI) m/z calculated for $C_{13}H_{16}O_2$ $(M+Na)^+$: 227.1047, found: 227.1040

2-Benzyl-2-hydroxy-7-methyl-3,4-dihydronaphthalen-1(*2H*)-one (13s): The reaction of 2-benzyl-7-methyl-3,4-dihydronaphthalen-1(2*H*)-one (62.5 mg, 0.25 mmol), KO-*t*-Bu (28 mg, 0.25 mmol), in DMSO (1.0 mL), at 25 ^{o}C, under air, for 24 h, afforded (45 mg, 68%) of **13s** as a light yellow solid.

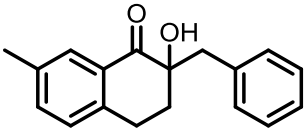

^{1}H NMR (400 MHz, $CDCl_3$) δ 7.93 (d, *J* = 8.0 Hz, 1H), 7.30-7.15 (m, 6H), 7.11 (s, 1H), 3.80 (bs, 1H), 3.23 (ddd, *J* = 18.0, 12.7, 5.5 Hz, 1H), 3.01-2.96 (m, 2H), 2.90 (d, *J* = 14 Hz, 1H), 2.43 (s, 3H), 2.28-2.13 (m, 2H). **^{13}C NMR** (100 MHz, $CDCl_3$) δ 200.69, 145.32, 143.40, 135.61, 130.51, 129.66, 128.29, 128.23, 128.21, 128.12, 126.96, 76.10, 42.17, 33.94, 26.46, 21.96. **FTIR** (neat): 3484, 2925, 1681, 1288 cm^{-1}. **HRMS** (ESI) m/z calculated for $C_{18}H_{18}O_2$ $(M+Na)^+$: 289.1204, found: 289.1213.

2-Benzyl-5-fluoro-2-hydroxy-3,4-dihydronaphthalen-1(2*H*)-one (13u): The reaction of 2-benzyl-5-fluoro-3,4-dihydronaphthalen-1(2*H*)-one (63.5 mg, 0.25 mmol), KO-*t*-Bu (28 mg, 0.25 mmol), in DMSO (1.0 mL), at 25 ^{o}C, under air, for 24 h, afforded (29 mg, 43%) of **13u** as a light yellow solid. **^{1}H NMR** (400 MHz, $CDCl_3$) δ 7.82 (dd, *J* = 7.7, 1.1 Hz, 1H), 7.34-7.27 (m, 5H), 7.12 (m, 2H), 3.72 (bs, 1H), 3.18 (ddd, *J* = 18.5, 4.1, 1.9 Hz, 1H), 3.07 (dd, *J* = 12.5, 5.6 Hz, 1H), 2.99 (m, 1H) 2.92 (d, *J* = 13.8 Hz, 1H), 2.33 (ddd, *J* = 13.7, 5.5, 2.1 Hz, 1H), 2.22 – 2.13 (m, 1H). **^{13}C NMR** (100 MHz, $CDCl_3$) δ 200.12, 160.31 (d, *J* = 246 Hz), 135.13, 132.42 (d, *J* = 4.6 Hz), 130.47, 129.46 (d, *J* = 5 Hz), 128. 36 (d, *J* = 10 Hz), 127.80, 127.14, 123.69 (d, *J* = 3.3 Hz), 120.60 (d, *J* = 21.3 Hz), 77.10, 42.08, 33.07, 19.74(d, *J* = 3.2 Hz). **FTIR** (neat): 3489, 2925.62, 1689, 1279 cm^{-1}. **HRMS** (ESI) m/z calculated for $C_{17}H_{15}FO_2$ $(M+Na)^+$: 293.0953, found: 293.0956.

2-Benzyl-7-chloro-2-hydroxy-3,4-dihydronaphthalen-1(2*H*)-one (13v): The reaction of 2-benzyl-7-chloro-3,4-dihydronaphthalen-1(2*H*)-one (67.5 mg, 0.25 mmol), KO-*t*-Bu (28 mg, 0.25 mmol), in DMSO (1.0 mL), at 25 ^{o}C, under air, for 24 h, afforded (35.8 mg, 50%) of **13v** as a yellow liquid. **^{1}H NMR** (400 MHz, $CDCl_3$) δ 7.99 (d, *J* = 2.3 Hz, 1H), 7.52 (dd, *J* = 8.2, 2.3 Hz, 1H), 7.31 – 7.25 (m, 3H), 7.13 (dd, *J* = 7.5, 1.7 Hz, 2H), 3.66 (s, 1H), 3.21 (ddd, *J* = 17.9, 12.7, 5.5 Hz, 1H), 3.05 – 2.96 (m, 2H), 2.91 (d, *J* = 13.8 Hz, 1H), 2.28 (ddd, *J* = 13.6, 5.5, 2.4 Hz, 1H), 2.23 – 2.13 (m, 1H). **^{13}C NMR** (100 MHz, $CDCl_3$) δ 199.86, 141.55, 135.09, 134.22, 133.50, 131.85, 130.84, 130.48, 128.34, 127.75, 127.16, 76.15, 42.05, 33.83, 26.04. **FTIR** (neat): 3484, 2925.57, 1689, 1296 cm^{-1}. **HRMS** (ESI) m/z calculated for $C_{17}H_{15}ClO_2$ $(M+Na)^+$: 309.0658, found: 309.0658.

3-Benzyl-3-hydroxyindolin-2-one (15a): The reaction of 3-benzylindolin-2-one (55.75 mg, 0.25 mmol), KO-*t*-Bu (28 mg, 0.25 mmol), in toluene (1.0 mL), at 25 ^{o}C, under air, for 24 h, afforded (55.5, mg 93%) of **15a** as a white solid. **^{1}H NMR** (400 MHz, $CDCl_3$): δ 7.47 (bs, 1H), 7.23-7.12 (m, 5H), 7.05-6.98 (m, 3H), 6.71 (d, *J* = 7.7 Hz, 1H), 3.30 (d, *J* = 12.8 Hz, 1H), 3.14 (d, *J* = 12.8 Hz, 1H), 3.02 (bs, 1H). **^{13}C NMR** (100 MHz, $CDCl_3$) δ 179.60, 140.28, 133.92, 130.57, 129.85, 129.73, 128.06, 127.12, 125.11, 122.99, 110.19, 77.36, 44.79. **FTIR** (neat): 3261, 1714 cm^{-1}. **HRMS** (ESI) m/z calculated for $C_{15}H_{13}NO_2$ $(M+Na)^+$: 262.0844, found: 262.0847

3-Hydroxy-3-(4-methoxybenzyl)indolin-2-one (15b): The reaction of 3-(4-methoxybenzyl)indolin-2-one (63.25 mg, 0.25 mmol), KO-*t*-Bu (28 mg, 0.25 mmol), in toluene (1.0 mL), at 25 ^{o}C, under air, for 24 h, afforded (61 mg, 90%) of **15b** as a yellow solid. **^{1}H NMR** (400 MHz, $CDCl_3$): δ 7.23 (m, 1H), 7.18 (m, 1H), 7.06-7.02 (dt, *J* = 7.6, 0.9 Hz, 1H), 6.90 (d, *J* = 8.4 Hz, 2H), 6.72-6.67 (m, 3H), 3.73 (s, 3H), 3.24 (d, *J* = 13.2 Hz, 1H), 3.08 (d, *J* = 13.2 Hz, 1H), 2.82 (bs, 1H). **^{13}C NMR**

(100 MHz, $CDCl_3$) δ 179.58, 158.67, 140.27, 131.55, 129.82, 125.85, 125.05, 122.98, 113.45, 110.18, 77.36, 55.25, 43.92. **FTIR** (neat): 3262, 1712 cm^{-1}. **HRMS** (ESI) m/z calculated for $C_{16}H_{15}NO_3$ $(M+Na)^+$: 292.0949, found: 292.0963.

3-Hydroxy-3-(3-methoxybenzyl)indolin-2-one (15c): The reaction of 3-(3-methoxybenzyl)indolin-2-one (63.25 mg, 0.25 mmol), KO-*t*-Bu (28 mg, 0.25 mmol), in toluene (1.0 mL), at 25 ^oC, under air, for 24 h, afforded (60 mg, 89%) of **15c** as a light brown solid. **^{1}H NMR** (400 MHz, $CDCl_3$) δ 7.89 (bs, 1H), 7.20-7.17 (m, 2H), 7.03(m, 2H), 6.70-6.68 (m, 2H), 6.57 (m, 1H), 6.48 (m, 1H), 3.61 (s, 3H), 3.43 (bs,1H), 3.28 (d, *J* = 12.8 Hz, 1H), 3.11(d, *J* = 13.2 Hz, 1H). **^{13}C NMR** (100 MHz, $CDCl_3$) δ 180.34, 159.44, 140.74, 135.75, 130.25, 130.14, 129.3, 125.34, 123.35, 123.27, 115.96, 113.44, 110.70, 77.95, 55.51, 45.04. **FTIR** (neat): 3229, 1705 cm^{-1}. **HRMS** (ESI) m/z calculated for $C_{16}H_{15}NO_3$ $(M+Na)^+$: 292.0949, found: 292.0948.

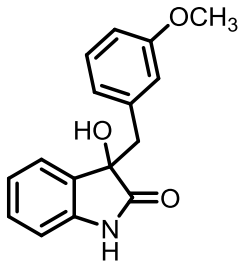

3-Hydroxy-3-(2-methylbenzyl)indolin-2-one (15d): The reaction of 3-(2-methylbenzyl)indolin-2-one (59.25 mg, 0.25 mmol), KO-*t*-Bu (28 mg, 0.25 mmol), in toluene (1.0 mL), at 25 ^oC, under air, for 24 h, afforded (42 mg, 66%) of **15d** as a cream colour solid. **^{1}H NMR** (400 MHz, $CDCl_3$+ Methanol-*d4*) δ 7.38 (bs, 1H), 7.25-7.21 (m, 1H), 7.15-7.07 (m ,4H), 6.96 (t, *J* = 7.5 Hz, 1H), 6.88 (d, *J* = 8 Hz, 1H), 6.80 (d, *J* = 8 Hz, 1H), 3.29 (d, *J* =13.9 Hz, 1H), 3.12 (d, *J* = 13.9Hz, 1H), 2.76 (bs, 1H), 2.03 (s, 3H). **^{13}C NMR** (100 MHz, $CDCl_3$) δ 179.18, 139.93, 137.23, 132.52, 130.88, 129.85, 129.75, 129.04, 126.59, 124.96, 124.62, 122.10, 109.58, 76.91, 39.76, 19.36. **FTIR** (neat): 3237, 1707 cm^{-1}. **HRMS** (ESI) m/z calculated for $C_{16}H_{15}NO_2$ $(M+Na)^+$: 276.1000, found: 276.1003.

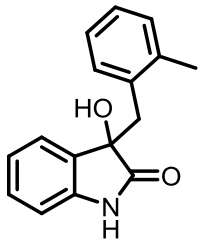

3-Hydroxy-3-(3-methylbenzyl)indolin-2-one (15e): The reaction of 3-(3-methylbenzyl)indolin-2-one (59.25 mg, 0.25 mmol), KO-*t*-Bu (28 mg, 0.25 mmol), in toluene (1.0 mL), at 25 ^oC, under air, for 24 h, afforded (55 mg, 87%) of **15e** as a cream colour solid. **^{1}H NMR** (400 MHz, $CDCl_3$) δ 7.73 (bs, 1H), 7.23-7.15 (m, 2H), 7.05-6.96 (m, 3H), 6.81-6.71 (m, 3H), 3.26 (d, *J* =13 Hz, 1H), 3.19 (bs, 1H), 3.08 (d, *J* = 13 Hz, 1H), 2.20 (s, 3H). **^{13}C NMR** (100 MHz, $CDCl_3$) δ 179.73, 140.31, 137.59, 133.79, 131.38, 129.88, 129.79, 127.90, 127.85, 127.58, 125.15, 122.91, 110.19, 44.72, 21.41. **FTIR** (neat): 3258, 1714 cm^{-1}. **HRMS** (ESI) m/z calculated for $C_{16}H_{15}NO_2$ $(M+Na)^+$: 276.1000, found: 276.1007.

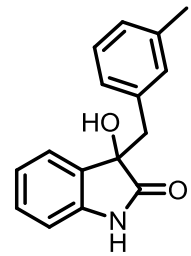

3-Hydroxy-3-(4-methylbenzyl)indolin-2-one (15f): The reaction of 3-(4-methylbenzyl)indolin-2-one (59.25 mg, 0.25 mmol), KO-*t*-Bu (28 mg, 0.25 mmol), in toluene (1.0 mL), at 25 ^oC, under air, for 24 h, afforded (41 mg, 64%) of **15f** as a light brown solid. **^{1}H NMR** (400 MHz, $CDCl_3$) δ 7.58 (bs, 1H), 7.23-7.17 (m, 2H), 7.04 (dt, *J* = 8.4, 4.2

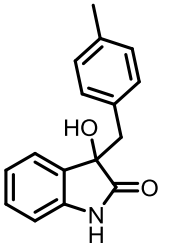

Hz, 1H), 6.95 (d, *J* = 7.9 Hz, 2H), 6.87 (d, *J* = 8 Hz, 2H), 6.72 (d, *J* = 7.8, 1H), 3.26 (d, *J* =13 Hz, 1H), 3.10 (d, *J* = 13 Hz, 1H), 3.06 (bs, 1H), 2.25 (s, 3H). **^{13}C NMR** (100 MHz, $CDCl_3$) δ 179.59, 140.29, 136.70, 130.70, 130.41, 129.85, 129.80, 128.80, 125.09, 122.96, 110.17, 44.37, 21.20. **FTIR** (neat): 3271, 3313, 1713 cm^{-1}. **HRMS** (ESI) m/z calculated for $C_{16}H_{15}NO_2$ $(M+Na)^+$: 276.1000, found: 276.1009.

3-([1,1'-Biphenyl]-4-ylmethyl)-3-hydroxyindolin-2-one (15g): The reaction of 3-([1,1'-biphenyl]-4-ylmethyl)indolin-2-one (74.75 mg, 0.25 mmol), KO-*t*-Bu (28 mg, 0.25 mmol), in toluene (1.0 mL), at 25 ^oC, under air, for 24 h, afforded (72 mg, 91%) of **15g** as a white solid. **^{1}H NMR** (400 MHz, $CDCl_3$) δ 7.58-7.49 (m, 2H), 7.42-7.39 (m, 3H), 7.34-7.30 (m, 1H), 7.22-7.19 (m, 3H), 7.08-7.04 (m, 3H), 6.72 (d, *J* = 8 Hz, 1H), 3.35 (d, *J* =12.9 Hz, 1H), 3.18 (d, *J* = 13 Hz, 1H), 2.81 (bs, 1H). **^{13}C NMR** (100 MHz, $CDCl_3$ + Methanol-*d4*) δ 180.44, 140.70, 139.47, 133.33, 130.82, 130.20, 129.49, 128.71, 127.17, 127.06, 126.86, 126.38, 124.77, 122.58, 110.10, 43.79. **FTIR** (neat): 3333, 2923, 1711 cm^{-1}. **HRMS** (ESI) m/z calculated for $C_{21}H_{17}NO_2$ $(M+Na)^+$: 338.1157, found: 338.1161.

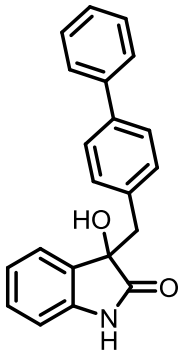

3-Butyl-3-hydroxyindolin-2-one (15h): The reaction of 3-butylindolin-2-one (47.25 mg, 0.25 mmol), KO-*t*-Bu (28 mg, 0.25 mmol), in toluene (1.0 mL), at 25 ^oC, under air, for 24 h, afforded (26 mg, 51%) of **15h** as a light yellow solid. **^{1}H NMR** (400 MHz, $CDCl_3$) δ 8.33 (bs, 1H), 7.36 (d, *J* = 7.4 Hz, 1H), 7.28-7.24 (m, 1H), 7.10-7.06 (dt, *J* = 7.6, 0.9 Hz, 1H), 6.89 (d, *J* = 7.7 Hz, 1H), 3.18 (bs, 1H), 1.99-1.93 (m, 2H), 1.29 - 1.04 (m, 4H), 0.82 (t, *J* = 7.2 Hz, 3H). **^{13}C NMR** (100 MHz, $CDCl_3$) δ 180.74, 140.60, 130.69, 129.72, 124.43, 123.27, 110.40, 38.44, 25.32, 22.86, 13.95. **FTIR** (neat) 3678, 3183, 1710 cm^{-1}. **HRMS** (ESI) m/z calculated for $C_{12}H_{15}NO_2$ $(M+Na)^+$: 228.1000, found: 228.1010.

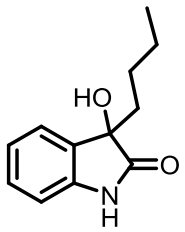

3-Hexyl-3-hydroxyindolin-2-one (15i): The reaction of 3-hexylindolin-2-one (54.25 mg, 0.25 mmol), KO-*t*-Bu (28 mg, 0.25 mmol), in toluene (1.0 mL), at 25 ^oC, under air, for 24 h, afforded (34 mg, 58%) of **15i** as a white solid. **^{1}H NMR** (400 MHz, $CDCl_3$) δ 8.30 (bs, 1H), 7.35 (d, *J* = 7.3 Hz, 1H), 7.27-7.23 (m, 1H), 7.07 (dd, *J* = 7.6 Hz, 0.8 Hz, 1H), 6.88 (d, *J* = 7.7 Hz, 1H), 3.15 (bs, 1H), 1.96-1.93 (m, 2H), 1.22-1.19 (m, 8H), 0.82 (t, J = 6.8 Hz, 3H). **^{13}C NMR** (100 MHz, $CDCl_3$) δ 181.01, 140.62, 130.72, 129.68, 124.37, 123.25, 110.49, 77.25, 38.60, 31.63, 29.40, 23.14, 22.63, 14.14. **FTIR** (neat) 3260, 2926, 1714, 1621 cm^{-1}. **HRMS** (ESI) m/z calculated for $C_{14}H_{19}NO_2$ $(M+H)^+$: 234.1494, found: 234.1492.

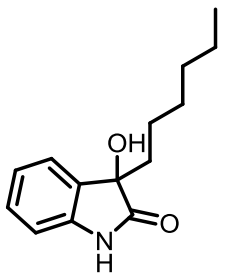

3-Hydroxy-3-isopropylindolin-2-one (15j): The reaction of 3-isopropylindolin-2-one (43.75 mg, 0.25 mmol), KO-*t*-Bu (28 mg, 0.25 mmol), in toluene (1.0 mL), at 25 ^oC, under air, for 24 h, afforded (17 mg, 35%) of **15j** as a brown solid. **^{1}H NMR** (400 MHz,

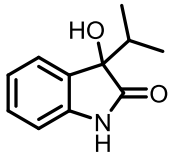

$CDCl_3$) δ 7.76 (bs, 1H), 7.38-7.36 (m, 1H), 7.27-7.25 (m, 1H), 7.09-7.05 (dt, *J* = 7.6, 1.0 Hz, 1H), 6.88-6.88 (m, 1H), 2.75 (bs, 1H), 2.24 (sep, 1H), 1.12 (d, *J* = 6.9 Hz, 3H), 0.81 (d, *J* = 6.8 Hz, 3H). **^{13}C NMR** (100 MHz, $CDCl_3$) δ 180.44, 140.93, 129.70, 129.04, 125.33, 123.00, 122.99, 110.13, 79.76, 36.24, 16.43, 15.90. **FTIR** (neat) 3268, 2965, 1713, 1620 cm^{-1}. **HRMS** (ESI) m/z calculated for $C_{11}H_{13}NO_2$ $(M+Na)^+$: 214.0843, found: 214.0849.

3-Hydroxy-3-octylindolin-2-one (15k): The reaction of 3-octylindolin-2-one (61.25 mg, 0.25 mmol), KO-*t*-Bu (28 mg, 0.25 mmol), in toluene (1.0 mL), at 25 ^oC, under air, for 24 h, afforded (42 mg, 67%) of **15k** as a light yellow solid. **^{1}H NMR** (400 MHz, $CDCl_3$) δ 7.58 (bs, 1H), 7.36 (d, *J* = 7.2 Hz, 1H), 7.29-7.25 (m, 1H), 7.10-7.06 (dt, *J* = 7.6, 0.8 Hz, 1H), 6.87 (d, *J* = 7.8 Hz, 1H), 2.71 (bs, 1H), 1.97-1.90 (m, 2H), 1.25-1.19 (m, 12H), 0.85 (t, J = 7.2 Hz, 3H). **^{13}C NMR** (100 MHz, $CDCl_3$) δ 180.31, 140.51, 130.56, 129.75, 124.46, 123.28, 110.29, 77.07, 38.72, 31.91, 29.74, 29.41, 29.28, 23.20, 22.75, 14.23. **FTIR** (neat) 3268, 1713 cm^{-1}. **HRMS** (ESI) m/z calculated for $C_{16}H_{23}NO_2$ $(M+H)^+$: 262.1807, found: 262.1808.

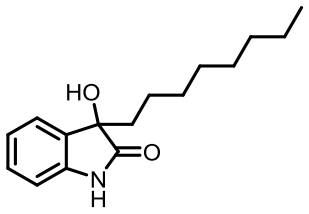

1,3-Dibenzyl-3-hydroxyindolin-2-one (15l): The reaction of 1,3-dibenzylindolin-2-one (78 mg, 0.25 mmol), KO-*t*-Bu (28 mg, 0.25 mmol), in toluene (1.0 mL), at 25 ^oC, under air, for 24 h, afforded (78 mg, 94%) of **15l** as a white solid. **^{1}H NMR** (400 MHz, $CDCl_3$): δ 7.37 (d, *J* = 7.2 Hz, 1H), 7.20-7.05 (m, 8H), 6.95 (d, *J* = 7.4 Hz, 2H), 6.72 (d, *J* = 6.6 Hz, 2H), 6.44 (d, *J* = 7.7 Hz, 1H), 5.00 (d, *J* = 16.0 Hz, 1H), 4.45 (d, *J* = 16.0 Hz, 1H), 3.42 (d, *J* = 12.7 Hz, 1H), 3.30 (d, *J* = 12.7 Hz, 1H), 3.08 (bs, 1H). **^{13}C NMR** (100 MHz, $CDCl_3$) δ 177.69, 142.86, 135.04, 133.94, 130.56, 129.93, 129.25, 128.79, 128.23, 127.47, 127.09, 126.79, 124.51, 123.09, 109.72, 77.64, 44.97, 43.86. **FTIR** (neat): 3333, 1691, 1171 cm^{-1}. **HRMS** (ESI) m/z calculated for $C_{22}H_{19}NO_2$ $(M+Na)^+$: 352.1313, found: 352.1312.

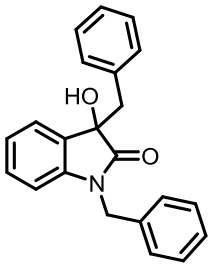

1-Benzyl-3-hydroxy-3-(2-methylbenzyl)indolin-2-one (15m): The reaction of 1-benzyl-3-(2-methylbenzyl)indolin-2-one (81.75 mg, 0.25 mmol), KO-*t*-Bu (28 mg, 0.25 mmol), in toluene (1.0 mL), at 25 ^oC, under air, for 24 h, afforded (85 mg, 99%) of **15m** as a white solid. **^{1}H NMR** (400 MHz, $CDCl_3$): δ 7.22-7.19 (m, 3H), 7.18-7.12 (m, 3H), 7.08 (d, *J* = 8 Hz, 1H), 7.02-6.96 (m, 3H), 6.89-6.87 (m, 2H), 6.54 (d, *J* = 7.8Hz, 1H), 5.05 (d, *J* = 15.9 Hz, 1H), 4.54 (d, *J* = 15.8 Hz, 1H), 3.39 (d, *J* = 13.6 Hz, 1H), 3.29 (d, *J* = 13.6 Hz, 1H), 2.95 (bs, 1H), 2.10 (s, 3H). **^{13}C NMR** (100 MHz, $CDCl_3$) δ 178.23, 142.66, 137.85, 135.25, 132.53, 131.22, 130.62, 129.88, 129.57, 128.88, 127.58, 127.28, 126.91, 125.68, 124.75, 122.99, 109.61, 43.92, 41.02, 20.05. **FTIR** (neat): 3612, 3389, 2923, 1708, 1614 cm^{-1}. **HRMS** (ESI) m/z calculated for $C_{23}H_{21}NO_2$ $(M+Na)^+$: 366.1469, found: 366.1474.

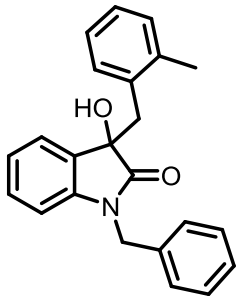

1-Benzyl-3-hydroxy-3-(3-methylbenzyl)indolin-2-one (15n): The reaction of 1-benzyl-3-(3-methylbenzyl)indolin-2-one (81.75 mg, 0.25 mmol), KO-*t*-Bu (28 mg, 0.25 mmol), in toluene (1.0 mL), at 25 ^{o}C, under air, for 24 h, afforded (77 mg, 90%) of **15n** as a light yellow crystals. **^{1}H NMR** (400 MHz, $CDCl_3$): δ 7.37 (dd, *J* = 7.3 Hz, 1.0 Hz, 1H), 7.21 – 7.11 (m, 4H), 7.07 (dt, *J* = 7.6 Hz, 1.1 Hz, 1H), 7.03 – 6.95 (m, 2H), 6.77 (s, 1H), 6.70 (m, 3H), 6.43 (d, *J* = 7.4 Hz, 1H), 5.03 (d, *J* = 16.0Hz, 1H), 4.43 (d, *J* = 16.0 Hz, 1H), 3.38 (d, *J* = 12.7 Hz, 1H), 3.24 (d, *J* = 12.7 Hz, 1H), 3.00 (bs, 1H), 2.16 (s, 3H). **^{13}C NMR** (100 MHz, $CDCl_3$) δ 177.69, 142.91, 137.82, 135.10, 133.81, 131.30, 129.88, 129.35, 128.77, 128.09, 127.84, 127.56, 127.45, 126.68, 124.52, 123.02, 109.69, 77.63, 44.93, 43.85, 21.39. **FTIR** (neat): 3360, 2922, 1702, 1614 cm^{-1}. **HRMS** (ESI) m/z calculated for $C_{23}H_{21}NO_2$ $(M+H)^+$: 344.1651, found: 344.1660.

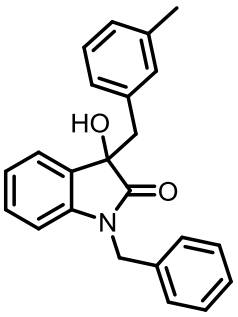

1-Benzyl-3-hydroxy-3-(4-methylbenzyl)indolin-2-one (15o): The reaction of 1-benzyl-3-(4-methylbenzyl)indolin-2-one (81.75 mg, 0.25 mmol), KO-*t*-Bu (28 mg, 0.25 mmol), in toluene (1.0 mL), at 25 ^{o}C, under air, for 24 h, afforded (72 mg, 84%) of **15o** as a cream colour solid. **^{1}H NMR** (400 MHz, $CDCl_3$): δ 7.40 (dd, *J* = 7.3, 1.1 Hz, 1H), 7.24-7.13 (m, 4H), 7.09 (dt, *J* = 7.6 Hz, 1H), 6.95 (d, *J* = 7.9 Hz, 2H), 6.85 (d, *J* = 8.0 Hz, 2H), 6.76 (d, *J* = 6.8 Hz, 2H), 6.47 (d, *J* = 7.6 Hz, 1H), 5.06 (d, *J* = 15.9 Hz, 1H), 4.46 (d, *J* = 16.0 Hz, 1H), 3.39 (d, *J* = 12.7 Hz, 1H), 3.27 (d, *J* = 12.8 Hz, 1H), 2.96 (bs, 1H), 2.31 (s, 3H). **^{13}C NMR** (100 MHz, $CDCl_3$) δ 177.72, 142.91, 136.61, 135.10, 130.78, 130.43, 129.88, 129.36, 128.95, 128.67, 127.46, 126.87, 124.49, 123.05, 109.70, 77.36, 44.54, 43.88, 21.29. **FTIR** (neat): 3465, 3355, 2920, 1692, 1616 cm^{-1}. **HRMS** (ESI) m/z calculated for $C_{23}H_{21}NO_2$ $(M+H)^+$: 344.1651, found: 344.1654.

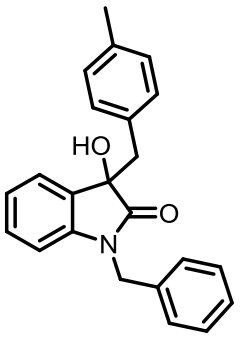

3-([1,1'-Biphenyl]-4-ylmethyl)-1-benzyl-3-hydroxyindolin-2-one (15p): The reaction of 3-([1,1'-biphenyl]-4-ylmethyl)-1-benzylindolin-2-one (97.25 mg, 0.25 mmol), KO-*t*-Bu (28 mg, 0.25 mmol), in toluene (1.0 mL), at 25 ^{o}C, under air, for 24 h, afforded (99 mg, 98%) of **15p** as a white solid. **^{1}H NMR** (400 MHz, $CDCl_3$): δ 7.57-7.50 (m, 1H), 7.45-7.30 (m, 3H), 7.16 (dt, *J* = 7.7 Hz, 1.4Hz, 1H), 7.12-6.97 (m, 3H), 6.74 (d, *J* = 6.3 Hz, 2H), 6.46 (d, *J* = 7.3 Hz, 1H), 5.04 (d, *J* = 15.9 Hz, 1H), 4.45 (d, *J* = 16.0 Hz, 1H), 3.46 (d, *J* = 12.7 Hz, 1H), 3.32 (d, *J* = 12.7 Hz, 1H), 2.92 (bs, 1H). **^{13}C NMR** (100 MHz, $CDCl_3$) δ 177.58, 142.94, 140.65, 139.83, 135.00, 133.03, 131.00, 130.01, 129.24, 128.91, 128.78, 127.48, 127.44, 127.05, 126.79, 126.78, 124.51, 123.13, 109.83, 77.36, 44.61, 43.94. **FTIR** (neat): 3564, 3360, 2920, 1700, 1615 cm^{-1}. **HRMS** (ESI) m/z calculated for $C_{28}H_{23}NO_2$ $(M+Na)^+$: 428.1626, found: 428.1623.

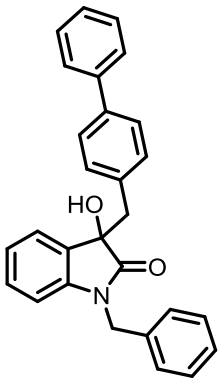

5-Benzyl-5-hydroxy-1,3-dimethylpyrimidine-2,4,6(1*H*,3*H*,5*H*)-trione (15q): The reaction of 5-benzyl-1,3-dimethylpyrimidine-2,4,6(1*H*,3*H*,5*H*)-trione (50 mg, 0.203 mmol), KO-*t*-Bu (28 mg, 0.25 mmol), in toluene (1.0 mL), at 25 ^{o}C, under air, for 24 h, afforded 93% of **15q** as a white powder without column purification, yield was determined by subtracting the theoretical weight of the by product. **^{1}H NMR** (400 MHz, DMSO-d_6) δ 7.20 (dd, *J* = 7.9 Hz, 1.0 Hz, 2H), 7.11 (dd, *J* = 10.6 Hz, 4.4 Hz, 2H), 7.03 – 6.97 (m, 1H), 3.44 (s, 2H), 3.04 (s, 6H). **^{13}C NMR** (100 MHz, DMSO-*d6*) δ 162.17, 153.03, 145.39, 128.32, 127.31, 124.30, 84.70, 39.52, 30.26, 26.97. **FTIR** (neat): 3501, 2934, 1740, 1660, 1052 cm^{-1}. **HRMS** (ESI) m/z calculated for $C_{13}H_{14}N_2O_4$ $(M+H)^+$: 263.1032, found: 263.1040.

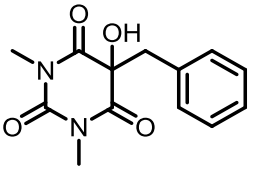

5-Hydroxy-1,3-dimethyl-5-(4-methylbenzyl)pyrimidine-2,4,6(1*H*,3*H*,5*H*)-trione (15r): The reaction of 1,3-dimethyl-5-(4-methylbenzyl)pyrimidine-2,4,6(1*H*,3*H*,5*H*)-trione (33 mg, 0.126 mmol), KO-*t*-Bu (28 mg, 0.25 mmol), in toluene (1.0 mL), at 25 ^{o}C, under air, for 24 h, afforded 82% of **15r** as a white powder without column purification, yield was determined by subtracting the theoretical weight of the by product. **^{1}H NMR** (400 MHz, DMSO-d_6) δ 7.07 (d, *J* = 7.9 Hz, 2H), 6.91 (d, *J* = 7.9 Hz, 2H), 3.38 (s, 2H), 3.03 (s, 6H), 2.20 (s, 3H). **^{13}C NMR** (100 MHz, DMSO-*d6*) δ 162.10, 153.01, 142.30, 132.79, 128.19, 127.83, 84.86, 79.19, 39.52, 29.78, 26.92, 20.64. **FTIR** (neat): 3329, 2927, 1741, 1662, 1219, 1055 cm^{-1}. **HRMS** (ESI) m/z calculated for $C_{14}H_{16}N_2O_4$ $(M+Na)^+$: 299.1008, found: 299.0989.

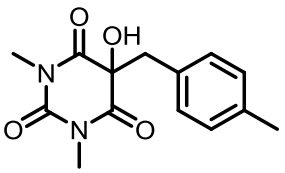

5-Hydroxy-1,3-dimethyl-5-(3-methylbenzyl)pyrimidine-2,4,6(1*H*,3*H*,5*H*)-trione (15s): The reaction of 1,3-dimethyl-5-(3-methylbenzyl)pyrimidine-2,4,6(1*H*,3*H*,5*H*)-trione (54 mg, 0.2078 mmol), KO-*t*-Bu (54 mg, 0.25 mmol), in toluene (1.0 mL), at 25 ^{o}C, under air, for 24 h, afforded 91% of **15s** as a white powder without column purification, yield was determined by subtracting the theoretical weight of the by product. **^{1}H NMR** (400 MHz, DMSO-d_6) δ 7.01 – 6.98 (m, 3H), 6.81 (s, 1H), 3.40 (s, 2H), 3.04 (s, 6H), 2.20 (s, 3H). **^{13}C NMR** (100 MHz, DMSO-*d6*) δ 162.14, 153.03, 145.33, 135.93, 128.94, 127.21, 125.55, 124.96, 84.71, 39.52, 30.21, 26.97, 21.21. **FTIR** (neat): 3265, 2930, 1734, 1672, 1054 cm^{-1}. **HRMS** (ESI) m/z calculated for $C_{14}H_{16}N_2O_4$ $(M+Na)^+$: 299.1008, found: 299.0996.

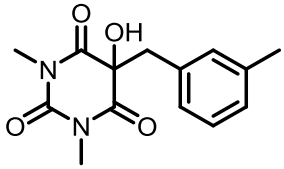

5-Hydroxy-5-(3-methoxybenzyl)-1,3-dimethylpyrimidine-2,4,6(1*H*,3*H*,5*H*)-trione (15t): The reaction of 5-(3-methoxybenzyl)-1,3-dimethylpyrimidine-2,4,6(1*H*,3*H*,5*H*)-trione (69 mg, 0.25 mmol), KO-*t*-Bu (28 mg, 0.25 mmol), in toluene (1.0 mL), at 25 ^{o}C, under air, for 24 h, afforded 81% of **15t** as a white powder without column purification, yield was determined by

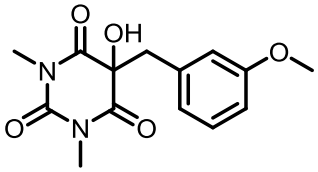

subtracting the theoretical weight of the by product. **^{1}H NMR** (400 MHz, DMSO-d_6) δ 7.02 (t, J = 7.9 Hz, 1H), 6.81 – 6.76 (m, 2H), 6.61 – 6.56 (m, 1H), 3.66 (s, 3H), 3.41 (s, 2H), 3.04 (s, 6H). **^{13}C NMR** (100 MHz, DMSO-*d6*) δ 162.17, 158.76, 153.02, 147.04, 128.16, 120.83, 114.27, 109.44, 84.58, 54.71, 39.52, 39.52, 30.32, 26.97. **FTIR** (neat): 3405, 2932, 1735, 1662, 1054 cm^{-1}. **HRMS** (ESI) m/z calculated for $C_{14}H_{16}N_2O_5$ $(M+Na)^+$: 315.0957, found: 315.0952.

2B.8.5. Appendix II: Copies of ^{1}H and ^{13}C NMR spectra of representative compounds

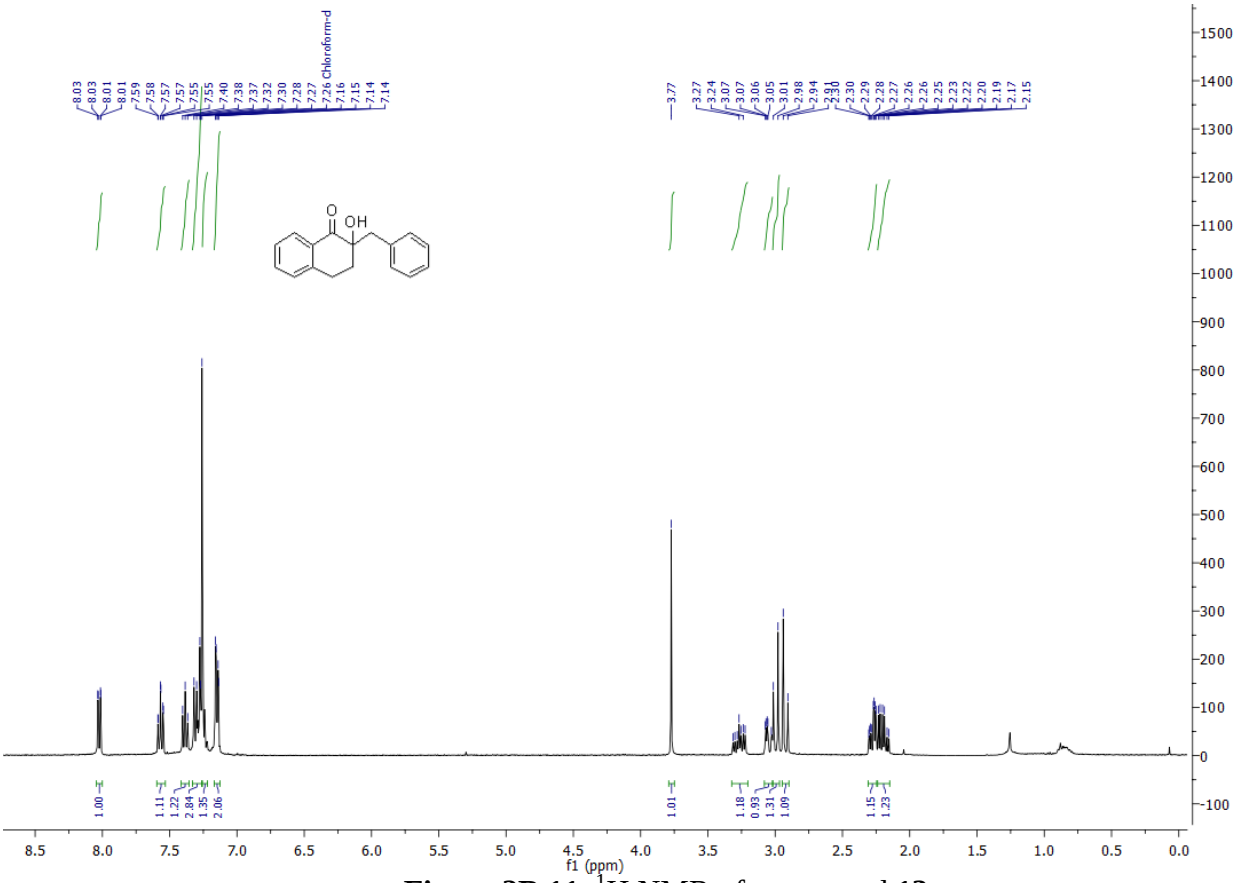

Figure 2B.11. ^{1}H NMR of compound **13a**

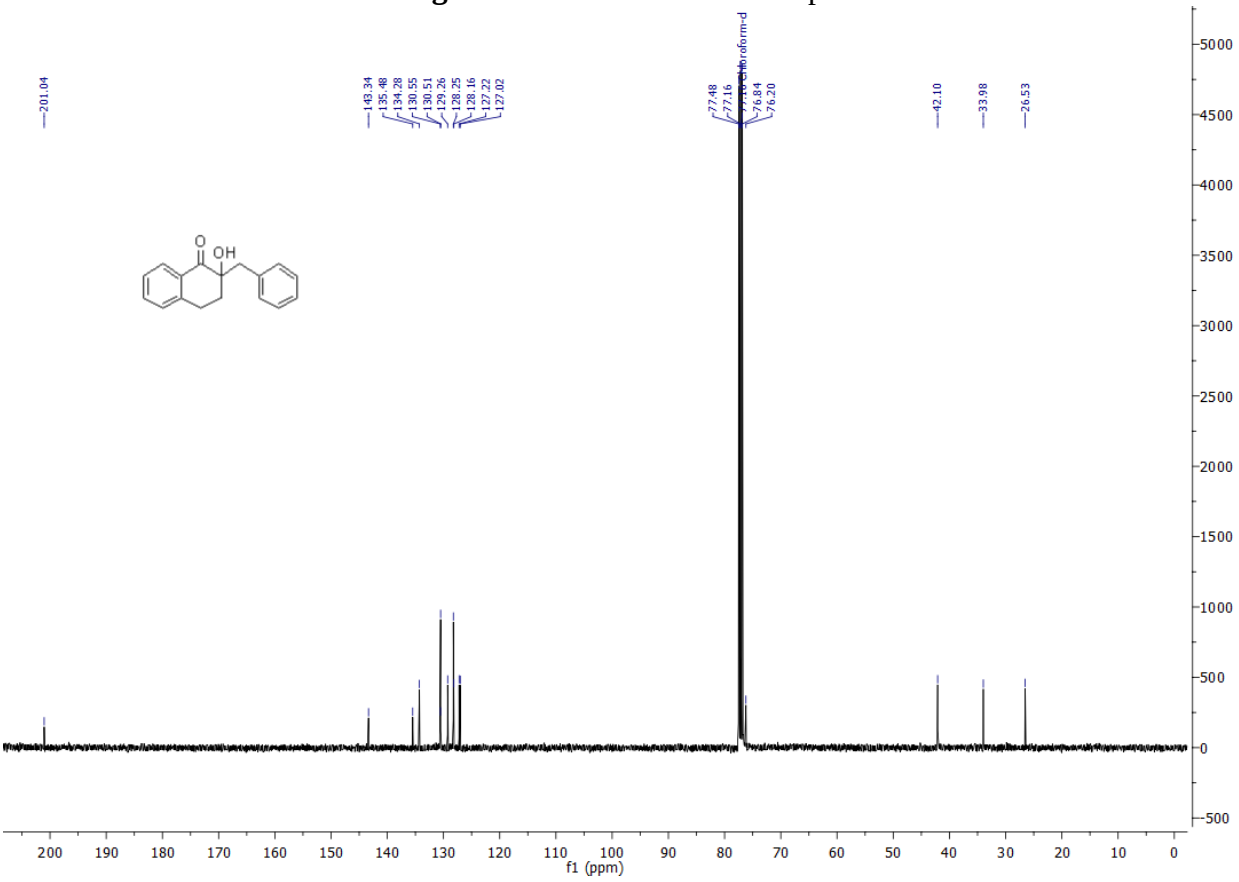

Figure 2B.12. ^{13}C NMR of compound **13a**

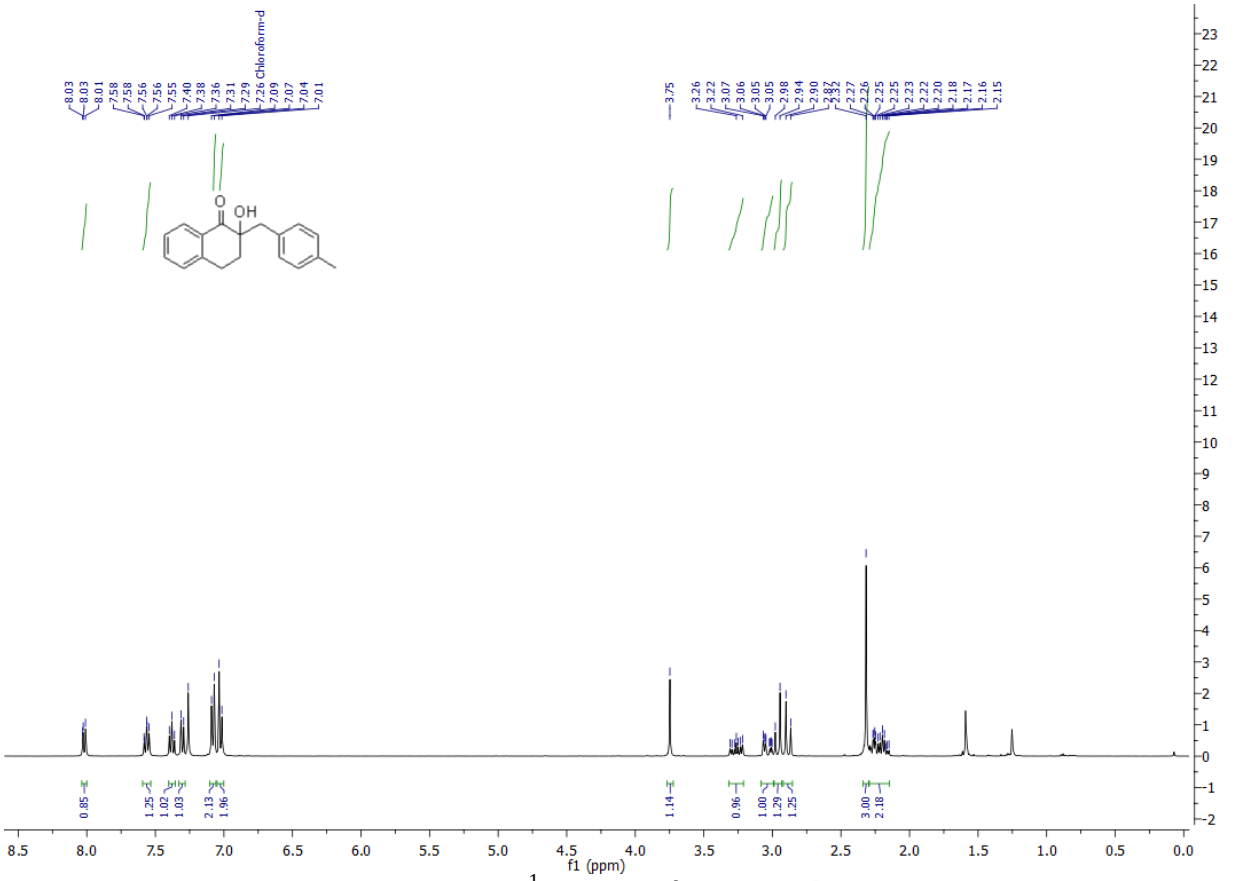

Figure 2B.13. ^{1}H NMR of compound **13e**

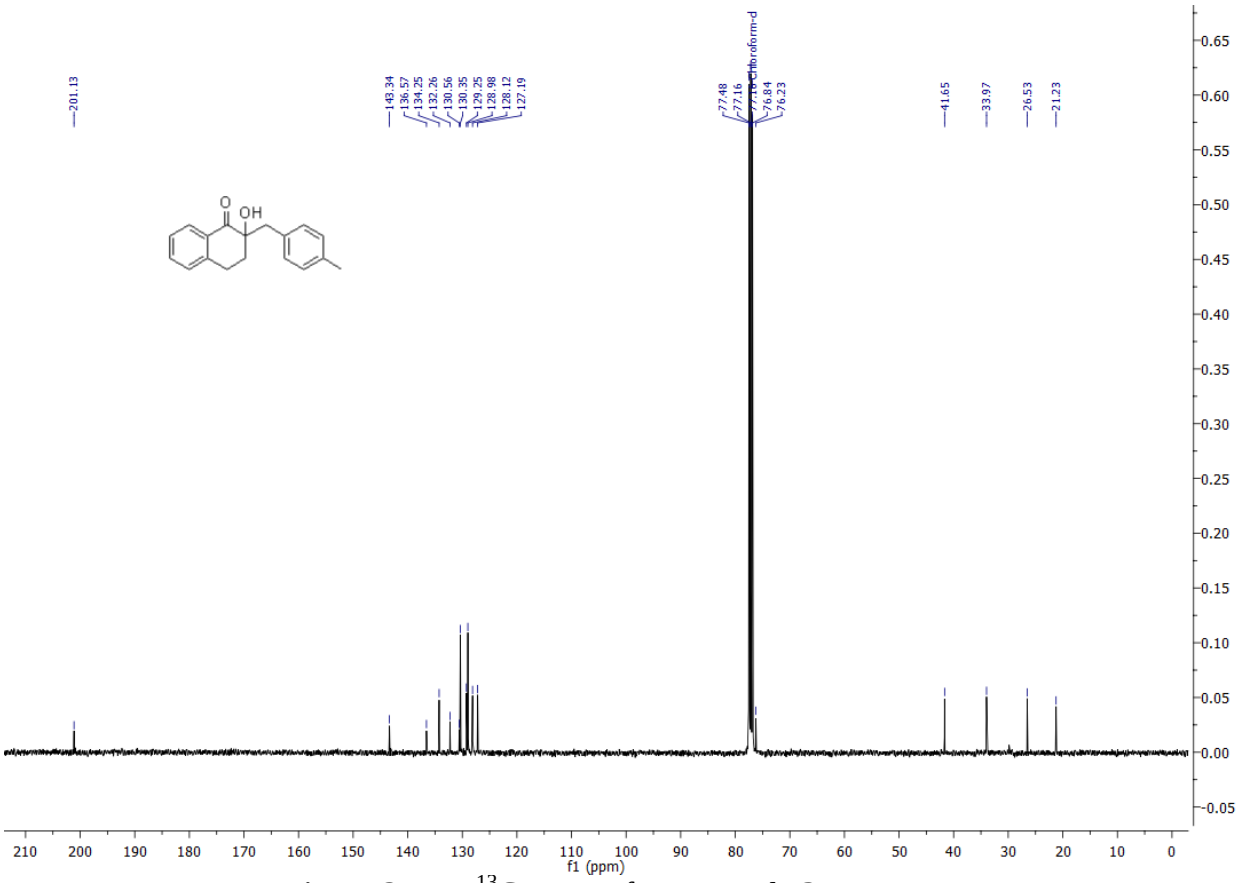

Figure 2B.14. ^{13}C NMR of compound **13e**

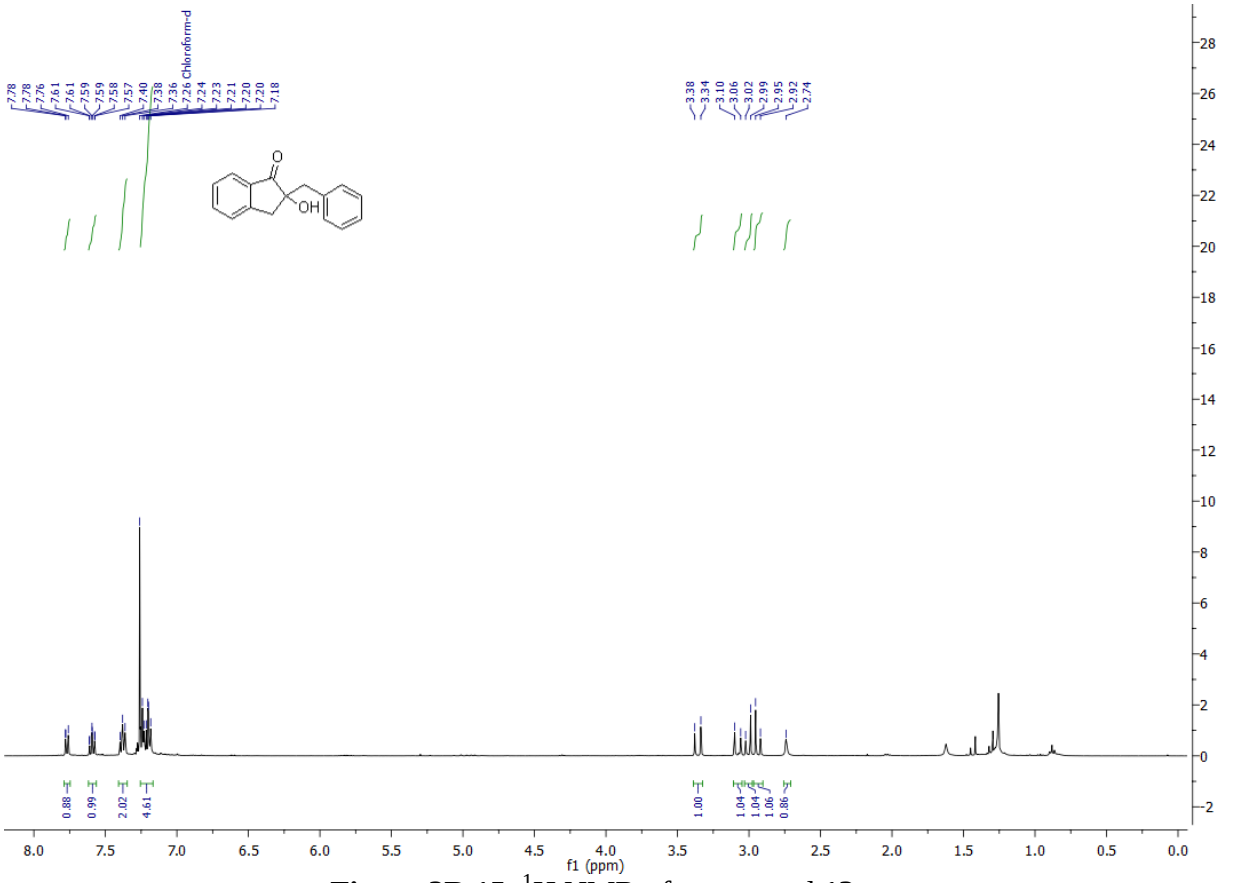

Figure 2B.15. ^{1}H NMR of compound **13m**

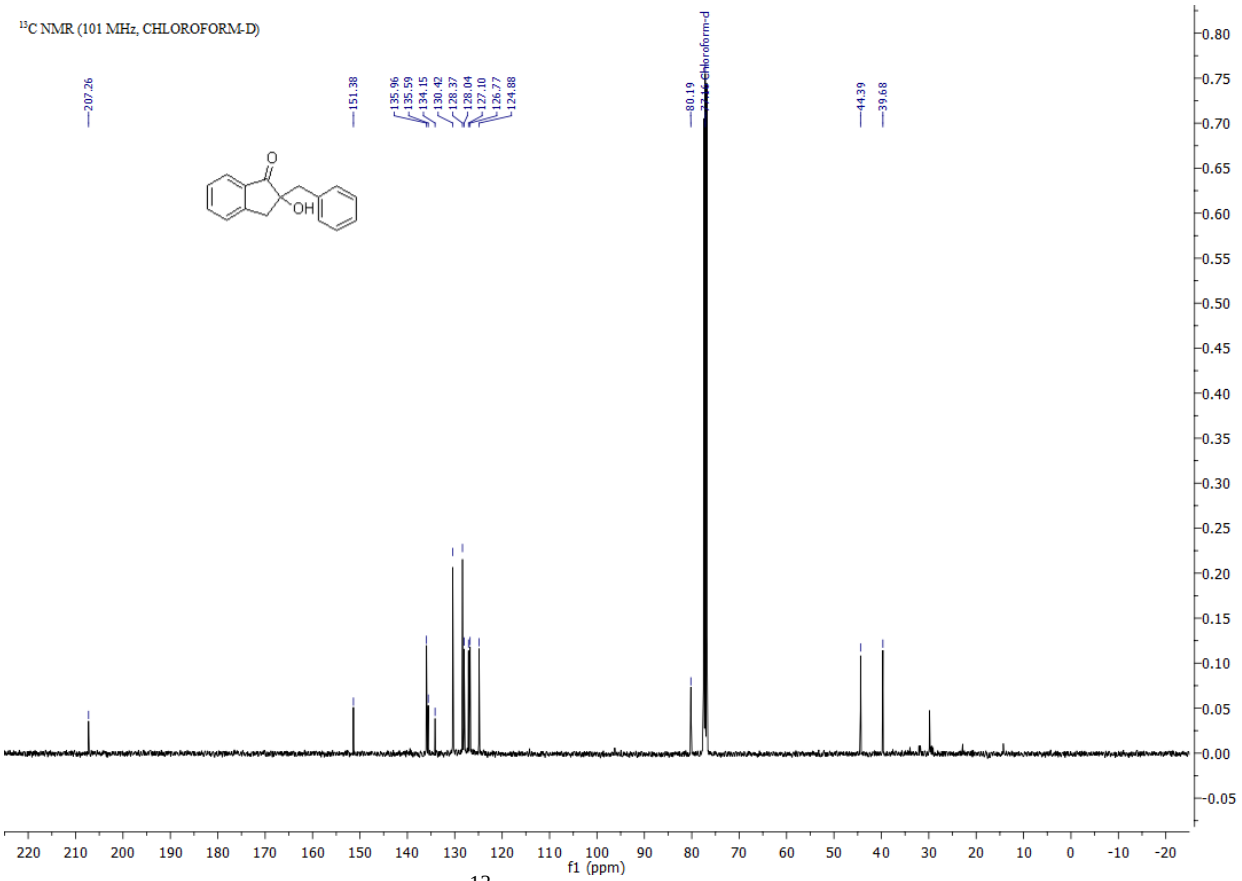

Figure 2B.16. ^{13}C NMR of compound **13m**

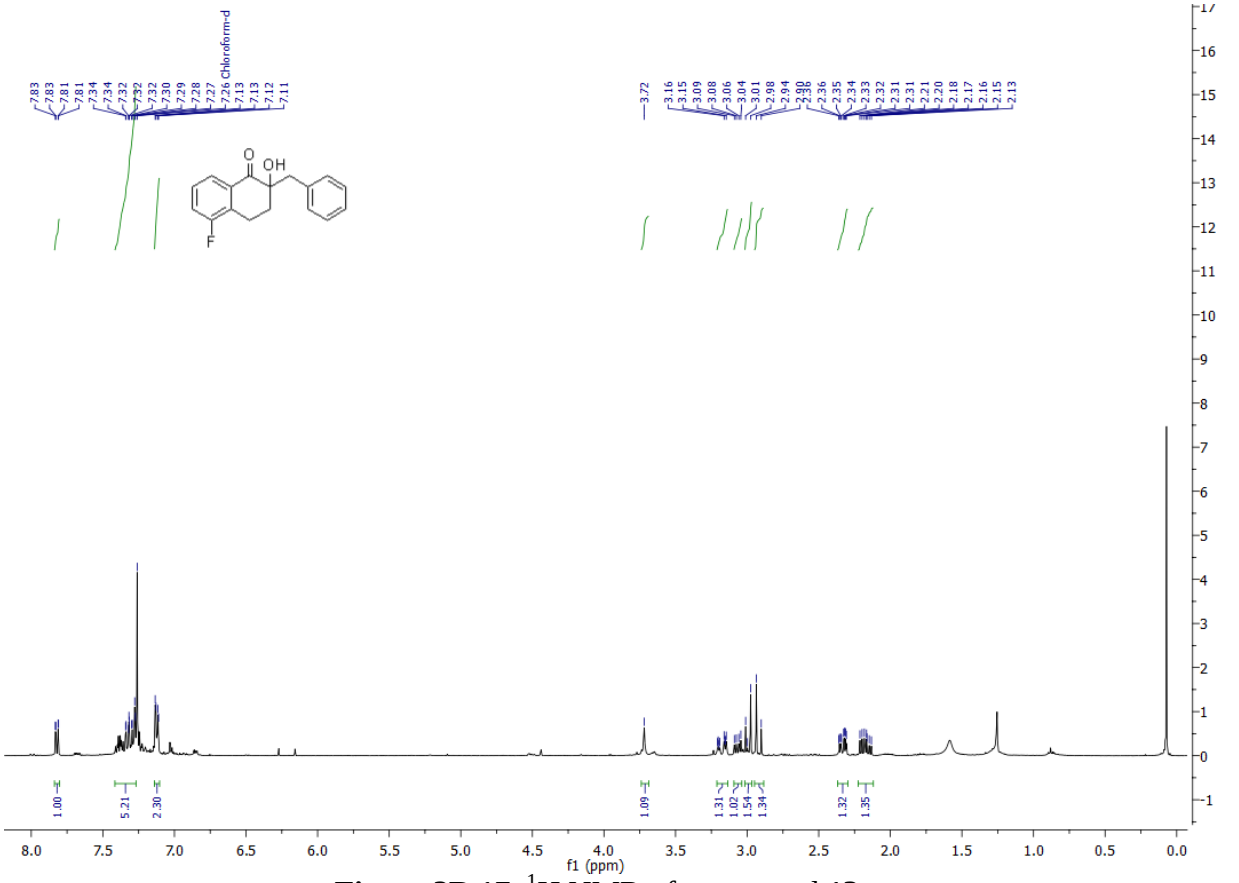

Figure 2B.17. ^{1}H NMR of compound **13u**

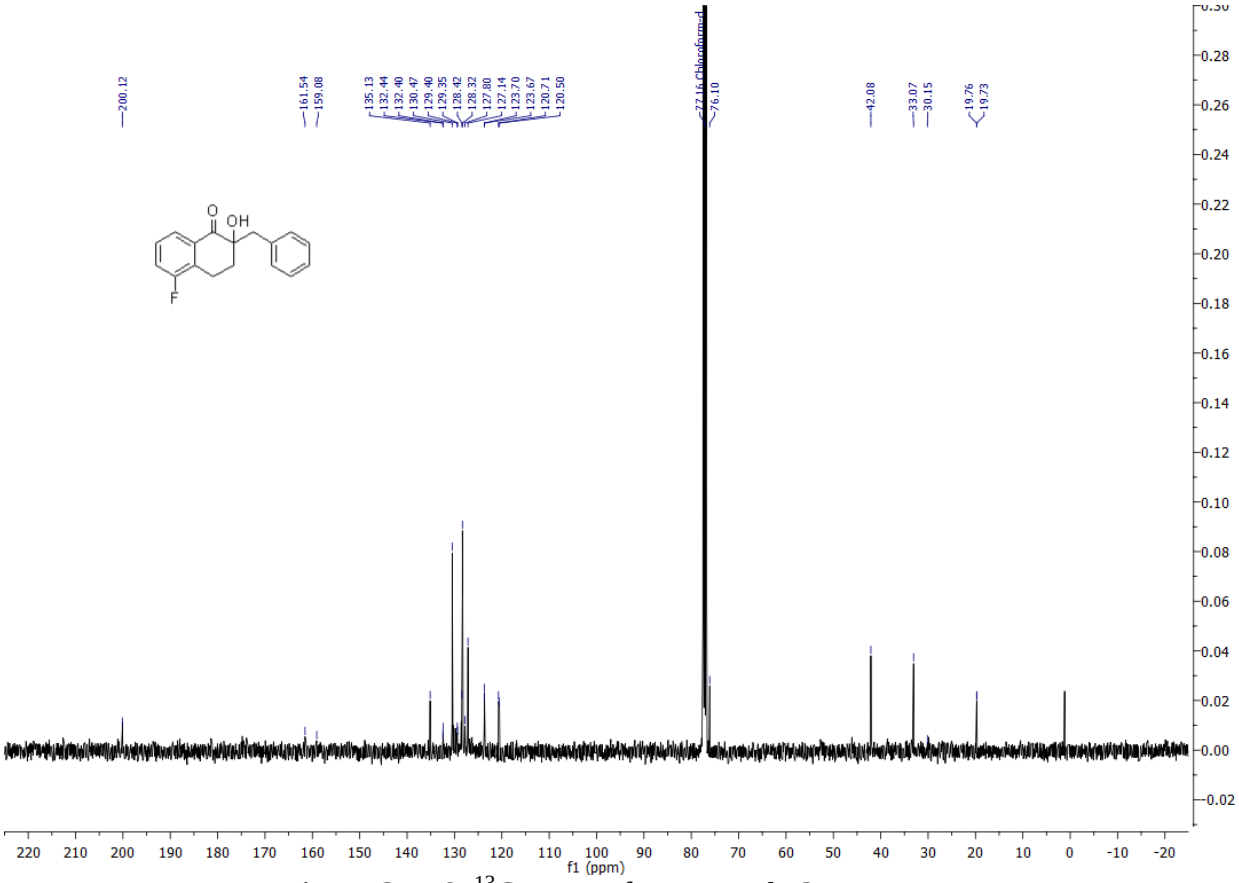

Figure 2B.18. ^{13}C NMR of compound **13u**

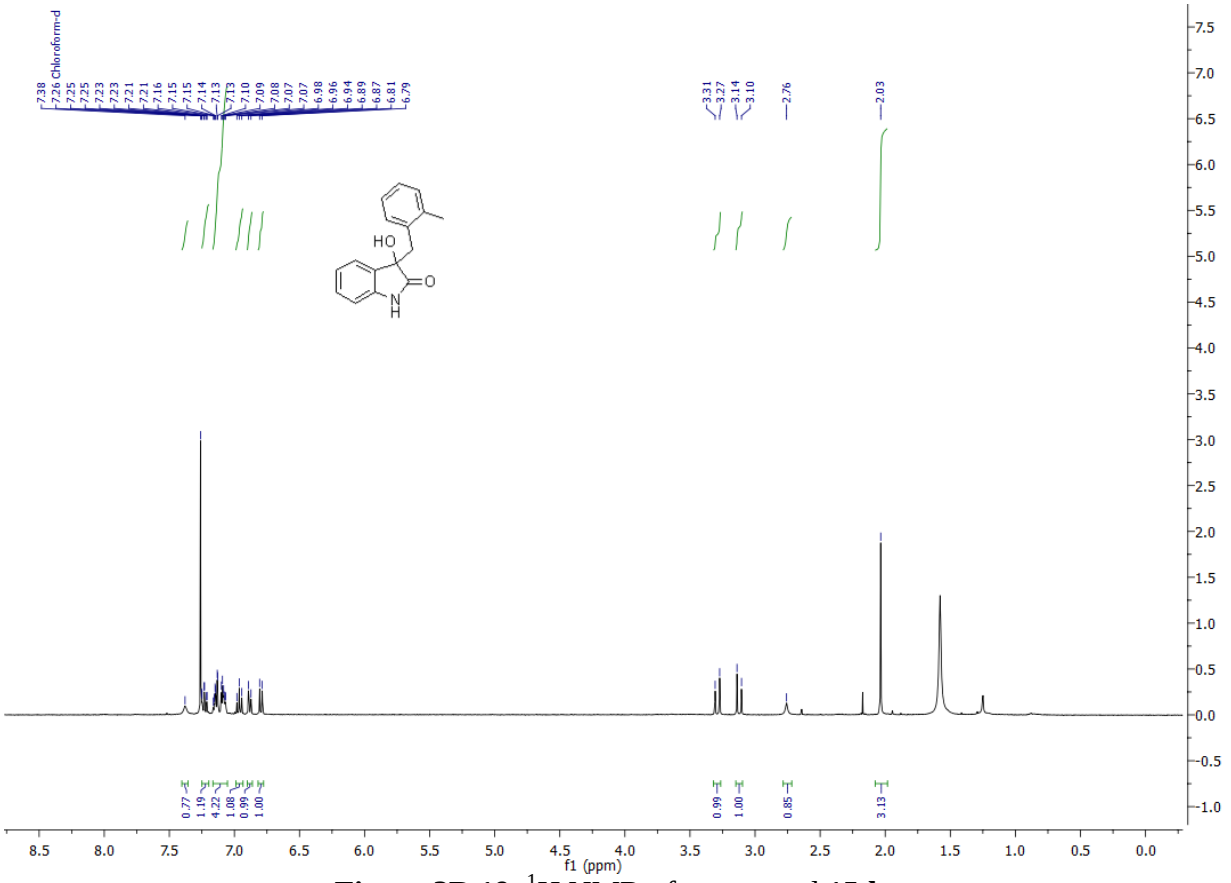

Figure 2B.19. ^{1}H NMR of compound **15d**

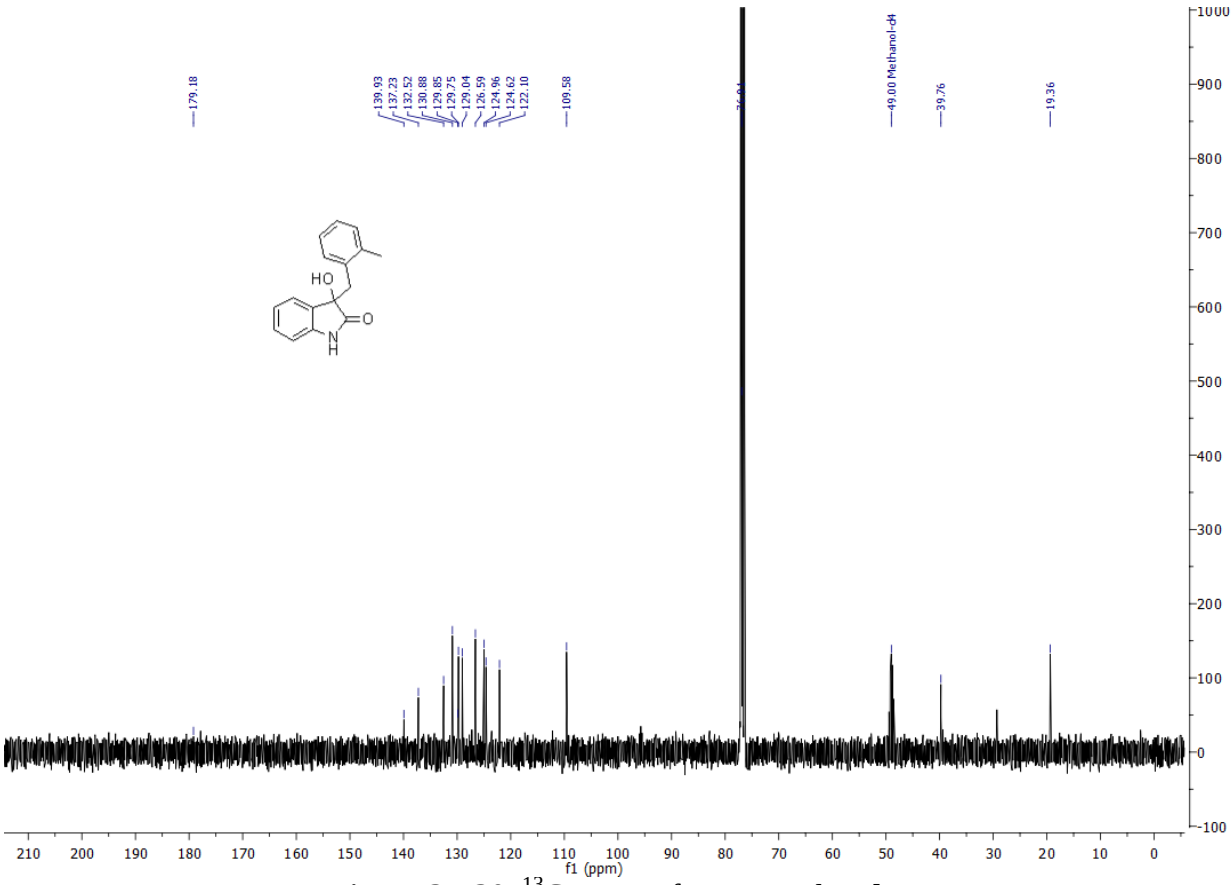

Figure 2B.20. ^{13}C NMR of compound **15d**

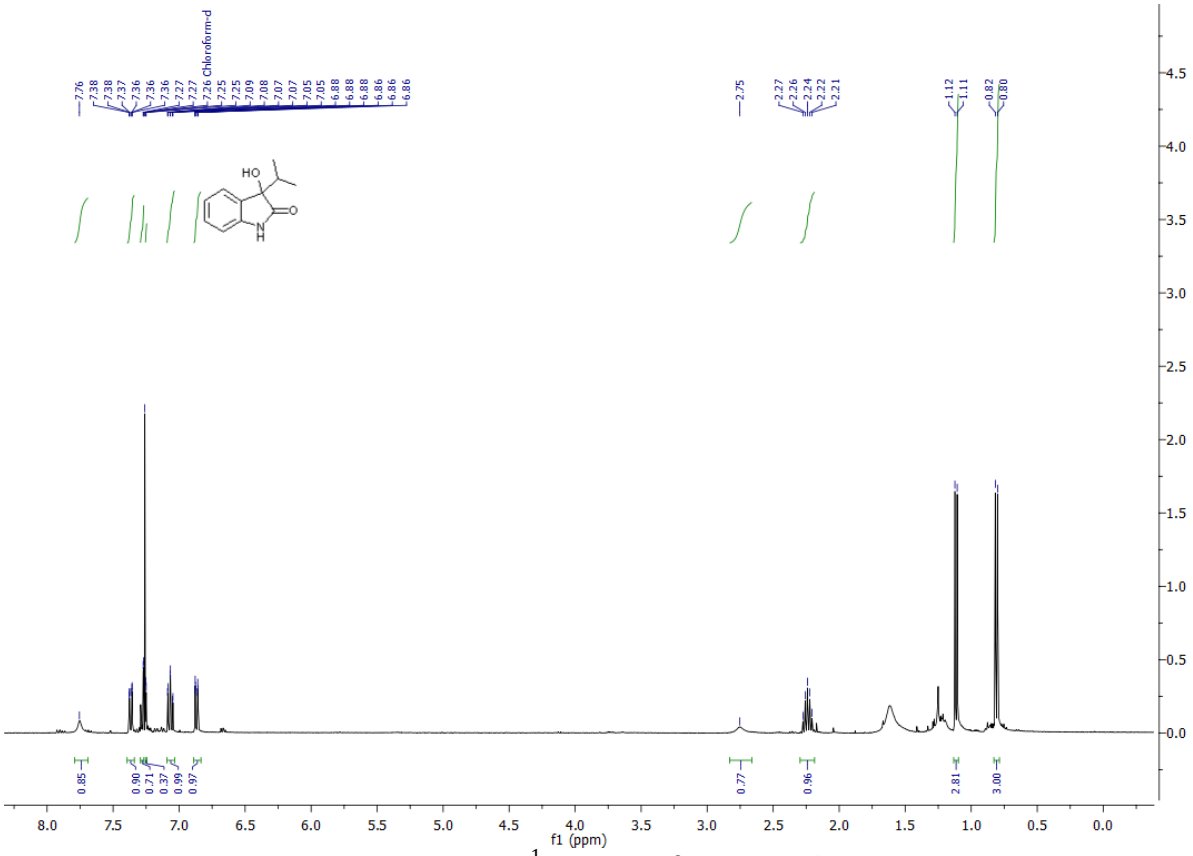

Figure 2B.21. ^{1}H NMR of compound **15j**

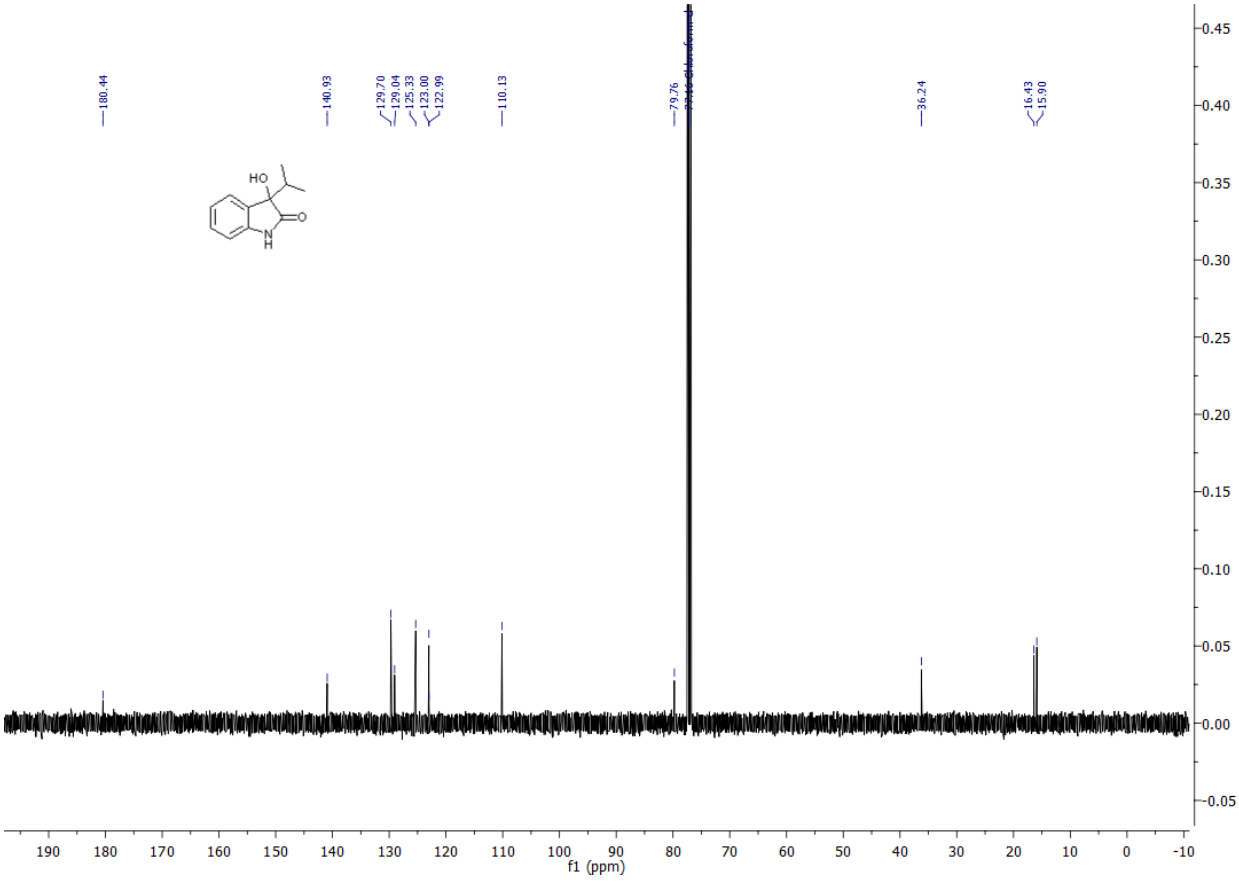

Figure 2B.22. ^{13}C NMR of compound **15j**

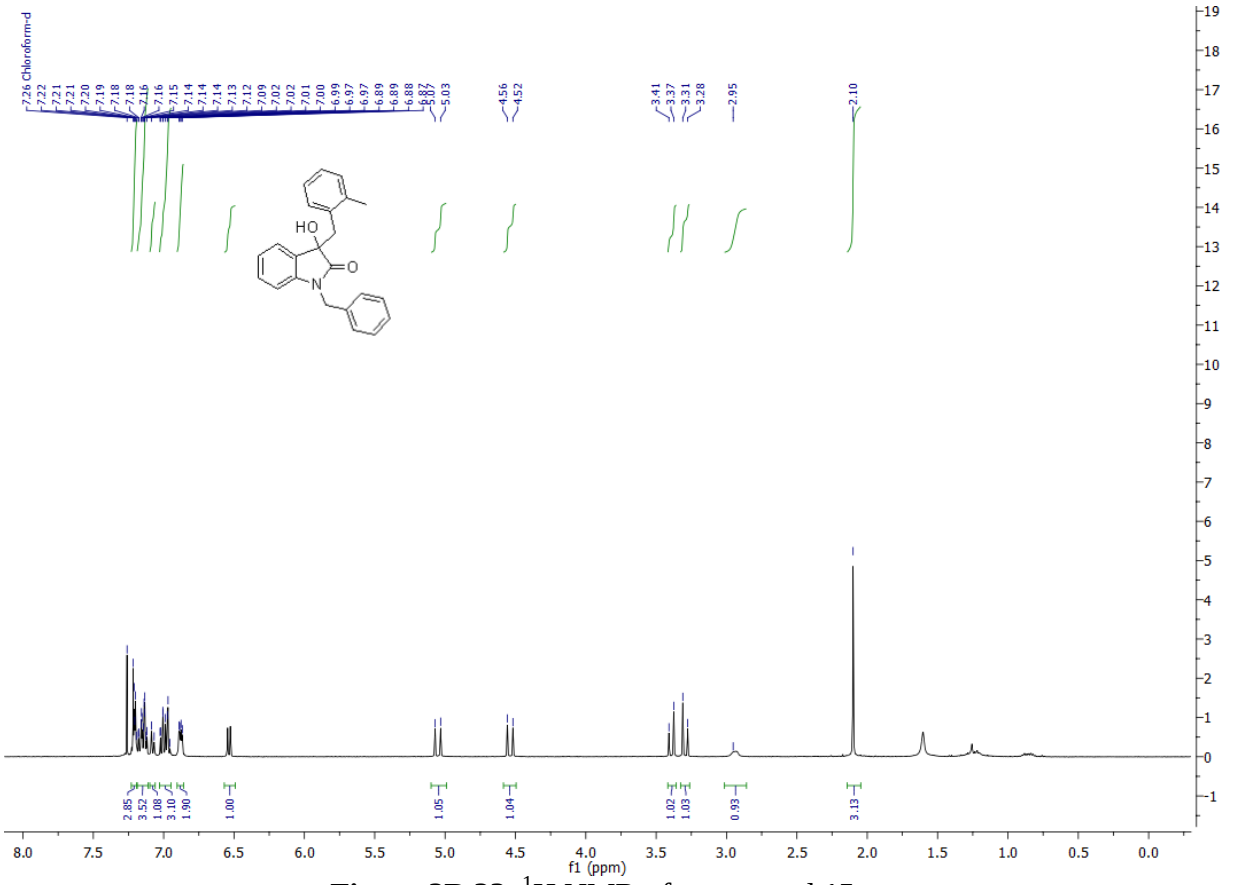

Figure 2B.23. ^{1}H NMR of compound **15m**

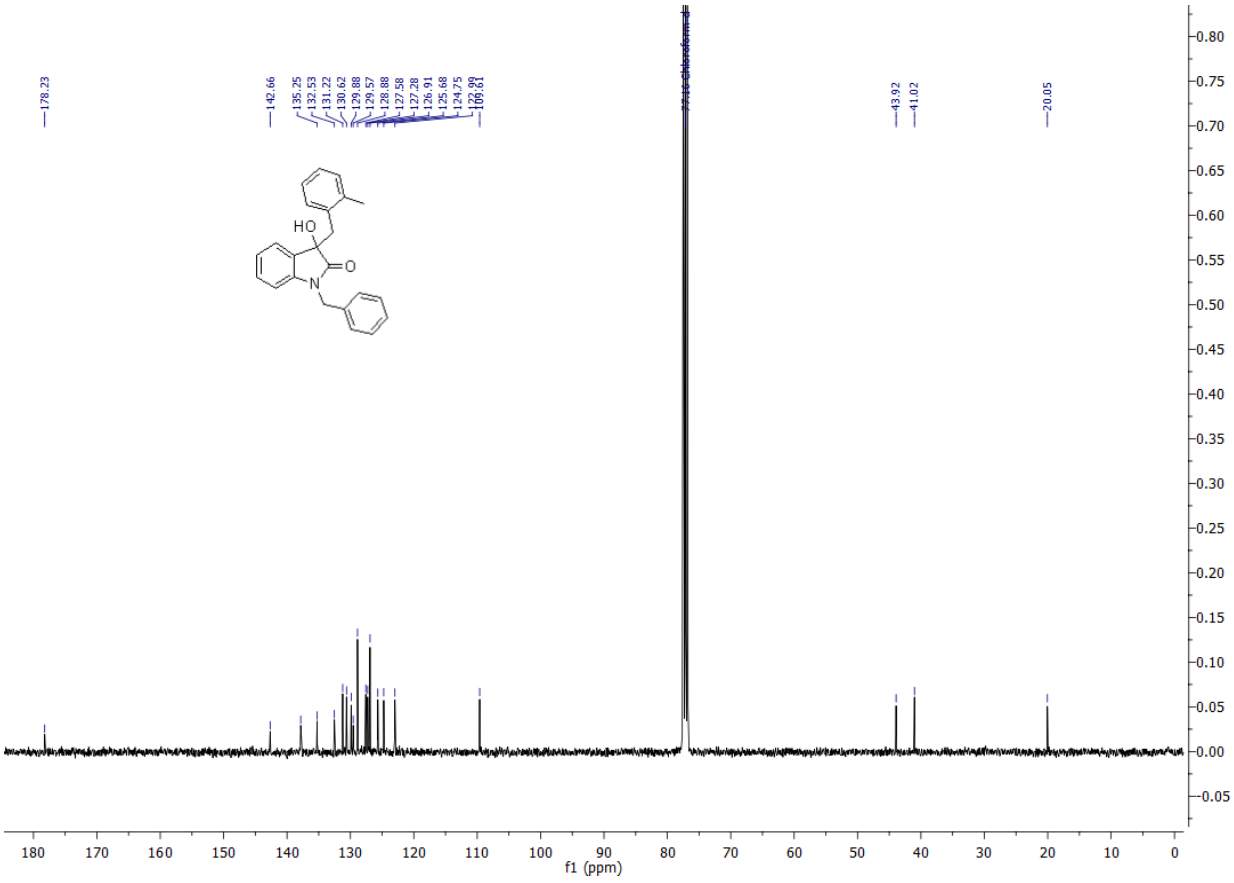

Figure 2B.24. ^{13}C NMR of compound **15m**

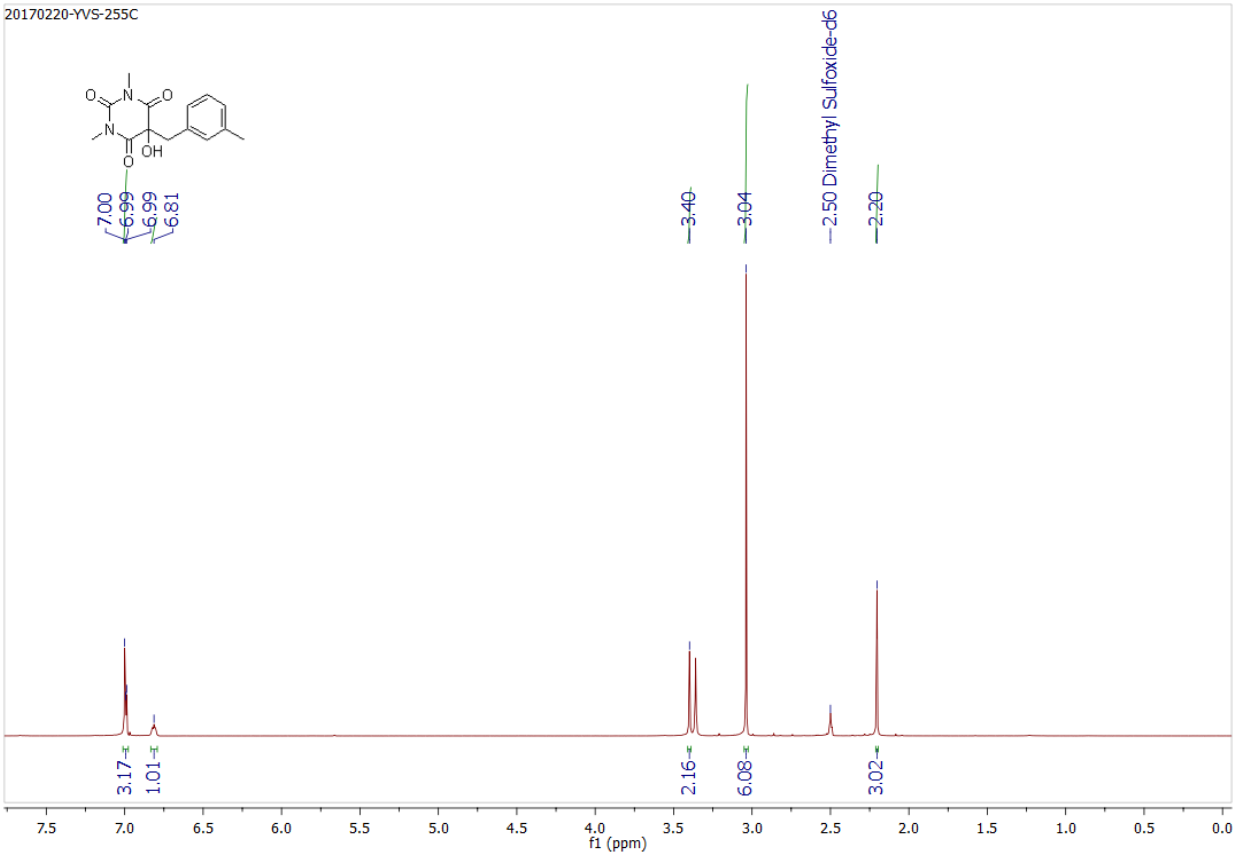

Figure 2B.25. ^{1}H NMR of compound **15s**

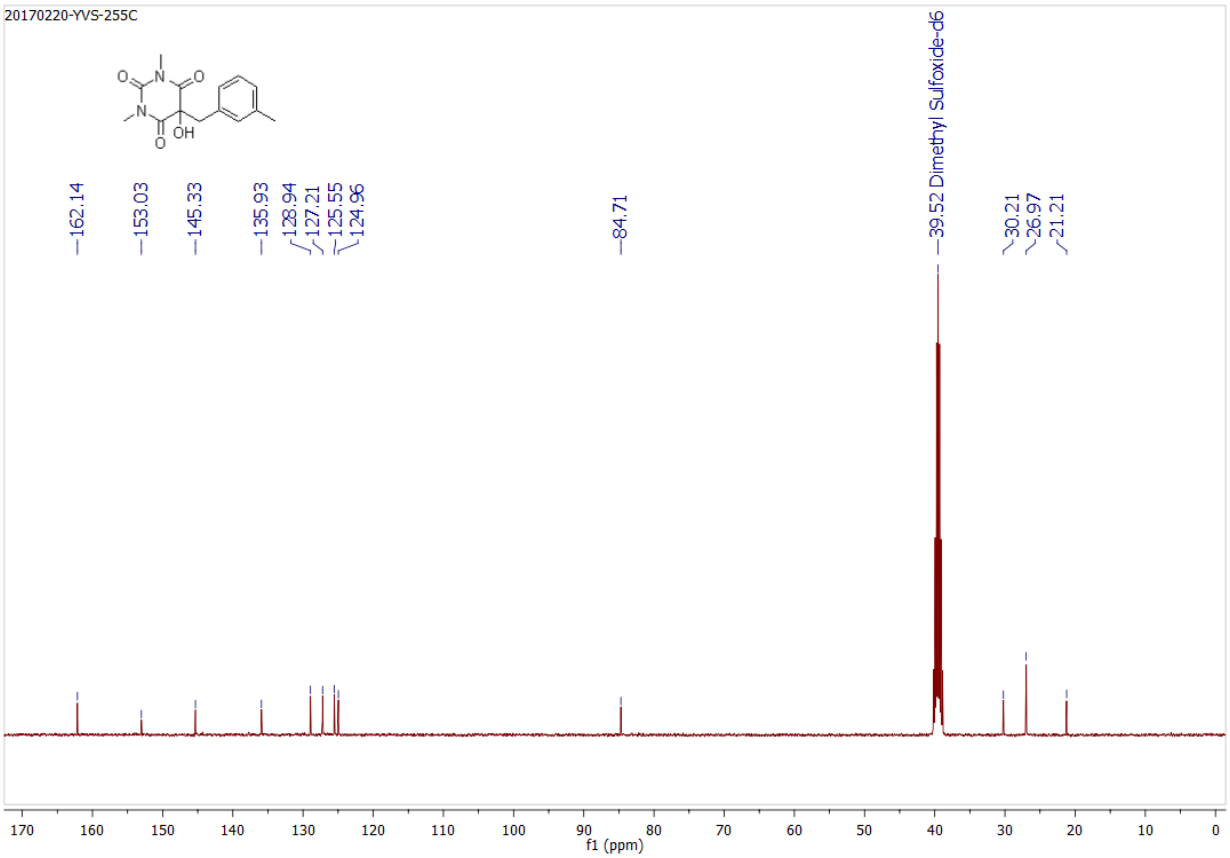

Figure 2B.26. ^{13}C NMR of compound **15s**

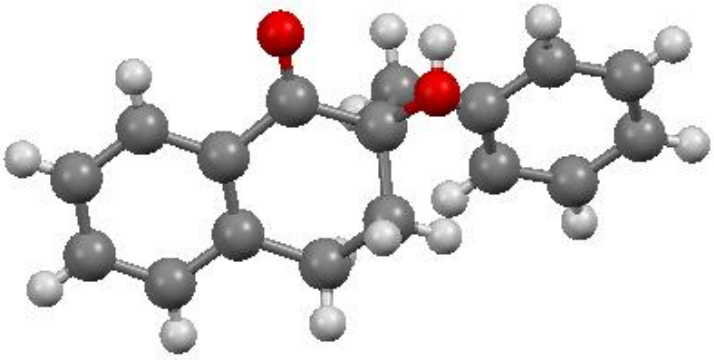

Figure 2B.27. Single crystal structure for compound **13a**

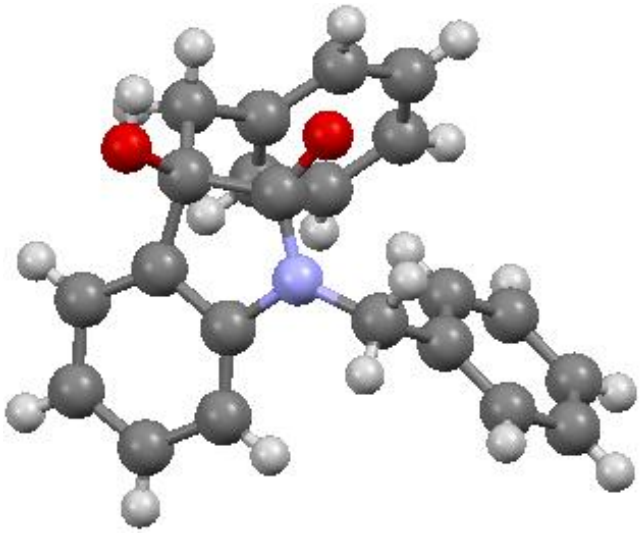

Figure 2B.28. Single crystal structure for compound **15l**

2B.9. References:

(1) Chen, B.-C.; Zhou, P.; Davis, F. A.; Ciganek, E. *Organic Reactions*, Vol. 62 (Ed.: L. E. Overman), Wiley, New York, 2003, p. 1.
(2) Matsuda, H.; Yoshida, K.; Miyagawa, K.; Asao, Y.; Takayama, S.; Nakashima, S.; Xu, F.; Yoshikawa, M. *Bioorg. Med. Chem*. **2007**, *15*, 1539.
(3) Olack, G.; Morrison, H. *J. Org. Chem*. **1991**, *56*, 4969.
(4) Chen, B. C.; Zhao, R.; Gove, S.; Wang, B.; Sundeen, J. E.; Salvati, M. E.; Barrish, J. C. *J. Org. Chem.* **2003**, *68*, 10181.
(5) Hewawasam, P.; Meanwell, N. A.; Gribkoff, V. K.; Dworetzky, S. I.; Boissard, C. G. *Bioorg. Med. Chem. Lett*. **1997**, *7*, 1255.
(6) Rasmussen, H. B.; MacLeod, J. K. *J. Nat. Prod*. **1997**, *60*, 1152.
(7) Dietliker, K.; Murer, P.; Hsler, R.; Jung, T. PCT Int. Appl. US 20100104979, 2010.
(8) Decker, C.; Viet, T. N. T.; Decker, D.; Weber-Koehl, E. *Polymer* **2001**, *42*, 5531.
(9) Nagase, H.; Hagio, H.; Ishikawa, H.; Shimoju, N.; Yoshida, A.; Naito, Y. PCT Int. Appl. US 20150185368A1, 2015.
(10) (a) Davis, F. A.; Chen, B.-C. *Chem. Rev.* **1992**, *92*, 919. (b) Voutyritsa, E.; Theodorou, A.; Kokotos, C. G. *Org. Biomol. Chem.* **2016**, *14*, 5708. (c) Wang, T.; Jiao, N. *J. Am. Chem. Soc.* **2013**, *135*, 11692. (d) Brodsky, B. H.; Bois, J. D. *J. Am. Chem. Soc.* **2005**, *127*, 15391. (e) Odagi, M.; Furukori, K.; Yamamoto, Y.; Sato, M.; Iida, K.; Yamanaka, M.; Nagasawa, K. *J. Am. Chem. Soc.* **2015**, *137*, 1909. (f) Watanabe, T.; Odagi, M.; Furukori, K.; Nagasawa, K. *Chem. Eur. J.* **2014**, *20*, 591. (g) Yang, Y.; Moinodeen, F.; Chin, W.; Ma, T.; Jiang, Z.; Tan, C. H. *Org. Lett.* **2012**, *14*, 4762.
(11) Use of oxygen/air-mediated transformation review: (a) Stahl, S. S. *Science* **2005**, *309*, 1824. (b) Que, L.; Tolman, W. B. *Nature* **2008**, *455*, 333. (c) Punniyamurthy, T.; Velusamy, S.; Iqbal, J. *Chem. Rev.* **2005**, *105*, 2329. (d) Zhang, C.; Tang, C.; Jiao, N. *Chem. Soc. Rev.* **2012**, *41*, 3464.
(12) Examples of O_2 fixation see: (a) Pattillo, C. C.; Strambeanu, L. I.; Calleja, P.; Vermeulen, N. A.; Mizuno, T.; White, M. C. *J. Am. Chem. Soc.* **2016**, *138*, 1265. (b) Saha, D.; Saha, D. Guin, J. *ACS Catal.* **2016**, *6*, 6050. (c) Anson, C. W.; Ghosh, S.; Hammes-Schiffer, S; Stahl, S. S. *J. Am. Chem. Soc*. **2016**, *138*, 4186. (d) Brink, G.-J. T; Arends, I. W. C. E.; Sheldon, R. A. *Science* **2000**, 287, 1636. (e) Brice, J. L.; Harang , J. E.; Timokhin, V. I.; Anastasi, N. R.; Stahl, S. S. *J. Am. Chem. Soc.* **2005**, *127*, 2868. (f) Zhang, Y.-H., Yu, J.-Q. *J. Am. Chem. Soc.* **2009**, *131*, 14654. (g) Chiba, S.; Zhang, L.; Lee, J.-Y. *J. Am. Chem. Soc.* **2010**, *132*, 7266. (h) Lyons, T. W.; Reinhard, C. T.; Planavsky, N. J. *Nature* **2012**, *506*, 307.
(13) El-Qisairi, A. K.; H. A. Qaseer, *J. Organomet. Chem.* **2002**, *659*, 50.
(14) Chuang, G. J.; Wang, W.; Lee, E.; Ritter, T. *J. Am. Chem. Soc.* **2011**, *133*, 1760.
(15) Liang, Y-F.; Jiao, N. *Angew. Chem. Int. Ed.* ***2014***, *53*, 548.
(16) Sui-Boon, D. S.; Wang, M.; Zhao, Y. *ACS Catal*. **2015**, *5*, 3609.
(17) Tsang, A. S-K.; Kapat, A.; Schoenebeck, F. *J. Am. Chem. Soc.* **2016**, *138*, 518.

(18) Ishimaru, T.; Shibata, N.; Nagai, J.; Nakamura, S.; Toru, T.; Kanemasa, S. *J. Am. Chem. Soc*. **2006**, *128*, 16488.
(19) Sano, D; Nagata, K.; Itoh, T. *Org. Lett*. **2008**, *10*, 1593.

Chapter 3

Section A:

Iron-Catalyzed Batch/Continuous Flow Synthesis of Peroxides and Evaluation of Anticancer Property

3A. Iron-Catalyzed Batch/Continuous Flow Synthesis of Peroxides and Evaluation of Anticancer Property

3A.1. Abstract

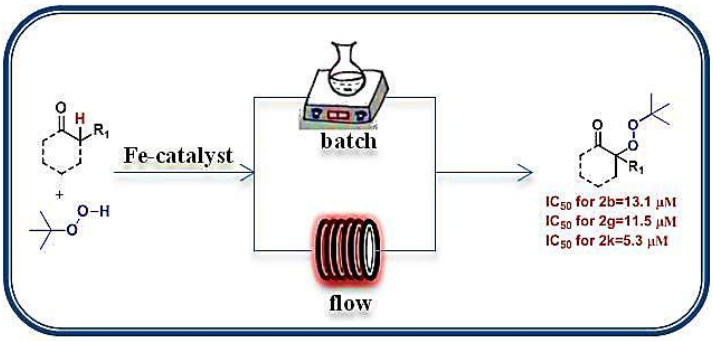

In this chapter, we have demonstrated for the first time, Iron-catalyzed C-H peroxidation of carbonyl compounds under batch/continuous flow. Using the present protocol, a library of linear alkylated and arylated peroxides is synthesized in good to excellent yield. This protocol is highly selective and general for a range of biologically important derivatives of 2-oxindole, barbituric acid, and 4-hydroxy coumarin with a good functional group tolerance and avoiding the cleavage of the peroxide bond. To minimize the explosive hazards of peroxides, we have transformed this reaction to a continuous flow. Moreover, the current peroxidation reaction is scalable to grams and also synthesizable in a continuous flow with increased safety in a short duration. In mechanistic studies, we found that Fe-(II) undergoes a redox type process to generate the radical intermediates, which subsequently recombine selectively to form the stable peroxides. Finally, the potential of peroxides is evaluated by cell viability assay and exhibits good anticancer activity with minimum IC_{50}= 5.3 μM.

3A.2. Introduction to continuous flow chemistry

Continuous flow chemistry is a new paradigm in organic synthesis. The homogeneous and heterogeneous catalysis both are suitable for this newly emerged technique, where recycling of catalyst is imperative. The continuous-flow reactor is a powerful synthetic tool in the bulk chemical, petrochemical, and pharmaceutical industry. The continuous flow chemistry tools meet most of the principles of green chemistry.[1,2] The continuous-flow reactor allows greater process windows, more efficiency, better safety, and superior mass transfer feature than traditional batch reactions.[3-6] Moreover, the flow chemistry emerged as a powerful synthesis tool for

handling obnoxious or hazardous material and exothermic reactions with greater safety.

(a) **(b)**

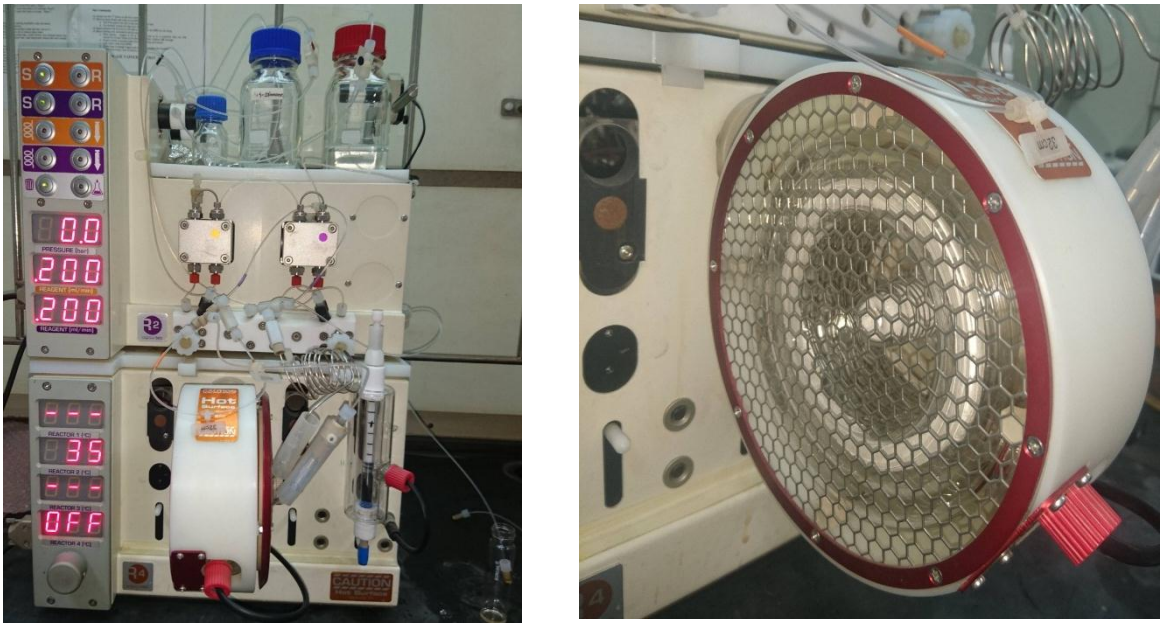

Figure 3A.1. (a) The full setup for the Vapourtec R-series reactor from our laboratory; (b) Image for the coiled reactor.

A typical continuous-flow reactor consists of following parts:

(a) **Pumps**: The commonly employed pumps for continuous flow reactors involve piston, peristaltic, or syringe pumps. The primary function of a pump is to transport the reagents, reactant, or solvent from a vessel or bottle into reaction loops.

(b) **Reaction loops**: The reaction loops are placed to introduce a small volume of reagents or reactants. Loops feed the reagents or solvent into a mixing junction.

(c) **T-piece**: T-piece or mixing piece is a very important component in the continuous flow setup. It is the primary mixing point where two reagent streams are getting mixed and passed into a reactor.

(d) **Coil reactor**: There are many types of reactors are available to conduct a continuous flow operation. The coiled reactors are mainly used for homogeneous reaction conditions. The coil reactor provides heating or cooling and retention time for a reaction, and its length and width varied from case to case.

(e) **Column reactor**: In this type, a reactor is the hollow vertical glass or metal tube packed with a solid catalyst or reagents or scavengers.

(f) **Back pressure regulator**: The back pressure regulator (BPR) controls the pressure in the system. Using the BPR, the superheating of a solvent is possible. For instance,

dichloromethane (DCM) is having a boiling point of 39.6 ^{o}C, but we can heat the DCM well beyond its boiling point.

(g**) Downstream unit**: The *in-line* analytics or reaction monitoring is possible using a continuous flow system by integrating it with various instruments such as IR, UV, and NMR, *etc.*

Designing of the continuous flow synthesis for industrially important molecules which were traditionally synthesized in batch conditions has attracted much attention due to its greater process windows, efficiency, environmentally benign properties, and better safety.[7a-d] Hence, we envision to develop the C-H peroxidation reaction in a continuous flow, which can overcome the explosive hazards.

3A.3. Introduction on peroxidation

Peroxidation can be defined as the addition of the R-O-O- group across the desired functionality. In the realm of science, peroxide bond (C-O-O) is a key pharmacophore due to its omnipresence in a variety of biologically active anticancer,[8a-d] anti-HIV,[9] anthelmintics,[10a-b] and antimalarial,[11a-d,] etc. pharmaceuticals, natural products, and drugs. For instance, Artemisinin constituting cyclic peroxide has been used in curing the malaria. Many of the organic peroxides constituted C-O-O bonds, which are readily cleaved by heat, light, and metals. In such processes, organic peroxides, superoxides, hydroperoxy radicals, hydroxyl radicals, and hydrogen peroxides are cleaved to form the reactive oxygen species (ROS).[12] In the past decades, organic peroxides have proven themselves as potential drug candidates for cellular evaluation. Oxidation has a significant role in living organisms defense system, but on the contrary, it can also be damaging to the cell *via* oxidative stress, where peroxides act as the pro-oxidants.[13]

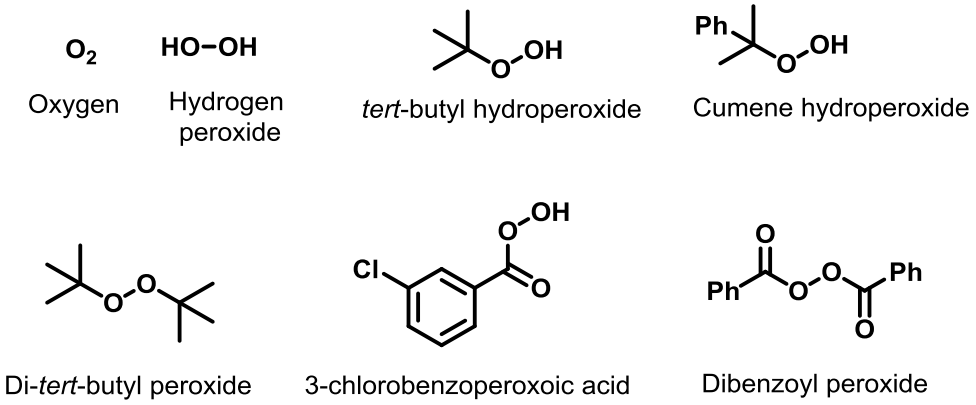

Figure 3A.2. Commonly available peroxylating reagents

Unfortunately, cancer is the second foremost reason for the death of ~8.8 million people per year, the quandary associated with cancer is an inaccessible or late-

stage diagnosis, and higher economic cost makes it one of the lethal diseases. The existing drugs such as docetaxel, doxorubicin, mitomycin, daunorubicin or antibodies, etc. are being used to treat cancer, but their synthesis or isolation is a challenging task.

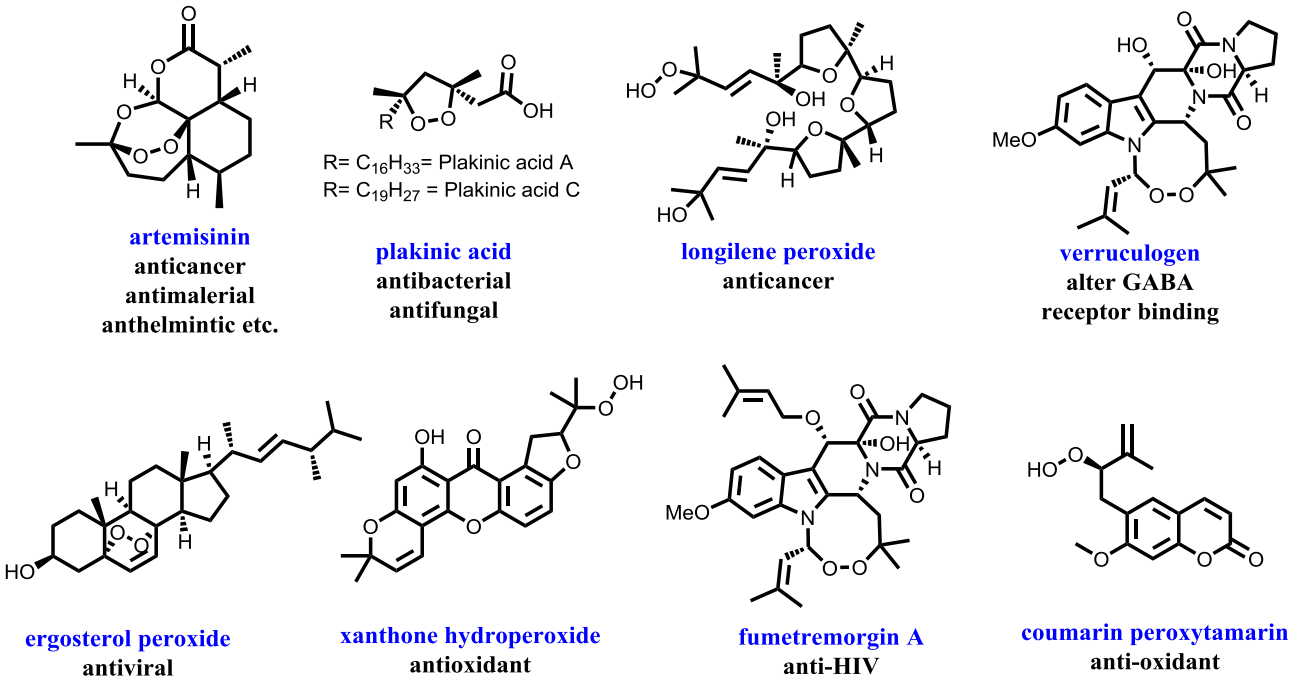

Figure 3A.3. Compounds showing peroxide linkage

On the other hand, *Plasmodium* species is one of the lethal pathogens which cause malaria; according to the World Health Organization (WHO), malaria is responsible for the death of ~4.35 million peoples globally.[14] In past decades varieties of metabolites and naturally occurring peroxy compounds have been isolated, and several of them are highly potent for biological activities. The effective cure for malaria is jeopardized due to escalating resistance against known peroxy compounds.[15] Therefore there is an urgent requirement to develop an efficient and simple protocol for the on-demand synthesis of novel antimalarial drug candidates.

3A.4. Literature background on peroxidation

In 1958, Morris S. Kharasch and George Sosnovsky[16] reported the metal-catalyzed peroxidation reaction of allylic olefin using a copper catalyst and *tert*-butyl benzoperoxoate. By employing this strategy, several reports were established for the peroxidation reaction.

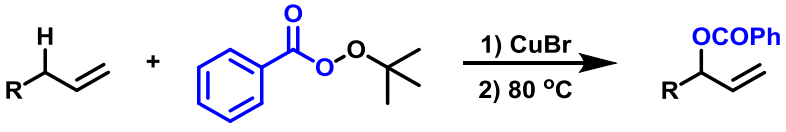

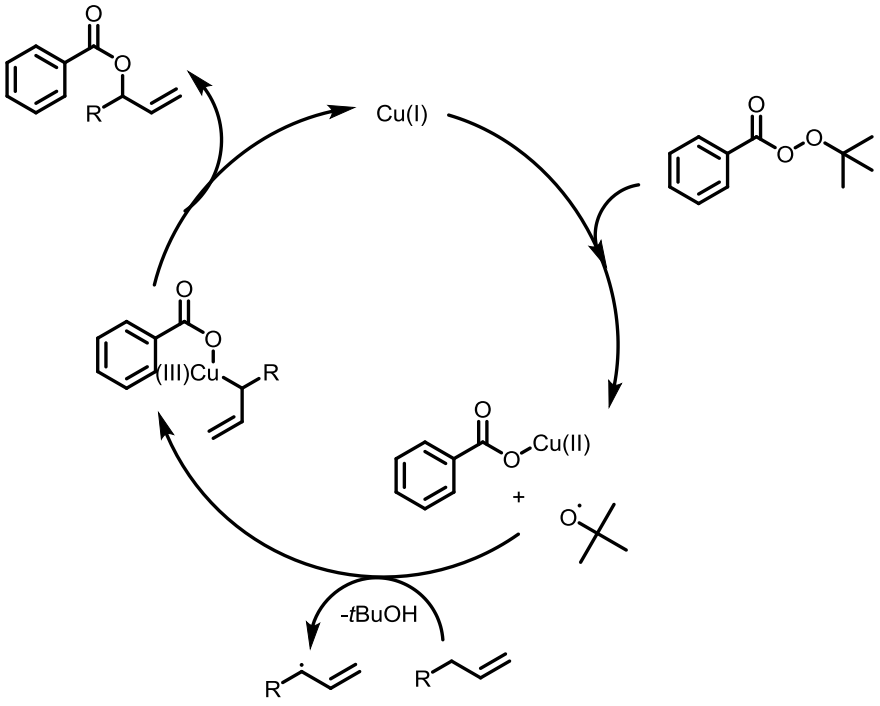

Scheme 3A.1. Kharasch and Sosnovsky reaction

The mechanism of the Kharasch reaction follows a radical pathway. The reaction of metal salts with peroxides undergoes oxidation and gives the alkoxy radical. The alkoxy radical abstracts the hydrogen from the olefin to afford allylic radical. The recombination of alkoxy radical and allylic radical produces the final product and catalyst is regenerated for catalytic cycle.[17]

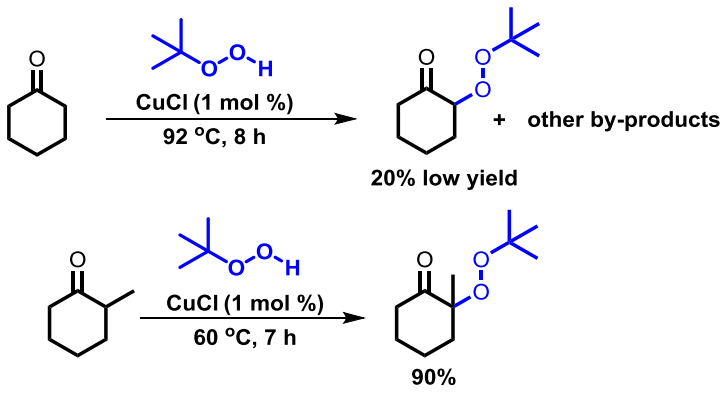

Scheme 3A.2. Kharash-Sosnovsky's approach for peroxidation of carbonyl compounds

In this context, the peroxidation of heterocyclic compounds using ruthenium catalyst and TBHP was achieved by Murahashi and co-workers.[18]

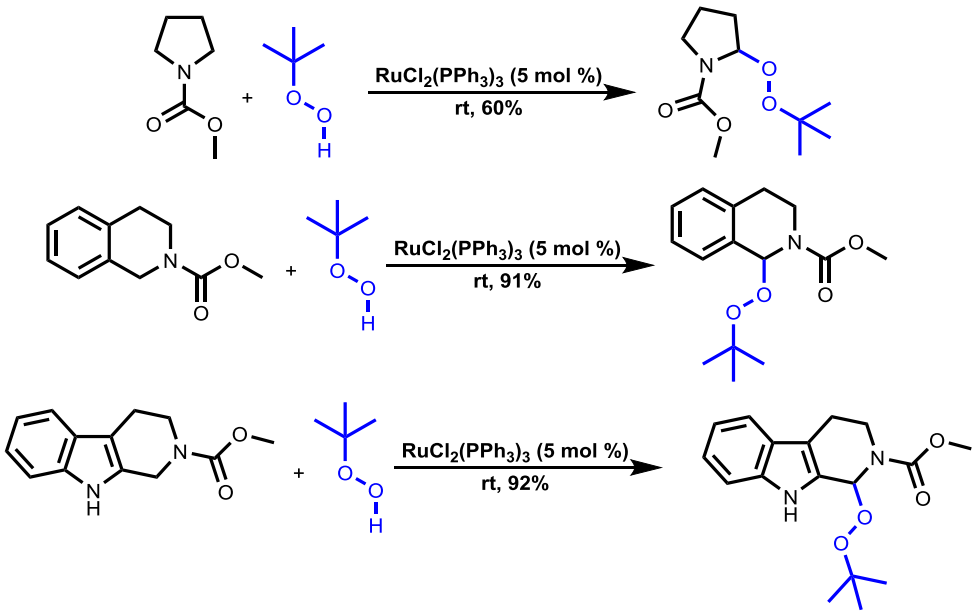

Scheme 3A.3. Murahashi's approach for peroxidation of heterocyclic compounds

Likewise, varieties of metals have been used for the bisperoxidation or difunctionalization reactions.[19-21]

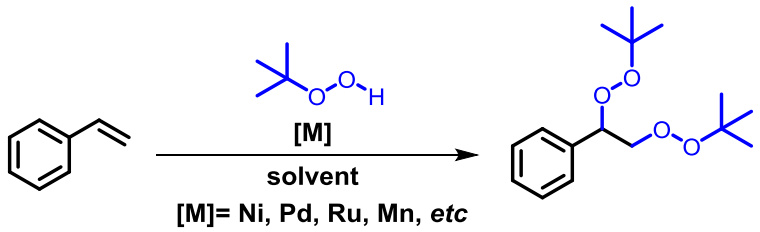

Scheme 3A.4. Miscellaneous approaches for bisperoxidation of olefins using peroxide and metal

Moreover, the difunctionalization reactions of olefins such as carbonylation-peroxidation,[22] carbamoylation-peroxidation,[23] phosphorylation–peroxidation,[24] alkoxycarbonylation–peroxidation,[25] azidation-peroxidation,[26] alkylation-peroxidation,[27] sulfonylation-peroxidation,[28] perfluoroalkylation-peroxidation,[29] trifluoromethylation-peroxidation,[30] and nitration-peroxidation[31] *etc*. using metals are extensively studied in the literature (Scheme 3A.5).

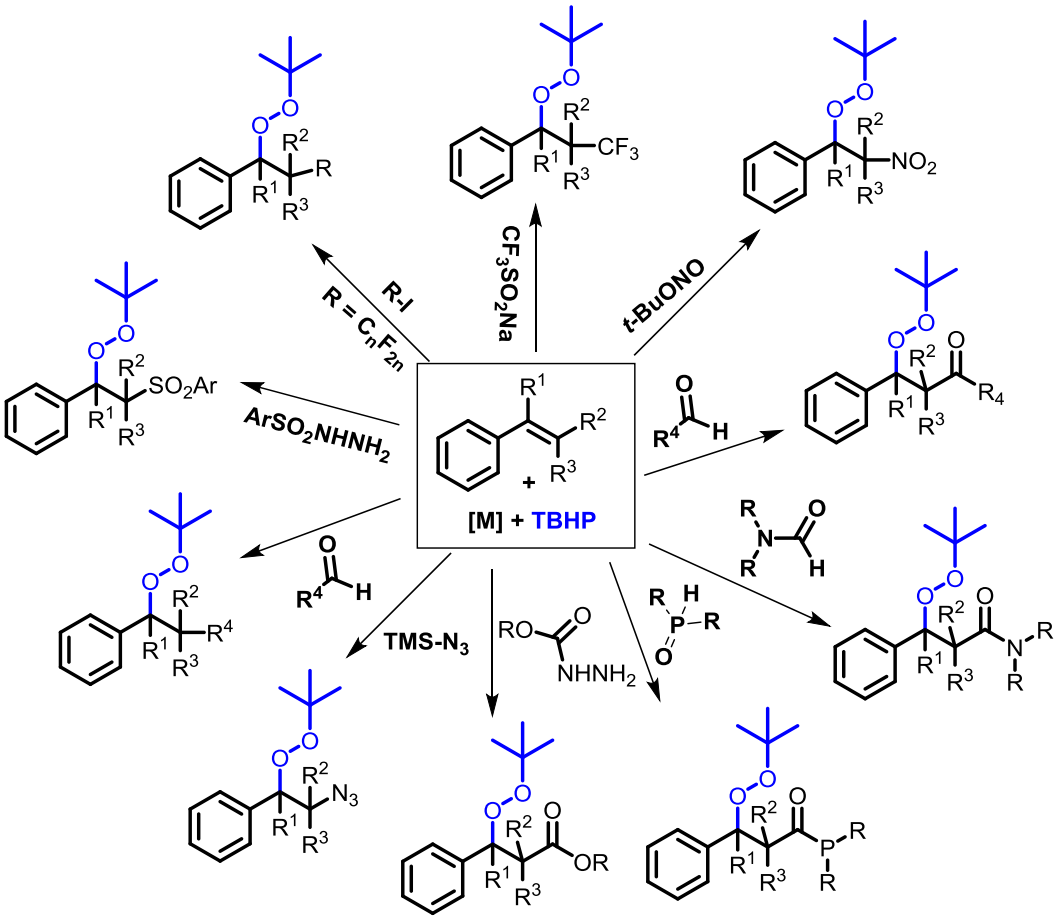

Scheme 3A.5. Miscellaneous approaches for difunctionalization of olefins using peroxide and metal

Interestingly, the peroxidation of dicarbonyl compounds was reported by Terent'ev and co-workers.[32]

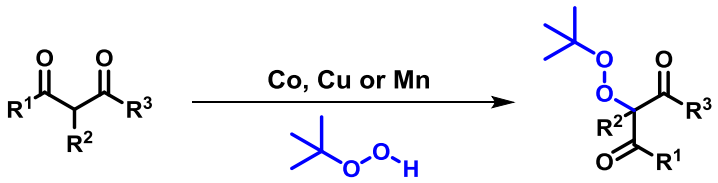

Scheme 3A.6. Terente'ev approach for peroxidation of di-keto compounds

Patel and co-workers demonstrated the cycloalkylation-peroxidation of coumarins using Cu_2O and TBHP.[33]

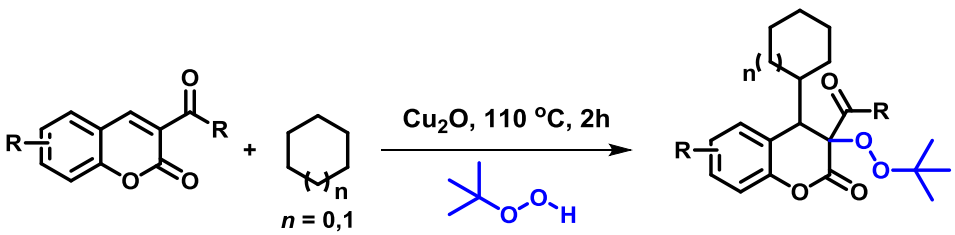

Scheme 3A.7. Patel's approach for cycloalkylation-peroxidation of coumarins

Accordingly, there were only two reports for the direct C-H peroxidation of tertiary carbons, which provides quaternary peroxides. In particular, for the C-H peroxidation of C3-substituted-2-oxindoles, the first report was demonstrated by Liu and co-workers.[34] They have used TBHP, Cobalt-Salen complex in the water at 55 ^{o}C to afford peroxyoxindoles in excellent yield. However, heating is required, and the substrate scope was restricted to 2-oxindole moiety only.

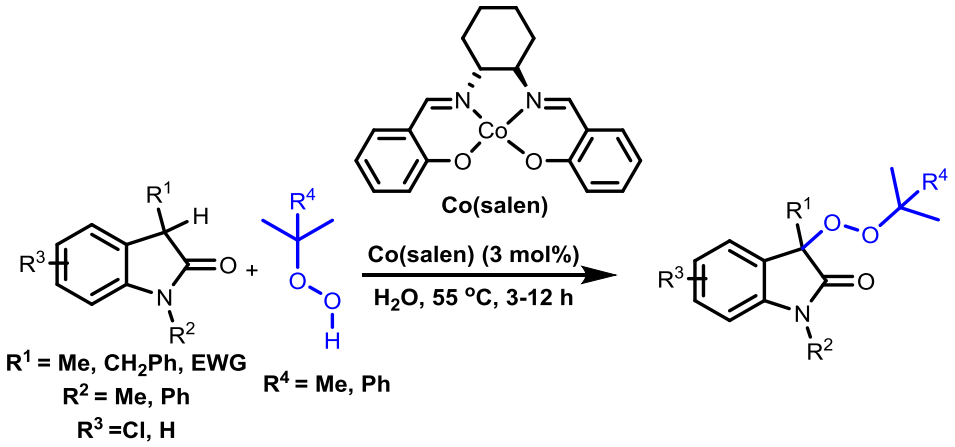

Scheme 3A.8. Peroxidation of 2-oxindole derivatives using cobalt

Later, in the same year, Stoltz and co-workers reported a similar C-H peroxidation reaction of C3-substituted-2-oxindoles using TBHP, CuCl in DCM at rt.[35] In this report, the substrates were limited to 2-oxindole derivatives only.

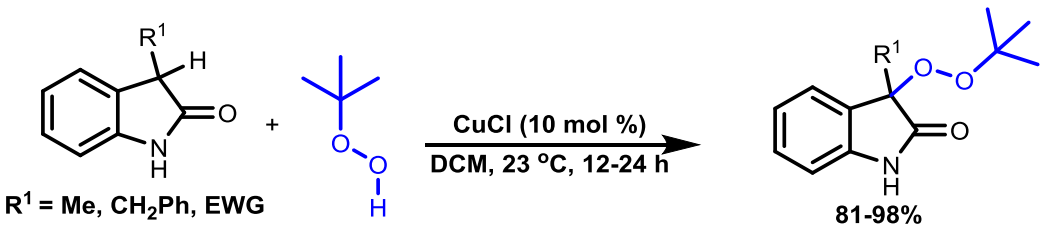

Scheme 3A.9. Peroxidation of 2-oxindole derivatives using Copper

A.5. The rationale of present work

Even though there are several drugs available for the treatment of cancer and malaria, it requires tedious steps for the synthesis of their complex skeleton. Thus it is an inducement for us to develop the new drugs, which should consist of straightforward chemical synthesis, and overcome the resistance, lower cost, and specific activity towards target disease. On the other hand, we observed that the handling of peroxides in large-scale reactions has associated with critical challenges due to its reactive and explosive nature, which motivated us to transform the batch C-H peroxidation into continuous flow method. Furthermore, we have sought to extend

the substrates scope of our protocol to other pharmacophores such as 2-oxindole, barbituric acid[36a-c,] and coumarin[37a−c] derivatives. Due to extensive bioactive properties peroxide chemistry has gained substantial attention not only by the chemists but also by the biologists. As mentioned above the pioneering work was reported by Liu's group, in which Co(salen) complex (3 mol%) catalyzed C−H peroxidation of 2-oxindole.[34] Notably, the Stoltz and co-workers developed an elegant method for the C−H peroxidation of 2-oxindoles using CuCl (10 mol%) and further showed that the substrates undergo skeletal rearrangement.[35] In both the protocols the substrate scope is restricted to 2-oxindole derivatives, furthermore higher catalyst loading and higher temperature are the notable drawbacks. Despite the existing methods, there is requisite to develop a variant and effective protocol which would overcome the above limitations and give access to the *on-demand synthesis* of bioactive compounds. Keeping this all in mind we inspired to develop a mild and efficient protocol in batch/continuous flow for the C-H peroxidation reaction.

3A.6. Results and discussion

As a part of our research on sustainable catalysis, we have discovered a very simple protocol to synthesize derivatives of peroxyoxindoles, peroxybarbiturates, and tested their anticancer activity. The alkyl hydroperoxides are sometimes used in conjunction with transition metals to generate alkoxy radical where the metal undergoes one redox type reaction (Scheme 3A.10.).[38] Peroxides are the reactive intermediates which react with metal vigorously to form metal hydroxide and alkylperoxo metal species. During this process, we cannot rule out the possibility of some amount of TBHP decomposition. Therefore it is necessary to add an excess of TBHP during such a process. Getting inspiration from this precedented reaction, we envisioned to use $FeCl_2$ for the radical generation of organic hydroperoxides and heterocyclic substrates.

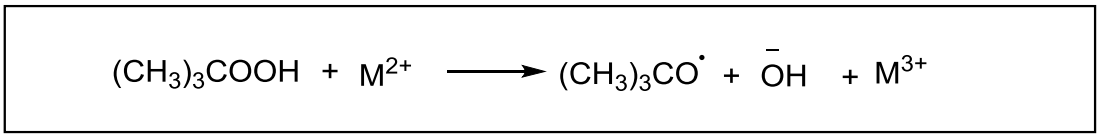

Scheme 3A.10. The reaction of metal with peroxide

3A.6.1 Optimization studies in batch

Table. 3A.1. Optimization of reaction conditions for C-H peroxidation

For instance, 3-benzylindolin-2-one **1a** was selected as a model substrate, and optimization exercise was conducted. The control experiment was performed by stirring amide **1a**, 5.0-6.0M TBHP in decane (*tert*-Butyl hydroperoxide), in the

absence of Fe catalyst and ligand in CH_3CN at rt for 16 h, which showed no reaction (Table. 3A.1, entry 1).

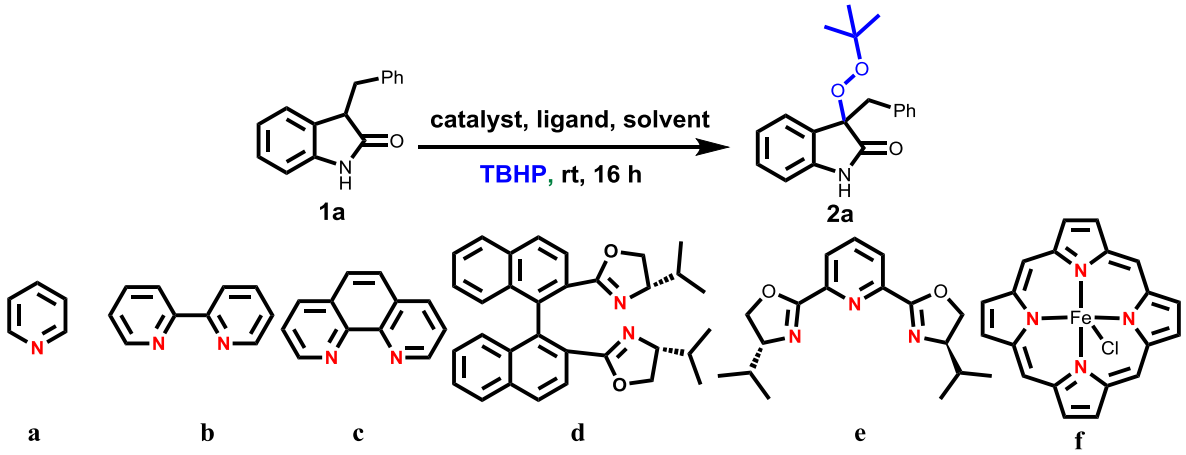

Entry	Catalyst	Ligand	Yield 2a [%]
1	-	-	no reaction
2[a]	-	-	trace
3	$FeCl_3$	-	71
4	$FeCl_2$	-	70
5	$FeCl_2$	a	36
6	$FeCl_2$	b	76
7	$FeCl_2$	c	67
8	$FeCl_2$	d	28
9	$FeCl_2$	e	95
10	$FeCl_3$	e	73
11	catalyst f	-	82
12[b]	$FeCl_2$	e	37
13[c]	$FeCl_2$	e	10
14[d]	$FeCl_2$	e	88

Reaction condition: Metal (0.0125 mmol), ligand (0.0125 mmol), TBHP (4 equiv), solvent (1.5 mL) and carbonyl compound (0.25 mmol) were stirred at rt for 16 h. [a)] heated at 80 ^oC. [b)] DCE as a solvent. [c)] THF as a solvent. [d)] dichloromethane (DCM) as a solvent.

Interestingly, the addition of 5 mol% of $FeCl_2$ or $FeCl_3$ to the reaction mixture led to C-H peroxidation to give the product **2a** in 70 and 71%, respectively. To identify an optimal reaction condition, we have screened a variety of ligands in combination with the iron catalyst (results summarized in Table. 3A.1). To our

delight, addition 5 mol% $FeCl_2$ catalyst, 5 mol% (2,6-Bis[(*4S*)-(−)-isopropyl-2-oxazolin-2-yl]pyridine) (pybox), 4 equiv of TBHP in acetonitrile solvent at rt for 16 h afforded the best yield for the peroxide **2a** (Table 3A.1, entry 9); the resultant structure was unambiguously characterized by spectroscopic techniques.

3A.6.2. The substrate scope of 2-oxindole derivatives in batch

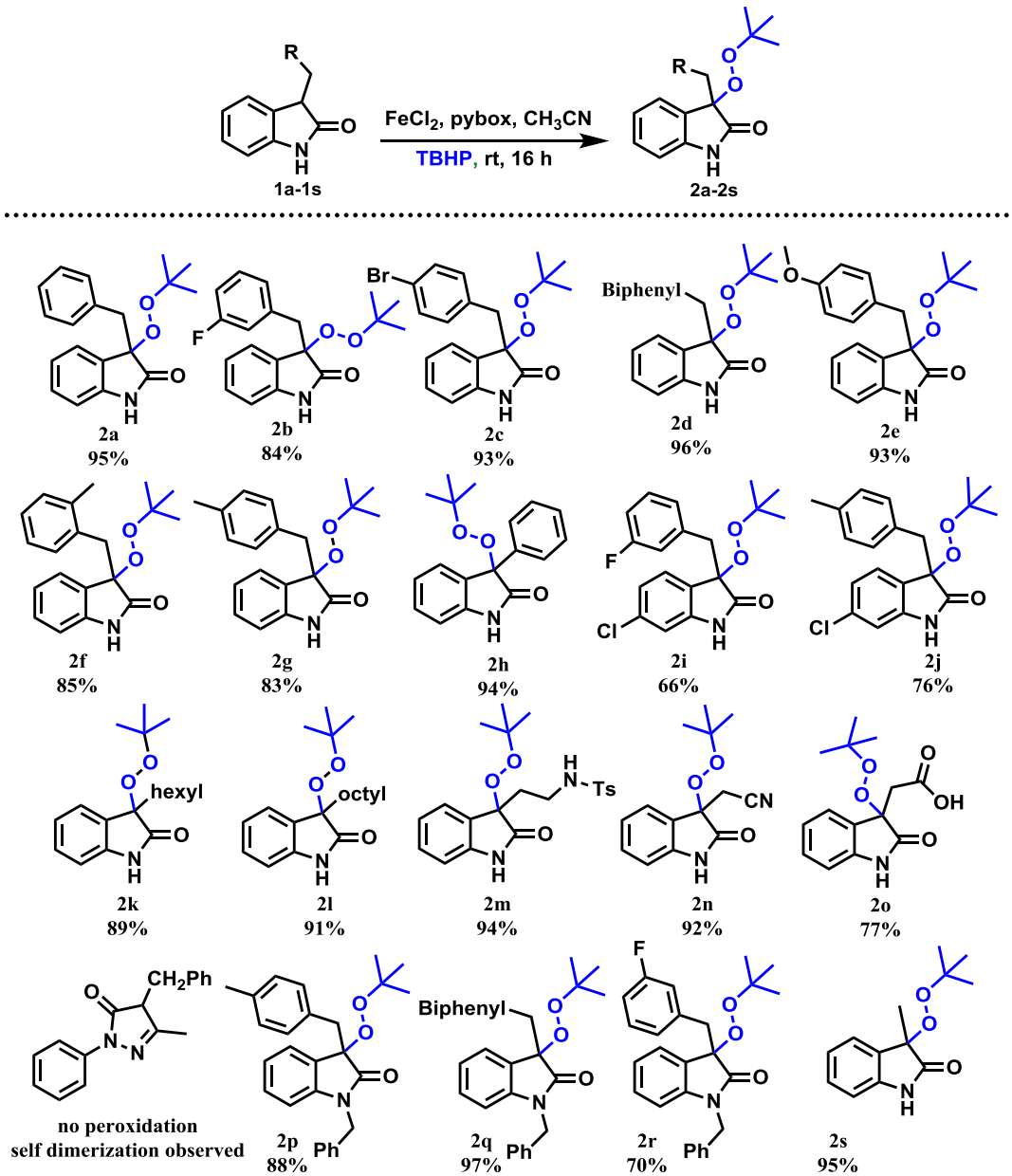

Figure 3A.4. Substrate scope for peroxidation with C3-substituted-2-oxindole in batch

Reaction condition: $FeCl_2$ (0.0125 mmol), ligand (**e**) (0.0125 mmol), TBHP (4 equiv), acetonitrile (1.5 mL) and C3-substituted-2-oxindole (0.25 mmol) were stirred at rt for 16 h.

Later, we have applied the optimized reaction conditions that were applied to a variety of substrates to afford desired peroxides. Reaction with electron-withdrawing substituents on *meta* or *para* position afforded **2b**, **2c** in excellent yield (Figure 3A.4.). Furthermore, the electron-donating substrates worked well to afford peroxide **2d-2g** in excellent yield (Figure 3A.4.). The decent yield was obtained with α-arylated 2-oxindole, **2h**. Next, the reaction with the electron-withdrawing 2-oxindole skeleton also afforded a good yield of peroxide **2i** and **2j** (Figure 3A.4.). While exploring the substrate scope, we found out that the variety of more challenging substrates such as aliphatic substituent (**2k**,**l**), *N*-Tosyl (**2m**), cyano (**2n**), acid (**2o**) (Figure 3A.4.) on 2-oxindole reacts smoothly to afford the corresponding peroxide in good to excellent yield. Moreover, the yield of the reaction was not affected by the *N*-substitution, *viz N*-protected 2-oxindoles efficiently reacts with TBHP to give peroxides **2p-r** in excellent yield (Figure 3A.4.). Additionally, α-methyl-substituted 2-oxindole was also successfully undergone C-H peroxidation to give the product **2s** in 95% yield.

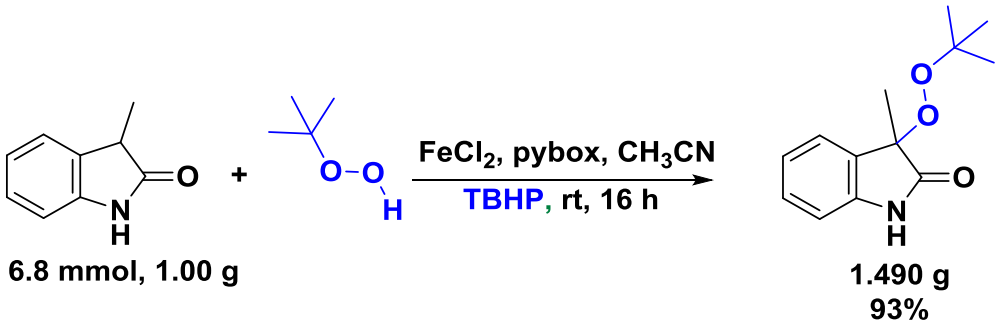

Scheme 3A.11. Upscaling of reaction in a batch process

Furthermore, we have demonstrated the reaction on a gram scale. Thus, 1.0 g of α-methyl-2-oxindole was subjected with 4 equiv of TBHP (6.0 M in decane) under an optimized condition (see Table. 3A.1., entry 9) afforded the product **2s** in 93% yield (1.49 gm, Scheme 3A.11.).

3A.6.3. Optimization studies in a continuous flow

When we were trying to perform the reaction on the gram scale, we observed the exothermic reaction. To this context, we observed that the handling of peroxides in large-scale reactions has associated with critical challenges due to its reactive and explosive nature, which motivated us to transform the batch C-H peroxidation into a continuous flow method. Initial efforts without the catalyst or ligand and varying the temperature were failed to give expected product **2a** (Table. 3A.2. entries 1-4).

Table. 3A.2. Optimization of reaction conditions for C-H peroxidation in flow

Entry	Flow rate in mL/min	Catalyst/ligand	Substrate:TBHP	t_R/ number of runs	Yield
1	0.1 each	-	0.1M :0.4M	60/3	-
2	0.2 each	-	0.1M :0.4M	30/3	-
3[a]	0.1 each	-	0.1M :0.4M	60/3	trace
4[a]	0.2 each	-	0.1M :0.4M	30/3	trace
5	0.1 each	$FeCl_2$	0.1M :0.4M	60/3	70
6	0.2 each	$FeCl_2$	0.1M :0.4M	30/3	74
7[b]	0.1 each	$FeCl_2$/**e**	0.1M :0.4M	60/3	55
8[b]	0.2 each	$FeCl_2$/**e**	0.1M :0.4M	30/3	63
9	0.1 each	$FeCl_3$	0.1M :0.4M	60/3	82
10	0.2 each	$FeCl_3$	0.1M :0.4M	30/3	88

Reaction condition: 0.1 M solution of **1a** in 25 mL CH_3CN + metal (0.125 mmol) and 0.4 M solution prepared from (5.0-6.0M TBHP in decane) in 25 mL CH_3CN were flown through the 12 mL SS tubular reactor (Vapourtec R-series) at 35^oC. [a)] Heated at 85 ^oC. [b)] 0.1245 mmol of ligand used, t_R= residence time. The following formula can calculate the residence time: Residence time= reactor volume / flow rate.

Next, the use of $FeCl_2$ alone afforded 70 and 74% yield of **2a** after 3 runs (Table 3A.2., entry 5, 6)**.** Later, we have applied previously optimized batch conditions *viz* $FeCl_2$+ligand **e** into a flow reactor where we have observed moderate yield of product **2a** (Table 3A.2., entry 7, 8). Thus, after switching the catalyst from $FeCl_2$ to $FeCl_3$ without the addition of any ligand was effective to give the productive yield of peroxyoxindole (Table 3A.2., entry 9). Hence, with the 0.2 mL flow rate of **1a** (0.1 M of 2-oxindole+ 5 mol% $FeCl_3$) and 0.2 mL flow rate of (0.4 M solution prepared from 5.0-6.0M TBHP in decane), at 35 ^oC afforded **2a** in 88% yield (Table 3A.2., entry 10) after running three cycles with the residence time of 30 minutes for each cycle.

3A.6.4. The substrate scope of 2-oxindole derivatives in a continuous flow

Further, the generality of this method was expanded with other substrates. Thus the reaction of 3-(2-methylbenzyl)indolin-2-one under standard reaction conditions afforded **2f** in 80% yield after 3 runs with 30 min of residence time. Likewise, the product **2e** and **2s** obtained in good yield (Figure 3A.5.).

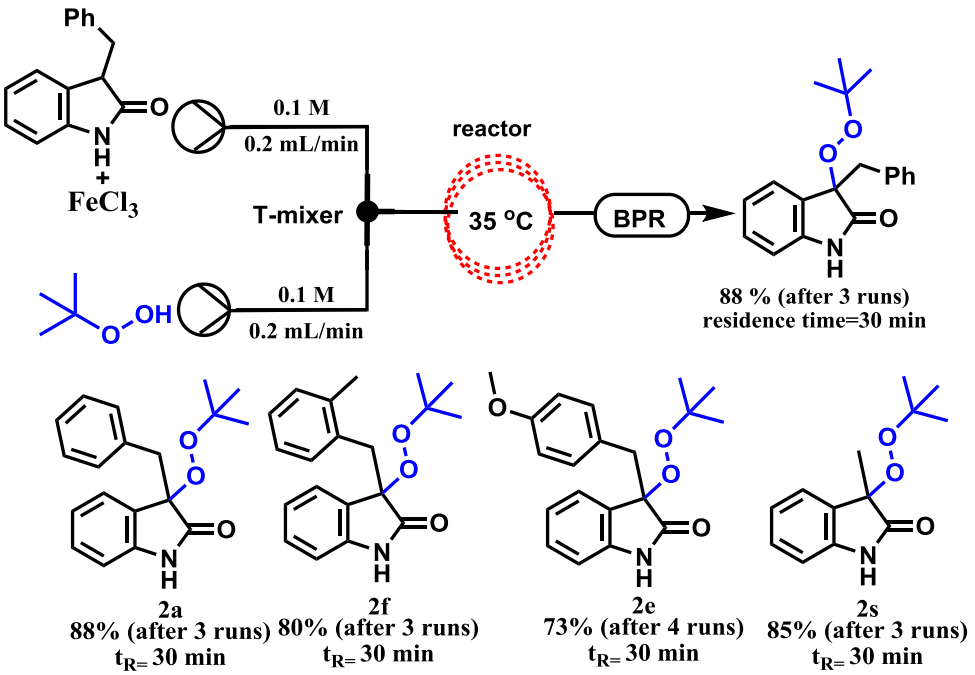

Figure 3A.5. Substrate scope for peroxidation with C3-substituted-2-oxindole in a continuous flow

Reaction condition: 0.1 M solution of **1** in 25 mL CH_3CN + $FeCl_3$ (0.125 mmol) and 0.4 M solution prepared from (5.0-6.0 6M TBHP in decane) in 25 mL CH_3CN were flown through the 12 mL SS tubular reactor (Vapourtec R-series) at 35 ^oC, t_R= residence time.

3A.6.5. The substrate scope of barbituric acid and coumarin derivatives in batch

Next, we have performed the reaction in batch with barbituric acid derivatives since it is a biologically active core in therapeutic design (CNS agent) and having less reactive amide C-H group. Thus, 5-benzyl-1,3-dimethylpyrimidine-2,4,6(1*H*,3*H*,5*H*)-trione was reacted under optimized reaction conditions to afford C-H peroxidation product **4a** in a 97% yield (Figure 3A.6.). Furthermore, these fruitful results were generalized with a wide substrate scope. Electron releasing groups such as methoxy, methyl, phenyl on the aromatic part of the barbituric acid derivatives under this experimental condition smoothly undergoes the C-H peroxidation to afford the respective products **4b-e** in good to excellent yield (Figure 3A.6.). Similar results were obtained while using the Fluorine and Bromine substituted substrates led to the respective products **4f, g** in 81%, and 60% (Figure 3A.6.). While using the alkyl substituent on the barbituric acid, moderate to the good yield of the products **4h, i** was observed.

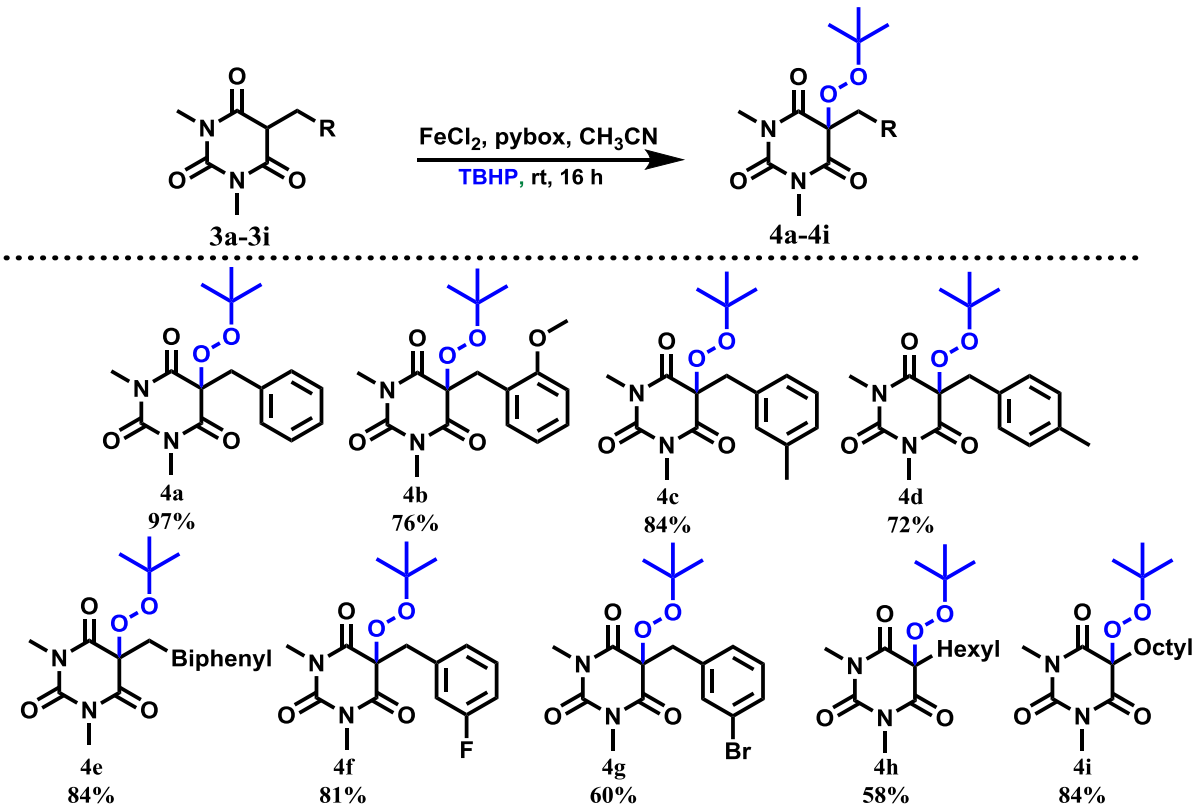

Figure 3A.6. Substrate scope for peroxidation with barbituric acid derivatives in batch.

Reaction condition: $FeCl_2$ (0.0125 mmol), ligand **(e)** (0.0125 mmol), TBHP (4 equiv), acetonitrile (1.5 mL) and barbiturate (0.25 mmol) were stirred at rt for 16 h.

This methodology was further generalized with hydroxyl coumarin derivatives (Figure 3A.7.). Fe-pybox catalyzed peroxidation reaction was performed with 3-benzylchromane-2,4-dione. Allowing this reaction mixture in the presence of TBHP at rt for 16 h, followed by column purification, afforded the product **6a** in 80% yield (Figure 3A.7.). Series of coumarin derivatives were subjected to the C-H peroxidation reactions to afford the corresponding C-H peroxylated products **6b-d** in very good yields (Figure 3A.7.). NMR and mass analysis techniques completely support the structure of the isolated peroxy compound **6**.

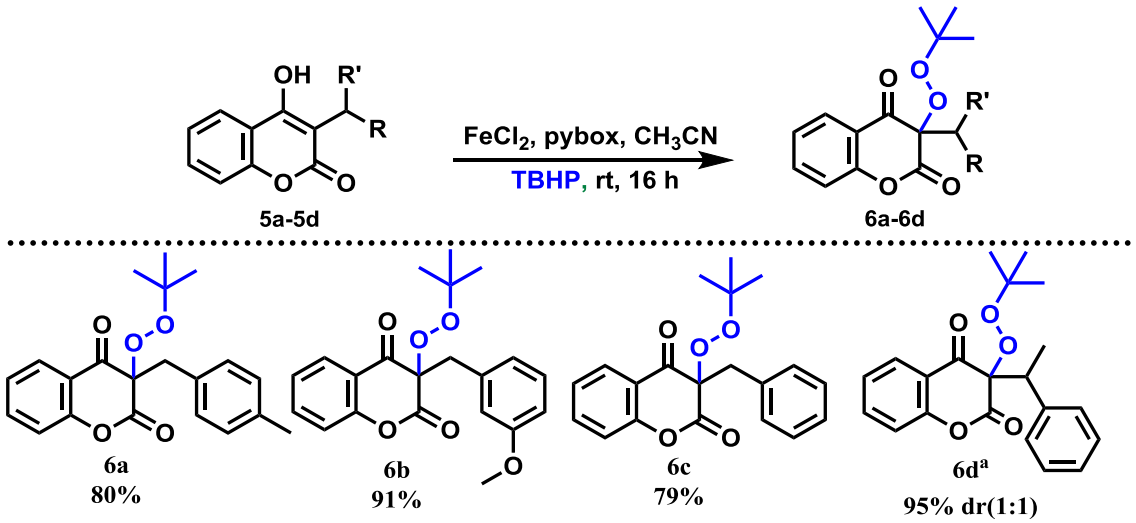

Figure 3A.7. Substrate scope for peroxidation with coumarin derivatives in batch **Reaction condition:** $FeCl_2$ (0.0125 mmol), pybox **(e)** (0.0125 mmol), 5.0-6.0M TBHP in decane (4 equiv), acetonitrile (1.5 mL) and coumarin derivatives **5a-5d** (0.25 mmol) were stirred at rt for 16 h. [a)] heated at 60 ^{o}C

3A.7. Mechanistic investigations

3A.7.1. Radical quenching experiments

To show the involvement of radical in our reaction, we have performed radical quenching studies. For instance, under the standard reaction conditions with TEMPO ((2,2,6,6-tetramethylpiperidin-1-yl)oxidanyl) afforded desired product **2a** in 78% isolated yield.

Table. 3A.3. Radical quenching experiments

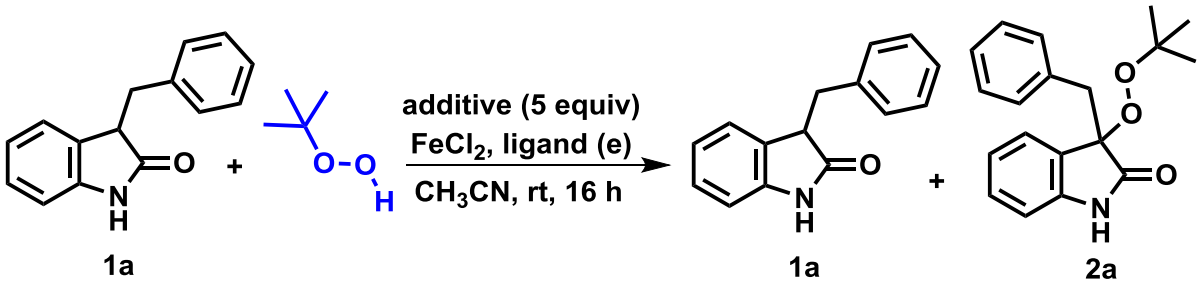

Additive	Recovered 1a %	Yield of 2a %
None	0	95
TEMPO	20	78
1,1-diphenylethylene	80	18
α-methylstyrene	40	47
O_2	37	58

Accordingly, an iron-catalyzed peroxidation reaction of 3-benzylindolin-2-one was performed in the presence of 1,1-diphenylethylene, and we observed a drastic decrease in yield of the product **2a**. Furthermore, the reaction in the presence of α-methyl styrene and molecular oxygen produced **2a** in 47 and 58 %, respectively (Table 3A.3.). The considerable decrease in the yield of the product suggests the involvement of radical pathways in this transformation.

3A.7.2. EPR measurements

To show the evidence for radical involvement, we have recorded EPR (Electron Paramagnetic Resonance) spectra for the reaction mixture. To record the spectra, a mixture of iron(II) chloride (0.0125 mmol, 5 mol%) and pybox (**e**) (0.0125 mmol, 5 mol%) in acetonitrile: DCM (1:1) was stirred at rt for 20-30 minutes. The prepared deep red solution was added in a quartz EPR tube, and EPR were recorded at -196 ^{o}C. After recording EPR for the iron-complex, in the same tube appropriate amount of the oxidant (*t*-BuOOH) was added, and after shaking, the resulting solution was analyzed using EPR at liquid nitrogen temperature. Finally, substrate **1a** was added to the above-completed sample and again recorded EPR at -196 ^{o}C. The presence of *g* value around 2.003 indicates[39] the formation of organic radical *viz tert*-Butoxy radical (Figure 3A.8).

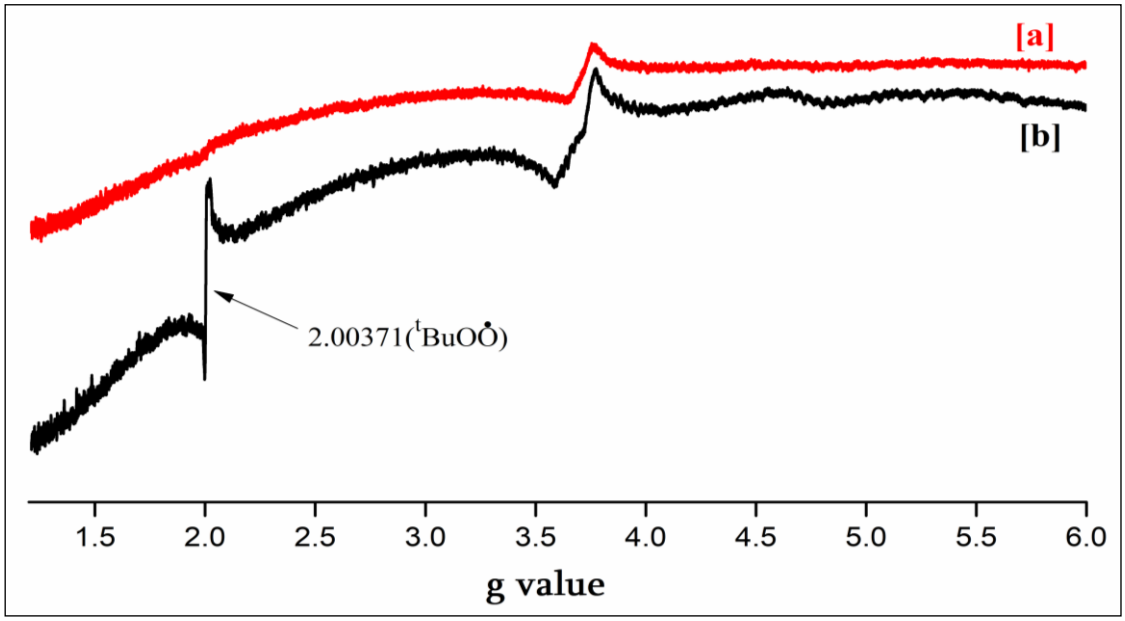

Figure 3A.8. EPR spectrum of [a] $FeCl_2$ + ligand **e**, [b] $FeCl_2$ + ligand **e** + TBHP in (1:1) DCM-CH_3CN at −196 °C.

3A.8. The possible reaction mechanism

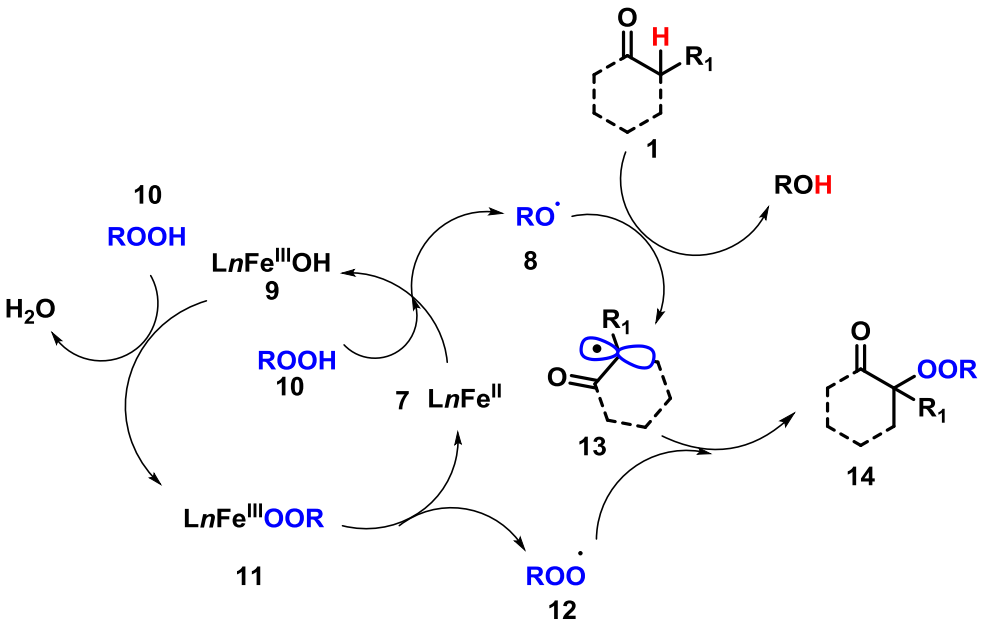

Figure 3A.9. The possible reaction mechanism

We propose the possible reaction mechanism based on radical quenching experiments, EPR measurements and previous literature reports (Figure 3A.9). [17] In the first step, **7** reacts with TBHP **10** to give the reactive alkoxide radical **8** and HO-Fe(III) complex **9**. This intermediate **9** on reaction with another equiv of TBHP produces the peroxylated Fe(III) intermediate **11** by the elimination of water. This peroxylated intermediate **11** undergo redox type reaction to give **7** and produces a peroxy radical **12**. EPR spectra of the reaction mixture display the radical involvement (Figure 3A.8.). The alkoxy radical **8** produced in this transformation abstracts α-C-H proton of the carbonyl compound to give the respective radical **13**. Further recombination of α-radical of the carbonyl compound **13** and the peroxyl radical **12** afforded the C-H peroxylated product **14**.

3A.9. Biological evaluation

It is documented in the literature reports that the presence of an oxygen-oxygen (O-O) bond can exhibit interesting biological properties.[11] We imagined that the synthesized peroxy compounds might show the biological properties. We have collaborated with Dr. Sudipta Basu of IISER, Pune and evaluated the anticancer activity on HeLa cervical cancer cells. HeLa cells were treated with 30 μM concentration of library members for 24 h and the cell viability was determined by MTT assay. It was found that 2-oxindole derivatives **2b**, **2g,** and **2k** killed HeLa

cells significantly compared to the other library members (cell viability = 29.5 ±1.6%, 24.2 ±1.0% and 21.2 ±0.5% respectively) (Figure 3A.10.).

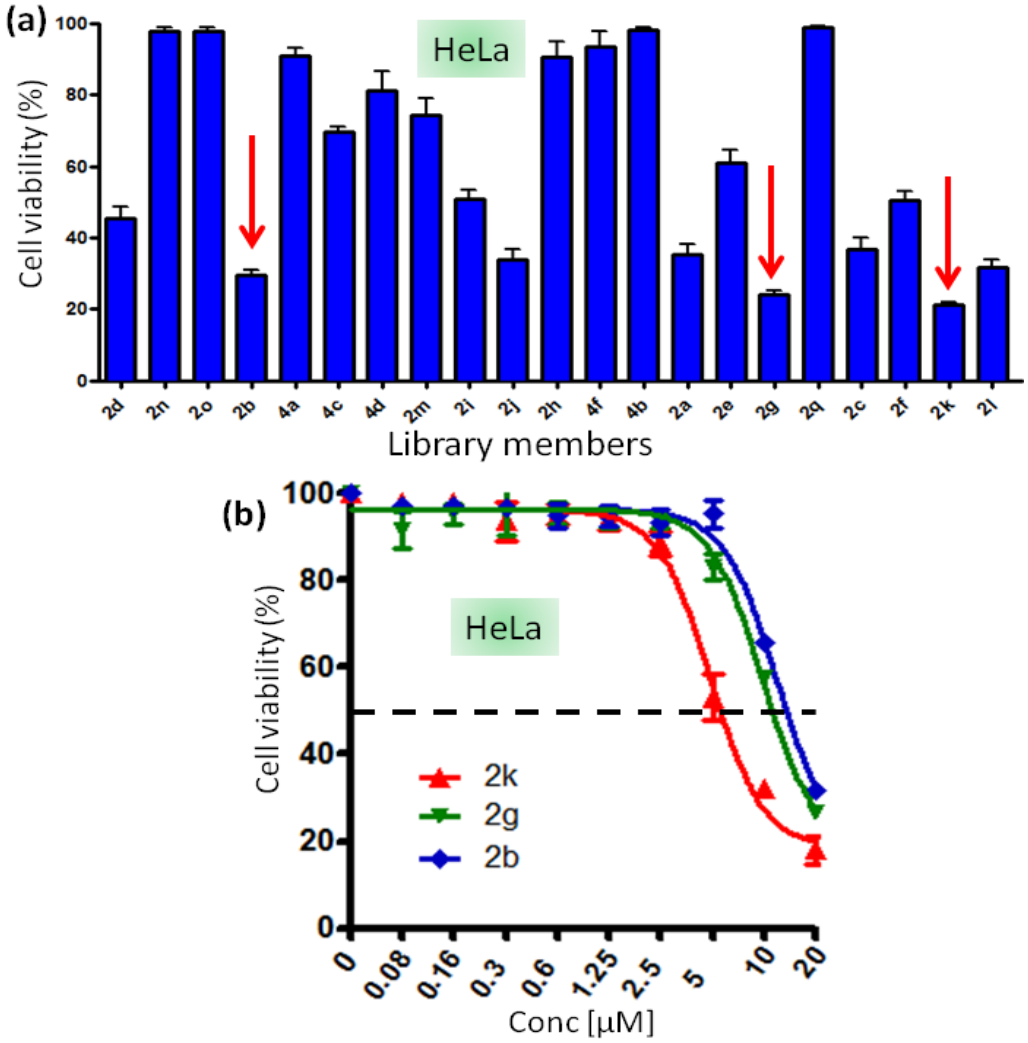

Figure 3A.10. Dose-dependent cell viability assay in HeLa cells.

We chose to evaluate the dose-dependent cancer cell killing ability of **2k**, **2g**, and **2b** further. We treated HeLa cells with compound **2b**, **2g**, and **2k** with varying dosages for 24 h and evaluated the cell viability by MTT assay. Interestingly, compound **2k** showed much lower IC_{50} = 5.3 μM (cell viability = 17.9 ± 3.1 % at 20 μM concentration) compared to IC_{50} = 11.5 μM (cell viability = 26.6 ± 0.9 % at 20 μM concentration) and 13.1 μM (cell viability = 31.6 ± 1.4 % at 20 μM concentration) for compound **2g** and **2b** respectively (Figure 3A.10.). These cell viability assays confirmed that compounds **2b**, **2g,** and **2k** showed better anti-cancer activity against cervical cancer cells as compared to other substrates.

3A.10. Conclusion

In conclusion, we have developed a Fe-catalyzed peroxidation of carbonyl compounds *via* C-H functionalization. The present method is highly useful for the

synthesis of quaternary peroxy derivatives of 2-oxindole, barbituric acid, and coumarin substrates. Moreover, this method is demonstrated with gram scale synthesis. To minimize the explosive hazards, we have transformed the batch reaction conditions to continuous flow. Based on preliminary results, the mechanistic investigations revealed that the radical generated from peroxide and oxindole initiated by the Fe-catalyst afforded the peroxylated 2-oxindole derivative *via* selective recombination process. Among several other ligands screened, pybox ligand is highly efficient to form the peroxylated product. The biological activity of the various peroxylated 2-oxindole was tested against the cancerous cell lines, showing potential activity. To our delight (**2b**, **2g**, and **2k**) was found to be highly active against HeLa cells among the other substrates.

3A.11. Experimental section and characterization data

3A.11.1. General information and data collection

The 2-oxindole, barbituric acid, and 4-hydroxy coumarin were purchased from Sigma-Aldrich or Alfa-Aesar. Deuterated solvents were used as received. All the solvents used were dry grade and stored over 4Å molecular sieves. Column chromatographic separations performed over 100-200 Silica-gel. Visualization was accomplished with UV light and PMA, CAM stain followed by heating. The Iron(II) chloride 98% (product number- 372870), *tert*-Butyl hydroperoxide (TBHP) 5.0-6.0 M in decane solution, and pybox (407151) ligand was purchased from Sigma-Aldrich. All the experiments with metal and pybox ligands were carried out without maintaining inert condition. The flow chemistry experiments were carried on Vapourtec R-series. ^{1}H and ^{13}C NMR spectra were recorded on 400 and 100 MHz, respectively, using a Bruker 400 MHz or JEOL 400 MHz spectrometers. Abbreviations used in the NMR follow-up experiments: b, broad; s, singlet; d, doublet; t, triplet; q, quartet; m, multiplet. High-resolution mass spectra were recorded with Waters- synapt G2 using electrospray ionization (ESI-TOF). Fourier-transform infrared (FT-IR) spectra were obtained with a Bruker Alpha-E Fourier transform infrared spectrometer. The **Melting point**s were measured using the **Melting point** apparatus- VEEGO, model- VMP-D. The EPR spectra are recorded on JES - FA200 ESR Spectrometer with X and Q band at SAIF, IIT- Bombay, India.

Note: "Although the reaction of a metal salt with organic peroxides leads to an explosive reaction, we have not faced any issue even at gram scale."

3A.11.2. Experimental procedure

(A) General experimental procedure for C-H peroxidation of carbonyl compounds:

In a 5 mL round bottom flask mixture of iron(II) chloride (0.0125 mmol, 5 mol%) and (2,6-Bis[(4*S*)-(−)-isopropyl-2-oxazolin-2-yl]pyridine) (pybox) ligand (0.0125 mmol, 5 mol%) in acetonitrile 1.5 mL was stirred at rt for 20-30 min. To the obtained deep-red solution was added 5.0-6.0 M *tert*-Butyl hydroperoxide (TBHP) in decane solution (1.0 mmol, 4 equiv) and finally, respective carbonyl compound (0.25 mmol, 1 equiv) was added, and septum placed over it. The resulting solution was stirred at rt for 16 h without maintaining any special conditions such as the inert atmosphere. After completion of the reaction, a volatile component was evaporated using a vacuum. The residue was directly purified by silica gel chromatography (EtOAc: hexane= 15:85 or 20:80).

(B) Experimental procedure for C-H peroxidation of amide (1 mmol scale):

3-benzyl-3-(*tert*-butylperoxy)indolin-2-one (**2a**): In a 25 mL round bottom flask mixture of iron(II) chloride (6.3 mg, 0.05 mmol, 5 mol%) and pybox (15.05 mg, 0.05 mmol, 5 mol%) in acetonitrile 4 mL was stirred at rt for 20-30 min. To the obtained deep-red solution was added *tert*-butyl hydroperoxide (TBHP) 5.0-6.0 M in decane solution (4.0 mmol, 4 equiv) and finally, 3-benzylindolin-2-one (223 mg, 1 mmol) was added and septum placed over it. The resulting solution was stirred at rt 16 h without maintaining any special conditions such as the inert atmosphere. After reaction completion, the volatile solvent was removed using a vacuum, and the crude reaction mixture was directly purified by column chromatography on silica gel with eluent (EtOAc: n-hexane= 10:90) afforded (290 mg 93%) of **2a** as a white solid.

(C) **Experimental procedure for C-H peroxidation of amide (gram-scale synthesis):**

3-(*tert*-butylperoxy)-3-methylindolin-2-one (**2s**): In a 100 mL round bottom flask mixture of iron(II) chloride (42.8 mg, 0.34 mmol, 5 mol%) and pybox (L) (102 mg, 0.340 mmol, 5 mol%) in acetonitrile 15 mL was stirred at rt for 20-30 min. To the obtained deep-red solution was added *tert*-Butyl hydroperoxide (TBHP) 5.0-6.0 M in decane solution (27.2 mmol, 4 equiv) and finally, 3-methyl-2-oxindole (1000 mg, 6.80 mmol) was added, and the resulting solution was stirred at rt 16 h without maintaining any special conditions such as the inert atmosphere. After reaction completion, the volatile solvent was removed using a vacuum, and the crude reaction mixture was directly purified by column chromatography on silica gel with eluent (EtOAc: n-hexane=12:88) afforded (1490 mg 93%) of **2s** as a white solid.

(D) Experimental procedure for radical inhibition:

Mixture of iron(II) chloride (6.3 mg, 0.05 mmol, 5 mol%) and pybox (15.05 mg, 0.05 mmol, 5 mol%) in acetonitrile 4 mL was stirred at rt for 20-30 min. To the obtained deep-red solution was added *tert*-butyl hydroperoxide (TBHP) 5.0-6.0 M in decane solution (4.0 mmol, 4 equiv), 2,2,6,6-tetramethylpiperidine-1-oxyl (TEMPO) (5 equiv) or 1,1-diphenylethylene (5 equiv) or α-methylstyrene (5 equiv) and finally 3-

benzylindolin-2-one (223 mg, 1 mmol) was added and resulting solution was stirred at rt 16 h. After reaction completion, the volatile solvent was removed using a vacuum, and the crude reaction mixture was directly purified by column chromatography on silica gel with eluent (EtOAc: n-hexane= 10:90). The drastic decrease in the yield of the product **2a** in the presence of 1,1-diphenylethylene or α-methyl styrene suggests the involvement of radical pathway in the reaction.

(E) Experimental procedure for EPR Analysis:

Mixture of iron(II) chloride (0.0125 mmol, 5 mol%) and pybox (0.0125 mmol, 5 mol%) in acetonitrile : DCM (1:1) was stirred at rt for 20-30 minutes. The prepared deep red solution was added in a quartz EPR tube, and EPR spectra was recorded at -196 ^{o}C. After recording EPR for complex, in the same tube appropriate amount of the oxidant (*t*-BuOOH) was added, and after shaking, the resulting solution was analyzed using EPR at liquid nitrogen temperature. Finally, substrate **1a** was added to the above-completed sample and again recorded EPR at -196 ^{o}C. The presence of *g* value around 2.003 indicates the formation of organic radical (*tert*-butoxy radical).

3A.11.3. Spectroscopic data

3-Benzyl-3-(*tert*-butylperoxy)indolin-2-one (**2a**)[34]: Prepared according to general procedure A, using 3-benzylindolin-2-one (55.7 mg, 0.25 mmol) to afford peroxyoxindole **2a** (74 mg, 95% yield) as a white solid. **Melting point**: 152-154 ^{o}C. **^{1}H NMR** (400 MHz, $CDCl_3$): δ 7.61 (bs, 1H), 7.20 – 7.10 (m, 4H), 7.02 (dd, *J* = 7.5, 2.0 Hz, 2H), 6.98 – 6.91 (m, 2H), 6.68 (d, *J* = 7.5 Hz, 1H), 3.34 (d, *J* = 13.2 Hz, 1H), 3.06 (d, *J* = 13.2 Hz, 1H), 1.13 (s, 9H). **^{13}C NMR** (100 MHz, $CDCl_3$) δ 176.2, 141.1 , 133.6, 130.9, 129.5, 127.9, 127.7, 127.0, 125.9, 122.1, 109.8, 85.6, 80.7, 40.5, 26.7. **FTIR** (neat): 3254, 2978, 2926, 2112, 1726, 1112 cm^{-1}. **HRMS** (ESI-TOF) *m/z*: $[M + Na]^+$ calcd for $C_{19}H_{21}NO_3Na$ 334.1418; found 334.1423.

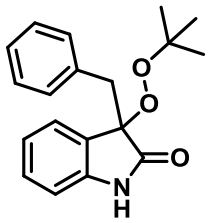

3-(*tert*-Butylperoxy)-3-(3-fluorobenzyl)indolin-2-one (**2b**): Prepared according to general procedure A, using 3-(3-fluorobenzyl)indolin-2-one (60.2 mg, 0.25 mmol) to afford peroxyoxindole **2b** (74 mg, 84% yield) as a light yellow solid. M elting Point: 145-147^{o}C. **^{1}H NMR** (400 MHz, $CDCl_3$): δ 8.57 (bs, 1H), 7.19 (ddd, *J* = 7.8, 6.7, 2.2 Hz, 1H), 7.10 (td, *J* = 7.9, 6.1 Hz, 1H), 6.98 – 6.91 (m, 2H), 6.89 – 6.83 (m, 1H), 6.81 (d, *J* = 7.7 Hz, 1H), 6.78 – 6.73 (m, 2H), 3.34 (d, *J* = 13.3 Hz, 1H), 3.04 (d, *J* = 13.3 Hz, 1H), 1.12 (s, 9H). **^{13}C NMR** (100 MHz, $CDCl_3$) δ 176.7, 162.3 (d, *J* = 245.2 Hz), 141.2, 136.2 (d, *J* = 7.7 Hz), 129.7, 129.3 (d, *J* = 8.2 Hz), 127.4, 126.6 (d, *J* = 2.8 Hz), 125.7, 122.1, 117.7 (d, *J* = 21.6 Hz), 114.0 (d, *J* = 21.0 Hz), 110.1, 85.4, 80.8, 40.2 (d, *J* = 1.5 Hz), 26.6. **FTIR** (neat): 3258, 2977, 2924, 1730, 1189 cm^{-1}. **HRMS** (ESI-TOF) *m/z*: $[M + Na]^+$ calcd for $C_{19}H_{20}FNO_3Na$ 352.1321; found 352.1319.

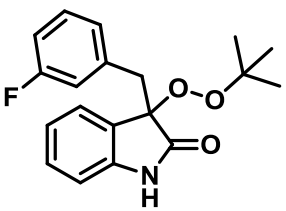

3-(4-Bromobenzyl)-3-(*tert*-butylperoxy)indolin-2-one (**2c**): Prepared according to general procedure A, using 3-(4-bromobenzyl)indolin-2-one (75.25 mg, 0.25 mmol) to afford peroxyoxindole **2c** (91 mg, 93% yield) as a light yellow solid. **Melting point**: 128-131 °C. **^{1}H NMR** (400 MHz, $CDCl_3$) δ 8.00 (bs, 1H), 7.27 -7.25 (m, 2H), 7.23 – 7.16 (m, 1H), 6.96 (dd, *J* = 5.8, 4.2 Hz, 2H), 6.89 (d, *J* = 8.4 Hz, 2H), 6.73 (d, *J* = 7.8 Hz, 1H), 3.28 (d, *J* = 13.3 Hz, 1H), 3.02 (d, *J* = 13.3 Hz, 1H), 1.12 (s, 9H). **^{13}C NMR** (100 MHz, $CDCl_3$) δ 176.2, 141.0, 132.6, 132.6, 131.1, 129.7, 127.4, 125.7, 122.2, 121.2, 110.0, 85.3, 80.8, 39.9, 26.6. **FTIR** (neat): 3257, 2925, 2857, 1727, 1112 cm^{-1}. **HRMS** (ESI-TOF) *m/z*: $[M + Na]^+$ calcd for $C_{19}H_{20}BrNO_3Na$ 412.0524; found 412.0524.

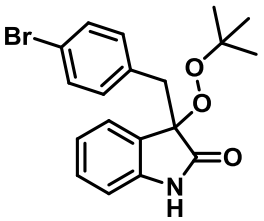

3-([1,1'-Biphenyl]-4-ylmethyl)-3-(*tert*-butylperoxy)indolin-2-one (**2d**): Prepared according to general procedure A, using 3-([1,1'-biphenyl]-4-ylmethyl)indolin-2-one (74.7 mg, 0.25 mmol) to afford peroxyoxindole **2d** (93 mg, 96% yield) as a white solid. **Melting point**: 162-164 °C. **^{1}H NMR** (400 MHz, $CDCl_3$) δ 8.26 (bs, 1H), 7.54 (dd, *J* = 5.2, 3.3 Hz, 2H), 7.44 – 7.36 (m, 4H), 7.34 – 7.29 (m, 1H), 7.20 (ddd, *J* = 7.5, 1.6 Hz, 1H), 7.09 (d, *J* = 8.2 Hz, 2H), 7.02 – 6.95 (m, 2H), 6.75 (d, *J* = 7.8 Hz, 1H), 3.39 (d, *J* = 13.2 Hz, 1H), 3.09 (d, *J* = 13.3 Hz, 1H), 1.14 (s, 9H). **^{13}C NMR** (100 MHz, $CDCl_3$) δ 176.7, 141.2, 140.8, 139.7, 132.7, 131.3, 129.5, 128.8, 127.7, 127.3, 127.0, 126.5, 125.8, 122.0, 110.0, 85.66, 80.75, 40.17, 26.64. **FTIR** (neat): 3256, 2974, 2924, 1731, 1116 cm^{-1}. **HRMS** (ESI-TOF) *m/z*: $[M + Na]^+$ calcd for $C_{25}H_{25}NO_3Na$ 410.1731; found 410.1727.

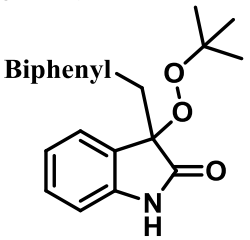

3-(*tert*-Butylperoxy)-3-(4-methoxybenzyl)indolin-2-one (**2e**): Prepared according to general procedure A, using 3-(4-methoxybenzyl)indolin-2-one (63.2 mg, 0.25 mmol) to afford peroxyoxindole **2e** (79 mg, 93% yield) as a yellow solid. **Melting point**: 141-143 °C. **^{1}H NMR** (400 MHz, $CDCl_3$) δ 7.83 (bs, 1H), 7.18 (ddd, *J* = 7.8, 6.9, 2.2 Hz, 1H), 6.99 – 6.94 (m, 2H), 6.94 – 6.90 (m, 2H), 6.70 (d, *J* = 7.8 Hz, 1H), 6.68 – 6.65 (m, 2H), 3.73 (s, 3H), 3.28 (d, *J* = 13.4 Hz, 1H), 3.00 (d, *J* = 13.4 Hz, 1H), 1.12 (s, 9H). **^{13}C NMR** (100 MHz, $CDCl_3$) δ 176.5, 158.6, 141.1, 131.9, 129.4, 127.9, 125.8, 125.5, 122.0, 113.3, 109.8, 85.8, 80.7, 55.2, 39.7, 26.6. **FTIR** (neat): 3402, 3366, 2921, 2854, 1732, 1183 cm^{-1}. **HRMS** (ESI-TOF) *m/z*: $[M + H]^+$ calcd for $C_{20}H_{24}NO_4$ 342.1705; found 342.1702.

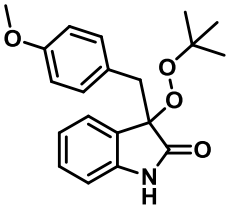

3-(*tert*-Butylperoxy)-3-(2-methylbenzyl)indolin-2-one (**2f**): Prepared according to general procedure A, using 3-(2-methylbenzyl)indolin-2-one (59.2 mg, 0.25 mmol) to afford peroxyoxindole **2f** (69 mg, 85% yield) as a light yellow solid. **Melting point**: 167-169 °C. **^{1}H NMR** (400 MHz, $CDCl_3$) δ 8.00 (bs, 1H), 7.20 (td, *J* = 7.8, 1.3 Hz, 1H), 7.16 – 7.05 (m, 4H), 6.85 (dd, *J* = 7.8, 7.3 Hz, 1H), 6.80 (d, *J* = 7.7 Hz, 1H), 6.56 (d, *J* = 7.6 Hz, 1H), 3.40 (d, *J* = 14.3 Hz, 1H), 3.00 (d, *J* = 14.3 Hz, 1H), 2.01 (s, 3H), 1.11 (s, 9H). **^{13}C NMR** (100 MHz, $CDCl_3$) δ 177.2, 140.8, 137.9, 132.7, 131.9, 130.3, 129.4, 127.7, 127.3, 126.2, 125.4, 121.9, 109.8, 85.3, 80.7, 37.2, 26.7,

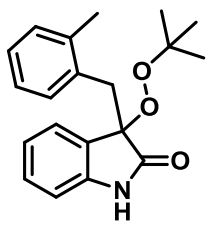

20.0. **FTIR** (neat): 3255, 2975, 2924, 2856, 1728, 1117 cm^{-1}. **HRMS** (ESI-TOF) *m/z*: $[M + Na]^+$ calcd for $C_{20}H_{23}NO_3Na$ 348.1575; found 348.1584.

3-(*tert*-Butylperoxy)-3-(4-methylbenzyl)indolin-2-one (**2g**): Prepared according to general procedure A, using 3-(4-methylbenzyl)indolin-2-one (59.2 mg, 0.25 mmol) to afford peroxyoxindole **2g** (67 mg, 83% yield) as a yellow solid. **Melting point**: 122-125 °C. **^{1}H NMR** (400 MHz, $CDCl_3$) δ 8.32 (bs, 1H), 7.21 – 7.15 (m, 1H), 6.97 – 6.93 (m, 4H), 6.92 – 6.88 (m, 2H), 6.73 (d, *J* = 7.7 Hz, 1H), 3.31 (d, *J* = 13.3 Hz, 1H), 3.01 (d, *J* = 13.3 Hz, 1H), 2.25 (s, 3H), 1.12 (s, 9H). **^{13}C NMR** (100 MHz, $CDCl_3$) δ 176.9, 141.2, 136.5, 130.8, 130.4, 129.4, 128.6, 125.8, 121.9, 109.9, 85.8, 80.7, 40.0, 26.6, 21.2. **FTIR** (neat): 3260, 2924, 2857, 1725, 1112 cm^{-1} . **HRMS** (ESI-TOF) *m/z*: $[M + Na]^+$ calcd for $C_{20}H_{23}NO_3Na$ 348.1575; found 348.1575.

3-(*tert*-Butylperoxy)-3-phenylindolin-2-one (2h)[35]: Prepared according to general procedure A, using 3-phenylindolin-2-one (52 mg, 0.25 mmol) to afford peroxyoxindole **2h** (69.5 mg, 94% yield) as a yellow solid. **Melting point**: 139-141 °C. **^{1}H NMR** (400 MHz, $CDCl_3$) δ 8.28 (s, 1H), 7.47 – 7.41 (m, 2H), 7.34 – 7.28 (m, 5H), 7.09 (t, *J* = 7.5 Hz, 1H), 6.89 (dd, *J* = 7.7, 4.3 Hz, 1H), 1.19 (s, 9H). **^{13}C NMR** (100 MHz, $CDCl_3$) δ 176.2, 141.7, 136.1, 129.9, 129.3, 129.1, 128.6, 127.2, 126.6, 122.7, 110.2, 86.5, 81.0, 26.7. **FTIR** (neat): 3255, 2978, 2926, 2857, 1730, 1 111 cm^{-1}. **HRMS** (ESI-TOF) *m/z*: $[M + Na]^+$ calcd for $C_{18}H_{19}NO_3Na$ 320.1262; found 320.1266.

3-(*tert*-Butylperoxy)-6-chloro-3-(3-fluorobenzyl)indolin-2-one (**2i**): Prepared according to general procedure A, using 6-chloro-3-(3-fluorobenzyl)indolin-2-one (68.7 mg, 0.25 mmol) to afford peroxyoxindole **2i** (60 mg, 66% yield) as a white solid. **Melting point**: 172-174 °C. **^{1}H NMR** (400 MHz, $CDCl_3$) δ 7.86 (bs, 1H), 7.17 – 7.10 (m, 1H), 6.94 (dd, *J* = 8.2, 1.7 Hz, 1H), 6.93 – 6.87 (m, 1H), 6.84 – 6.74 (m, 4H), 3.32 (d, *J* = 13.4 Hz, 1H), 3.02 (d, *J* = 13.4 Hz, 1H), 1.13 (s, 9H). **^{13}C NMR** (100 MHz, $CDCl_3$) δ 175.9, 162.4 (d, *J* = 245.6 Hz), 142.0, 135.7 (d, *J* = 7.7 Hz), 135.3, 129.4 (d, *J* = 8.0 Hz), 126.6, 125.8, 122.2, 117.7 (d, *J* = 21.5 Hz), 114.2 (d, *J* = 20.9 Hz), 110.6, 84.8, 81.0, 39.9, 26.5. **FTIR** (neat): 3308, 3257, 2922, 2854, 1732, 1124 cm^{-1}. **HRMS** (ESI-TOF) *m/z*: $[M + Na]^+$ calcd for $C_{19}H_{19}ClFNO_3Na$ 386.0934; found 386.0934.

3-(*tert*-Butylperoxy)-6-chloro-3-(3-fluorobenzyl)indolin-2-one (**2j**): Prepared according to general procedure A, using 6-chloro-3-(4-methylbenzyl)indolin-2-one (67.7 mg, 0.25 mmol) to afford peroxyoxindole **2j** (68.5 mg, 76% yield) as a yellow green solid. **Melting point**: 156-158 °C. **^{1}H NMR** (400 MHz, $CDCl_3$) δ 7.98 (bs, 1H), 6.97 (d, *J* = 7.8 Hz, 2H), 6.93 (dd, *J* = 8.0, 1.8 Hz, 1H), 6.89 (d, *J* = 8.0 Hz, 2H), 6.83 (d, *J* = 8.0 Hz , 1H), 6.74 (d, *J* = 1.7 Hz, 1H), 3.28 (d, *J* = 13.4 Hz, 1H), 2.98 (d, *J* = 13.4 Hz, 1H), 2.27 (s, 3H), 1.12 (s, 9H).

^{13}C NMR (100 MHz, $CDCl_3$) δ 176.5, 142.2, 136.8, 135.0, 130.7, 130.1, 128.8, 126.7, 126.3, 122.1, 110.5, 85.3, 80.9, 39.9 26.6, 21.2. **FTIR** (neat): 3256, 2978, 2926, 2859, 1733, 1120 cm^{-1}. **HRMS** (ESI-TOF) *m/z:* $[M + Na]^+$ calcd for $C_{20}H_{22}ClNO_3Na$ 382.1185; found 382.1189.

3-(*tert*-Butylperoxy)-3-hexylindolin-2-one (**2k**): Prepared according to general procedure A, 3-hexylindolin-2-one (54.2 mg, 0.25 mmol) to afford peroxyoxindole **2k** (68 mg, 89% yield) as an light orange solid. **Melting point**: 77-79 °C. **^{1}H NMR** (400 MHz, $CDCl_3$) δ 8.52 (bs, 1H), 7.30 – 7.27 (m, 1H), 7.23 (td, *J* = 7.7, 1.3 Hz, 1H), 7.04 (td, *J* = 7.6, 1.0 Hz, 1H), 6.86 (d, *J* = 7.7 Hz, 1H), 1.90 (ddd, *J* = 13.0, 9.6, 4.4 Hz, 2H), 1.25 – 1.15 (m, 8H), 1.10 (s, 9H), 0.81 (t, *J* = 6.9 Hz, 3H). **^{13}C NMR** (100 MHz, $CDCl_3$) δ 177.5, 141.4, 129.4, 129.0, 124.7, 122.4, 110.0, 85.7, 80.4, 34.2, 31.5, 29.5, 26.6, 22.8, 22.6, 14.1. **FTIR** (neat): 3257, 2925, 2858, 1728, 1196 cm^{-1}. **HRMS** (ESI-TOF) *m/z:* $[M + Na]^+$ calcd for $C_{18}H_{27}NO_3Na$ 328.1888; found 328.1883.

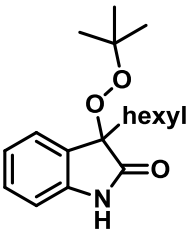

3-(*tert*-Butylperoxy)-3-octylindolin-2-one (**2l**): Prepared according to general procedure A, 3-octylindolin-2-one (61.2 mg, 0.25 mmol) to afford peroxyoxindole **2l** (76 mg, 91% yield) as a yellow liquid. **^{1}H NMR** (400 MHz, $CDCl_3$) δ 8.23 (bs, 1H), 7.29 (d, *J* = 7.3 Hz, 1H), 7.23 (dt, *J* = 7.7, 3.9 Hz, 1H), 7.04 (td, *J* = 7. 6, 0.8 Hz, 1H), 6.84 (d, *J* = 7.7 Hz, 1H), 1.97 – 1.84 (m, 2H), 1.28 – 1.14 (m, 12H), 1.10 (s, 9H), 0.84 (t, *J* = 7.0 Hz, 3H). **^{13}C NMR** (100 MHz, $CDCl_3$) δ 177.1, 141.2, 129.2, 128.9, 124.6, 122.3, 109.8, 85.5, 80.3, 34.1, 31.8, 29.7, 29.2, 29.1, 26.4, 22.7, 22.6, 14.0. **FTIR** (neat): 3254, 2925, 2858, 1726, 1196 cm^{-1}. **HRMS** (ESI-TOF) *m/z:* $[M + Na]^+$ calcd for $C_{20}H_{31}NO_3Na$ 356.2201; found 356.2206.

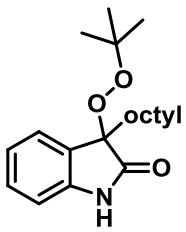

***N*-(2-(3-(*tert*-Butylperoxy)-2-oxoindolin-3-yl)ethyl)-4-methylbenzenesulfonamide** (**2m**): Prepared according to general procedure A, 4-methyl-N-(2-(2-oxoindolin-3-yl)ethyl)benzene-sulfonamide (82.5 mg, 0.25 mmol) to afford peroxyoxindole **2m** (98 mg, 94% yield) as a yellow liquid. **^{1}H NMR** (400 MHz, $CDCl_3$) δ 8.01 (bs, 1H), 7.73 – 7.69 (m, 2H), 7.29-7.24 (m, 4H), 7.19 (d, *J* = 7.1 Hz, 1H), 7.04 (td, *J* = 7.6, 0.8 Hz, 1H), 6.83 (d, *J* = 7.7 Hz, 1H), 5.54 (t, *J* = 6.1 Hz, 1H), 3.17 – 3.07 (m, 2H), 2.41 (s, 3H), 2.28 – 2.19 (m, 1H), 2.05 – 1.95 (m, 1H), 1.08 (s, 9H). **^{13}C NMR** (100 MHz, $CDCl_3$) δ 176.4, 143.4, 140.8, 136.9, 130.1, 129.8, 128.2, 127.2, 124.7, 122.9, 110.4, 83.9, 81.0, 38.2, 34.1, 26.5, 21.6. **FTIR** (neat): 3265, 2976, 2925, 2861, 1724, 1158 cm^{-1}. **HRMS** (ESI-TOF) *m/z:* $[M + H]^+$ calcd for $C_{21}H_{27}N_2O_5S$ 419.1640; found 419.1639.

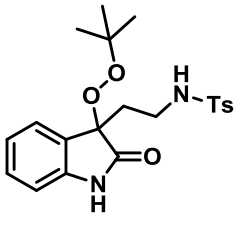

2-(3-(*tert*-Butylperoxy)-2-oxoindolin-3-yl)acetonitrile (2n)[34]: Prepared according to general procedure A, 2-(2-oxoindolin-3-yl)acetonitrile (50 mg, 0.29 mmol) to afford peroxyoxindole **2n** (69.5 mg, 92% yield) as a pale yellow solid. **Melting point**: 114-116 °C. **^{1}H NMR** (400 MHz, $CDCl_3$) δ 8.18 (bs, 1H), 7.61 (d, *J* = 7.3 Hz, 1H), 7.35 (td, *J* = 7.8, 1.1 Hz, 1H), 7.13 (td, *J* = 7.5, 0.7 Hz, 1H), 6.91 (d, *J* = 7.7 Hz, 1H), 3.17 (d, *J* =

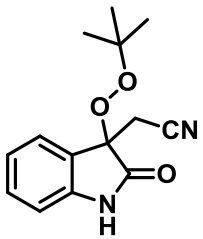

16.8 Hz, 1H), 2.82 (d, *J* = 16.9 Hz, 1H), 1.16 (s, 9H). **^{13}C NMR** (100 MHz, $CDCl_3$) δ 173.9, 140.9, 131.1, 125.7, 125.6, 123.3, 114.9, 110.6, 8 1.9, 80.3, 26.4, 23.3. **FTIR** (neat): 3266, 2978, 2925, 2115, 1733, 1107 cm^{-1}. **HRMS** (ESI-TOF) *m/z:* $[M + Na]^+$ calcd for $C_{14}H_{16}N_2O_3Na$ 283.1058; found 283.1067.

2-(3-(*tert*-Butylperoxy)-2-oxoindolin-3-yl)acetic acid (2o)[35]: Prepared according to general procedure A, 2-(2-oxoindolin-3-yl)acetic acid (48 mg, 0.25 mmol) to afford peroxyoxindole **2o** (54 mg, 77% yield) as a creamy solid. **Melting point**: 188-190 °C. **^{1}H NMR** (400 MHz, DMSO-*d6*) δ 12.29 (s, 1H), 10.36 (s, 1H), 7.36 (d, *J* = 7.3 Hz, 1H), 7.22 (dt, *J* = 7.7, 1.2 Hz, 1H), 6.93 (dt, *J* = 7.6, 0.9 Hz, 1H), 6.77 (d, *J* = 7.7 Hz, 1H), 3.02 (d, *J* = 15.7 Hz, 1H), 2.93 (d, *J* = 15.7 Hz, 1H), 1.01 (s, 9H). **^{13}C NMR** (100 MHz, DMSO-*d6*) δ 173.9, 169.3, 143.5, 129.8, 127.2, 124.9, 121.0, 109.4, 81.7, 79.9, 37.6, 26.1. **FTIR** (neat): 3368, 2922, 2855, 1725, 1188 cm^{-1}. **HRMS** (ESI-TOF) *m/z:* $[M + H]^+$ calcd for $C_{14}H_{18}NO_5$ 280.1185; found 280.1179.

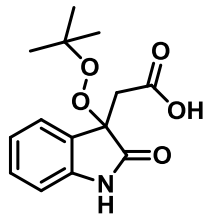

1-Benzyl-3-(*tert*-butylperoxy)-3-(4-methylbenzyl)indolin-2-one (**2p**): Prepared according to general procedure A, 1-benzyl-3-(4-methylbenzyl)indolin-2-one (81.7 mg, 0.25 mmol) to afford peroxyoxindole **2p** (91.5 mg, 88% yield) as a white solid. **Melting point**: 124-126 °C. **^{1}H NMR** (400 MHz, $CDCl_3$) δ 7.18 – 7.06 (m, 5H), 6.99 – 6.87 (m, 7H), 6.40 (d, *J* = 7.7 Hz, 1H), 4.88 (d, *J* = 16.1 Hz, 1H), 4.72 (d, *J* = 16.1 Hz, 1H), 3.35 (d, *J* = 13.0 Hz, 1H), 3.14 (d, *J* = 13.0 Hz, 1H), 2.28 (s, 3H), 1.15 (s, 9H). **^{13}C NMR** (100 MHz, $CDCl_3$) δ 174.5, 143.3, 136.5, 135.5, 130.8, 130.4, 129.4, 128.7, 128.5, 127.5, 127.3, 126.8, 125.3, 122.0, 109.1, 85.7, 80.7, 43.5, 39.8, 26.7, 21.3. **FTIR** (neat): 3381, 2922, 2855, 1730, 1114 cm^{-1}. **HRMS** (ESI-TOF) *m/z:* $[M + Na]^+$ calcd for $C_{27}H_{29}NO_3Na$ 438.2044; found 438.2050.

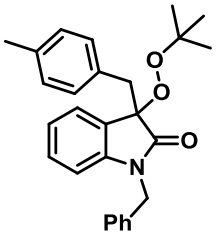

3-([1,1'-Biphenyl]-4-ylmethyl)-1-benzyl-3-(*tert*-butylperoxy)indolin-2-one (2q): Prepared according to general procedure A, 3-([1,1'-biphenyl]-4-ylmethyl)-1-benzylindolin-2-one (97 mg, 0.25 mmol) to afford peroxyoxindole **2q** (115 mg, 97% yield) as a yellow solid. **Melting point**: 122-125 °C. **^{1}H NMR** (400 MHz, $CDCl_3$) δ 7.56 (d, *J* =1.8 Hz, 2H), 7.45 – 7.38 (m, 4H), 7.33 (ddd, *J* = 7.3, 3.7, 1.2 Hz, 1H), 7.16 (d, *J* = 0.8 Hz, 1H), 7.14 – 7.07 (m, 6H), 7.01 – 6 .92 (m, 3H), 6.42 (d, *J* = 7.7 Hz, 1H), 4.90 (d, *J* = 16.1 Hz, 1H), 4.73 (d, *J* = 16.1 Hz, 1H), 3.44 (d, *J* = 13.0 Hz, 1H), 3.22 (d, *J* = 13.0 Hz, 1H), 1.18 (s, 9H). **^{13}C NMR** (100 MHz, $CDCl_3$) δ 174.41, 143.30, 140.72, 139.68, 135.40, 132.72, 131.40, 129.55, 128.88, 128.75, 128.61, 127.38, 127.30, 127.04, 126.79, 126.60, 125.29, 122.14, 109.26, 85.63, 80.77, 43.52, 39.85, 26.69. **FTIR** (neat): 3369, 2920, 1726, 1178 cm^{-1}. **HRMS** (ESI-TOF) *m/z:* $[M + Na]^+$ calcd for $C_{32}H_{31}NO_3Na$ 500.2201; found 500.2202.

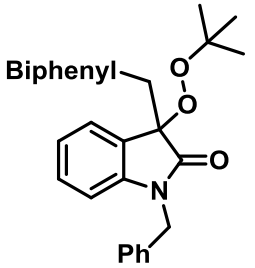

1-Benzyl-3-(*tert*-butylperoxy)-3-(3-fluorobenzyl)indolin-2-one (**2r**): Prepared according to general procedure A, 1-benzyl-3-(3-fluorobenzyl)indolin-2-one (82.7 mg, 0.25 mmol) to afford peroxyoxindole **2r** (73 mg, 70% yield) as a white solid. **Melting**

point: 98-100 °C. **^{1}H NMR** (400 MHz, $CDCl_3$) δ 7.19 (dd, *J* = 6.5, 3.5 Hz, 3H), 7.14 – 7.06 (m, 3H), 7.01 (dd, *J* = 6.2, 3.0 Hz, 2H), 6.97 (t, *J* = 7.5 Hz, 1H), 6.88 (td, *J* = 8.4, 2.2 Hz, 1H), 6.81 (d, *J* = 7.6 Hz, 1H), 6.75 (d, *J* = 9.9 Hz, 1H), 6.45 (d, *J* = 7.8 Hz, 1H), 4.96 (d, *J* = 16.0 Hz, 1H), 4.67 (d, *J* = 16.0 Hz, 1H), 3.39 (d, *J* = 13.1 Hz, 1H), 3.16 (d, *J* = 13.1 Hz, 1H), 1.16 (s, 9H). **^{13}C NMR** (100 MHz, $CDCl_3$) δ 174.2, 162.4 (d, *J* = 245.4 Hz), 143.2, 136.2 (d, *J* = 7.7 Hz), 135.4, 129.7, 129.4 (d, *J* = 8.2 Hz), 128.6, 127.4, 127.0, 126.8, 126.7 (d, *J* = 2.8 Hz), 125.2, 122.2, 117.7 (d, *J* = 21.5 Hz), 114.0 (d, *J* = 21.0 Hz), 109.3, 85.3, 80.9, 43.5, 39.9 (d, *J* = 1.5 Hz), 26.6 (s). **FTIR** (neat): 3383, 2920, 2853, 1730, 1182 cm^{-1}. **HRMS** (ESI-TOF) *m/z:* $[M + Na]^+$ calcd for $C_{26}H_{26}FNO_3Na$ 442.1794; found 442.1793.

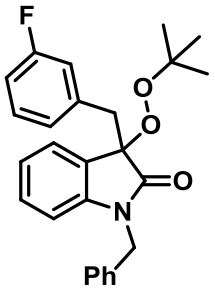

3-(*tert*-Butylperoxy)-3-methylindolin-2-one (2s): Prepared according to general procedure A, 3-methylindolin-2-one (36.7 mg, 0.25 mmol) to afford peroxyoxindole **2s** (73 mg, 95% yield) as a white solid. **Melting point**: 128-130 °C. **^{1}H NMR** (400 MHz, $CDCl_3$) δ 7.98 (s, 1H), 7.32 (d, *J* = 7.3 Hz, 1H), 7.24 (dd , *J* = 7.7, 1.2 Hz, 1H), 7.05 (td, *J* = 7.5, 0.7 Hz, 1H), 6.85 (dd, *J* = 7.8, 0.7 Hz, 1H), 1.54 (s, 3H), 1.11 (s, 9H). **^{13}C NMR** (100 MHz, $CDCl_3$) δ 192.3, 140.7, 130.2, 129.5, 124.5, 122.6, 110.0, 82.2, 80.5, 26.6, 20.4. **FTIR** (neat): 3257, 2979, 2927, 1728, 1111 cm^{-1}. **HRMS** (ESI-TOF) *m/z:* $[M + H]^+$ calcd for $C_{13}H_{18}NO_3$ 236.1287; found 236.1298.

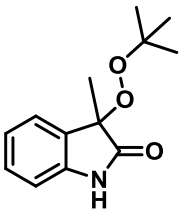

5-Benzyl-5-(*tert*-butylperoxy)-1,3-dimethylpyrimidine-2,4,6(1*H*,3*H*,5*H*)-trione (4a): Prepared according to general procedure A, 5-benzyl-1,3-dimethylpyrimidine-2,4,6(1*H*,3*H*,5*H*)-trione (61.5 mg, 0.25 mmol) to afford peroxybarbiturate **4a** (81 mg, 97% yield) as a colorless crystals. **Melting point**: 67-70 °C. **^{1}H NMR** (40.00 MHz, $CDCl_3$) δ 7.24 – 7.22 (m, 3H), 7.01 – 6.98 (m, 2H), 3.28 (s, 2H), 3.11 (s, 6H), 1.24 (s, 9H). **^{13}C NMR** (100 MHz, $CDCl_3$) δ 168.3, 150.2, 130.9, 129.6, 128.9, 128.5, 84.1, 82.4, 41.9, 28.6, 26.5. **FTIR** (neat): 3432, 2978, 2926, 2857, 1688 cm^{-1}. **HRMS** (ESI-TOF) *m/z:* $[M + H]^+$ calcd for $C_{17}H_{23}N_2O_5$ 335.1607; found 335.1610.

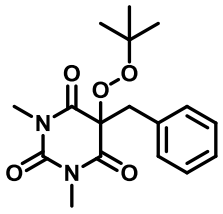

5-(*tert*-Butylperoxy)-5-(2-methoxybenzyl)-1,3-dimethylpyrimidine-2,4,6(1*H*,3*H*,5*H*)-trione (**4b**): Prepared according to general procedure A, 5-(2-methoxybenzyl)-1,3-dimethylpyrimidine-2,4,6(1*H*,3*H*,5*H*)-trione (69 mg, 0.25 mmol) to afford peroxybarbiturate **4b** (69 mg, 76% yield) as a pale yellow liquid. **^{1}H NMR** (400 MHz, $CDCl_3$) δ 7.22 (td, *J* = 8.2, 1.7 Hz, 1H), 7.01 (dd, *J* = 7.5 , 1.5 Hz, 1H), 6.84 (td, *J* = 7.4, 0.8 Hz, 1H), 6.77 (d, *J* = 8.3 Hz, 1H), 3.72 (s, 3H), 3.28 (s, 2H), 3.10 (s, 6H), 1.26 (s, 9H). **^{13}C NMR** (100 MHz, $CDCl_3$) δ 167.9, 157.6, 150.7, 132.1, 129.9, 120.7, 119.8, 110.3, 83.7, 82.1, 55.4, 37.1, 28.6, 26.6. **FTIR** (neat): 3396, 2979, 1685, 1065 cm^{-1}. **HRMS** (ESI-TOF) *m/z:* $[M + Na]^+$ calcd for $C_{18}H_{24}N_2O_6Na$ 387.1532; found 387.1536.

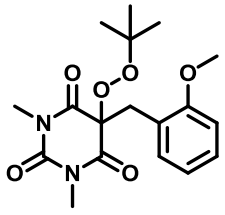

5-(*tert*-Butylperoxy)-1,3-dimethyl-5-(3-methylbenzyl)pyrimidine-2,4,6(1*H*,3*H*,5*H*)-trione (**4c**): Prepared according to general procedure A, 1,3-dimethyl-5-(3-methylbenzyl)pyrimidine-2,4,6(1*H*,3*H*,5*H*)-trione (65 mg, 0.25 mmol) to afford peroxybarbiturate **4c** (73 mg, 84% yield) as a white solid. **Melting point**: 61-63 °C. **^{1}H NMR** (400 MHz, $CDCl_3$) δ 7.10 (t, *J* = 7.5 Hz, 1H), 7.03 (d, *J* = 7.6 Hz, 1H), 6.81 – 6.76 (m, 2H), 3.22 (s, 2H), 3.10 (s, 6H), 2.25 (s, 3H), 1.23 (s, 9H). **^{13}C NMR** (100 MHz, $CDCl_3$) δ 168.7, 150.2, 138.6, 130.7, 130.2, 129.1, 128.7, 126.6, 84.2, 82.3, 42.0, 28.5, 26.5, 21.3. **FTIR** (neat): 2979, 2925, 2857, 1692, 1106 cm^{-1}. **HRMS** (ESI-TOF) *m/z:* $[M + H]^+$ calcd for $C_{18}H_{25}N_2O_5$ 349.1763; found 349.1769.

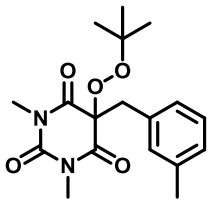

5-(*tert*-Butylperoxy)-1,3-dimethyl-5-(4-methylbenzyl)pyrimidine-2,4,6(1*H*,3*H*,5*H*)-trione (**4d**): Prepared according to general procedure A, 1,3-dimethyl-5-(4-methylbenzyl)pyrimidine-2,4,6(1*H*,3*H*,5*H*)-trione (65 mg, 0.25 mmol) to afford peroxybarbiturate **4d** (63 mg, 72% yield) as a colorless solid. **Melting point**: 72-74 °C. **^{1}H NMR** (400 MHz, $CDCl_3$) δ 7.01 (d, *J* = 7.8 Hz, 2H), 6.86 (d, *J* = 8.0 Hz, 2H), 3.22 (s, 2H), 3.12 (s, 6H), 2.26 (s, 3H), 1.22 (s, 9H). **^{13}C NMR** (100 MHz, $CDCl_3$) δ 168.4, 150.3, 138.1, 129.5, 127.7, 84.1, 82.3, 41.5, 2 8.5, 26.5, 21.2. **FTIR** (neat): 3429, 2923, 1688, 1106 cm^{-1}. **HRMS** (ESI-TOF) *m/z:* $[M + H]^+$ calcd for $C_{18}H_{25}N_2O_5$ 349.1763; found 349.1773.

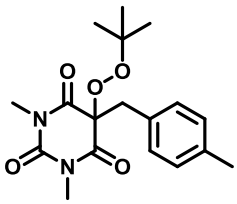

5-([1,1'-Biphenyl]-4-ylmethyl)-5-(*tert*-butylperoxy)-1,3-dimethylpyrimidine-2,4,6(1*H*,3*H*,5*H*)-trione (**4e**): Prepared according to general procedure A, 5-([1,1'-biphenyl]-4-ylmethyl)-1,3-dimethylpyrimidine-2,4,6(1*H*,3*H*,5*H*)-trione (80.5 mg, 0.25 mmol) to afford peroxybarbiturate **4e** (86 mg, 84% yield) as a white solid. **Melting point**: 106-108 °C. **^{1}H NMR** (400 MHz, $CDCl_3$) δ 7.53 (d, *J* = 7.2 Hz, 2H), 7.46 (d, *J* = 8.4 Hz, 2H), 7.45 – 7.40 (m, 2H), 7.37 – 7.32 (m, 1H), 7.08 (d, *J* = 8.4 Hz, 2H), 3.33 (s, 2H), 3.16 (s, 6H), 1.25 (s, 9H). **^{13}C NMR** (100 MHz, $CDCl_3$) δ 168.4, 150.3, 141.2, 140.3, 130.1, 129.9, 128.9, 127.7, 127.5, 127.2, 83.9, 82.4, 41.4, 28.7, 26.5. **FTIR** (neat): 3377, 2923, 2854, 2315, 1695, 1188 cm^{-1}. **HRMS** (ESI-TOF) *m/z:* $[M + H]^+$ calcd for $C_{23}H_{27}N_2O_5$ 411.1920; found 411.1917.

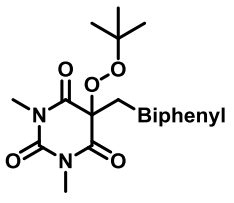

5-(*tert*-Butylperoxy)-5-(3-fluorobenzyl)-1,3-dimethylpyrimidine-2,4,6(1*H*,3*H*,5*H*)-trione (**4f**): Prepared according to general procedure A, 5-(3-fluorobenzyl)-1,3-dimethylpyrimidine-2,4,6(1*H*,3*H*,5*H*)-trione (66 mg, 0.25 mmol) to afford peroxybarbiturate **4f** (71 mg, 81% yield) as a colorles s semisolid. **Melting point**: 51-54 °C. **^{1}H NMR** (400 MHz, $CDCl_3$) δ 7.20 (dd, *J* = 14.0, 7.9 Hz, 1H), 6.97 – 6.91 (m, 1H), 6.81 – 6.77 (m, 1H), 6.74 (d, *J* = 9.3 Hz, 1H), 3.27 (s, 2H), 3.15 (s, 6H), 1.22 (s, 9H). **^{13}C NMR** (100 MHz, $CDCl_3$) δ 168.1, 162.8 (d, *J* = 247.8 Hz), 150.2, 133.4 (d, *J* = 7.4 Hz), 130.4 (d, *J* = 8.1 Hz), 125.4 (d, *J* = 2.6 Hz), 116.7 (d, *J* = 21.6 Hz), 115.5 (d, *J* = 20.9 Hz), 83.6, 82.5,

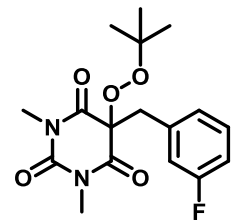

41.1, 28.6, 26.5. **FTIR** (neat): 3431, 2980, 2927, 1688, 1104 cm^{-1}. **HRMS** (ESI-TOF) *m/z:* $[M + H]^+$ calcd for $C_{17}H_{22}FN_2O_5$ 353.1512; found 353.1524.

5-(3-Bromobenzyl)-5-(*tert*-butylperoxy)-1,3-dimethylpyrimidine-2,4,6(1*H*,3*H*,5*H*)-trione (**4g**): Prepared according to general procedure A, 5-(3-bromobenzyl)-1,3-dimethylpyrimidine-2,4,6(1*H*,3*H*,5*H*)-trione (81.2 mg, 0.25 mmol) to afford peroxybarbiturate **4g** (62 mg, 60% yield) as a colorless liquid. **^{1}H NMR** (400 MHz, $CDCl_3$) δ 7.40 – 7.37 (m, 1H), 7.19 (t, *J* = 1.7 Hz , 1H), 7.11 (t, *J* = 7.8 Hz, 1H), 6.95 (d, *J* = 7.7 Hz, 1H), 3.24 (s, 2H), 3.16 (s, 6H), 1.23 (s, 9H). **^{13}C NMR** (100 MHz, $CDCl_3$) δ 168.1, 150.1, 133.3, 132.8, 131.6, 130.3, 128.3, 122.9, 83.7, 82.6, 41.2, 28.6, 26.5. **FTIR** (neat): 3364, 2922, 2854, 1693, 1188 cm^{-1}. **HRMS** (ESI-TOF) *m/z:* $[M + Na]^+$ calcd for $C_{17}H_{21}BrN_2O_5Na$ 435.0532; found 435.0550.

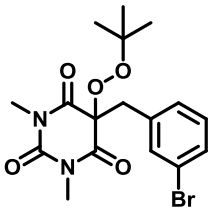

5-(*tert*-Butylperoxy)-5-hexyl-1,3-dimethylpyrimidine-2,4,6(1*H*,3*H*,5*H*)-trione (**4h**): Prepared according to general procedure A, 5-hexyl-1,3-dimethylpyrimidine-2,4,6(1*H*,3*H*,5*H*)-trione (60 mg, 0.25 mmol) to afford peroxybarbiturate **4h** (48 mg, 58% yield) as a yellow liquid. **^{1}H NMR** (400 MHz, $CDCl_3$) δ 3.34 (s, 6H), 2.00 – 1.95 (m, 2H), 1.25-1.20 (6H), 1.17 (s, 9H), 1.12– 1.06 (m, 2H), 0.83 (t, *J* = 6.9 Hz, 3H). **^{13}C NMR** (100 MHz, $CDCl_3$) δ 168.8, 151.0, 82.9, 82.0, 35.5, 31.3, 29.1, 28.9, 26.4, 22.9, 22.5, 14.0. **FTIR** (neat): 2928, 2861, 1687, 1190 cm^{-1}. **HRMS** (ESI-TOF) *m/z:* $[M + H]^+$ calcd for $C_{16}H_{29}N_2O_5$ 329.2076; found 329.2078.

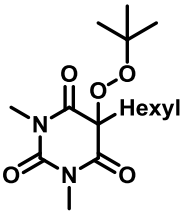

5-(*tert*-Butylperoxy)-1,3-dimethyl-5-octylpyrimidine-2,4,6(1*H*,3*H*,5*H*)-trione (4i): Prepared according to general procedure A, 1,3-dimethyl-5-octylpyrimidine-2,4,6(1*H*,3*H*,5*H*)-trione (67 mg, 0.25 mmol) to afford peroxybarbiturate **4i** (75 mg, 84% yield) as a colorless liquid. **^{1}H NMR** (400 MHz, $CDCl_3$) δ 3.35 (s, 6H), 2.02 – 1.95 (m, 2H), 1.29 – 1.19 (m, 10H), 1.18 (s, 9H), 1.13 – 1.04 (m, 2H), 0.85 (t, *J* = 7.0 Hz, 3H). **^{13}C NMR** (100 MHz, $CDCl_3$) δ 192.6, 168.8, 151.1, 83.0, 82.1, 35.5, 31.8, 29.4, 29.2, 29.1, 28.9, 26.5, 22.9, 22.7, 14.2. **FTIR** (neat): 3417, 2926, 2859, 1693, 1192 cm^{-1}. **HRMS** (ESI-TOF) *m/z:* $[M + Na]^+$ calcd for $C_{18}H_{32}N_2O_5Na$ 379.2209; found 379.2211.

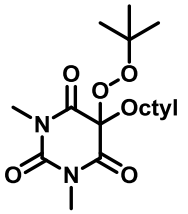

3-(*tert*-Butylperoxy)-3-(4-methylbenzyl)chromane-2,4-dione (6a): Prepared according to general procedure A, 4-hydroxy-3-(4-methylbenzyl)-2*H*-chromen-2-one (66.5 mg, 0.25 mmol) to afford **6a** (71 mg, 80% yield) as a yellow liquid. We observed that, if reaction mixture loaded on silica gel and kept more time in column then it started decomposing. Therefore quick separation is needed from silica gel column to avoid side product. **Melting point**: 99-102 °C. **^{1}H NMR** (400 MHz, $CDCl_3$) δ 7.86 (dd, *J* = 7.8, 1.7 Hz, 1H), 7.52 – 7.48 (m, 1H), 7.16 (dt, *J* = 13.9, 3.4 Hz, 1H), 6.95 – 6.88 (m, 5H), 3.32 (d, *J* = 12.6 Hz, 1H), 3.28 (d, *J* = 12.6 Hz, 1H), 2.16 (s, 3H), 1.23 (s, 9H). **^{13}C NMR** (100 MHz, $CDCl_3$) δ 191.0, 167.4, 154.3, 137.6, 137.1, 130.2, 129.3, 127.3, 126.9, 124.9,

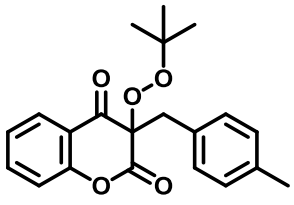

120.0, 117.6, 88.0 , 82.3, 42.0, 26.5, 21.1. **FTIR** (neat): 3400, 2921 2854, 1737, 1651, 1193 cm^{-1}. **HRMS** (ESI-TOF) *m/z:* $[M + H]^+$ calcd for $C_{21}H_{23}N_2O_5Na$ 355.1545; found 355.1557.

2-(*tert*-Butylperoxy)-2-(3-methoxybenzyl)naphthalene-1,3(2*H*,4*H*)-dione (6b): Prepared according to general procedure A, 4-hydroxy-3-(3-methoxybenzyl)naphthalen-2(1*H*)-one (70 mg, 0.25 mmol) to afford **6b** (84 mg, 91% yield) as a colorless liquid. We observed that, if reaction mixture loaded on silica gel and kept more time in column then it started decomposing. Therefore quick separation is needed from silica gel column to avoid side product. 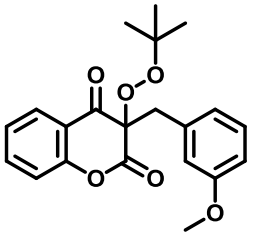 **^{1}H NMR** (400 MHz, $CDCl_3$) δ 7.86 (dd, *J* = 7.8, 1.7 Hz, 1H), 7.53 – 7.47 (m, 1H), 7.20 – 7.14 (m, 1H), 7.03 – 6.93 (m, 2H), 6.64 – 6.60 (m, 2H), 6.57 – 6.55 (m, 1H), 3.64 (s, 3H), 3.34 (d, *J* = 12.5 Hz, 1H), 3.30 (d, *J* = 12.4 Hz, 1H), 1.23 (s, 9H). **^{13}C NMR** (100 MHz, $CDCl_3$) δ 191.0 , 167.6, 159.5, 154.3, 137.2, 131.9, 129.7, 126.9, 124.9, 122.7, 120.1, 117.7, 115.4, 114.1, 87.8, 82.4, 55.2, 42.5, 26.5. **FTIR** (neat): 3416, 2926, 2857, 1712, 1606, 1202 cm^{-1}. **HRMS** (ESI-TOF) *m/z:* $[M + K]^+$ calcd for $C_{21}H_{22}O_6K$ 409.1053; found 409.1059.

3-Benzyl-3-(*tert*-butylperoxy)chromane-2,4-dione (**6c**): Prepared according to general procedure A, 3-benzyl-4-hydroxy-2*H*-chromen-2-one (62 mg, 0.25 mmol) to afford **6c** (67 mg, 79% yield) as a yellow liquid. We observed that, if reaction mixture loaded on silica gel and kept more time in column then it started decomposing. Therefore quick separation is needed from silica gel column to avoid side product. 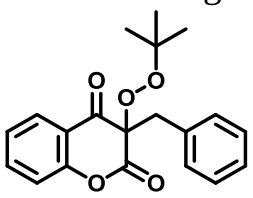 **^{1}H NMR** (400 MHz, $CDCl_3$) δ 7.85 (dd, *J* = 7.8, 1.7 Hz, 1H), 7.50 – 7.45 (m, 1H), 7.18 – 7.13 (m, 1H), 7.10 – 7.02 (m, 1H), 6.92 (dd, *J* = 8.3, 0.7 Hz, 1H), 3.38 – 3.30 (m, 1H), 1.23 (s, 1H). **^{13}C NMR** (100 MHz, $CDCl_3$) δ 190.9, 167.6, 154.3, 137.2, 130.4, 130.3, 128.6, 127.9, 126.9, 124.9, 120.0, 117.6, 87.9, 82.4, 42.5, 26.5. **FTIR** (neat): 3402, 2924, 2854, 1717, 1611, 1149, 1104 cm^{-1}. **HRMS** (ESI-TOF) *m/z:* $[M + K]^+$ calcd for $C_{20}H_{20}O_5K$ 379.0948; found 379.0947.

3-(*tert*-Butylperoxy)-3-(1-phenylethyl)chromane-2,4-dione (**6d**): Prepared according to general procedure A, 4-hydroxy-3-(1-phenylethyl)-2*H*-chromen-2-one (66.5 mg, 0.25 mmol) to afford **6d** (84 mg, 95% yield) as a pale yellow liquid (obtained as a 1:1 diastereomeric mixture, dr is determined by NMR) after silica-gel column purification. 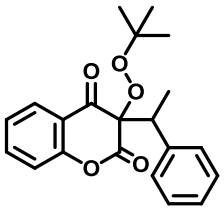 **^{1}H NMR** for major isomer (400 MHz, $CDCl_3$) = 7.73 (dd, *J* = 7.8, 1.7 Hz, 1H), 7.40 – 7.37 (m, 1H), 7.17 – 7.11 (m, 1H), 7.08 – 6.94 (m, 5H), 6.81 (t, *J* = 9.0 Hz, 2H), 3.59 – 3.54 (m, 1H), 1.54 (d, *J* = 7.2 Hz, 3H), 1.26 (s, 9H). **^{13}C NMR** for major isomer (100 MHz, $CDCl_3$) δ 191.5, 167.9, 154.3, 136.8, 136.2, 128.9, 128.4, 126.8, 124.7, 120.9, 117.3, 90.2, 82.3, 48.0, 26.5, 14.5. **FTIR** (neat): 2980, 2928, 1783, 1703, 1608, 1141 cm^{-1}. **HRMS** (ESI) *m/z:* $[M + K]^+$ calcd for $C_{21}H_{22}O_5K$ 393.1101; found 393.1111.

3A.11.4. Appendix III: Copies of ^{1}H and ^{13}C NMR spectra of representative compounds

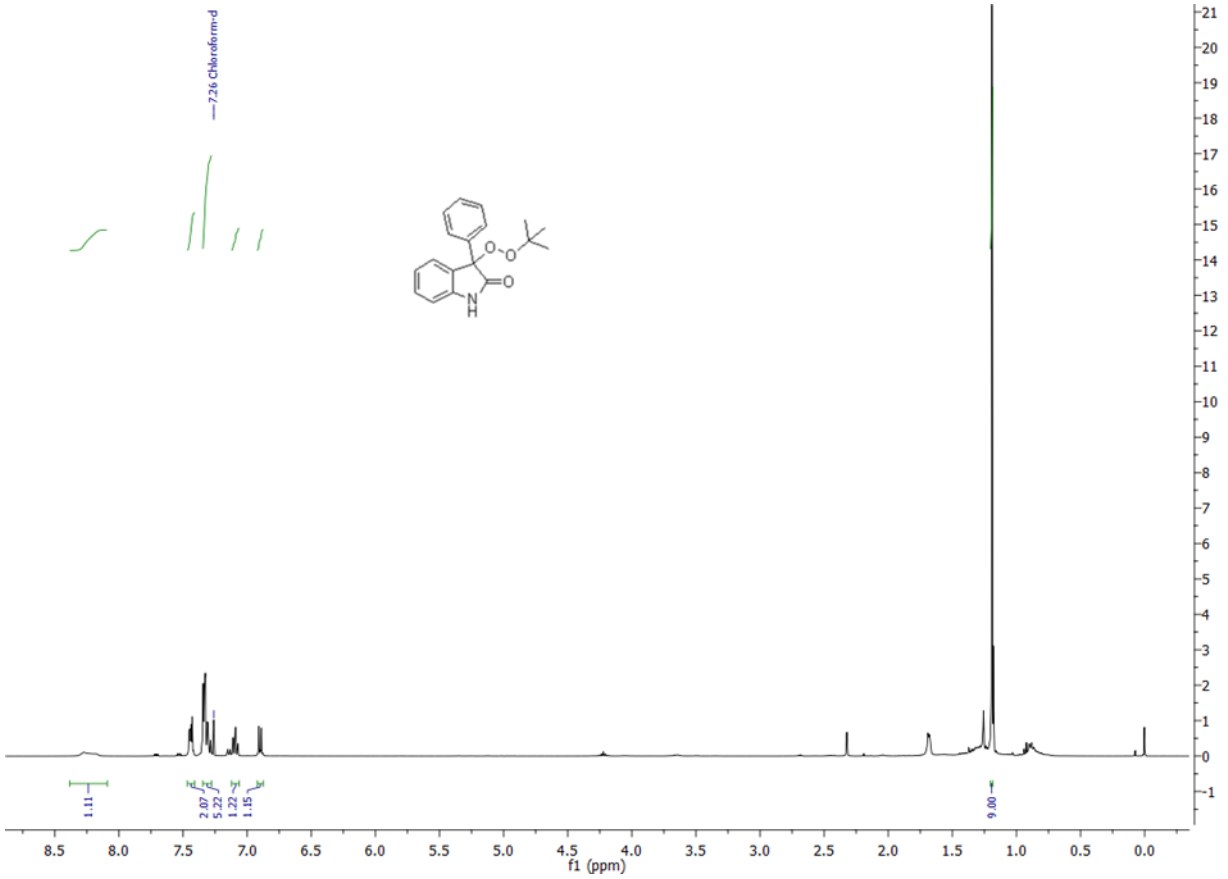

Figure 3A.11. ^{1}H NMR of compound **2h**

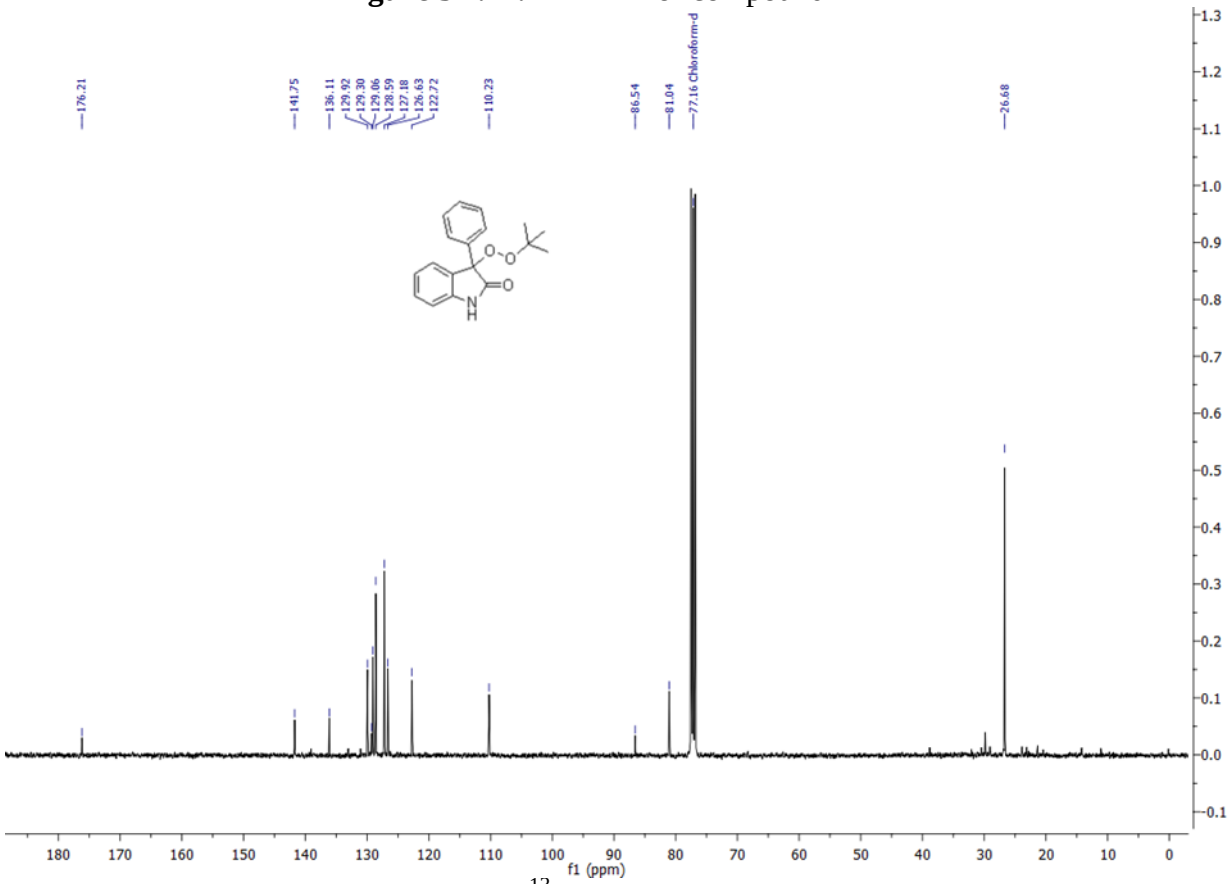

Figure 3A.12. ^{13}C NMR of compound **2h**

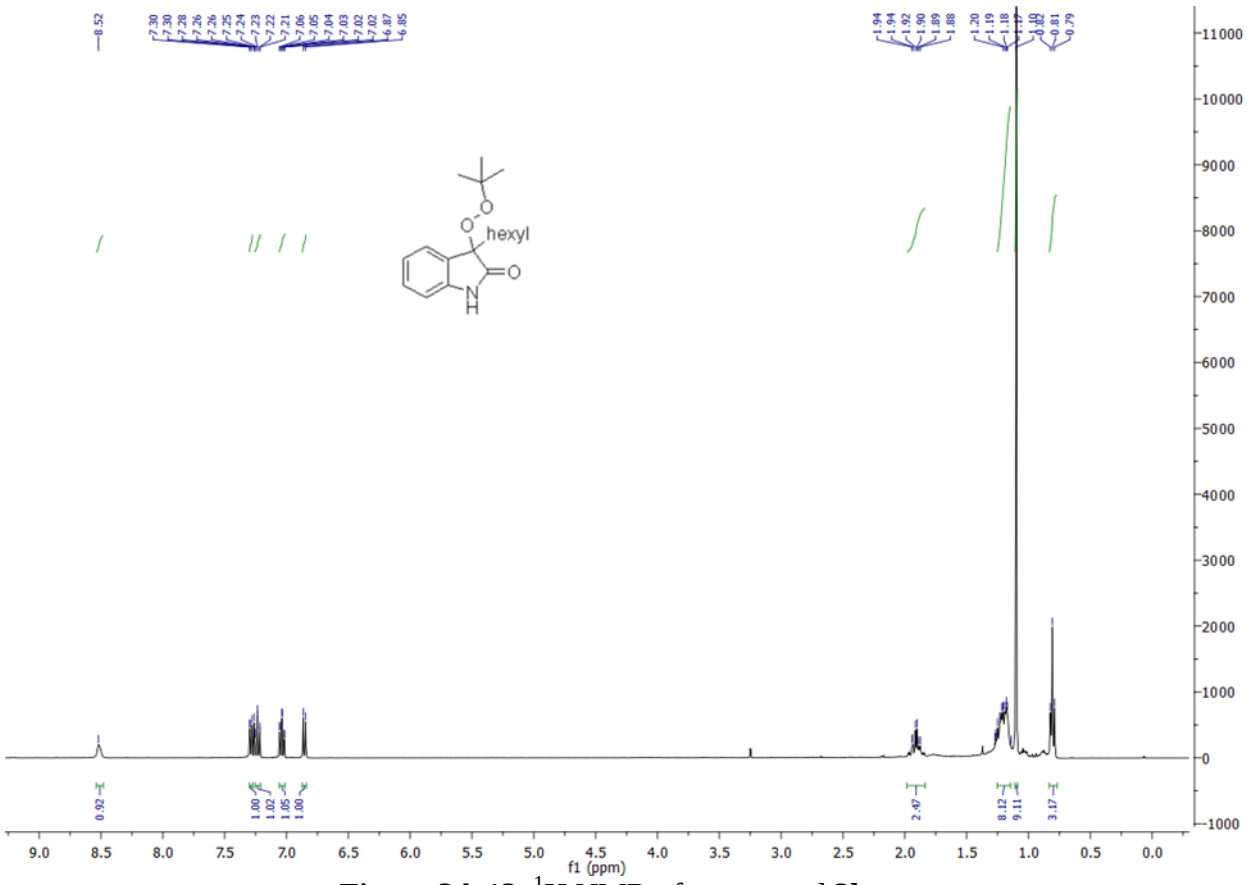

Figure 3A.13. ^{1}H NMR of compound **2k**

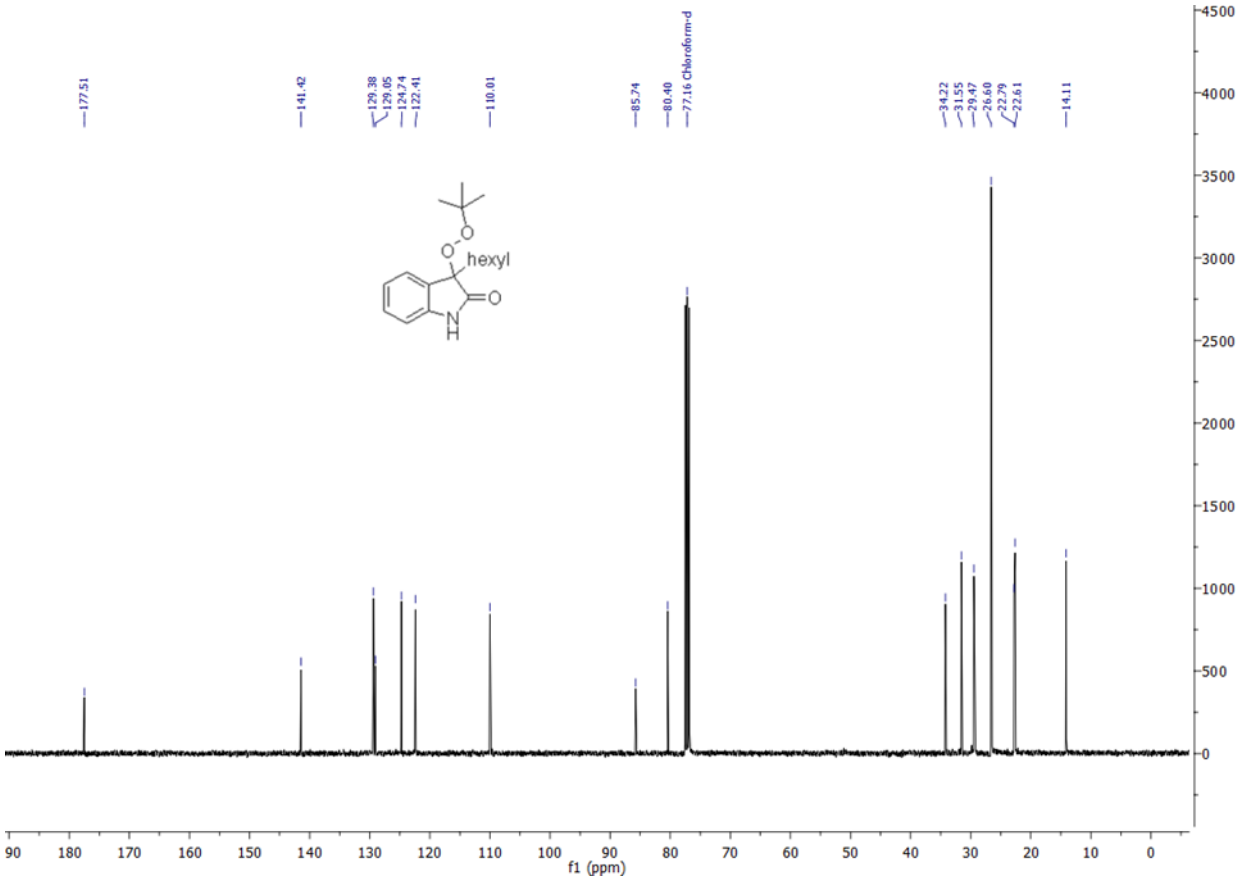

Figure 3A.14. ^{13}C NMR of compound **2k**

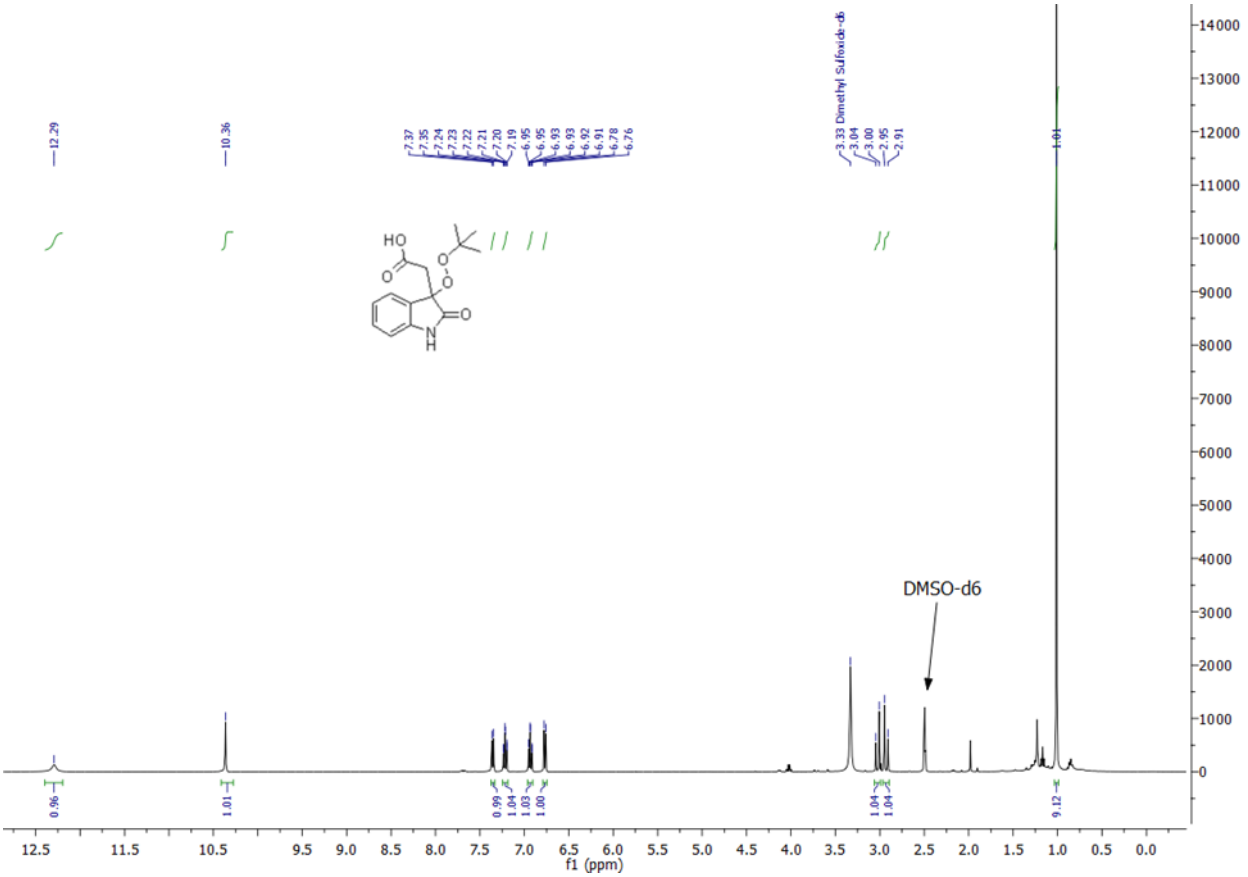

Figure 3A.15. ^{1}H NMR of compound **2o**

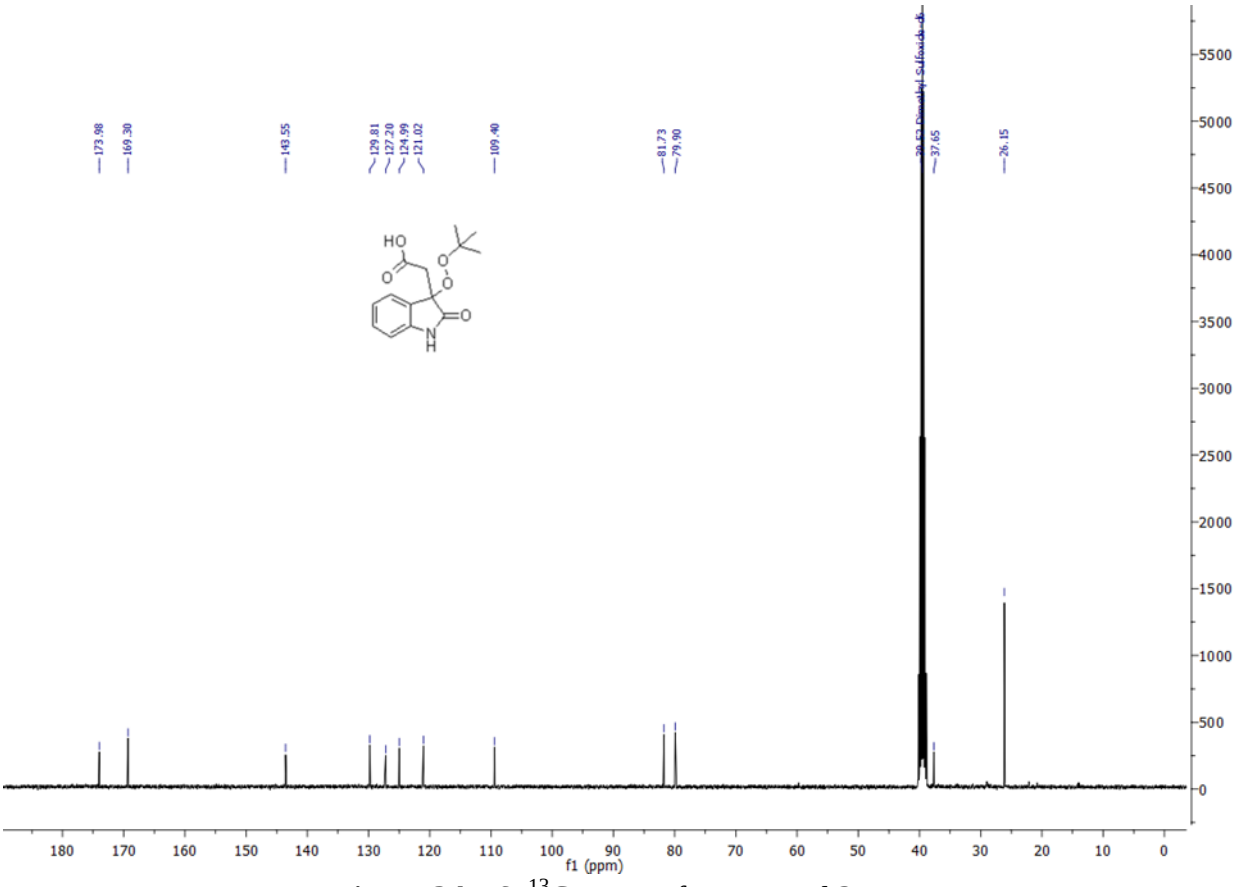

Figure 3A.16. ^{13}C NMR of compound **2o**

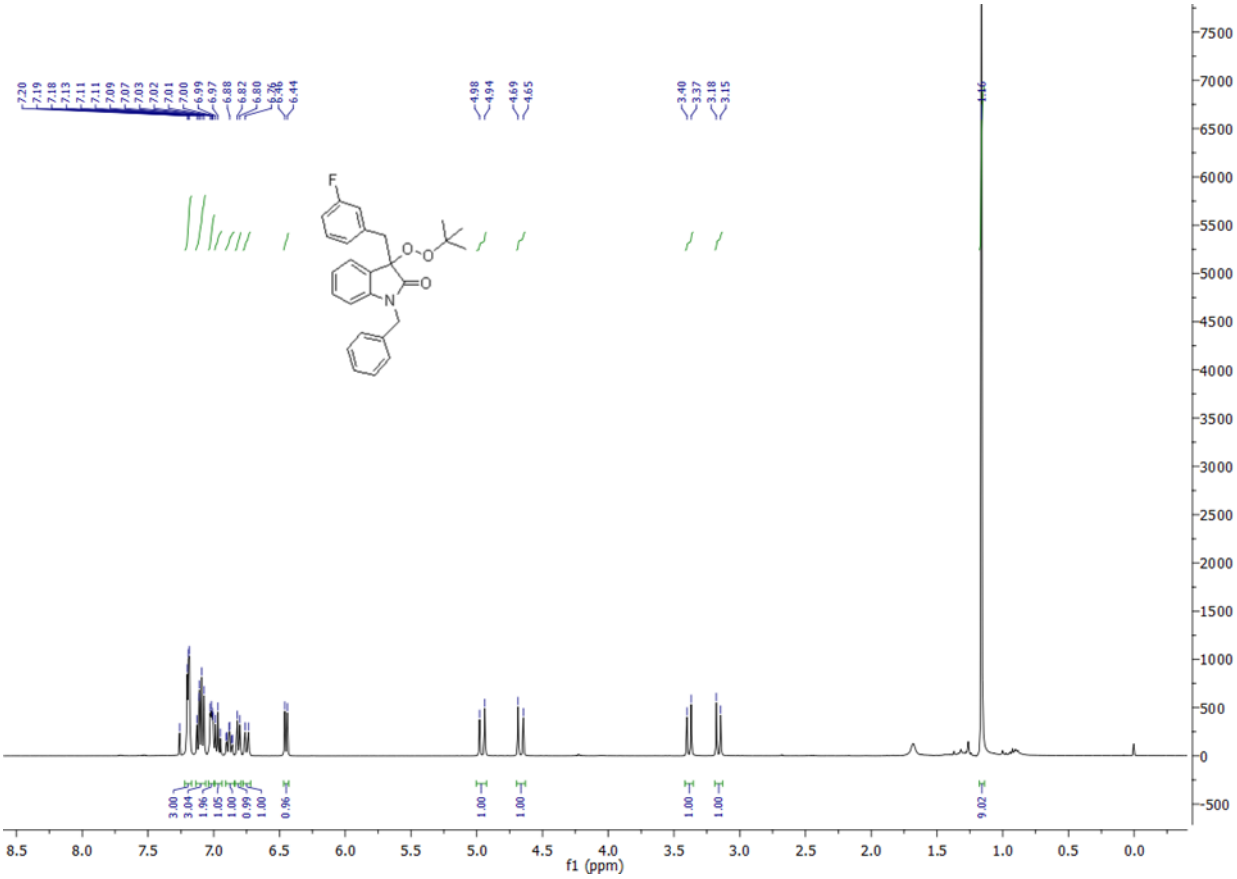

Figure 3A.17. ^{1}H NMR of compound **2r**

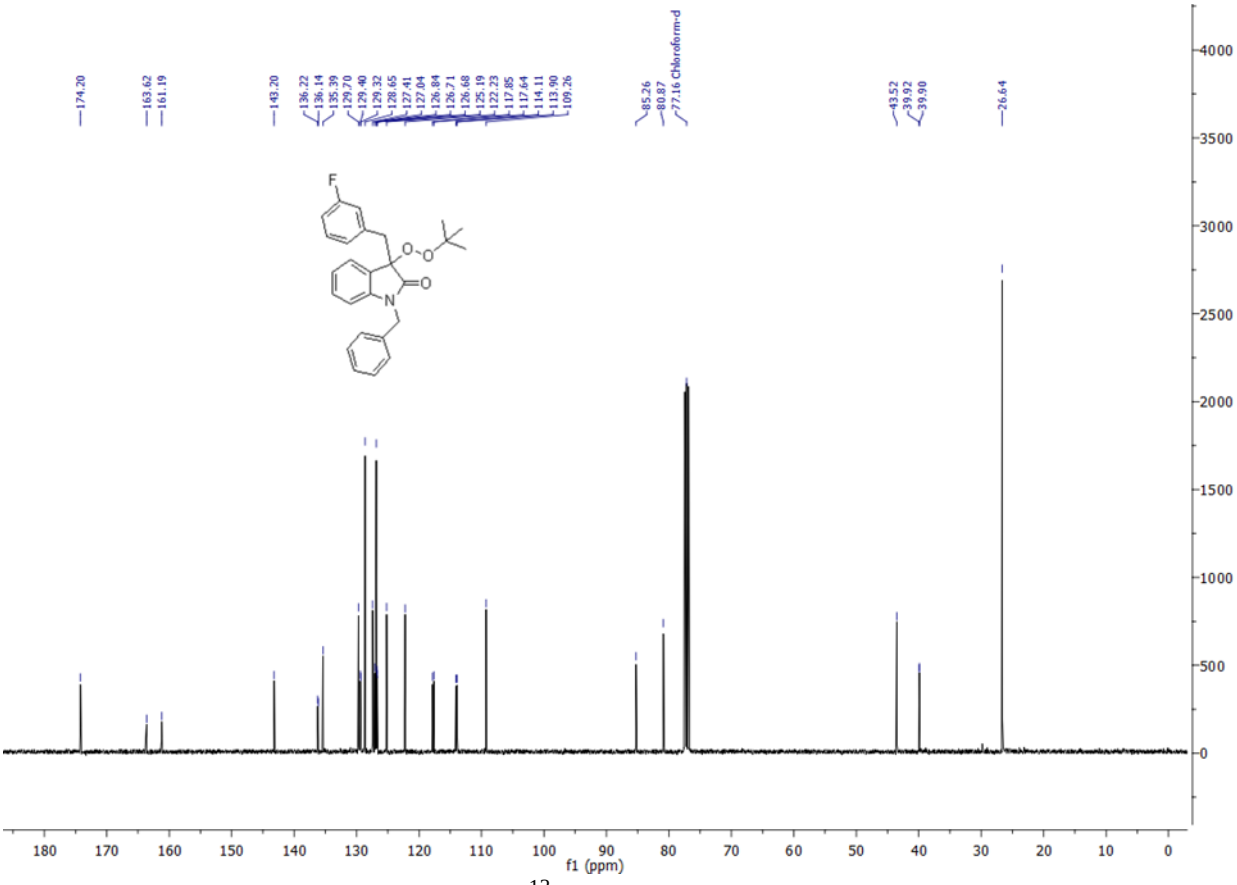

Figure 3A.18. ^{13}C NMR of compound **2r**

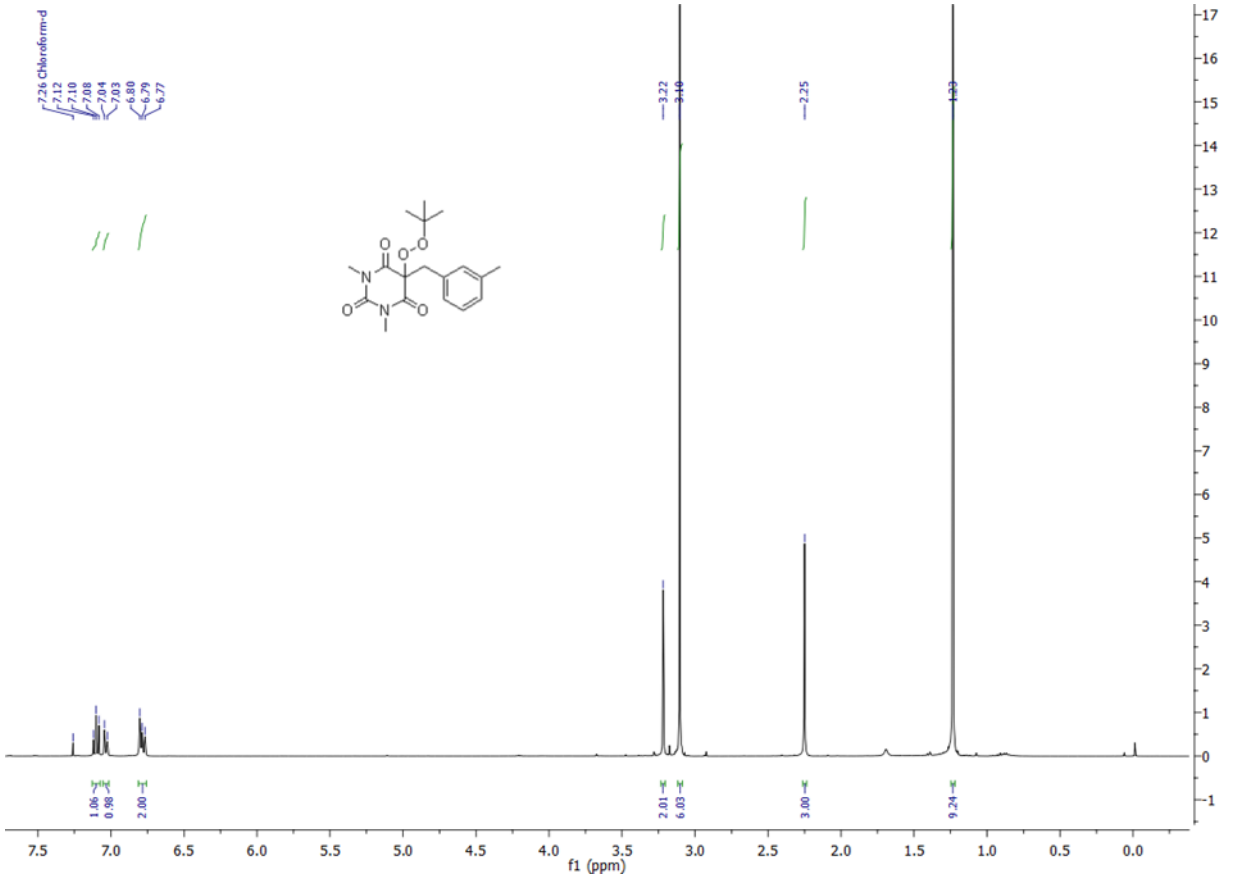

Figure 3A.19. ^{1}H NMR of compound **4c**

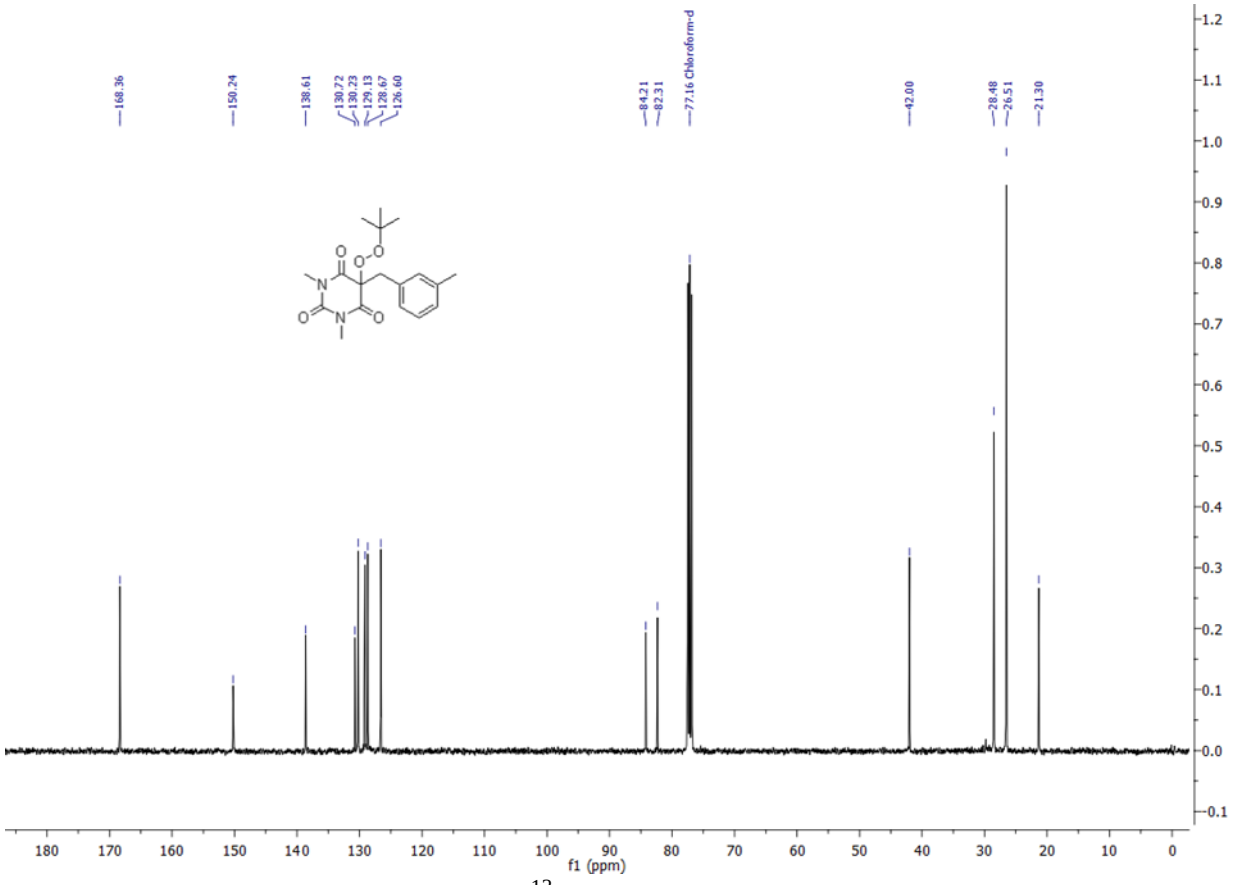

Figure 3A.20. ^{13}C NMR of compound **4c**

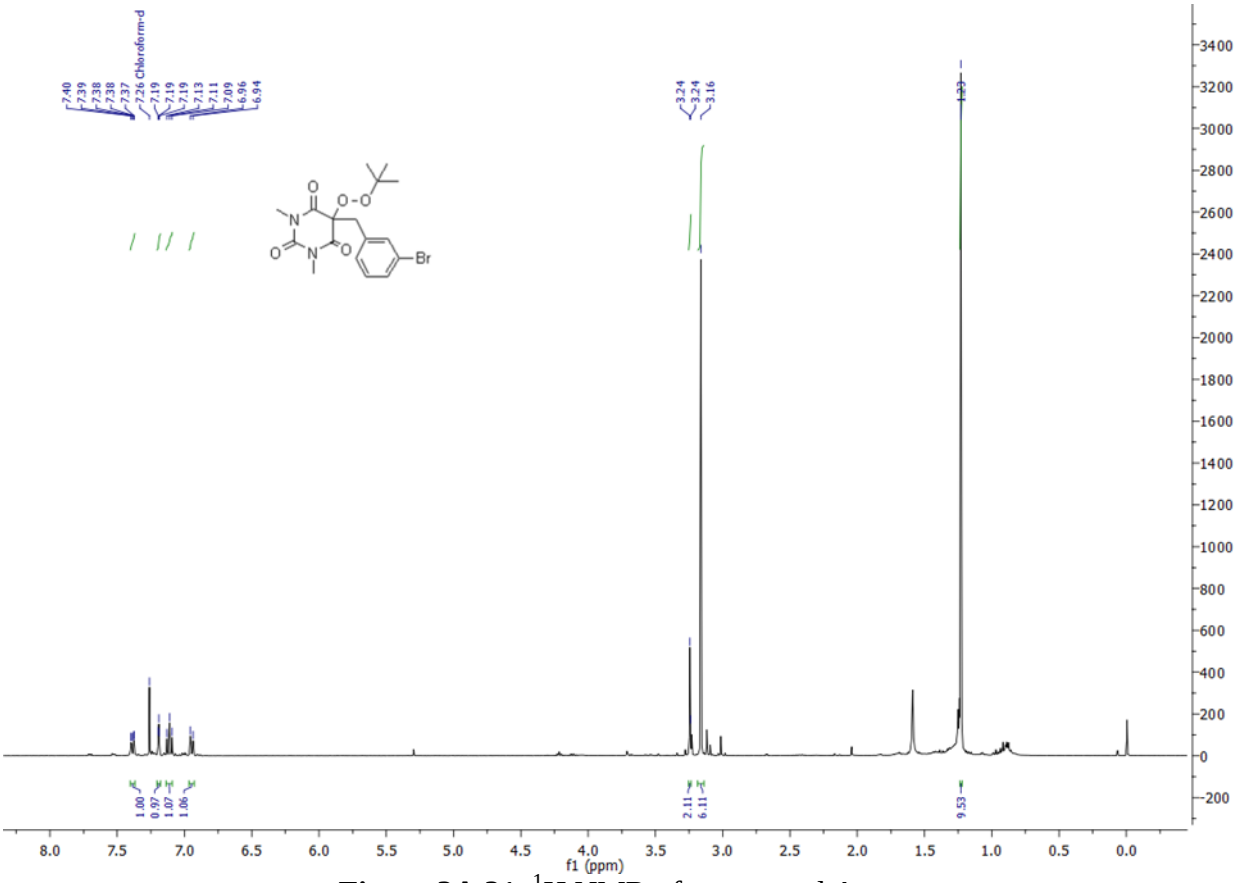

Figure 3A.21. ^{1}H NMR of compound **4g**

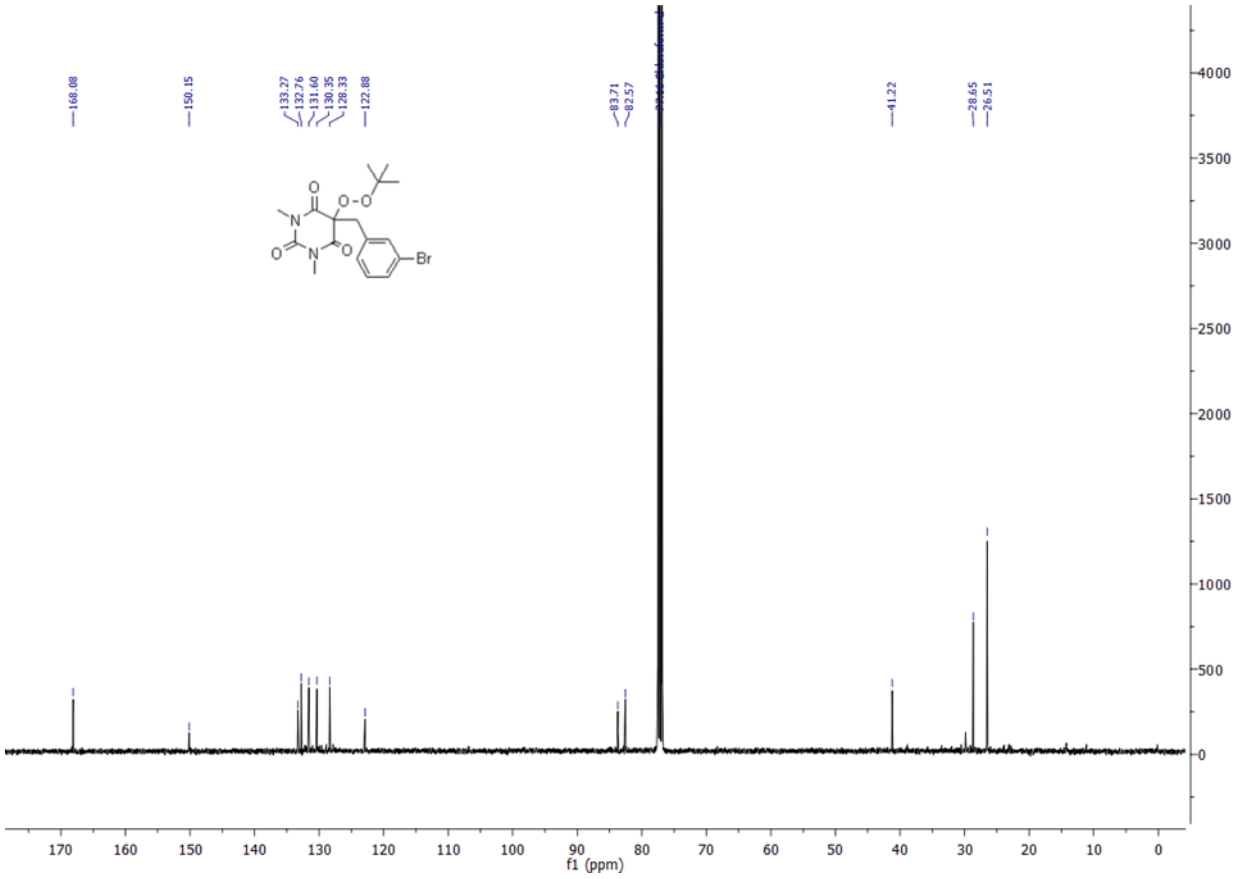

Figure 3A.22. ^{13}C NMR of compound **4g**

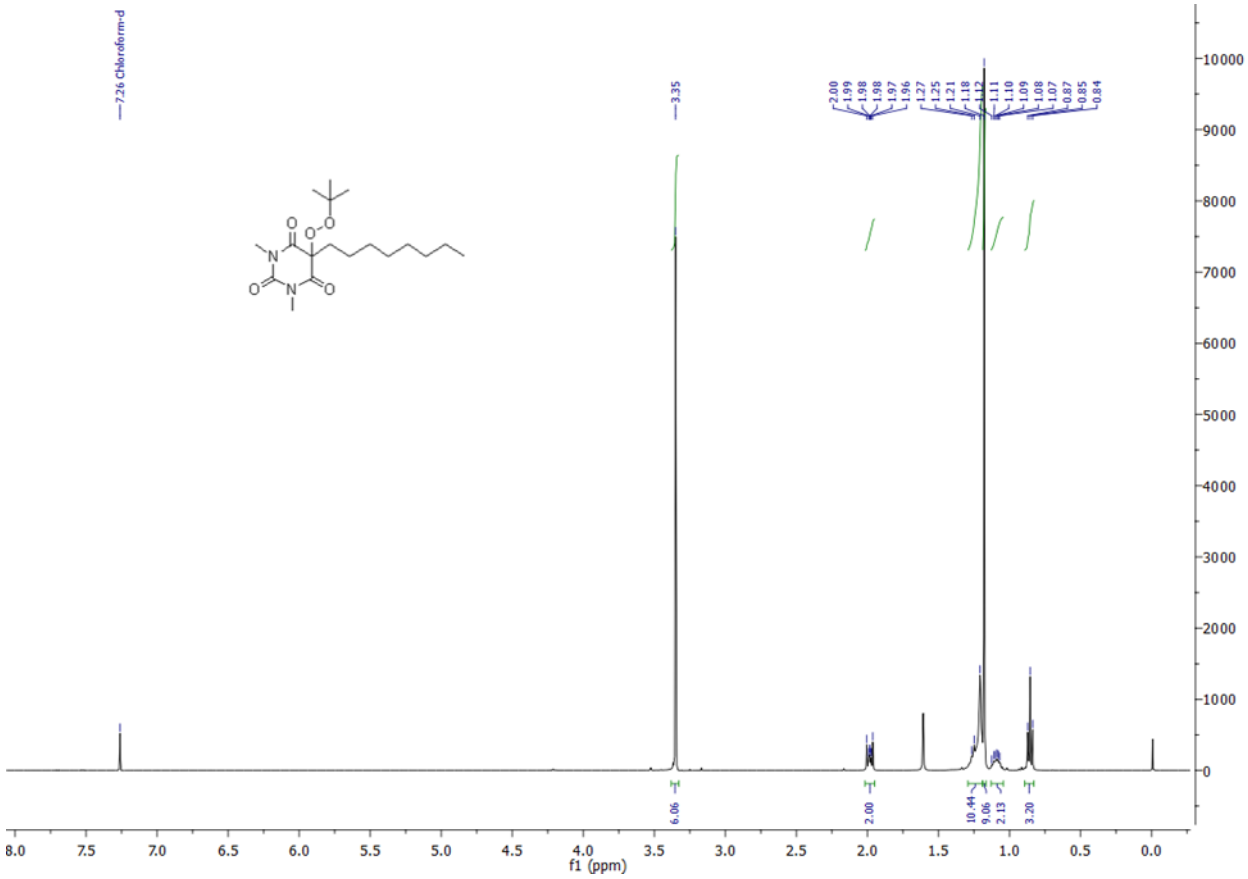

Figure 3A.23. ^{1}H NMR of compound **4i**

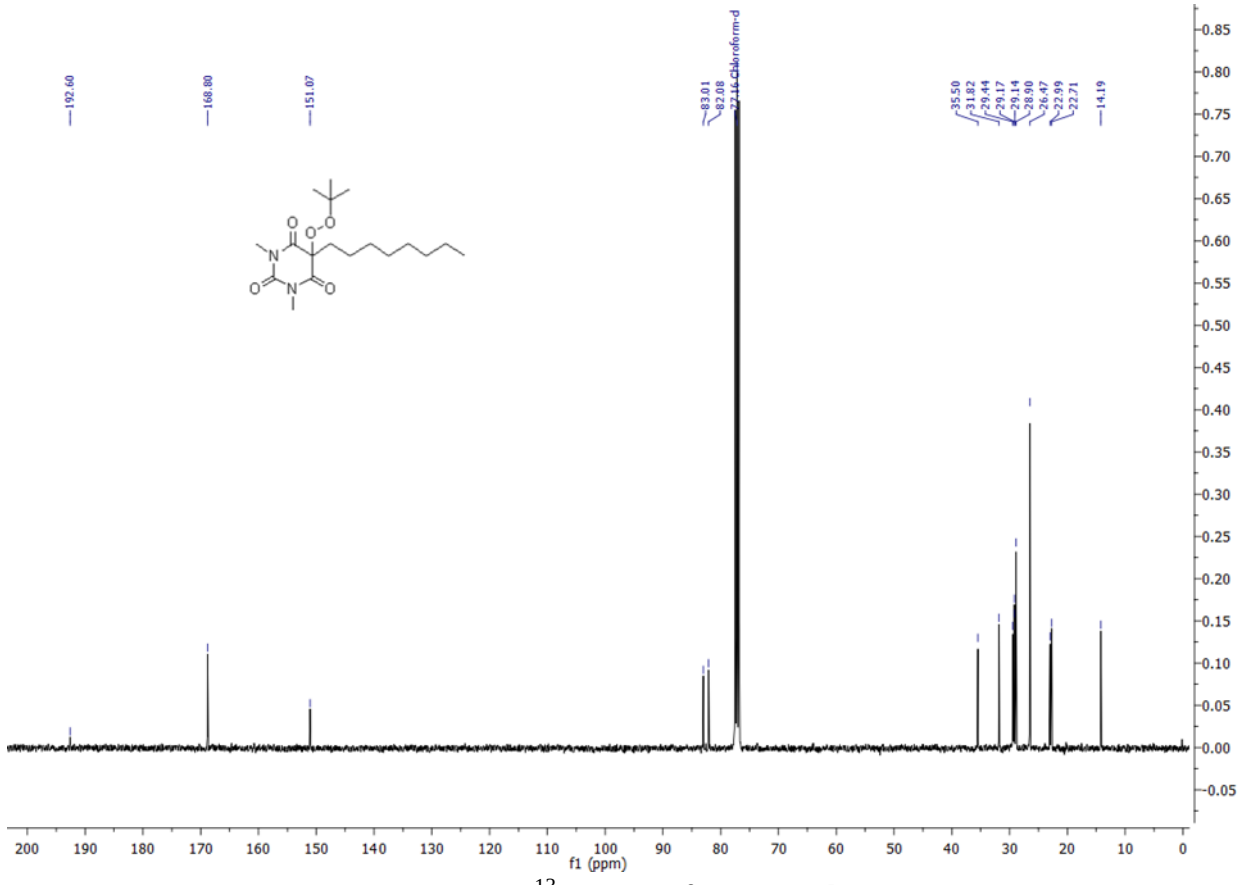

Figure 3A.24. ^{13}C NMR of compound **4i**

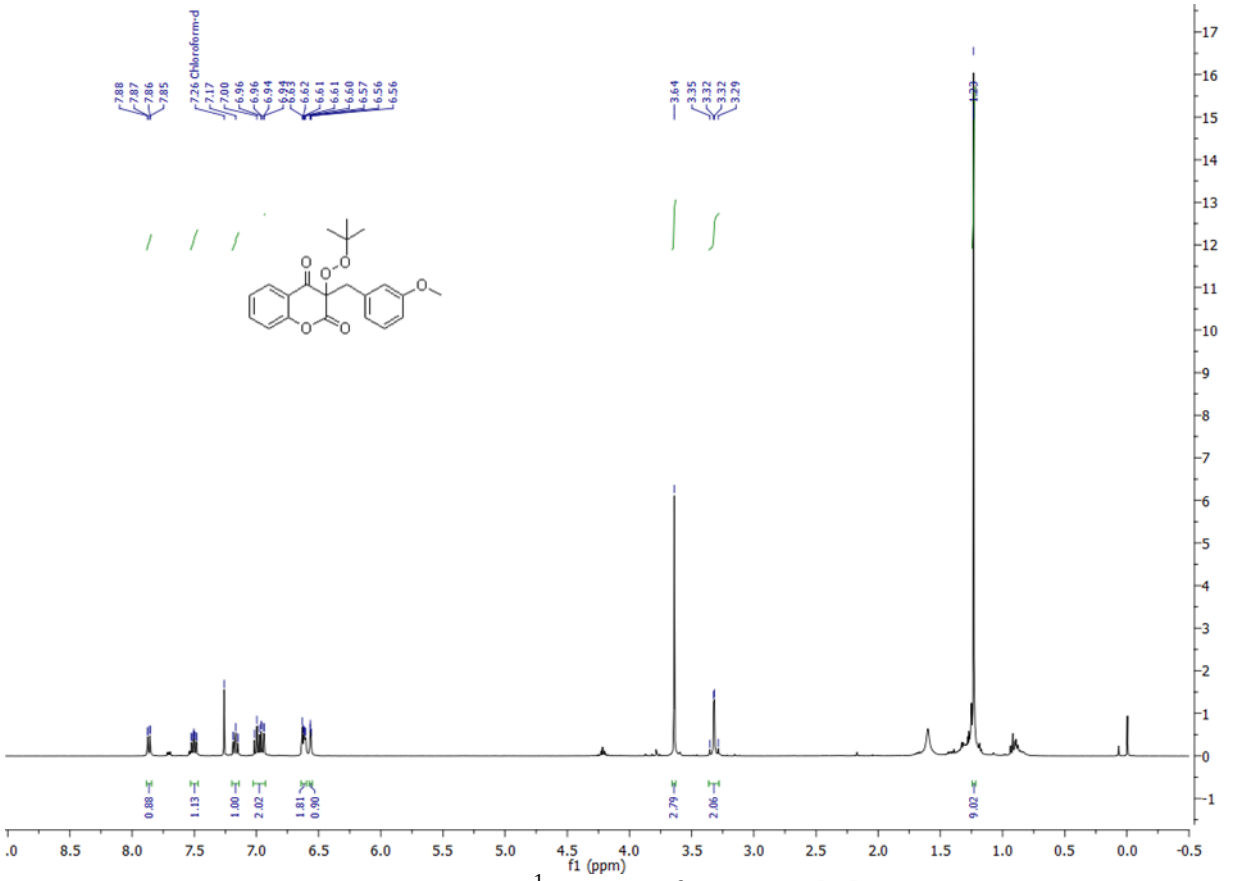

Figure 3A.25. ^{1}H NMR of compound **6b**

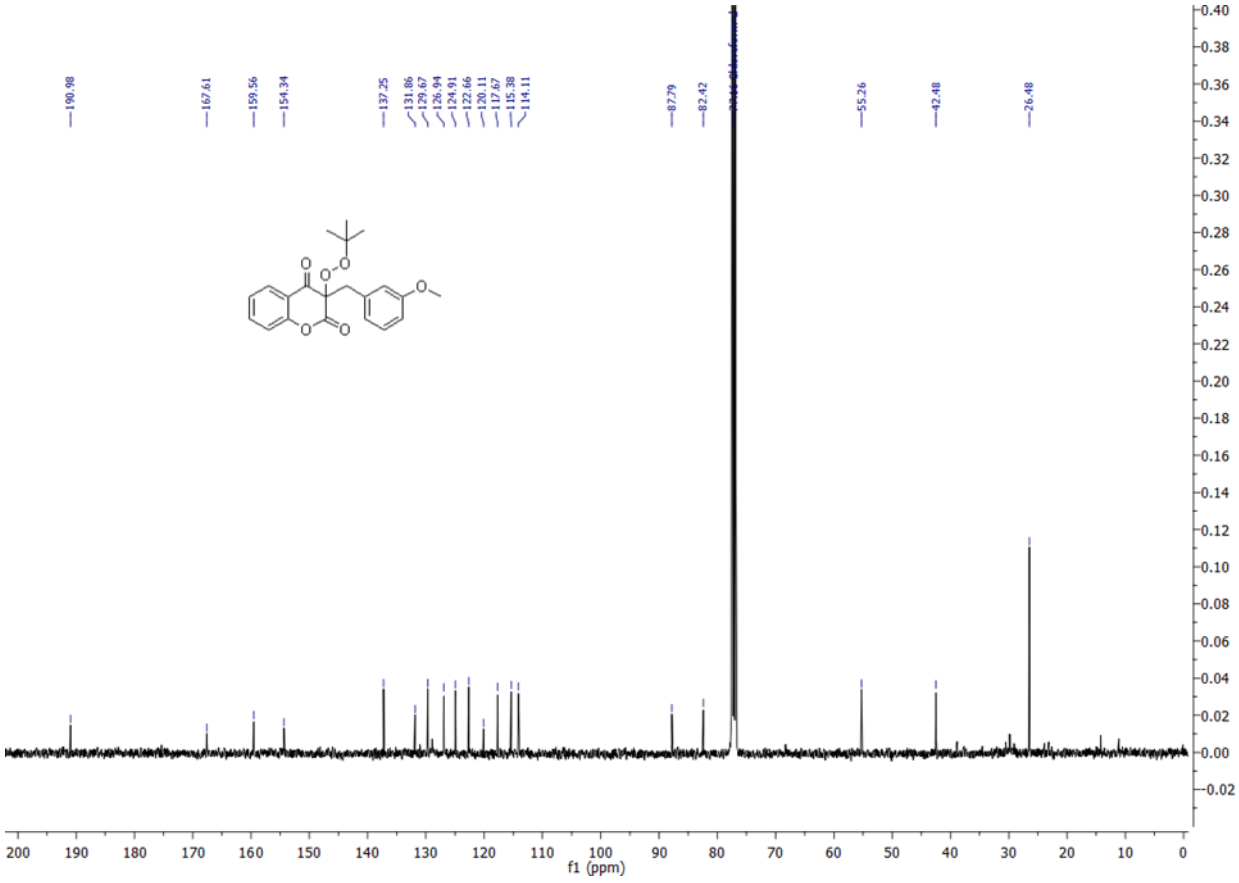

Figure 3A.26. ^{13}C NMR of compound **6b**

3A.12. References

(1) Ley, S. V. ; Fitzpatrick, D. E.; Ingham, R. J.; Myres, R. M. *Angew. Chem. Int. Ed*. **2015**, *54*, 3449.
(2) Ley, S. V. *Chem. Rec.* **2012**, *12*, 378.
(3) Tsubogo, T.; Oyamada, H.; Kobayashi, S. *Nature* **2015**, *520*, 329.
(4) Hartman, R. L.; McMullen, J. P.; Jensen, K. F. *Angew. Chem. Int. Ed.* **2011**, *50*, 7502.
(5) Webb, D.; Jamison, T. F. *Chem. Sci.* **2010**, *1*, 675.
(6) Bédard, A.-C.; Adamo, A.; Aroh, K. C.; Russell, M. G.; Bedermann, A. A.; Torosian, J.; Yue, B.; Jensen, K. F.; Jamison, T. F. *Science* **2018**, *361*, 1220.
(7) (a) Webb, D.; Jamison, T. F. *Chem. Sci.* **2010**, *1*, 675. (b) Wegner, J.; Ceylan, S.; Kirschning, A. *Chem. Commun.* **2011**, *47*, 4583. (c) Wegner, J.; Ceylan, S.; Kirschning, A. *Adv. Synth. Catal*. **2012**, *354*, 17. (d) Pastre, J. C.; Browne, D. L.; Ley, S. V. *Chem. Soc. Rev.* **2013**, *42*, 8849.
(8) (a) Dembitsky, V. M. *Eur. J. Med. Chem.* **2008,** *43*, 223. (b) Dembitsky, V. M.; Gloriozova, T. A.; Poroikov, V.V. *Mini-Rev. Med. Chem.* **2007,** *7*, 571. (c) Del Sol Jimenez, M.; Garzón, S. P.; Rodr guez, A. D. *J. Nat. Prod.* **2003**, *66*, 655. (d) Dwivedi, A.; Mazumder, A.; du Plessis, L.; du Preez, J. L.; Haynes, R. K.; du Plessis, J. *Nanomedicine* **2015,** *11*, 2041.
(9) Camuzat-Dedenis, B.; Provot, O.; Cointeaux, L.; Perroux, V.; Jean-Francois, B.; Bories, C.; Loiseau, P. M.; Mayrargue, J. *Eur. J. Med. Chem.* **2001**, *36*, 837.
(10) (a) Ingram, K.; Yaremenko, I. A.; Krylov, I. B.; Hofer, L.; Terent'ev, A. O.; Keiser, J. *J. Med. Chem.* **2012,** *55*,8700. (b) Keiser, J.; Ingram, K.; Vargas, M.; Chollet, J.; Wang, X.; Dong, Y.; Vennerstrom, J. L. *Antimicrob. Agents Chemother.* **2012**, *56*, 1090.
(11) (a) Tu, Y. *Nature Medicine* **2011**, *17*, 1217. (b) Fernández, I.; Robert, A. *Org. Biomol. Chem.* **2011**, *9*, 4098. (c) Winzeler, E. A.; Manary, M. J. *Genome Biology* **2014**, *15*, 544. (d) Jefford, C. W. *Curr. Top. Med. Chem.* **2012,** *12*, 373.
(12) Nosaka, Y.; Nosaka, A. Y. *Chem. Rev.* **2017**, *117*, 11302.
(13) Peter, C. A. *Science* **1985**, *227*, 375.
(14) World Health Organization. World malaria report 2018; https://www.who.int/malaria/media/world-malaria-report-2018/en/
(15) Fairhurst, R. M.; Dondorp, A. M. *Microbiol Spectr.* **2016**, *4*, 3.
(16) Kharasch, M. S.; Sosnovsky, G. *J. Am. Chem. Soc*. **1958**, *80*, 756.
(17) Kharasch, M. S.; Fono, A. *J. Org. Chem*. **1959**, *24*, 72.
(18) Murahashi, S.; Naota, T.; Kuwabara, T.; Saito, T.; Kumobayashi, H.; Akutagawa, S. *J. Am. Chem. Soc.* **1990**, *112*, 7820.
(19) Rispens, M. T.; Gelling, O. J.; de Vries, A. H. M.; Meetsma, A.; van Bolhuis, F.; Feringa, B. L. *Tetrahedron* **1996**, *52*, 3521.
(20) Yu, J. Q.; Corey, E. J. *Org. Lett*. **2002**, *4*, 2727.
(21) Terent'ev, A. O.; Sharipov, M. Y.; Krylov, I. B.; Gaidarenko, D. V.; Nikishin, G. I. *Org. Biomol. Chem*. **2015**, *13*, 1439.

(22) Liu, W.; Li, Y.; Liu, K.; Li, Z. *J. Am. Chem. Soc.* **2011**, *133*, 10756.
(23) Cheng, J.-K.; Shen, L.; Wu, L.-H.; Hu, X.-H.; Loh. T.-P. *Chem. Commun*. **2017**, *53*, 12830.
(24) Chen, Y.; Chen, Y.; Lua, S.; Li, Z. *Org. Chem. Front*. **2018**, *5*, 972.
(25) Zong, Z.; Lu, S.; Wang, W.; Li, Z. *Tetrahedron Lett*. **2015**, *56*, 6719.
(26) Chen, Y.; Tiana, T.; Li, Z. *Org. Chem. Front*. **2019**, *6*, 632.
(27) Wu, C.-S.; Li, R.; Wang, Q.-Q.; Yang, L. *Green Chem*. **2019**, *21*, 269.
(28) Xu, R.; Li, Z. *Tetrahedron Lett*. **2018**, 59, 3942.
(29) Shi, E.; Liu, J.; Liu, C.; Shao, Y.; Wang, H.; Lv, Y.; Ji, M.; Bao, X.; Wan, X. *J. Org. Chem*. **2016**, *81*, 5878.
(30) Zhang, H.-Y.; Ge, C.; Zhao, J.; Zhang, Y. *Org. Lett*. **2017**, *19*, 5260.
(31) Chen, Y.; Ma, Y.; Li, L.; Jiang, H.; Li, Z. *Org. Lett*. **2019**, *21*, 1480.
(32) Terent'ev, A. O.; Borisov, D. A.; Yaremenko, I. A.; Chernyshev, V. V.; Nikishin, G. I. *J. Org. Chem*. **2010**, *75*, 5065.
(33) Banerjee, A.; Santra, S. K.; Mishra, A.; Khatun, N.; Patel, B. K. *Org. Biomol. Chem.* **2015**, *13*, 1307.
(34) Kong, D.-L.; Cheng, L.; Yue, T.; Wu, H.-R.; Feng, W.-C.; Wang, D.; Liu, L. *J. Org. Chem*. **2016**, *81*, 5337.
(35) Klare, H. F. T.; Goldberg, A. F. G.; Duquette, D. C.; Stoltz, B. M. *Org. Lett.* **2017**, *19*, 988.
(36) (a) Jeong, Y. C.; Moloney, G. M. *Molecules* **2015**, *20*, 3582. (b) Hutchings, A. D.; Widdop, B. Drugs of Abuse. In The *Immunoassay Handbook*, 4th ed.; Wild, D., Ed.; Elsevier: Oxford, U.K., 2013; Chapter 9.23, pp 963-987. (c) D'Hulst, C.; Atack, J. R.; Kooy, R. F. *Drug Discovery Today* **2009**, *14*, 866.
(37) (a) Musa, M. A.; Cooperwood, J. S.; Khan, M.; Omar, F. *Curr. Med. Chem.* **2008**, *15*, 2664. (b) Jung, J.-C.; Lee, J.-H.; Oh, S.; Lee, J.-G.; Park, O.-S. *Bioorg. Med. Chem. Lett.* **2004**, *14*, 5527. (c) Stanchev, S.; Hadjimitova, V.; Traykov, T.; Boyanov, T.; Manolov, I. *Eur. J. Med. Chem.* **2008**, *43*, 67.
(38) Richardson, W. H. *J. Am. Chem. Soc.* **1965**, *87*, 247.
(39) Zima, A. M.; Lykin, O. Y.; Ottenbacher, R. V.; Bryliakov, K. P.; Talsi, E. P. *ACS Catal*. **2017**, 7, 60.

The content of the Chapter 3A is reproduced from Ref. "*J. Org. Chem.* **2018**, *83*, 1358" with permission from the American Chemical Society.

Chapter 3

Section B:

Magnetic Iron Nanoparticle Catalyzed C-H Peroxidation of Carbonyls under Batch/Flow System: Evaluation of Antimalarial Property

3B. Magnetic Iron Nanoparticle Catalyzed C-H Peroxidation of Carbonyls under Batch/Flow System: Evaluation of Antimalarial Property

3B.1. Abstract

The immobilization of Fe on the magnetite (Fe_3O_4) surface rendered magnetic $Fe(OH)_3@Fe_3O_4$ nanoparticles (Fe-MNP) using earth-abundant and inexpensive precursors. To exploit the catalyst efficacy, "flow nanocatalysis" was used as a process intensification tool for rapid C(sp^3)-H peroxidation of carbonyl compounds in a continuous-flow reactor. This unified strategy is very facile for the peroxidation of various 2-oxindole derivatives to obtain bioactive quaternary peroxy compounds in very good yield with 7.9 minutes of residence time in a continuous flow. Additionally, the explosion hazards of TBHP (*tert*-Butyl hydroperoxide) were minimized in a continuous-flow reactor by keeping the critical volume low. Moreover, we have shown the removal of the *tert*-butyl group by using heterogeneous Brønsted acid under continuous flow.

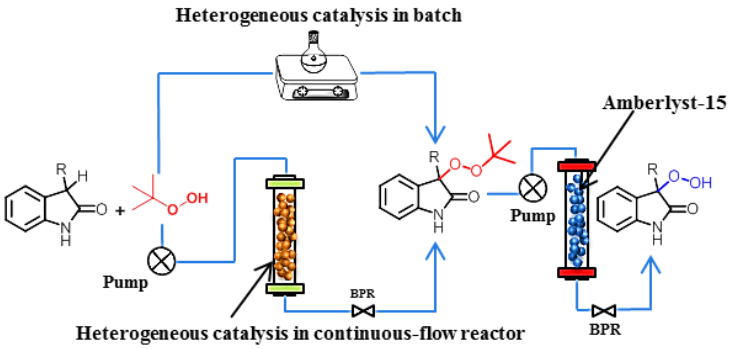

Introduction and literature background on C-H peroxidation and continuous flow chemistry

The introduction and literature background on continuous flow and C-H peroxidation process is discussed in Section 3A.2, 3A.3, 3A.4 of chapter 3A.

3B.2. Heterogeneous catalysis in a continuous flow

Heterogeneous catalysis is the backbone of continuous manufacturing processes in the chemical industry. Approximately 85-90% of the finished products of the chemical industry are made using catalytic routes.[1] Supported-heterogeneous catalysts are indispensable tools in catalysis science and technology and are most important in the production of natural products, active pharmaceutical ingredients, and petrochemicals.[2a-d] Consequently, it is imperative to project the synthesis of supported catalytic systems for organic transformations in continuous-flow or batch and

industrially vital reactions; where the most crucial parameter is recycling of the used catalyst. Interestingly, the iron oxides, silica, carbon, alumina, or zirconia were used as catalyst support for metals, organocatalyst, and metal oxides nanoparticles.[3] Specifically, a superparamagnetic iron oxide nanoparticle (SPION), e.g., core /shell structure has proven a track record of success in the heterogeneous catalysis due to its excellent ferromagnetism, ease of separation, abundant, inexpensive, environmentally benign nature and well-studied properties.[4a-d] However, the immobilization of metals on iron oxides has gained substantial attention due to the possibility of anchoring, greater surface area, and high stability.[5-7] Particularly, the pioneering work using $Fe(OH)_3@Fe_3O_4$ was demonstrated by Song *et al.* for aldol reaction and by Heydari and co-workers for transamidation.[8] The coating on Fe_3O_4 is essential since bare Fe_3O_4 nanoparticles are susceptible to aerial oxidation even at rt which results in loss of magnetism.[9]

Interestingly, the integration of supported catalysts with continuous flow reactors (nano-catalysis in flow) has a history of more than 100 years, which gives access to robust process intensification. The pioneering example includes the synthesis of ammonia by Haber–Bosch process from N_2 and H_2 under high pressure and temperature in the presence of magnetite (Fe_3O_4) catalyst. However, the recent advances emphasizing on the use of the Ru/C catalyst for better conversion and results.[2d] However, in current practices, the chemical engineering aspects improved the design, safety, automated operations of the continuous flow reactors. The significant transformations have been achieved using placing supported catalyst in packed bed reactors. [10]

In 2010, Reiser and co-workers reported the Magnetite@silica-immobilized azabis(oxazoline)-Copper(II) complex for kinetic resolution of 1,2-Diphenylethane-1,2-diol under batch/continuous flow (Scheme 3B.1).[11]

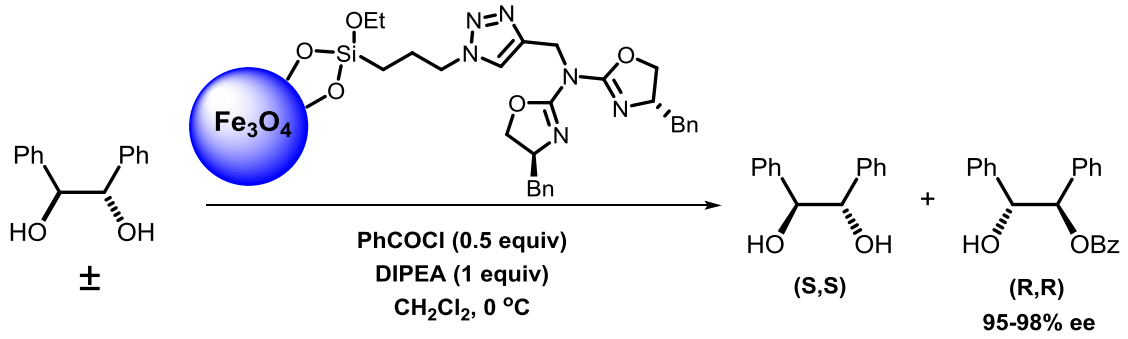

Scheme 3B.1. Reiser's approach for monobenzoylation of racemic diol

In 2011, Pericas and co-workers demonstrated the functionalization of Fe_3O_4 magnetic nanoparticles with (S)-α,α-Diphenylprolinol trimethylsilyl ether for asymmetric, organocatalytic Michael addition reactions (Scheme 3B.2).[6]

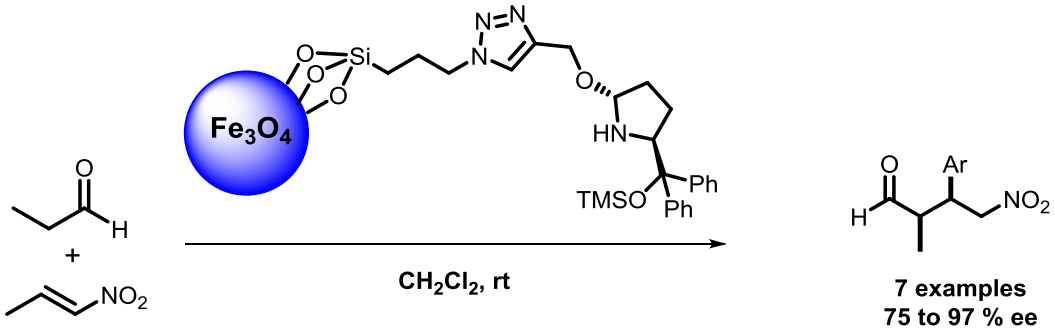

Scheme 3B.2. Pericàs approach for asymmetric Michael reaction using nano-catalysis

Kappe and co-workers reported the aerobic oxidation of benzyl alcohol using Fe/Al-SBA15 under continuous flow (Scheme 3B.3). [12]

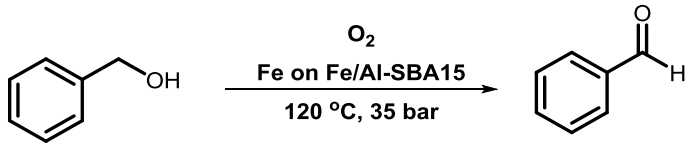

Scheme 3B.3. Aerobic oxidation of benzyl alcohol using a supported catalyst

Kappe and co-workers developed a nano-Fe_3O_4 catalyzed reduction of nitro compounds to produce a variety of amine derivatives in continuous flow (Scheme 3B.4.).[13]

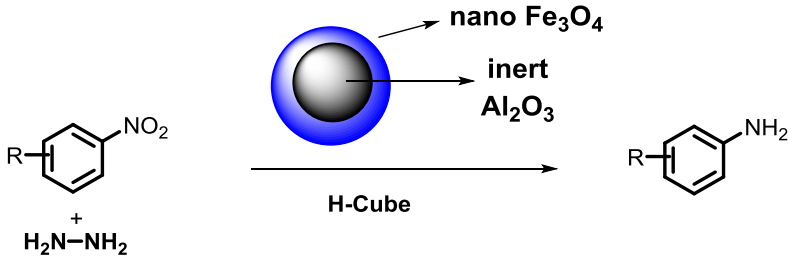

Scheme 3B.4. Kappe's approach for reduction of a nitro group using nano-catalysis

Kirschning and co-workers developed a Pd-nanoparticle catalyzed Suzuki-Miyaura and Heck-Mizoroki reaction in continuous flow (Scheme 3B.5.).[14]

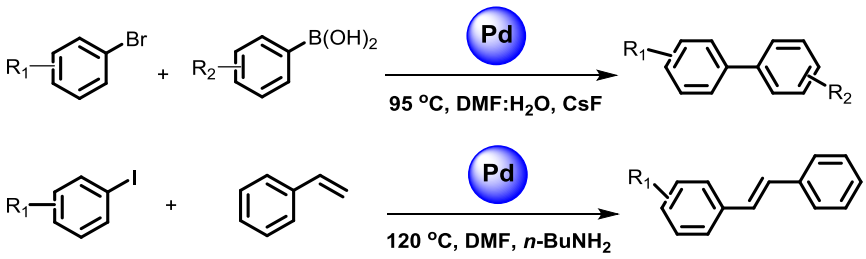

Scheme 3B.5. Kirschning's approach for cross-coupling reactions in a continuous flow

3B.3. The rationale of present work

The homogeneous catalysts suffer from difficulty in recovery and reusing of the catalyst, ensuing in poor atom efficiency. There are varieties of transformations such as oxidation-reduction, cross-coupling, and Michael or aldol addition, *etc*. are known using flow nano-catalysis. However, in the collective report until today, there is no report for C-H peroxidation using a supported catalyst in batch/flow. In extension to our previous determination for C-H peroxidation using homogeneous catalysis, we have envisaged exploring the $Fe(OH)_3@Fe_3O_4$ (magnetic iron oxide nanoparticles) as a supported catalyst for C-H peroxidation to synthesize antimalarial scaffolds in a continuous flow and batch process. In a batch reaction, the metal reacts vigorously with peroxides, which may lead to explosive and exothermic reactions. However, the use of continuous flow set up allows safer reaction is owing to the controlled addition of peroxides by keeping critical volumes small. The present protocol comprises of following advantages: (i) Rapid on-demand synthesis of antimalarial peroxides using continuous flow; (ii) Use of eco-friendly solvent *viz* ethyl acetate; (iii) Reduced explosive hazards by controlled addition in continuous flow; (iv) Simple magnetic decantation can recover the catalyst from the reaction mixture (batch reactions); (v) Easy catalyst packing and removal in a packed bed reactor due magnetic nature of the catalyst (flow conditions); (vi) *in vitro* antimalarial evaluation against *Plasmodium falciparum*.

3B.4. Results and discussion

Catalyst preparation and characterization

At the outset, the catalyst was prepared using reported protocols[8] and characterization of $Fe(OH)_3@Fe_3O_4$ composite material using XPS, TGA, HR-TEM, FE-SEM, PXRD, and EDAX analysis. In a powder XRD pattern, we detected 2θ values as 23.6 °, 30.7 °, 36.1 °, 38.1 °, 44.4 °, 57.7 °, 63.3 ° and, 71.7 °, which correspond to Fe_3O_4 nanoparticles (JCPDS- 00-011-0614). No $Fe(OH)_3$ component was observed,

indicating that $Fe(OH)_3$ is amorphous (Figure 3B.1). The size and morphology of the nanocomposites were evaluated by TEM and FE-SEM analysis and found the average particle size 11.3 nm for fresh catalysts and 10.7 nm for the used catalyst (Figure 3B.1). In X-ray Photoelectron Spectroscopy data of magnetic iron oxide nanoparticles, the Fe 2p showed peaks at 711 and 724.3 eV along with satellite peaks at 720 and 732.9 eV (Figure 3B.1).[15]

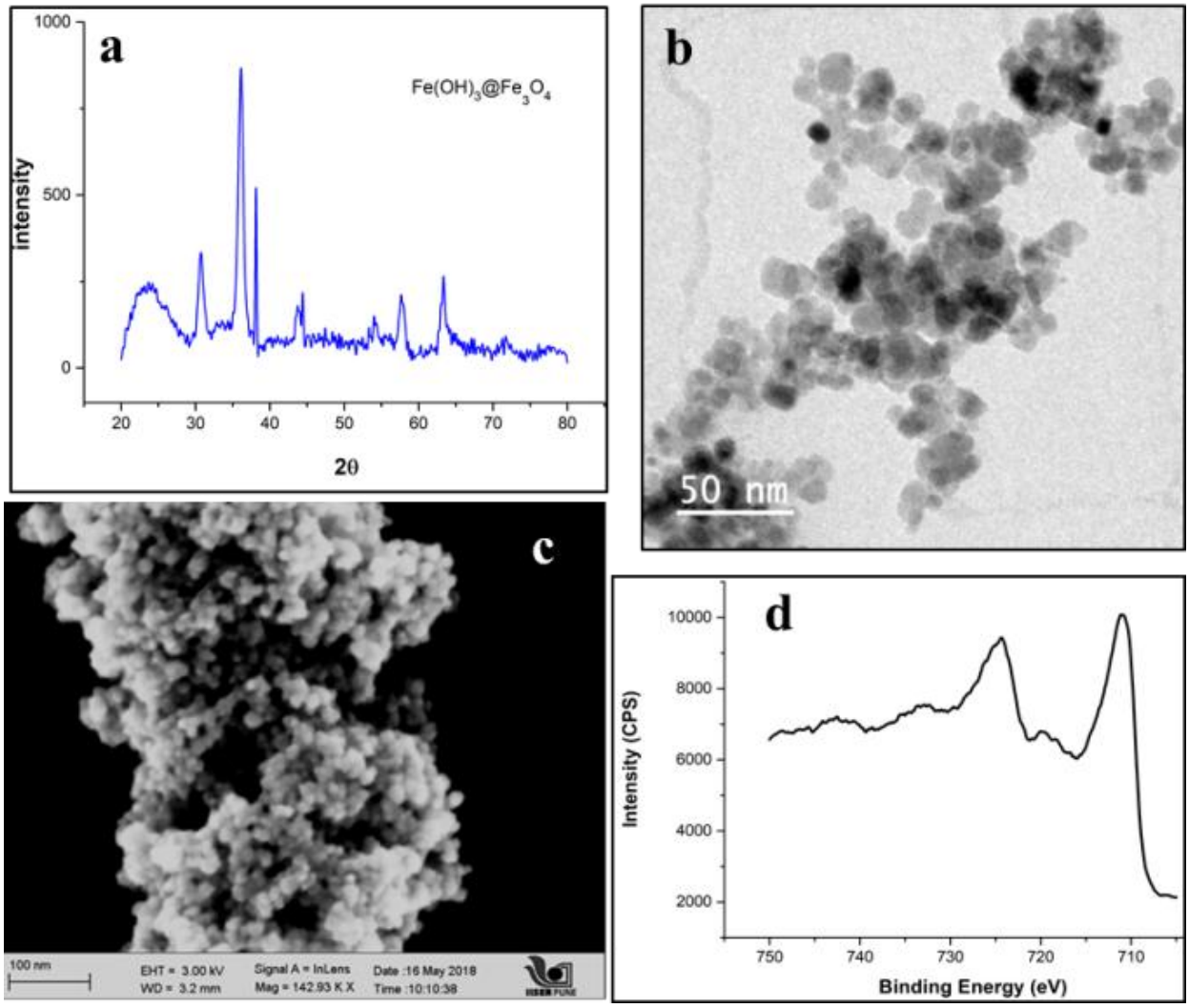

Figure 3B.1. (a) P-XRD pattern, (b) TEM image, (c) SEM image, (d) Oxygen 2p XPS data for $Fe(OH)_3Fe_3O_4$

To gain more insights into XPS pattern, the XPS spectra for O 1s was recorded which showed the peaks at 530, and 531.2 eV corresponds to Fe_3O_4 and $Fe(OH)_3$ and resembles with the literature values (Figure 3B.2).[16]

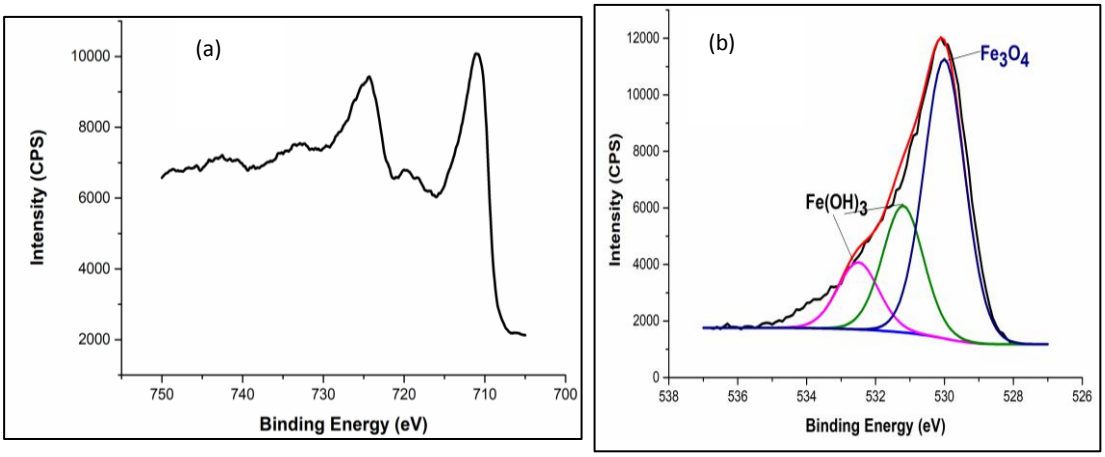

Figure 3B.2. Oxygen 1s XPS data for $Fe(OH)_3$ on Fe_3O_4

Next, the % amount of immobilization of $Fe(OH)_3$ on Fe_3O_4 was checked by using thermogravimetric analysis (TGA). The TGA was carried out for Fe_3O_4 and magnetic iron oxide nanoparticles, and we found the 38 wt % of $Fe(OH)_3$ and 62 wt % of Fe_3O_4 (Figure 3B. 3).

$$\frac{9.62\ g\ H_2O}{100\ g\ cat.} \times \frac{1\ mol\ H_2O}{18\ g\ H_2O} \times \frac{2\ mol\ Fe(OH)_3}{3\ mol\ H_2O} \times \frac{106.87\ g\ Fe(OH)_3}{1\ mol\ Fe(OH)_3} \times \frac{38\ g\ Fe(OH)_3}{100\ g\ cat.} = 38\ \%\ Fe(OH)_3$$

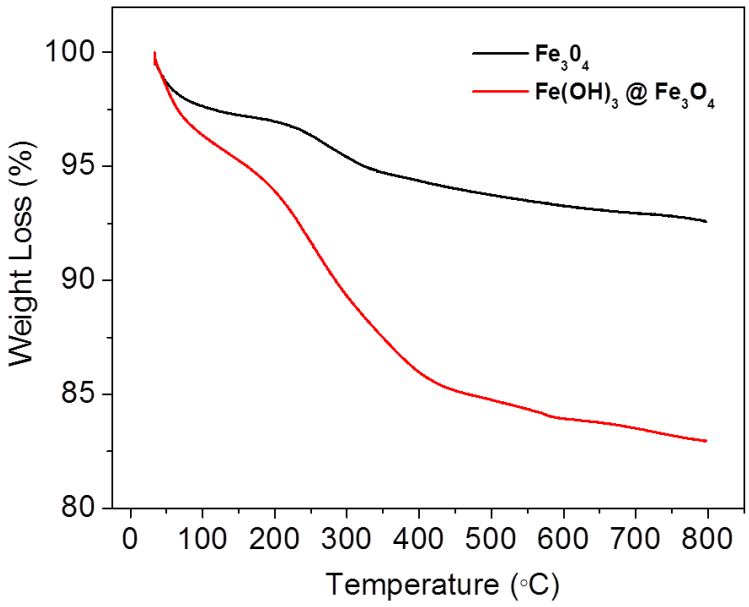

Figure 3B.3. TGA data for $Fe(OH)_3$@Fe_3O_4 and bare Fe_3O_4

3B.4. Optimization studies (Batch chemistry for C-H peroxidation)

Table 3B.1. Optimization of C-H peroxidation

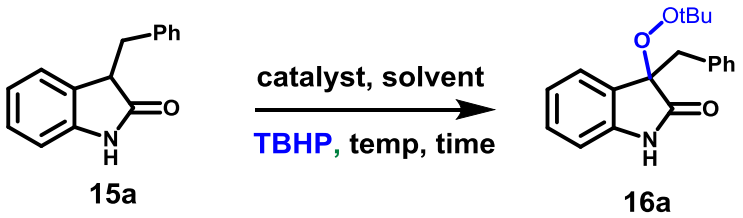

15a 16a

Entry	Catalyst	Solvent	Temp (^{o}C)	Time	Yield (%)
		batch conditions			
1	-	acetonitrile	rt	4 h	no reaction
2[a]	-	acetonitrile	80	4 h	traces
3	Fe-MNP	acetonitrile	rt	4 h	10
4	Fe-MNP	acetonitrile	60	4 h	48
5	Fe-MNP	acetonitrile	80	4 h	66
6[b]	Fe-MNP	acetonitrile	80	4 h	67
7	Fe-MNP	ethyl acetate	rt	4 h	08
8	Fe-MNP	ethyl acetate	40	4 h	21
9	Fe-MNP	ethyl acetate	60	4 h	42
10[c]	Fe-MNP	ethyl acetate	80	4 h	26
11[d]	Fe-MNP	ethyl acetate	80	4 h	62
12	**Fe-MNP**	**ethyl acetate**	**80**	**4 h**	**81**
13	Fe-MNP	H_2O	80	4 h	44
14	Fe-MNP	dimethyl carbonate	80	4 h	75
15	Fe-MNP	tert-butanol	80	4 h	59
16	Fe-MNP	1,4-dioxane	80	4 h	10
17	Fe-MNP	dimethoxyethane	80	4 h	57
18	Fe-MNP	dimethylformamide	80	4 h	39
		continuous-flow conditions (time in min)[e]			
19	-	ethyl acetate	rt	-	no reaction
20	-	ethyl acetate	80	-	traces
21	Fe-MNP	acetonitrile	rt	7.9	no reaction
22	Fe-MNP	acetonitrile	80	3.9	55
23	Fe-MNP	acetonitrile	80	7.9	64
24	Fe-MNP	ethyl acetate	80	3.9	66
25	**Fe-MNP**	**ethyl acetate**	**80**	**7.9**	**75**

Reaction condition: 15a (0.25 mmol), Fe-MNP (30 mg), TBHP (4 equiv) and solvent (1 mL) were stirred in a resealable tube. [a)] in the absence of Fe-MNP [b)] 70% aqueous TBHP was used. [c)] 10 mg of Fe-MNP catalyst was added. [d)] 20 mg of Fe-MNP catalyst was added. [e)] 0.1 M substrate in ethyl acetate (5 mL) and TBHP (4 equiv) were premixed and flown through Omnifit® (6.6 x 150 mm) packed bed (Fe-MNP filled up to 2.3 cm, 800 mg) at 80 ^{o}C with 0.1 or 0.2 mL/min flow rate with 3-4 bar pressure.

For instance, **15a** was chosen as a model substrate for the C-H peroxidation reaction. In a control experiment in the absence of catalyst, traces of product **16a** was observed at 80 ^{o}C in acetonitrile (ACN) (Table 3B.1, entry 2). In the presence of $Fe(OH)_3@Fe_3O_4$, its decisive role was observed when reaction performed at 60 ^{o}C, and 80 ^{o}C in ACN for 4 h afforded 100% conversion with **16a** in 48 and 66% yield respectively (Table 3B.1, entries 4, 5). Due to the highly reactive nature of TBHP with metal, we cannot rule out the possibility of some amount of TBHP decomposition. Therefore, it is necessary to add an excess of TBHP during such a process. The reaction with a 70% aqueous solution of TBHP also gave comparable yield (Table 3B.1, entry 6). To our delight, better results were observed when low cost, commonly used, and less toxic ethyl acetate used as a solvent[17] to afford **16a** in 81% at 80 ^{o}C in 4 h (Table 3B.1, entry 12). Next, the concentration effect of a catalyst on the outcome of reaction progress was investigated (Table 3B.1, entries 10-11). Furthermore, we have tested the other green or less hazardous solvents for C-H peroxidation, and results are summarized in Table 3B.1, entries 10-12. The low yield of the product was observed in other solvents like 1,4-dioxane, DME, and DMF (Table 3B.1, entries 16-18).

3B.4.2. Substrate scope

Having optimized conditions in hand, we aimed to explore the substrate scope for the C-H peroxidation. Our protocol was general to the variety of electron-donating as well as electron-withdrawing substituents, which afforded good to a very good yield of peroxides **16a-j** (Figure 3B.4). Also, an aliphatic alkyl group at the C3 position of 2-oxindole provided corresponding peroxides **16k-o** (Figure 3B.4) in good yield. Notably, the substrate scope was not only limited to 2-oxindole, but the derivatives of substituted barbituric acid also afforded a good yield of product **16p** and **16q** (Figure 3B.4). To our delight, the reaction conditions were tolerant for sensitive groups such as *N*-tosyl (**16t**) and nitrile (**16u**); afforded peroxylated products in reasonable yield (Figure 3B.4).

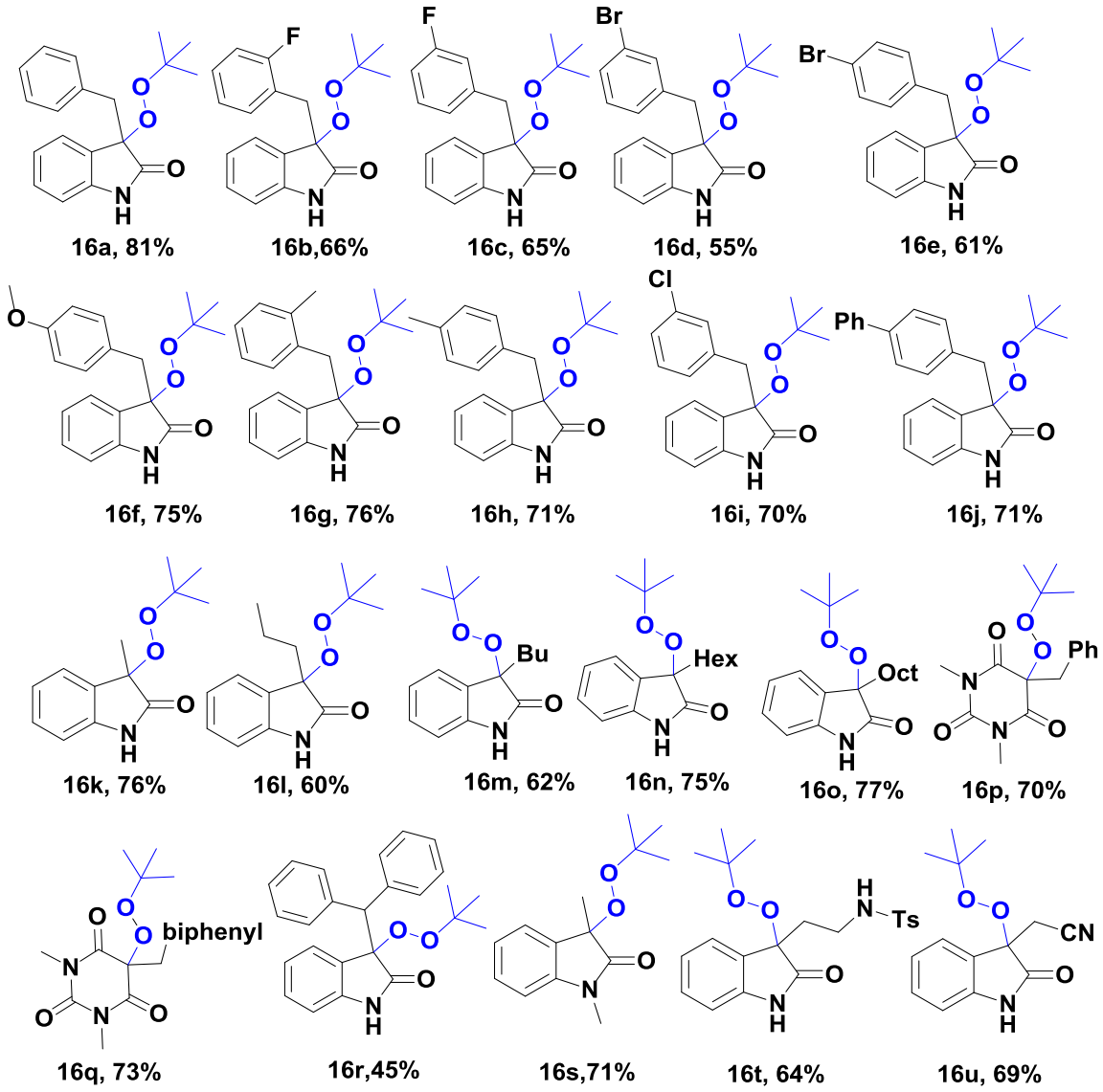

Figure 3B. 4. Substrate scope for the C-H peroxidation in batch

Reaction condition: C3-substituted-2-oxindole or barbiturate (0.25 mmol), Fe-MNP (30 mg), TBHP (4 equiv) and ethyl acetate (1 mL) were stirred in a re-sealable tube at 80 ^{o}C for 4 h. The mentioned yields are isolated yields.

Moreover, a sterically hindered phenyl group as a C3-substituent on 2-oxindole afforded a 45% yield of the product **16r** (Figure 3B.4) (50% starting material recovered). *N*-protected 2-oxindole also worked well to provide a 71% yield of **16s**. The recyclability studies for magnetic iron oxide nanoparticles were performed for compound **15a**. To check the leaching of iron, the MP-AES of the sample after the reaction was recorded and found 0.16 ppm and 0.13 ppm of iron in batch and continuous flow, respectively, which confirms the high stability of the nanostructured iron oxide particles. Furthermore, we have checked the recyclability of the prepared

Fe-MNP catalyst. The nanostructured iron oxide particle catalyst can be recycled up to 10 times (a catalyst is still active and can be used for other reactions) with some loss in the yield of peroxy product (Figure 3B.5).

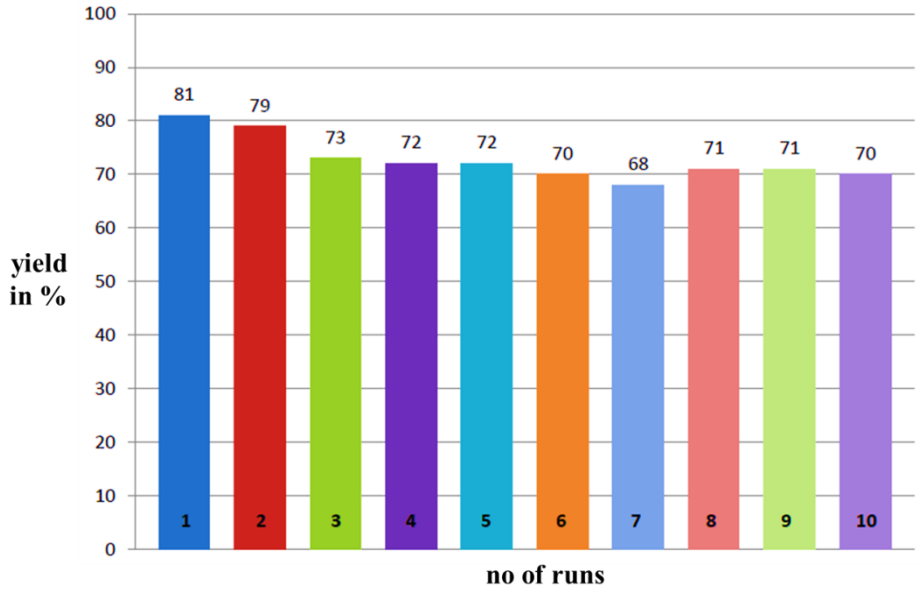

Figure 3B.5. Recyclability data for $Fe(OH)_3@Fe_3O_4$

Continuous flow chemistry for C-H peroxidation:

After getting the productive results in batch conditions, we focused our attention on continuous flow mode. We aimed for continuous flow to reduce the explosive hazards of TBHP[18] and avoid the mechanical degradation of magnetic iron oxide nanoparticles in batch conditions. The flow setup was worked out according to the requirement of reaction conditions (Figure 3B.6). Time mentioned for flow is residence time; Residence time = reactor volume / flow rate.

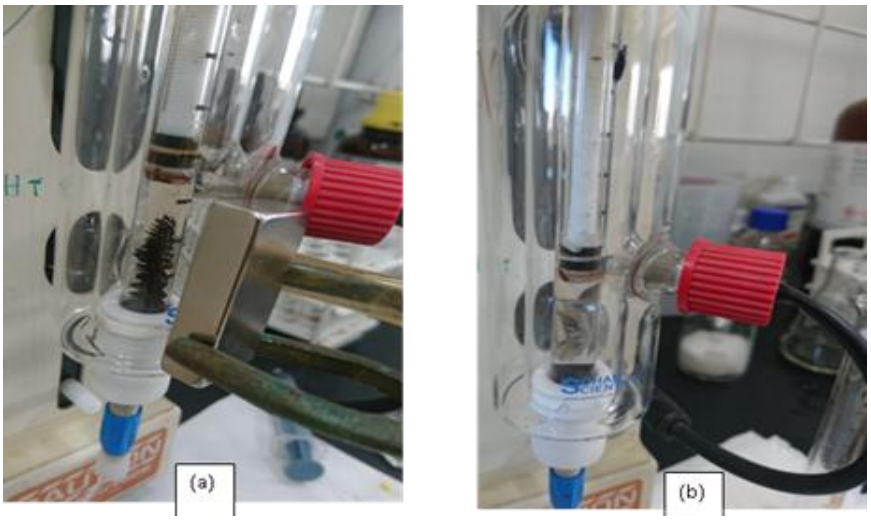

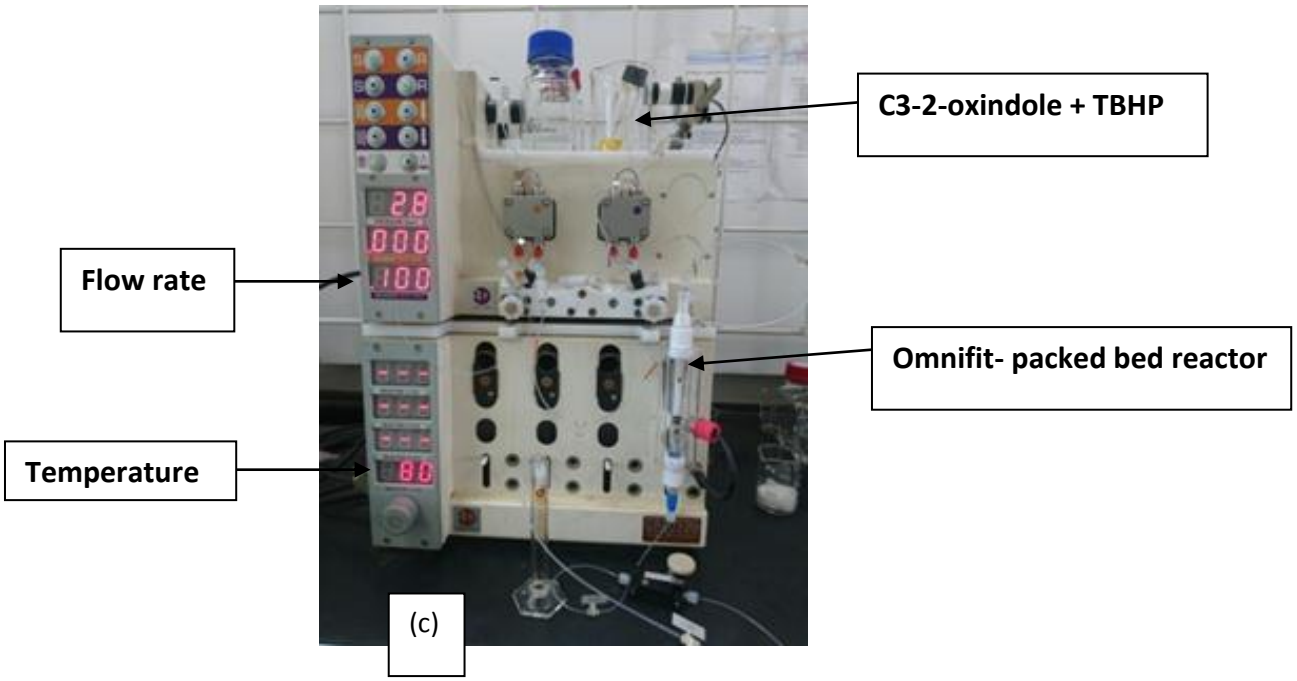

Figure 3B.6. (a) Packed bed reactor in the presence of a magnet; (b) Packed bed reactor in the absence of magnet (Omnifit®) (c) The full setup for Vapourtec R-series continuous-flow reactor.

The reagents were pumped directly from the flask. The glass column (Omnifit®, 6.6 x 150 mm) was packed with $Fe(OH)_3Fe_3O_4$, up to 2.3 cm in height. A frit (30 μm) was placed into the lower thread of the glass column to provide the support for the catalyst The catalyst is a composite material ($Fe(OH)_3Fe_3O_4$ nanoparticles tend to agglomerate owing to their magnetic property) hence the use of 30 μm frit does not allow the leaching of nanostructured iron oxide particles. Sometimes, the aggregation in magnetic iron oxide nanoparticles is problematic as it may block the flow of liquid. Although we have not observed any blocking issue, to overcome the blocking issue, the magnets with rotatory motor near the packed bed reactor can be placed, which will avoid the aggregation of nanoparticles. Only traces of product **16a** were observed when the control experiment performed in the absence of nanostructured iron oxide particles at 80 ^oC (Table 3B.1, entry 20). Subsequently, the solution of **15a** (0.1M) and TBHP (4 equiv) in 5 mL ACN flown through the packed bed reactor with a flow rates of 0.2 and 0.1 mL/min at 80 ^oC; afforded 55 and 64 % yield of the product **16a** with a residence time of 3.9 and 7.9 min respectively (Table 3B.1, entries 22, 23). The improvement in yield was observed when ethyl acetate was used as a solvent over ACN. To our delight, a solution of 0.1M **15a** and 4 equiv of TBHP flown through the (magnetic iron oxide nanoparticles = 800 mg, 2.3

cm) packed bed reactor at 0.2, and 0.1 mL/min flow rate at 80 ^{o}C provided **16a** in 66 and 75 % yield (Table 3B.1, entries 24, 25). Furthermore, a long run experiment was investigated by packing 300 mg of catalyst in a packed bed reactor (1.1 cm bed height). The solution of 3-methylindolin-2-one (24 mmol) and TBHP (96 mmol) was dissolved in 240 mL of ethyl acetate and flown through the magnetic iron oxide nanoparticle catalyst bed at 80 ^{o}C continuously up to 40 h. To our delight, after 40 h of continuous peroxidation reaction, we have isolated **16k** (13.19 mmol) with TON = 12.37 and productivity of 0.309 mmol $_{\text{product}}$ mmol $_{\text{magnetic iron oxide nanoparticles}}^{-1}$ h^{-1}. Unfortunately, during a long time experiment, the drop in conversion was observed from 95 % to 38 % (by TLC and NMR) periodically for the C-H peroxidation reaction (Figure 3B.7). The results for the long-time experiment indicates that the catalyst can afford ~95% conversion up to 2 h and after that gradual drop in conversion. To get a good yield in the continuous flow, it is necessary to wash and dry the catalyst after 2 h.

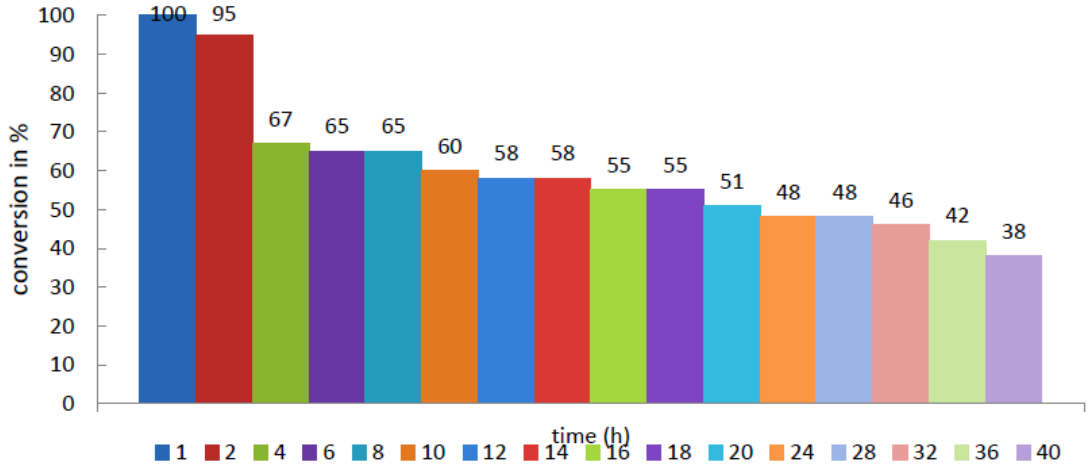

Figure 3B.7. Long-time experiment chart for entry **16k**

After a 40 h long run experiment, the catalyst was washed with ethyl acetate and dried and further used for various substrates, which fall into the scope of this protocol (Figure 3B.8). Following this strategy, the C-H peroxidation reaction was studied with several derivatives of C3-substituted 2-oxindole derivatives. The substituent is bearing electron-withdrawing **16b-d** and **16i,** and electron-donating **16f-h** (Figure 3B.8) afforded good to very good yield in a continuous-flow system. C3-alkyl substituted 2-oxindole derivatives also reacted smoothly to afford **16k, n, o** in good yield.

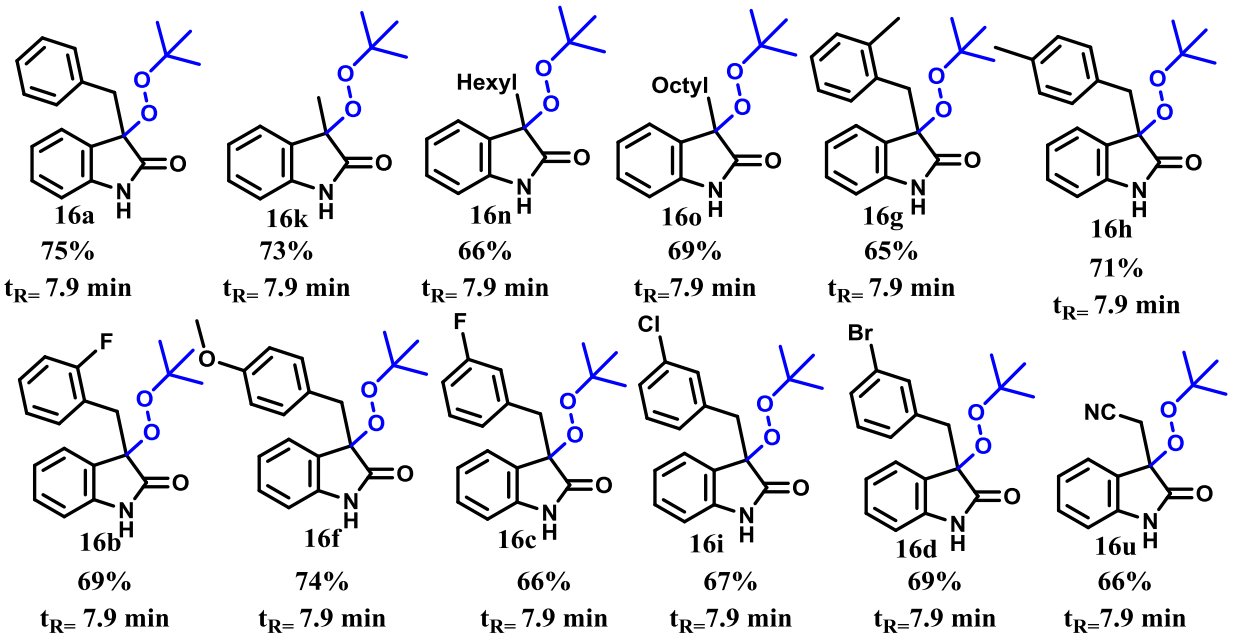

Figure 3B.8. Substrate scope for the C-H peroxidation in a continuous flow

Reaction condition: 0.1 M substrate in ethyl acetate (5 mL) and TBHP (4 equiv) were premixed and flown through packed bed of magnetic iron oxide nanoparticles (800 mg, bed height= 2.3 cm) with the 3-4 bar pressure at 0.1 mL/min at 80 ^{o}C. Reagents were pumped directly from the flask. The mentioned yields are isolated yields.

3B.5. The removal of *tert*-butyl group under a continuous flow

In the past decades, varieties of hydroperoxides were isolated and grabbed significant attention due to their interesting properties. In this regard, we sought to demonstrate the utility of synthesized peroxylated compounds by removal of the *tert*-butyl group using Amberlyst 15 *via* C-O bond cleavage in a continuous-flow reactor. The Omnifit column packed with 500 mg of Amberlyst-15 (Dry form) and solution of 0.1 M peroxy derivatives flown through it. For each substrate new bed of Amberlyst-15 was used. We have tried to telescope the two flow reactions (C-H peroxidation and removal of the *tert*-butyl group) to get **17b** starting from 3-methyl-2-oxindole by avoiding solvent switch and isolation, but unfortunately, we did not observe the deprotected product. A variety of 3-oxyl-2-oxindole derivatives (**17a-17e**) were synthesized using this novel transformation under mild reaction conditions in a continuous-flow process (Figure 3B.9). The large-scale reaction of (0.50 gm of the substrate, 1 gm of Amberlyst-15) was proceeded smoothly with **16k** to afford hydroperoxy compound **17b** in 84% isolated yield. The low yields for the products **17a** and **17c-17e** are attributed to the formation of the rearranged product.[20]

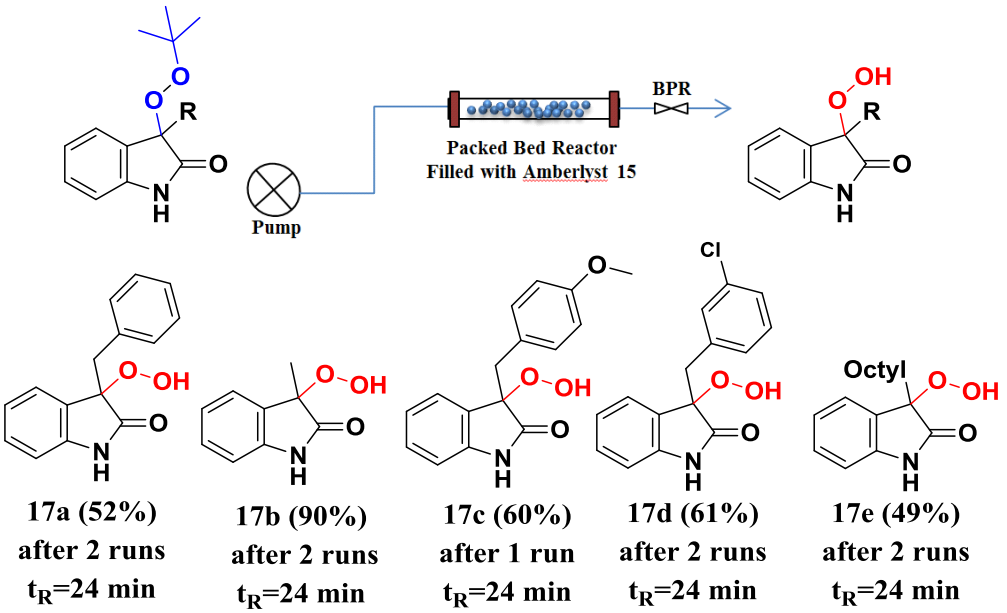

Figure 3B.9. The schematic representation for the removal of the *tert*-Butyl group in a continuous flow

Reaction condition: A solution of 0.1 M peroxyoxindole derivatives in 5 mL acetonitrile was flown through the packed bed of Amberlyst-15 (Dry form) (bed height 5-5.5 cm, 500 mg) with the 2-3 bar at 0.1 mL/min at 26 ^{o}C.

3B.6. The possible reaction mechanism

On the basis of literature reports, a plausible mechanism for the Fe-MNP catalyzed C-H peroxidation is depicted in in Figure 3B.10.[21]

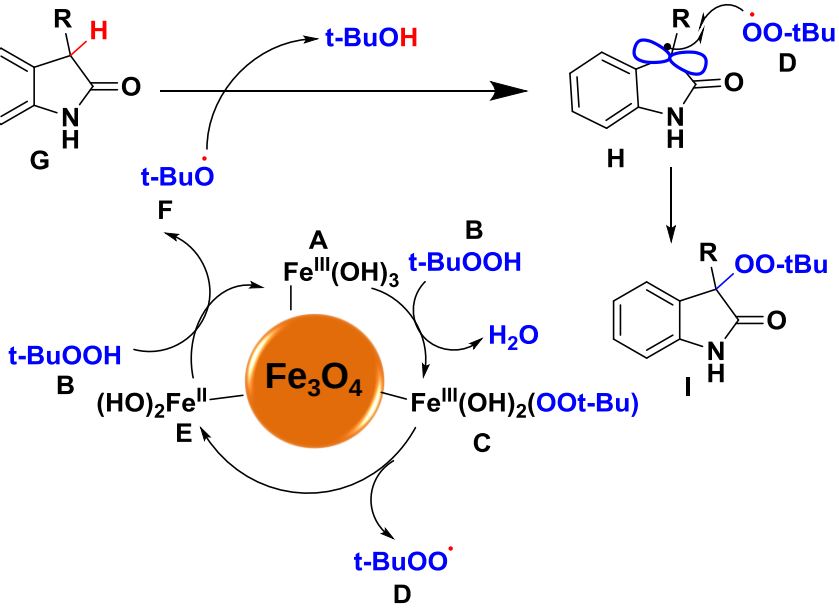

Figure 3B.10. The possible reaction mechanism

Initially, TBHP **B** reacts with $Fe^{III}(OH)_3$ **A** to provide intermediate $Fe^{III}(OH)_2$(OOt-Bu) **C** *via* the elimination of water. The $Fe^{III}(OH)_2$(OOt-Bu) **C** undergoes redox type reaction to produce *t*-Butylperoxy radical **D** and $Fe^{II}(OH)_2$ **E**. Next, another equiv of TBHP **B** reacts with $Fe^{II}(OH)_2$ **E** and produces a reactive *t*-Butoxy radical **F** and $Fe^{III}(OH)_3$ complex **A**. On the other hand, the *t*-Butoxy radical **F** abstracts the α-C-H proton from carbonyl compound **G** to give radical species **H** with elimination of *tert*-butanol. Finally, selective recombination of α-radical of the carbonyl compound **H** and *tert*-butyl peroxy radical **D**, give the C-H peroxylated product **I**.

3B.7. Biological evaluation

In collaboration with Dr. Krishanpal Karmodiya, IISER Pune, we have evaluated the antimalarial activity of some synthesized peroxy derivatives against malarial parassite *Plasmodium falciparum 3D7*. *In vitro* antimalarial activity was evaluated by SYBR green assay with concentration ranging from 0.156 µM to 20 µM of the peroxides. It was found that upon screening the seven derivatives, all were active against the malarial parasite, but compounds **16n** and **16o** killed parasites efficiently compared to the congeners. Particularly, **16n** and **16o** exhibited the lowest IC_{50} value of 2.93 µM and 3.2 µM, respectively (Figure 3B.11). The known antimalarial compounds such as Betulinic acid, Artemisinin, Lupeol, Chloroquine shows the IC_{50} values 18 µM, 0.0039 µM, 27.7 µM, 0.045 µM respectively.[19]

Entry	**16a**	**16c**	**16e**	**16h**	**16j**	**16n**	**16o**
IC_{50}	28.3	9.3	21.8	10.3	41.4	2.9	3.2

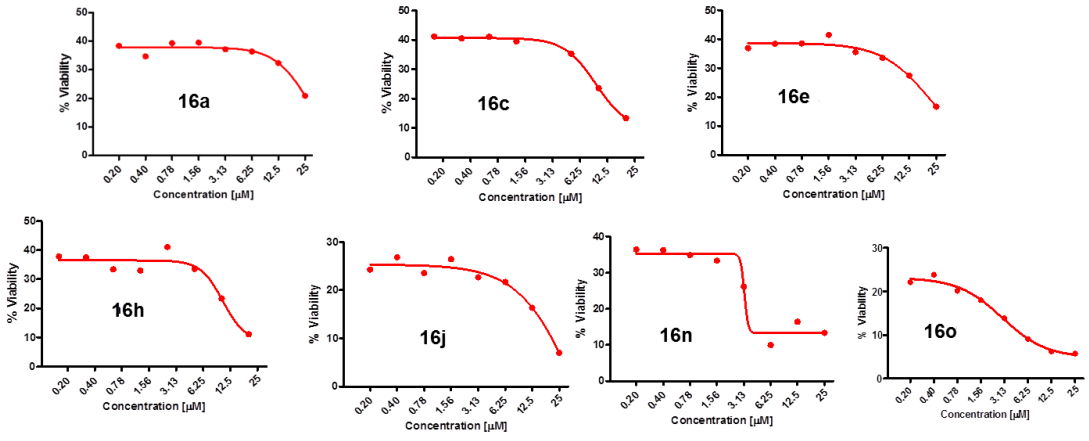

Figure 3B.11. Dose-dependent viability assay in *Plasmodium falciparum*

3B.8. Conclusion

In conclusion, the first heterogeneous Fe-MNP-catalyzed C-H peroxidation of carbonyl compounds with peroxide under batch/continuous flow process is reported. In divergence with documented methods, the current protocol does not require additional ligand and prolonged reaction time. The protocol is general and broad substrate scope is achieved with gram scale synthesis in a continuous-flow and batch conditions. In batch conditions, catalyst was recycled and reused up to 10 runs without much loss in its catalytic activity. In continuous-flow, the efficiency and stability of the catalyst were exploited by a long flow experiment (40 h) with the productivity of 0.309 mmol $_{product}$ mmol $_{Fe\text{-}MNP}^{-1}h^{-1}$. Later, the catalyst was recycled and used for the synthesis of a library of peroxy compounds. Moreover, the synthesized peroxides were tested against viability of malarial parasite, and found to be potentially active. Upon screening the library of peroxides, compounds **16n** and **o** exhibited best antiplasmodial activity against *Plasmodium falciparum 3D7 in vitro* with IC_{50} value 2.93 μM and 3.2 μM respectively.

3B.9. Experimental procedure

(A) General experimental procedure for C-H peroxidation of 2-oxindole and barbituric acid derivatives in batch:

In a 20 mL re-sealable vial was added $Fe(OH)_3Fe_3O_4$ (30 mg), ethyl acetate 1 mL, 5.0-6.0 M *tert*-Butyl hydroperoxide (TBHP) in decane solution (1.0 mmol, 4 equiv) and finally, C3- substituted-2-oxindole (0.25 mmol, 1 equiv) was added and tube is sealed with a cap using crimper. The reaction mixture was heated at 80 ^oC in an oil bath for 4 h. After reaction completion, magnetic nanoparticles were separated by magnetic decantation. A volatile component was evaporated using a vacuum. The residue was directly purified by silica gel chromatography (EtOAc: hexane = 15:85 or 20:80).

(B) Experimental procedure C-H peroxidation of C3-substituted-2-oxindole in continuous-flow:

The catalyst used for long run experiment was recycled and used to prepare library of peroxylated compounds. In a typical procedure, the 0.1M solution of C3-2-oxindole derivative in 5 mL ethyl acetate + 4 equiv of (5.0-6.0M TBHP in decane) was premixed and flown through Omnifit® (6.6 x 150 mm) packed bed column ($Fe(OH)_3Fe_3O_4$ filled up to 2.3 cm, 800 mg) at 80 ^oC with 0.1 mL/min flow rate at 2-3 bar pressure. After reaction completion, the catalyst bed was washed with ethyl acetate (3-4 times), and dried at 100 ^oC in the oven for 3- 4 h and reused for the next substrate.

A volatile component was evaporated using a vacuum. The residue was directly purified by silica gel chromatography (EtOAc: hexane= 15:85 or 20:80). **Note**: For preventive measurement we have filtered the solution through syringe filter before pumping it through pumps. (Filtration carried out using nylon syringe filter (0.22 µm)). Time mentioned in flow is residence time (t_R); residence time can be calculated by following formula: reactor volume/flow rate.

(C) General experimental procedure for removal of the *tert*-butyl group using Amberlyst 15:

A solution of 0.1 M peroxyoxindole in 5 mL acetonitrile was flown through the packed bed of Amberlyst-15 (Dry) (bed height 5.5 cm, 500 mg) with 2-3 bar pressure at 0.1 mL/min at 26 ^{o}C to afford hydroperoxy-2-oxindole **17a-17e**. (As there was some unreacted starting material left in 1st run, therefore, reaction mixture was subjected to 2nd run (depend on the substrate) in the same packed bed). For each substrate fresh Amberlyst-15 bed was used. After reaction completion, a volatile component was evaporated using a vacuum. The residue was directly purified by silica gel chromatography (EtOAc : hexane= 20:80 or 30:70).

3B.9.1. Spectroscopic data for the product

3-(*tert*-Butylperoxy)-3-(2-fluorobenzyl)indolin-2-one (**16b**): 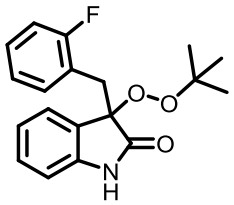

Prepared according to general procedure A, using 3-(2-fluorobenzyl)indolin-2-one (60.2 mg, 0.25 mmol) to afford peroxyoxindole **16b** (54.5 mg, 66% yield) as a cream colored solid. **^{1}H NMR** (400 MHz, $CDCl_3$): δ 8.54 (bs, 1H), 7.27 – 7.12 (m, 3H), 7.01 – 6.84 (m, 4H), 6.78 – 6.74 (m, 1H), 3.41 (d, *J* = 13.7 Hz, 1H), 3.16 (d, *J* = 13.7 Hz, 1H), 1.12 (s, 9H). **^{13}C NMR** (100 MHz, $CDCl_3$) δ 176.84, 161.32 (d, *J* = 247.1 Hz), 141.04, 132.82 (d, *J* = 3.6 Hz), 129.58, 129.01 (d, *J* = 8.2 Hz), 127.44, 125.69, 123.67 (d, *J* = 3.6 Hz), 122.10, 121.12 (d, *J* = 15.2 Hz), 115.16 (d, *J* = 22.5 Hz), 109.90, 85.12, 80.79, 32.63, 26.60. **FTIR** (neat): 3265, 2979, 2924, 1728, 1626, 1227, 1112 cm^{-1}. **HRMS** (ESI) m/z calculated for $C_{19}H_{20}FNO_3$ $(M+Na)^+$: 352.1325, found: 352.1331.

3-(4-Bromobenzyl)-3-(*tert*-butylperoxy)indolin-2-one (16d): Prepared according to general procedure A, using 3-(3-bromobenzyl)indolin-2-one (75.25 mg, 0.25 mmol) to afford peroxyoxindole **16d** (54 mg, 55% yield) as a light yellow solid. **^{1}H NMR** (400 MHz, $CDCl_3$) δ 8.19 (bs, 1H), 7.33 – 7.29 (m, 1H), 7.23 – 7.18 (m, 2H), 7.03 (t, *J* = 7.7 Hz, 1H), 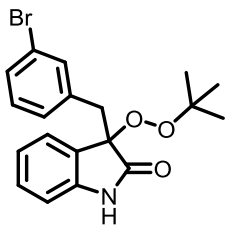

6.99 – 6.95 (m, 2H), 6.93 – 6.90 (m, 1H), 6.76 (d, *J* = 7.8 Hz, 1H), 3.32 (d, *J* = 13.3 Hz, 1H), 2.99 (d, *J* = 13.4 Hz, 1H), 1.13 (s, 9H). **^{13}C NMR** (100 MHz, $CDCl_3$) δ 176.28, 141.03, 136.04, 133.91, 130.21, 129.76, 129.55, 129.44, 127.32, 125.75, 122.20, 121.89, 110.08, 85.25, 80.90, 40.12, 26.63. **FTIR** (neat): 3259, 2979, 2926, 2859, 1728, 1620, 1365, 1195, 1115 cm^{-1}. **HRMS** (ESI) m/z calculated for $C_{19}H_{20}BrNO_3$ $(M+Na)^+$: 412.0524, found: 412.0521.

3-(*tert*-Butylperoxy)-3-(3-chlorobenzyl)indolin-2-one (16i): Prepared according to general procedure A, using 3-(3-chlorobenzyl)indolin-2-one (64.25 mg, 0.25 mmol) to afford peroxyoxindole **16i** (60.5 mg, 70% yield) as a yellow solid. **^{1}H NMR** (400 MHz, $CDCl_3$) δ 8.36 (bs, 1H), 7.20 (dt, *J* = 7.6, 1.4 Hz, 1H), 7.17 – 7.13 (m, 1H), 7.08 (t, *J* = 7.8 Hz, 1H), 7.04 (t, *J* = 1.7 Hz, 1H), 6.96 (t, *J* = 7.5 Hz, 1H), 6.93 – 6.90 (m, 2H), 6.76 (d, *J* = 7.7 Hz, 1H), 3.32 (d, *J* = 13.3 Hz, 1H), 3.01 (d, *J* = 13.3 Hz, 1H), 1.12 (s, 9H). **^{13}C NMR** (100 MHz, $CDCl_3$) δ 176.46, 141.10, 135.74, 133.67, 130.97, 129.75, 129.14, 127.29, 125.72, 122.18, 110.13, 85.29, 80.89, 40.13, 26.62. **FTIR** (neat): 3315, 3201, 2977, 2443, 1731, 1622, 1213 cm^{-1}. **HRMS** (ESI) m/z calculated for $C_{19}H_{20}ClNO_3$ $(M+Na)^+$: 368.1029, found: 368.1035.

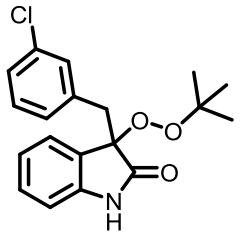

3-(*tert*-Butylperoxy)-3-propylindolin-2-one (16l): Prepared according to general procedure A, using 3-propylindolin-2-one (43.7mg, 0.25 mmol) to afford peroxyoxindole **16l** (20 mg, 30% yield) as yellow liquid. **^{1}H NMR** (400 MHz, $CDCl_3$) δ 8.15 (bs, 1H), 7.30 (d, *J* = 7.3 Hz, 1H), 7.26 – 7.21 (m, 1H), 7.04 (dt, *J* = 7.6, 0.7 Hz, 1H), 6.85 (d, *J* = 7.8 Hz, 1H), 2.03 – 1.74 (m, 2H), 1.34 – 1.26 (m, 2H), 1.11 (s, 9H), 0.85 (t, *J* = 7.3 Hz, 3H). **^{13}C NMR** (100 MHz, $CDCl_3$) δ 177.25, 141.30, 129.39, 129.07, 124.81, 122.44, 109.90, 85.62, 80.42, 36.38, 26.60, 16.43, 14.32. **FTIR** (neat): 3261, 2969, 1726, 1621, 1197, 1136 cm^{-1}. **HRMS** (ESI) m/z calculated for $C_{15}H_{21}NO_3$ $(M+Na)^+$: 286.1419, found: 286.1425.

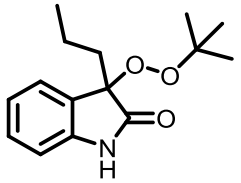

3-Butyl-3-(*tert*-butylperoxy)indolin-2-one (16m): Prepared according to general procedure A, using 3-butylindolin-2-one (47.2 mg, 0.25 mmol) to afford peroxyoxindole **16m** (43 mg, 62% yield) as yellow semisolid. **^{1}H NMR** (400 MHz, $CDCl_3$) δ 8.59 (bs, 1H), 7.29 (d, *J* = 7.4 Hz, 1H), 7.26 – 7.21 (m, 1H), 7.04 (dd, *J* = 10.0, 5.1 Hz, 1H), 6.88 – 6.84 (m, 1H), 2.00 – 1.84 (m, 2H), 1.30 – 1.17 (m, *J* = 7.0, 3.4 Hz, 4H), 1.10 (s, 9H), 0.80 (t, *J* = 7.1 Hz, 3H). **^{13}C NMR** (100 MHz, $CDCl_3$) δ 177.57, 141.44, 129.39, 129.00, 124.73, 122.40, 110.05, 85.73, 80.41, 33.98, 26.59, 24.95,

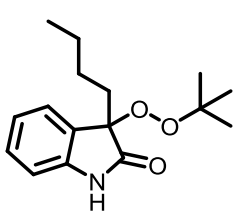

22.93, 13.89. **FTIR** (neat): 3260, 2965, 2869, 1725, 1619, 1362, 1140, 1027, 747 cm^{-1}. **HRMS** (ESI) m/z calculated for $C_{16}H_{23}NO_3$ $(M+Na)^+$: 300.1576, found: 300.1572.

3-Benzhydryl-3-(*tert*-butylperoxy)indolin-2-one (16r): Prepared according to general procedure A, using 3-benzhydrylindolin-2-one (74.7 mg, 0.25 mmol) to afford peroxyoxindole **16r** (54 mg, 45% yield) as a yellow solid. **^{1}H NMR** (400 MHz, $CDCl_3$) δ 7.38 – 7.33 (m, 2H), 7.29 – 7.24 (m, 4H), 7.20 (bs, 1H), 7.17 – 7.11 (m, 3H), 6.97 (dd, *J* = 7.8, 1.7 Hz, 2H), 6.89 (dt, *J* = 7.6, 1.0 Hz, 1H), 6.73 (d, *J* = 7.7 Hz, 1H), 6.53 (d, *J* = 7.5 Hz, 1H), 4.80 (s, 1H), 1.09 (s, 9H). **^{13}C NMR** (100 MHz, $CDCl_3$) δ 175.54, 142.09, 137.90, 137.18, 130.67, 130.03, 129.88, 128.39, 127.78, 127.45, 127.20, 127.12, 127.06, 121.92, 109.60, 86.64, 80.79, 55.49, 26.73. **FTIR** (neat): 3211, 2925, 1732, 1618, 1465, 1194, 1118 cm^{-1}. **HRMS** (ESI) m/z calculated for $C_{25}H_{25}NO_3$ $(M+H)^+$: 388.1913, found: 388.1902.

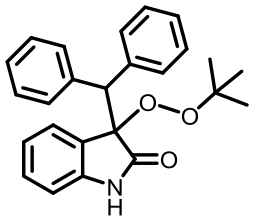

3-(*tert*-Butylperoxy)-1,3-dimethylindolin-2-one (16s): Prepared according to general procedure A, using 1,3-dimethylindolin-2-one (40.2 mg, 0.25 mmol) to afford peroxyoxindole **16s** (44 mg, 71% yield) as yellow liquid. **^{1}H NMR** (400 MHz, $CDCl_3$) δ 7.35 – 7.29 (m, 2H), 7.07 (dt, *J* = 7.7, 0.9 Hz, 1H), 6.80 (d, *J* = 7.7 Hz, 1H), 3.20 (s, 3H), 1.52 (s, 3H), 1.10 (s, 9H). **^{13}C NMR** (100 MHz, $CDCl_3$) δ 175.34, 143.71, 129.83, 129.51, 124.03, 122.56, 108.07, 81.99, 80.37, 26.57, 26.29, 20.44. **FTIR** (neat): 3058, 2980, 2930, 1727, 1613, 1360, 1115, 1063, 747 cm^{-1}. **HRMS** (ESI) m/z calculated for $C_{14}H_{19}NO_3$ $(M+Na)^+$: 272.1263, found: 272.1275.

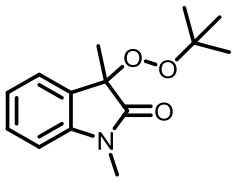

3-Benzyl-3-hydroperoxyindolin-2-one (17a): Prepared according to general procedure C, a solution of 0.1 M 3-benzyl-3-(*tert*-butylperoxy)indolin-2-one (155.5 mg, 0.5 mmol) in 5 mL acetonitrile was flown through the packed bed of Amberlyst 15 (bed height 5.5 cm) with 2-3 bar at 0.1 mL/min at 26 ^oC to afford hydroperoxy-2-oxindole **17a** (66 mg, 52% yield) as a white solid (2 runs). **Melting point**: 166-170 ^oC. **^{1}H NMR** (400 MHz, Methanol-*d4*) δ 7.38 – 7.34 (m, 2H), 7.25 – 7.13 (m, 3H), 6.97 – 6.89 (m, 3H), 6.86 – 6.82 (m, 1H), 3.50 (d, *J* = 13.8 Hz, 1H), 3.19 (d, *J* = 13.8 Hz, 1H). **^{13}C NMR** (100 MHz, Methanol-*d4*) δ 166.17, 143.00, 136.21, 132.03, 128.77, 127.71, 127.68, 124.60, 123.40, 118.40, 116.33, 98.75, 43.48. **FTIR** (neat): 3654, 3364, 3305, 3142, 2975, 2343, 1689, 1499, 1450, 1228, 1070, 755 cm^{-1}. **HRMS** (ESI) m/z calculated for $C_{15}H_{13}NO_3$ $(M+Na)^+$: 278.0793, found: 278.0801.

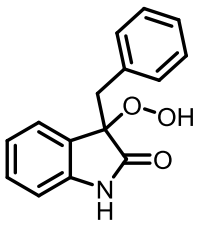

3-Hydroperoxy-3-methylindolin-2-one (17b): Prepared according to general procedure C, a solution of 0.1 M 3-(*tert*-butylperoxy)-3-methylindolin-2-one (117 mg, 0.5 mmol) in 5 mL acetonitrile was flown through the packed bed of Amberlyst 15 (bed height 5.5 cm) with 2-3 bar at 0.1 mL/min at 26 ^{o}C to afford hydroperoxy-2-oxindole **17b** (80 mg, 90% yield) as a white solid (2 runs). The data for this compound is in agreement with that reported. **Melting point**: 178-181 ^{o}C. **^{1}H NMR** (400 MHz, Methanol-*d4*) δ 6.98 – 6.95 (m, 3H), 6.94 – 6.89 (m, *J* = 3.8, 2.1 Hz, 1H), 1.71 (s, 3H). **^{13}C NMR** (100 MHz, Methanol-*d4*) δ 166.85, 143.22, 128.39, 124.59, 123.52, 118.57, 116.47, 96.86, 23.46. **FTIR** (neat): 3649, 3417, 3066, 2969, 2924, 2347, 1656, 1560, 1355, 1226, 1119, 747 cm^{-1}. **HRMS** (ESI) m/z calculated for $C_9H_9NO_3$ $(M+Na)^+$: 202.0479, found: 202.0475.

3-Hydroperoxy-3-(4-methoxybenzyl)indolin-2-one (17c): Prepared according to general procedure C, a solution of 0.1 M 3-(*tert*-butylperoxy)-3-(4-methoxybenzyl)indolin-2-one (170.5 mg, 0.5 mmol) in 5 mL acetonitrile was flown through the packed bed of Amberlyst-15 (bed height 5.5 cm) with 2-3 bar at 0.1 mL/min at 26 ^{o}C to afford hydroperoxy-2-oxindole **17c** (86 mg, 60% yield) as a white solid (1 run). **Melting point**: 167-169 ^{o}C. **^{1}H NMR** (400 MHz, Methanol-*d4*) δ 7.26 (dd, *J* = 8.8 Hz, 2H), 6.98 – 6.89 (m, 3H), 6.85 – 6.81 (m, 1H), 6.78 (*J* = 8.8 Hz, 2H), 3.73 (s, 3H), 3.43 (d, *J* = 13.9 Hz, 1H), 3.12 (d, *J* = 13.9 Hz, 1H). **^{13}C NMR** (100 MHz, Methanol-*d4*) δ 166.26, 160.04, 143.07, 133.01, 128.11, 127.70, 124.59, 123.35, 118.37, 116.31, 114.24, 98.83, 55.58, 42.66. **FTIR** (neat): 3665, 3460, 3299, 2976, 2344, 1690, 1605, 1504, 1362, 1243, 1167, 1035, 993, 751 cm^{-1}. **HRMS** (ESI) m/z calculated for $C_{16}H_{15}NO_4$ $(M+Na)^+$: 308.0899, found: 308.0895.

3-(3-Chlorobenzyl)-3-hydroperoxyindolin-2-one (17d): Prepared according to general procedure C, a solution of 0.1 M 3-(*tert*-butylperoxy)-3-(3-chlorobenzyl)indolin-2-one (172.5 mg, 0.5 mmol) in 5 mL acetonitrile was flown through the packed bed of Amberlyst-15 (bed height 5.5 cm) with 2-3 bar at 0.1 mL/min at 26 ^{o}C to afford hydroperoxy-2-oxindole **17d** (88 mg, 61% yield) as a white solid (2 runs). **Melting point**: 173-175 ^{o}C. **^{1}H NMR** (400 MHz, Methanol-*d4*) δ 7.40 – 7.36 (m, 1H), 7.32 – 7.27 (m, 1H), 7.24 – 7.15 (m, *J* = 9.1, 5.1 Hz, 2H), 6.98 – 6.90 (m, 3H), 6.89 – 6.83 (m, 1H), 3.49 (d, *J* = 13.8 Hz, 1H), 3.19 (d, J = 13.8 Hz, 1H). **^{13}C NMR** (100 MHz, Methanol-*d4*) δ 165.93, 142.87, 138.61, 134.56, 131.96,

130.49, 130.21, 127.81, 127.73, 124.69, 123.57, 118.47, 116.42, 98.48, 43.04. **FTIR** (neat): 3693, 3650, 3417, 3191, 2345, 1679, 1599, 1456, 1336, 1215, 1164, 1076, 1011, 756 cm^{-1} **HRMS** (ESI) m/z calculated for $C_{15}H_{12}ClNO_3$ $(M+Na)^+$: 312.0403, found: 312.0414.

3-Hydroperoxy-3-octylindolin-2-one (17e): Prepared according to general procedure C, a solution of 0.1 M 3-(*tert*-butylperoxy)-3-octylindolin-2-one (166.5 mg, 0.5 mmol) in 5 mL acetonitrile was flown through the packed bed of Amberlyst-15 (bed height 5.5 cm) with 2-3 bar at 0.1 mL/min at 26 ^oC to afford hydroperoxy-2-oxindole **17e** (68 mg, 49% yield) as a white solid (2 runs). **Melting point**: 130-133 ^oC. **^{1}H NMR** (400 MHz, Methanol-*d4*) δ 6.99 – 6.94 (m, 3H), 6.93 – 6.87 (m, 1H), 2.15 (ddd, *J* = 13.7, 11.3, 4.8 Hz, 1H), 1.90 (ddd, *J* = 13.7, 11.3, 5.0 Hz, 1H), 1.60 – 1.41 (m, 2H), 1.39 – 1.22 (m, 10H), 0.90 (t, *J* =7.2 Hz, 3H). **^{13}C NMR** (100 MHz, Methanol-d*4*) δ 166.72, 143.29, 128.03, 124.63, 123.42, 118.49, 116.38, 98.79, 37.52, 33.02, 30.81, 30.56, 30.34, 24.42, 23.72, 14.44. **FTIR** (neat): 3573, 3425, 3184, 2919, 2855, 2355, 1719, 1648, 1588, 1453, 1371, 1287, 1218, 1039, 978, 743 cm^{-1}. **HRMS** (ESI) m/z calculated for $C_{16}H_{23}NO_3$ $(M+Na)^+$: 300.1576, found: 300.1568.

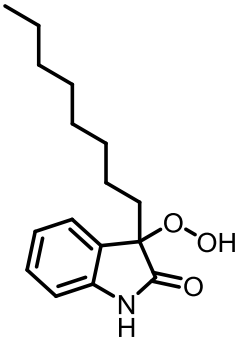

3B.9.2. Appendix IV: Copies of ^{1}H and ^{13}C NMR spectra of representative compounds

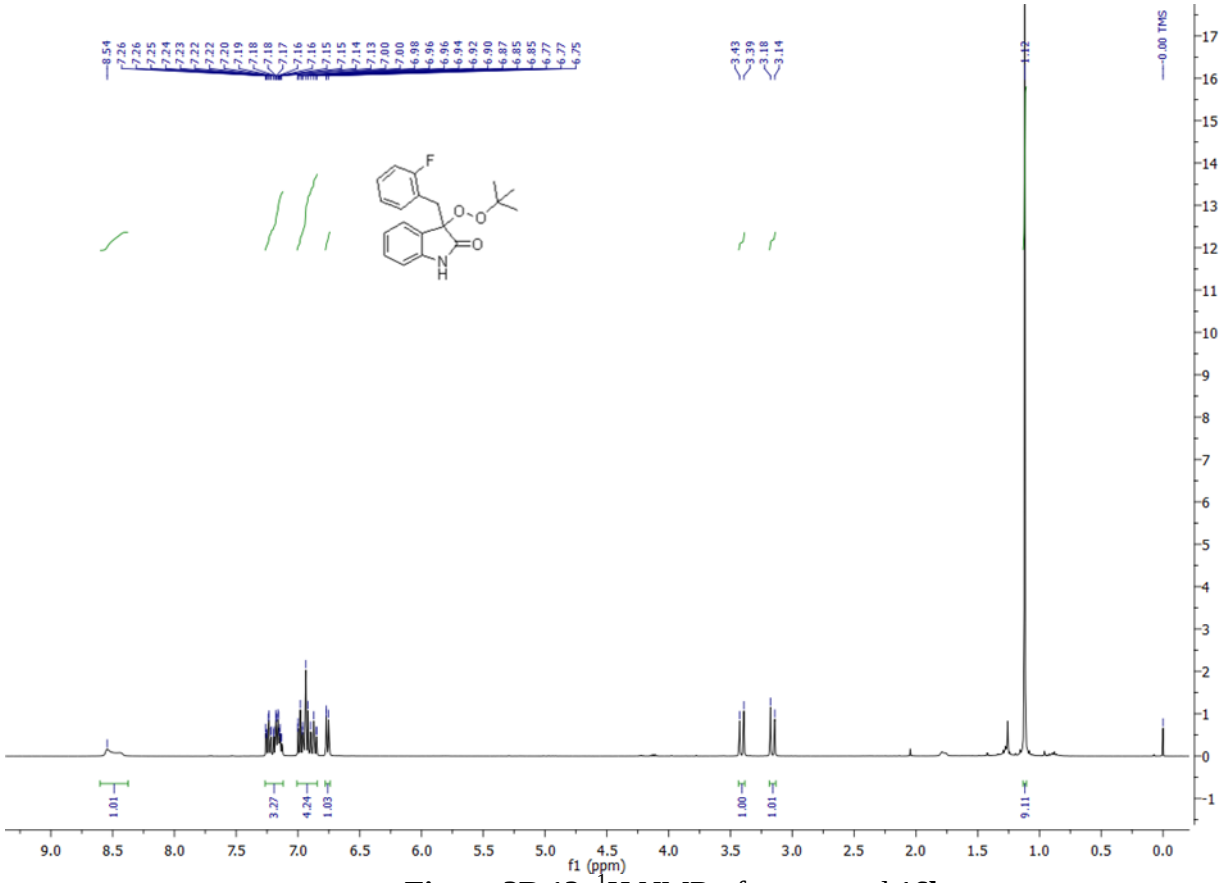

Figure 3B.12. ^{1}H NMR of compound **16b**

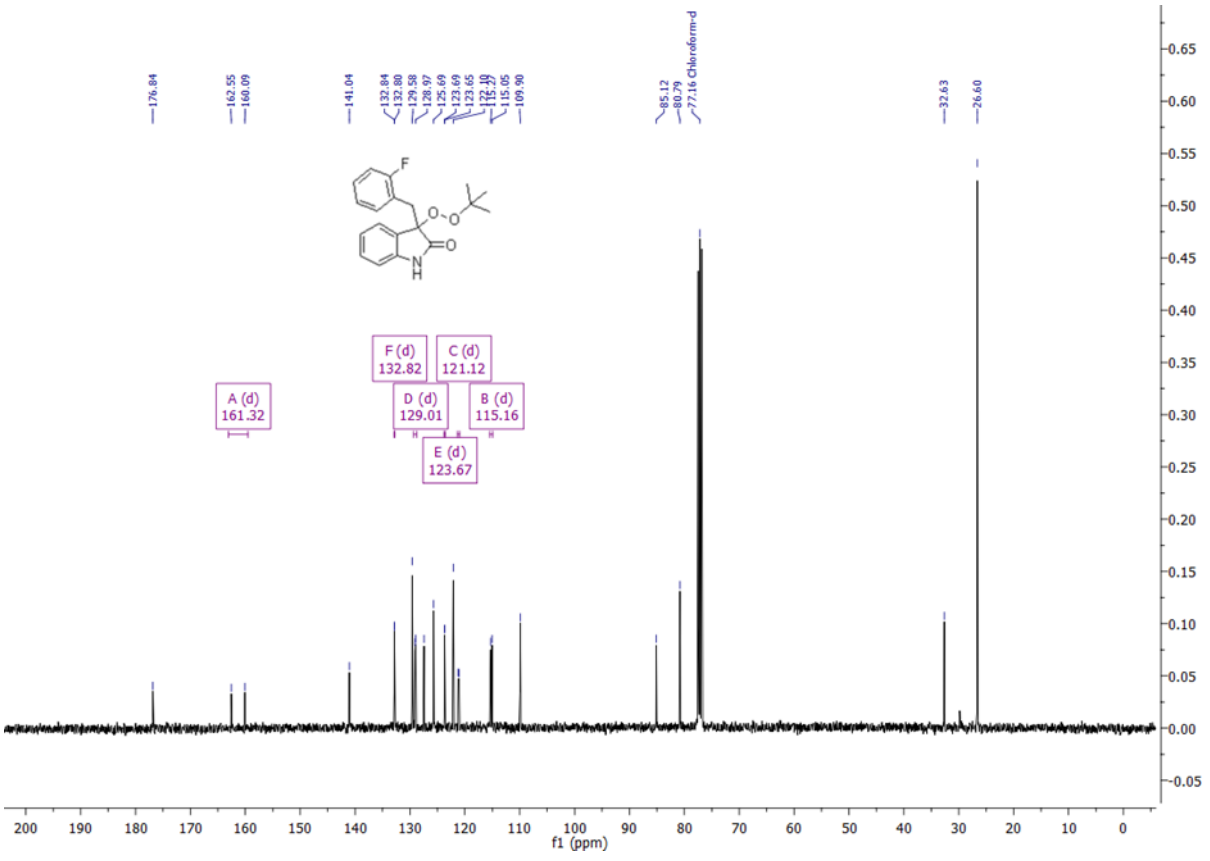

Figure 3B.13. ^{13}C NMR of compound **16b**

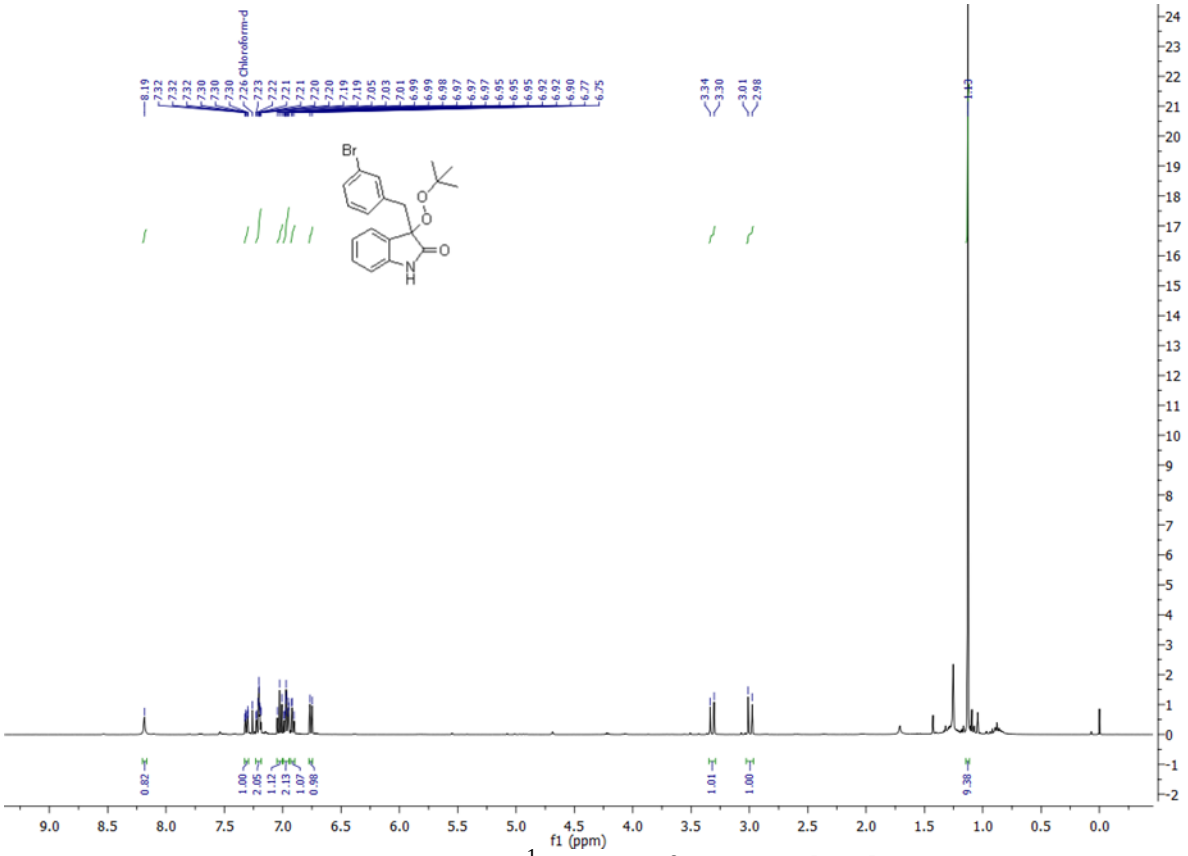

Figure 3B.14. ^{1}H NMR of compound **16d**

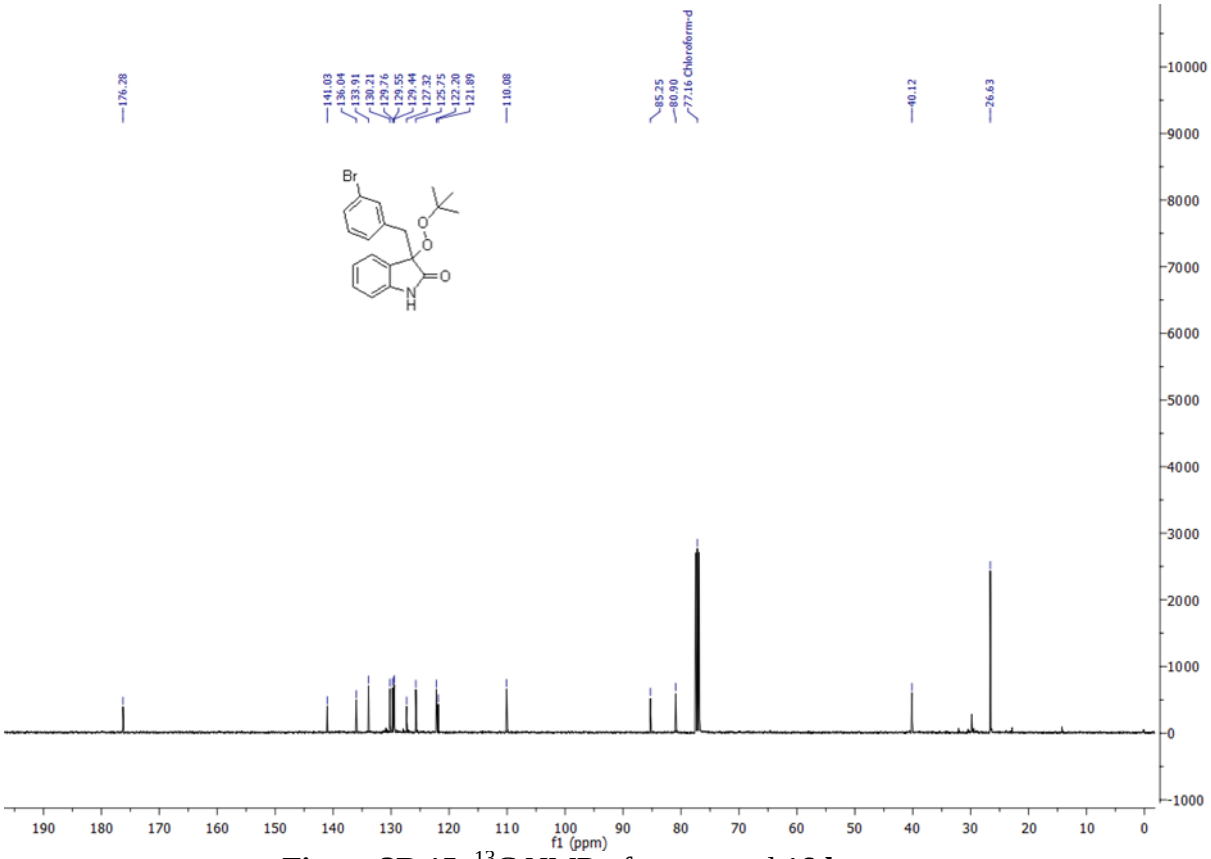

Figure 3B.15. ^{13}C NMR of compound **16d**

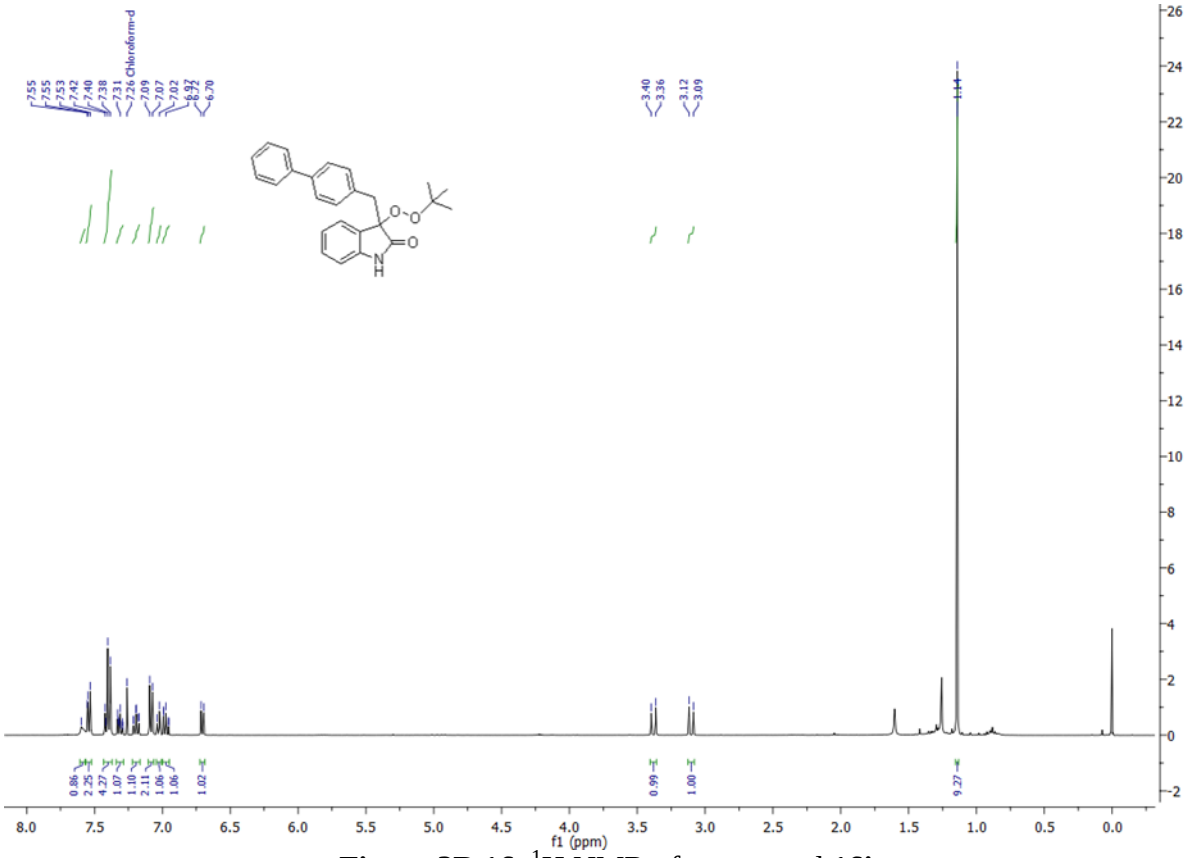

Figure 3B.16. ^{1}H NMR of compound **16i**

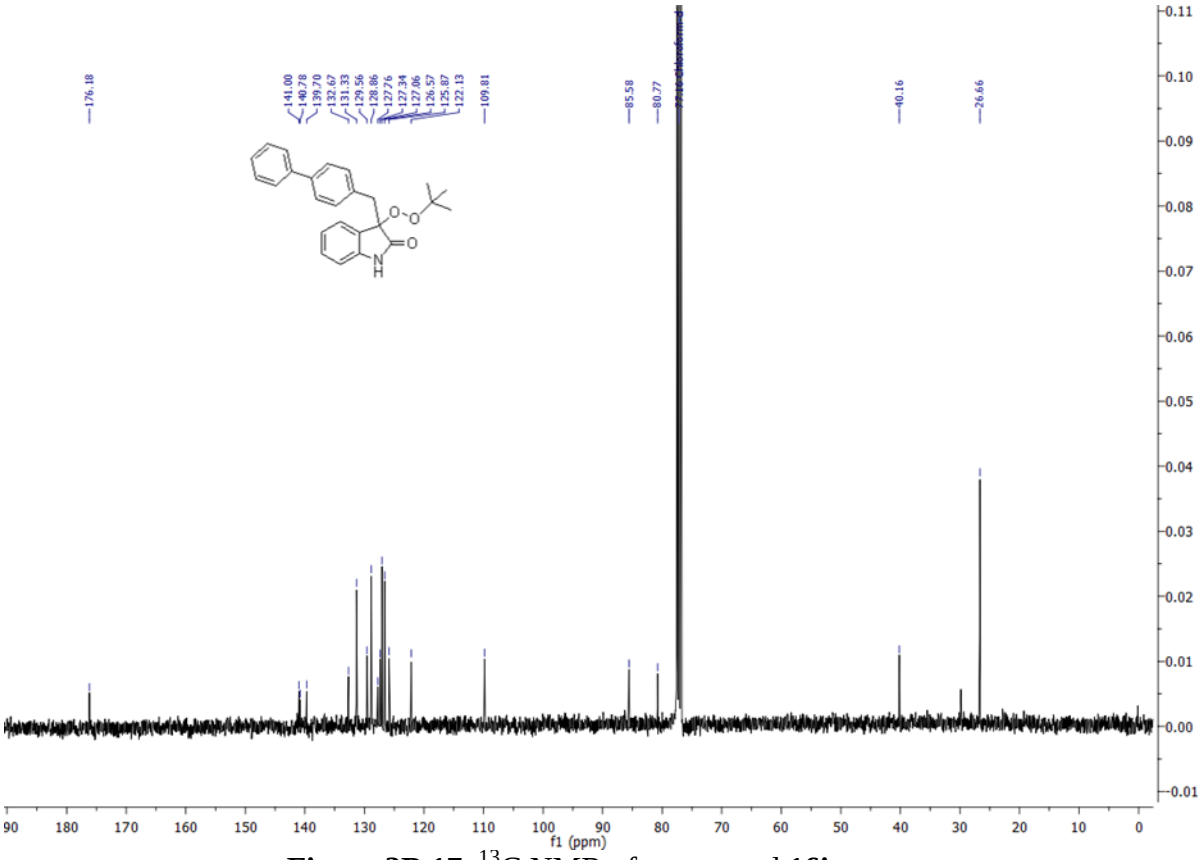

Figure 3B.17. ^{13}C NMR of compound **16i**

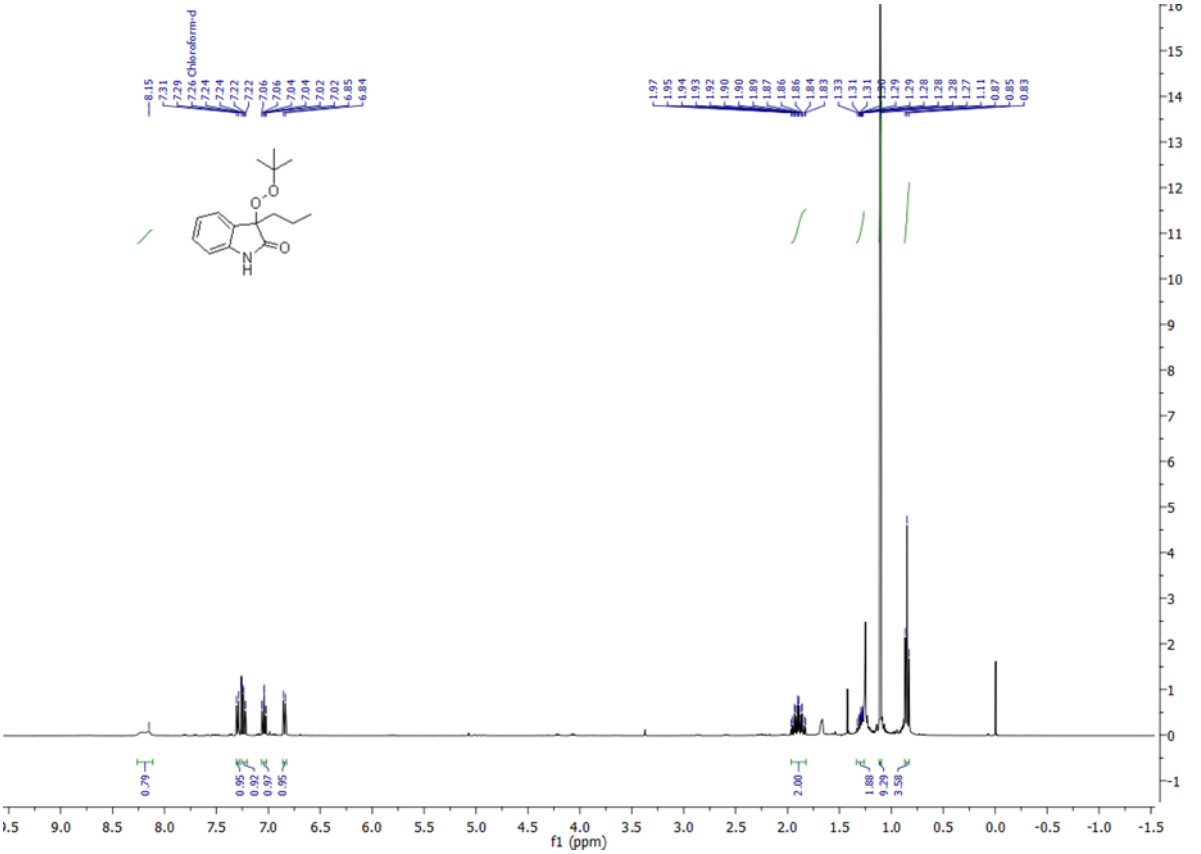

Figure 3B.18. ^{1}H NMR of compound **16l**

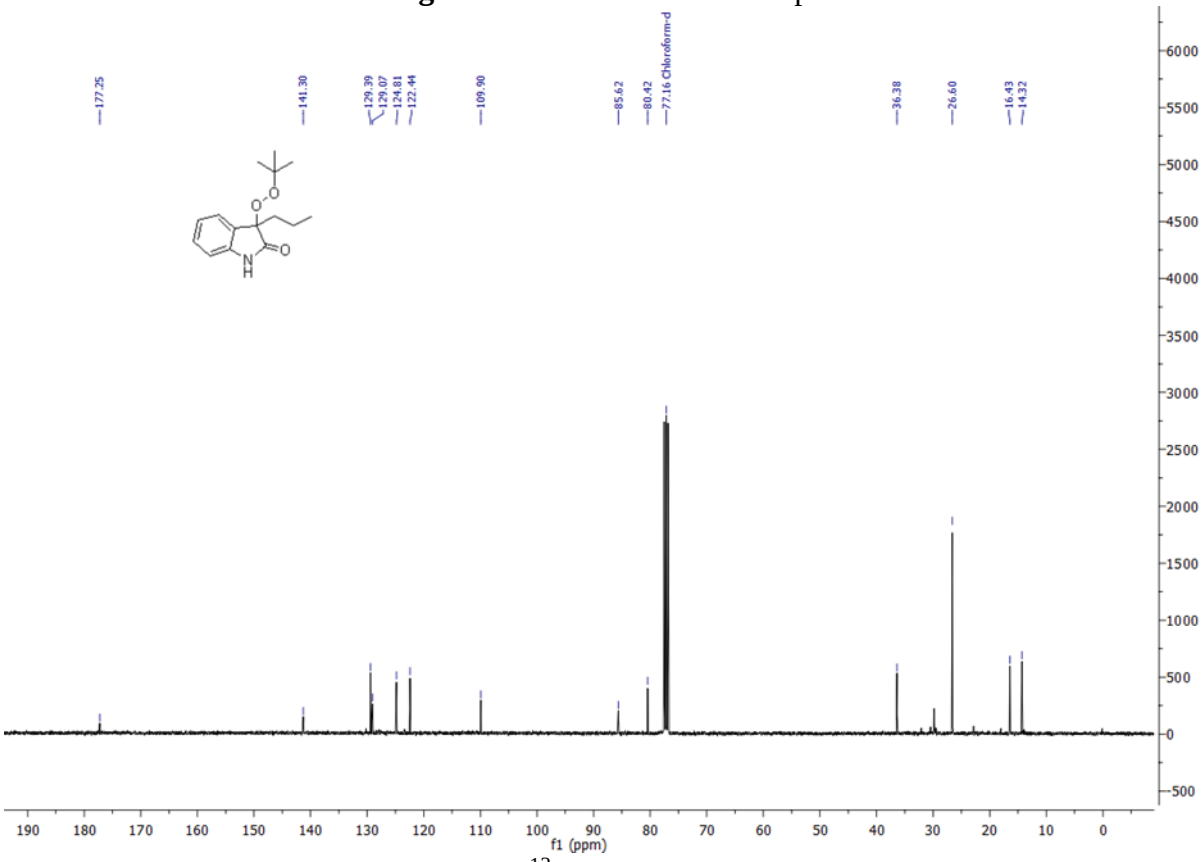

Figure 3B.19. ^{13}C NMR of compound **16l**

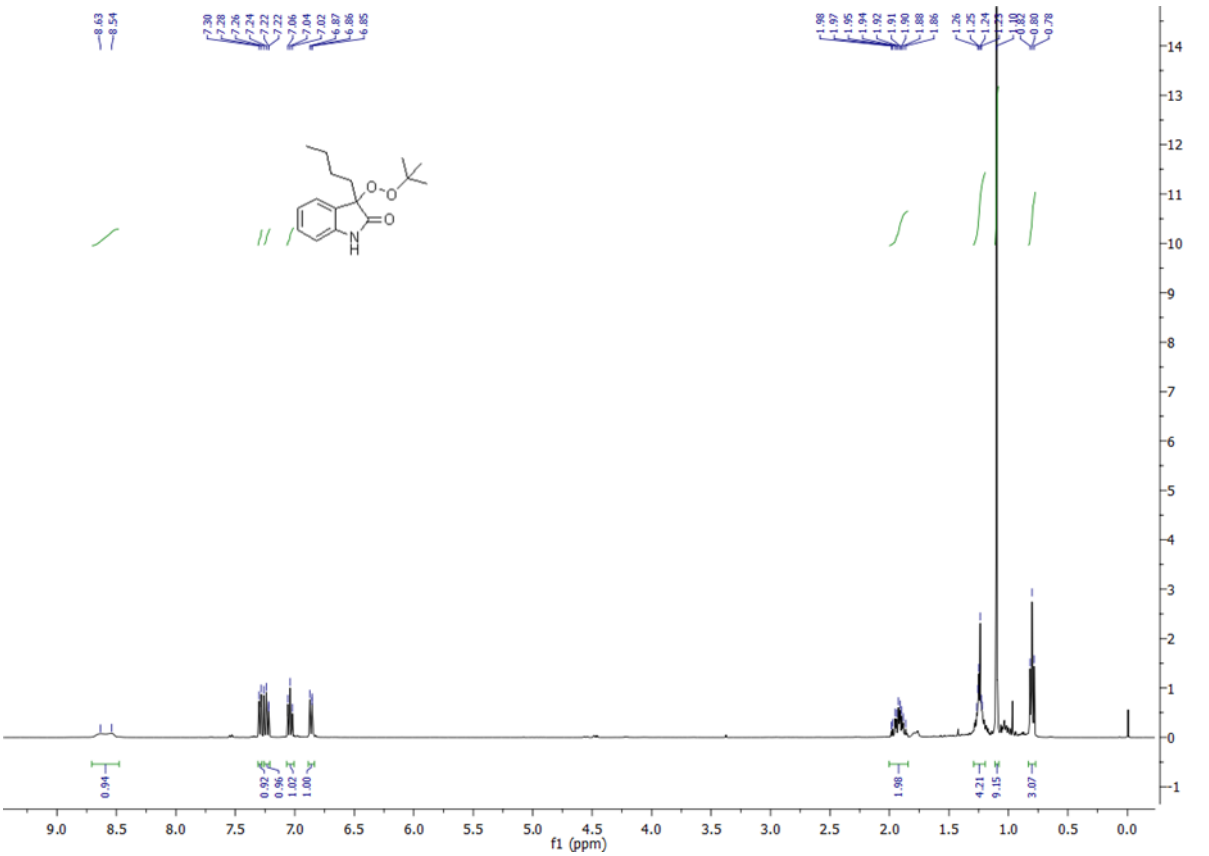

Figure 3B.20. ^{1}H NMR of compound **16m**

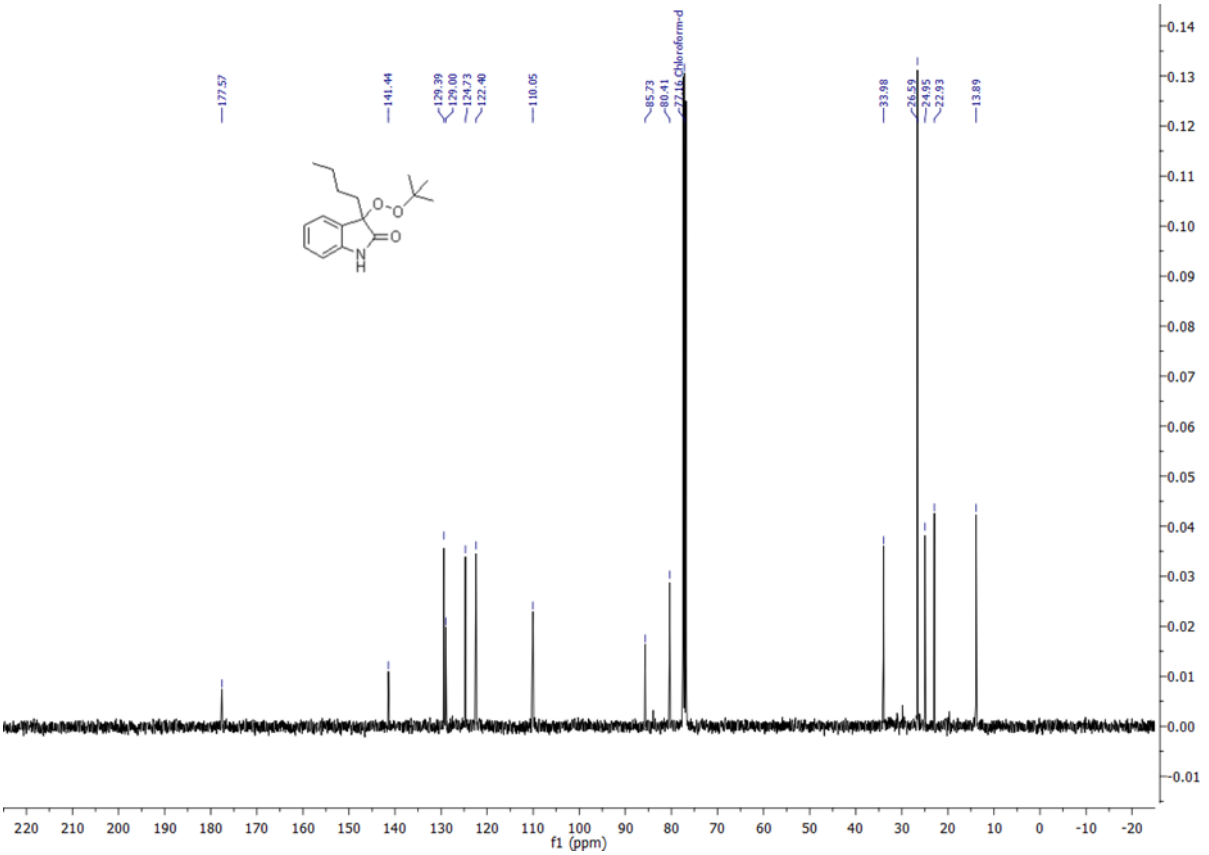

Figure 3B.21. ^{1}H NMR of compound **16m**

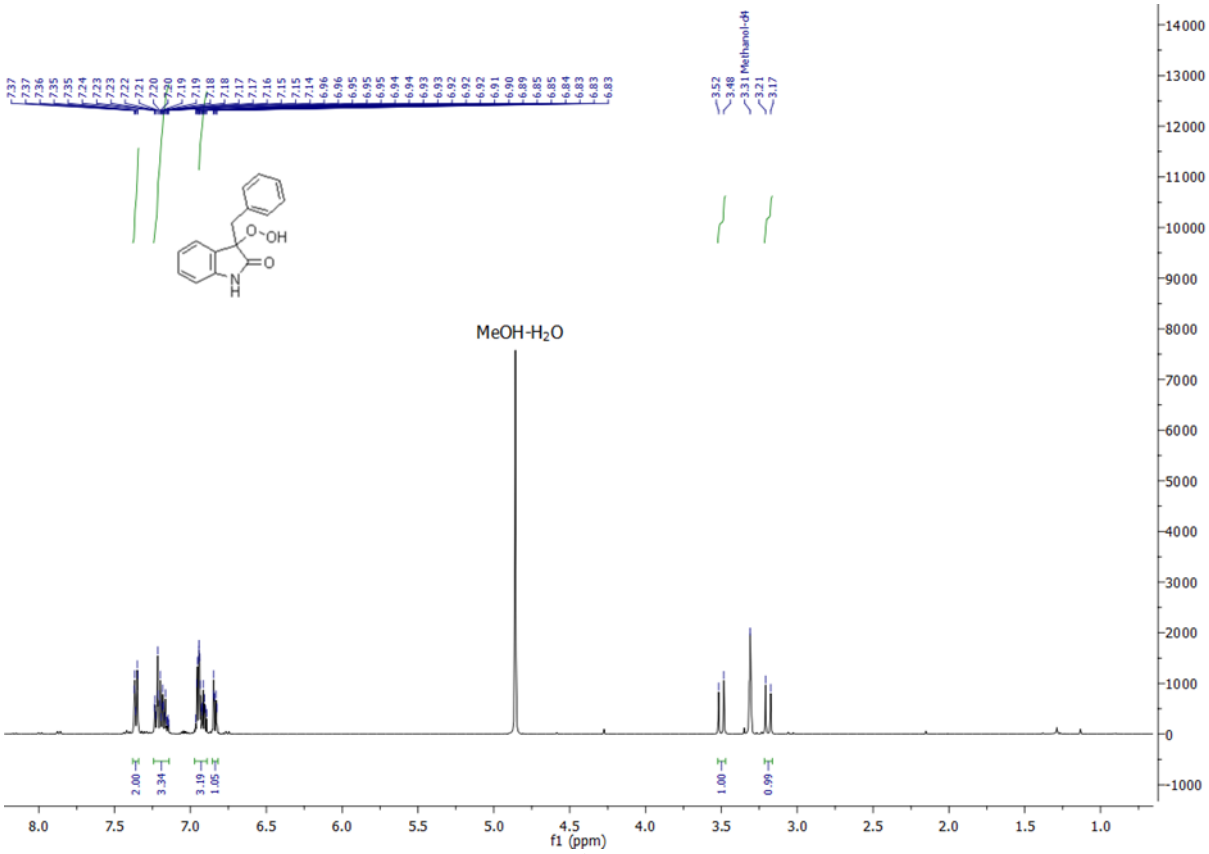

Figure 3B.22. ^{1}H NMR of compound **17a**

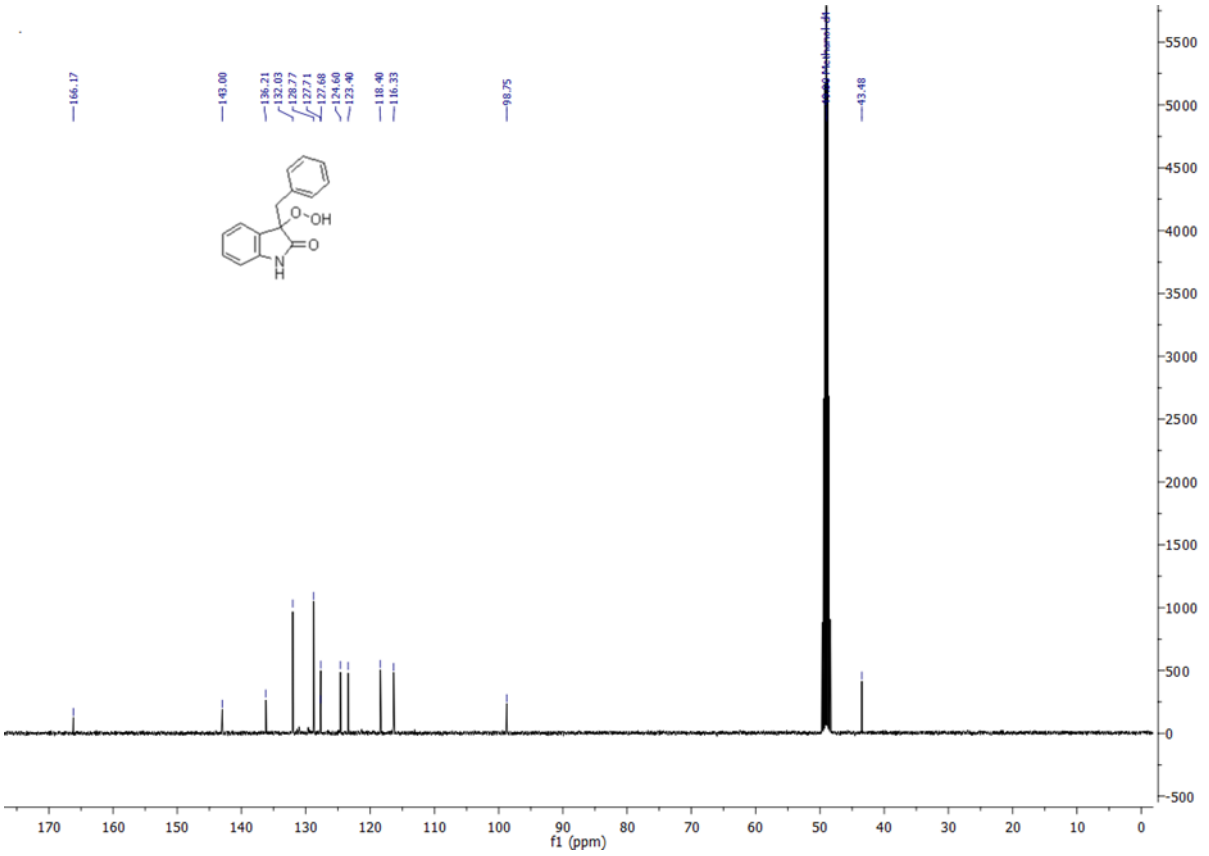

Figure 3B.23. ^{13}C NMR of compound **17a**

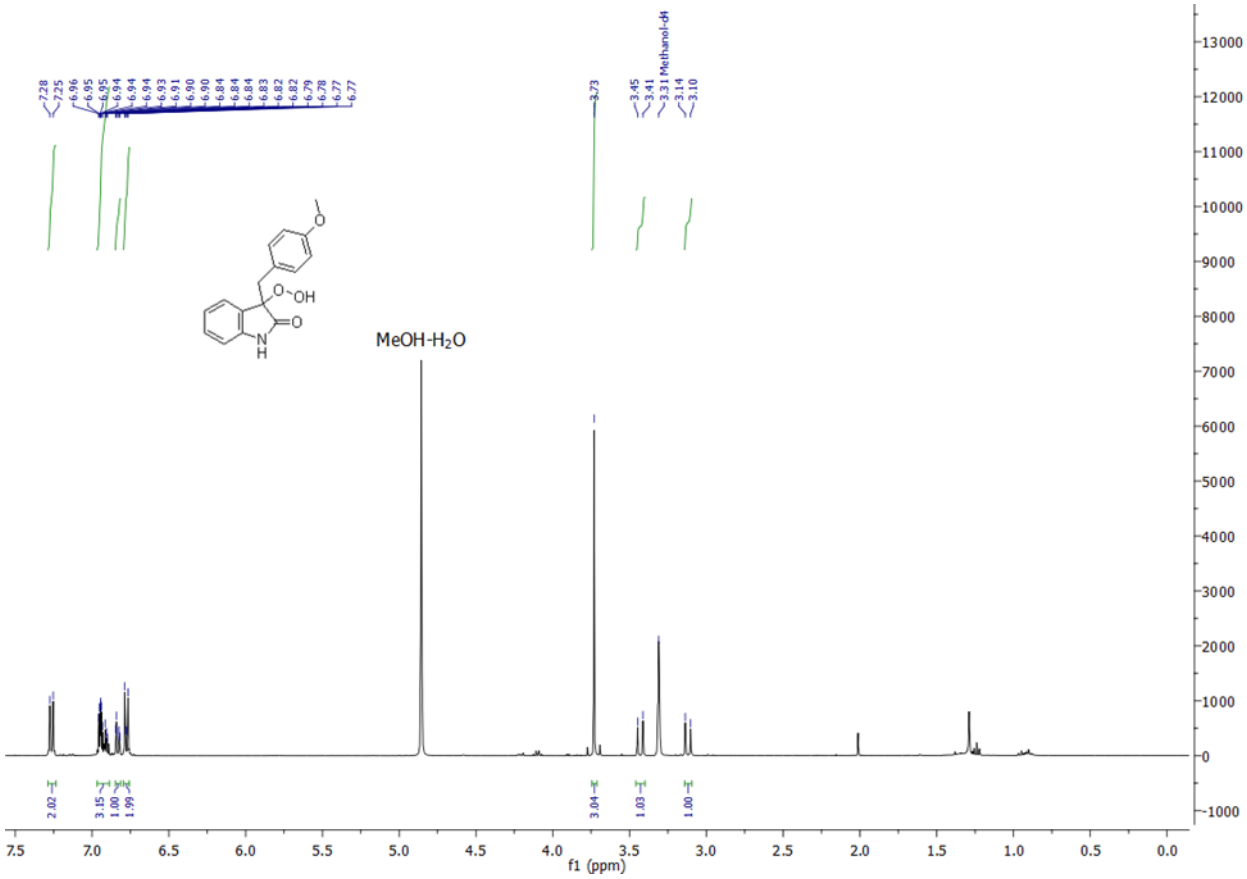

Figure 3B.24. ^{1}H NMR of compound **17c**

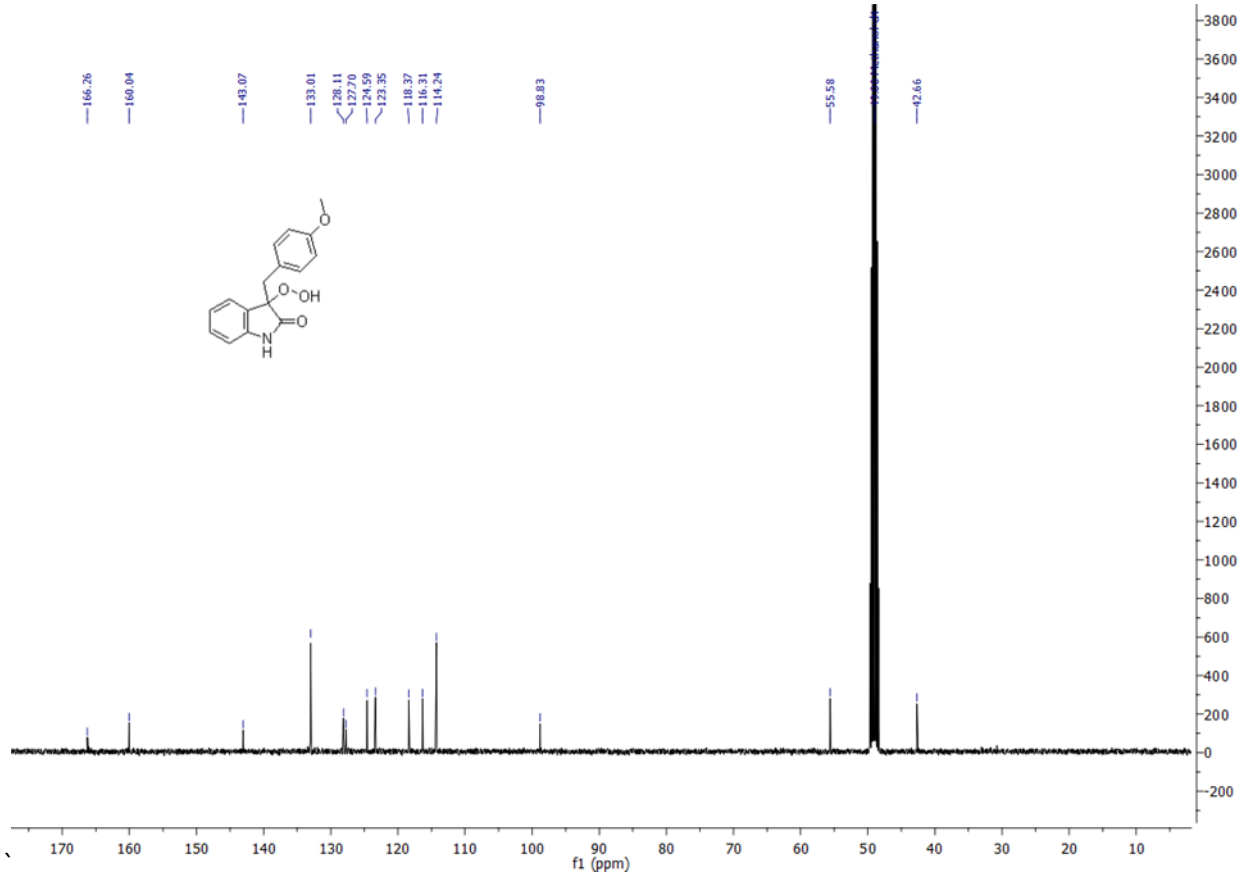

Figure 3B.25. ^{13}C NMR of compound **17c**

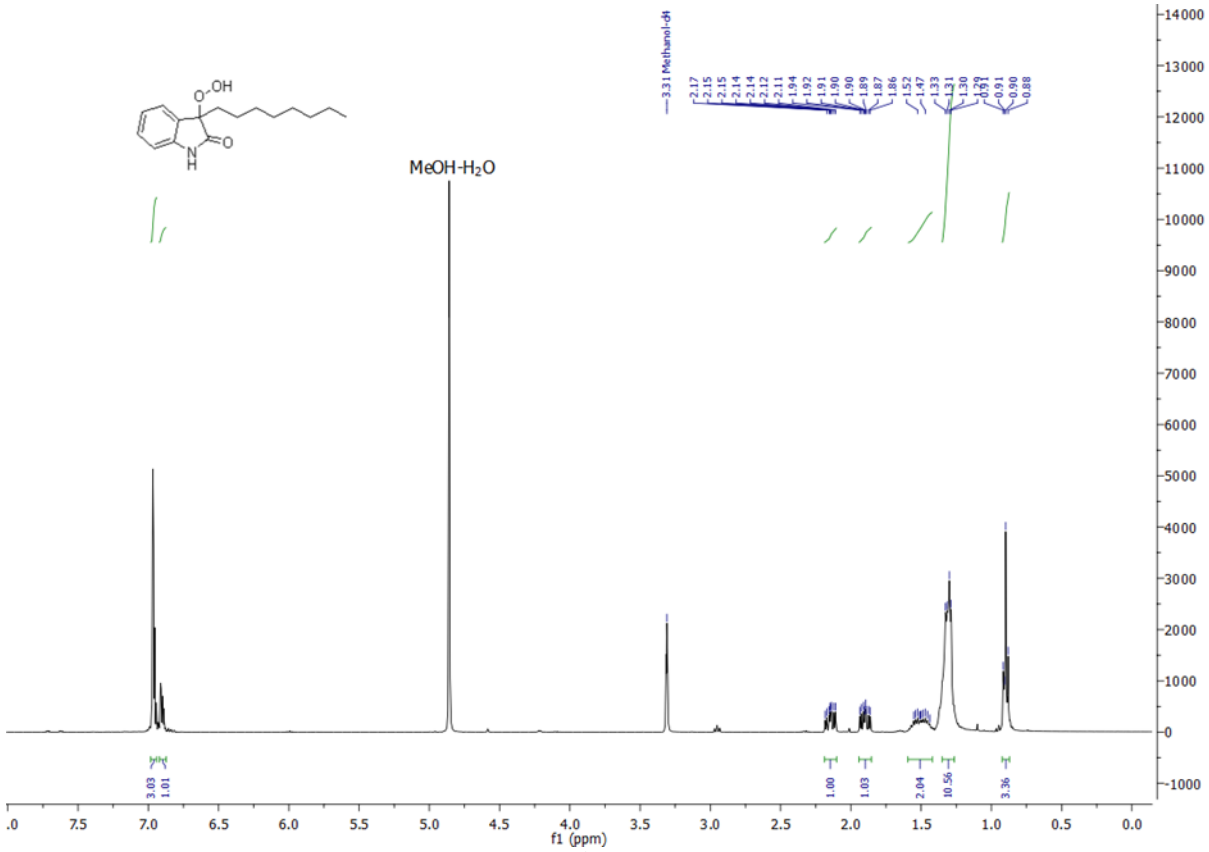

Figure 3B.26. ^{1}H NMR of compound **17e**

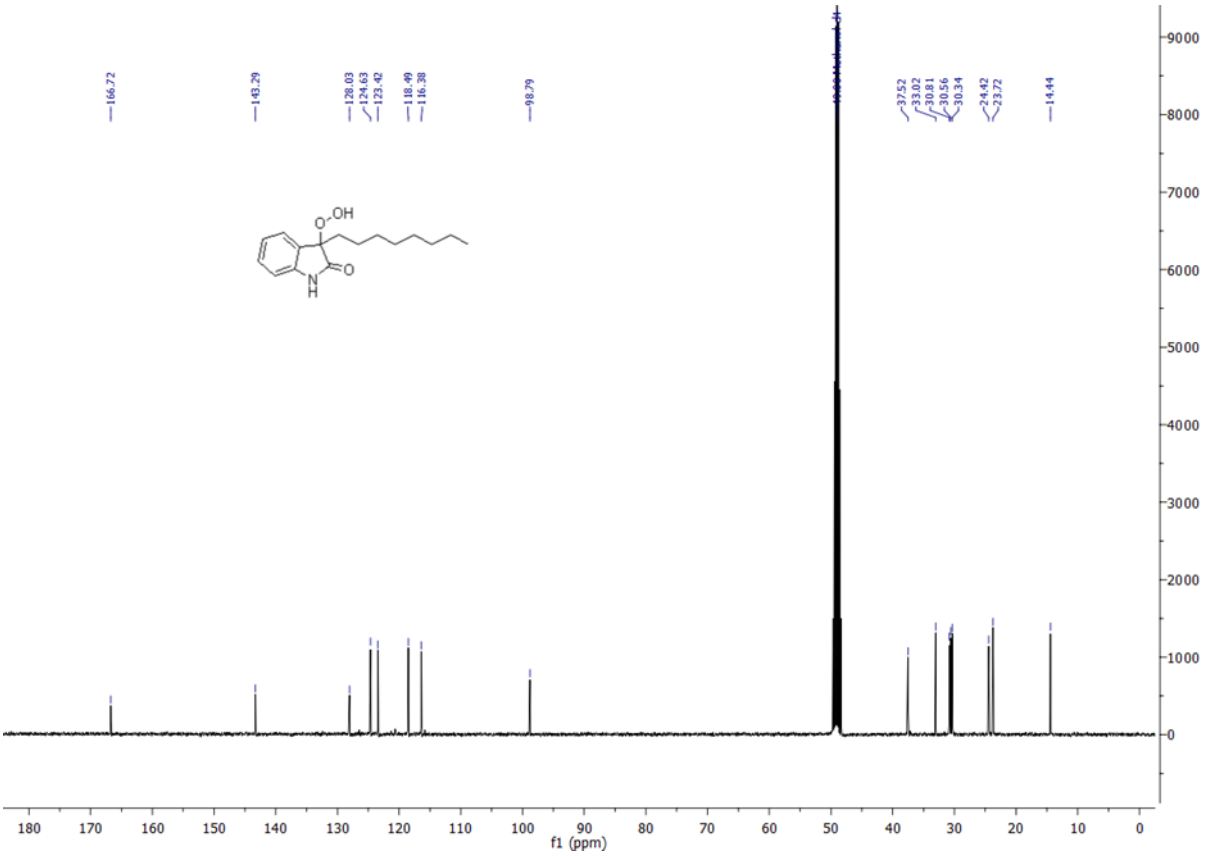

Figure 3B.27. ^{13}C NMR of compound **17e**

3B.9. References:

(1) I. Chorkendorff, J. W. Niemantsverdriet, *Concepts of Modern Catalysis and Kinetics*, Wiley-VCH Verlag GmbH & Co. KGaA Weinheim, 2003.
(2) (a) Climent, M. J.; Corma, A.; Iborra, S. *Chem. Rev.* **2011**, *111*, 1072. (b) Corma, A.; Garcia, H. *Chem. Soc. Rev.* **2008**, *37*, 2096. (c) Blaser, H. U. *Catal. Today* **2000**, *60***,** 161. (d) M. Appl. Ammonia, 2. Production Processes. In *Ullmann's Encyclopedia of Industrial Chemistry*, Wiley-VCH Verlag GmbH & Co. KGaA, 2011. DOI: 10.1002/14356007.o02_o11.
(3) (a) Munirathinam, R.; Huskens, J.; Verboom, W. *Adv. Synth. Catal.*, **2015**, *357*, 1093. (b) Munnik, P.; de Jongh, P. E.; de Jong, K. P. *Chem. Rev*. **2015**, *115*, 6687.
(4) (a) Gawande, M. B.; Brancoa, P. S.; Varma, R. S. *Chem. Soc. Rev*. **2013**, *42*, 3371. (b) Gupta, A. K.; Gupta, M. *Biomaterials* **2005**, *26*, 3995. (c) Teja, A. S.; Koh, P.-Y. *Prog. Cryst. Growth Charact. Mater.* **2009**, *55*, 22. (d) Nie, S.; Starodub, E.; Monti, M.; Siegel, D. A.; Vergara, L.; Gabaly, F. E.; Bartelt, N. C.; de la Figuera, J.; McCarty, K. F. *J. Am. Chem. Soc.* **2013**, *135*, 10091.
(5) Ranjbar, S.; Riente, P.; Rodríguez-Escrich, C.; Yadav, J.; Ramineni, K.; Pericàs, M. A. *Org. Lett.* **2016**, *18*, 1602.
(6) Riente, P.; Mendoza, C.; Pericàs, M. A. *J. Mater. Chem.* **2011**, *21*, 7350.
(7) Hu, A.; Yee, G. T.; Lin, W. *J. Am. Chem. Soc*. **2005**, *127*, 12486.
(8) (a) Niu, F.; Zhang, L.; Luo, S. Z.; Song, W. G. *Chem. Commun.* **2010**, *46*, 1109. (b) Arefi, M.; Saberi, D.; Karimi, M.; Heydari, A. *ACS Comb. Sci.* **2015**, *17*, 341.
(9) Mohammadi, A.; Barikani, M. *Mater. Charact.* **2014**, *90*, 88.
(10) Ricciardi, R.; Huskens, J.; Verboom, W. *ChemSusChem*. **2015**, *8*, 2586.
(11) Schatz, A.; Grass, R. N.; Kainz, Q.; Stark, W. J.; Reiser, O. *Chem. Mater*. **2010**, *22*, 305.
(12) Obermayer, D.; Balu, A. M.; Romero, A. A.; Goessler, W.; Luque, R.; Kappe, C. O. *Green Chem*. **2013**, *15*, 1530.
(13) Moghaddam, M. M.; Pieber, B.; Glasnov, V.; Kappe, C.O. *ChemSusChem* **2014**, *7*, 312.
(14) Mennecke, K.; Kirschning, A. *Beilstein J. Org. Chem*. **2009**, *5*, 21.
(15) Yamashita, T.; Hayes, P. *Appl. Surf. Sci.* **2008**, *254*, 2441.
(16) Zabarskas, V.; Tamulevičius, S.; Prosyčevas, I.; Puišo, J. *Mater. Sci-Medzg.* **2004**, *10*, 147.
(17) (a) Prat, D.; Wells, A.; Hayler, J.; Sneddon, H.; McElroy, C. R.; Abou-Shehadad, S.; Dunn, P. J. *Green Chem*. ***2016***, *18*, 288. (b) Kerton, F. M.; Marriott, R. *Alternative Solvents for Green Chemistry* 2nd edition; Royal Society of Chemistry: Cambridge, UK, 2013.
(18) Wang, Y. W.; Duh, Y. S.; Shu, C. M. *Proc. Safety Prog.* **2007**, *26*, 299.
(19) (a) Ziegler, H. L.; Staerk, D.; Christensen, J.; Hviid, L.; Hägerstr, H.; Jaroszewski, J. W. *Antimicrob. Agents Chemother*. **2002**, *46*, 1441. (b) Bhattacharya, A.; Mishra, L. C.; Bhasin, V. K.; *Am. J. Trop. Med. Hyg*. **2008**, *78*, 721. (c) Innocente,

A. M.; Silva, G. N. S.; Cruz, L. N.; Moraes, M. S.; Nakabashi, M.; Sonnet, P.; Gosmann, G.; Garcia, C. R. S.; Gnoatto, S. C. B. *Molecules* **2012**, *17*, 12003.
(20) Chaudhari, M. B.; Chaudhary, A.; Kumar, V.; Gnanaprakasam, B. *Org. Lett*. **2019**, *21*, 1617.
(21) Kong, D. L.; Cheng, L.; Yue, T.; Wu, H. R.; Feng, W. C.; Wang, D.; Liu, L. *J. Org. Chem.* **2016**, *81*, 5337.

The content of the Chapter 3B is reproduced from Ref. "*React. Chem. Eng.* **2019**, *4*, 1277" with permission from the Royal Society of Chemistry.

Chapter 4

Section A:

The Rearrangement of Peroxides for the Construction of Fluorophoric 1,4-Benzoxazin-3-one Derivatives

4A. The Rearrangement of Peroxides for the Construction of Fluorophoric 1,4-Benzoxazin-3-one Derivatives

4A.1. Abstract

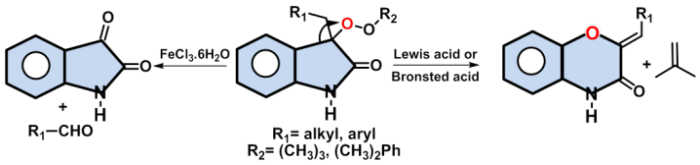

In this chapter, we have discovered a novel skeletal rearrangement of 3-(*tert*-butylperoxy)indolin-2-one using a Sn-catalyst. This rearrangement is highly selective to afford a series of fluorophoric (Z)-2-arylidene and alkylidene-2*H*benzo[*b*][1,4]oxazin-3(4*H*)-one derivatives in good to excellent yield. On the other hand, the reaction of 3-(*tert*-butylperoxy)indolin-2-one derivatives in the presence of $FeCl_3$ produces the Hock fragmentation product *via* C–C bond cleavage.

4A.2. Literature background on the rearrangement of peroxides

Rearrangement reactions give an alternative route for the synthesis of complex building blocks.[1] A variety of rearrangement of peroxides such as (acid-catalyzed, base-catalyzed, or radical-mediated) are reported in the literature (Figure 4A.1, Figure 4A.2, Figure 4A.3).[2] Synthetically, the Hock process is the best method for synthesizing phenol from cumene hydroperoxide and is one of the path-breaking examples for rearrangement of organic peroxide, which can be attributed to the acidic source.[3] In biochemistry, lipid peroxidation is an important research area; as a result, attracting the scientific community from across many disciplines. The naturally occurring oxylipins constitute a family of oxygenated natural products, which is ubiquitous in plants, animals, and fungi. Enzymatically, in oxylipin metabolism, hydroperoxide lyase (HPL) converts fatty acid hydroperoxides into hemiacetal derivatives *via* hock type rearrangement that spontaneously decomposes to the aldehydes.[4a-e]

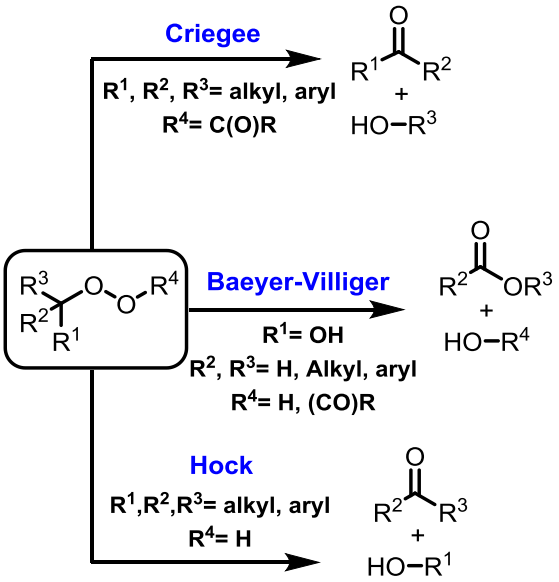

Figure 4A.1. Acid-catalyzed rearrangement of peroxides

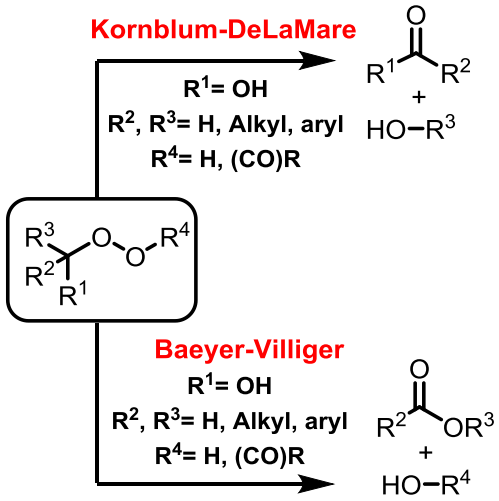

Figure 4A.2. Base-catalyzed rearrangement of peroxides

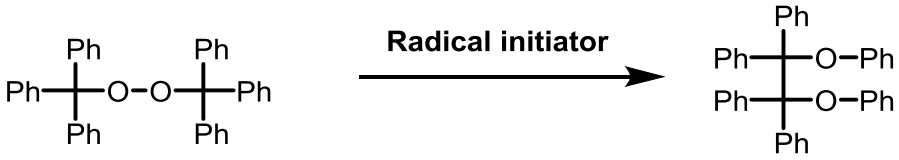

Figure 4A.3. Radical rearrangement of peroxide

In past decades, varieties of named[5] and unnamed[6] rearrangement of organic peroxides are documented in the literature. However, the migration of aryl or alkyl group towards electron-deficient oxygen atom has been widely studied for the Baeyer-Villiger oxidation,[7a-f] and Criegee solvolysis of peresters.[8a-d]

In 1899, Baeyer & Villiger reported the conversion of the ketone to ester in the presence of peracid *via* 1,2-migration. Till today, it is one of the most widely studied reaction due to its applications and new insights into the chemistry (Scheme 4A.1).[7]

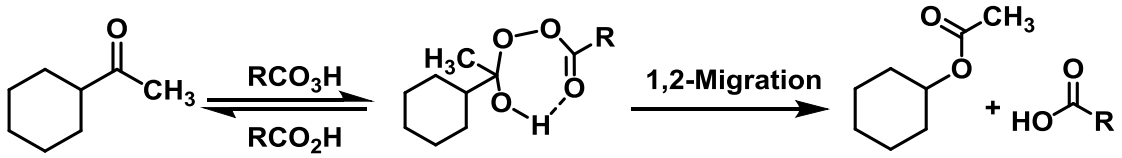

Scheme 4A.1. Baeyer-Villigar rearrangement

Later, Criegee tried to elucidate the mechanism of Baeyer-Villiger reaction, and he found an interesting intermediate. Thus, the intermediate (perester) is named after his name. The Criegee rearrangement involves the conversion of hydroperoxide into perester and further rearrangement to afford the corresponding ester (Scheme 4A.2.).[8]

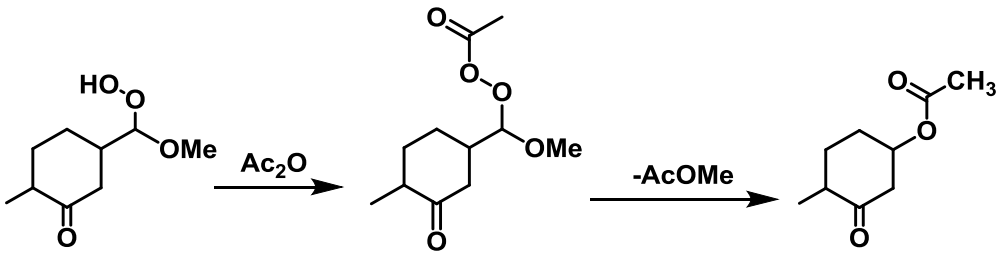

Scheme 4A.2. Criegee rearrangement

The Hock rearrangement involves the decomposition of cumene hydroperoxide to phenol and acetone. This reaction is highly important at the industrial level since it is used for commercial production of acetone and phenol.[3]

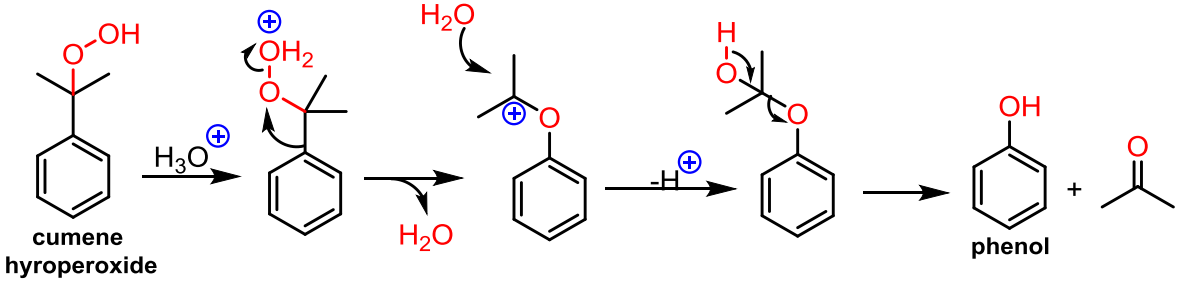

Scheme 4A.3. Mechanism of Hock rearrangement

In 1951, Kornblum and DeLaMare reported the rearrangement of peroxides. This reaction involves the rearrangement of (1-(*tert*-butylperoxy)ethyl)benzene to acetophenone and *tert*-butanol in the presence of a base.[9]

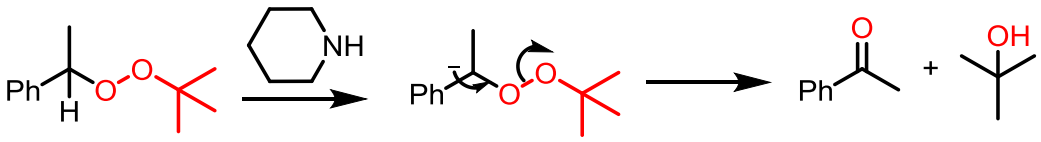

Scheme 4A.4. Kornblum-DeLaMare rearrangement

Apart from the famous named rearrangement reactions, there are several unnamed reactions are also documented in the literature. For instance, Murahashi and co-workers have reported the ruthenium-catalyzed oxidation of phenols via migration of alkyl group.[6a]

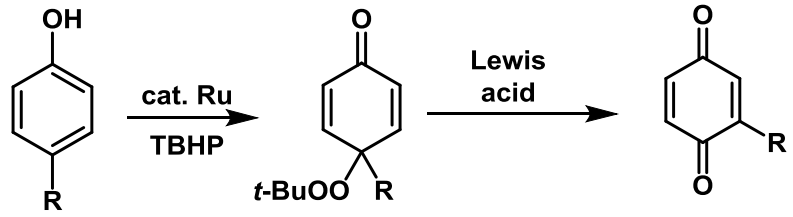

Scheme 4A.5. Oxidation of phenol using ruthenium catalyst and Lewis acid

In 2013, Li and co-workers reported the rearrangement of *tert*-butylperoxides to produce the 2,3-disubstituted furans *via* 1,2-aryl migration in the presence of acid.[6c]

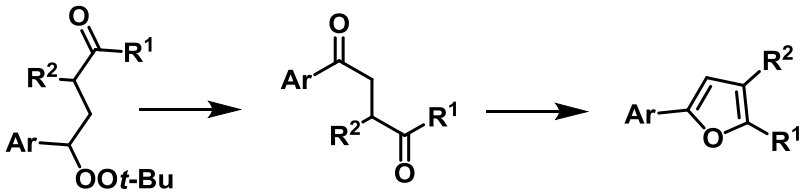

Scheme 4A.6. The rearrangement of peroxides to synthesize furan derivatives

Interestingly, the Hock rearrangement is found in plant metabolism. The enzymatic oxylipin metabolism is initiated by oxygenation of linoleic acid by lipoxygenase. Later, the (10*E*,12*Z*,15*Z*)-9-hydroperoxyoctadeca-10,12,15-trienoic acid (hydroperoxide) undergo Hock rearrangement to afford 9-oxononanoic acid and (3Z,6Z)-nona-3,6-dienal.[4]

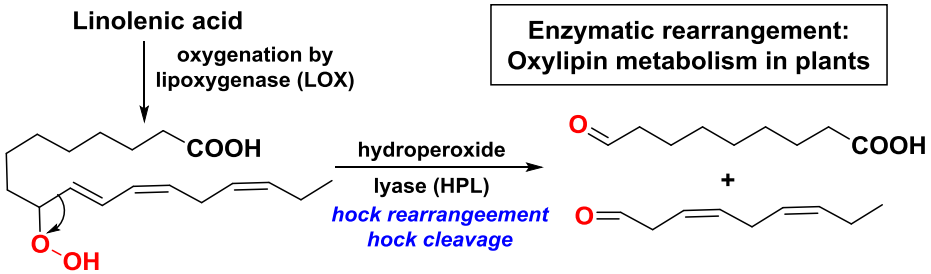

Scheme 4A.7. Enzymatic Hock rearrangement of peroxide

Next, the very important transformation which involves Hock rearrangement is the formation of secosterol aldehyde from cholesterol, which is responsible for Atherosclerosis. In this example, first the cholesterol undergo peroxidation in presence of oxygen to afford (3S,8S,9S,10R,13R,14S,17R)-5-hydroperoxy-10,13-dimethyl-17-((R)-6-methylheptan-2-yl)-2,3,4,5,8,9,10,11,12,13,14,15,16,17-tetradecahydro-1*H*-cyclopenta[*a*]phenanthren-3-ol (peroxy compound). This peroxy compound on further treatment with acid produces Hock rearranged (ring expansion) products. Finally, the hydrolysis, cleavage, and cyclization produce the secosterol aldehyde.[4]

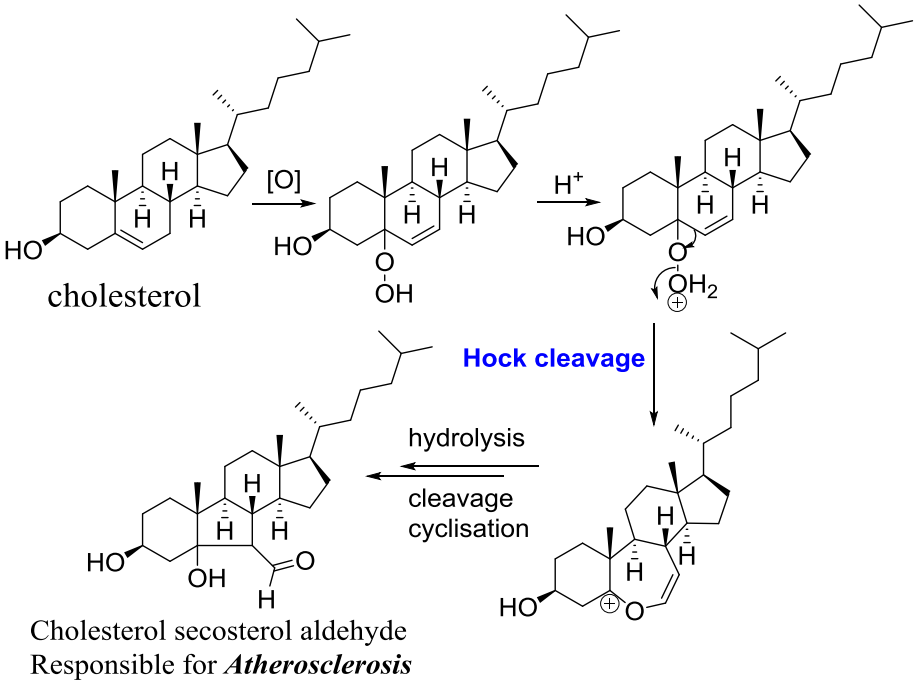

Scheme 4A.8. Enzymatic Hock rearrangement in cholesterol

4A.3. The rationale of present work

The syntheses of heterocyclic compounds have great importance in the chemistry owing to their interesting biological properties. In particular, 1,4-benzoxazin-3-one derivatives show the central nervous system (CNS) depressant,[10] antiproliferative,[11] neuroprotective properties.[12] By keeping this in mind we sought to employ the peroxyindoles as a precursor for the synthesis of 1,4-benzoxazin-3-one *via* rearrangement. On the other hand, despite there are several acids or base-catalyzed rearrangements of peroxides documented in the literature; there is no report on the metal-catalyzed ring expansion of 2-oxindole derivatives.

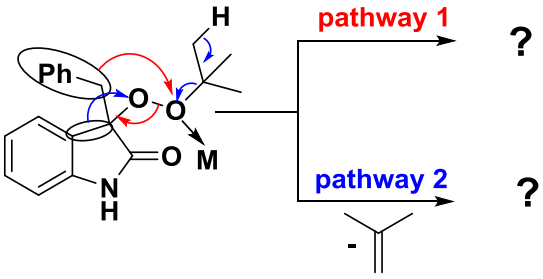

Figure 4A.4. Our hypothesis for a novel rearrangement of peroxide

Thus it was an inducement for us to develop the fundamental transformation for the rearrangement reaction. To our delight, by changing the metal from Tin (Sn) to Iron (Fe), it is possible to achieve the Hock rearrangement. Such type of reactions can also be used to distinguish the homolytic or heterolytic cleavage reactions.

4A.4. Results and discussion

4A.4.1. Optimization studies

Table 4A.1. Optimization for the rearrangement of peroxide[a]

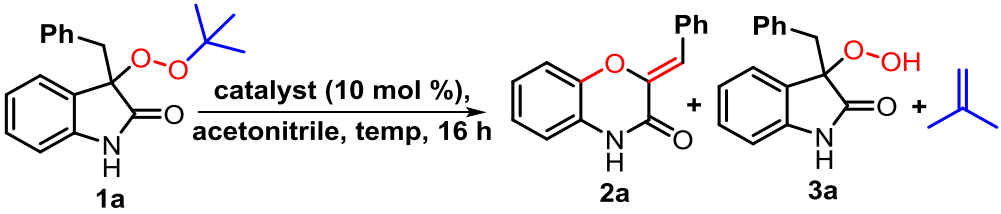

Entry	Catalyst 10 mol %	Temp in ^{o}C	Yield [%] 2a:3a
1	none	rt	no reaction
2	none	100	no reaction
3	$Sc(OTf)_3$	rt	00:52
4	$Sc(OTf)_3$	100	40:49
5	Ag(OTf)	100	no reaction
6	$Sn(OTf)_{2-}$	rt	00:57
7	$Sn(OTf)_2$	60	00:60
8	$Sn(OTf)_2$	100	90:00
9	$BF_3.OEt_2$	100	30:63
10	$Cu(OTf)_2$	100	28:51
11[b]	Amberlyst-15	100	31:39
12[c]	Amberlyst-15	100	87:00
13[d]	Amberlyst-15	100	81:10

[a]**Reaction conditions:** 0.25 mmol (**1a**), catalyst (10 mol %) in a 2 mL acetonitrile was heated at a specified temperature for 16 h in a sealed tube. With Amberlyst-15, 0.25 mmol/ 78 mg of a substrate (**1a**) and [b]26 mg, [c]156 mg, [d]78 mg of Amberlyst-15 was used (w/w substrate to Amberlyst-15 ratio is taken). Amberlyst-15 (Dry) form is used. The mentioned yields are isolated yields.

At the outset, a variety of Lewis acids were tried to get the rearrangement of **1a** and best-optimized condition (Table 4A.1). We commenced our investigation with the 3-benzyl-3-(*tert*-butylperoxy)indolin-2-one **1a** as a model molecule for the rearrangement. In control experiments, **1a** in acetonitrile (MeCN) was stirred at rt and 100 ^{o}C in the absence of acid source, which did not provide any product (Table 4A.1, entries 1, 2). Next, in the presence of 10 mol % $Sc(OTf)_3$, we observed only removal of *tert*-butyl group from **1a** to afford hydroperoxy compound **3a** (52%) and no rearranged product **2a** at rt (Table 4A.1, entry 3). However, increasing the temp to 100 ^{o}C we observed two products, rearranged **2a** and deprotected **3a** in a 40% and 49% isolated yield respectively with the liberation of isobutylene in 16 h (Table 4A.1, entry 4). The structure of the compound was unambiguously characterized by single-crystal X-ray diffraction (CCDC Number: 1889817). Next, the use of Ag(OTf) did not afford any product or by-product formation (Table 4A.1, entry 5). The copper triflate provided a 28% yield of the rearranged product **2a** and 51% yield of the deprotected compound **3a**. Among the different Lewis acids used, $Sn(OTf)_2$ was noticeably better in terms of selectivity and yield (Table 4A.1, entry 8). To our delight, the rearranged product **2a** was achieved using Brønsted acid, Amberlyst-15, with a comparable yield to that of Lewis acid (Table 4A.1, entry 12). The selection of Amberlyst-15 for the rearrangement is rational since it is mild, easy to measure, safe to handle, and easily separable at the end of the reaction.

4A.4.2. $FeCl_3$-catalyzed Hock rearrangement of peroxide

Interestingly, in contrast to $Sn(OTf)_2$, when $FeCl_3$ was used as Lewis acid source with **1a**, we observed Hock-rearrangement which results in the formation of aldehyde and isatin (Scheme 4A.9). We proposed that the peroxide **1a** will react *via* Hock rearrangement. The two possible pathways A and B are depicted in Scheme 4A.9. In pathway A, the migration of a phenyl group on the oxygen will generate isatin and (*tert*-butoxymethyl)benzene. The isobutylene will serve as a leaving group to afford isobutylene and benzaldehyde as a cleaved product.[13] However, the existence of pathway B is unlikely owing to the absence of benzyl alcohol in the reaction mixture. Furthermore, to rule out the possibility of pathway B, the reaction of **3a** was carried out with $FeCl_3$, which afforded the traces of rearranged product **2a** and not even traces of benzaldehyde or benzyl alcohol (most of the **3a** was recovered back).

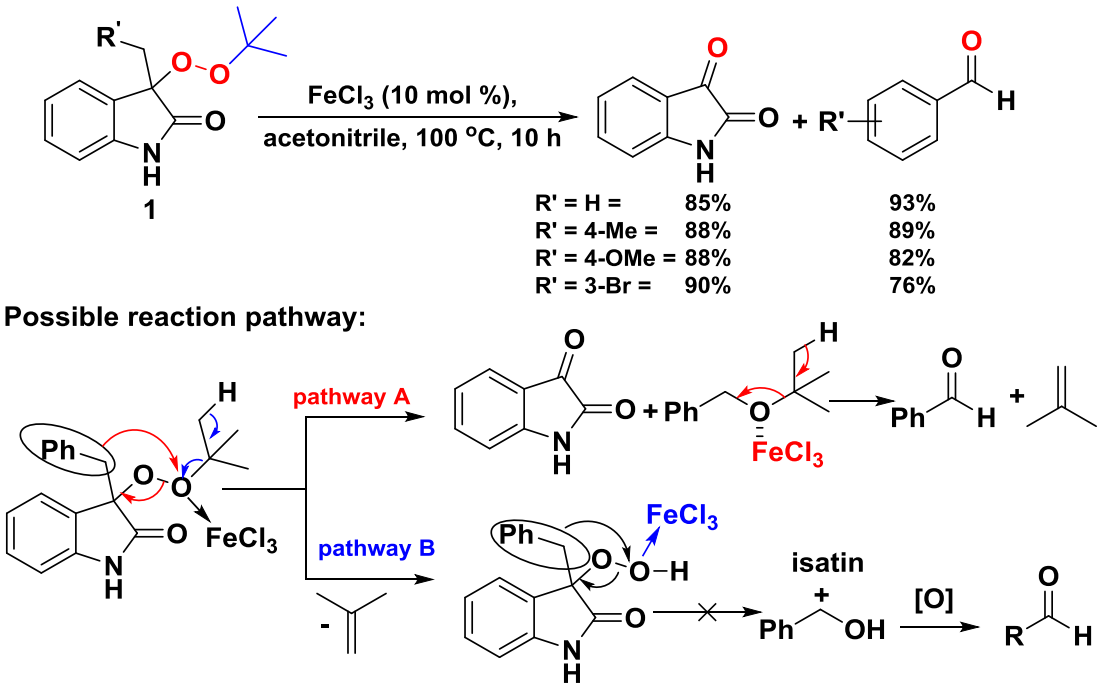

Scheme 4A.9. $FeCl_3$-catalyzed Hock-rearrangement of peroxides.

4A.4.3. Substrate scope for novel rearrangement of peroxide using $Sn(OTf)_2$

After stabilizing the optimized reaction conditions, the scope of Sn-catalyzed and Amberlyst-15 mediated novel rearrangement reaction was investigated (Scheme 4A.10). A series of alkyl or benzyl substituted peroxyoxindoles were subjected for rearrangement reaction. Benzyl group bearing electron-donating groups afforded the rearranged products (**2a-2d**) with good to excellent yield (Scheme 4A.10). Gratifyingly, the reaction of 3-(*tert*-butylperoxy)-3-cyclohexylindolin-2-one and 3-(*tert*-butylperoxy)-3-hexylindolin-2-one afforded **2e**, **2f** in 78% and 75% yield respectively using $Sn(OTf)_2$. However, the use of Amberlyst-15 provided **2e** and **2f** in 82% and 87% isolated yield respectively. In the case of ethyl 2-(3-(*tert*-butylperoxy)-2-oxoindolin-3-yl)acetate instead of rearrangement, only isobutylene removal was observed (Scheme 4A.10, **2g**). Additionally, the rearrangement reaction tolerated a wide variety of electron-withdrawing substituents to give products (**2h-2k**) in very good yield (Scheme 4A.10). The reaction of C3-substituted-6-chloro-2-oxindole derivatives gives a moderate yield of the product **2l** and **2m** (starting material recovered). The low yield of the product is maybe due to electronic destabilization by the negative inductive effect of the chlorine. Moreover, the *N*-protected peroxy compound reacted smoothly to afford rearranged product **2n** in a very good yield (Scheme 4A.10).

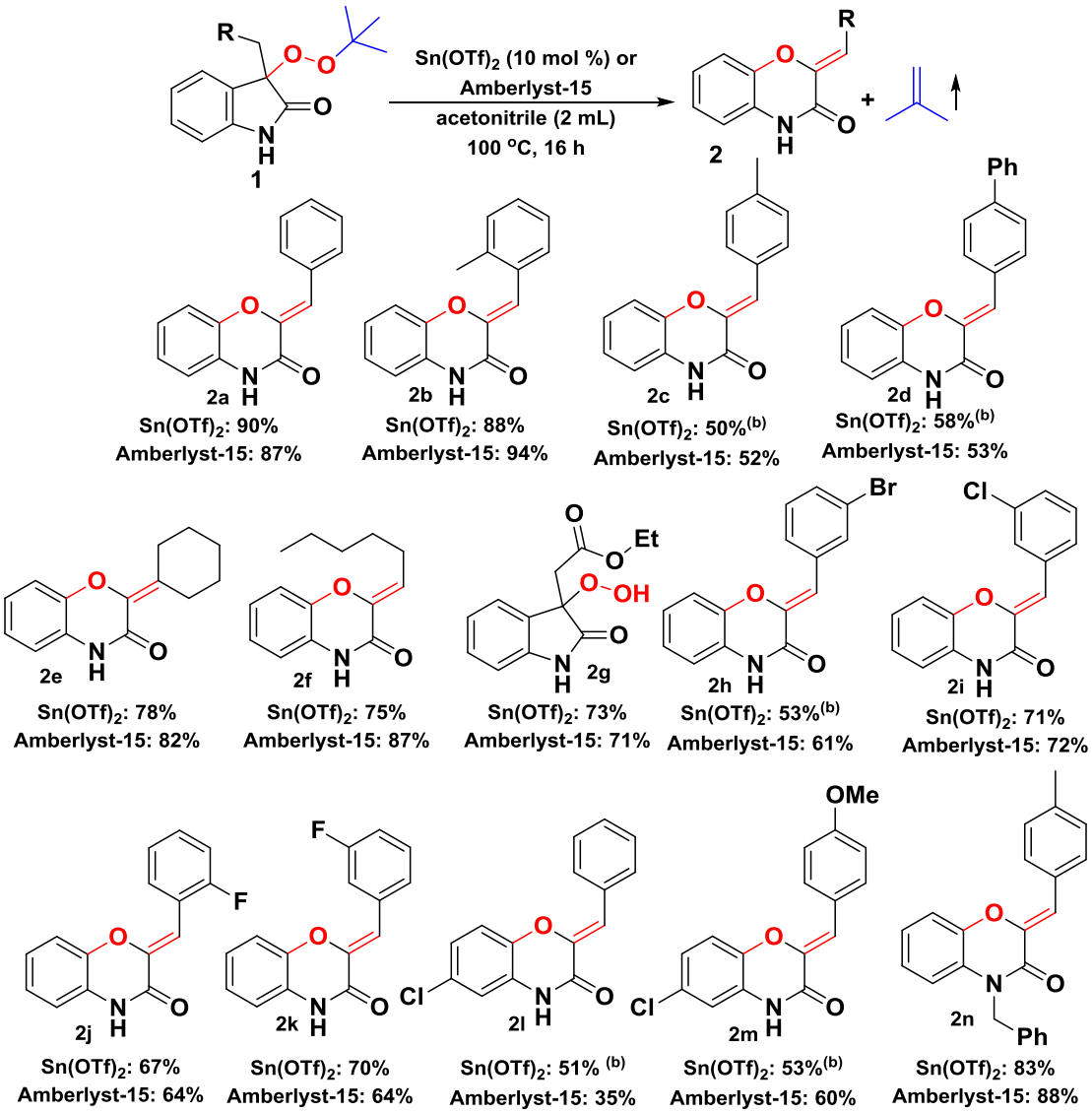

Scheme 4A.10. Substrate scope for rearrangement

[a]**Reaction conditions:** 0.25 mmol (**1a**), $Sn(OTf)_2$ (10 mol %) or Amberlyst-15 (w/w ratio to the substrate) in a 2 mL acetonitrile was heated at 100 °C for 16 h in a sealed tube. [b)]20 mol % of $Sn(OTf)_2$ was used and heated for 36 h. The mentioned yields are isolated yield.

Next, the reaction of 3-aryl-3-((2-phenylpropan-2-yl)peroxy)indolin-2-one derivatives **1aa** afforded (*Z*)-2-arylidine-2*H*-benzo[*b*][1,4]oxazin-3(4*H*)-ones in moderate to good yield with the removal of α-methyl styrene (Scheme 4A.11.) (starting material recovered).

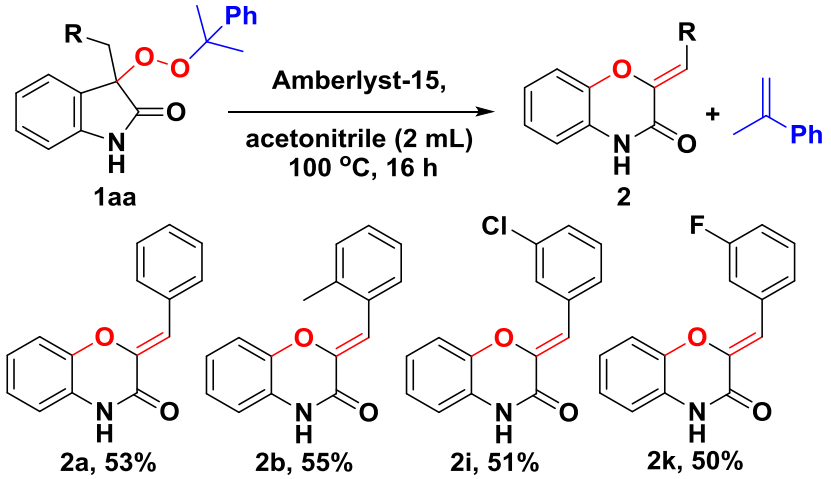

Scheme 4A.11. Substrate scope for the rearrangement of peroxide **4** with the removal of α-methyl styrene.

Reaction condition: 0.25 mmol (**1aa**), Amberlyst-15 (w/w ratio to the substrate) in a 2 mL acetonitrile was heated at 100 °C for 16 h in a sealed tube.

4A.5. Mechanistic investigations

To shed light on the reaction parameters, a model reaction was carried out with 3-(*tert*-butylperoxy)-3-methylindolin-2-one and 3-hydroperoxy-3-methylindolin-2-one which does not afford any rearranged product. Next, the reaction of 0.25 mmol of 3-benzhydryl-3-(*tert*-butylperoxy)indolin-2-one with $Sn(OTf)_2$ (10 mol %) provided a complicated reaction mixture (Scheme 4A.12). The above studies indicate the need for $–(CH_2)-$ group at the C3-position of peroxyoxindole. (Scheme 4A.12).

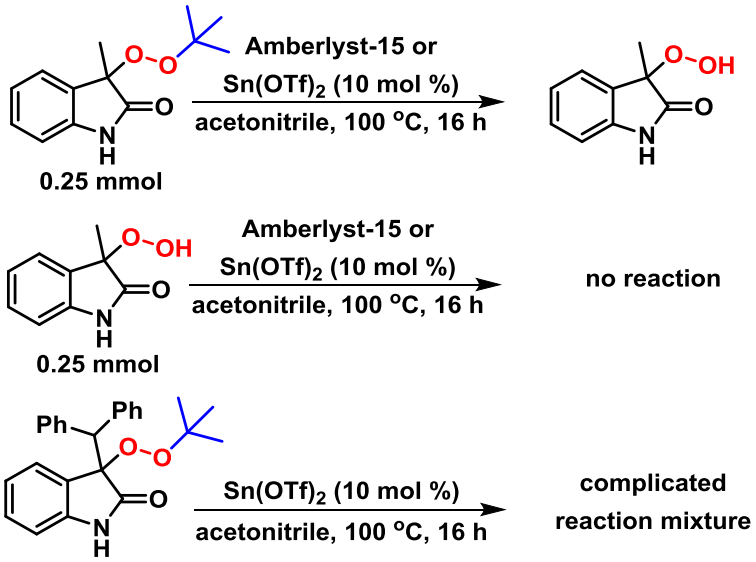

Scheme 4A.12. Control experiments for mechanistic studies

4A.5.1 Detection of isobutylene liberation using GC-MS

Later, the GC-MS spectra of a reaction mixture of 3-benzyl-3-(*tert*-butylperoxy)indolin-2-one under established reaction conditions were analyzed. After reaction completion, the gaseous component of the reaction mixture was taken using a gas-tight syringe and injected in the instrument. The GC-MS spectra showed a peak with *m/e* = 56 which corresponds to the isobutylene gas (Figure 4A.5).

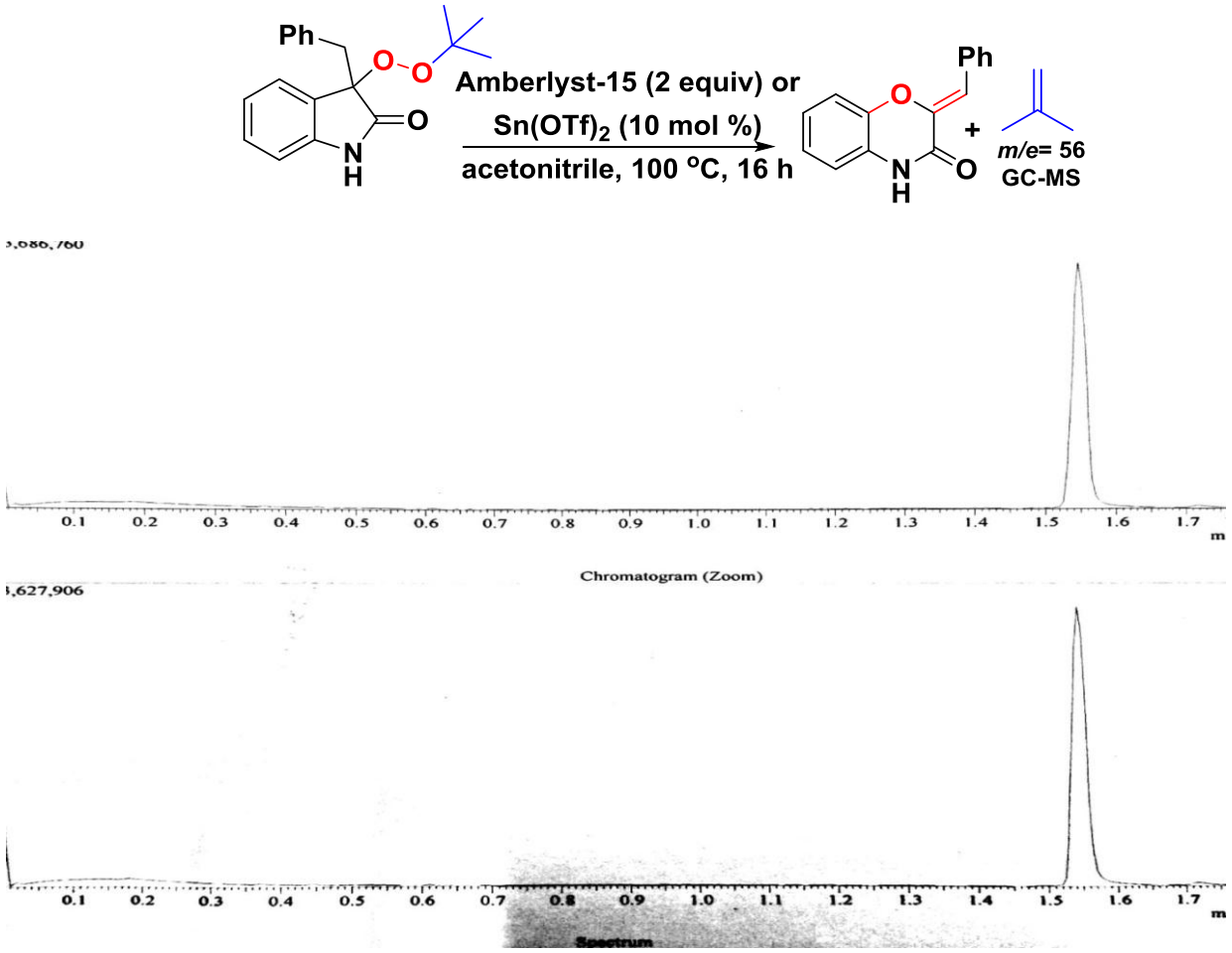

Figure 4A.5. GC-MS spectra of the gaseous phase of a reaction mixture

4A.5.2. Kinetic isotope effect: K_H/K_D

To get the idea about reaction steps and rate-determining step, we have performed deuterium labeling experiments. Initially, the deuterated compounds were prepared using a catalytic approach.

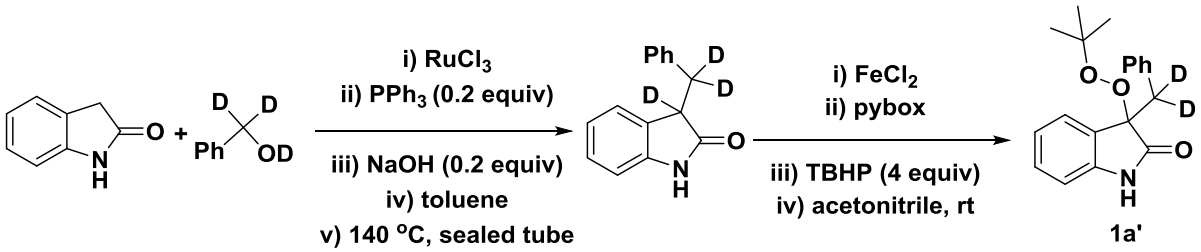

Scheme 4A.13. Synthesis of deuterated starting material

The parallel reaction was carried out with labeled (**1a'**), and unlabeled peroxy (**1a**) compound and analyzed by crude ^{1}H NMR using 1,3,5-trimethoxybenzene as an internal standard. A normal primary kinetic isotope effect (KIE) of 1.75 was detected, representing that the H-atom transfer is involved in the rate-determining step (Scheme 4A.14).[14] The k_H/k_D ratio was calculated using ^{1}H NMR with 1,3,5-trimethoxybenzene as an internal standard. The ratio for the labeled and unlabeled compounds: 1.17/0.67= 1.75 (Figure 4A.11 and Figure 4A.12).

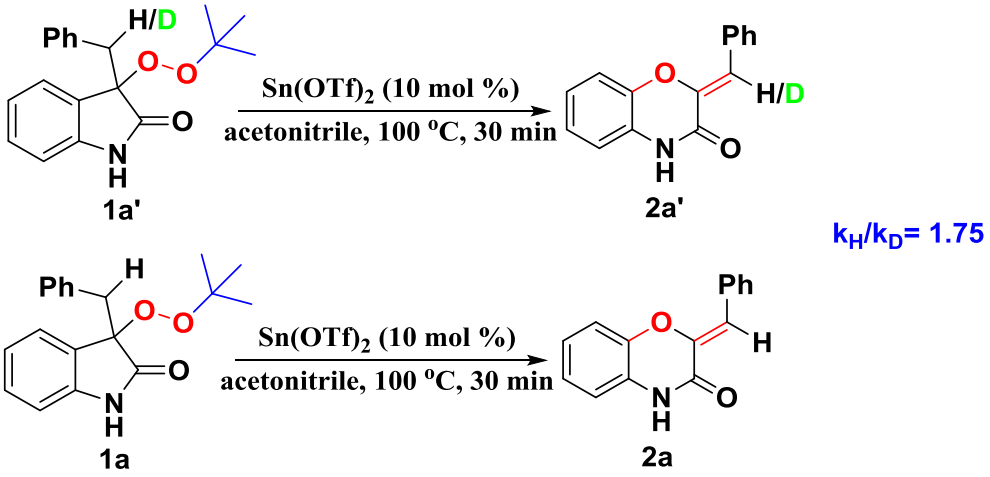

Scheme 4A.14. Deuterium labeling studies for novel rearrangement reaction

To gain insight into the reaction mechanism, the hydroperoxy compound **3a** was prepared separately and subjected to standard reaction condition. The expected product **2a** was isolated with a 86% yield, which suggests that the reaction proceeded *via* **3a** as an intermediate (Scheme 4A.15.).

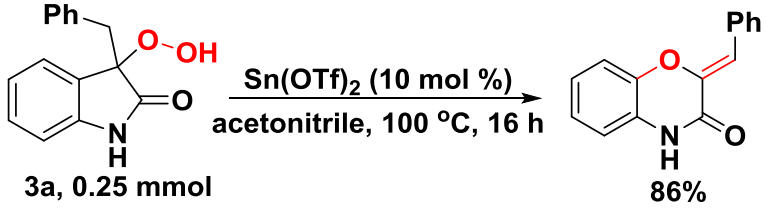

Scheme 4A.15. Detection of intermediate

Furthermore, the reaction of $Sn(OTf)_2$ and 3-benzyl-3-(*tert*-butylperoxy)indolin-2-one in acetonitrile-*d3* was carried out in an NMR tube. The notable peaks were observed at 6.82, singlet, which belongs to alkene C-H of arylidine product **2a**. Moreover, at 4.66 ppm (septet) and 1.71 (triplet) was also observed which arises due to the presence of isobutylene.

4A.6. The possible reaction mechanism

Based on our experimental observations and literature reports, [15a-b] a possible reaction mechanism for Sn-catalyzed novel rearrangement is depicted in Figure 4A.6. Mechanistically, the catalytic cycle initiated by the coordination of the peroxy O-O bond of **1** with **A** to give **B**. The deprotonation of **B** commenced by *in situ* generated triflate anion give **D** with the liberation of isobutylene **C** (confirmed by GC-MS and NMR). Following the protonation of SnOTf-chelated oxygen **D** with TfOH, endoperoxide **E** is obtained. A ring expansion is owing to the C3-C4 carbon shift onto oxygen of HO-SnOTf in **E** to give the carbocation **F** and Sn(OH)OTf in a concerted passion. The triflate anion abstracts the proton from **F** to stabilize the carbocation and afforded product **2**. Subsequently, catalyst **A** is regenerated by the reaction of Sn(OH)OTf and Tf-OH.

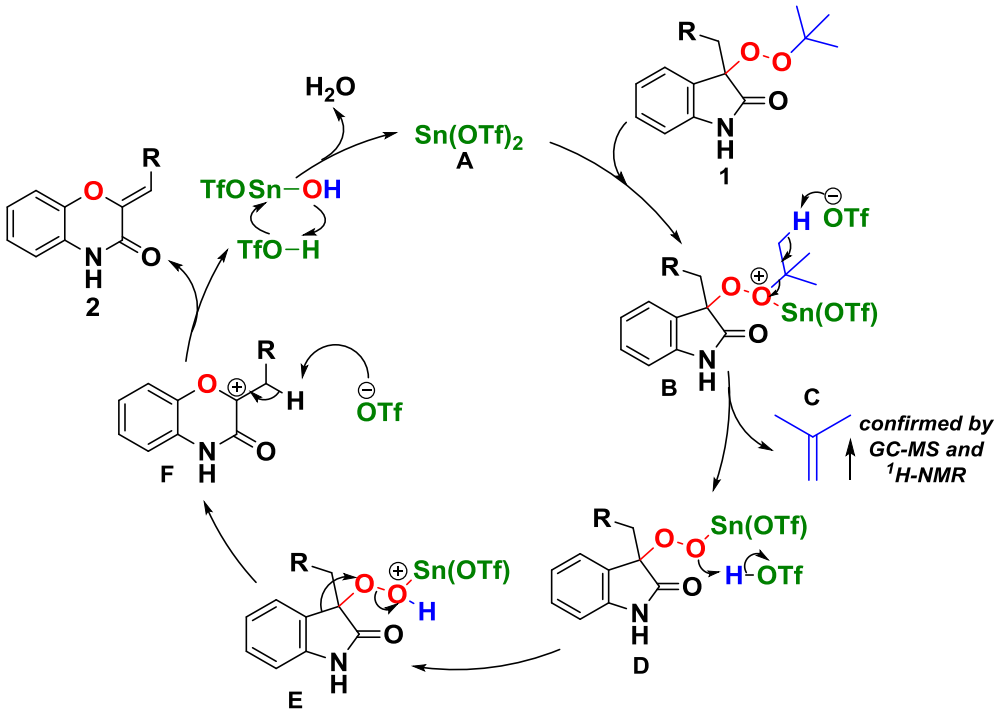

Figure 4A.6. The possible reaction mechanism

Photo-physical studies

While isolating the compounds, it was observed that these compounds show the fluorescent property. Thus to show the application of the synthesized compounds, we

have recorded emission spectra for the selected compounds (Figure 4A.7). The compound displayed a fluorescent emission band around 430-450 nm (**2k**, 454 nm; **2a**, 452 nm; **2f**, 428 nm) in the DMSO solvent. The fluorescent emission band for **2f** and **2a** showed a bathochromic shift (about 26 nm). This shift attributed to the presence of extended conjugation in the aromatic rings as compared to **2k**. The prepared compounds could be employed as a fluorescent motif to understand the complex mode of action in the biological processes.[10-11]

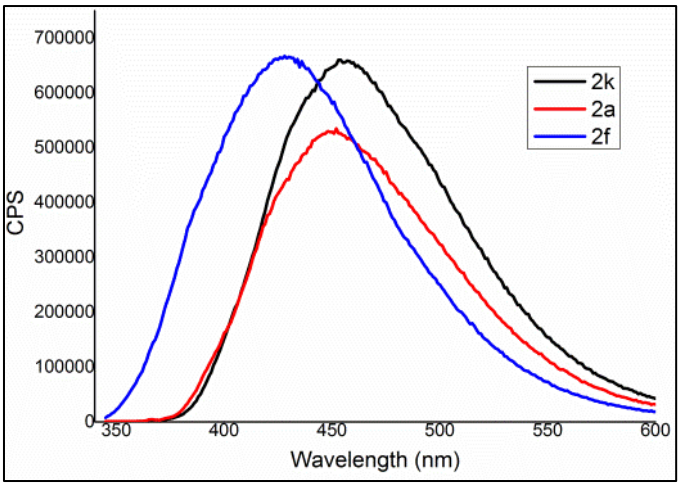

Figure 4A.7. Emission spectra for the selected compounds in DMSO

4A.7. Conclusion

In conclusion, we have established and novel protocol for unprecedented biomimetic cascade rearrangement of 3-peroxy-2-oxindoles, which produces predominantly (*Z*)-2-arylidene or alkylidene-2*H*-benzo[*b*][1,4]oxazin-3(4*H*)-one derivatives in the presence of Lewis/Brønsted acid. Fascinatingly, if we use a catalytic amount of $FeCl_3$, a Hock-rearrangement of was observed, which can be used to probe the homolytic *vs.* heterolytic cleavage. A variety of substrates demonstrated the generality of the protocol. The synthesized compounds showed good fluorescent activity, which may be of interest for understanding the complex biological process through cell imaging. Finally, based on experimental observations, a possible mechanism for rearrangement reaction has been proposed.

4A.8. Experimental section and characterization data

4A.8.1. General information and data collection

Column chromatographic separations were performed over 100-200 mesh size silica-gel. Visualization was accomplished with UV light and PMA, CAM stain followed by heating. The Amberlyst-15 (Dry form), $Sn(OTf)_2$, and other metal triflates were purchased from Sigma-Aldrich. The dry solvents were used in all experiments.

The ^{1}H and ^{13}C NMR spectra were recorded on 400 and 100 MHz, respectively, using a Bruker or JEOL spectrometers. Abbreviations used in the NMR follow-up experiments: b, broad; s, singlet; d, doublet; t, triplet; q, quartet; m, multiplet. High-resolution mass spectra were recorded with Waters- synapt G2 using electrospray ionization (ESI). The emission spectra was recorded on Horiba scientfic, model no-fluoromx-4.

4A.8.2. Experimental procedure

(A) General experimental procedure for the rearrangement reaction (with $Sn(OTf)_2$):

In a 20 mL re-sealable vial (equipped with a rubber septum and N_2 balloon) was added $Sn(OTf)_2$ (10 mol%), acetonitrile (2 mL), and finally, peroxy compound (**1**) (0.25 mmol, 1 equiv). The tube was purged with N_2 and sealed with a cap using a crimper. The reaction mixture was heated at 100 ^{o}C in an oil bath for 16 h. After 16 h (conversion checked by TLC, if the reaction is not completed, then continued until better conversion) added methanol and a volatile component was evaporated using a vacuum and residue was directly purified by silica gel chromatography (EtOAc: hexane= 15:85 to 30:70).

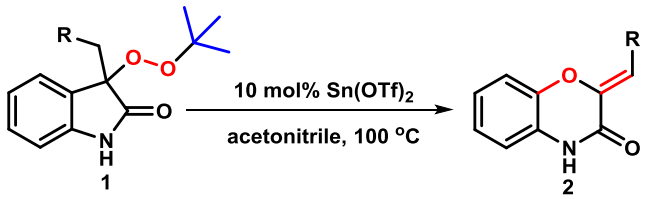

(B) General experimental procedure for the rearrangement reaction (with Amberlyst-15):

In a 20 mL re-sealable vial (equiped with rubber septum and N_2 balloon) was added Amberlyst-15 (substrate to Amberlyst-15 weight ratio of 1:2), aceotnitrile 2 mL, and finally, peroxy compound (**1**) (0.25 mmol). The tube was purged with N_2 and sealed with a cap using crimper. The reaction mixture was heated at 100 ^{o}C in an oil bath for 16 h. After reaction completion methanol was added in the reaction mixture and filtered to remove Amberlyst-15 and volatile component was evaporated using a vacuum. The residue was directly purified by silica gel chromatography (EtOAc : hexane= 15:85 to 30:70).

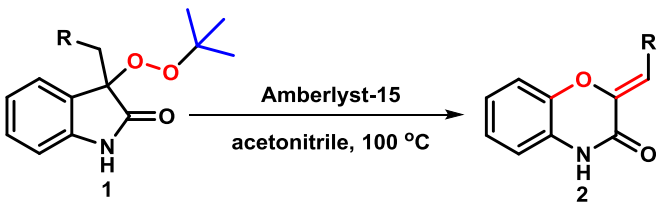

(C) Experimental procedure for 1 mmol scale:

In a 20 mL re-sealable vial (equipped with a rubber septum and N_2 balloon) was added Amberlyst-15 (622 mg) (substrate to Amberlyst-15 weight ratio of 1:2), acetonitrile (8 mL), and finally, 3-benzyl-3-(*tert*-butylperoxy)indolin-2-one (**1a**) (1 mmol, 311 mg). The tube was purged with N_2 and sealed with a cap using a crimper. The reaction mixture was heated at 100 ^oC in an oil bath until the reaction completion. After reaction completion, methanol was added in the reaction mixture and filtered to remove Amberlyst-15, and the volatile component was evaporated using a vacuum. The residue was directly purified by silica gel chromatography to afford (*Z*)-2-benzylidene-2*H*-benzo[*b*][1,4]oxazin-3(4*H*)-one **2a** (190 mg, 80%) using Amberlyst-15 as a faint yellow solid (EtOAc: hexane= 15:85).

(D) General experimental procedure for Hock rearrangement reaction:

In a 20 mL re-sealable vial was added $FeCl_3.6H_2O$ (10 mol %), acetonitrile (2 mL), and finally, peroxy compound (**1**) (0.25 mmol). The tube was sealed with a cap using a crimper. The reaction mixture was heated at 100 ^oC in an oil bath for 10 h. After reaction completion, the volatile component was evaporated using a vacuum, and the residue was directly purified by silica gel chromatography to afford isatin and aldehyde.

(E) Procedure for detection of *iso*-butylene gas liberation using GC-MS:

In a 20 mL re-sealable vial (equipped with a rubber septum and N_2 balloon) was added $Sn(OTf)_2$ (10 mol %), acetonitrile (2 mL), and finally, 3-benzyl-3-(*tert*-butylperoxy)indolin-2-one (**1a**) (0.25 mmol, 1 equiv). The tube was purged with N_2 and sealed with a cap using a crimper. The reaction mixture was heated at 100 ^oC in an oil bath for 16 h. After reaction completion, the gaseous component was taken using a Gas-tight syringe and injected into a GC-MS instrument. The presence of m/e= 56 corresponds to *iso*-butylene gas.

(F) Procedure for reaction monitoring using NMR:

In a NMR tube was added $Sn(OTf)_2$ (10 mol%), acetonitrile-*d3* 0.6 mL, and finally, 3-benzyl-3-(*tert*-butylperoxy)indolin-2-one (**1a**) (20 mg, 0.06 mmol, 1 equiv). The tube was purged with N_2 and closed using a cap. The reaction mixture was heated at 100 ^oC. After 2 h, the NMR tube was cooled and subjected to ^1H NMR. The notable peaks were observed at 6.82, singlet which belongs to alkene C-H of arylidine product **2a**. Moreover, at 4.66 ppm (septet) and 1.71 (triplet) was also observed which arises due to the presence of isobutylene (Figure 4A.8).

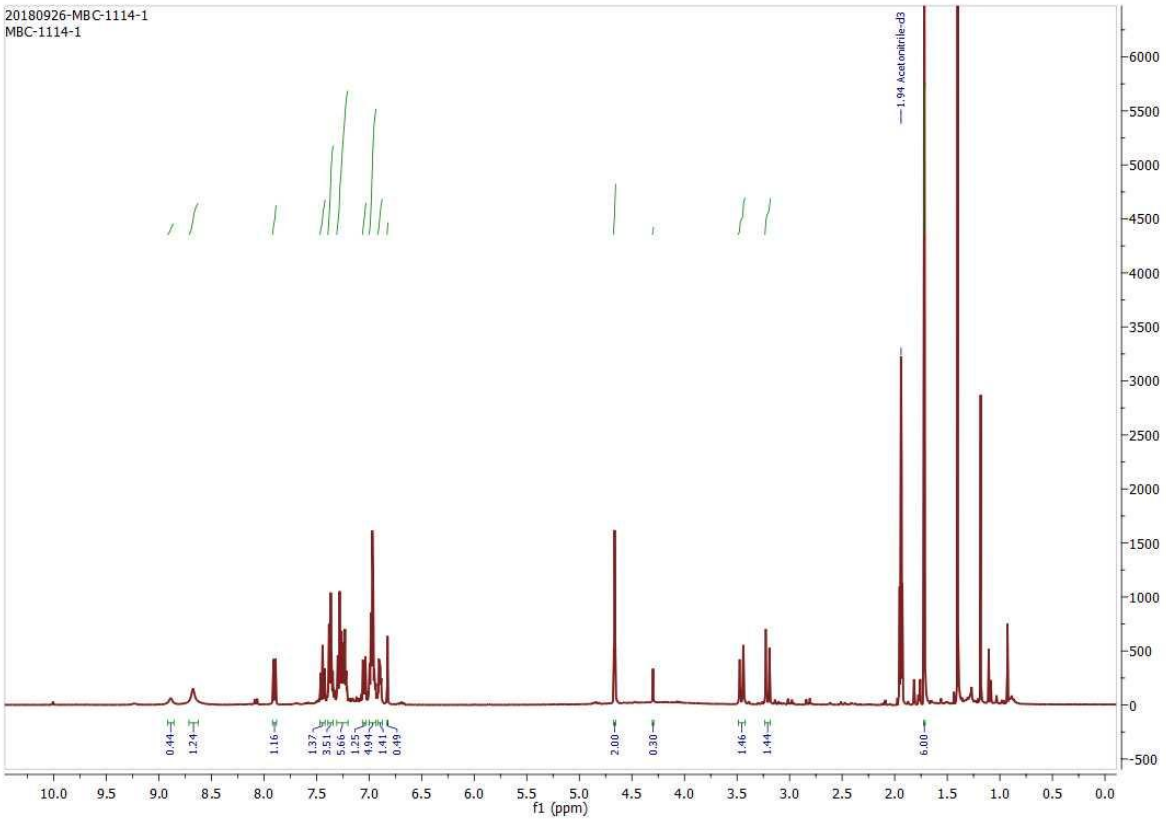

Figure 4A.8. ^{1}H NMR spectra of the crude reaction mixture

(G) Procedure for deuteration experiments:

(i) Procedure for synthesis of benzyl alcohol-*d3*:

The deuterated benzyl alcohol was prepared by using the reported procedure with few modifications by Gunanathan *et al*.[1] In a typical procedure, benzyl alcohol (2 mmol), Ru-MACHO (0.004 mmol), KO*t*Bu (0.001 mmol) were charged in a 20 mL resealable vial which was equipped with a rubber septum and N_2 balloon. The D_2O (1.6 mL) was added using a syringe and reaction mixture purged with N_2, and the tube was sealed with a cap using a crimper and heated at 60 ^{o}C in an oil bath. The reaction was stopped after 6 h, and the reaction mixture was extracted with dichloromethane and the combined organic layer is washed with brine solution. The removal of the solvent under reduced pressure provided pure products for further reaction. The ^{1}H NMR data resembles the previous report and showed 96 % deuterium incorporation (Figure 4A.9).

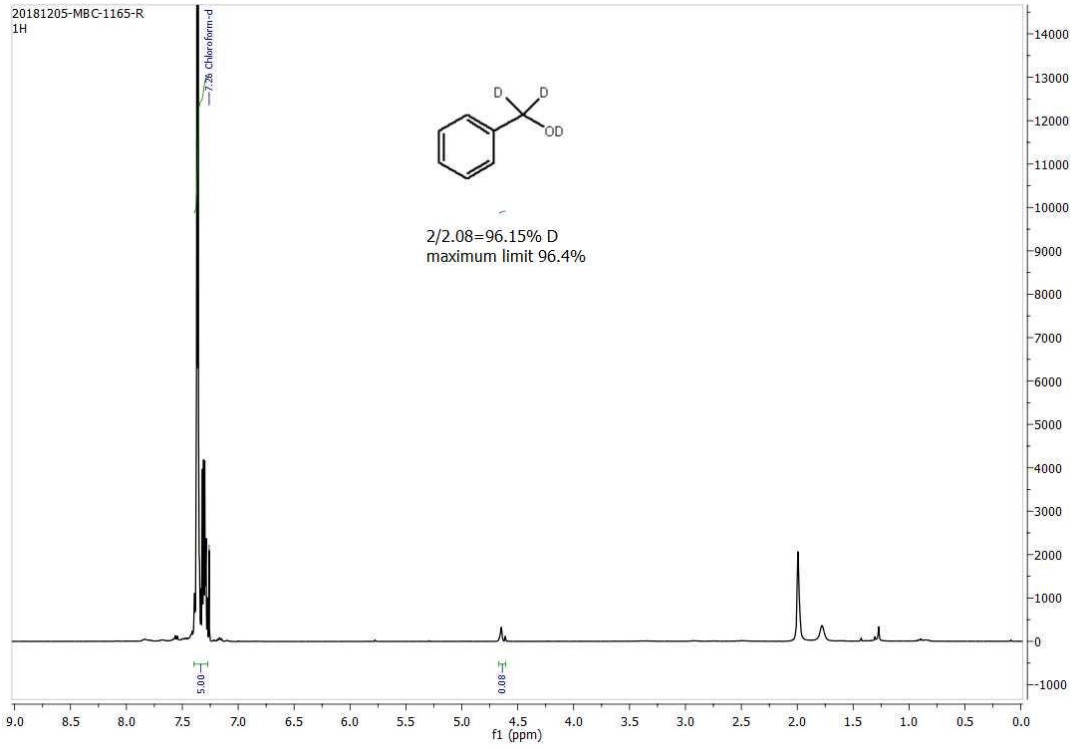

Figure 4A.9. ^{1}H NMR spectrum of benzyl alcohol-*d3* (400 MHz, $CDCl_3$)

(ii) Procedure for the synthesis of 3-(Phenylmethyl-*d2*)indolin-2-one-3*d*:

(a) In a 20 mL resealable tube added $RuCl_3.{}_nH_2O$ (0.162 mmol), PPh_3 (0.324 mmol), NaOH (0.324 mmol), 2-oxindole (1.297 mmol) and benzyl alcohol-*d3* (1.62 mmol, 1 equiv) after addition the vial was purged with N_2 and sealed with cap using crimper and heated at 140 ^{o}C for 24 h. The reaction mixture was cooled, and the volatile component was evaporated using a vacuum and directly purified column chromatography (Ethyl acetate: Pet ether= 18: 82).

(b) For C3-peroxidation, In a 5 mL round-bottom flask mixture of iron(II) chloride (0.031 mmol, 5 mol%) and (2,6-Bis[(4*S*)-(−)-isopropyl-2-oxazolin-2-yl]pyridine) (0.031 mmol, 5 mol%) in acetonitrile 3 mL was stirred at rt for 20−30 min. To the obtained deep-red solution was added 5.0−6.0 M *tert*-butyl hydroperoxide (TBHP) in decane solution (2.48 mmol, 0.45 mL) and finally, 3-(phenylmethyl-*d2*)indolin-2-one-3-*d* (0.62 mmol, 1 equiv) was added, and septum placed over it. The resulting solution was stirred at rt for 16 h without maintaining any special conditions such as the inert atmosphere. After completion of the reaction, a volatile component was evaporated using a vacuum. The residue was directly purified by silica gel chromatography (EtOAc: hexane= 15:85). The deuterium incorporation was measured by ^{1}H NMR analysis, which showed 57% deuterium incorporation (Figure 4A.10).

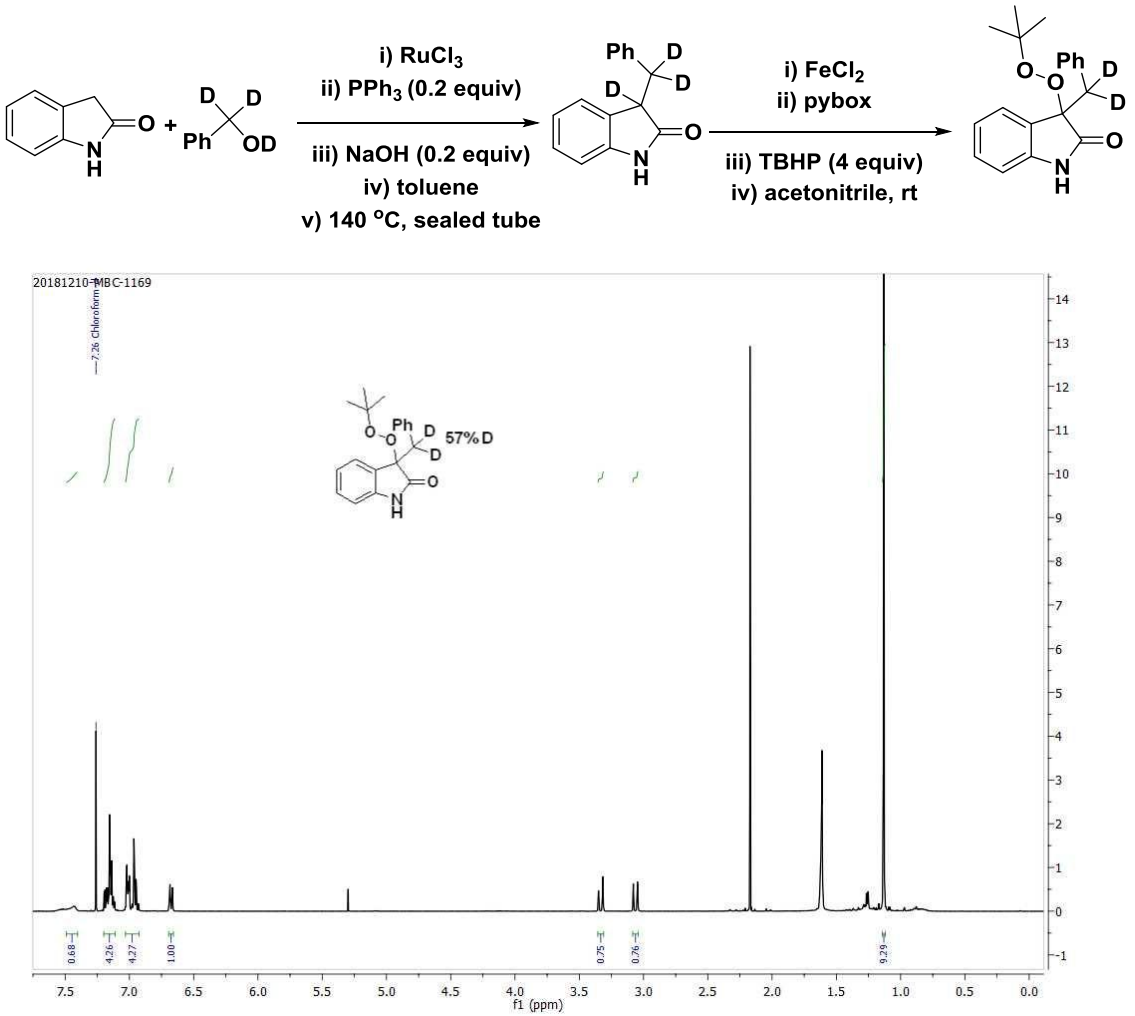

Figure 4A.10. ^{1}H NMR spectrum of 3-(*tert*-butylperoxy)-3-(phenylmethyl-d_2)indolin-2-one (400 MHz, $CDCl_3$)

(iii) Procedure for the catalytic H/D exchange reaction (Parallel reaction):

Reaction with isotope labeled peroxide:

In a 20 mL re-sealable vial (equipped with a rubber septum and N_2 balloon) was added $Sn(OTf)_2$ (5.32 mg, 10 mol%), acetonitrile 2 mL, and finally, deuterated 3-benzyl-3-(*tert*-butylperoxy)indolin-2-one (**1a'**) (40 mg, 0.1277 mmol, 1 equiv). The tube was purged with N_2 and sealed with a cap using a crimper. The reaction mixture was heated at 100 ^{o}C in an oil bath for 30 min. After reaction completion, a volatile component was evaporated using a vacuum and analyzed by crude ^{1}H NMR using 1,3,5-trimethoxybenzene as an internal standard.

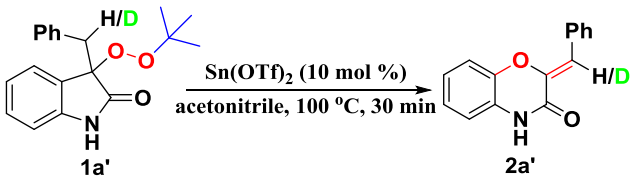

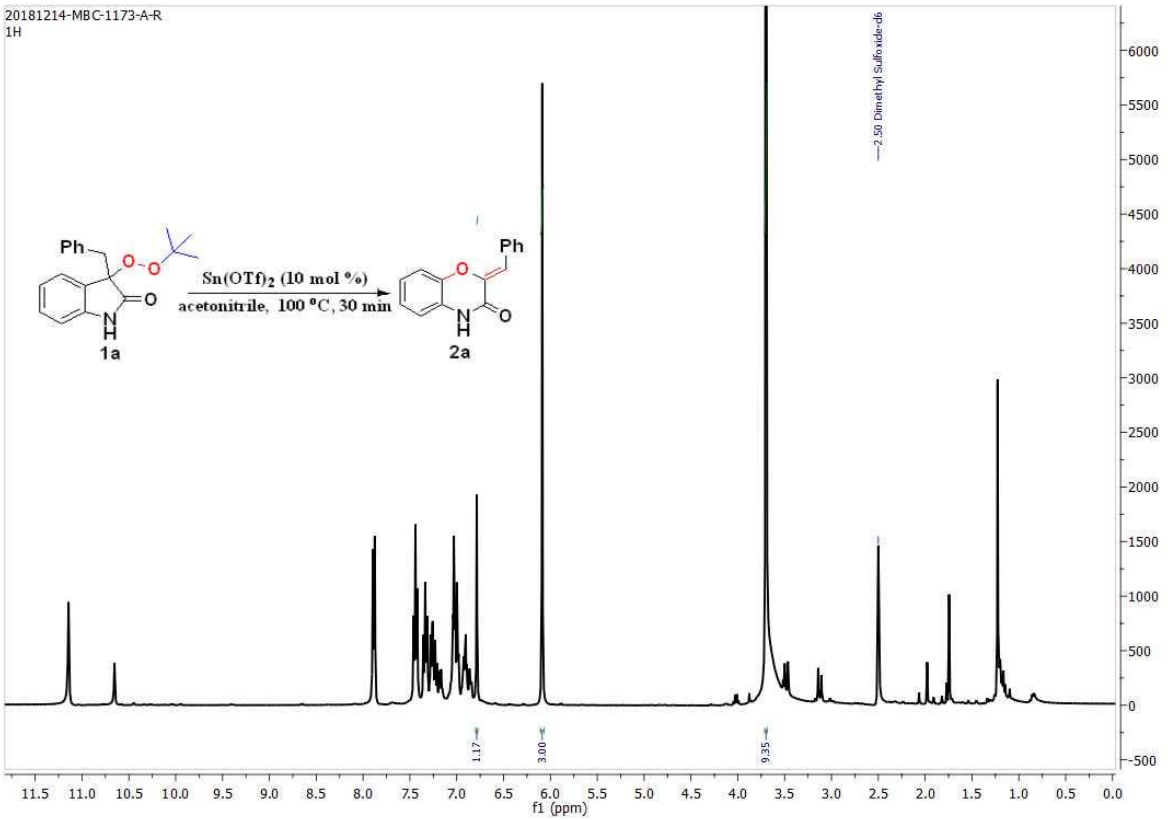

Figure 4A.11. ^{1}H NMR for crude reaction mixture of unlabeled peroxide

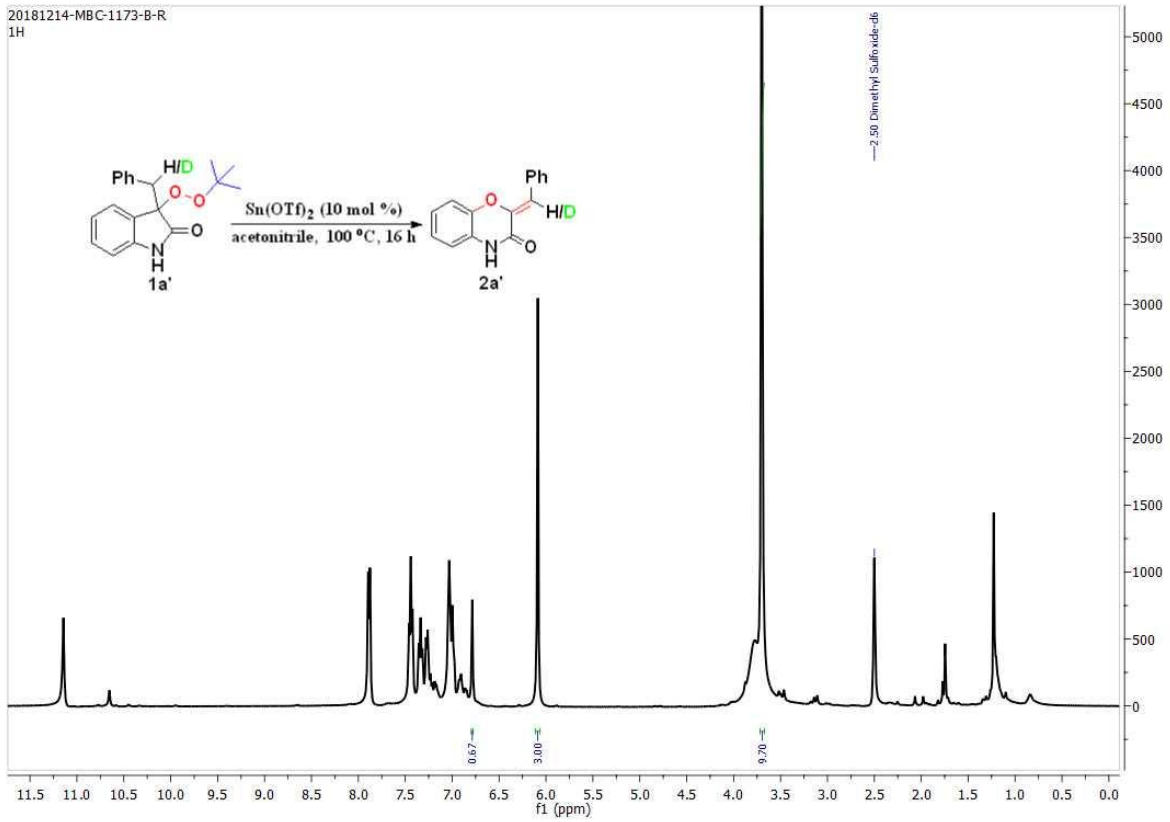

Figure 4A.12. ^{1}H NMR for crude reaction mixture of labeled peroxide

Reaction with unlabeled peroxide:

In a 20 mL re-sealable vial (equipped with a rubber septum and N_2 balloon) was added $Sn(OTf)_2$ (5.32 mg, 10 mol%), acetonitrile 2 mL, and finally, 3-benzyl-3-(*tert*-butylperoxy)indolin-2-one (**1a**) (40 mg, 0.1277 mmol, 1 equiv). The tube was purged with N_2 and sealed with a cap using a crimper. The reaction mixture was heated at 100 ^oC in an oil bath for 30 min. After reaction completion, a volatile component was evaporated using a vacuum and analyzed by crude ^1H NMR using 1,3,5-trimethoxybenzene as an internal standard. The K_H/K_D ratio was calculated by ^1H NMR analysis and found k_H/k_D= 1.17/0.67= 1.75 (Figure 4A.11 and Figure 4A.12).

4A.8.3. Spectroscopic data

(*Z*)-2-Benzylidene-2*H*-benzo[*b*][1,4]oxazin-3(4*H*)-one (2a): Prepared according to general procedure (A) and (B), using 3-benzyl-3-(*tert*-butylperoxy)indolin-2-one (77.7 mg, 0.25 mmol) to afford (*Z*)-2-benzylidene-2*H*-benzo[*b*][1,4]oxazin-3(4*H*)-one **2a** (53.8 mg, 90%) using $Sn(OTf)_2$ and (51.6 mg, 87%) using Amberlyst-15 as a faint yellow solid. 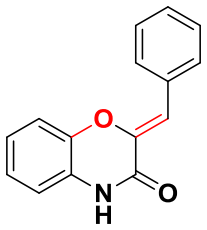

^{1}H NMR (400 MHz, DMSO-*d6*): δ 11.15 (bs, 1H), 7.90-7.88 (m, 2H), 7.46-7.42 (m, 2H), 7.37-7.32 (m, 1H), 7.30-7.27 (m, 1H), 7.06-7.02 (m, 2H), 7.01-6.97 (m, 1H), 6.78 (s, 1H). **^{13}C NMR** (100 MHz, DMSO-*d6*) δ 156.26, 141.78, 140.44, 133.24, 129.74, 128.68, 128.18, 125.37, 123.49, 123.20, 115.57, 115.55, 110.50. **FTIR** (KBr): 3175, 2974, 2897, 1692, 1638, 1498, 1387, 1109 cm^{-1}. **HRMS** (ESI) m/z calculated for $C_{15}H_{11}NO_2$ $(M+H)^+$: 238.0868, found: 238.0869.

(*Z*)-2-(2-Methylbenzylidene)-2*H*-benzo[*b*][1,4]oxazin-3(4*H*)-one (2b): Prepared according to general procedure (A) and (B), using 3-(*tert*-butylperoxy)-3-(2-methylbenzyl)indolin-2-one (81.2 mg, 0.25 mmol) to afford (*Z*)-2-(2-methylbenzylidene)-2*H*-benzo[*b*][1,4]oxazin-3(4*H*)-one **2b** (55 mg, 88%) using $Sn(OTf)_2$ and (59 mg, 94%) using Amberlyst-15 as a cream colored solid. 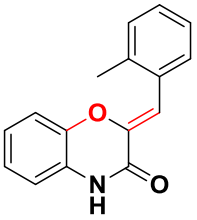

^{1}H NMR (400 MHz, DMSO-*d6*): δ 11.19 (bs, 1H), 8.08 (d, *J* = 7.8 Hz, 1H), 7.32-7.21 (m, 3H), 7.18-7.16 (m, 1H), 7.06-6.97 (m, 3H), 6.91 (s, 1H), 2.36 (s, 3H). **^{13}C NMR** (100 MHz, DMSO-*d6*): δ 156.39, 141.68, 140.39, 136.71, 131.65, 130.24, 129.00, 128.02, 126.06, 125.39, 123.42, 123.21, 115.54, 115.47, 107.49, 19.90. **FTIR** (KBr): 3180, 2962, 2920, 1688, 1634, 1503, 1387, 1112 cm^{-1} **HRMS** (ESI) m/z calculated for $C_{16}H_{13}NO_2$ $(M+H)^+$: 252.1025, found: 252.1024.

(*Z*)-2-(4-Methylbenzylidene)-2*H*-benzo[*b*][1,4]oxazin-3(4*H*)-one (2c): Prepared according to general procedure (A) and (B), using 3-(*tert*-butylperoxy)-3-(4-methylbenzyl)indolin-2-one (81.2 mg, 0.25 mmol) to afford (*Z*)-2-(4-methylbenzylidene)-2*H*-benzo[*b*][1,4]oxazin-3(4*H*)-one **2c** (31.7 mg, 50%) using $Sn(OTf)_2$ and (32.6 mg, 52%) using Amberlyst-15 as a cream colored solid. 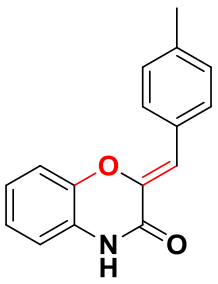

^{1}H NMR (400 MHz, DMSO-*d6*): 11.09 (bs, 1H), 7.78 (d, *J* = 8.0 Hz,

2H), 7.26-7.24 (3H), 7.06 – 6.94 (m, 3H), 6.75 (s, 1H), 2.34 (s, 3H). **^{13}C NMR** (100 MHz, $CDCl_3$) δ 156.39, 141.16, 140.50, 137.81, 130.44, 129.72, 129.29, 125.42, 123.39, 123.13, 115.52, 115.49, 110.67, 21.00. **FTIR** (KBr): 3150, 2919, 1687, 1635, 1504, 1387, 1112 cm^{-1}. **HRMS** (ESI) m/z calculated for $C_{16}H_{13}NO_2$ $(M+H)^+$: 252.1025, found: 252.1027.

(*Z*)-2-([1,1'-Biphenyl]-4-ylmethylene)-2*H*-benzo[*b*][1,4]oxazin-3(4*H*)-one (2d): Prepared according to general procedure (A) and (B), using 3-([1,1'-biphenyl]-4-ylmethyl)-3-(*tert*-butylperoxy)indolin-2-one (96.7 mg, 0.25 mmol) to afford (*Z*)-2-([1,1'-biphenyl]-4-ylmethylene)-2*H*-benzo[*b*][1,4]oxazin-3(4*H*)-one **2d** (45.9 mg, 58%) using $Sn(OTf)_2$ and (41.5 mg, 53%) using Amberlyst-15 as a cream colored solid.

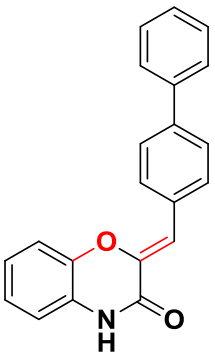

^{1}H NMR (400 MHz, DMSO-*d6*) δ 11.16 (bs, 1H), 7.99 (d, *J* =8.4 Hz, 2H), 7.77-7.72 (m, 4H), 7.51-7.47 (m, 2H), 7.41-7.37 (m, 1H), 7.32-7.29 (m, 1H), 7.07 – 7.03 (m, 2H), 7.01 – 6.98 (m, 1H), 6.84 (s, 1H). **^{13}C NMR** (100 MHz, DMSO-*d6*) δ 156.24, 141.92, 140.46, 139.55, 139.46, 132.45, 130.33, 129.03, 127.69, 126.82, 126.57, 125.41, 123.52, 123.21, 115.59, 115.53, 110.10. **FTIR** (KBr): 3150, 2959, 2920, 1679, 1635, 1500, 1387, 1106 cm^{-1}. **HRMS** (ESI) m/z calculated for $C_{21}H_{15}NO_2$ $(M+H)^+$: 314.1181, found: 314.1183.

2-Cyclohexylidene-2*H*-benzo[*b*][1,4]oxazin-3(4*H*)-one (2e): Prepared according to general procedure (A) and (B), using 3-(*tert*-butylperoxy)-3-cyclohexylindolin-2-one (75.8 mg, 0.25 mmol) to afford 2-cyclohexylidene-2*H*-benzo[*b*][1,4]oxazin-3(4*H*)-one **2e** (45 mg, 78%) using $Sn(OTf)_2$ and (47 mg, 82%) using Amberlyst-15 as a white solid.

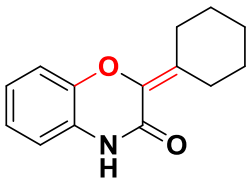

^{1}H NMR (400 MHz, DMSO-*d6*): δ 10.65 (bs, 1H), 7.03 – 6.99 (m, 1H), 6.96 – 6.90 (m, 2H), 6.89 – 6.85 (m, 1H), 2.88-2.84 (m, 2H), 2.46 – 2.43 (m, 2H), 1.58-1.52 (m, 6H). **^{13}C NMR** (100 MHz, DMSO-*d6*) δ 158.72, 142.67, 134.09, 133.72, 126.47, 122.75, 122.62, 115.00, 114.87, 28.32, 27.52, 27.22, 27.11, 25.77. **FTIR** (KBr): 3181, 2985, 2920, 1677, 1628, 1451, 1387, 1117 cm^{-1}. **HRMS** (ESI) m/z calculated for $C_{14}H_{15}NO_2$ $(M+H)^+$: 230.1181, found: 230.1187.

(*Z*)-2-Hexylidene-2*H*-benzo[*b*][1,4]oxazin-3(4*H*)-one (2f): Prepared according to general procedure (A) and (B), using 3-(*tert*-butylperoxy)-3-hexylindolin-2-one (76 mg, 0.25 mmol) to afford (*Z*)-2-hexylidene-2*H*-benzo[*b*][1,4]oxazin-3(4*H*)-one **2f** (43 mg, 75%) using $Sn(OTf)_2$ and (50.5 mg, 87%) using Amberlyst-15 as a white solid.

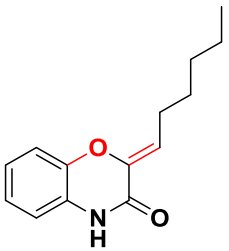

^{1}H NMR (400 MHz, DMSO-*d6*): δ 10.88 (bs, 1H), 7.04 – 7.00 (m, 1H), 6.97 – 6.90 (m, 3H), 5.87 (t, *J* = 7.7 Hz, 1H), 2.24 (q, *J* = 7.5 Hz, 2H), 1.47 – 1.39 (m, 2H), 1.34 – 1.26 (m, 4H), 0.86 (t, *J* = 6.9 Hz, 3H). **^{13}C NMR** (100 MHz, DMSO-*d6*) δ 156.26, 141.98, 140.99, 125.37, 123.03, 122.82, 115.44, 115.15, 114.69, 30.92, 27.85, 23.92, 21.89, 13.90. **FTIR** (KBr): 3168, 2948, 2919, 1692, 1653, 1504, 1394, 1288 cm^{-1}. **HRMS** (ESI) m/z calculated for $C_{14}H_{17}NO_2$ $(M+H)^+$: 232.1338, found: 232.1339.

Ethyl 2-(3-hydroperoxy-2-oxoindolin-3-yl)acetate (2g): Prepared according to general procedure (A) and (B), using ethyl 2-(3-(*tert*-butylperoxy)-2-oxoindolin-3-yl)acetate (76.7 mg, 0.25 mmol) to afford ethyl 2-(3-hydroperoxy-2-oxoindolin-3-yl)acetate **2g** (46 mg, 73%) using $Sn(OTf)_2$ and (44.5 mg, 71%) using Amberlyst-15 as a white solid. 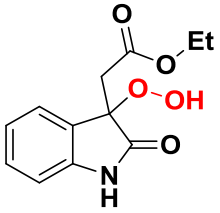

^{1}H NMR (400 MHz, DMSO-*d6*): δ 10.74 (bs, 1H), 7.68 (bs, 1H), 6.96 – 6.88 (m, 4H), 4.01 (q, *J* = 7.1 Hz, 2H), 3.31 (d, *J* = 16.4 Hz, 1H), 2.90 (d, *J* = 16.4 Hz, 1H), 1.13 (t, *J* = 7.1 Hz, 3H). **^{13}C NMR** (100 MHz, DMSO-*d6*) δ 168.28, 162.96, 140.84, 126.85, 122.81, 122.19, 116.95, 115.25, 95.16, 59.98, 41.34, 13.98. **FTIR** (KBr): 3416, 2923, 1691, 1630, 1580, 1384 cm^{-1}. **HRMS** (ESI) m/z calculated for $C_{12}H_{13}NO_5$ $(M+Na)^+$:274.0691, found: 274.0698.

(*Z*)-2-(3-Bromobenzylidene)-2*H*-benzo[*b*][1,4]oxazin-3(4*H*)-one (2h): Prepared according to general procedure (A) and (B), using 3-(3-bromobenzyl)-3-(*tert*-butylperoxy)indolin-2-one (97.2 mg, 0.25 mmol) to afford (*Z*)-2-(3-bromobenzylidene)-2*H*-benzo[*b*][1,4]oxazin-3(4*H*)-one **2h** (42 mg, 53%) using $Sn(OTf)_2$ and (48 mg, 61%) using Amberlyst-15 as a white solid. 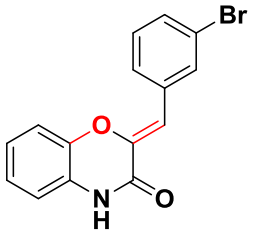

^{1}H NMR (400 MHz, DMSO-*d6*): δ 11.22 (bs, 1H), 8.04 (t, *J* = 1.6 Hz, 1H), 7.93 (d, *J* = 7.9 Hz, 1H), 7.55 – 7.51 (m, 1H), 7.40 (t, *J* = 7.9 Hz, 1H), 7.26 – 7.22 (m, 1H), 7.08 – 7.03 (m, 2H), 7.01 – 6.98 (m, 1H), 6.77 (s, 1H). **^{13}C NMR** (100 MHz, DMSO-*d6*) δ 155.85, 142.79, 140.22, 135.70, 131.90, 130.76, 130.66, 128.48, 125.28, 123.67, 123.28, 121.88, 115.66, 115.46, 108.71. **FTIR** (KBr): 3180, 2979, 2920, 1685, 1642, 1501, 1393, 1110 cm^{-1}. **HRMS** (ESI) m/z calculated for $C_{15}H_{10}BrNO_2$ $(M+H)^+$: 315.9973, found: 315.9969.

(*Z*)-2-(3-Chlorobenzylidene)-2*H*-benzo[*b*][1,4]oxazin-3(4*H*)-one (2i): Prepared according to general procedure (A) and (B), 3-using (*tert*-butylperoxy)-3-(3-chlorobenzyl)indolin-2-one (86.4 mg, 0.25 mmol) to afford (*Z*)-2-(3-chlorobenzuylidene)-2*H*-benzo[*b*][1,4]oxazin-3(4*H*)-one **2i** (48 mg, 71%) using $Sn(OTf)_2$ and (49 mg, 72%) using Amberlyst-15 as a white solid. 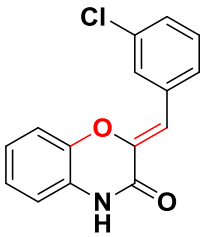

^{1}H NMR (400 MHz, DMSO-*D6*) δ 11.23 (bs, 1H), 7.91 – 7.87 (m, 2H), 7.47 (t, *J* = 7.8 Hz, 1H), 7.40 (ddd, *J* = 8.0, 2.0, 1.0 Hz, 1H), 7.26 (dd, *J* = 7.4, 1.9 Hz, 1H), 7.08-7.04 (m, 2H), 7.01 – 6.97 (m, 1H), 6.78 (s, 1H). **^{13}C NMR** (100 MHz, DMSO-*d6*) δ 155.88, 142.81, 140.25, 135.42, 133.28, 130.50, 129.01, 128.17, 127.81, 125.29, 123.69, 123.29, 115.66, 115.53, 108.80. **FTIR** (KBr): 3147, 3083, 2921, 1694, 1641, 1502, 1390, 1111 cm^{-1}. **HRMS** (ESI) m/z calculated for $C_{15}H_{10}ClNO_2$ $(M+H)^+$: 272.0478, found: 272.0481.

(*Z*)-2-(2-Fluorobenzylidene)-2*H*-benzo[*b*][1,4]oxazin-3(4*H*)-one (2j): Prepared according to general procedure (A) and (B), using 3-(*tert*-butylperoxy)-3-(2-fluorobenzyl)indolin-2-one (82.3 mg, 0.25 mmol) to afford (*Z*)-2-(2-fluorobenzylidene)-2*H*-benzo[*b*][1,4]oxazin-3(4*H*)-one **2j** (43 mg, 67%) using $Sn(OTf)_2$ and (41 mg, 64%) using Amberlyst-15 as a white solid. 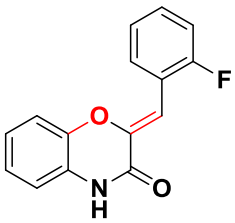

^{1}H NMR (400 MHz, DMSO-

d6) δ 11.27 (bs, 1H), 8.31 (td, *J* = 7.8, 1.7 Hz, 1H), 7.41 (tdd, *J* = 7.3, 5.5, 1.8 Hz, 1H), 7.34 – 7.26 (m, 3H), 7.09 – 7.03 (m, 2H), 7.03 – 6.98 (m, 1H), 6.91 (s, 1H). **^{13}C NMR** (100 MHz, DMSO-*d6*) δ 159.64 (d, *J* = 249.1 Hz), 155.81, 143.19 (d, *J* = 1.9 Hz), 140.23, 130.09, 130.01, 129.96, 125.26, 124.80 (d, *J* = 3.5 Hz), 123.67, 123.26, 120.69 (d, *J* = 11.1 Hz), 115.64 (d, *J* = 1.8 Hz), 115.31 (d, *J* = 22.0 Hz), 100.53 (d, *J* = 8.2 Hz). **FTIR** (KBr): 3150, 2920, 1687, 1635, 1500, 1391, 1127 cm^{-1}. **HRMS** (ESI) m/z calculated for $C_{15}H_{10}FNO_2$ $(M+H)^+$: 256.0774, found: 256.0776.

(*Z*)-2-(3-Fluorobenzylidene)-2*H*-benzo[*b*][1,4]oxazin-3(4*H*)-one (2k): Prepared according to general procedure (A) and (B), using 3-(*tert*-butylperoxy)-3-(3-fluorobenzyl)indolin-2-one (82.3 mg, 0.25 mmol) to afford (*Z*)-2-(3-fluorobenzylidene)-2*H*-benzo[*b*][1,4]oxazin-3(4*H*)-one **2k** (45 mg, 70%) using $Sn(OTf)_2$ and (41 mg, 64%) using Amberlyst-15 as a white solid.

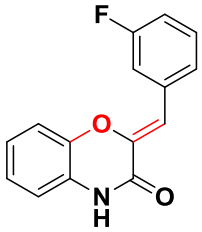

^{1}H NMR (400 MHz, DMSO-*d6*) δ 11.22 (bs, 1H), 7.74 – 7.68 (m, 2H), 7.48 (td, *J* = 8.1, 6.4 Hz, 1H), 7.30 (dd, *J* = 7.4, 2.0 Hz, 1H), 7.21 – 7.15 (m, 1H), 7.09 – 7.03 (m, 2H), 7.02 – 6.98 (m, 1H), 6.80 (s, 1H). **^{13}C NMR** (100 MHz, DMSO-*d6*) δ 162.15 (d, *J* = 242.7 Hz), 155.91, 142.68, 140.27, 135.55 (d, *J* = 8.5 Hz), 130.53 (d, *J* = 8.6 Hz), 125.95 (d, *J* = 2.6 Hz), 125.27, 123.66, 123.27, 115.83, 115.63, 115.62, 114.88 (d, *J* = 21.3 Hz), 109.09 (d, *J* = 2.7 Hz). **FTIR** (KBr): 3183, 2920, 1694, 1641, 1501, 1390, 1110 cm^{-1}. **HRMS** (ESI) m/z calculated for $C_{15}H_{10}FNO_2$ $(M+H)^+$: 256.0774, found: 256.0775.

(*Z*)-2-Benzylidene-6-chloro-2*H*-benzo[*b*][1,4]oxazin-3(4*H*)-one (2l): Prepared according to general procedure (A) and (B), using 3-benzyl-3-(*tert*-butylperoxy)-6-chloroindolin-2-one (86.5 mg, 0.25 mmol) to afford (*Z*)-2-benzylidene-6-chloro-2*H*-benzo[*b*][1,4]oxazin-3(4*H*)-one **2l** (35 mg, 51%) using $Sn(OTf)_2$ and (24 mg, 35%) using Amberlyst-15 as a white solid. (Low yield due to formation of 30% and 38% deprotected hydroperoxy compound respectively).

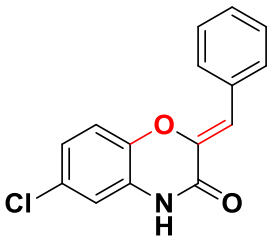

^{1}H NMR (400 MHz, DMSO-*d6*) δ 11.22 (s, 1H), 7.89 – 7.86 (m, 2H), 7.44 (m, 2H), 7.38 – 7.31 (m, 2H), 7.06 (dd, *J* = 8.4, 2.5 Hz, 1H), 6.97 (d, *J* = 2.5 Hz, 1H), 6.79 (s, 1H). **^{13}C NMR** (100 MHz, DMSO-*d6*) δ 156.08, 141.22, 139.41, 132.99, 129.86, 128.68, 128.34, 126.96, 126.76, 122.55, 117.13, 114.82, 111.08. **FTIR** (KBr): 3175, 2924, 1683, 1635, 1494, 1380, 1240 cm^{-1}. **HRMS** (ESI) m/z calculated for $C_{15}H_{10}ClNO_2$ $(M+H)^+$: 272.0478, found: 272.0493.

(*Z*)-6-Chloro-2-(4-methoxybenzylidene)-2*H*-benzo[*b*][1,4]oxazin-3(4*H*)-one (2m): Prepared according to general procedure (A) and (B), using 3-(*tert*-butylperoxy)-6-chloro-3-(4-methoxybenzyl)indolin-2-one (94 mg, 0.25 mmol) to afford (*Z*)-6-chloro-2-(4-methoxybenzylidene)-2*H*-benzo[*b*][1,4]oxazin-3(4*H*)-one **2m** (40 mg, 53%) using $Sn(OTf)_2$ and (45 mg, 60%) using Amberlyst-15 as a white solid. (Low yield due to formation of 24% and 20% deprotected peroxy compound respectively).

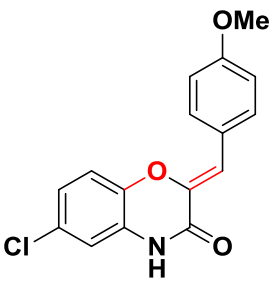

^{1}H NMR (400 MHz, DMSO-*d6*) δ 11.10 (bs, 1H), 7.84 (d, *J* = 8.8 Hz, 2H), 7.29

(d, *J* = 8.7 Hz, 1H), 7.04 (dd, *J* = 8.7, 2.5 Hz, 1H), 7.01 – 6.98 (m, 2H), 6.95 (d, *J* = 2.5 Hz, 1H), 6.75 (s, 1H), 3.80 (s, 3H). **^{13}C NMR** (100 MHz, DMSO-*d6*) δ 159.30, 156.39, 139.58, 139.56, 131.56, 127.09, 126.60, 125.62, 122.47, 117.02, 114.75, 114.17, 111.29, 55.18. **FTIR** (KBr): 3149, 2925, 1686, 1637, 1509, 1396, 1119 cm^{-1}. **HRMS** (ESI) m/z calculated for $C_{16}H_{12}ClNO_3$ $(M+H)^+$: 302.0584, found: 302.0586.

(*Z*)-4-Benzyl-2-(4-methylbenzylidene)-2*H*-benzo[*b*][1,4]oxazin-3(4*H*)-one (2n): Prepared according to general procedure (A) and (B), using 1-benzyl-3-(*tert*-butylperoxy)-3-(4-methylbenzyl)indolin-2-one (94 mg, 0.25 mmol) to afford (*Z*)-4-benzyl-2-(4-methylbenzylidene)-2*H*-benzo[*b*][1,4]oxazin-3(4*H*)-one **2n** (71 mg, 83%) using $Sn(OTf)_2$ and (75 mg, 88%) using Amberlyst-15 as a white solid.

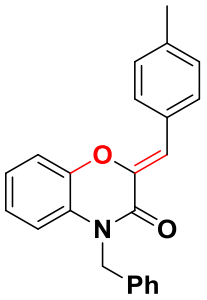

^{1}H NMR (400 MHz, DMSO-*d6*) 7.82 (d, *J* = 8.2 Hz, 2H), 7.34-7.32 (m, 5H), 7.29-7.26 (m, 3H), 7.10 – 6.99 (m, 3H), 6.90 (s, 1H), 5.28 (s, 2H), 2.35 (s, 3H). **^{13}C NMR** (100 MHz, DMSO-*d6*) δ 156.54, 141.18, 140.28, 138.03, 136.03, 130.44, 129.82, 129.35, 128.71, 127.23, 126.61, 126.02, 123.80, 123.38, 115.88, 115.59, 112.11, 44.34, 21.02. **FTIR** (KBr): 3059, 2922, 1671, 1628, 1503, 1394, 1112 cm^{-1}. **HRMS** (ESI) m/z calculated for $C_{23}H_{19}NO_2$ $(M+H)^+$: 342.1494, found: 342.1486.

4A.8.4. Appendix V: Copies of ^{1}H and ^{13}C NMR spectra of representative compounds

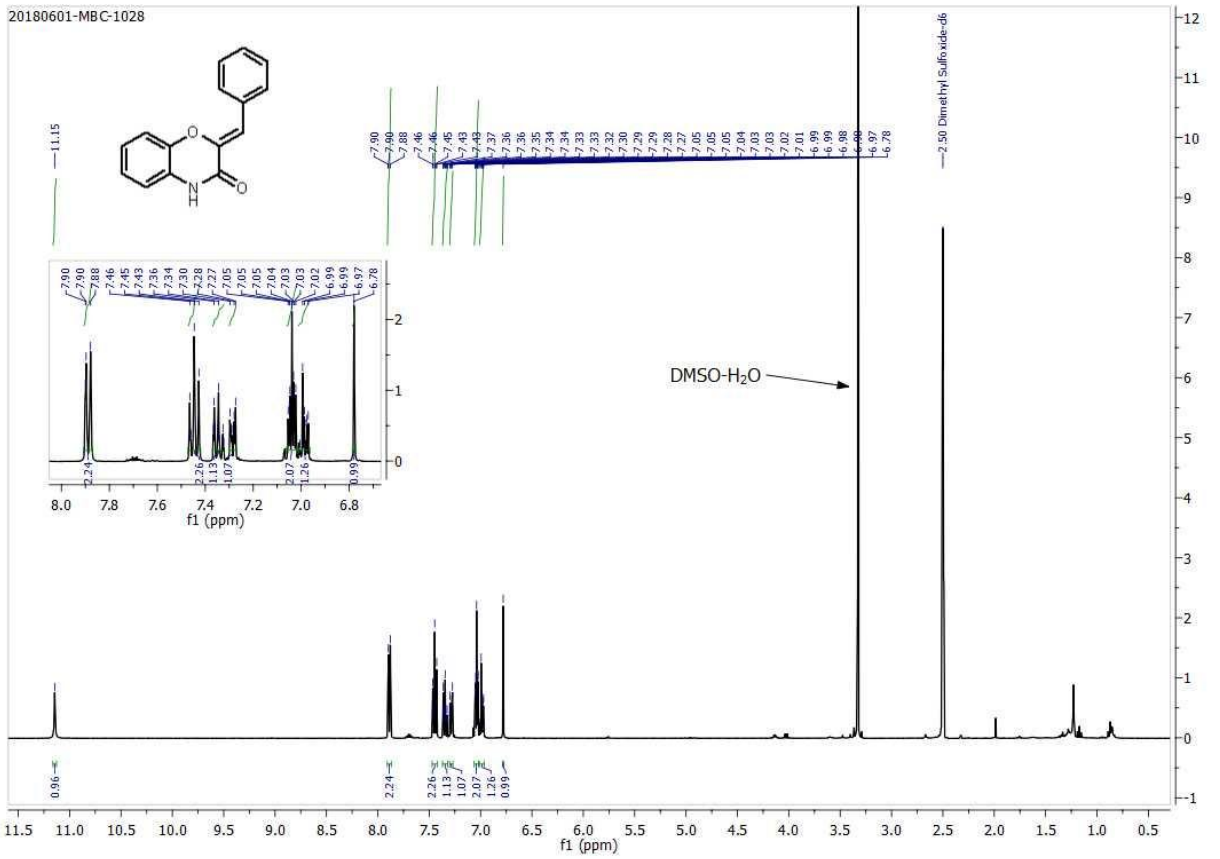

Figure 4A.13. ^{1}H NMR of compound **2a**

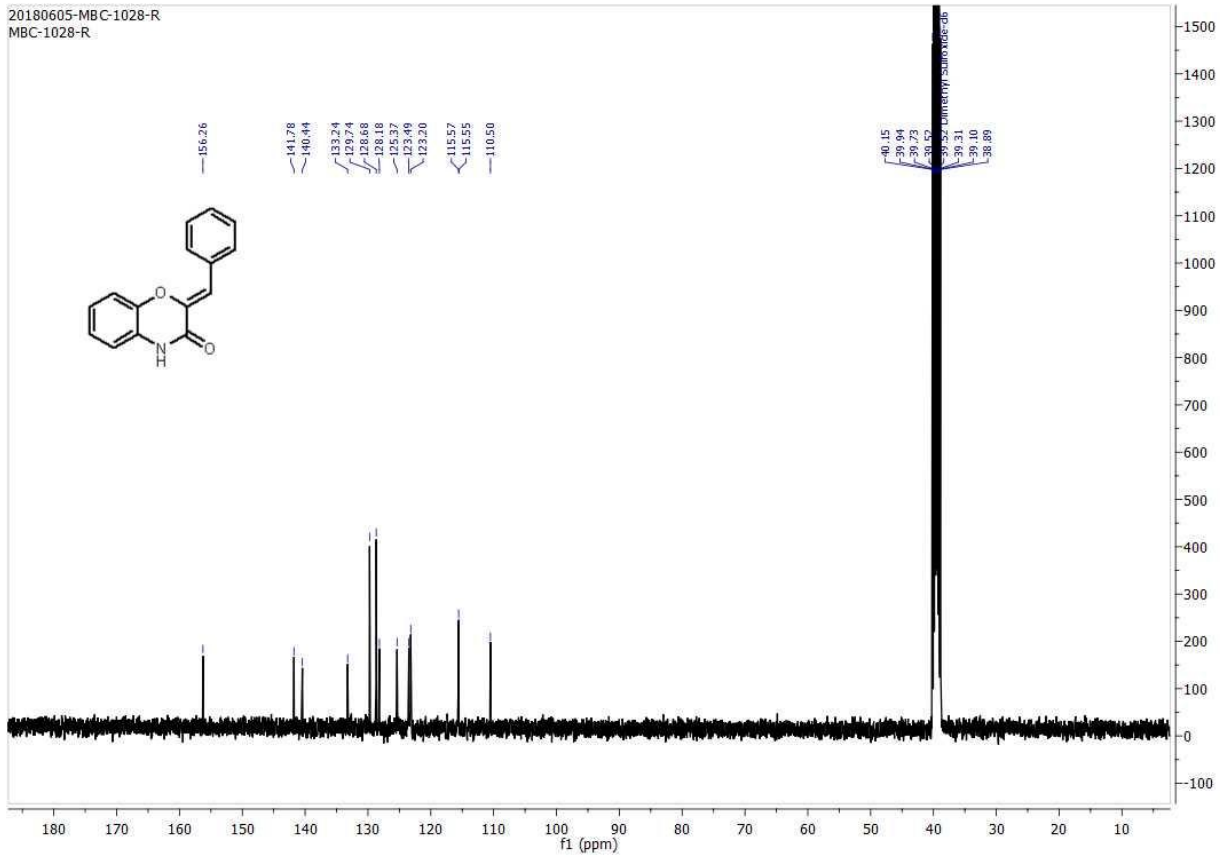

Figure 4A.14. ^{13}C NMR of compound **2a**

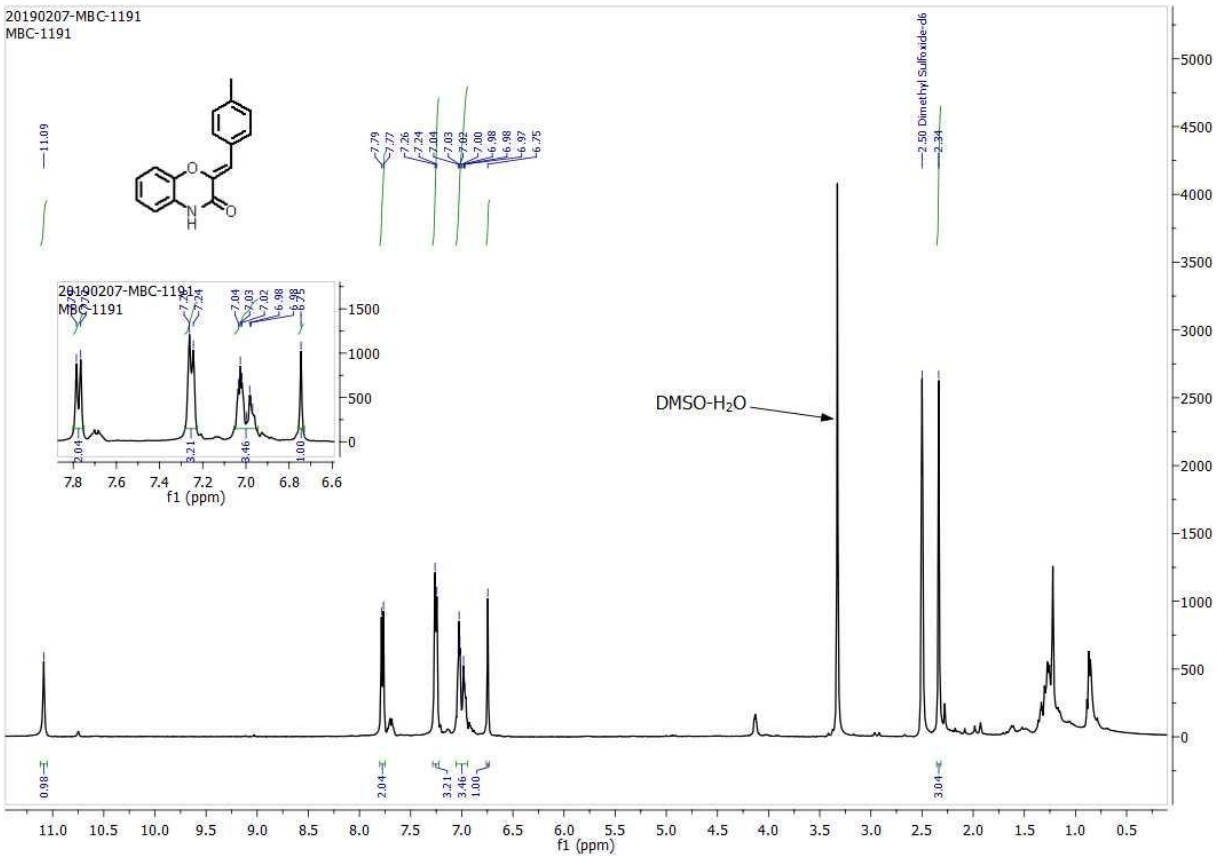

Figure 4A.15. ^{1}H NMR of compound **2c**

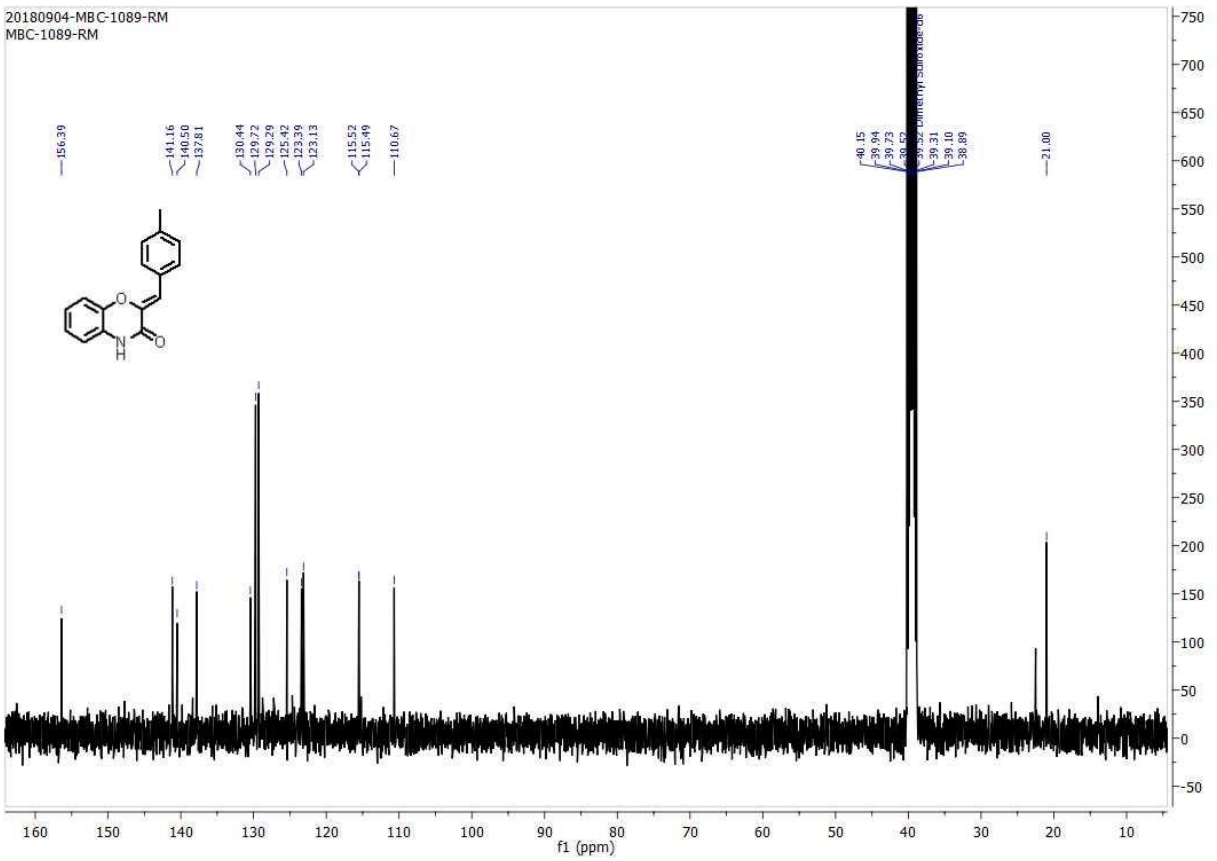

Figure 4A.16. ^{13}C NMR of compound **2c**

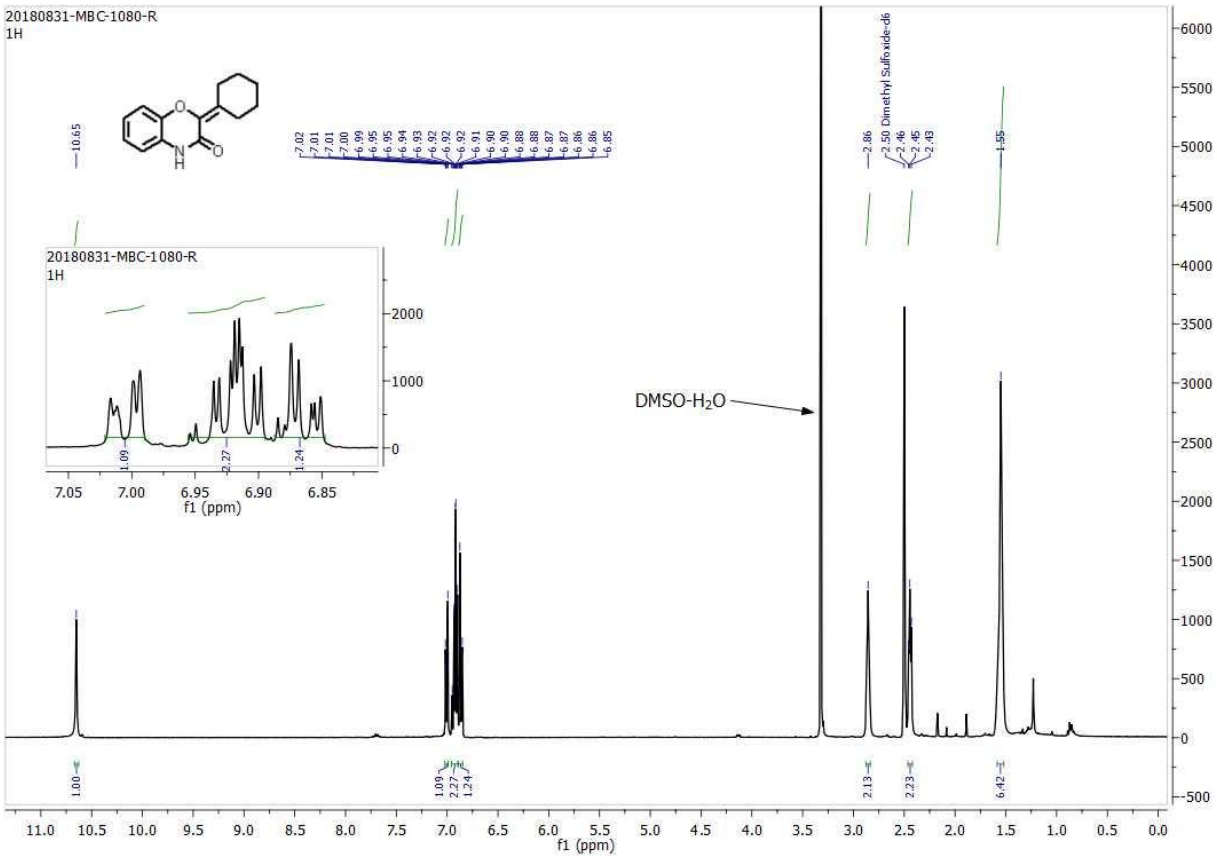

Figure 4A.17. ^{1}H NMR of compound **2e**

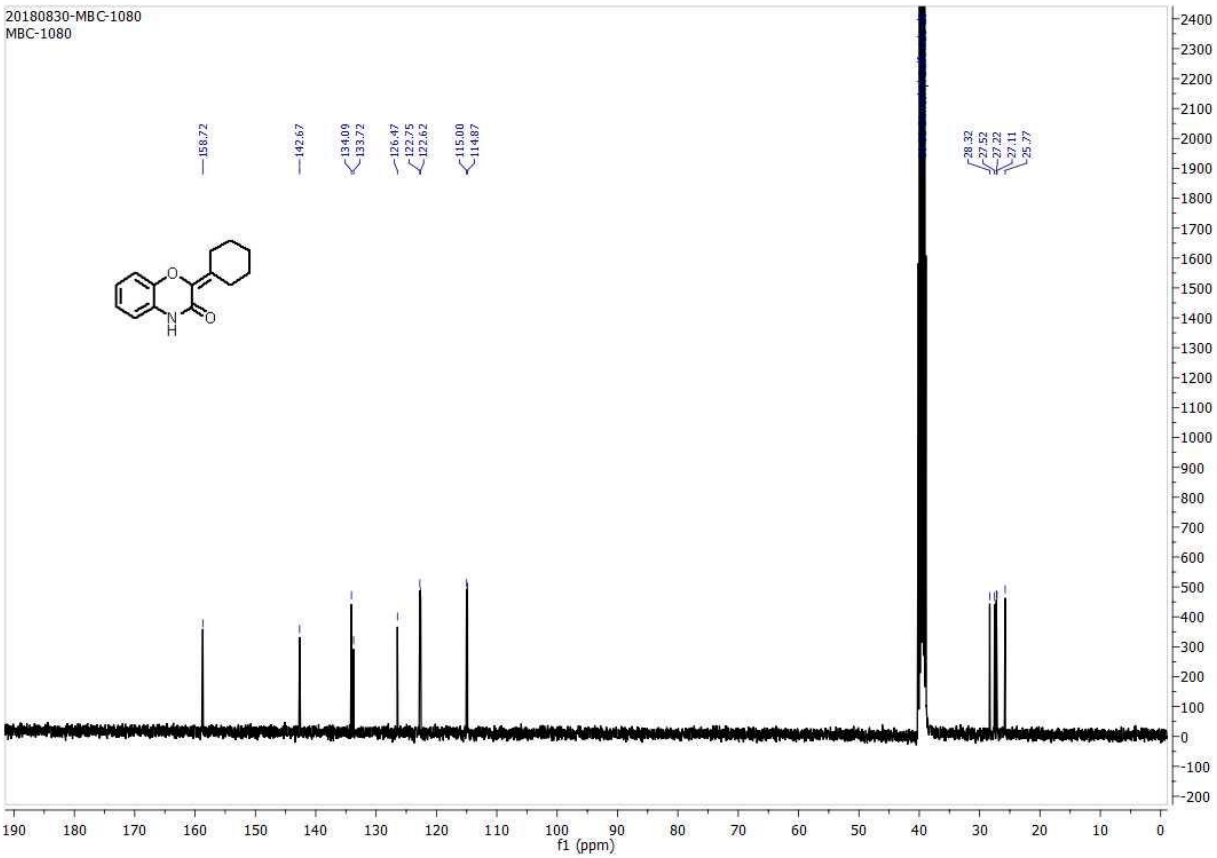

Figure 4A.18. ^{13}C NMR of compound **2e**

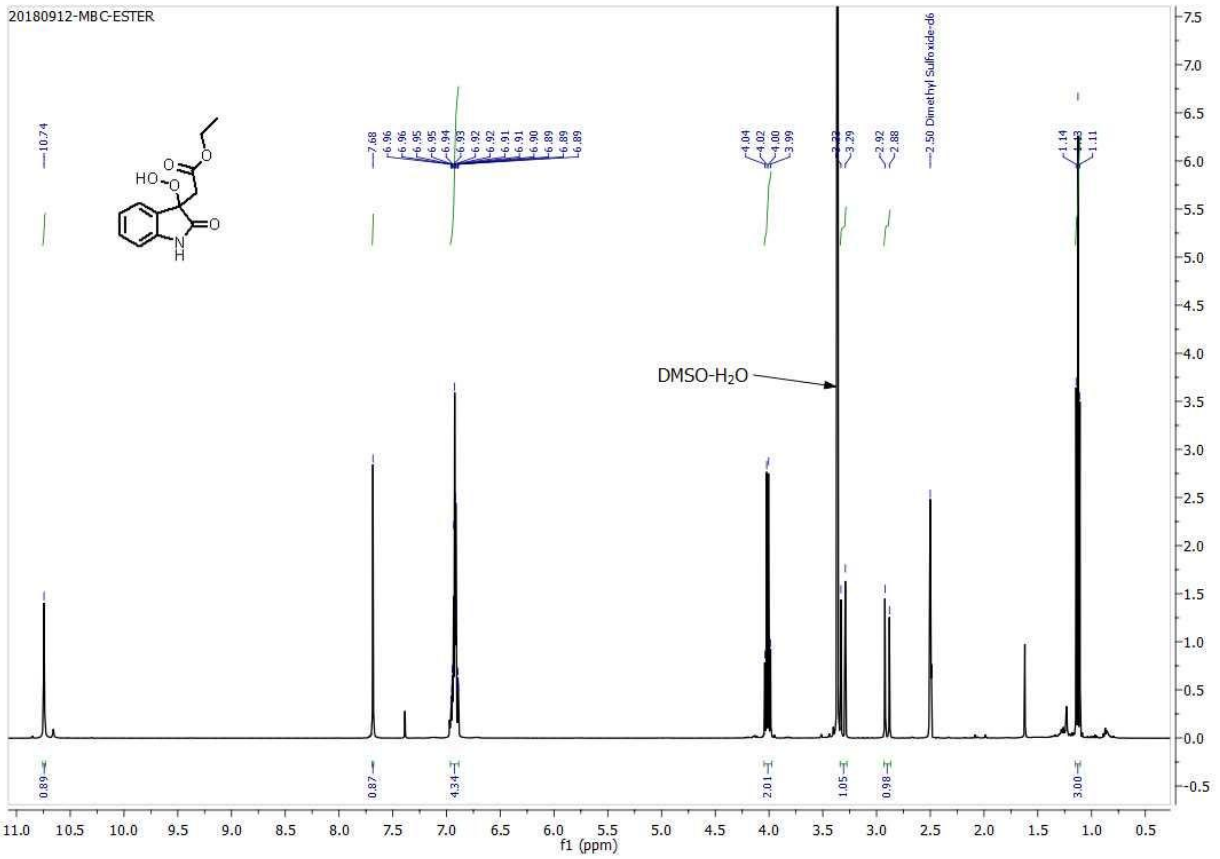

Figure 4A.19. ^{1}H NMR of compound **2g**

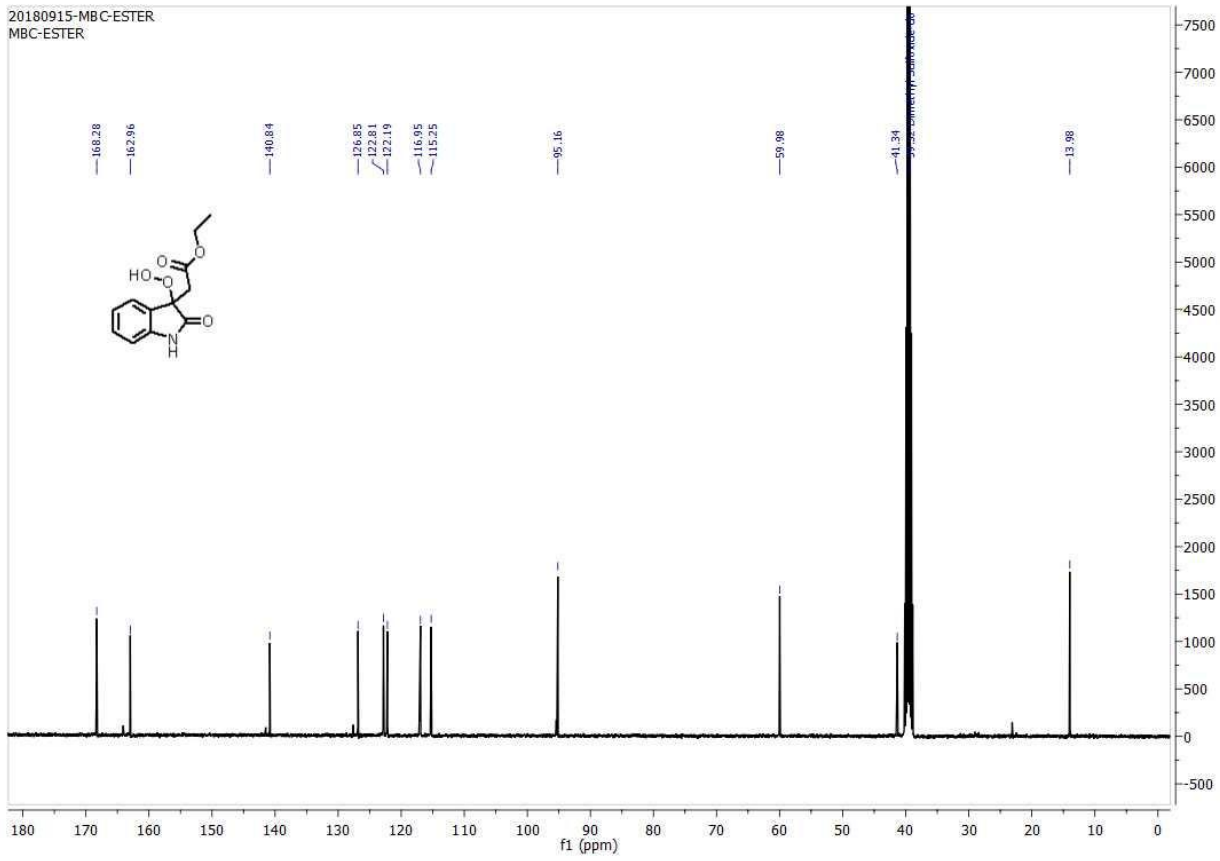

Figure 4A.20. ^{13}C NMR of compound **2g**

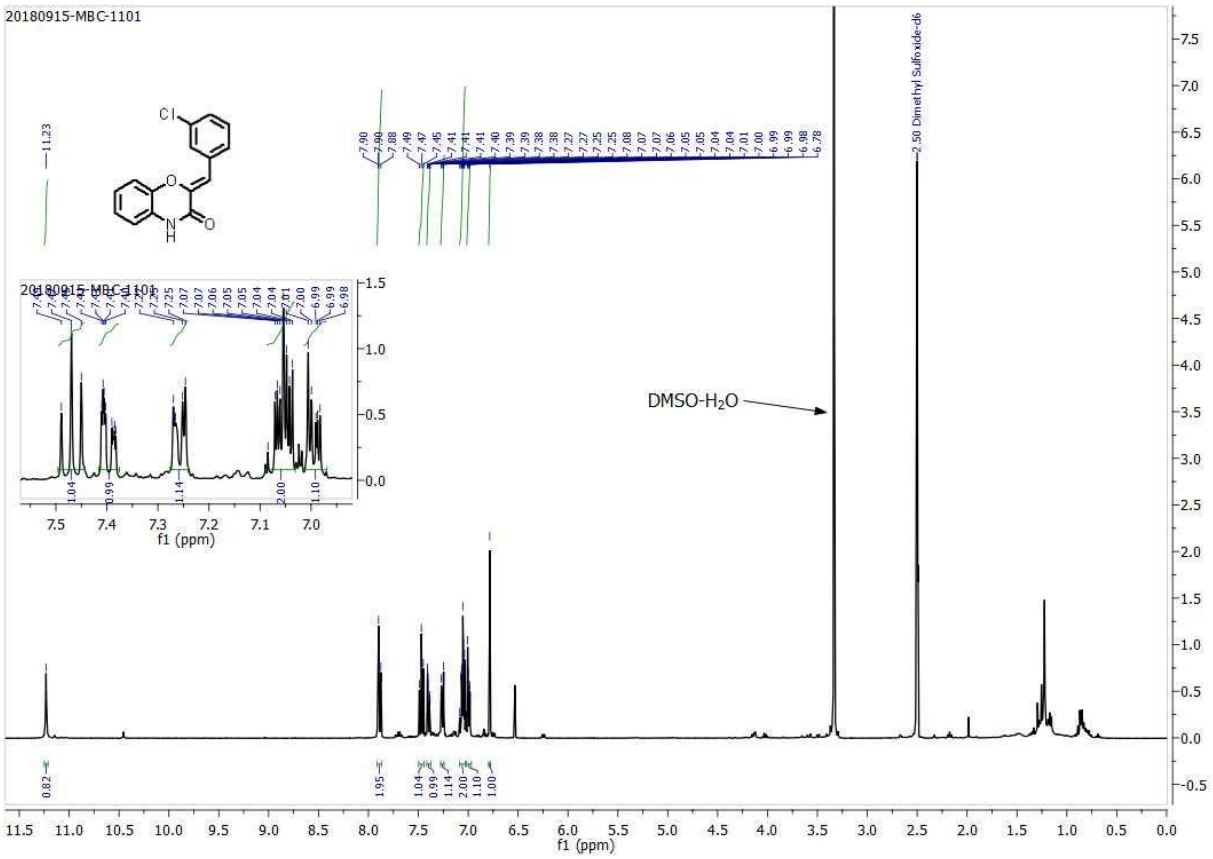

Figure 4A.21. ^{1}H NMR of compound **2i**

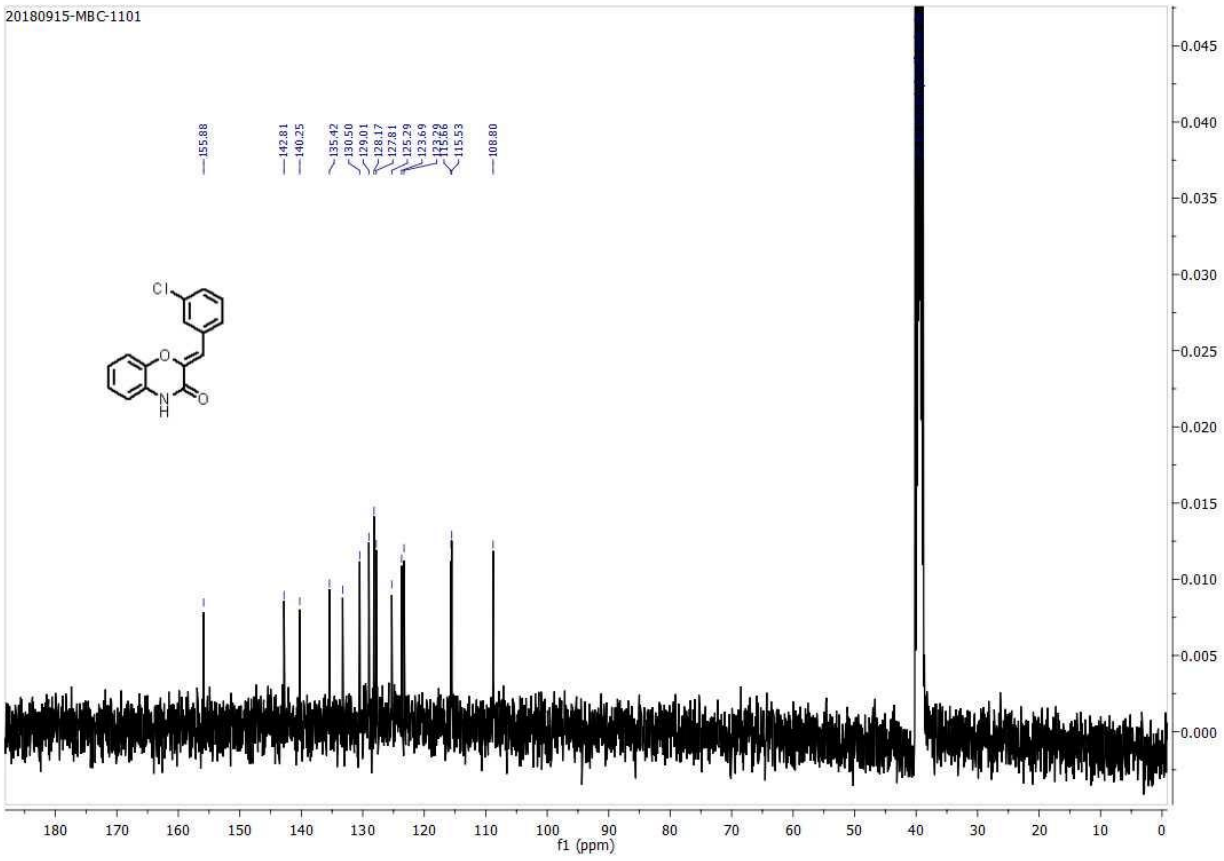

Figure 4A.22. ^{13}C NMR of compound **2i**

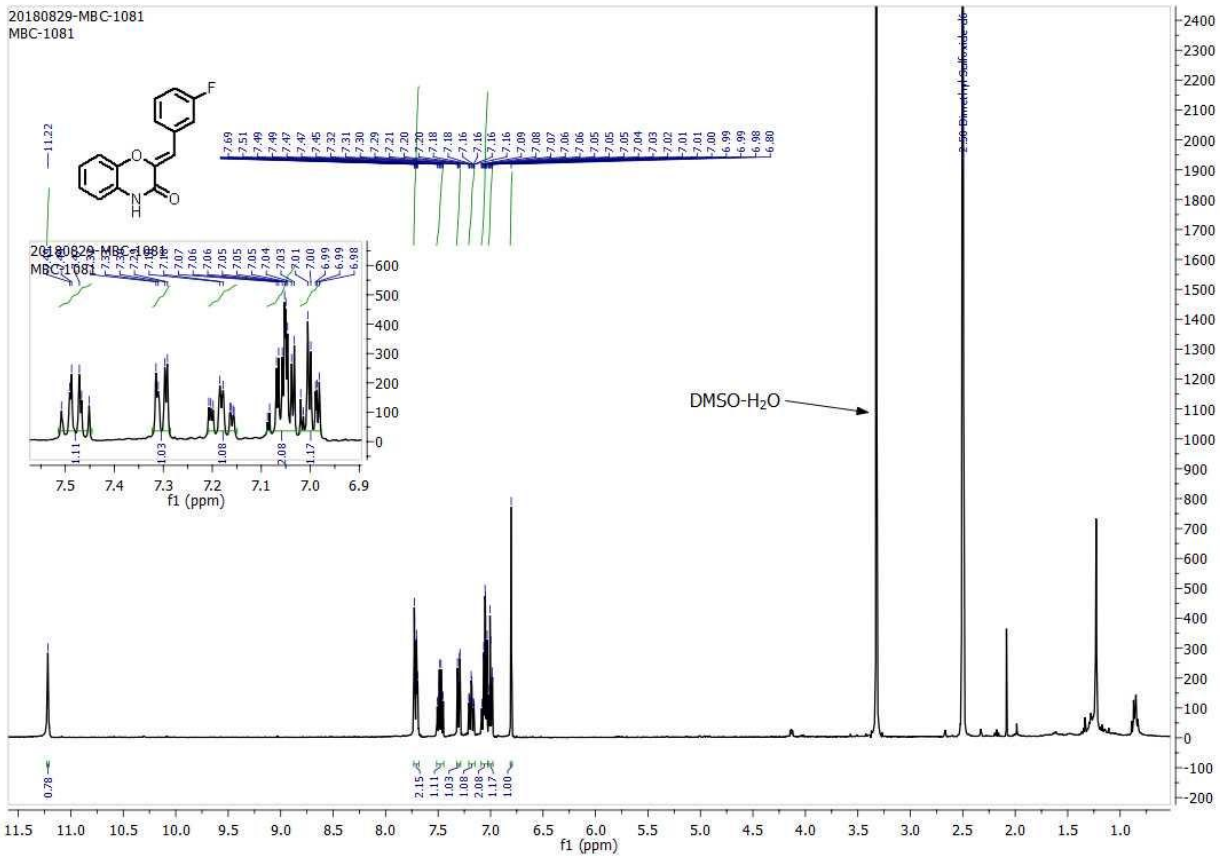

Figure 4A.23. ^{1}H NMR of compound **2k**

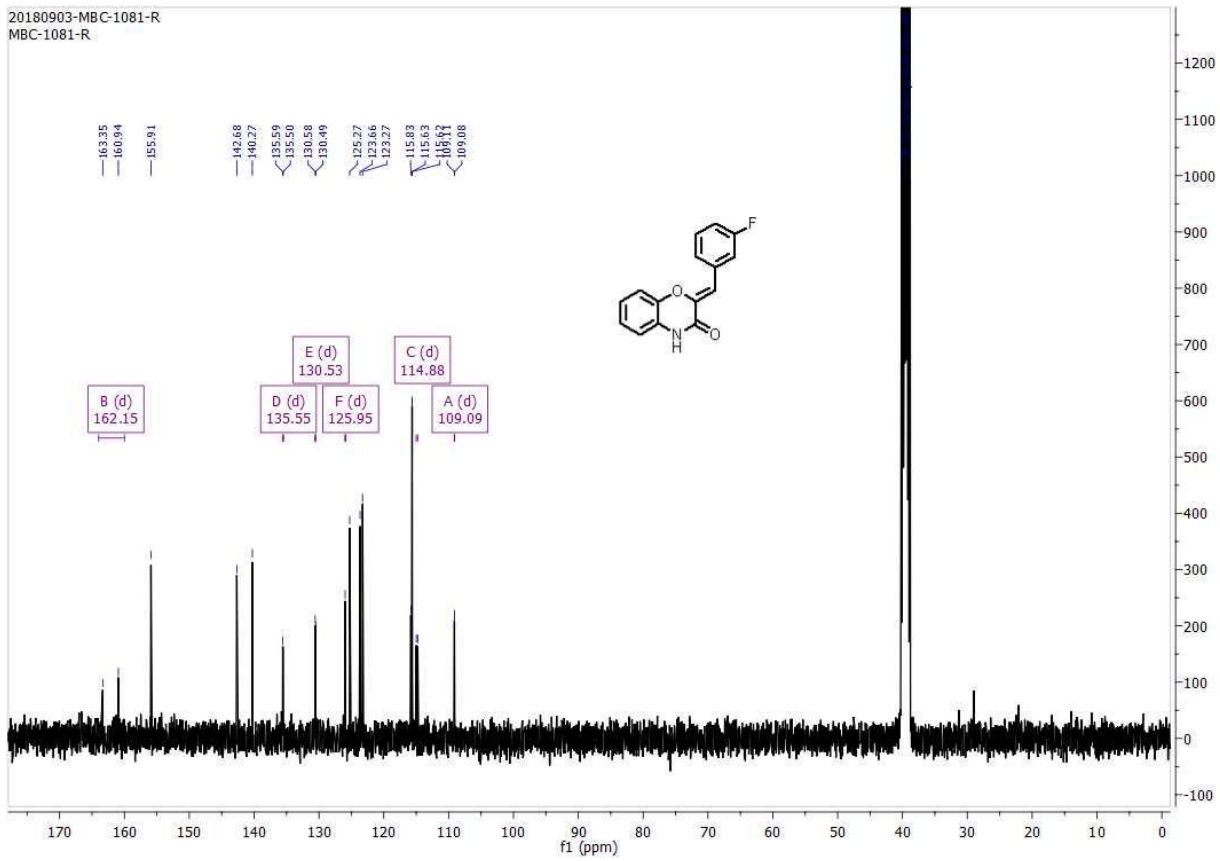

Figure 4A.24. ^{13}C NMR of compound **2k**

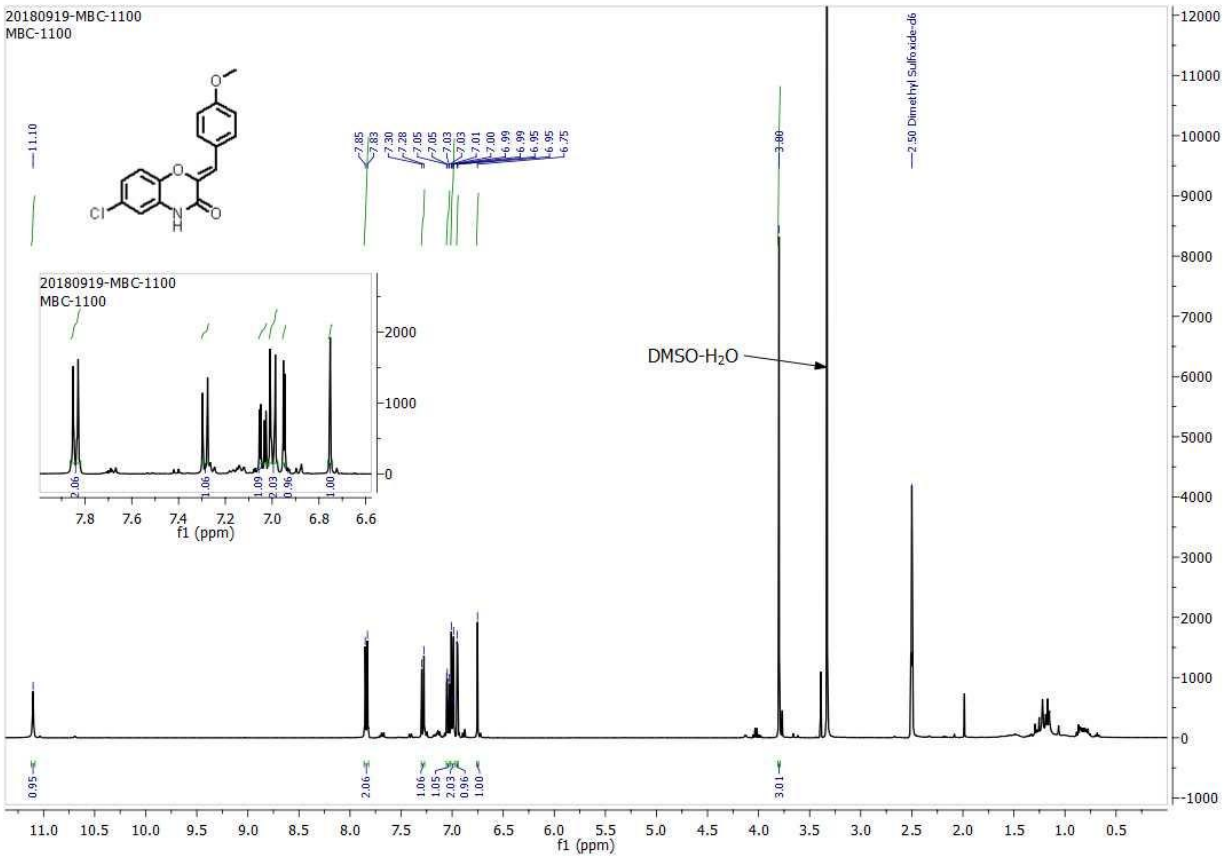

Figure 4A.25. ^{1}H NMR of compound **2m**

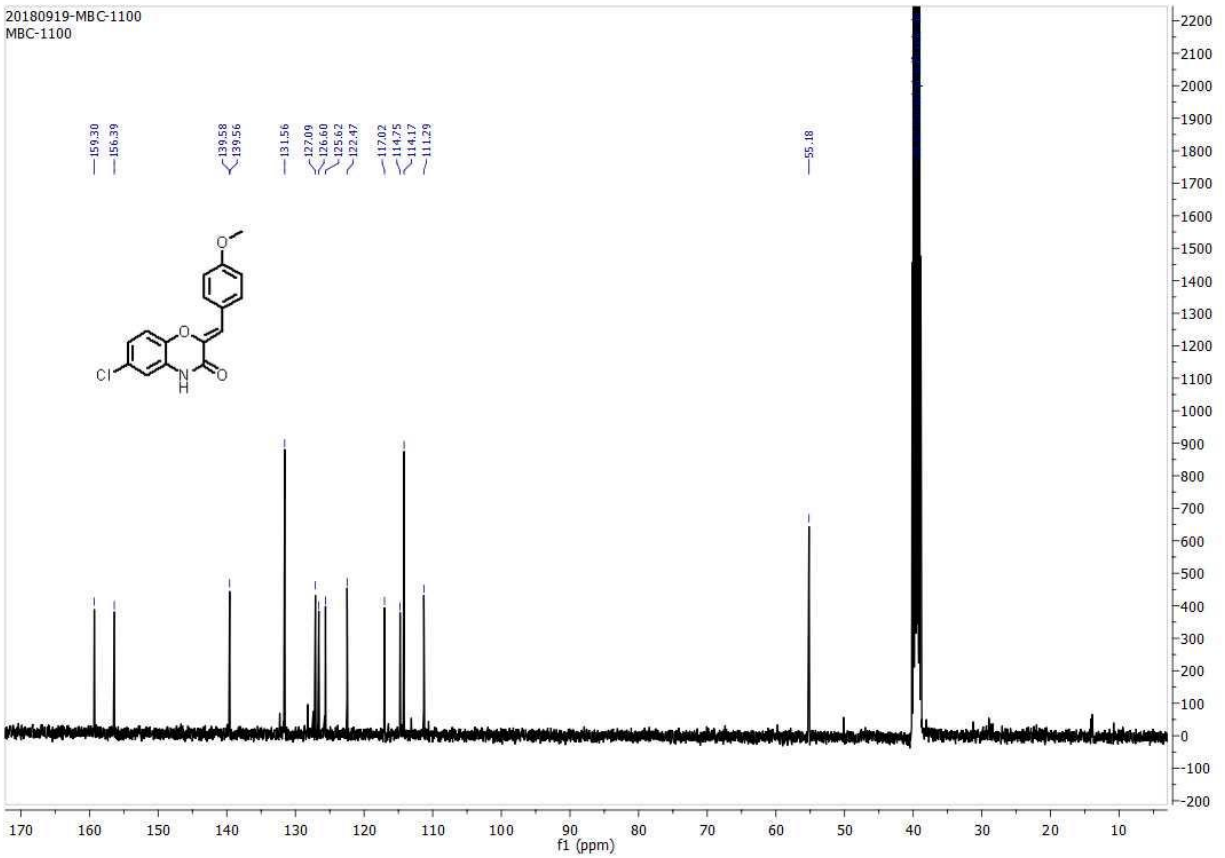

Figure 4A.26. ^{13}C NMR of compound **2m**

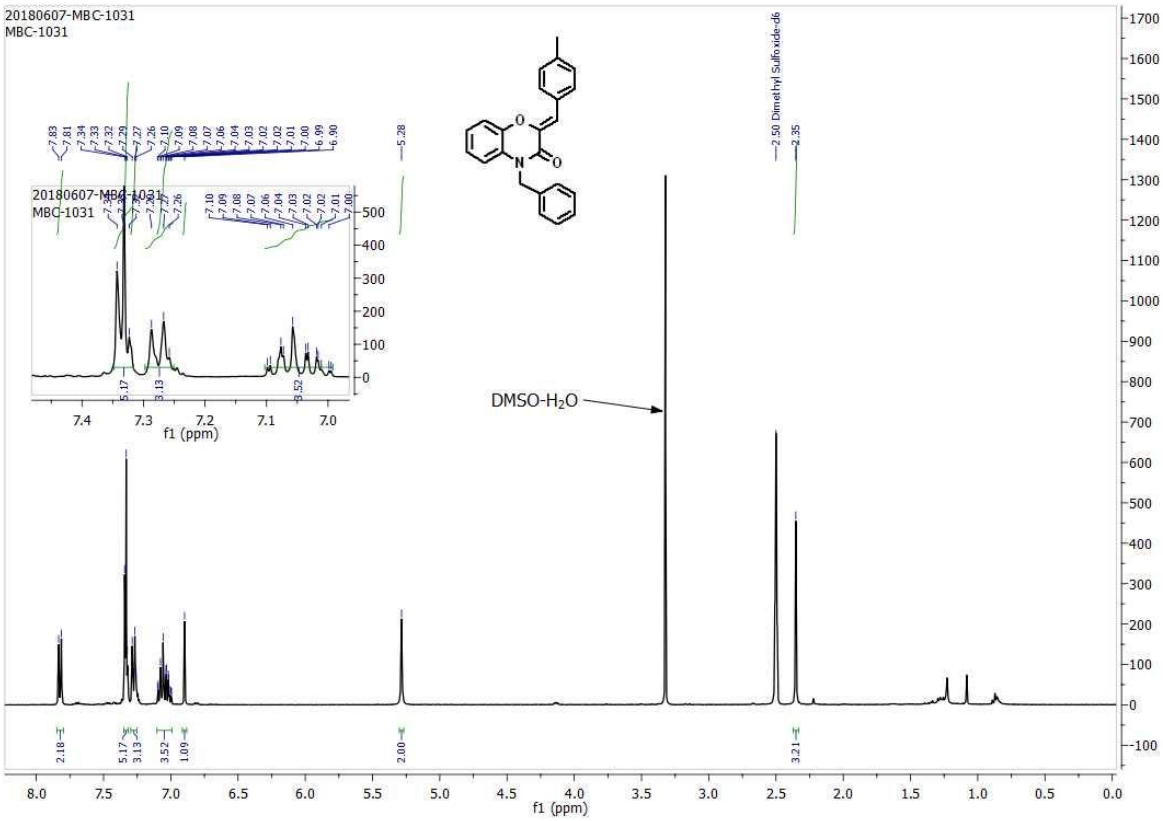

Figure 4A.27. ^{1}H NMR of compound **2n**

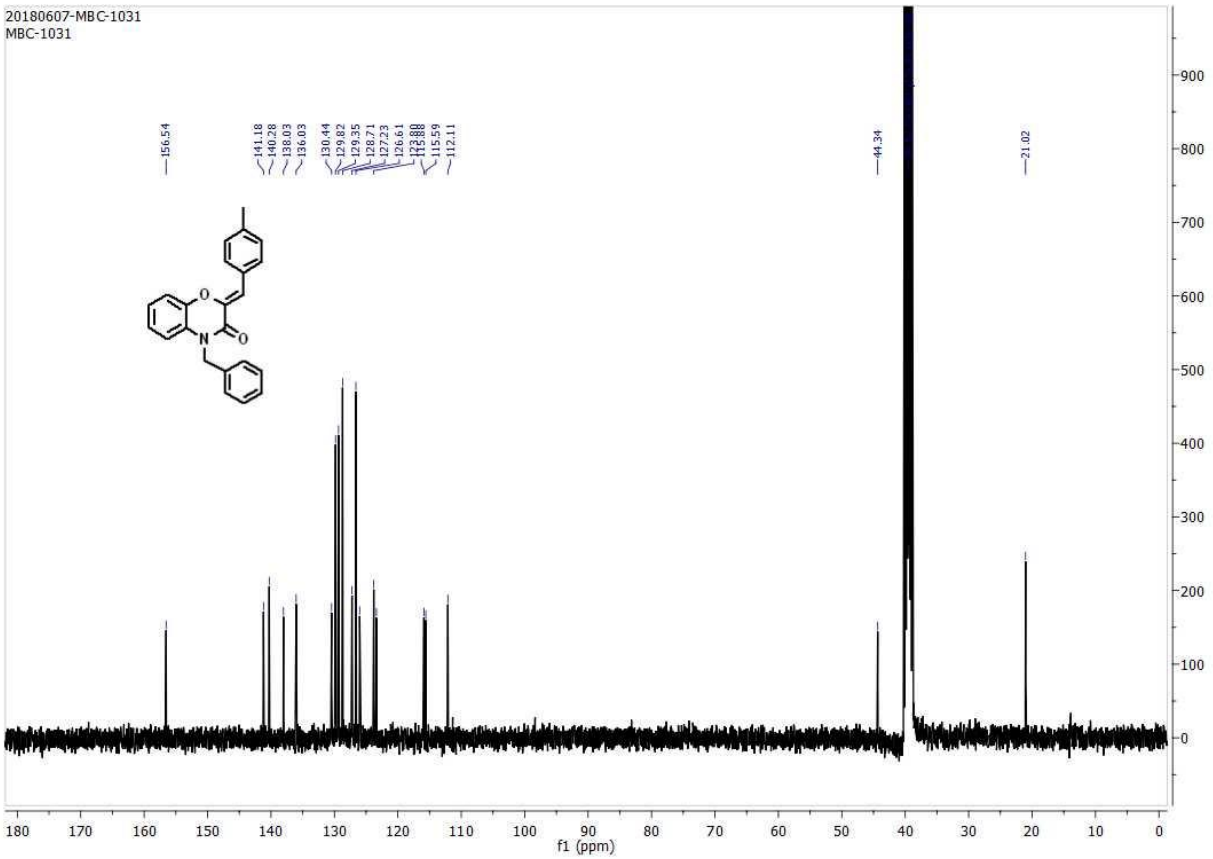

Figure 4A.28. ^{13}C NMR of compound **2n**

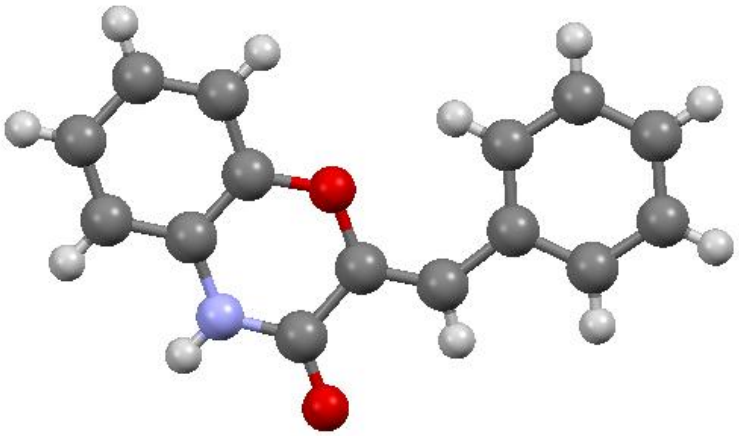

Figure 4A.29. Single crystal structure for compound **2a**

4A.9. References

(1) (a) *Molecular Rearrangements in Organic Synthesis*, ed by Christian M. Rojas, John Wiley & Sons. Inc., Hoboken, New Jersey, **2015**. (b) Moulay, S. *Chem. Educ. Res. Pract*. **2002**, *3*, 33.

(2) Yaremenko, I. A.; Vil', V. A.; Demchuk, D. V.; Terent'ev, A. O. *Beilstein J. Org. Chem.* **2016**, *12*, 1647.

(3) Hock, H.; Lang, S. *Ber*. **1944**, *77*, 257.

(4) (a) Brinkhorst, J.; Nara, S. J.; Pratt, D. A. *J. Am. Chem. Soc.* **2008**, *130*, 12224. (b) Yin, H.;. Xu, L; Porter, N. A. *Chem. Rev.* **2011**, *111*, 5944. (c) Spickett, C. M. *Redox Bio.* **2013**, *1*, 145. (d) Grechkin, A. N.; Brühlmann, F.; Mukhtarova, L. S.; Gogolev, Y. V.; Hamberg, M. *Biochim. Biophys. Acta*. **2006,** *1761*, 1419. (e) Mita, G.; Quarta, A.; Fasano, P.; De Paolis, A.; Di Sansebastiano, G. P.; Perrotta, C.; Iannacone, R.; Belfield, E.; Hughes, R.; Tsesmetzis, N.; Casey, R.; Santino, A. *J. Exp. Bot.* **2005**, *56*, 2321.

(5) (a) Yablokov, V. A. *Russ. Chem. Rev.* **1980**, *49*, 833. (b) Yaremenko, I. A.; Vil', V. A.; Demchuk, D. V.; Terent'ev, A. O. *Beilstein J. Org. Chem.* **2016**, *12*, 1647.

(6) (a) Murahashi, S.-I.; Naota, T.; Miyaguchi, N.; Noda, S. *J. Am. Chem. Soc.* **1996,** *118*, 2509. (b) Terent'ev, A. O.; Platonov, M. M.; Kashin, A. S.; Nikishin, G. I. *Tetrahedron* **2008,** *64*, 7944. (c) Zheng, X.; Lu, S.; Li, Z. *Org. Lett*. **2013**, *15*, 5432. (d) Klare, H. F. T.; Goldberg, A. F. G.; Duquette, D. C.; Stoltz, B. M. *Org. Lett.* **2017**, *19*, 988.

(7) (a) Baeyer, A.; Villiger, V. *Ber. Dtsch. Chem. Ges.* **1899**, *32*, 3625. (b) Baeyer, A.; Villiger, V. *Ber. Dtsch. Chem. Ges.* **1900**, *33*, 858. (c) "The Baeyer–Villiger Oxidation of Ketones and Aldehydes": Krow, G. R. in *Organic Reactions, Vol. 43* (Ed.:L. A. Paquette), Wiley, NewYork, 1993, pp. 251 –79. (d) Vil, V. A.; dos P. Gomes, G.; Bityukov, O. V.; Lyssenko, K. A.; Nikishin, G. I.; Alabugin, I. V.; Terent'ev, A. O. *Angew. Chem. Int. Ed.* **2018**, *57*, 3372. (e) Zhou, L.; Liu, X.; Ji, J.; Zhang, Y.; Hu, X.; Lin, L.; Feng, X. *J. Am. Chem. Soc*. **2012**, *134*, 17023. (f) Strukul, G. *Angew. Chem. Int. Ed.* **1998**, *37*, 1198. (g) Wang, Z. Baeyer–Villiger Oxidation. *Comprehensive Organic Name Reactions and Reagents;* John Wiley & Sons, 2010; pp 150–155

(8) (a) Criegee, R. *Justus Liebigs Ann. Chem.* **1948**, *560*, 127. (b) Davies, A. G. "*Organic Peroxides*," Butterworths, London, **1961**. (c) Ogibin, Y. N.; Terent'ev, A. O.; Kutkin, A. V.; Nikishin, G. I. *Tetrahedron Lett*. **2002**, *43*, 1321. (d) Schweitzer-Chaput, B.; Kurtén, T.; Klussmann, M. *Angew. Chem. Int. Ed*. **2015**, *54*, 11848.

(9) Kornblum, N.; DelaMare, H. E. *J. Am. Chem. Soc*. **1951**, *73*, 880.

(10) Turk, C. F.; Krapcho, J.; Michel, I. M.; Weinryb, I. *J. Med. Chem.* **1977**, *20*, 729.

(11) Honda, T.; Terao, T.; Aono, H.; Ban, M . *Bioorg. Med. Chem.* **2009**, *17*, 699.

(12) Ankati, H.; Akubathini, S. K.; D'Mello, S. R.; Biehl, E. R. *Synth. Commun*. **2010**, *40*, 2364.

(13) Kraus, G. A.; Fulton, B. S. *J. Org. Chem*. **1985**, *50*, 1784.

(14) Gomez-Gallego, M.; Sierra, M. A. *Chem. Rev.* **2011**, *111*, 4857.

(15) (a) Chan, C.-K.; Chen, Y.-H.; Chang, M.-Y. *Tetrahedron* **2016**, *72*, 5121. (b) Chan, C.-K.; Wang, H.-S.; Tsai, Y.-L.; Chang, M.-Y. *RSC Adv.* **2017**, *7*, 29321.
(16) For rearrangements, see: (a) Xu, G.-C.; Liu, L.-P.; Lu, J.-M.; Shi, M. *J. Am. Chem. Soc*. **2005**, *127*, 14552. (b) Xu, G.-C.; Ma, M.; Liu, L.-P.; Shi, M. *Synlett*, **2005**, 1869. (c) Lambert, T. H.; MacMillan, D. W. C. *J. Am. Chem. Soc*. **2002**, *124*, 13646. (d) Kranz, D. P.; zu Greffen, A. M.; Sheikh, S. E.; Neudörfl, J. M.; Schmalz, H.-G. *Eur. J. Org. Chem*. **2011**, 2860.
(17) For C-O and O-O bond cleavage, see: (a) Olah, G. A.; Parker, D. G.; Yoneda, N.; Pelizza, F. *J. Am. Chem. Soc.* **1976**, *98*, 2245. (b) Olah, G. A.; Parker, D. G.; Yoneda, N. *Angew. Chem. Int. Ed. Engl*. **1978**, *17*, 909. (c) L. Liguori, Bjørsvik, H.-R.; Fontana, F.; Bosco, D.; Galimberti, L.; Minisci, F. *J. Org. Chem.* **1999**, *64*, 8812.

Chapter 4

Section B:

Domino Rearrangement of Peroxides for the Ring Expansion Enabled by Catalytic Dual Activation of Esters and Peroxides

4B. Domino Rearrangement of Peroxides for The Ring Expansion Enabled by Catalytic Dual Activation of Esters and Peroxides

4B.1. Abstract

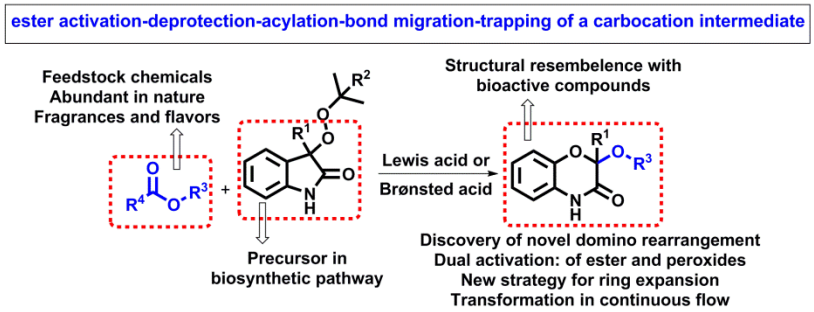

In this chapter, we have reported the Sn-catalyzed novel ring expansion strategy *via* rearrangement of peroxides to produce the substituted-2*H*-benzo[*b*][1,4]oxazin-3(4*H*)-one derivatives. The present rearrangement reaction proceeds via *in situ* generations of perester from peroxides. The peresters are generated by employing naturally abundant feedstock chemicals such as esters. A possible mechanism has been proposed based on labeling and spectroscopic studies. Overall, present rearrangement reaction proceeds *via* five elementary steps: ester activation-deprotection-acylation-bond migration-trapping of a carbocation intermediate in a domino fashion.

Introduction and literature background on rearrangement reactions of peroxides

The introduction and literature background on the rearrangement of peroxides is discussed in section 4A.2 of chapter 4.

4B.2. The rationale of present work

In the Poaceae (family of a plant), 2-oxindole exhibits an important role in the biosynthesis of cyclic hydroxamic acids. The 1,4-benzoxazin-3-one scaffolds are the secondary metabolites of grasses and play a crucial role in the biosynthetic pathway of the plant defense process by means of synthesizing the anti-insecticidal compounds. In particular, 2,4-dihydroxy-7-methoxy-1,4-benzoxazin-3-one (DIMBOA) mostly found in wheat and maize, whereas 2,4-dihydroxy-1,4-benzoxazin-3-one (DIBOA) is observed in the rye (Figure 4B.1).). [1] Moreover, the unique structure of 1,4-benzoxazin-3-ones shows resemblance with biologically important molecules (Figure 4B.2). [2] In this context, the peroxyindole can be employed as a precursor for the ring

expansion reaction to synthesize the substituted-2*H*-benzo[*b*][1,4]oxazin-3(4*H*)-one derivatives.

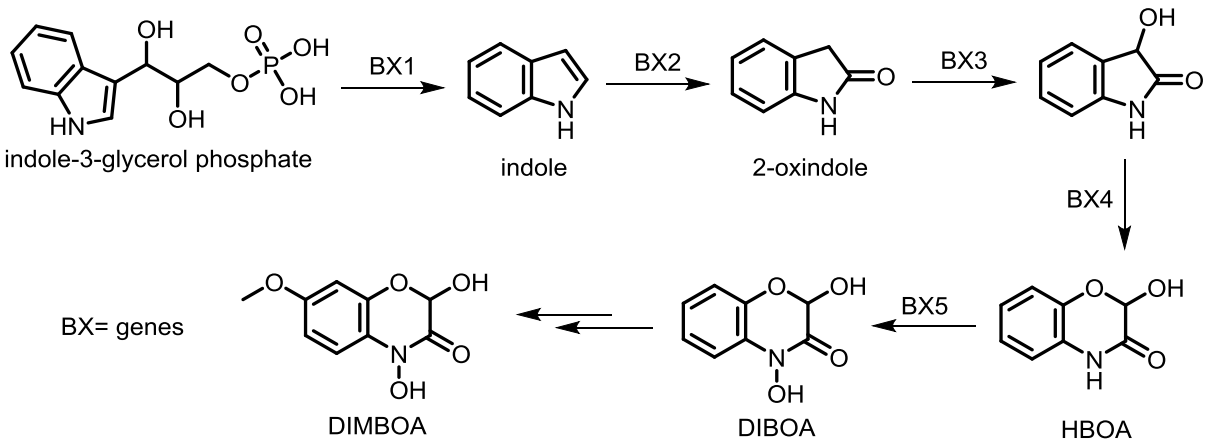

Figure 4B.1. Biosynthetic pathway for the synthesis of HBOA, DIBOA, and DIMBOA

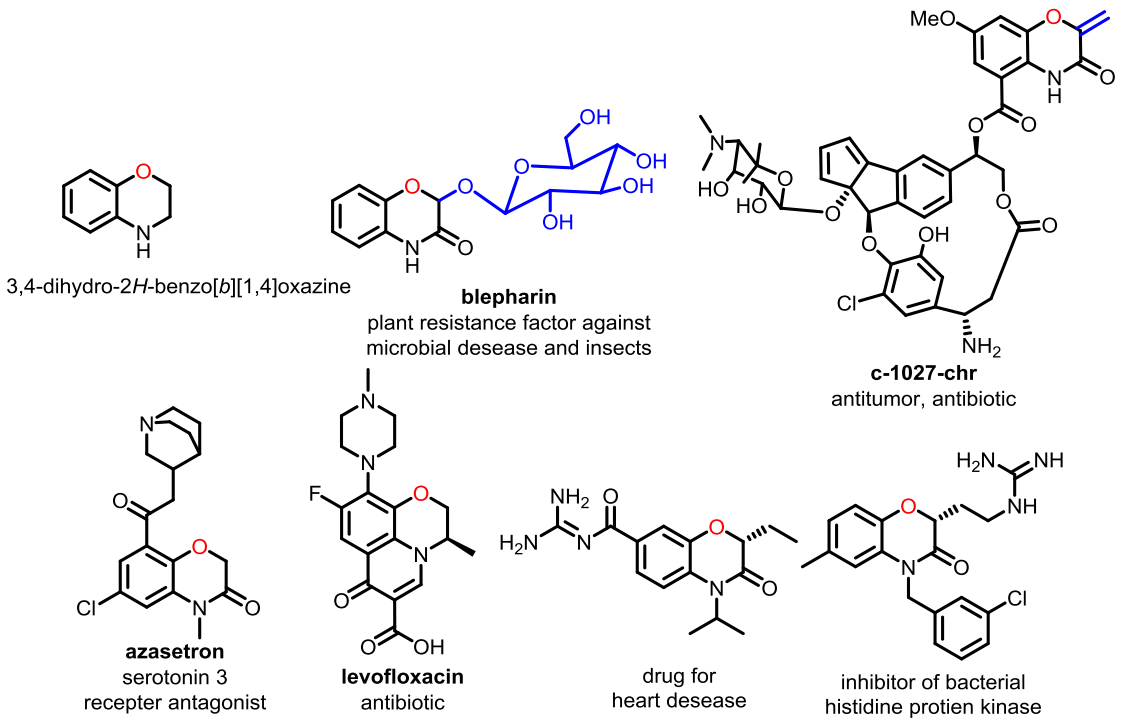

Figure 4B.2. Bioactive compounds having benzo-[1,4]oxazine core

In the literature variety of rearrangements were reported in the past decades.[3] The most studied rearrangements involve the peroxide moiety.[4-7] In particular, the rearrangement of peroxyindoles has also been reported.[8a] By keeping this in mind, we inspired to develop a biomimetic metal-catalyzed approach for rearrangement reaction to offer the ring expansion product. Thus we have used esters as a source of acyl group as they are feedstock chemicals. Next, the Sn was chosen as a catalyst for dual

activation of esters as well as peroxides. In the course of our reaction, we envisioned the migration of a bond from C3-C3a to electron-deficient oxygen to generate the carbocation and its trapping the *in situ* formed alkoxy group.

4B.3. Results and discussion

4B.3.1. Optimization studies

Based on our previous work (Chapter 4A), which involves the synthesis of (Z)-2-arylidene and alkylidene-2*H*benzo[*b*][1,4]oxazin-3(4*H*)-one derivatives starting from peroxyindoles. The previous research finding involves the rearrangement in the presence of Sn or Amberlyst-15; this is attributed to the construction of a more stable C-O bond through shifting of C(3)-C(3a) bond on weak O-O bond.[9] During this process, the carbocation is generated, which was stabilized by the deprotonation of an adjacent proton to it. Principally, the presence of -CH_2- group is necessary for ring expansion to occur. Interestingly, if we replace the -CH_2- group with CH_3- group, then this rearrangement does not occur. Thus we were interested in manipulating the reactivity of 3-hydroperoxy-3-methylindolin-2-one with alkyl or phenyl substituents and trapping of carbocation by means of nucleophile/alkoxide using rearrangement reaction. We have commenced our investigation by taking 3-(*tert*-butylperoxy)-3-methylindolin-2-one as a model substrate and a variety of metals (Table 4B.1).

In the initial control experiments, the reaction of peroxide **4** and ethyl acetate in the absence of catalyst at rt and at 80 ^oC was tested, which does not afford any product formation (Table 4B.1, entries 1 and 2). The use of $Cu(OTf)_2$ at 60 ^oC was not effective for this rearrangement reaction (Table 4B.1, entry 3). The other metal triflates such as $Sc(OTf)_3$, Ag(OTf), and $Sn(OTf)_3$ afforded 24%, 0%, and 89% yield of **6a** respectively at 60 ^oC (Table 4B.1, entry 4, 5, and 9). However, the $FeCl_3$ afforded a 45% yield of the rearranged product **6a** in 53 h. Increasing the temperature from 60 ^oC to 80 ^oC, a decrease in the yield of a product **6a** was observed in the presence of $Sn(OTf)_2$ (Table 4B.1, entry 10). Next, we have tested the equiv of ethyl acetate for this transformation. The use of THF as a solvent and 2 equiv of ethyl acetate produced **6a** in 15% yield (Table 4B.1, entry 11). Similarly, the use of 10 equiv of ethyl acetate produced **6a** in 24% yield (Table 4B.1, entry 12). To our delight, this reaction can be achieved by using Amberlyst-15 as a source of the proton, which afforded product **6a** in 85% yield (Table 4B.1, entry 13).

Table 4B.1. Optimization for the rearrangement of peroxide

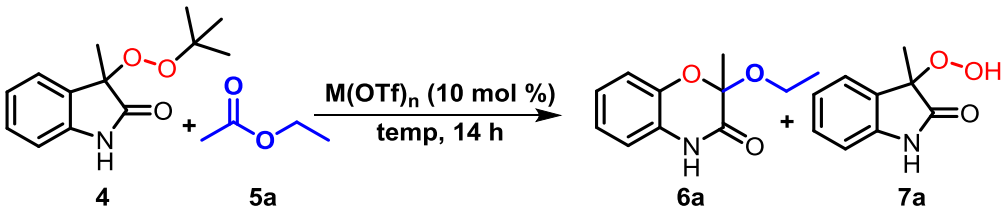

Entry	Catalyst	Temp in ^{o}C	Yield [%] 4:6a:7a
1	none	rt	no reaction
2	none	80	no reaction
3	$Cu(OTf)_2$	60	00:00:00
4	$Sc(OTf)_3$	60	55:24:traces
5	Ag(OTf)	60	no reaction
6[b]	$FeCl_3$	60	00:45:38
7	$Pd(TFA)_2$	60	no reaction
8	$Sn(OTf)_2$	rt	08:58:27
9	$Sn(OTf)_2$	60	00:89:09
10	$Sn(OTf)_2$	80	00:62:10
11[c]	$Sn(OTf)_2$	60	00:15:70
12[d]	$Sn(OTf)_2$	60	00:24:62
13[e]	Amberlyst-15	60	00:85:10

[a)]**Reaction conditions**: All reactions were carried out at 50 mg of **4a** in ethyl acetate (1 mL) using 10 mol % of catalyst at a specified temperature for 14 h in a re-sealable tube. [b)]heated for 53 h, [c)]THF was used a solvent and added 2 equiv of ethyl acetate, [d)]THF was used a solvent and added 10 equiv. of ethyl acetate, [e)](w/w ratio x 2) of substrate/Amberlyst®-15 was taken. The mentioned yields are isolated yields.

4B.3.2. Substrate scope for novel rearrangement of peroxide

After getting the best-optimized condition, we moved to show the generality of this protocol. The reaction underwent very smoothly, and a variety of fragrances, flavoring agents, and solvents were utilized as a source of the acyl group. The commonly and commercially available esters such as ethyl acetate (**5a**), methyl acetate (**5b**), propyl acetate (**5c**), butyl acetate (**5d**), pentyl acetate (**5e**), 2-ethylhexyl acetate (**5f**), octyl acetate (**5g**) and 2-ethoxy ethyl acetate (**5h**) were smoothly reacted with 3-(*tert*-butylperoxy)-3-methylindolin-2-one (**4a)** to produce rearranged products **6a-6h** in good to excellent yield (Table 4B.2).

Table 4B.2. Substrate scope for the rearrangement of peroxides

Starting material	Ester	Product	Yield	Starting Material	Ester	Product	Yield
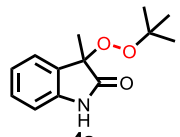 4a	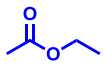 5a	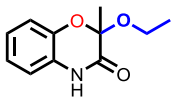 6a	89				
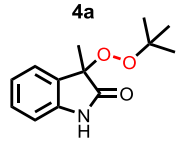 4a	 5b	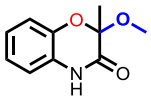 6b	82	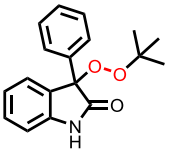 4b	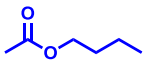 5d	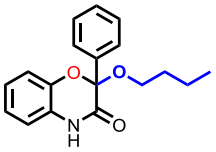 6k	81
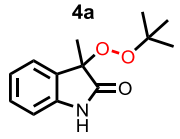 4a	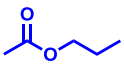 5c	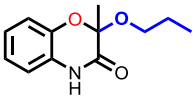 6c	70	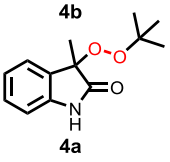 4a	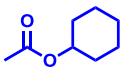 5i	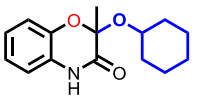 6l	37
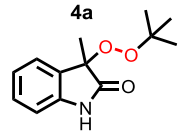 4a	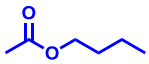 5d	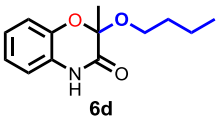 6d	73	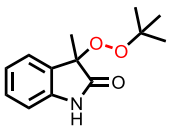 4a	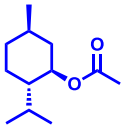 5j	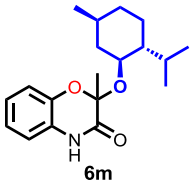 6m	19
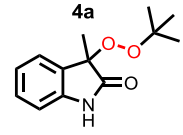 4a	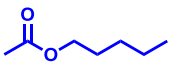 5e	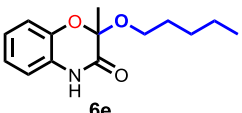 6e	72	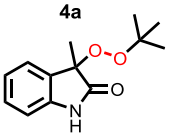 4a	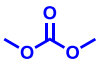 5k	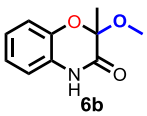 6b	49
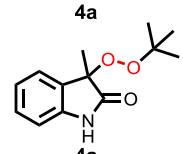 4a	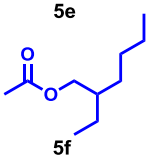 5f	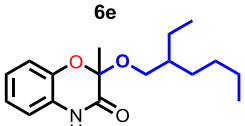 6f[b]	45	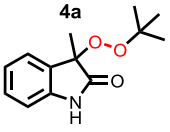 4a	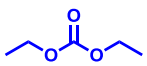 5l	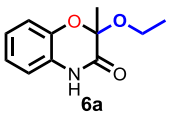 6a	39
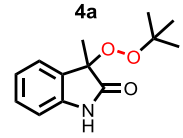 4a	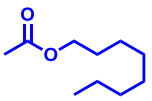 5g	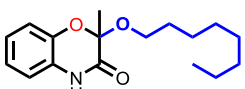 6g	65	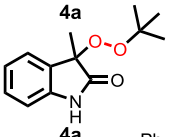 4a	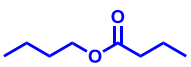 5m	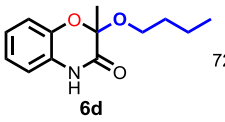 6d	72
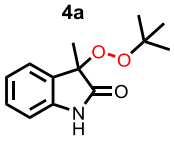 4a	5h	6h	70	4c	5a	6a	94
4b	5a	6i	73	4a	5n	6n	88
4b	5b	6j	90	4a	5o	6o	84

[a]**Reaction Condition:** 0.2 mmol of starting material peroxide **4a-4c**, 10 mol % of $Sn(OTf)_2$ in 1 mL ester (**5a-5o**) was heated at 60 °C for 14 h in re-sealable tube. [b]heated at 80 °C. The mentioned yields are isolated yields.

The ring expansion reaction not only works with the 3-(*tert*-butylperoxy)-3-methylindolin-2-one, but it also works with the 3-(*tert*-butylperoxy)-3-phenylindolin-2-one. In the ester part, the reaction of cyclohexyl acetate and menthyl acetate afforded 37% and 19% yield of the product. The aromatic esters such as benzyl acetate and 3-phenylpropyl acetate delivered ring expansion products **6n** and **6o** in 88 and 84% yield, respectively. Surprisingly, in the NMR spectrum of product **6n**, two types of signals were observed. These signals attributed to the equilibrium form between **6n** and benzyl alcohol. To get a clear understanding, we have confirmed the structure of **6n** and evidenced the structure by single-crystal XRD, NMR, and HRMS. In the case of **6o**, the presence of 3-phenylpropan-1-ol was confirmed by NMR and GC-MS.

4B.3.3. Transformation in a continuous flow

The present reaction works smoothly with heterogeneous acid, Amberlyst-15. Thus we envisioned transforming the batch reaction in a continuous flow.

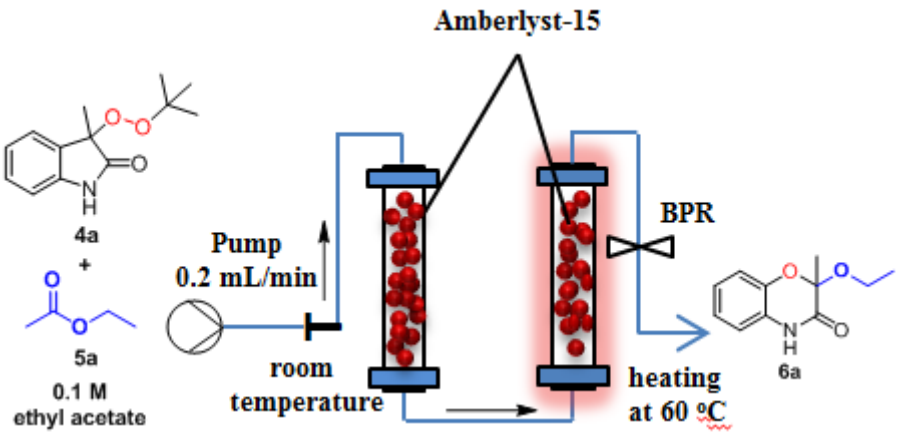

Figure 4B.3. Continuous flow setup for rearrangement reaction

To achieve the ring expansion in a continuous flow, we have used the Vapourtec-R series reactor. To reach a better yield and selectivity (Omnifit®, 6.6 x 150 mm) glass columns were packed with Amberlyst-15 (1 gm). Later, the solution of **4a** (0.1 M) in 5 mL ethyl acetate flowed through the packed bed reactors with the flow rate of 0.2 mL/min to afford rearranged product **6a** in 84% yield with residence time (t_R) = 22 min (Figure 4B.3).

4B.4. Mechanistic investigations

To shed light on the mechanism, the reaction of **4a** and **7a** with ethanol instead of ethyl acetate was performed, in which the desired product **6a** is not observed (Scheme 4B.1, eq 1 and 2). Furthermore, to gain insights into the mechanistic aspects,

the gaseous component of a reaction mixture was subjected to GC-MS analysis and observed *m/e* = 56 owing to the formation of isobutylene gas. Furthermore, the reaction of **4a** with butyl butyrate under standard conditions afforded product **6d** and butanoic acid (detected by GC-MS, *m/e* = 88) (Scheme 4B.1, eq 3 and 4).

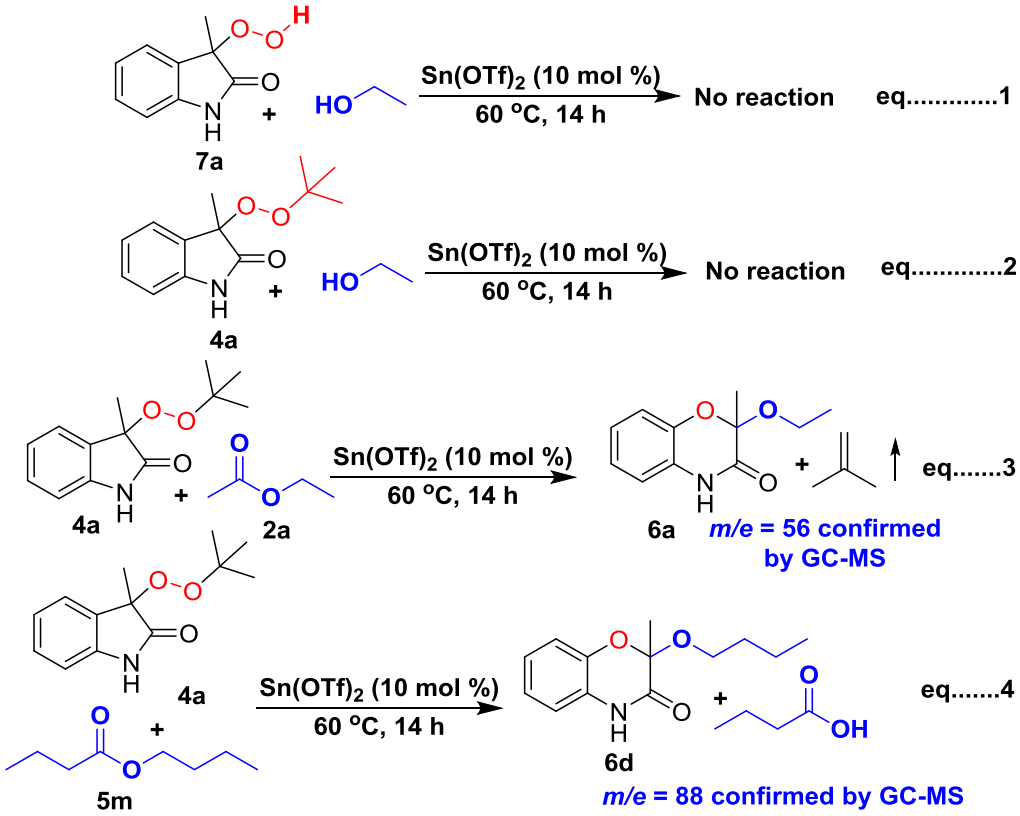

Scheme 4B.1. Experiments for mechanistic studies

Moreover, the reaction of **7a** with ethyl acetate in the presence of $Sn(OTf)_2$ afforded the desired product in 89% yield (Scheme 4B.2, eq 1). Furthermore, 3-methyl-2-oxoindolin-3-yl ethaneperoxoate (**4a'**) was synthesized separately and reacted with ethanol and isotope-labeled methanol (CD_3-OD) under standard conditions; which provided rearranged product **6a** and **6b'** in 80% and 75% yield (Scheme 4B.2, eq 2 and 3). The reaction of **4a** with isotopically labeled acetate (octyl-1,1-*d2* acetate) proceeded smoothly to afford 2-methyl-2-((octyl-1,1-*d2*)oxy)-2*H*-benzo[*b*][1,4]oxazin-3(4*H*)-one (**6g'**) in 72% yield with 64.5 % deuterium incorporation (Scheme 4B.2, eq 4). The above experiments prove that the **4a'** is a key intermediate in this transformation.

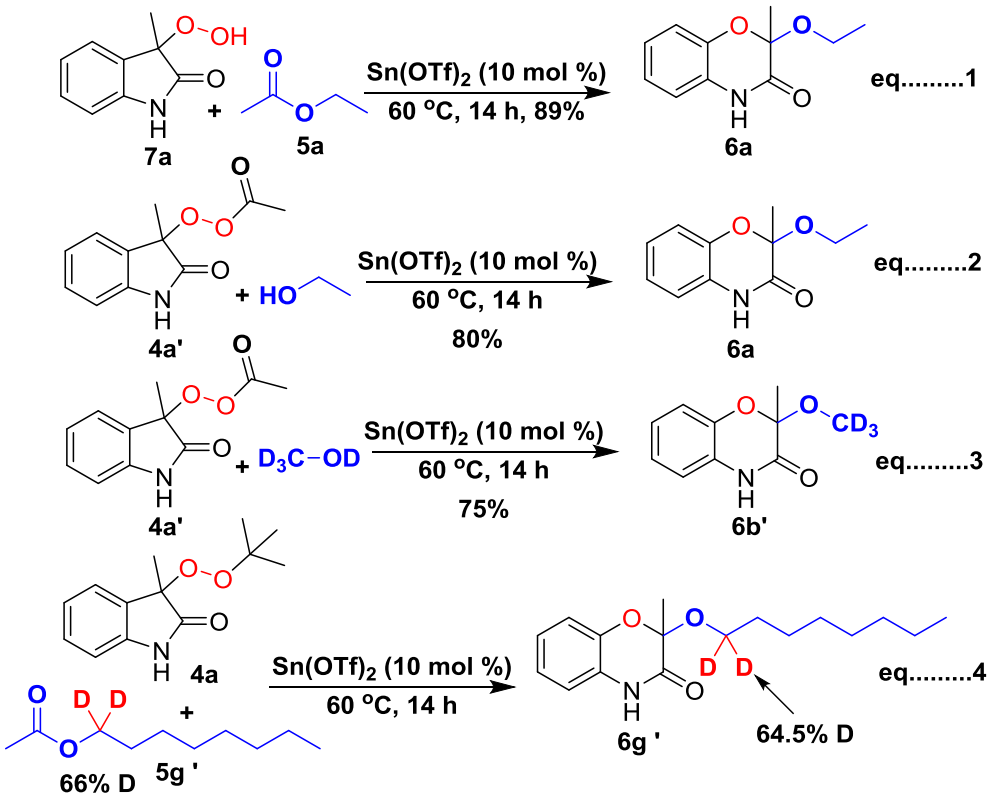

Scheme 4B.2. Experiment for mechanistic studies

4B.4.1. Detection of isobutylene liberation using GC-MS

Accordingly, we have investigated the liberation of isobutylene using GC-MS and found the *m/e*= 56. To perform this reaction, the gaseous component of the reaction mixture was subjected to analysis and the chromatogram was recorded.

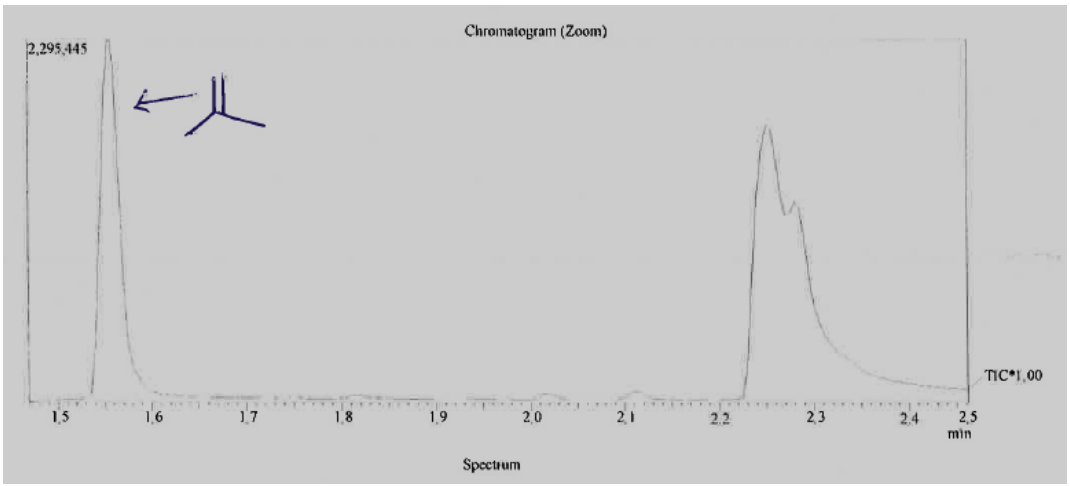

Figure 4B.4. GC-MS spectra of the gaseous phase of the reaction mixture

4B.4.2. Detection of carboxylic acid using GC-MS

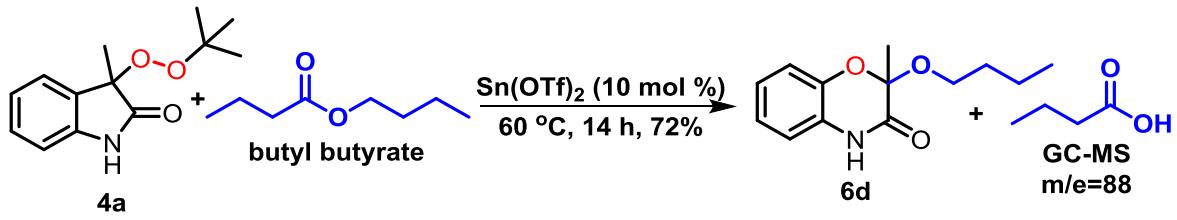

Scheme 4B.3. Evidence for formation of butanoic acid

Furthermore, the reaction of **4a** with butyl butyrate under standard conditions produced product **6d** and butanoic acid (detected by GC-MS, *m/e* = 88). This experiment proves the removal of acid during the reaction.

4B.5. The possible reaction mechanism

The possible reaction mechanism for a novel rearrangement reaction is proposed on the foundation of our experimental results and literature reports (Figure 4B.5).[7g,10] We believe that the present novel rearrangement reaction proceeds in a concerted fashion. Initially, the coordination of $Sn(OTf)_2$ with ester may lead to form the Sn-chelated ester (**B**). On the other hand, the coordination of another molecule of $Sn(OTf)_2$ with peroxide (**D**) assists in the removal of olefin (liberation of isobutylene detected by GC-MS) leads to offer hydroperoxide (**F**). The perester (**G**) is formed by the attack of peroxide (**F**) on chelated ester (**B**). Interestingly, the ring expansion (**H**) is attributed to the formation of stable C-O bond through favorable overlap of donor C(3)-C(3a) σ bond with acceptor O-O σ* orbital. After bond migration, carboxylic acid leaves, and the catalyst is regenerated for the next cycle. During this process, the carbocation (**H**) is generated, which is trapped by an *in situ* formed alkoxy group to afford the rearranged product (**I**). Overall, this concerted reaction involves ester activation-deprotection-acylation-bond migration-trapping of a carbocation in a domino fashion.

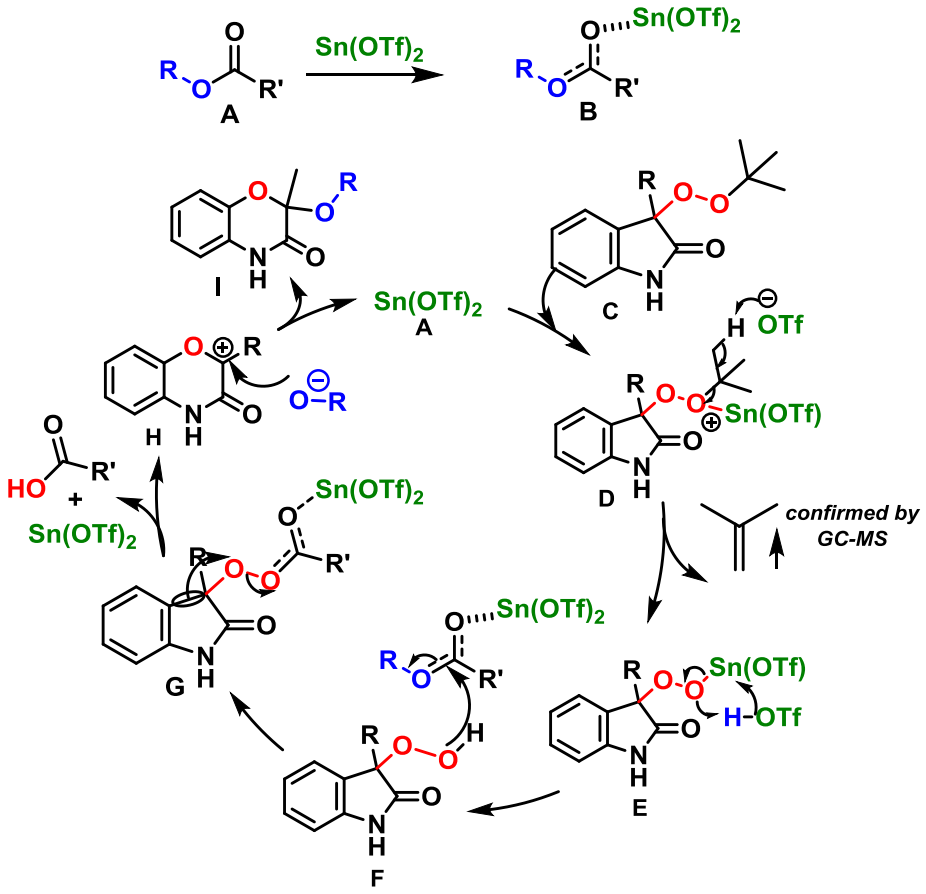

Figure 4B.5. The possible reaction mechanism

4B.6. Conclusion

In summary, we have discovered a novel rearrangement of peroxides for the first, and it is very important for the construction of valuable substituted-2*H*-benzo[*b*][1,4]oxazin-3(4*H*)-one derivatives using mild conditions *via* ester activation-deprotection-acylation-bond migration-trapping of a carbocation in a domino fashion. The *in situ* generations of perester has been achieved by using easily available esters as a source of an acetyl group. Additionally, the carbocation is trapped by an *in situ* generated alkoxy group. Furthermore, we have shown the incorporation of -OCD_3 or –OEt group using $Sn(OTf)_2$ on perester moiety. To show the application in a continuous flow, the heterogeneous version of the rearrangement reaction is developed by integrating the Amberlyst-15 in a continuous flow to obtain the rapid synthesis of ring expanded product in 22 min of residence time.

4B.7. Experimental section and characterization data

4B.7.1. General information and data collection

All the solvents used were dry grade and stored over 4 Å molecular sieves. The acetates were brought from Sigma Aldrich, Rankem, and AVRA chemicals. Deuterated solvents were used as received. Column chromatographic separations performed over 100-200 Silica-gel. Visualization was accomplished with UV light and PMA, CAM stain followed by heating. The Amberlyst-15 (Dry form), $Sn(OTf)_2$, and other metal triflates were purchased from Sigma-Aldrich. The flow chemistry experiments were carried on the Vapourtec R-series. ^1H and ^{13}C NMR spectra were recorded on 400 and 100 MHz, respectively, using a Bruker 400 MHz or JEOL 400 MHz spectrometers. Abbreviations used in the NMR follow-up experiments: b, broad; s, singlet; d, doublet; t, triplet; q, quartet; m, multiplet. High-resolution mass spectra were recorded with Waters- synapt G2 using electrospray ionization (ESI). Fourier-transform infrared (FT-IR) spectra were obtained with a Bruker Alpha-E Fourier transform infrared spectrometer.

4B.7.2. Experimental procedure

A) General experimental procedure for the synthesis of starting material:

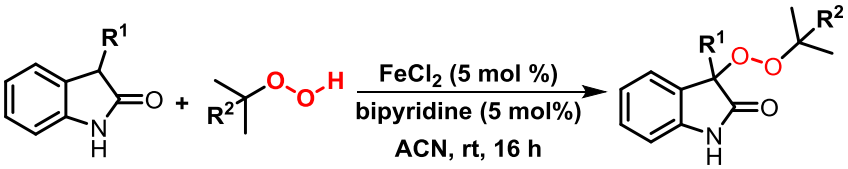

The substituted peroxides were synthesized *via* a procedure reported by Chaudhari[11] *et al.* with little modifications. In a glass vessel, the mixture of iron(II) chloride (5 mol%) and bypyridine ligand (5 mol%) in 2 mL acetonitrile (ACN) was stirred at rt for 20−30 min. To the obtained deep-red solution was added 5.0−6.0 M *tert*-butyl hydroperoxide (TBHP) in decane solution (4 equiv) and finally, respective carbonyl compound (1 equiv) was added, and septum placed over it. The resulting solution was stirred at rt for 16 h without maintaining any special conditions such as the inert atmosphere. After completion of the reaction, a volatile component was evaporated using a vacuum. The residue was directly purified by silica gel chromatography (EtOAc: hexane=15:85 or 20:80).

B) General experimental procedure for the rearrangement reaction using $Sn(OTf)_2$):

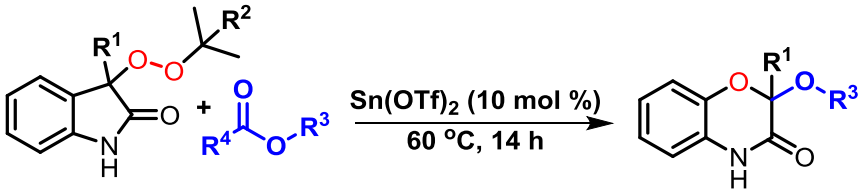

In a 20 mL re-sealable vial (equipped with a stir bar, rubber septum, and N_2 balloon) was added $Sn(OTf)_2$ (10 mol%), acetate (1 mL), and finally, peroxy compound (**4**) (50 mg, 1 equiv). The tube was purged with N_2 and sealed with a cap using a crimper. The reaction mixture was heated at 60 ^oC in an oil bath for 14 h. After 14 h, the volatile component was evaporated using a vacuum and residue was directly purified by silica gel chromatography (EtOAc: hexane= 15:85).

C) Experimental procedure for the rearrangement reaction using Amberlyst-15:

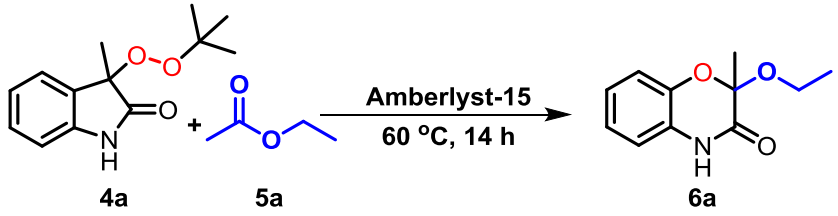

In a 20 mL re-sealable vial (equipped with a stir bar, rubber septum and N_2 balloon) was added Amberlyst-15 (Dry) (100 mg) (substrate to Amberlyst-15 weight ratio of 1:2), ethyl acetate (1 mL), and finally, 3-(*tert*-butylperoxy)-3-methylindolin-2-one (**4a**) (50 mg, 0.21 mmol). The tube was purged with N_2 and sealed with a cap using a crimper. The reaction mixture was heated at 60 ^oC in an oil bath for 14 h. After 14 h, the reaction mixture filtered to remove solid Amberlyst-15. The volatile component was evaporated using a vacuum and residue was directly purified by silica gel chromatography (EtOAc: hexane= 15:85) to afford **6a** (37.5 mg, 85%) as a white solid.

D) Experimental procedure for one mmol scale:

In a 20 mL re-sealable vial (equipped with a stir bar, rubber septum and N_2 balloon) was added $Sn(OTf)_2$ (41.7 mg, 0.1 equiv, 10 mol%), ethyl acetate (4 mL), and finally, 3-(*tert*-butylperoxy)-3-methylindolin-2-one (1 mmol, 235 mg, 1 equiv). The tube was purged with N_2 and sealed with a cap using a crimper. The reaction mixture was heated at 60 ^oC in an oil bath for 14 h. After 14 h, the volatile component was evaporated using a vacuum, and the residue was directly purified by silica gel chromatography (EtOAc: hexane= 15:85) to afford **6a** (170 mg, 82%) as a white solid.

E) Detection of isobutylene gas using GC-MS:

In a 20 mL re-sealable vial (equipped with a stir bar, rubber septum and N_2 balloon) was added $Sn(OTf)_2$ (8.9 mg, 0.1 equiv, 10 mol%), ethyl acetate (1 mL), and finally, 3-(*tert*-butylperoxy)-3-methylindolin-2-one (50 mg, 0.21 mmol, 1 equiv). The tube was purged with N_2 and sealed with a cap using a crimper. The reaction mixture was heated at 60 ^oC in an oil bath for 14 h. After reaction completion, the gaseous component was taken using a gastight syringe and injected into a GCMS instrument. The presence of peak at retention time = 1.55 and m/e = 56 corresponds to *iso*-butylene gas.

F) Evidance for formation of butanoic acid:

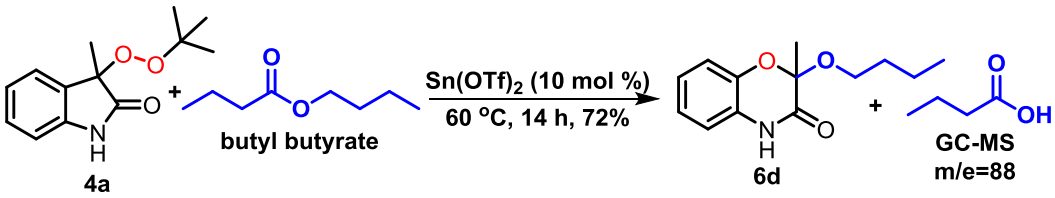

In a 20 mL re-sealable vial (equipped with a stir bar, rubber septum and N_2 balloon) was added $Sn(OTf)_2$ (8.9 mg, 0.1 equiv, 10 mol%), butyl acetate (1 mL), and finally, 3-(*tert*-butylperoxy)-3-methylindolin-2-one (50 mg, 0.21 mmol, 1 equiv). The tube was purged with N_2 and sealed with a cap using a crimper. The reaction mixture was heated at 60 ^oC in an oil bath for 14 h. After reaction completion, the reaction mixture was injected into a GCMS instrument. The presence of a peak at retention time = 8.47 and m/e = 88 corresponds to butanoic acid.

G) Deuteration experiments:

(i) Procedure for the synthesis of octanol-*d3*:

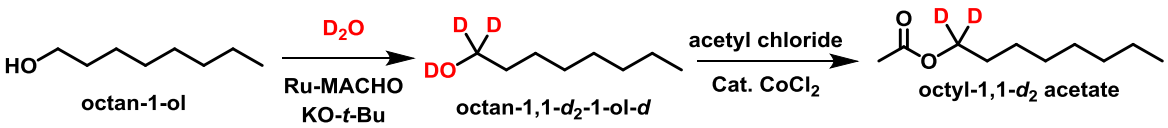

The deuterated beznyl alcohol was prepared by using reported procedure with few modifications by Gunanathan *et al.*[3] In a typical procedure, octanol (7.69 mmol), Ru-MACHO (0.005 mmol), KO-*t*-Bu (0.005 mmol) were charged in a 20 mL resealable vial which was equiped rubber septum and N_2 balloon. The D_2O (3 mL) was added using syringe and reaction mixture purged with N_2 and tube is sealed with cap using crimper and heated at 80 ^oC in a oil bath. The reaction was stopped after 6 h and reaction mixture is extracted with dichloromethane and the combined organic layer is washed with brine solution. The removal of solvent under reduced pressure

provided pure product for further reaction. The ^{1}H NMR data showed 68 % deuterium incorporation for octanol-*d3*.

(ii) Procedure for the synthesis of octyl-1,1-*d2* acetate:

In a typical procedure, octanol-*d3* (1 mL), acetyl chloride (1.2 equiv), $CoCl_2$ (10 mol%) were added in round bottom flask containing 50 mL of DCM; the reaction mixture was stirred at rt until completion. After reaction completion, the reaction mixture was quenched by addition of water. The organic layer was collected and washed with solution of Na_2CO_3. The The volatile component was evoporated using vaccum and crude reaction mixture passed through silica gel column to afford octyl-1,1-*d2* acetate in 71% yield. The ^{1}H NMR data showed 66% deuterium incorporation for octyl-1,1-*d2* acetate (Figure 4B.6).

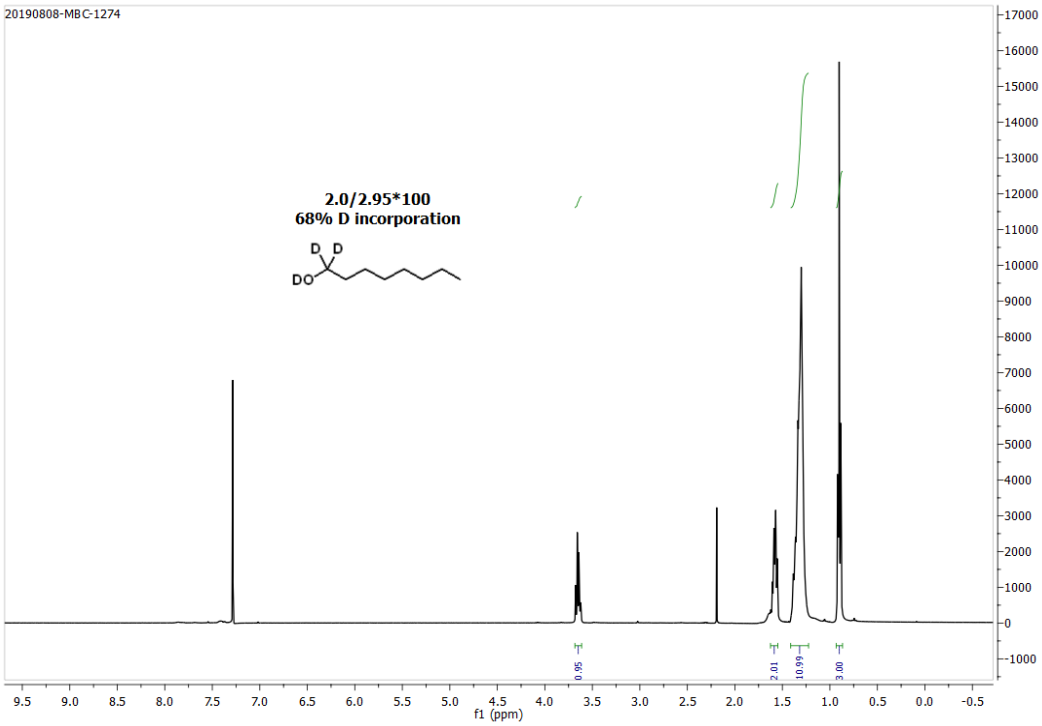

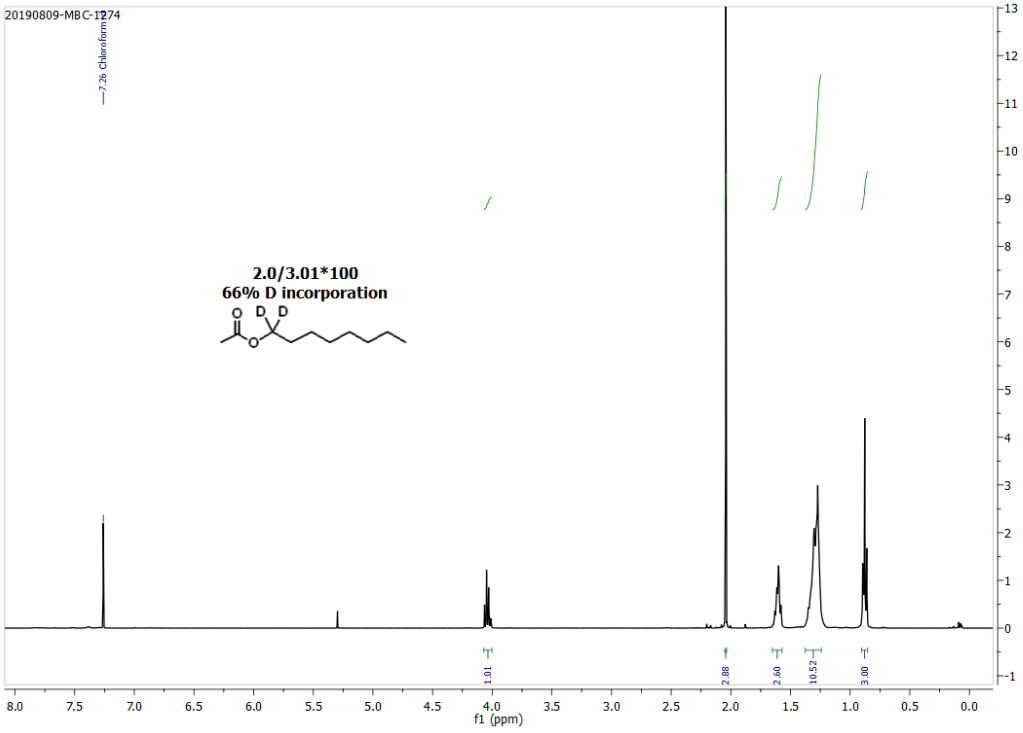

Figure 4B.6. ^{1}H NMR spectrum of octanol-*d3* and octyl-1,1-*d2* acetate (400 MHz, $CDCl_3$)

(iii) Procedure for the synthesis of 2-methyl-2-((octyl-1,1-*d2*)oxy)-2*H*-benzo[*b*][1,4]oxazin-3(4*H*)-one using isotope labeled ester:

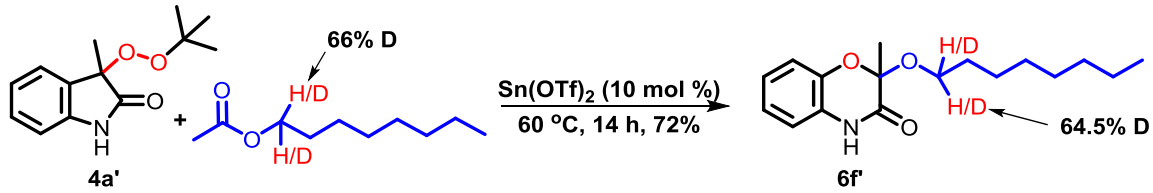

In a 20 mL re-sealable vial (equiped with stirr bar, rubber septum and N_2 balloon) was added $Sn(OTf)_2$ (8.9 mg, 0.1 equiv, 10 mol%), octyl-1,1-*d2* acetate (1 mL), and finally, 3-(*tert*-butylperoxy)-3-methylindolin-2-one (50 mg, 0.21 mmol, 1 equiv). The tube was purged with N_2 and sealed with a cap using crimper. The reaction mixture was heated at 60 ^{o}C in an oil bath for 14 h. The residue was directly purified by silica gel chromatography (EtOAc: hexane= 15:85) to afford **6f'** in 72% yield as a white solid. The ^{1}H NMR data showed 64.5% deuterium incorporation (Figure 4B.7). **HRMS** (ESI) m/z calculated for $C_{17}H_{23}D_2NO_3$ $(M+H)^+$: 294.2038, found: 294.2294.

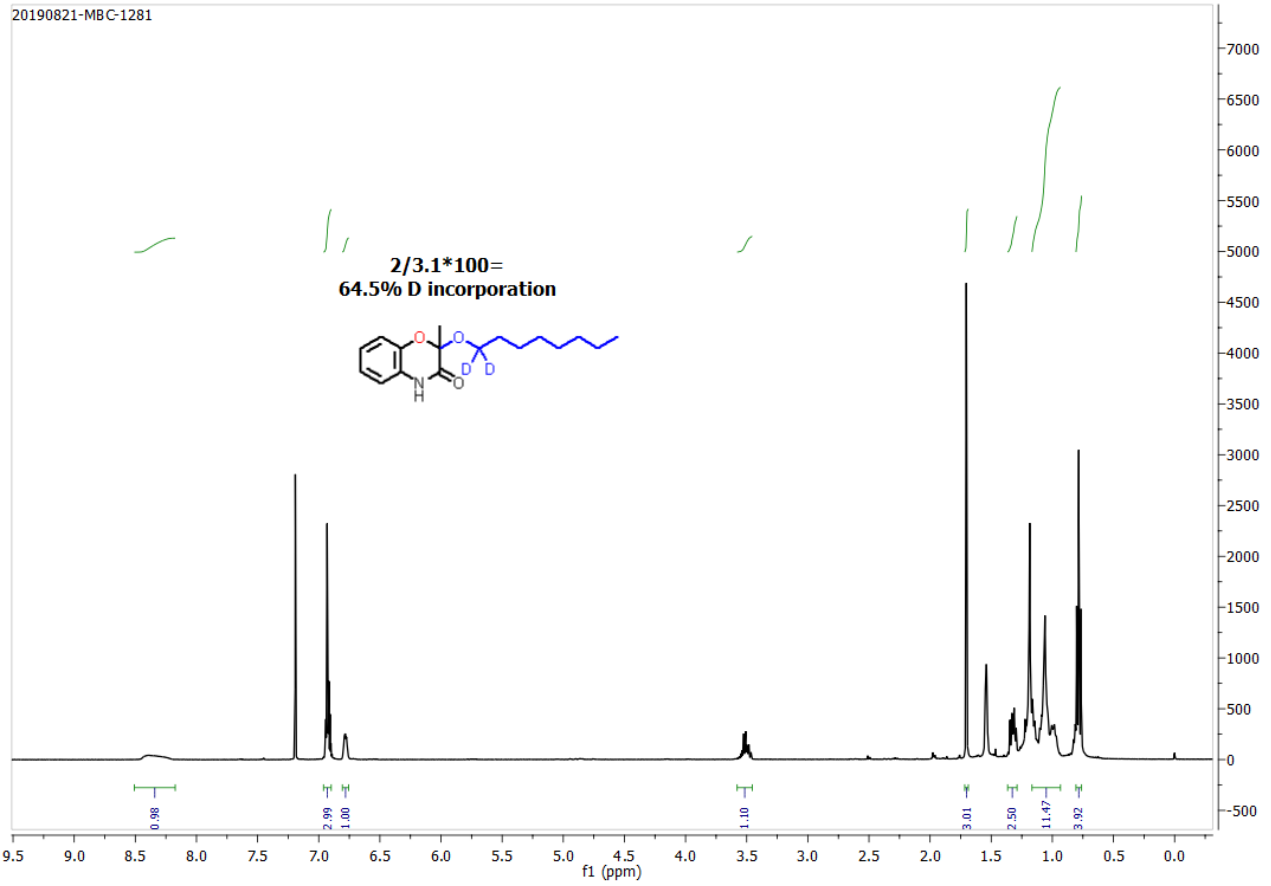

Figure 4B.7. ^{1}H NMR for 2-methyl-2-((octyl-1,1-*d2*)oxy)-2*H*-benzo[*b*][1,4]oxazin-3(4*H*)-one

(iv) Procedure for the synthesis of 2-(methoxy-*d3*)-2-methyl-2*H*-benzo[*b*][1,4]oxazin-3(4*H*)-one using deuterated methanol:

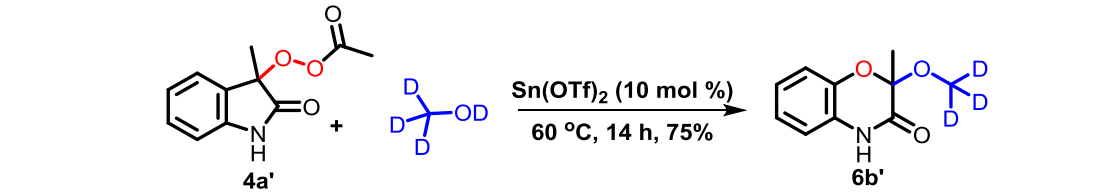

4a'
3-methyl-2-oxoindolin-3-yl ethaneperoxoate

6b'
2-(methoxy-d_3)-2-methyl-2*H*-benzo-[*b*][1,4]oxazin-3(4*H*)-one

In a 20 mL re-sealable vial (equiped with stirr bar, rubber septum and N_2 balloon) was added $Sn(OTf)_2$ (10 mol%), Methanol-*d4* (0.75 mL), and finally, 3-methyl-2-oxoindolin-3-yl ethaneperoxoate (0.18 mmol, 40 mg, 1 equiv). The tube was purged with N_2 and sealed with a cap using crimper. The reaction mixture was heated at 60 ^{o}C in an oil bath for 14 h. After 14 h, volatile component was evaporated using a vacuum and residue was directly purified by silica gel chromatography to afford 2-(methoxy-

d3)-2-methyl-2*H*-benzo[*b*][1,4]oxazin-3(4*H*)-one **6b'** in 75% isolated yield. **HRMS** (ESI) m/z calculated for $C_{10}H_8D_3NO_3$ $(M+H)^+$: 197.1005, found: 197.1001.

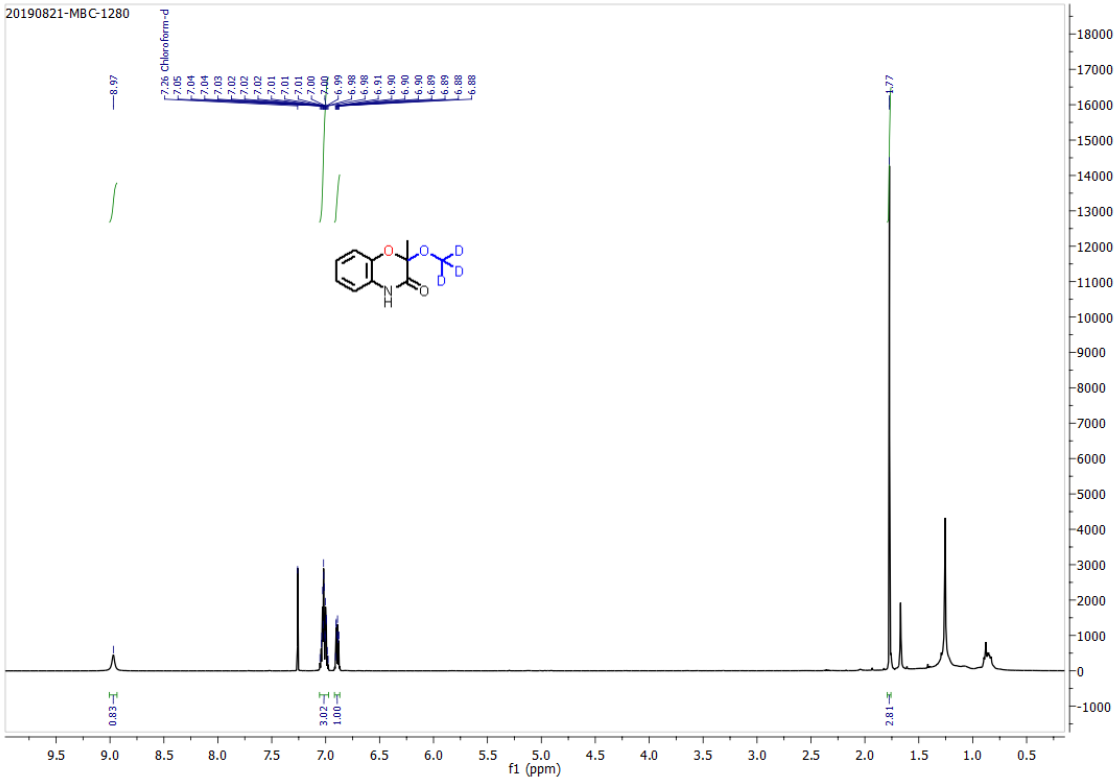

Figure 4B.8. ^{1}H NMR for 2-(methoxy-*d3*)-2-methyl-2*H*-benzo[*b*][1,4]oxazin-3(4*H*)-one

4B.7.3. Spectroscopic data

2-Ethoxy-2-methyl-2*H*-benzo[*b*][1,4]oxazin-3(4*H*)-one (6a): Prepared according to general procedure (B), using 3-(*tert*-butylperoxy)-3-methylindolin-2-one (50 mg, 0.21 mmol) to afford 2-ethoxy-2-methyl-2*H*-benzo[*b*][1,4]oxazin-3(4*H*)-one **6a** (39 mg, 89%) as a whitle solid. 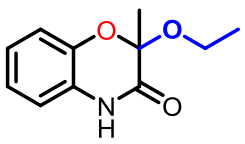
Melting point: 126-128 °C. **^{1}H NMR** (400 MHz, $CDCl_3$): δ 8.84 (bs, 1H), 7.03 – 6.96 (m, 3H), 6.90 – 6.85 (m, 1H), 3.74 – 3.62 (m, 2H), 1.78 (s, 3H), 1.06 (t, *J* = 7.1 Hz, 3H). **^{13}C NMR** (100 MHz, $CDCl_3$) δ 164.7, 141.7, 126.6, 124.1, 122.9, 117.4, 115.7, 99.3, 58.3, 19.6, 15.3. **FTIR** (KBr): 3452, 1712, 1506, 1398, 1246, 1172, 1108, 1046 cm^{-1}. **HRMS** (ESI) m/z calculated for $C_{11}H_{13}NO_3$ $(M+Na)^+$: 230.0793, found: 230.0795.

2-Methoxy-2-methyl-2*H*-benzo[*b*][1,4]oxazin-3(4*H*)-one (6b): Prepared according to general procedure (B), using 3-(*tert*-butylperoxy)-3-methylindolin-2-one (50 mg, 0.21 mmol) to afford 2-methoxy-2-methyl-2*H*-benzo[*b*][1,4]oxazin-3(4*H*)-one **6b** (33.5 mg, 82%) as a whitle solid. 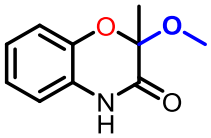
Melting point: 110-112 °C. **^{1}H NMR** (400 MHz, $CDCl_3$): δ 9.28 (bs, 1H), 7.06 – 6.97 (m, 3H), 6.93 – 6.89 (m, 1H), 3.35 (s, 3H), 1.78 (s, 3H).

^{13}C NMR (100 MHz, $CDCl_3$): δ 164.7, 141.5, 126.5, 124.2, 123.0, 117.4, 115.9, 99.3, 49.9, 18.9. **FTIR** (KBr): 3533, 1699, 1506, 1245, 1171, 1109 cm^{-1}. **HRMS** (ESI) m/z calculated for $C_{10}H_{11}NO_3$ $(M+Na)^+$: 216.0637, found: 216.0640.

2-Methyl-2-propoxy-2*H*-benzo[*b*][1,4]oxazin-3(4*H*)-one (6c): Prepared according to general procedure (**B**), using 3-(*tert*-butylperoxy)-3-methylindolin-2-one (50 mg, 0.21 mmol) to afford 2-methyl-2-propoxy-2*H*-benzo[*b*][1,4]oxazin-3(4*H*)-one **6c** (33 mg, 70%) as a whitle solid. **Melting point**: 115-117 °C. **^{1}H NMR** (400 MHz, $CDCl_3$): δ 9.12 (s, 1H), 7.03 – 6.96 (m, 3H), 6.92 – 6.87 (m, 1H), 3.56 (qt, *J* = 8.8, 6.5 Hz, 2H), 1.78 (s, 3H), 1.48 – 1.39 (m, 2H), 0.69 (t, *J* = 7.4 Hz, 3H). **^{13}C NMR** (100 MHz, $CDCl_3$) δ 164.8, 141.7, 126.7 124.0, 122.8, 117.4, 115.7, 99.1, 64.0, 22.9, 19.4, 10.5. **FTIR** (KBr): 3078, 2925, 1714, 1614, 1505, 1398, 1107 cm^{-1}. **HRMS** (ESI) m/z calculated for $C_{12}H_{15}NO_3$ $(M+H)^+$: 222.1130, found: 222.1121.

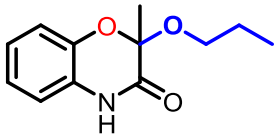

2-Butoxy-2-methyl-2*H*-benzo[*b*][1,4]oxazin-3(4*H*)-one (6d): Prepared according to general procedure (B), using 3-(*tert*-butylperoxy)-3-methylindolin-2-one (50 mg, 0.21 mmol) to afford 2-butoxy-2-methyl-2*H*-benzo[*b*][1,4]oxazin-3(4*H*)-one **6d** (36.5 mg, 73%) as a whitle solid. **Melting point**: 98-100 °C. **^{1}H NMR** (400 MHz, $CDCl_3$): δ 8.98 (bs, 1H), 7.03 – 6.96 (m, 3H), 6.91 – 6.85 (m, 1H), 3.65 – 3.54 (m, 2H), 1.78 (s, 3H), 1.44 – 1.35 (m, 2H), 1.18 – 1.07 (m, 2H), 0.76 (t, *J* = 7.4 Hz, 3H). **^{13}C NMR** (100 MHz, $CDCl_3$): δ 164.7, 141.7, 126.7, 124.0, 122.8, 117.5, 115.6, 99.1, 62.2, 31.6, 19.4, 19.1, 13.8. **FTIR** (KBr): 3407, 3224, 2917, 1714, 1619, 1505, 1398, 1105 cm^{-1}. **HRMS** (ESI) m/z calculated for $C_{16}H_{13}NO_2$ $(M+Na)^+$: 258.1106, found: 258.1110.

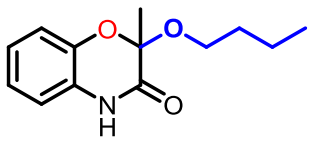

2-Methyl-2-(pentyloxy)-2*H*-benzo[*b*][1,4]oxazin-3(4*H*)-one (6e): Prepared according to general procedure (B), using 3-(*tert*-butylperoxy)-3-methylindolin-2-one (50 mg, 0.21 mmol) to afford 2-methyl-2-(pentyloxy)-2*H*-benzo[*b*][1,4]oxazin-3(4*H*)-one **6e** (38 mg, 72%) as a whitle solid. **Melting point**: 91-92 °C. **^{1}H NMR** (400 MHz, $CDCl_3$): δ 9.50 (bs, 1H), 7.02 – 6.95 (m, 3H), 6.94 – 6.89 (m, 1H), 3.64 – 3.54 (m, 2H), 1.78 (s, 3H), 1.45 – 1.37 (m, 2H), 1.16 (qd, *J* = 7.6, 1.4 Hz, 2H), 1.10 – 1.01 (m, 2H), 0.76 (t, *J* = 7.2 Hz, 3H). **^{13}C NMR** (100 MHz, $CDCl_3$): δ 165.1, 141.7, 126.7, 124.0, 122.8, 117.4, 115.8, 99.0, 62.4, 29.3, 28.1, 22.4, 19.5, 14.0. **FTIR** (KBr): 3452, 2938, 2583, 2363, 1714, 1614, 1504, 1396, 1246, 1102, cm^{-1}. **HRMS** (ESI) m/z calculated for $C_{14}H_{19}NO_3$ $(M+Na)^+$: 272.1263, found: 272.1268.

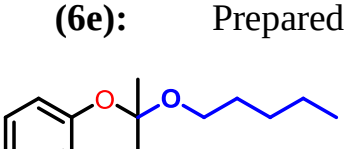

2-((2-Ethylhexyl)oxy)-2-methyl-2*H*-benzo[*b*][1,4]oxazin-3(4*H*)-one (6f): Prepared according to general procedure (B), using 3-(*tert*-butylperoxy)-3-methylindolin-2-one (50 mg, 0.21 mmol) to afford 2-((2-ethylhexyl)oxy)-2-methyl-2*H*-benzo[*b*][1,4]oxazin-3(4*H*)-one **6f** (28 mg, 45%) as a whitle solid. The obtained compound is diastereoisomer and distinguished by ^{13}C NMR. **Melting point**: 67-69 °C. **^{1}H NMR** (400 MHz, $CDCl_3$): δ 8.30 (bs, 1H), 7.03 – 6.96 (m,

3H), 6.88 – 6.81 (m, 1H), 3.51 – 3.42 (m, 2H), 1.78 (s, 3H), 1.34 – 1.28 (m, 1H), 1.17 – 1.00 (m, 8H), 0.83 – 0.76 (m, 3H), 0.73 – 0.67 (m, 3H). (The merging of two triplets in between the range of 0.83-0.76 and 0.73-0.67 ppm in ^{1}H NMR shows the presence of diastereoisomer. By NMR the dr ratio is ~50:50%). **^{13}C NMR** (100 MHz, $CDCl_3$): δ 164.3, 141.7, 126.8, 124.0, 122.8, 117.6, 115.4, 99.05, 64.61, 64.31*, 39.50, 39.48*, 30.40, 30.36*, 29.14, 28.92*, 23.65, 23.61*, 23.06, 23.05*, 19.15, 19.14*, 14.16, 11.16, 11.00*. (The starred peaks in ^{13}C NMR shows the presence of diastereoisomer). **FTIR** (KBr): 3486, 2929, 1693, 1503, 1399, 1242, 1099 cm^{-1}. **HRMS** (ESI) m/z calculated for $C_{17}H_{25}NO_3$ $(M+Na)^+$: 314.1732, found: 314.1733.

2-Methyl-2-(octyloxy)-2*H*-benzo[*b*][1,4]oxazin-3(4*H*)-one (6g): Prepared according to general procedure (B), using 3-(*tert*-butylperoxy)-3-methylindolin-2-one (50 mg, 0.21 mmol) to afford 2-methyl-2-(octyloxy)-2*H*-benzo[*b*][1,4]oxazin-3(4*H*)-one **6g** (40 mg, 65%) as a whitle solid. **Melting point**: 88-90 °C. **^{1}H NMR** (400 MHz, $CDCl_3$): δ 9.35 (bs, 1H), 7.02 – 6.95 (m, 3H), 6.93 – 6.88 (m, 1H), 3.64 – 3.54 (m, 2H), 1.78 (s, 3H), 1.45 – 1.36 (m, 2H), 1.29 – 1.01 (m, 10H), 0.85 (t, *J* = 7.1 Hz, 3H). **^{13}C NMR** (100 MHz, $CDCl_3$): δ 165.0, 141.7, 126.7, 124.0, 122.8, 117.4, 115.8, 99.1, 62.4, 31.9, 29.6, 29.3, 29.3, 26.0, 22.8, 19.4, 14.2. **FTIR** (KBr): 3400, 3168, 2326, 1717, 1620, 1502, 1409, 1102 cm^{-1}. **HRMS** (ESI) m/z calculated for $C_{17}H_{25}NO_3$ $(M+Na)^+$: 314.1732, found: 314.1735.

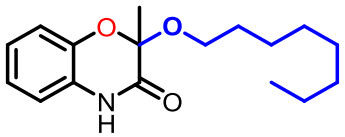

2-(2-Ethoxyethoxy)-2-methyl-2*H*-benzo[*b*][1,4]oxazin-3(4*H*)-one (6h): Prepared according to general procedure (B), using 3-(*tert*-butylperoxy)-3-methylindolin-2-one (50 mg, 0.21 mmol) to afford 2-(2-ethoxyethoxy)-2-methyl-2*H*-benzo[*b*][1,4]oxazin-3(4*H*)-one **6h** (37.5 mg, 70%) as a light yellow semisolid. **Melting point**: 65-67 °C. **^{1}H NMR** (400 MHz, $CDCl_3$): δ 9.42 (bs, 1H), 7.03 – 6.95 (m, 3H), 6.93 – 6.87 (m, 1H), 3.81 – 3.71 (m, 2H), 3.43 (t, *J* = 5.3 Hz, 2H), 3.39 – 3.28 (m, 2H), 1.79 (s, 3H), 1.04 (t, *J* = 7.0 Hz, 3H). **^{13}C NMR** (100 MHz, $CDCl_3$): δ 164.6, 141.5, 126.6, 124.1, 122.9, 117.4, 115.9, 99.1, 69.1, 66.7, 62.0, 19.5, 15.2. **FTIR** (KBr): 3427, 1713, 1609, 1504, 1399, 1259, 1124, 1063 cm^{-1}. **HRMS** (ESI) m/z calculated for $C_{13}H_{17}NO_4$ $(M+Na)^+$: 274.1055, found: 274.1058.

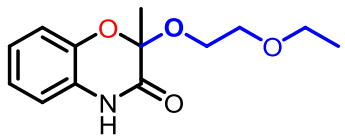

2-Ethoxy-2-phenyl-2*H*-benzo[*b*][1,4]oxazin-3(4*H*)-one (6i): Prepared according to general procedure (B), using 3-(*tert*-butylperoxy)-3-phenylindolin-2-one (50 mg, 0.17 mmol) to afford 2-ethoxy-2-phenyl-2*H*-benzo[*b*][1,4]oxazin-3(4*H*)-one **6i** (33 mg, 73%) as a white solid. **Melting point**: 187-188 °C. **^{1}H NMR** (400 MHz, $CDCl_3$): δ 9.00 (bs, 1H), 7.75 – 7.68 (m, 2H), 7.47 – 7.39 (m, 3H), 7.16 – 7.12 (m, 1H), 7.08 – 6.99 (m, 2H), 6.87 – 6.84 (m, 1H), 3.61 – 3.47 (m, 2H), 1.08 (t, *J* = 7.1 Hz, 3H). **^{13}C NMR** (100 MHz, $CDCl_3$): δ 163.7, 141.5, 135.1, 129.4, 128.2, 127.9, 126.6, 124.2, 123.1, 117.5, 115.8, 100.6, 59.8, 15.2. **FTIR** (KBr): 3369, 2847, 1723, 1630, 1502, 1267 cm^{-1}. **HRMS** (ESI) m/z calculated for $C_{16}H_{15}NO_3$ $(M+Na)^+$: 292.0950, found: 292.0950.

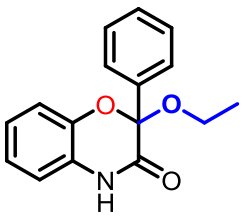

2-Methoxy-2-phenyl-2*H*-benzo[*b*][1,4]oxazin-3(4*H*)-one (6j): 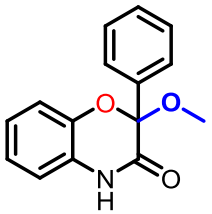
Prepared according to general procedure (B), using 3-(*tert*-butylperoxy)-3-phenylindolin-2-one (50 mg, 0.17 mmol) to afford 2-methoxy-2-phenyl-2*H*-benzo[*b*][1,4]oxazin-3(4*H*)-one **6j** (38.5 mg, 90%) as a white solid. **Melting point**: 178-180 ^{o}C. **^{1}H NMR** (400 MHz, $CDCl_3$): δ 8.6 (bs, 1H), 7.73 – 7.68 (m, 2H), 7.48 – 7.40 (m, 3H), 7.17 (d, *J* = 7.3 Hz, 1H), 7.12 – 7.00 (m, 2H), 6.88 – 6.83 (m, 1H), 3.25 (s, 3H). **^{13}C NMR** (100 MHz, $CDCl_3$): δ 163.3, 141.3, 134.2, 129.5, 128.3, 128.0, 126.6, 124.3, 123.3, 117.7, 115.7, 100.6, 51.1. **FTIR** (KBr): 3420, 3216, 2990, 2856, 1666, 1623, 1506, 1267, 1030 cm^{-1}. **HRMS** (ESI) m/z calculated for $C_{15}H_{13}NO_3$ $(M+Na)^+$: 278.0793, found: 278.0794.

2-Butoxy-2-phenyl-2*H*-benzo[*b*][1,4]oxazin-3(4*H*)-one (6k): Prepared according to general procedure (B), using 3-(*tert*-butylperoxy)-3-phenylindolin-2-one (50 mg, 0.17 mmol) to afford 2-butoxy-2-phenyl-2*H*-benzo[*b*][1,4]oxazin-3(4*H*)-one **6k** (40.5 mg, 81%) as a white solid. **Melting point**: 133-135 ^{o}C. **^{1}H NMR** (400 MHz, $CDCl_3$): δ 8.43 (bs, 1H), 7.73 – 7.69 (m, 2H), 7.47 – 7.41 (m, 3H), 7.15 (dd, *J* = 7.2, 2.1 Hz, 1H), 7.08 – 6.99 (m, 2H), 6.86 – 6.83 (m, 1H), 3.51 – 3.38 (m, 2H), 1.46 – 1.38 (m, 2H), 1.22 – 1.11 (m, 2H), 0.76 (t, *J* = 7.4 Hz, 3H). **^{13}C NMR** (100 MHz, $CDCl_3$): δ 163.4, 141.5, 134.9, 129.4, 128.2, 128.0, 126.6, 124.1, 123.1, 117.7, 115.5, 100.4, 63.5, 31.6, 19.2, 13.8. **FTIR** (KBr): 3425, 3301, 3152, 2959, 2930, 1705, 1622, 1506, 1384, 1252 cm^{-1}. **HRMS** (ESI) m/z calculated for $C_{18}H_{19}NO_3$ $(M+Na)^+$: 320.1263, found: 320.1262.

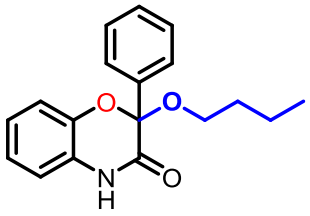

2-(Cyclohexyloxy)-2-methyl-2*H*-benzo[*b*][1,4]oxazin-3(4*H*)-one (6l): Prepared according to general procedure (B), using 3-(*tert*-butylperoxy)-3-methylindolin-2-one (50 mg, 0.21 mmol) to afford 2-(cyclohexyloxy)-2-methyl-2*H*-benzo[*b*][1,4]oxazin-3(4*H*)-one **6l** (20.5 mg, 37%) as a white solid. **Melting point**: 148-150 ^{o}C. **^{1}H NMR** (400 MHz, $CDCl_3$): δ 8.51 (bs, 1H), 7.03 – 6.95 (m, 3H), 6.87 – 6.83 (m, 1H), 3.94 – 3.84 (m, 1H), 1.80 (s, 3H), 1.73 – 1.54 (m, 4H), 1.37 – 1.27 (m, 2H), 1.22 – 1.01 (m, 4H). **^{13}C NMR** (100 MHz, $CDCl_3$): δ 164.4, 141.9, 126.6, 124.0, 122.7, 117.6, 115.6, 99.6, 72.2, 34.3, 33.8, 29.8, 25.5, 24.5, 20.2. **FTIR** (KBr): 3411, 2319, 1714, 1623, 1498, 1402, 1263, 1174 cm^{-1}. **HRMS** (ESI) m/z calculated for $C_{15}H_{19}NO_3$ $(M+Na)^+$: 284.1263, found: 284.1258.

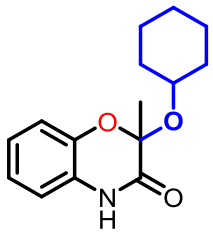

2-(((1S,2R,5S)-2-Isopropyl-5-methylcyclohexyl)oxy)-2-methyl-2*H*-benzo[*b*][1,4]oxazin-3(4*H*)-one (6m): Prepared according to general procedure (B), using 3-(tert-butylperoxy)-3-methylindolin-2-one (50 mg, 0.21 mmol) to afford **2**-(((1S,2R,5S)-2-isopropyl-5-methylcyclohexyl)oxy)-2-methyl-2*H*-benzo[*b*][1,4]oxazin-3(4*H*)-one **6m** (13 mg, 19%) as a white solid. **Melting point**: 109-111 ^{o}C. **^{1}H NMR** (400 MHz, $CDCl_3$): The compound exist in distereomeric form. The ^{1}H NMR values are given for only one type of isomer and marked with **X** in the NMR spectra : δ 8.27 (s, 1H), 7.03 – 6.93

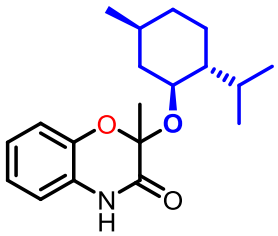

(m, 3H), 6.86 – 6.80 (m, , 1H), 3.74 – 3.63 (m, 1H), 2.08 – 1.97 (m, 2H), 1.84 (s, 3H), 1.60 – 1.53 (m, 3H), 1.12 –0.91 (m, 4H), 0.86 (d, *J* = 6.5 Hz, 6H), 0.72 (d, *J* = 6.9 Hz, 3H). **^{13}C NMR** (100 MHz, $CDCl_3$): Values are for distereomeric mixture δ 164.22, 163.87, 141.84, 126.57, 125.86, 123.91, 123.88, 122.53, 122.47, 117.77, 117.49, 115.53, 115.46, 99.84, 99.63, 74.55, 74.50, 48.54, 47.85, 43.75, 43.03, 34.28, 34.21, 31.78, 31.67, 29.85, 29.81, 25.27, 24.52, 23.34, 23.21, 22.85, 22.41, 21.74, 21.37, 21.18, 19.98, 16.29, 16.16. **FTIR** (KBr): 3361, 2851, 1701, 1506, 1381, 1167 cm^{-1}. **HRMS** (ESI) m/z calculated for $C_{19}H_{27}NO_3$ $(M+Na)^+$: 340.1889, found: 340.1892.

2-(Benzyloxy)-2-methyl-2*H*-benzo[*b*][1,4]oxazin-3(4*H*)-one (6n): Prepared according to general procedure (B), using 3-(*tert*-butylperoxy)-3-methylindolin-2-one (50 mg, 0.21 mmol) to afford 2-(benzyloxy)-2-methyl-2*H*-benzo[*b*][1,4]oxazin-3(4*H*)-one **6n** (50 mg, 88%) as a white solid. The presence of benzyl alcohol was confirmed by GC-MS and NMR.

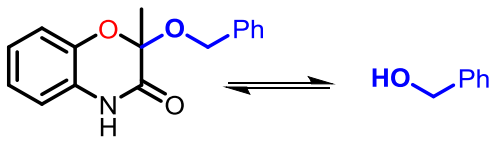

Interestingly, on TLC compound shows single spot but when submitted for NMR, then compound shows two type of protons in NMR. We have assigned one type of protons for rearranged product **6n** and other type of proton belongs to benyzl alcohol. The strucutre of the product **6n** supported by single crystal XRD and HRMS. **Melting point**: 163-165 ^{o}C. **^{1}H NMR** (400 MHz, $CDCl_3$): Values assigned for compound **6n** and benzyl alcohol: δ 8.83 (bs, 1H), 7.39 – 7.35 (m, 4H), 7.33 – 7.27 (m, 1H), 7.23 – 7.19 (m, 3H), 7.10 – 6.98 (m, 5H), 6.89 – 6.84 (m, 1H), 4.70 (s, 2H belongs to benzy alcohol), 4.67 (s, 1H, merged with adjacent peak), 4.65 (d, *J* = 11.1 Hz, 1H), 1.87 (s, 3H). **^{13}C NMR** (100 MHz, $CDCl_3$): Values assigned for compound **6n** and benzyl alcohol: δ 164.2, 141.5, 141.0, 137.1, 128.7, 128.4, 127.8, 127.8, 127.1, 126.7, 124.2, 123.1, 117.5, 115.8, 99.4, 65.5, 64.6, 19.7. **FTIR** (KBr): 3415, 2922, 1697, 1612, 1502, 1393, 1168, 1105 cm^{-1}. **HRMS** (ESI) m/z calculated for $C_{16}H_{15}NO_3$ $(M+Na)^+$: 292.0950, found: 292.0953.

2-Methyl-2-(3-phenylpropoxy)-2*H*-benzo[*b*][1,4]oxazin-3(4*H*)-one (6o): Prepared according to general procedure (B), using 3-(*tert*-butylperoxy)-3-methylindolin-2-one (50 mg, 0.21 mmol) to afford 2-methyl-2-(3-phenylpropoxy)-2*H*-benzo[*b*][1,4]oxazin-3(4*H*)-one **6o** (53 mg, 84%) as a white solid.

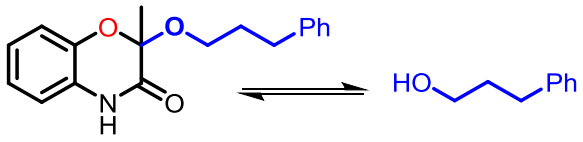

The presence of 3-phenylpropan-1-ol was confirmed by GC-MS and NMR. Interestingly, on TLC compound shows single spot but when submitted for NMR, then compound shows two type of protons in NMR. We have assigned one type of protons for rearranged product **6o** and other type of proton belongs to 3-phenylpropan-1-ol. The strucutre of the product **6o** supported by HRMS data. **Melting point**: 121-123 ^{o}C. **^{1}H NMR** (400 MHz, $CDCl_3$): Values assigned for compound **6o** and 3-phenylpropan-1-ol: δ 8.67 (bs, 1H), 7.32 – 7.27 (m, 2H), 7.24 – 7.24 (m, 6H), 7.18 – 7.12 (m, 1H), 7.04 – 6.98 (m, 5H), 6.89 – 6.86 (m, 1H), 3.69 (t, *J* = 6.4 Hz, 2H), 3.65 – 3.57 (m, 2H), 2.72 (t, *J* = 7.6 Hz, 2H), 2.42 (t, *J* = 7.6 Hz, 2H), 1.94 – 1.87 (m, 2H), 1.78 (s, 3H). **^{13}C NMR** (100 MHz, $CDCl_3$): Values assigned for compound **6o** and 3-

phenylpropan-1-ol: δ 164.3, 141.9, 141.8, 141.6, 128.6, 128.5, 128.5, 128.4, 126.6, 126.0, 125.9, 124.2, 123.0, 117.6, 115.6, 99.1, 62.4, 61.5, 34.4, 32.2, 32.1, 31.1, 19.3. **FTIR** (KBr): 3492, 2925, 2571, 1707, 1616, 1504, 1404, 1244, 1107 cm^{-1}. **HRMS** (ESI) m/z calculated for $C_{18}H_{19}NO_3$ $(M+H)^+$: 298.1443, found: 298.1442.

4B.7.4. Appendix VI: Copies of ^{1}H and ^{13}C NMR spectra of representative compounds

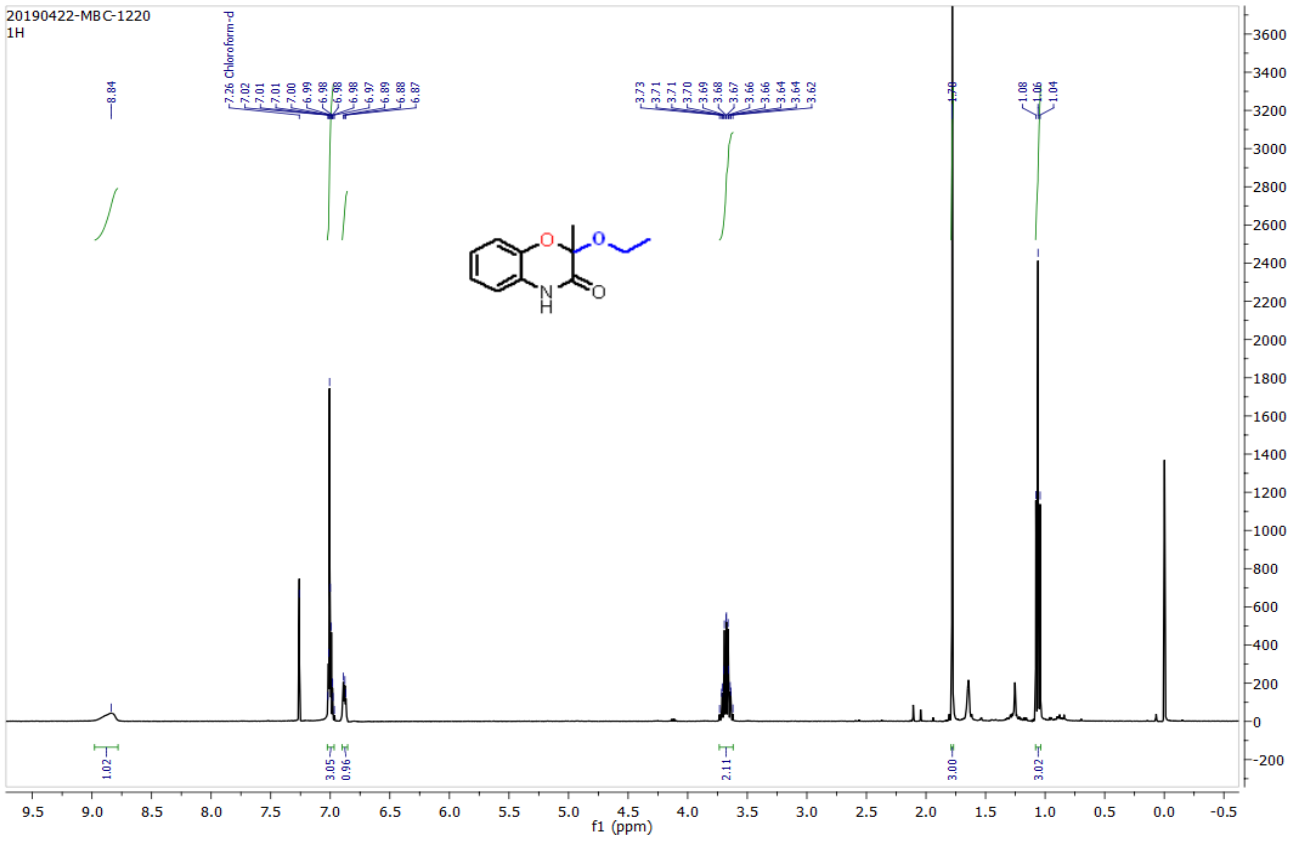

Figure 4B.9. ^{1}H NMR of compound **6a**

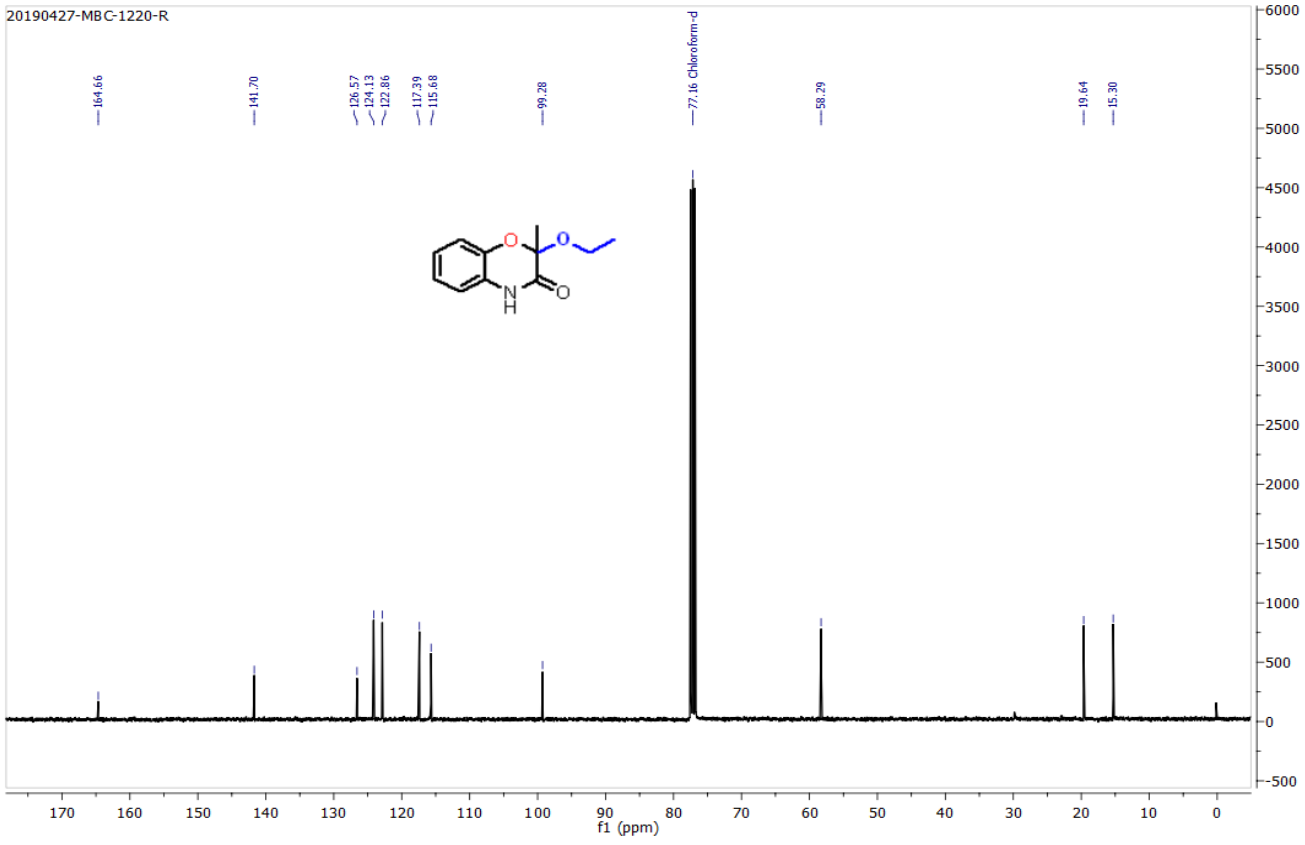

Figure 4B.10. ^{13}C NMR of compound **6a**

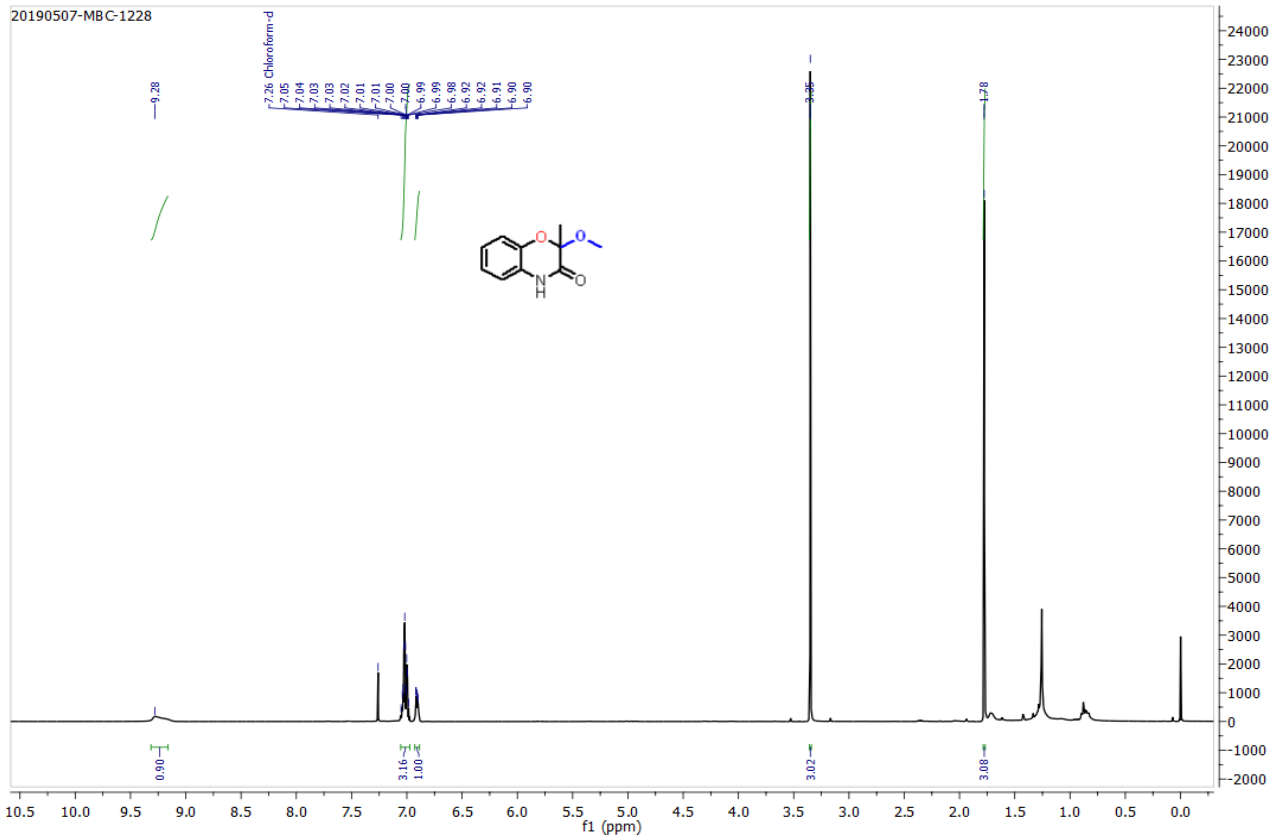

Figure 4B.11. ^{1}H NMR of compound **6b**

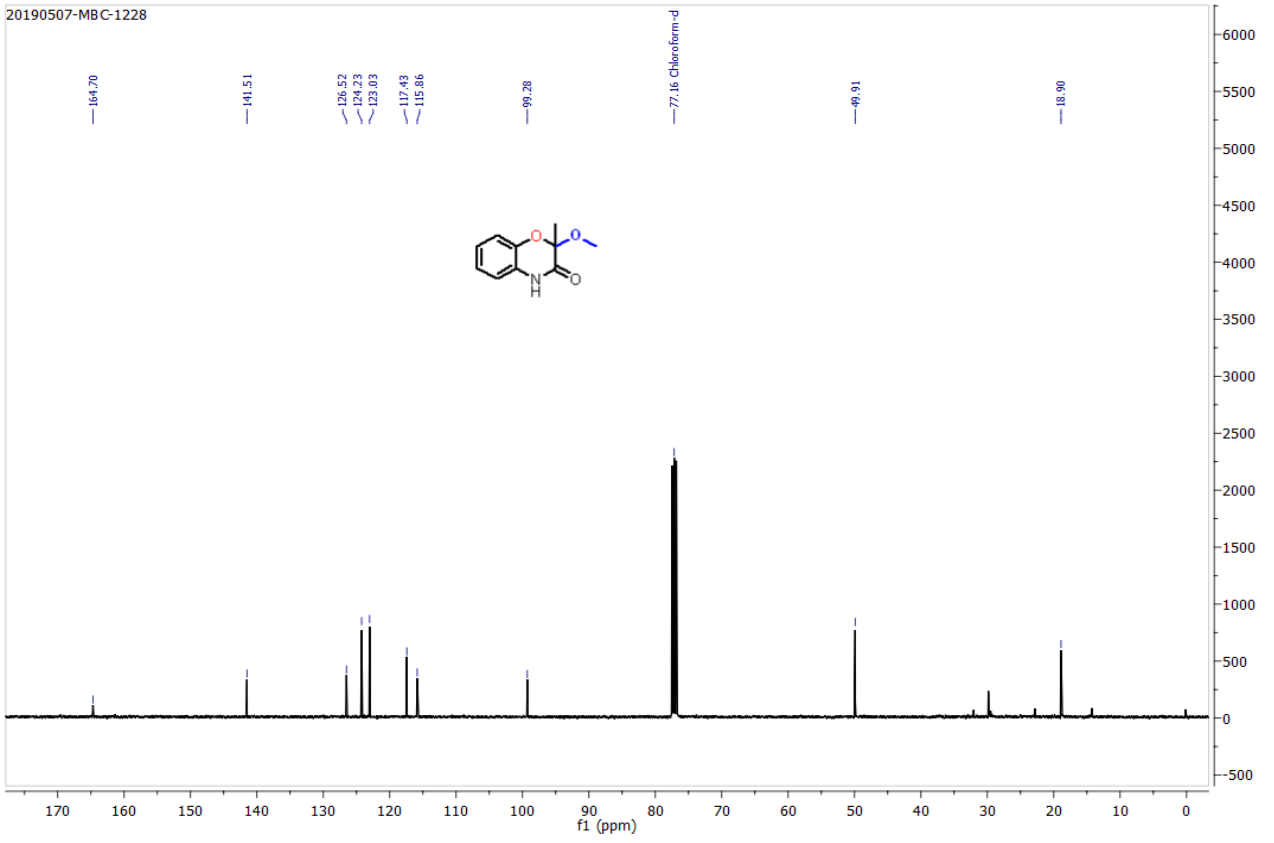

Figure 4B.12. ^{13}C NMR of compound **6b**

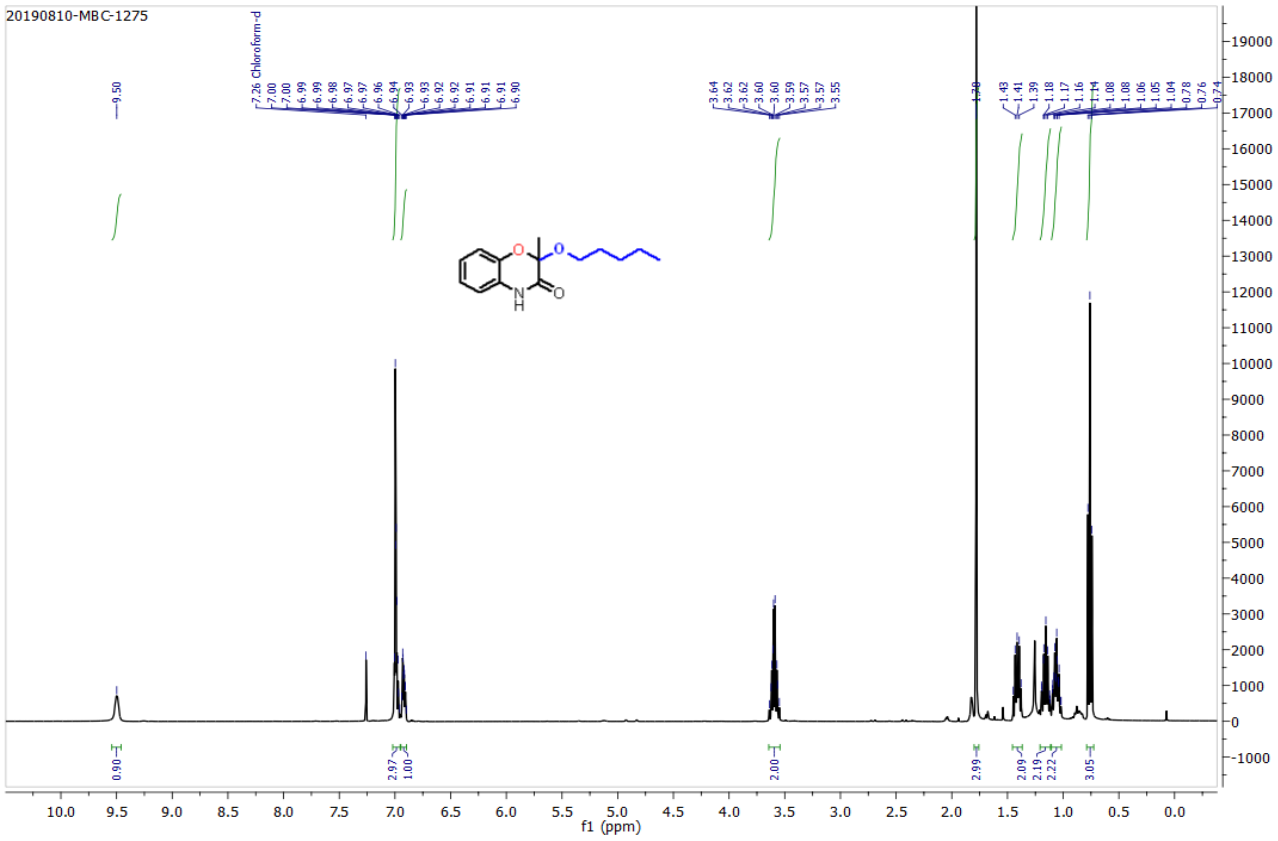

Figure 4B.13. ^{1}H NMR of compound **6e**

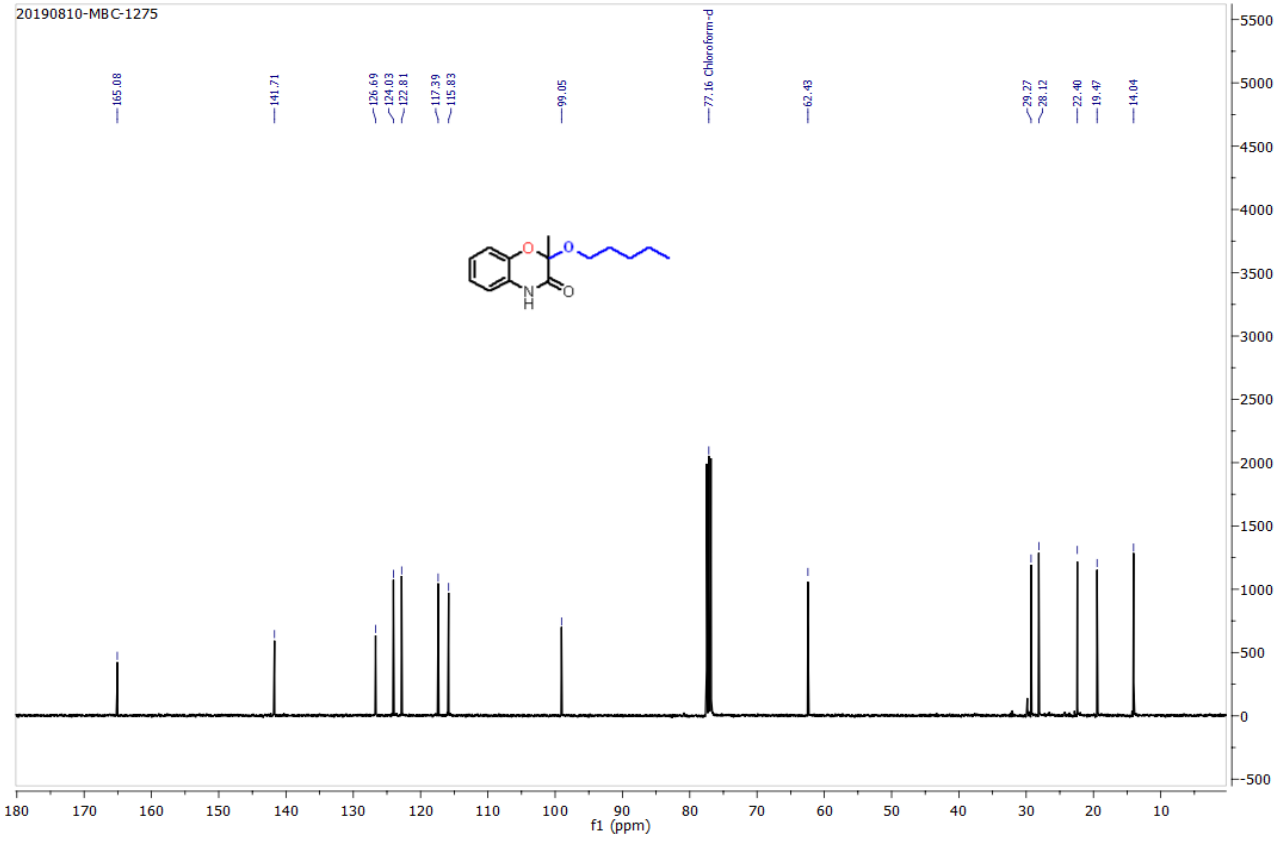

Figure 4B.14. ^{13}C NMR of compound **6e**

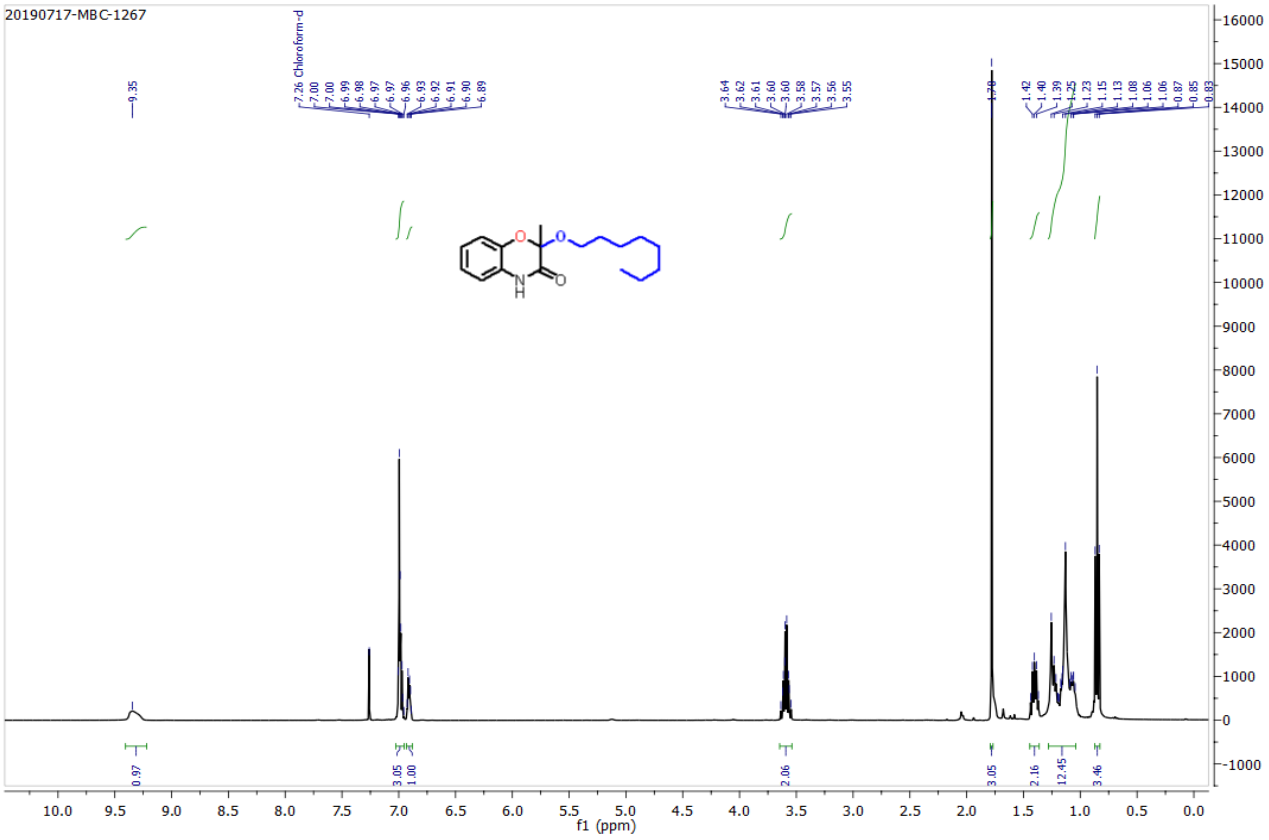

Figure 4B.15. ^{1}H NMR of ccompound **6g**

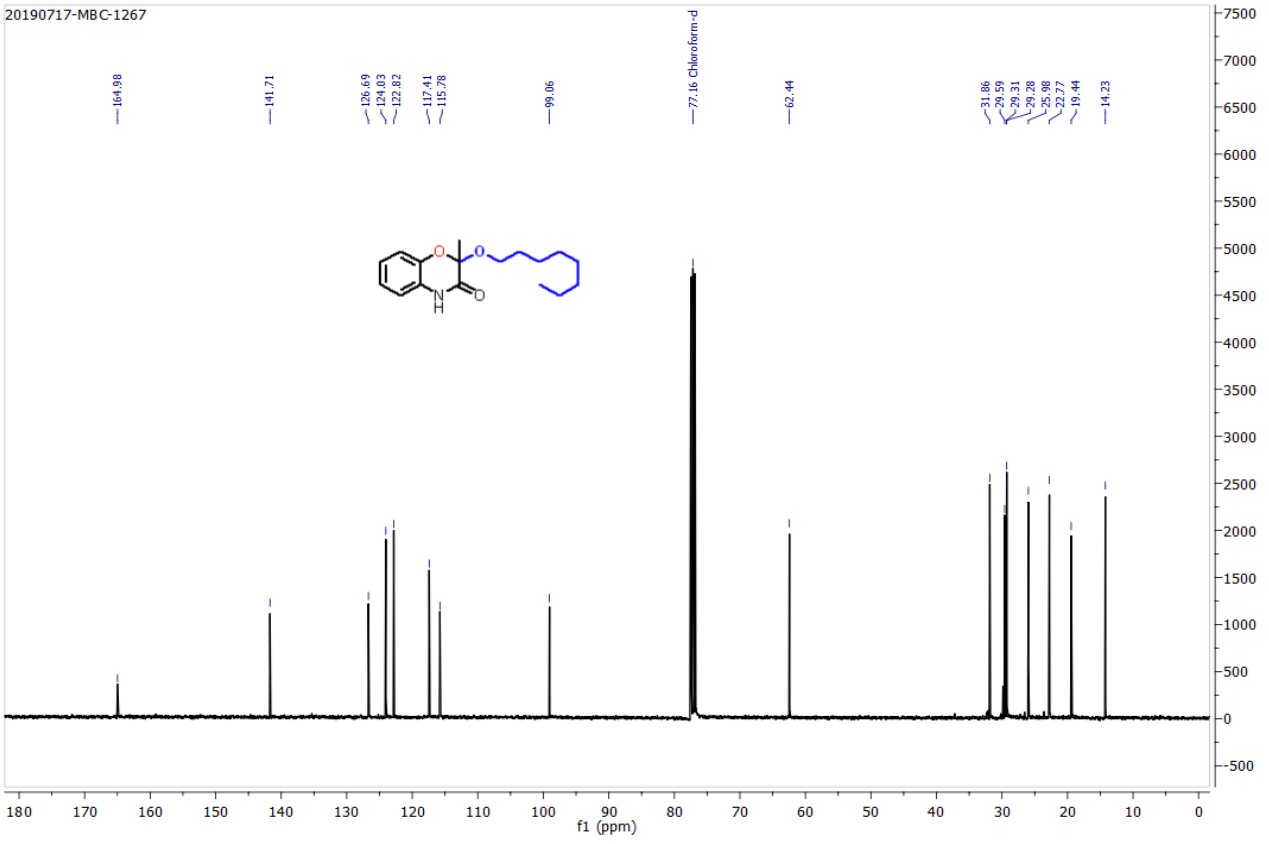

Figure 4B.16. ^{13}C NMR of compound **6g**

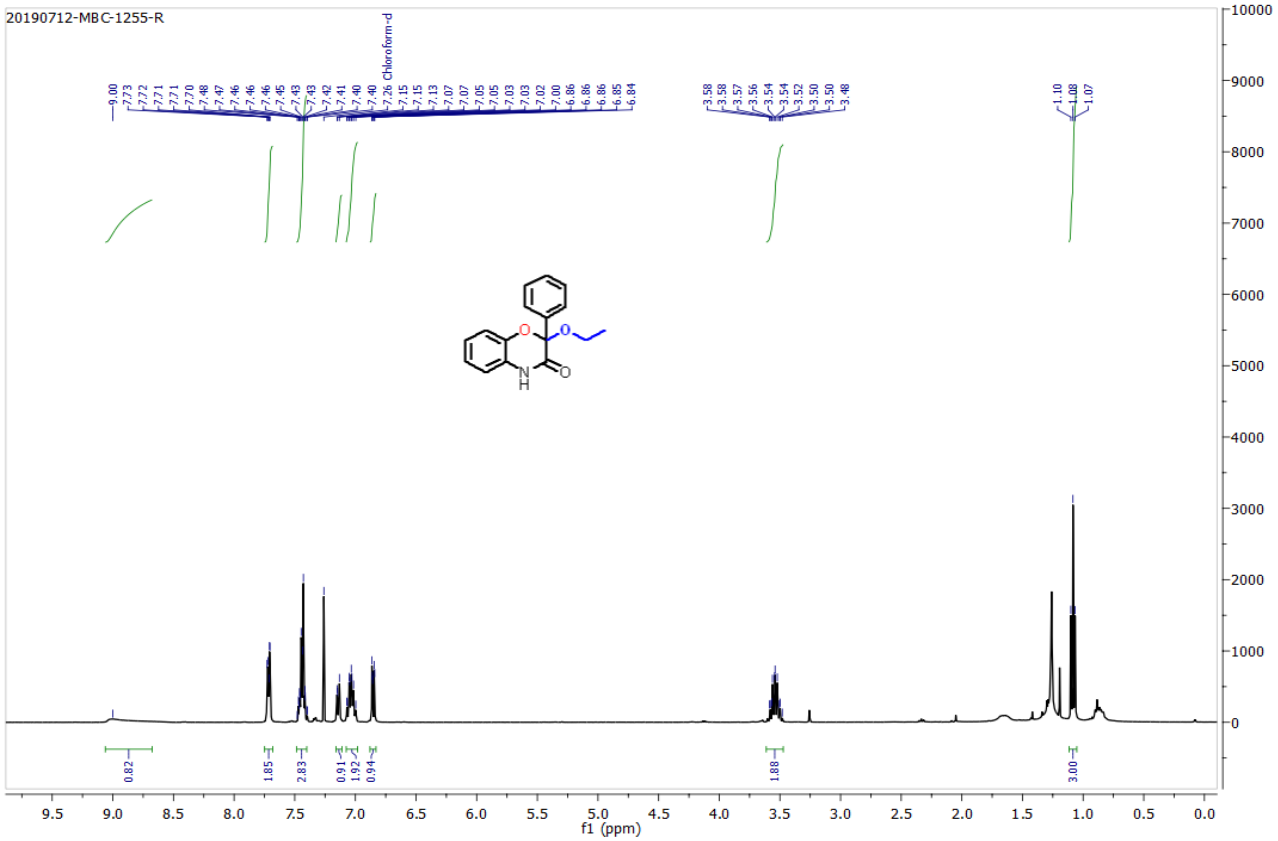

Figure 4B.17. ^{1}H NMR of compound **6i**

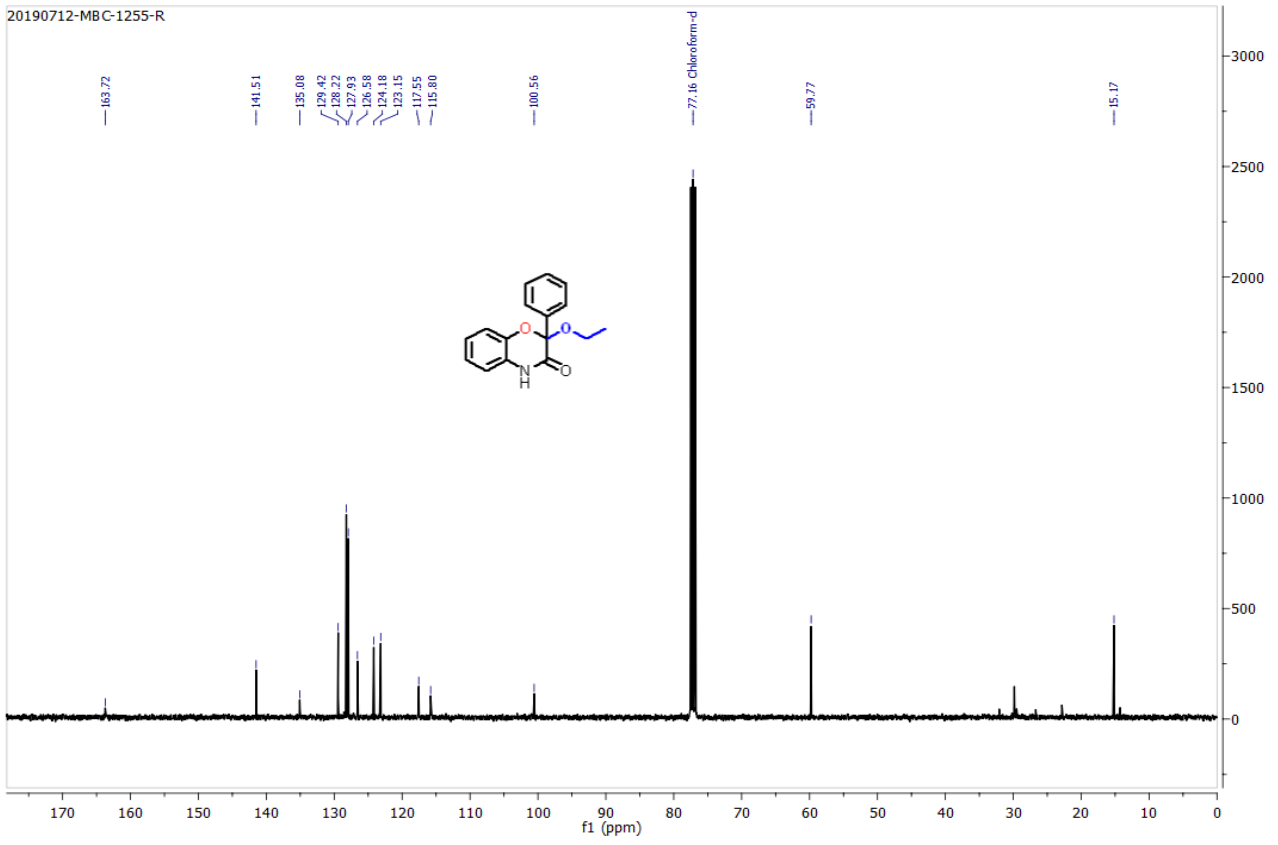

Figure 4B.18. ^{13}C NMR of compound **6i**

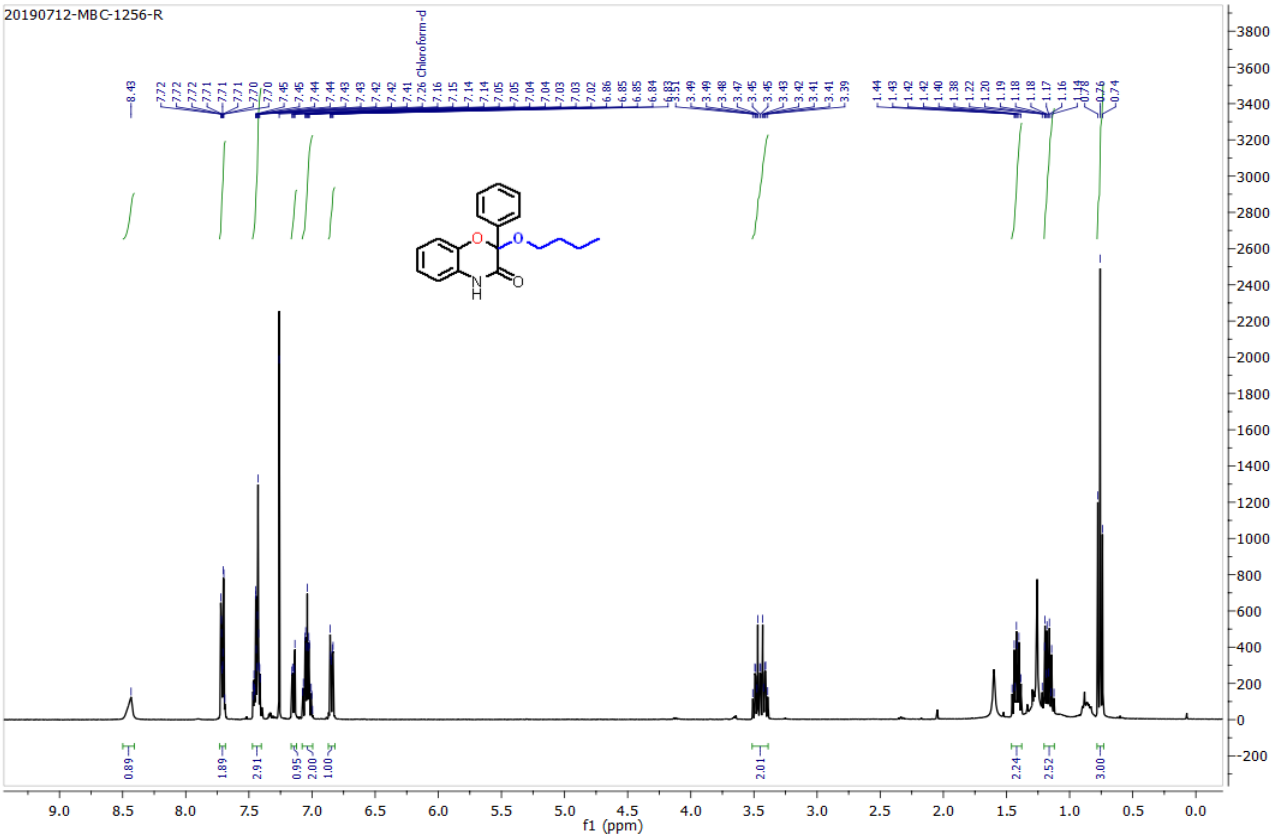

Figure 4B.19. ^{1}H NMR of compound **6k**

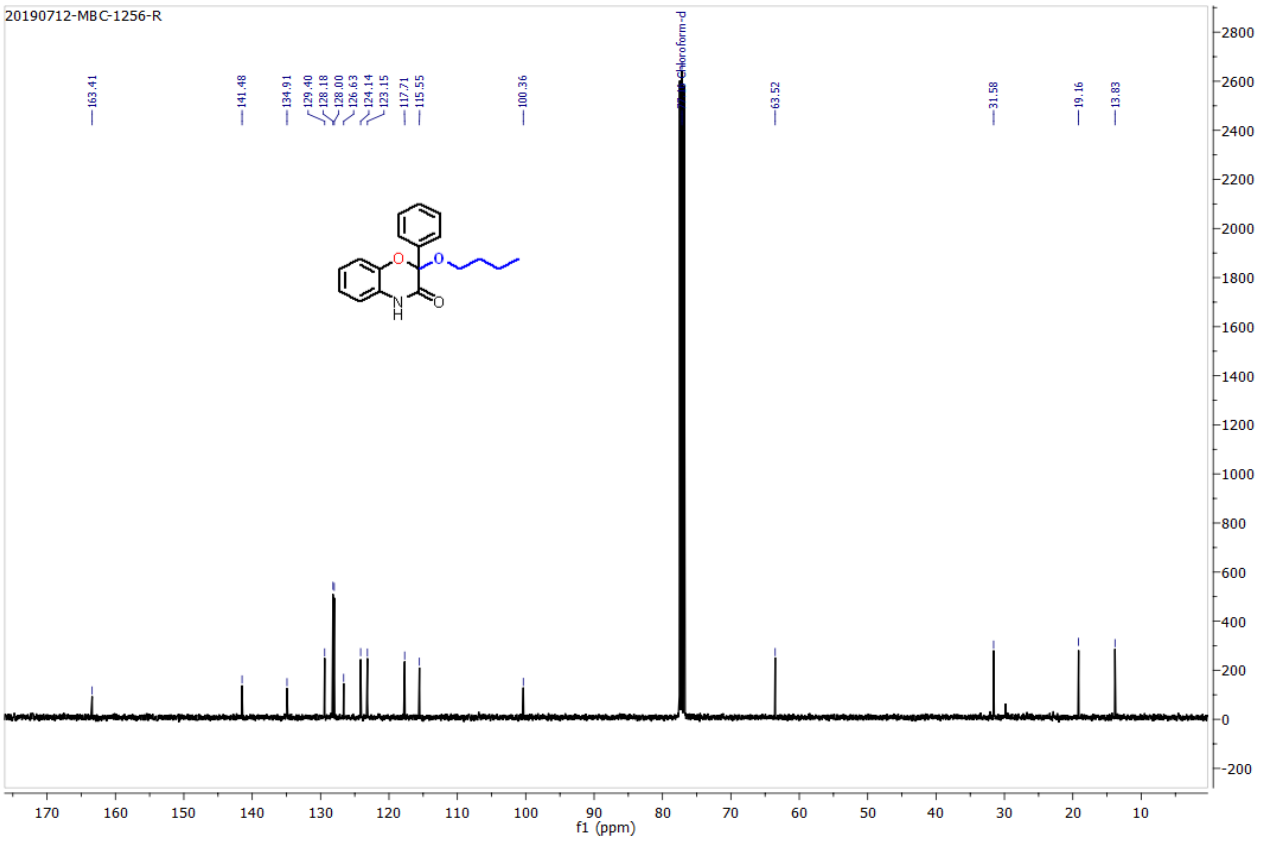

Figure 4B.20. ^{13}C NMR of compound **6k**

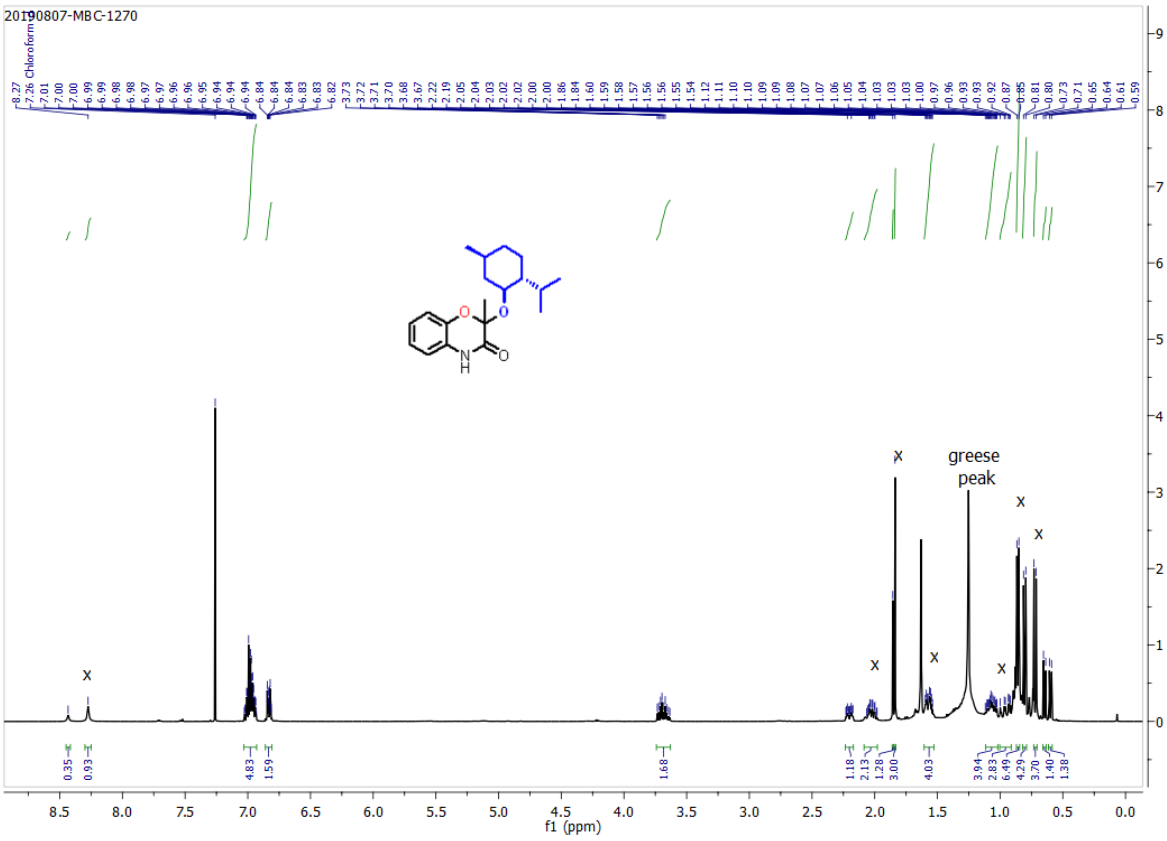

Figure 4B.21. ^{1}H NMR of compound **6m**

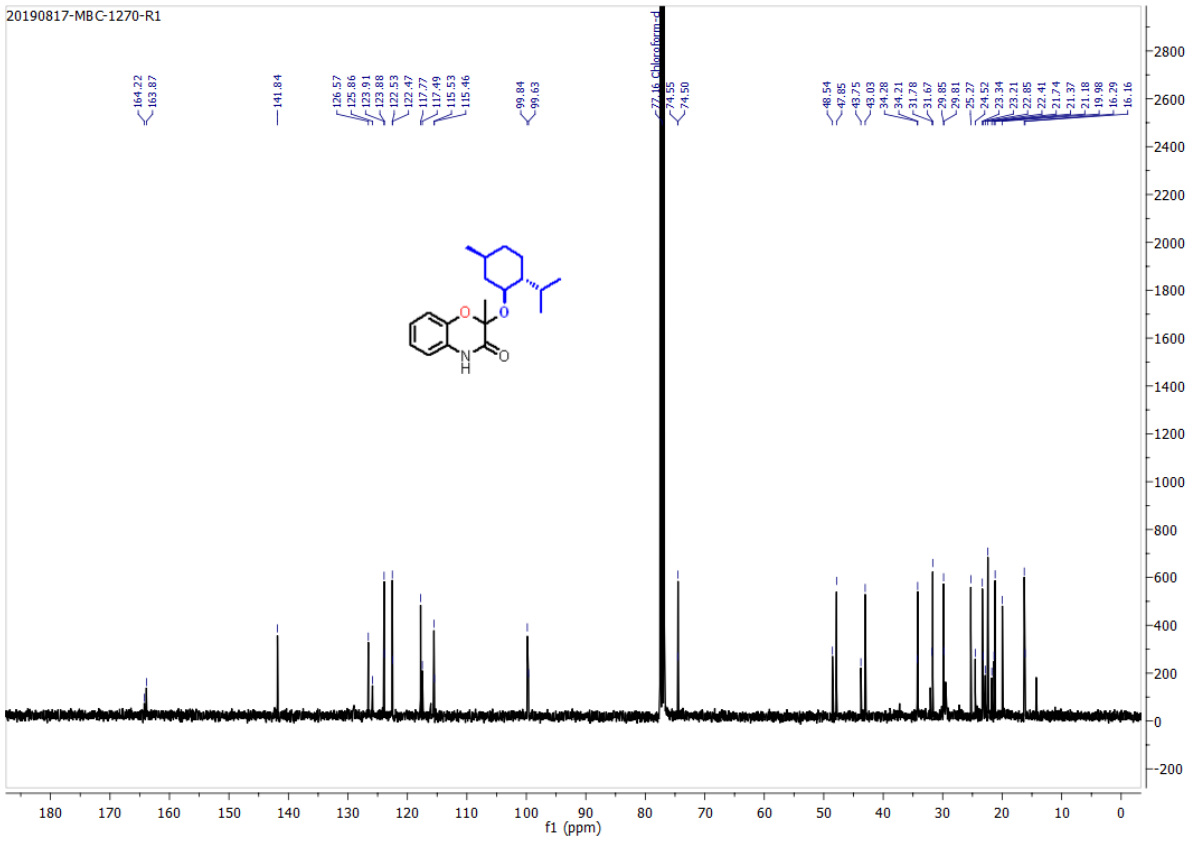

Figure 4B.22. ^{13}C NMR of compound **6m**

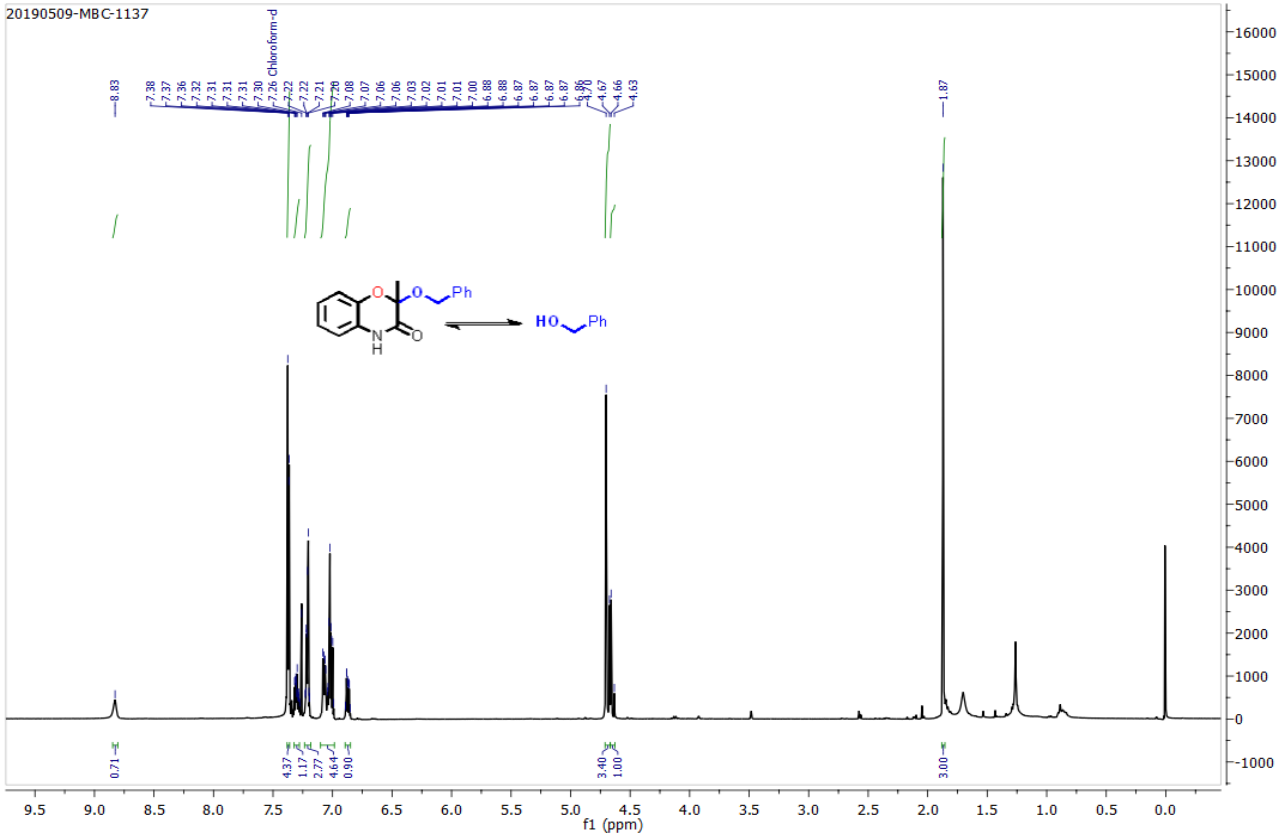

Figure 4B.23. ^{1}H NMR of compound **6n**

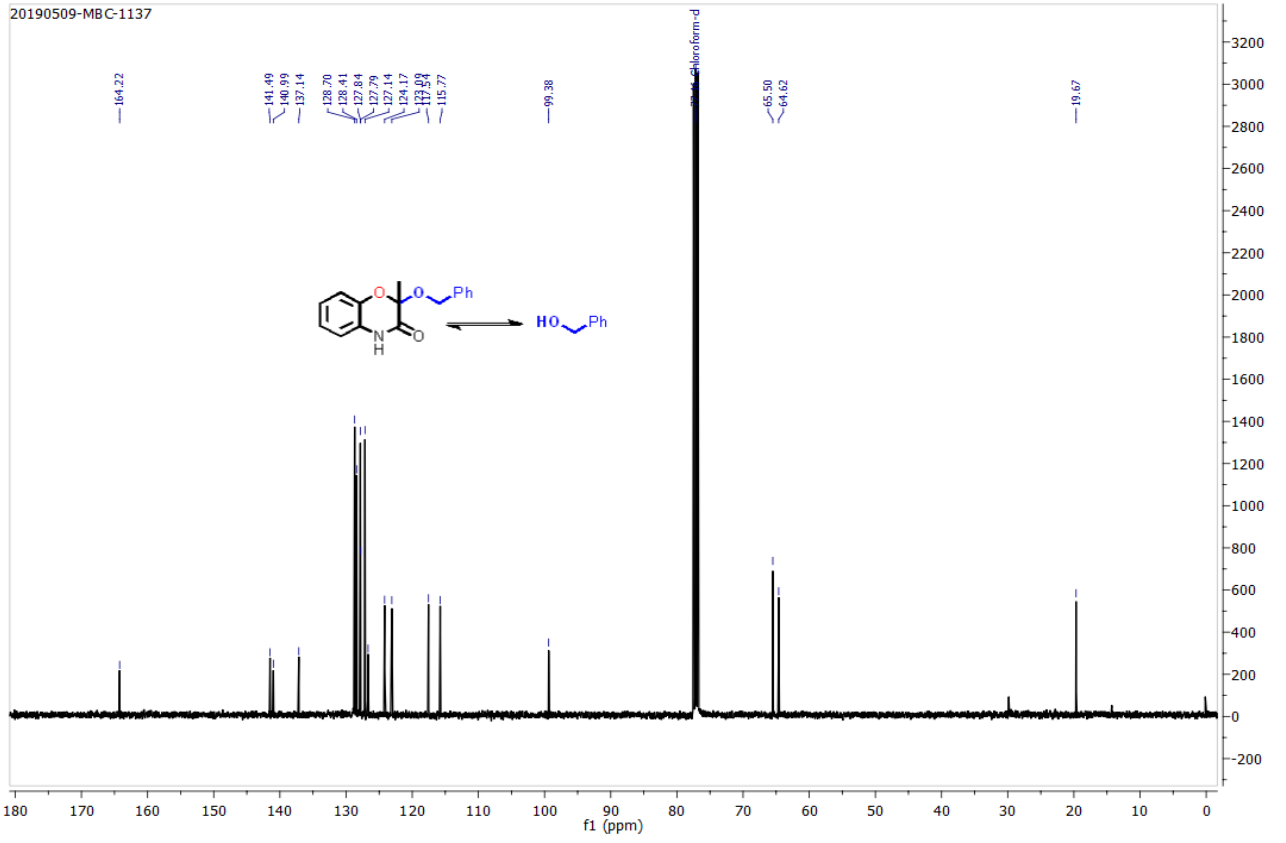

Figure 4B.24. ^{13}C NMR of compound **6n**

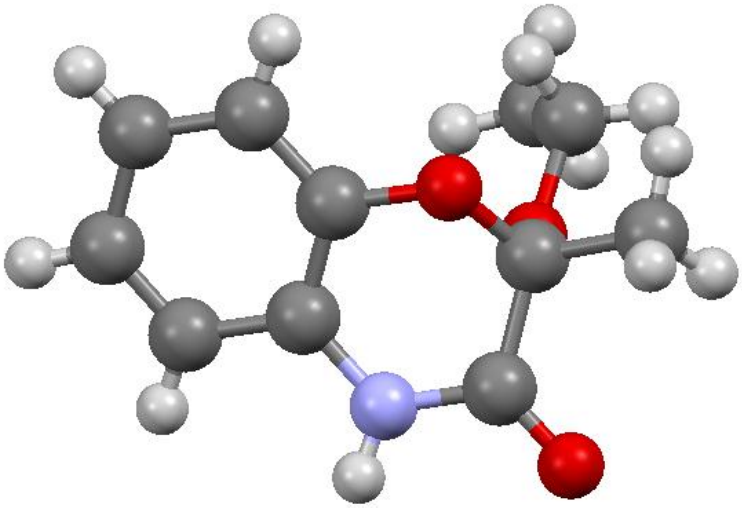

Figure 4B.25. Single crystal structure for compound **6a**

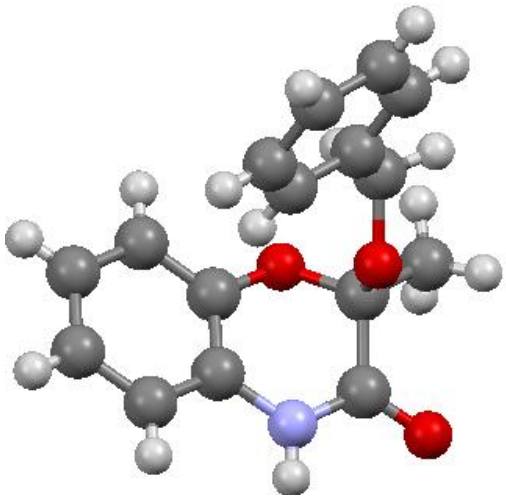

Figure 4B.26. Single crystal structure for compound **6n**

4B.8. References

(1) (a) Frey, M.; Chomet, P.; Glawischnig, E.; Stettner, C.; Grun, S.; Winklmair, A.; Eisenreich, W.; Bacher, A.; Meeley, R. B.; Briggs, S. P.; Simcox, K.; Gierl, A. *Science* **1997**, *277*, 696. (b) Dixon, R. A. *Nature* **2001**, *411*, 843. (c) Niemeyer, H. M. *J. Agric. Food Chem*. **2009**, *57*, 1677.
(2) (a) Warner, C. J. A.; Cheng, A. T.; Yildiz, F. H.; Linington, R. G. *Chem. Commun*. **2015**, *51*, 1305. (b) Minami, Y.; Yoshida, K-I.; Azuma, R.; Saeki, M.; Otani, T. *Tetrahedron Lett*. **1993**, *34*, 2633. (c) Beach, M.; Frechette, R. WO Patent Appl. 9728167, 1997. (d) Kikelj, D.; Suhadolc, E.; Rutar, A.; Pečar, S.; Punčuh, A.; Urleb, U.; Leskovšek, V.; Marc, G.; Sollner Dolenc, M.; Krbavčič, A.; Serša, G.; Novaković, S.; Povšič, L.; Štalc, A. European Patent EP0695308, 1996.
(3) (a) *Molecular Rearrangements in Organic Synthesis*, ed by Christian M. Rojas, John Wiley & Sons. Inc., Hoboken, New Jersey, **2015**. (b) Moulay, S. The Most Well-Known Rearrangements in Organic Chemistry at Hand. *Chem. Educ. Res. Pract*. **2002**, *3*, 33.
(4) (a) Hock, H.; Lang, S. *Ber*. **1944**, *77*, 257. (b) Yin, H.;. Xu, L; Porter, N. A. *Chem. Rev*. **2011**, *111*, 5944. (c) Mita, G.; Quarta, A.; Fasano, P.; De Paolis, A.; Di Sansebastiano, G. P.; Perrotta, C.; Iannacone, R.; Belfield, E.; Hughes, R.; Tsesmetzis, N.; Casey, R.; Santino, A. *J. Exp. Bot.* **2005**, *56*, 2321. (d) Yablokov, V. A. *Russ. Chem. Rev.* **1980**, *49*, 833. (e) Yaremenko, I. A.; Vil', V. A.; Demchuk, D. V.; Terent'ev, A. O. *Beilstein J. Org. Chem.* **2016**, *12*, 1647.
(5) (a) Baeyer, A.; Villiger, V. *Ber. Dtsch. Chem. Ges.* **1899**, *32*, 3625. (b) Strukul, G. *Angew. Chem. Int. Ed.* **1998**, *37*, 1198.
(6) (a) Criegee, R. *Ber. Dtsch. Chem Ges. A* **1945**, *77*, 722. (b) Wang, Z. Criegee Rearrangement. *Comprehensive Organic Name Reactions and Reagents;* John Wiley & Sons, **2010**; pp 770–774.
(7) (a) Olah, G. A.; Parker, D. G.; Yoneda, N.; Pelizza, F. *J. Am. Chem. Soc.* **1976**, *98*, 2245. (b) Murahashi, S.-I.; Naota, T.; Miyaguchi, N.; Noda, S. *J. Am. Chem. Soc.* **1996,** *118*, 2509. (c) Terent'ev, A. O.; Platonov, M. M.; Kashin, A. S.; Nikishin, G. I. *Tetrahedron* **2008,** *64*, 7944. (d) Brinkhorst, J.; Nara, S. J.; Pratt, D. A. *J. Am. Chem. Soc.* **2008**, *130*, 12224. (e) Valgimigli, L.; Amorati, R.; Fumo, M. G.; DiLabio, G. A.; Pedulli, G. F.; Ingold, K. U.; Pratt, D. A. *J. Org. Chem*. **2008**, *73*, 1830. (f) Zheng, X.; Lu, S.; Li, Z. *Org. Lett*. **2013**, *15*, 5432. (g) Chaudhari, M. B.; Chaudhary, A.; Kumar, V.; Gnanaprakasam, B. *Org. Lett.* **2019**, *21*, 1617.
(8) (a) Klare, H. F. T.; Goldberg, A. F. G.; Duquette, D. C.; Stoltz, B.M. *Org. Lett.* **2017**, *19*, 988. (b) Xiangbing, Q.; Hongli, B.; Tambar, U. K. *J. Am. Chem. Soc*. **2011**, *133*, 10050. (c) May, J. A.; Stoltz, B. *Tetrahedron* **2006**, *62*, 5262.
(9) (a) Chandrasekhar, C.; Roy, C. D. *Tetrahedron Lett*. **1987**, *28*, 6371. (b) Goodman, R. M.; Kishi, Y. *J. Am. Chem. Soc*. **1998**, *120*, 9392. (c) Hedaya, E.; Winstein, S. *Tetrahedron Lett*. **1962**, *3*, 563. (d) Crudeen, C. M.; Chen, A. C.; Calhoun, L. A. *Angew. Chem. Int. Ed.* **2000**, *39*, 2851. (e) Vil, V. A.; dos P. Gomes, G.; Bityukov, O.

V.; Lyssenko, K. A.; Nikishin, G. I.; Alabugin, I. V.; Terent'e v, A. O. *Angew. Chem. Int. Ed.* **2018**, *57*, 3372.
(10) (a) Ferreira, A. B.; Cardoso, A. L.; da Silva, M. J *ISRN Renewable Energy* **2012**, *2012*, 1. (b) Chan, C.-K.; Chen, Y.-H.; Chang, M.-Y. *Tetrahedron* **2016**, *72*, 5121. (c) Chan, C.-K.; Wang, H.-S.; Tsai, Y.-L.; Chang, M.-Y. *RSC Adv.* **2017**, *7*, 29321.
(11) Chaudhari, M. B.; Moorthy, S.; Patil, S.; Bisht, G. S.; Mohamed, H.; Basu, S.; Gnanaprakasam, B. *J. Org. Chem.* **2018,** *83*, 1358.

SUMMARY

The metal-catalyzed oxidative C-H functionalization offers a direct route to construct the C-C, C-O and C-N bond formation and gives access to novel bioactive compounds, commercial drugs, natural products, household products, petrochemicals, *etc.* In this thesis, we have presented our investigations on C-C bond formation by α-alkylation of unactivated amides, C-O bond formation *via* sp^3-C-H peroxidation, and hydroxylation of carbonyl compounds and novel rearrangement of peroxides to afford the biologically important scaffolds.

Chapter 2: Ruthenium-Catalyzed Direct α-Alkylation of Amides Using Alcohols and C-H Hydroxylation of Carbonyl Compounds

This chapter described the development of a highly efficient protocol for Ru-PNN catalyzed direct α-alkylation of amides using alcohol as an alkylating partner. This reaction proceeds *via* dehydrogenation–condensation–hydrogenation (domino sequence) with an excellent turnover number (TON). Moreover, we have developed a mild and operationally simple transition-metal free protocol for C-H hydroxylation of various ketones and amides using inexpensive- base and environmentally benign atmospheric air as an oxidant. This methodology delivers a broad array of substrates and provide an alternate route for the synthesis of hydroxylated ketones and amides by avoiding the use of hazardous phosphine based reductant and an expensive metal catalyst. DFT computations and isotope labeling studies support the mechanism.

Chapter 3: Metal-Catalyzed Batch/Continuous Flow Synthesis of Peroxides and Evaluation of Biological Properties

This chapter described the Fe-catalyzed peroxidation of carbonyl compounds *via* C-H functionalization. The present method is highly useful for the synthesis of quaternary peroxy derivatives of 2-oxindole, barbituric acid, and coumarin substrates. To minimize the explosive hazards, we have transformed the batch reaction conditions to continuous flow. The biological activity of the various peroxylated 2-oxindole was tested against the cancerous

cell lines, showing potential activity. On the other hand, to overcome the limitations of homogeneous catalysis and to increase the robustness of the catalytic process, the heterogeneous catalyst was prepared and implemented for C-H peroxidation in batch/continuous flow.

Chapter 4: The Novel Rearrangements of Peroxide on Electron Deficient Oxygen

In this chapter, for the first time, we have established a novel protocol for unprecedented biomimetic cascade rearrangement of 3-peroxy-2-oxindoles, which produces predominantly (*Z*)-2-arylidene or alkylidene-2*H*-benzo[*b*][1,4]oxazin-3(4*H*)-one derivatives in the presence of Lewis/Brønsted acid. Fascinatingly, if we use a catalytic amount of $FeCl_3$, a Hock-rearrangement was observed, which can be used to probe the homolytic *vs.* heterolytic cleavage. Interestingly, one more novel rearrangement of peroxides was developed for the construction of valuable substituted-2*H*-benzo[*b*][1,4]oxazin-3(4*H*)-one derivatives using mild conditions *via* ester activation-deprotection-acylation-bond migration-trapping of a carbocation in a domino fashion. The *in situ* generations of perester has been achieved by using easily available esters as a source of an acetyl group. Additionally, the carbocation is trapped by an *in situ* generated alkoxy group. To show the application under continuous flow, the heterogeneous version of the rearrangement reaction is developed by integrating the Amberlyst-15 in a continuous flow to obtain the rapid synthesis of ring expanded product in 22 min of residence time.

Title: Transition-Metal-Free C–H Hydroxylation of Carbonyl Compounds

Author: Moreshwar B. Chaudhari, Yogesh Sutar, Shreyas Malpathak, et al

Publication: Organic Letters

Publisher: American Chemical Society

Date: Jul 1, 2017

PERMISSION/LICENSE IS GRANTED FOR YOUR ORDER AT NO CHARGE

This type of permission/license, instead of the standard Terms & Conditions, is sent to you because no fee is being charged for your order. Please note the following:

- Permission is granted for your request in both print and electronic formats, and translations.
- If figures and/or tables were requested, they may be adapted or used in part.
- Please print this page for your records and send a copy of it to your publisher/graduate school.
- Appropriate credit for the requested material should be given as follows: "Reprinted (adapted) with permission from (COMPLETE REFERENCE CITATION). Copyright (YEAR) American Chemical Society." Insert appropriate information in place of the capitalized words.
- One-time permission is granted only for the use specified in your request. No additional uses are granted (such as derivative works or other editions). For any other uses, please submit a new request.

Title: Iron-Catalyzed Batch/Continuous Flow C–H Functionalization Module for the Synthesis of Anticancer Peroxides

Author: Moreshwar B. Chaudhari, Suresh Moorthy, Sohan Patil, et al

Publication: The Journal of Organic Chemistry

Publisher: American Chemical Society

Date: Feb 1, 2018

PERMISSION/LICENSE IS GRANTED FOR YOUR ORDER AT NO CHARGE

This type of permission/license, instead of the standard Terms & Conditions, is sent to you because no fee is being charged for your order. Please note the following:

- Permission is granted for your request in both print and electronic formats, and translations.
- If figures and/or tables were requested, they may be adapted or used in part.
- Please print this page for your records and send a copy of it to your publisher/graduate school.
- Appropriate credit for the requested material should be given as follows: "Reprinted (adapted) with permission from (COMPLETE REFERENCE CITATION). Copyright (YEAR) American Chemical Society." Insert appropriate information in place of the capitalized words.
- One-time permission is granted only for the use specified in your request. No additional uses are granted (such as derivative works or other editions). For any other uses, please submit a new request.

BACK CLOSE WINDOW

Title: The Rearrangement of Peroxides for the Construction of Fluorophoric 1,4-Benzoxazin-3-one Derivatives

Author: Moreshwar B. Chaudhari, Atul Chaudhary, Vishnupriya Kumar, et al

Publication: Organic Letters

Publisher: American Chemical Society

Date: Mar 1, 2019

PERMISSION/LICENSE IS GRANTED FOR YOUR ORDER AT NO CHARGE

This type of permission/license, instead of the standard Terms & Conditions, is sent to you because no fee is being charged for your order. Please note the following:

- Permission is granted for your request in both print and electronic formats, and translations.
- If figures and/or tables were requested, they may be adapted or used in part.
- Please print this page for your records and send a copy of it to your publisher/graduate school.
- Appropriate credit for the requested material should be given as follows: "Reprinted (adapted) with permission from (COMPLETE REFERENCE CITATION). Copyright (YEAR) American Chemical Society." Insert appropriate information in place of the capitalized words.
- One-time permission is granted only for the use specified in your request. No additional uses are granted (such as derivative works or other editions). For any other uses, please submit a new request.

BACK CLOSE WINDOW